Fundamentals of Compressible Flow with Aircraft and Rocket Propulsion

Third Edition

The subject of compressible flow or gas dynamics deals with the thermo-fluid dynamic problems of gases and vapours. It is now an important part of the undergraduate and postgraduate curricula. *Fundamentals of Compressible Flow* covers this subject in fourteen well organised chapters in a lucid style. A large mass of theoretical material and equations has been supported by a number of figures and graphical depictions. Author's sprawling teaching experience in this subject and allied areas is reflected in the clarity, and systematic and logical presentation.

SALIENT FEATURES

- Begins with basic definitions and formulas.
- Separate chapters on adiabatic flow, isentropic flow and rate equations.
- Includes basics of the atmosphere, and measuring techniques.
- Separate sections on wind tunnels, laser techniques, hot wires and flow measurement.
- Discusses applications in aircraft and rocket propulsion, space flights, and pumping of natural gas.
- Contains large number of solved and unsolved problems.

The present edition has an additional chapter (14) on miscellaneous problems in compressible flow (gas dynamics). This is designed to support the tutorials, practice exercises and examinations. Problems have been specially chosen for students and engineers in the areas of aerospace, chemical, gas and mechanical engineering.

S.M. Yahya is presently Emeritus Fellow in the Mechanical Engineering Department, I.I.T. Delhi. He obtained his doctoral degree in Turbomachinery from the University of Liverpool, England in 1965. He has been serving the Indian Institute of Technology, Delhi since 1967. He was the head of the Mechanical Engineering Department during 1987-90.

Professor Yahya has designed and taught courses in Gas Dynamics, Turbomachinery and Power Plants for undergraduate and postgraduate programmes. He also started and coordinated professional course programmes in Turbomachinery and Power Generation Technology at I.I.T. Delhi. He worked as a chair professor for the NTPC-sponsored master's programme in Power Generation Technology. Prof. Yahya served the Aligarh Muslim University as its Pro-vice Chancellor in 1991-92.

Besides numerous research publications he is also the author of *Turbomachines* (1972), *Elementary Gas Dynamics* (1973), *Gas Tables* (1978) and *Turbines, Compressors and Fans* (1983).

NEW AGE INTERNATIONAL (P) LIMITED, PUBLISHERS
New Delhi • Bangalore • Chennai • Guwahati
Hyderabad • Kolkata • Lucknow • Mumbai

ISBN 81-224-1468-0

S.M. YAHYA

Fundamentals of Compressible Flow

NEW AGE

Fundamentals of Compressible Flow SI Units with Aircraft and Rocket Propulsion

Third Edition

S.M. YAHYA

RAVI BOOK HOUSE
College Books Division
5, South Mada Street, Mylapore, Chennai - 4.
Phone : 24941751, 24617090, 24612376
url : WWW.ravibookhouse.com
E-mail : sales@ravibookhouse.com

NEW AGE INTERNATIONAL PUBLISHERS

formulas and units. A large number of unsolved examples with answers have also been given.

A financial grant from the Indian Institute of Technology, Delhi is gratefully acknowledged; it covered a part of the expenditures for preparing the manuscript. Thanks and appreciations are due to the staff of the New Age Publishers Pvt. Ltd. for their expertise and perseverance in bringing this title to completion.

Constructive criticism, attention to errors and suggestions for further improvements will be received with gratitute.

New Delhi — **S.M. YAHYA**

May, 1982

CONTENTS

Preface to the Third Edition v
Preface to the First Edition vii

PART I

1. DEFINITIONS AND BASIC RELATIONS 3
1.1 Fluid 4
1.2 System 4
1.3 Boundary 4
1.4 Control volume 4
1.5 State 4
1.6 Process 4
1.7 Cycle 5
1.8 Property 5
1.9 Continuum 5
1.10 Pure substance 6
1.11 Pressure 6
1.12 Density 6
1.13 Equilibrium 6
1.14 Temperature 7
1.15 Energy 7
1.16 Work 7
1.17 Heat 7
1.18 Zeroth law of thermodynamics 7
1.19 First law of thermodynamics 8
1.20 Specific heats of gases 9
1.21 Internal energy and enthalpy 10
1.22 Ideal gas 11
1.23 Equations of state 12
1.24 Real gases 13
1.25 Second law of thermodynamics 16
1.26 Reversible flow 17

1.27	Irreversible flow	17
1.28	Adiabatic process	17
1.29	Change of entropy	17
1.30	Third law of thermodynamics	18
1.31	Isentropic process	18
1.32	Bulk modulus of elasticity	18
1.33	Coefficient of compressibility	20
1.34	Fluid velocity	20
1.35	Streamline	21
1.36	Stream tube	21
1.37	Incompressible flow	21
1.38	Compressible flow	21
1.39	Steady flow	21
1.40	Unsteady flow	22
1.41	Flow process	22
1.42	Non-flow process	23
1.43	Viscosity	24
1.44	Reynolds number	25
1.45	Mach number	25
1.46	Laminar flow	26
1.47	Turbulent flow	26
1.48	Coefficient of skin friction	27
1.49	Properties of the atmosphere	30
2.	**THE ENERGY EQUATION**	**45**
2.1	Energy equation for a non-flow process	46
2.2	Energy equation for a flow process	47
2.3	The adiabatic energy equation	48
2.4	Stagnation velocity of sound	50
2.5	Stagnation pressure	51
2.6	Stagnation density	51
2.7	Stagnation state	51
2.8	Various regions of flow	52
2.9	Reference velocities	54
2.10	Bernoulli equation	59
2.11	Effect of Mach number on compressibility	60
3.	**RATE EQUATIONS FOR A CONTROL VOLUME**	**73**
3.1	Continuity equation (conservation of mass)	73
3.2	Momentum equation (conservation of momentum)	75

3.3	Moment of momentum equation	78
3.4	Energy equation (conservation of energy)	78
3.5	Entropy equation	80
4.	**ISENTROPIC FLOW WITH VARIABLE AREA**	**87**
4.1	Comparison of isentropic and adiabatic processes	87
4.2	Mach number variation	91
4.3	Stagnation and critical states	93
4.4	Area ratio as function of Mach number	96
4.5	Impulse function	98
4.6	Mass flow rate	100
4.7	Flow through nozzles	105
4.8	Flow through diffusers	110
4.9	Use of gas tables	111
5.	**WAVE MOTION**	**129**
5.1	Wave propagation in an elastic solid medium	129
5.2	Propagation of infinitesimal waves (sound waves)	131
5.3	Non-steep finite pressure waves	141
5.4	Steep finite pressure waves	145
5.5	Expansion waves	153
6.	**FLOW WITH NORMAL SHOCK WAVES**	**169**
6.1	Development of a shock wave	170
6.2	Rarefaction wave	171
6.3	The governing equations	172
6.4	Prandtl-Meyer relation	176
6.5	Mach number downstream of the normal shock wave	178
6.6	Static pressure ratio across the shock	179
6.7	Temperature ratio across the shock	180
6.8	Density ratio across the shock (the Rankine-Hugoniot equations)	181
6.9	Stagnation pressure ratio across the shock	184
6.10	Change in entropy across the shock	186
6.11	Impossibility of a shock in subsonic flow	187
6.12	Strength of a shock wave	188
6.13	Determination of Mach number of supersonic flows	190
6.14	Tables and charts for normal shock waves	192
6.15	Supersonic wind tunnels	193
6.16	Moving normal shock waves	198

7. FLOW WITH OBLIQUE SHOCK WAVES 219
- 7.1 Nature of flow through oblique shock waves 221
- 7.2 Fundamental relations 223
- 7.3 Prandtl's equation 226
- 7.4 Rankine-Hugoniot equation 227
- 7.5 Variation of flow parameters 229
- 7.6 Oblique shock relations from the normal shock equations 236
- 7.7 Mach waves 237
- 7.8 Gas tables for oblique shocks 238
- 7.9 Charts for oblique shocks 239
- 7.10 The shock polar diagram 243
- 7.11 Expansion of supersonic flow 250

8. FLOW IN CONSTANT AREA DUCTS WITH FRICTION 265
- 8.1 The Fanno curves 265
- 8.2 Fanno flow equations 268
- 8.3 Solution of Fanno flow equations 272
- 8.4 Variation of flow properties 275
- 8.5 Variation of Mach number with duct length 279
- 8.6 Tables for Fanno flow 280
- 8.7 Charts for Fanno flow 280
- 8.8 Isothermal flow with friction 282

9. FLOW IN CONSTANT AREA DUCTS WITH HEAT TRANSFER 309
- 9.1 The Rayleigh line 309
- 9.2 Fundamental equations 315
- 9.3 Rayleigh flow relations 317
- 9.4 Variation of flow properties 320
- 9.5 Maximum heat transfer 321
- 9.6 Tables for Rayleigh flow 323
- 9.7 Charts for Rayleigh flow 324

PART-II

10. MULTI-DIMENSIONAL FLOW 337
- 10.1 Cartesian coordinate system 338
- 10.2 Cylindrical coordinate system 349
- 10.3 Potential function 363
- 10.4 Stream function 370

11. METHODS OF MEASUREMENT 380
- 11.1 Pressure 380
- 11.2 Temperature 387
- 11.3 Density 393
- 11.4 Velocity 393
- 11.5 Hot-wire anemometer 397
- 11.6 Direction of flow 401
- 11.7 Flow rate 403
- 11.8 Wind tunnels 414
- 11.9 Flow visualization 424
- 11.10 Optical methods 425
- 11.11 Laser techniques 430

PART-III

12. AIRCRAFT PROPULSION 453
- 12.1 Early aircraft engines 454
- 12.2 Types of aircraft engines 456
- 12.3 Aircraft propulsion theory 465
- 12.4 Ramjet engine 483
- 12.5 Pulse jet engine 487

13. ROCKET PROPULSION 503
- 13.1 Early rocket engines 504
- 13.2 Types of rocket engines 506
- 13.3 Liquid propellant rocket engines 513
- 13.4 Solid propellant rocket motors 527
- 13.5 Rocket propulsion theory 538
- 13.6 Rocket applications 550
- 13.7 Space flights 555

14 MISCELLANEOUS PROBLEMS IN COMPRESSIBLE FLOW 587

Appendices 645

Bibliography 677

Index 680

PART-I

1

Definitions and Basic Relations

Fluid dynamics of compressible flows is generally referred to as Gas dynamics. This deals with the unified analysis of dynamics and thermodynamics of compressible flows. Fluid mechanic analyses of high speed flows of gases and vapours are inadequate without considering compressibility. Therefore, in applications like high speed aerodynamics, rocket and missile propulsion, steam and gas turbines, and high speed turbocompressors compressible fluid dynamics is used to obtain solutions of a number of design problems.

The properties of the fluid which are generally considered in compressible flow problems are temperature (T), pressure (p), density (ρ), internal energy (u), enthalpy (h), entropy (s) and viscosity (μ).

Some of the recent advances made in this area are in transonic, supersonic and hypersonic flows, and unsteady flows in rotating and reciprocating machines. A major portion covered by the fluid dynamics of compressible flows deals with the relations between force, mass and velocity. Therefore, following laws are frequently used in dealing with a variety of compressible flow problems:

(a) First law of thermodynamics (Energy equation)

(b) Second law of thermodynamics (Entropy relations)

(c) Law of conservation of mass (Continuity equation)

(d) Newton's second law of motion (Momentum equation).

Before dealing with the detailed analyses of compressible flows some basic definitions and fundamental relations in thermodynamics and fluid mechanics are summarized.

1.1 FLUID

A fluid is a substance which continuously deforms when shearing forces are applied. Liquids, gases, vapours and their mixtures are all fluids. A nonviscous or inviscid fluid is known as an ideal fluid. A real fluid is viscous.

A perfect fluid is inviscid as well as incompressible; such fluids do not stick to the surface with which they are in contact.

1.2 SYSTEM

A system is an arbitrary collection of matter which has a fixed identity. Things outside the system are known as surroundings.

Closed system: A system which has a fixed quantity of matter (fluid) is known as a closed system. There is no outflow or inflow of fluid from and to the system. But the system can interact with its surroundings through heat and work transfer. The boundaries of a closed system, containing a fixed mass of matter, can change.

Open system (control volume): A system through which there is continuous flow of matter (fluid) is known as an open system. It has a fixed space but does not contain a fixed mass of matter (fluid); instead, there is a continuous flow of mass through the open system.

Isolated system: If there is no flow of mass and energy to and from a system it is known as an isolated system.

1.3 BOUNDARY

Boundary is an imaginary surface which separates the system from its surroundings.

1.4 CONTROL VOLUME

This is an arbitrary volume fixed in space through which fluid flows; the identity of the fluid occupying the control volume changes with time. Therefore, control volume is an open system.

The surface which surrounds the control volume is known as control surface.

1.5 STATE

The state of a system is its condition which is defined by its properties.

1.6 PROCESS

A process is a change or a series of changes in the state of a system.

1.7 CYCLE

If the initial and final states of a system experiencing a series of processes, are identical it is said to be executing a cycle of a given number of processes.

1.8 PROPERTY

Property is an observable characteristic of a system such as pressure, volume and temperature. A property is independent of the process and is fixed by the end state of a system. Therefore, it is a point function. A quantity composed of different properties is also a property, e.g. enthalpy, entropy, Gibbs function and Helmholtz function.

A set of properties identify the state of a system.

Intensive property: A property which is independent of the mass or size of the system is referred to as an intensive property, e.g. pressure, density, temperature, viscosity and tension.

Extensive property: A property which depends on the mass or size of the system is known as an extensive property, e.g. length, area and volume.

1.9 CONTINUUM

Fluids like other substances are made of molecules which are always in motion corresponding to a given temperature. Statistical mechanics can determine the position of individual molecules in space and time for a given system. But in most of the engineering problems the behaviour of individual molecules in a system is of little importance. Generally, the problems concern the gross behaviour of the fluid in a control volume or a system. This requires the assumption of a 'continuum' which implies that the molecular density in the system (with minimum volume ΔV_c, area ΔA_c etc.) under consideration is large enough (the molecular density of gases is about 10^{19} molecules per cm^3) to consider the fluid as a continuous medium.

Though the assumption of a continuum is taken for granted throughout this book, it does not imply that this method is universal in dealing with all kinds of problems; the assumption of a continuum has some limitations. This is not valid under the following conditions:

(*a*) If the mean free path of the molecules is comparable with some characteristic length or distance in the system where the volume is less than ΔV_c or area less than ΔA_c.

(*b*) If the average time between molecular collisions is large.

The assumption of a continuum permits the use of macroscopic approach in a given problem. In case of molecular analysis microscopic approach is used.

Macroscopic approach: In macroscopic approach the quantities refer to the large scale properties or gross characteristics of the system. In this approach the assumption of a continuum is valid.

Microscopic approach: In microscopic approach the quantities refer to the microscopic properties in the system. Therefore, the assumption of the continuum is not valid.

1.10 PURE SUBSTANCE

Pure substance is a system which is homogeneous in composition and chemical aggregation. Some examples of pure substances are air, steam, air-fuel mixture etc.; in these systems the chemical elements are combined chemically in the same way in all parts of the system.

1.11 PRESSURE

Pressure (p) at a point surrounded by an elemental area ΔA is the force per unit area given by

$$p = \lim_{\Delta A \to \Delta A_c} \left(\frac{\Delta F}{\Delta A} \right) \tag{1.1}$$

Force ΔF is perpendicular to the area ΔA. Thus pressure is similar to stress in compression. The units of both pressure and stress are the same, *i.e.*, kgf/cm^2 or N/m^2; but all stresses are not similar to pressure.

1.12 DENSITY

Density (ρ) of a medium is the mass of fluid per unit volume. Thus

$$\rho = \lim_{\Delta V \to \Delta V_c} \left(\frac{\Delta m}{\Delta V} \right) \text{ kg/m}^3 \tag{1.2}$$

Specific volume is given by

$$v = \frac{1}{\rho} \text{ m}^3/\text{kg} \tag{1.3}$$

1.13 EQUILIBRIUM

If the changes in temperature with time in a system are absent it is said to be in thermal equilibrium. Similarly with the absence of changes in pressure or force with time the system is in mechanical equilibrium.

It is said to be in chemical equilibrium if all possible chemical reactions in the system have taken place and there is no change of phase with time.

When a system is in thermal, mechanical and chemical equilibrium it is said to be in thermodynamic equilibrium.

The treatment in the following chapters assumes thermodynamic equilibrium.

1.14 TEMPERATURE

When two systems in contact with each other are in thermal equilibrium one property common to both the systems has the same value; this property of the two systems is called temperature. Temperature is a measure of thermal potential of a system.

1.15 ENERGY

Energy is the capacity of exerting a force through a distance. The state of a system can be changed by adding or rejecting energy. In other words energy can be defined as the capacity of doing work.

Heat, work and energy can all be expressed in kilocalories, metre-kilograms, joules or kilowatt-hours.

1.16 WORK

Work is also energy in transit. When there is work transfer to or from a system the sole effect external to the system is the raising or lowering of a weight.

Work is done by a system on its surroundings when they are moved through a distance by the action of a force; this force is exerted by the system on the surroundings in the direction of the displacement of the surroundings. In simple mechanical terms work is force × distance in the direction of force. Work is a path function because it depends on the type of process. Therefore, it is not a property.

1.17 HEAT

Heat is that form of energy which transfers between the two systems by virtue of the temperature difference between them. Thus it is also energy in transit, and is not contained in any system. Heat transfer from and to a system changes its state.

Heat is a path function and therefore not a property.

1.18 ZEROTH LAW OF THERMODYNAMICS

Zeroth law of thermodynamics states that if two bodies are in thermal

equilibrium with a third body, they must also be in thermal equilibrium with each other. This is the basis of temperature measurement in which thermal equilibrium between two or more bodies and a thermometer or a thermocouple is used.

1.19 FIRST LAW OF THERMODYNAMICS

First law of thermodynamics states that when a system executes a cyclic process, the algebraic sum of the work transfers is proportional to the algebraic sum of the heat transfers. Symbolically it is expressed as

$$\oint dW \propto \oint dQ$$

$$\oint dW = J \oint dQ$$

If heat and work are in the same units

$$\oint dQ - \oint dW = 0 \tag{1.4}$$

Figure 1.1 shows three processes A, B and C occurring between two given state points on $p-v$ coordinates. State point 2 can be reached by two processes along the paths A and B. The return from State 2 to 1 is achieved through the process C. Equation (1.4) will now be considered for the two cycles.

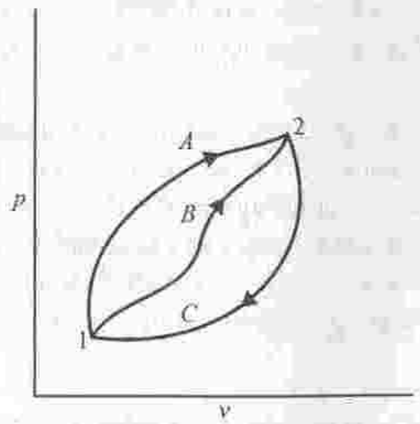

FIGURE 1.1 : Different processes between two state points

For the cycle 1A2C1

$$\oint (dQ - dW) = \int_{A1}^{2} (dQ - dW) + \int_{C2}^{1} (dQ - dW) = 0 \tag{1.5}$$

For the cycle 1B2C1

$$\oint (dQ - dW) = \int_{B1}^{2} (dQ - dW) + \int_{C2}^{1} (dQ - dW) = 0 \tag{1.6}$$

Subtracting Equation (1.6) from (1.5) and rearranging

$$\int_{A1}^{2} (dQ - dW) = \int_{B1}^{2} (dQ - dW) \tag{1.7}$$

Equation (1.7) shows that the quantity $(dQ - dW)$ is not a path function, *i.e.*, it does not depend on the path of the process. Therefore, the quantity $(dQ - dW)$ is the change in a property called "Energy" (E).

$$dE = dQ - dW$$

$$E_2 - E_1 = Q - W$$

$$Q = W + (E_2 - E_1) \tag{1.8}$$

This is the well known energy equation.

Heat transferred = Work done + change in energy.

With the help of Equation (1.8), first law can be restated as follows:

The energy of a system remains constant if the system is isolated from the surroundings as regards heat and work.

1.20 SPECIFIC HEATS OF GASES

Specific heat of a substance is its heat carrying capacity in a given process. It is defined by the amount of heat that is required to raise the temperature of a unit mass of a substance by one degree. Since in the present work we shall be dealing with gases their specific heats under two commonly used processes will be considered.

Specific heat at constant volume: The amount of heat required to raise the temperature of a unit mass of a gas by one degree at constant volume is known as the specific heat (c_v) at constant volume. It is given by

$$c_v = \left(\frac{\partial u}{\partial T}\right)_v = \left(\frac{\partial q}{\partial T}\right)_v \tag{1.9}$$

Specific heat at constant pressure: The amount of heat required to raise the temperature of a unit mass of a gas by one degree at constant pressure is known as the specific heat (c_p) at constant pressure.

It is given by

$$c_p = \left(\frac{\partial h}{\partial T}\right)_p = \left(\frac{\partial q}{\partial T}\right)_p \tag{1.10}$$

The specific heat of gases vary with temperature.

The ratio of specific heats: The ratio (γ) of specific heats at constant pressure and constant volume is given by

$$\gamma = \frac{c_p}{c_v} \tag{1.11}$$

From the kinetic theory of gases it can be shown that γ is related to the degrees of freedom (n) of the molecules by

$$\gamma = \frac{c_p}{c_v} = \frac{n+2}{n} \tag{1.12}$$

Values of γ for various gases, which are valid over a wide range of temperature are given in the following table:

TABLE 1.1: Values of γ for some gases

Gases	Degrees of Freedom	$\gamma = c_p/c_v$
Argon, Helium	$n = 3$	$5/3 = 1.67$
Air	$n = 5$	$7/5 = 1.4$
Steam, Carbon dioxide	$n = 6$	$8/6 = 1.33$
Ethane	$n = 8$	$10/8 = 1.25$

1.21 INTERNAL ENERGY AND ENTHALPY

Internal energy (u) of a gas is the energy stored in it by virtue of its molecular motion. If the internal energy is taken as zero at the absolute zero temperature its value at a temperature T is given by

$$u = c_v T$$

$$U = mc_v T \tag{1.13 (a)}$$

further assuming that c_v remains constant with temperature.

In compressible flows internal energy (u) often appears with the quantity (pv). Their sum is expressed by one single property called enthalpy (h). Thus

$$h = u + pv = u + \frac{p}{\rho} \tag{1.13 (b)}$$

For a perfect gas

$$h = c_v T + RT$$

$$h = (c_v + R)\, T$$

$$h = c_p T \tag{1.13 (c)}$$

1.22 IDEAL GAS

A gas which obeys the laws of Boyle and Charles is known as an ideal gas. Following relations hold for such a gas:

Boyle's law: At constant temperature

$$(pV)_T = \text{constant} \tag{1.14}$$

Charles' law: At constant pressure

$$\left(\frac{V}{T}\right)_p = \text{constant} \tag{1.15}$$

At constant volume

$$\left(\frac{p}{T}\right)_V = \text{constant} \tag{1.16}$$

It will be shown in the next section that the ideal gas follows a simple equation of state (1.22).

Semi-perfect gas: A semi-perfect gas is an ideal gas whose specific heats are functions of temperature.

$$c_p = f(T) \tag{1.17}$$

$$c_v = f(T) \tag{1.18}$$

Perfect gas: A perfect gas is an ideal gas whose specific heats remain constant at all temperatures.

$$\frac{d}{dT}(c_v) = 0 \tag{1.19}$$

$$c_v = \text{constant}$$

$$\frac{d}{dT}(c_p) = 0 \tag{1.20}$$

$$c_p = \text{constant}$$

Such a gas is also referred to as a calorically ideal gas.

1.23 EQUATIONS OF STATE

The state of a given system is fully defined by a certain minimum number of thermodynamic parameters. The relationship (equation) between these parameters (properties) is known as the equation of state. Other thermodynamic parameters can be determined by the known properties in the equation of state. As an example, equation of state for a system with variables p, V and T can be expressed in the following form

$$f(p,\ V,\ T) = 0 \tag{1.21}$$

For an ideal gas Equations (1.14), (1.15) and (1.16) can be combined to give

$$pV = mRT \tag{1.22}$$

where R is the gas constant.

$$p = \left(\frac{m}{V}\right) RT$$

$$p = \rho RT \tag{1.23}$$

Now $$m = n\overline{M} \tag{1.24}$$

Therefore, from Equations (1.22) and (1.24)

$$pV = n\,(\overline{M}R)\,T$$

But $$\overline{M}R = \overline{R}\ (\text{universal gas constant}) \tag{1.25}$$

Therefore, $$pV = n\overline{R}T \tag{1.26}$$

Gas properties based on one mole are known as molal or molar values such as molal volume and molal specific heats.

The volume of one mole or kilo mole (which has a mass numerically equal to the molecular weight of the given gas or substance) is 22.4 m^3 at $p = 1.0133$ bar and $T = 273$ K. Therefore, the value of the universal gas constant is

$$\overline{R} = \frac{pV}{nT}$$

$$R = \frac{1.0133 \times 10^5 \times 22.4}{1 \times 273 \times 1000}$$

$$\overline{R} = 8.314 \text{ kJ/k mol-K}$$

The gas constants are also given by

$$R = c_p - c_v \tag{1.27}$$

$$\overline{R} = \overline{M}R = \overline{M}\,(c_p - c_v) = \overline{c}_p - \overline{c}_v \tag{1.28}$$

From Equations (1.11) and (1.27)

$$c_p\left(1 - \frac{c_v}{c_p}\right) = R$$

$$c_p\left(1 - \frac{1}{\gamma}\right) = R$$

$$c_p = \frac{\gamma}{\gamma - 1} R \tag{1.29}$$

$$c_v = \frac{1}{\gamma - 1} R \tag{1.30}$$

Table 1.2 gives equations of state for some systems. Pairs of intensive and extensive properties along with the expressions for work done are also given.

TABLE 1.2: Pairs of intensive and extensive properties, work and equations of state

S. No.	System	Properties		Work	Equation of State
		Intensive	Extensive		
1.	Expansion in a cylinder	p	V	pdV	$p\frac{V}{T} = mR$
2.	Wire under tension	τ	L	τdL	$L_T = L_0\left[1 + \frac{\tau}{YA} + \alpha\,(T - T_0)\right]$
3.	Surface film	σ	A	σdA	$\sigma = \sigma_0 - k\,(T - T_0)$
4.	Reversible cell	$\in$	Z	$\in dZ$	$\in = a + bT + cT^2$
5.	Paramagnetic substance	H	M	HdM	$m = \frac{CVH}{T}$

1.24 REAL GASES

The behaviour of a real gas deviates from that of an ideal gas. Therefore, the equations of state (1.22), (1.23) etc. are not valid for real gases.

For real gases Equation (1.23) can be written as

$$p = Z\rho RT \tag{1.31}$$

The compressibility factor Z takes into account the deviation of a real gas behaviour from that of the ideal gas.

Some other equations of state for real gases are given in the following:

Van der Waals' Equation:

$$\left(p + \frac{a}{v^2}\right)(v - b) = RT \tag{1.32}$$

Plots of Equation (1.32) for various values of T are qualitatively shown in Figure 1.2. The parameters at the critical point are p_c, v_c and T_c.

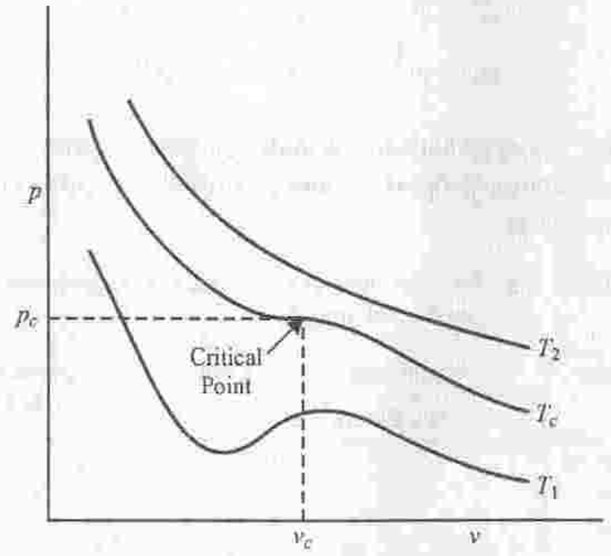

FIGURE 1.2 : Constant temperature plots of Van der Waals' equation

Following relations can be derived from Equation (1.32):

$$\frac{p_c v_c}{RT_c} = \frac{3}{8} \tag{1.33}$$

$$\left(p_r + \frac{3}{v_r^2}\right)(3v_r - 1) = 8T_r \tag{1.34}$$

where $p_r = \frac{p}{p_c}$, $v_r = \frac{v}{v_c}$ and $T_r = \frac{T}{T_c}$.

Equation (1.34) is independent of the gas constant R and constants a and b. Therefore, it is a universal equation for all the Van der Waals' gases.

Equation (1.34) can also be further reduced to the following form:

$$Z = f(p_r, T_r) \tag{1.35}$$

A plot of Equation (1.35) between Z and p_r at various values of T_r is shown in Figure 1.3. Such a chart can be used for determining various properties of real gases.

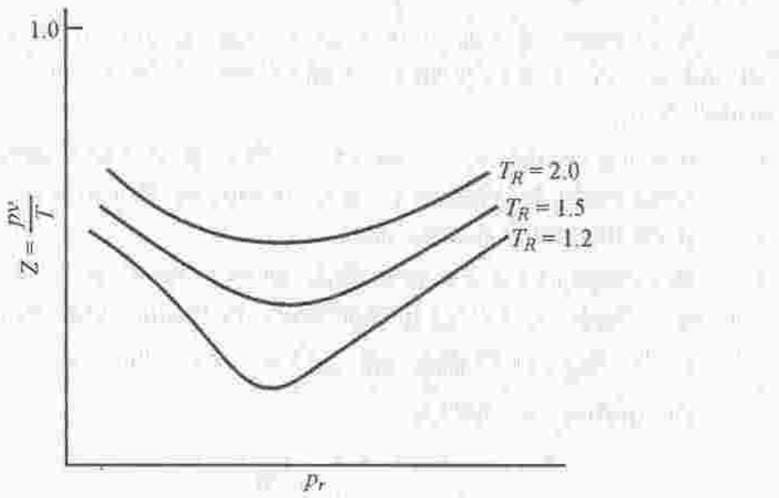

FIGURE 1.3 : Variation of compressibility factor with pressure ratio

Berthelot's equation:

$$p = \frac{\bar{R}T}{\bar{v} - b} - \frac{a}{T\bar{v}^2} \tag{1.36}$$

Dietrict's equation:

$$p = \frac{\bar{R}T}{\bar{v} - b} \exp\left(-\frac{a}{RT\bar{v}}\right) \tag{1.37}$$

Beattie-Bridgeman's equation:

$$p = \bar{R}T(1 - e)\ (\bar{v} + B)\,\bar{v}^{-2} - A\bar{v}^{-2} \tag{1.38}$$

where $A = A_0\left(1 - \frac{a}{\bar{v}}\right)$

$$B = B_0\left(1 - \frac{b}{v}\right)$$

$$e = \frac{c}{vT^3}.$$

1.25 SECOND LAW OF THERMODYNAMICS

The second law of thermodynamics provides a method of determining the efficiency of a given process; the real processes of energy transformation or transfer are compared with a standard "reference process", the ideal or the reversible process.

A number of statements have been provided to enunciate the second law of thermodynamics. Only some of these statements are mentioned here:

1. It is impossible to construct a heat engine which performs a complete cycle and delivers work exchanging heat from a single source (Kelvin-Planck's statement).
2. Heat cannot on its own flow from a body at lower temperature to a body at higher temperature (Clausius statement).

Following corollaries are derived from the second law:

Definition of entropy

$$S_2 - S_1 = \int_1^2 \frac{dQ_R}{T} \tag{1.39}$$

Clausius inequality

$$\oint \frac{dQ}{T} \le 0 \tag{1.40}$$

For any irreversible process

$$S_2 - S_1 > \int_1^2 \frac{dQ}{T} \tag{1.41}$$

For an irreversible adiabatic process

$$S_2 - S_1 > 0 \tag{1.42}$$

For any reversible cycle

$$\oint \frac{dQ_R}{T} = 0 \tag{1.43}$$

For isentropic or reversible adiabatic process

$$s_2 - s_1 = 0 \tag{1.44}$$

1.26 REVERSIBLE FLOW

A process is reversible if the system and its surroundings can be restored to their initial states by reversing the process. Quasistatic processes in the absence of solid or fluid friction and heat transfer with finite temperature difference are reversible. Some examples of reversible processes are compression of a spring, frictionless expansion or compression of a gas in a quasistatic adiabatic or an isothermal process.

A flow satisfying the conditions of a reversible process is referred to as a reversible or ideal flow. Such a flow is impossible to achieve in practice.

1.27 IRREVERSIBLE FLOW

A process which is not reversible is an irreversible process. In an irreversible process the system and the surroundings cannot be restored to their initial states by reversing the process. Some examples of irreversible processes are processes involving solid or fluid friction, heat transfer with finite temperature difference and free expansion. All real processes are irreversible. A real flow which does not satisfy the conditions of a reversible process is referred to as an irreversible flow.

1.28 ADIABATIC PROCESS

In an adiabatic process there is no heat transfer between the system and the surroundings. The work done in such a process between two states is given by

$$w_{nfp} = u_1 - u_2 \text{ (for non-flow processes)} \tag{1.45}$$

$$w_{fp} = h_1 - h_2 \text{ (for flow processes)} \tag{1.46}$$

In the absence of shaft work the stagnation enthalpy remains constant.

1.29 CHANGE OF ENTROPY

It can be shown that the integral of the quantity dq/T for any reversible process between two states is independent of the process; hence it is a property of the system called entropy (s). Its change in an infinitesimal process is given by

$$ds = \left(\frac{dq}{T}\right)_R \tag{1.47}$$

$$ds = \frac{p}{T}dv + c_v \frac{dT}{T} \tag{1.48}$$

For a finite process in a perfect gas

$$s_2 - s_1 = c_p \ln\left(\frac{T_2}{T_1}\right) - R \ln\left(\frac{p_2}{p_1}\right) \tag{1.49}$$

$$s_2 - s_1 = c_p \ln\left\{\frac{T_2/T_1}{(p_2/p_1)^{(\gamma-1)/\gamma}}\right\} \tag{1.50}$$

$$s_2 - s_1 = c_v \ln\left(\frac{T_2}{T_1}\right) + R \ln\left(\frac{v_2}{v_1}\right) \tag{1.51}$$

$$s_2 - s_1 = c_v \ln\left(\frac{p_2}{p_1}\right) + c_p \ln\left(\frac{v_2}{v_1}\right) \tag{1.52}$$

1.30 THIRD LAW OF THERMODYNAMICS

Third law of thermodynamics states that the entropy of a pure substance in complete thermodynamic equilibrium becomes zero at the absolute zero of temperature. This is included here only to fix the zero on the entropy-axis in the frequently occurring *h-s* or *T-s* diagrams.

1.31 ISENTROPIC PROCESS

An isentropic process is one in which there is no change in entropy. Such a process is a reversible adiabatic process; for this process, in the absence of shaft work, there is no change in the stagnation pressure and temperature.

Following relations hold for an isentropic process:

$$p v^{\gamma} = \text{constant} \tag{1.53}$$

$$\frac{T_1}{T_2} = \left(\frac{p_1}{p_2}\right)^{(\gamma-1)/\gamma} \tag{1.54}$$

$$\frac{v_1}{v_2} = \frac{\rho_2}{\rho_1} = \left(\frac{p_2}{p_1}\right)^{1/\gamma} \tag{1.55}$$

1.32 BULK MODULUS OF ELASTICITY

The bulk modulus of elasticity (K) of a fluid is defined by

$$K = \frac{\text{increase in pressure}}{\text{relative change in volume}}$$

Let the pressure change from p to $p + \Delta p$ in a system consisting of a fluid; the corresponding volume change is $-\frac{\Delta v}{v}$. Therefore,

$$K = \lim_{\Delta p \to 0} -\frac{v \Delta p}{\Delta v} = -v\frac{dp}{dv} \tag{1.56}$$

But $$v = \frac{1}{\rho}$$

$$dv = -\frac{d\rho}{\rho^2} \tag{1.57}$$

Therefore, $$K = \rho \frac{dp}{d\rho} \tag{1.58}$$

The value of $\frac{dp}{dv}$ or $\frac{dp}{d\rho}$ for gases and vapours depends on the process, *i.e.*, isothermal, adiabatic, etc.

Isothermal bulk modulus (K_T): For an ideal gas in an isothermal process

$$pv = \text{constant}$$

$$pdv + vdp = 0$$

$$-\frac{dp}{dv} = \frac{p}{v} \tag{1.59}$$

From Equations (1.56) and (1.59)

$$K_T = p \text{ (for an ideal gas)} \tag{1.60}$$

Adiabatic bulk modulus (K_s): For an ideal gas in reversible adiabatic process

$$pv^{\gamma} = \text{constant}$$

$$p(\gamma v^{\gamma-1})\,dv + v^{\gamma}\,dp = 0$$

$$-\frac{dp}{dv} = \frac{\gamma p}{v} \tag{1.61}$$

From Equations (1.56) and (1.61)

$$K_s = \gamma p \tag{1.62}$$

Equations (1.60) and (1.62) yield

$$K_s = \gamma K_T.$$

1.33 COEFFICIENT OF COMPRESSIBILITY

Coefficient of compressibility (β) of a fluid is defined as

$$\beta = \frac{\text{relative change in volume}}{\text{change in pressure}}$$

$$\beta = \lim_{\Delta p \to 0} -\frac{\Delta v}{v \Delta p} = -\frac{1}{v}\frac{dv}{dp} \tag{1.63}$$

Substituting for dv from Equation (1.57)

$$\beta = \frac{1}{\rho}\frac{d\rho}{dp} \tag{1.64}$$

Comparison of Equation (1.56) with (1.63), and Equation (1.58) with (1.64) shows that

$$K = \frac{1}{\beta} \tag{1.65}$$

Therefore, for ideal gases isothermal coefficient of compressibility is given by

$$\beta_T = \frac{1}{K_T} = \frac{1}{p} \tag{1.66}$$

The isentropic coefficient of compressibility is given by

$$\beta_s = \frac{1}{K_s} = \frac{1}{\gamma p} \tag{1.67}$$

$$\beta_T = \gamma \beta_s \tag{1.68}$$

For liquids the difference between the coefficients of compressibility (or bulk modulus) for isothermal and adiabatic processes is negligibly small.

1.34 FLUID VELOCITY

Fluid velocity (c) at a given point is the instantaneous velocity of the fluid particle passing through that point. Fluid velocity is a vector quantity.

1.35 STREAMLINE

A streamline is a curve in a flow field which is tangent to the direction of flow at all points. Streamlines do not cross each other.

1.36 STREAM TUBE

A stream tube is a collection of a number of streamlines forming an imaginary tube; this is shown in Figure 1.4. Therefore, there is no flow through the walls of a stream tube. There are no variations of flow parameters across the section of the stream tube. Flow through a stream tube is one-dimensional.

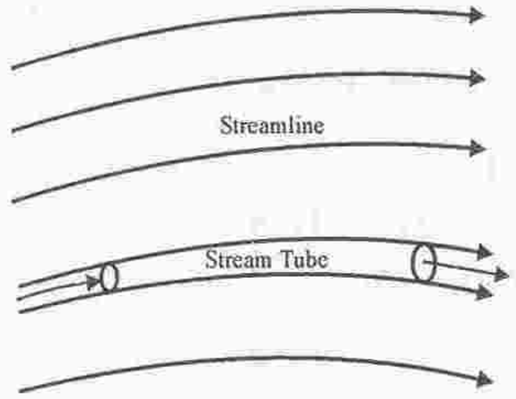

FIGURE 1.4 : One-dimensional flow

1.37 INCOMPRESSIBLE FLOW

If the relative change in density of a fluid in a process is negligibly small it is said to have incompressible flow; in such a flow velocity of sound is much larger than the flow velocity. Flow of gases at low Mach number (less than 0.3) can be assumed as incompressible.

1.38 COMPRESSIBLE FLOW

The relative changes in the density in compressible flows are appreciable and cannot be neglected. The fluid velocities in such flows are appreciable compared to the local velocity of sound. Flows at Mach numbers higher than 0.3 are considered as compressible.

1.39 STEADY FLOW

In steady flow the fluid properties (pressure, temperature, velocity, etc.)

in the control volume do not change with time. In mathematical terms, for steady flow,

$$\frac{\partial p}{\partial t}=\frac{\partial \rho}{\partial t}=\frac{\partial T}{\partial t}=\frac{\partial q}{\partial t}=\frac{\partial m}{\partial t}=0 \qquad (1.69)$$

The shape of the stream tube remains unaltered in a steady flow.

1.40 UNSTEADY FLOW

When one or more fluid property in the control volume change with time the flow is said to be unsteady.

1.41 FLOW PROCESS

A change or a series of changes in an open system is referred to as a "flow process". Some examples of such a process are: (*i*) flow through nozzles, diffusers and ducts, (*ii*) flow through a steam, gas or hydraulic turbine.

The work done in a steady flow process is given by

$$w_{fp}=-\int v\,dp \qquad (1.70)$$

This is shown in Figures 1.5 (*a*) and (*b*)

$$w_{fp}=-\int \frac{1}{\rho}dp=-\int dh \qquad (1.71)$$

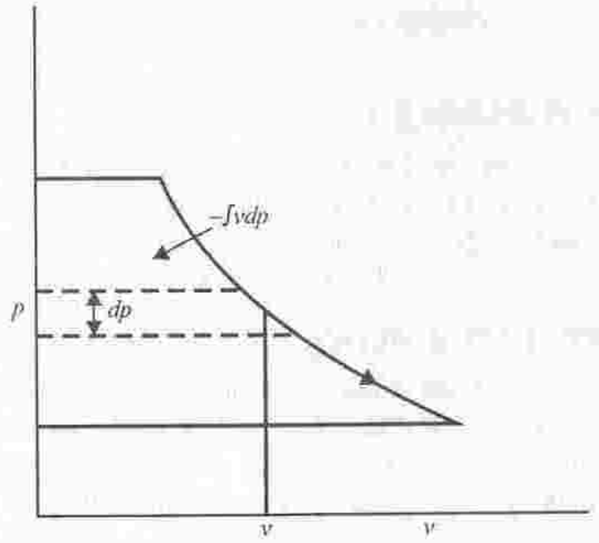

FIGURE 1.5 (*a*) : Work in a flow process (open system or a control volume)

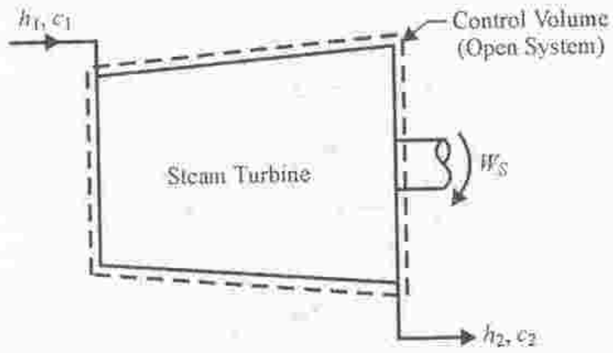

FIGURE 1.5 (*b*) : Steady flow of steam in a turbine (flow process)

For a perfect gas

$$w_{fp}=-c_p\int dT \qquad (1.72)$$

1.42 NON-FLOW PROCESS

A change or a series of changes in a closed system is referred to as a "non-flow process". Some examples of such a process are:

(*i*) Constant volume heating and cooling of a gas or a vapour.

(*ii*) Expansion or compression in reciprocating engines and compressors.

The work done in a reversible "non-flow process" is given by

$$w_{nfp}=\int p\,dv \qquad (1.73)$$

This is shown in Figures 1.6 (*a*) and (*b*).

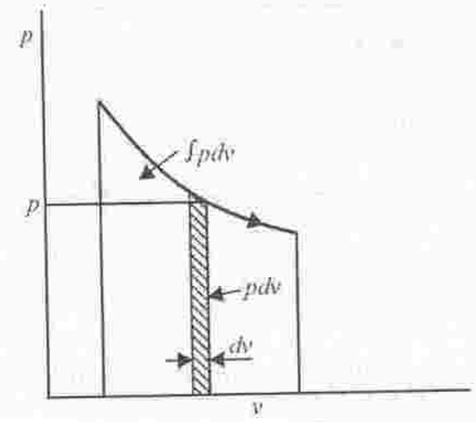

FIGURE 1.6 (*a*) : Work in a non-flow process (closed system)

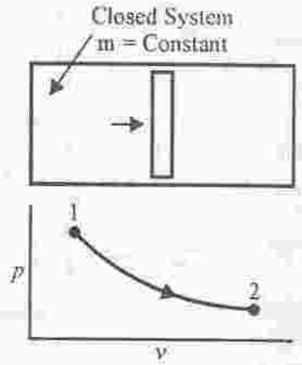

FIGURE 1.6 (*b*) : Expansion in an internal combustion engine cylinder (non-flow process)

1.43 VISCOSITY

The resistance to the shearing motion of two adjacent layers of a fluid is due to a fluid property called viscosity.

In a Newtonian fluid the relation between the shear stress and the angular deformation is linear. The deformation of such a fluid element $ABCD$ is shown in Figure 1.7. The angular deformation per unit time is given by

$$\frac{1}{t}\left(\frac{BE}{AB}\right)=\frac{1}{t}\left(\frac{t\,.\,dc}{dy}\right)=\frac{dc}{dy}$$

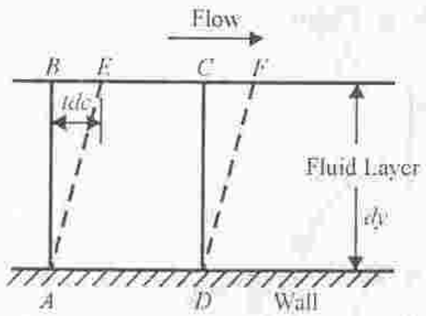

FIGURE 1.7 : Flow of a viscous fluid

Now the shear stress is proportional to the deformation. Therefore,

$$\tau \propto \frac{dc}{dy}$$

$$\tau = \mu \frac{dc}{dy} \tag{1.74}$$

In Equation (1.74) the constant of proportionality (μ) is known as the coefficient of viscosity. This is independent of velocity but varies considerably with temperature. Viscosities of gases vary little with pressure.

The kinematic viscosity ν is defined as the ratio of the dynamic viscosity and the density of the fluid.

$$\nu = \frac{\mu}{\rho}. \tag{1.75}$$

1.44 REYNOLDS NUMBER

This is a non-dimensional number defined as

$$\mathrm{Re} = \frac{\text{inertia force}}{\text{viscous force}}$$

$$= \frac{\rho A c^2}{\mu c l}$$

Here l is a characteristic length

$$A = l^2,\ \frac{\mu}{\rho} = \nu$$

Therefore, $$\mathrm{Re} = \frac{\rho c l}{\mu} = \frac{cl}{\nu} \tag{1.76}$$

1.45 MACH NUMBER

This is a non-dimensional number defined as

$$M^2 = \frac{\text{inertia force}}{\text{elastic force}}$$

$$= \frac{\rho A c^2}{KA} = \frac{\rho c^2}{K}$$

It will be shown later that $K = \rho a^2$. Therefore,

$$M^2 = \left(\frac{c}{a}\right)^2 \tag{1.77}$$

Equation (1.77) gives another definition of Mach number; this is the ratio of the fluid velocity and the local velocity of sound. It will

be seen in the following chapters that Mach number is an extremely important parameter in the analysis of compressible flows.

It is shown in Section 5.2 that the velocity of sound (a) in a medium at temperature T is given by

$$a = \sqrt{\left(\frac{\partial p}{\partial \rho}\right)} = \sqrt{\gamma RT} \tag{1.78}$$

Therefore, $$M = \frac{c}{a} = \frac{c}{\sqrt{\gamma RT}}. \tag{1.79}$$

1.46 LAMINAR FLOW

The flow of fluid over a body in orderly parallel layers without any component or components of fluctuations in the three directions is known as laminar flow. Here the surface frictional force which predominates keeps the flow parallel to the surface. Other slices of the flow slide on top of the other. Such a flow occurs at lower values of the Reynolds number.

1.47 TURBULENT FLOW

At higher values of the Reynolds number (greater than 2000 for circular pipes) the inertia force becomes predominant and fluid particles are no longer constrained to move in parallel layers; instead, they cross the parallel streamlines. Thus there are small scale fluctuation components (c'_x, c'_y and c'_z) in the three directions X, Y and Z which leads to a continuous mixing of the various layers of flow. The irregular fluctuations of velocity are superimposed on the mean flow. Such a flow is known as turbulent flow.

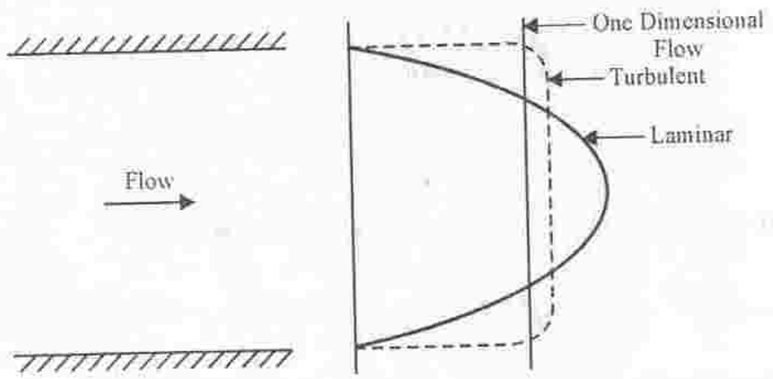

FIGURE 1.8 : Laminar and turbulent flows

Figure 1.8 shows the velocity profiles in laminar, turbulent and one dimensional flows in a duct.

Degree of turbulence: A measure of turbulence in the flow is given by the degree of turbulence or turbulence level; this is defined as the ratio of the arithmetic root mean square of the fluctuation components and the average bulk velocity.

$$\text{Degree of turbulence} = \frac{1}{c}\sqrt{\frac{1}{3}(c'^2_x + c'^2_y + c'^2_z)}. \tag{1.80}$$

1.48 COEFFICIENT OF SKIN FRICTION

Fanning's coefficient of skin friction (f) or friction factor is defined by

$$f = \frac{\tau_w}{\frac{1}{2}\rho c^2} \tag{1.81}$$

This is a non-dimensional factor and is a measure of frictional resistance to the flow. This is obtained by integrating the viscous stresses in the flow.

Figure 1.9 shows viscous flow in a circular duct of diameter D. The velocity at any radius r is c and the shear stress τ. The shear stress at the wall is τ_w and zero at the axis of the duct. The pressure gradient in the direction of flow is dp/dx.

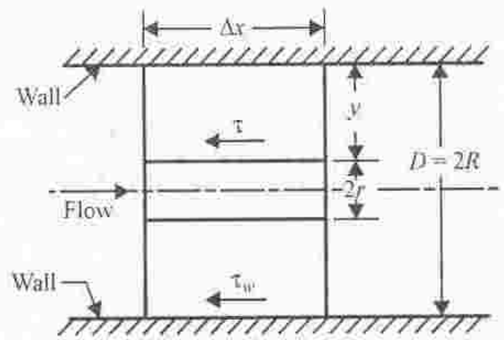

FIGURE 1.9 : Skin friction

Flow over the duct length Δx is now considered.

The pressure difference across this length is balanced by the shear force. Therefore,

$$\left\{p-\left(p+\frac{dp}{dx}\Delta x\right)\right\}\frac{\pi}{4}D^2=-(\pi D\Delta x)\,\tau_w$$

$$dp\cdot\frac{\pi}{4}D^2=\pi D dx\,.\,\tau_w \tag{1.82}$$

$$\tau_w=\frac{1}{4}D\frac{dp}{dx} \tag{1.83}$$

Substituting Equation (1.81) in (1.82) yields

$$dp=4f\cdot\frac{1}{2}\rho c^2\frac{dx}{D} \tag{1.84}$$

This is also expressed as

$$dp=f'\cdot\frac{1}{2}\rho c^2\frac{dx}{D} \tag{1.85}$$

where f' is the Darcy's friction factor.

$$f'=4f \tag{1.86}$$

Friction factor for laminar flow: From Equation (1.82) at $r=R$

$$dp\,.\,\pi R^2=2\pi R dx\tau_w \tag{1.87}$$

and at $r=r$

$$dp\,.\,\pi r^2=2\pi r dx\tau \tag{1.88}$$

Equations (1.87) and (1.88) give

$$\frac{\tau}{\tau_w}=\frac{r}{R} \tag{1.89}$$

From the definition of viscosity Equation (1.74) gives

$$\tau=\mu\frac{dc}{dy}$$

But in Figure 1.9

$$y=R-r$$
$$dy=-dr$$

Therefore, $$\tau=-\mu\frac{dc}{dr}$$

$$\frac{dc}{dr}=-\frac{\tau}{\mu} \tag{1.90}$$

Equations (1.89) and (1.90) give

$$\frac{dc}{dr}=-\frac{\tau}{\mu}=-\frac{r}{R}\frac{\tau_w}{\mu}$$

$$dc=-\frac{\tau_w}{R\mu}r dr \tag{1.91}$$

This equation on integration yields

$$c=-\frac{\tau_w}{R\mu}\frac{r^2}{2}+A$$

At $r=R,\ c=0.$

Therefore, $$A=\frac{\tau_w}{R\mu}\frac{R^2}{2}$$

$$c=\frac{\tau_w}{2R\mu}(R^2-r^2) \tag{1.92}$$

Equation (1.92) gives the local velocity c at radius r while the mean velocity is given by

$$\bar{c}=\frac{1}{\pi R^2}\int_0^R c\,(2\pi r dr) \tag{1.93}$$

Substituting for c from Equation (1.92)

$$\bar{c}=\frac{\tau_w}{\mu R^3}\int_0^R (R^2 r-r^3)\,dr$$

$$\bar{c}=\frac{\tau_w R}{4\mu} \tag{1.94}$$

Substituting for τ_w from Equation (1.81)

$$f=\frac{8\mu}{R\rho\bar{c}}$$

$$f=\frac{16}{\bar{c}D/(\mu/\rho)}$$

But $$\frac{\bar{c}D}{\mu/\rho}=\frac{\bar{c}D}{\nu}=\mathrm{Re}$$

Therefore, Fanning's friction factor

$$f = \frac{16}{\text{Re}} \tag{1.95}$$

and Darcy's friction factor

$$f' = \frac{64}{\text{Re}} \tag{1.96}$$

Friction factor for turbulent flow: When the flow enters into the turbulent region its velocity profile, besides other factors is also governed by the degree of turbulence and surface roughness; while in laminar region the viscous forces are predominant and the friction factor does not vary with roughness.

Some empirical relations for the friction factor in a turbulent flow are given here.

(*i*) For a smooth wall

$$\left(\frac{2}{f}\right)^{0.5} = 2.5 \ln [0.5\text{Re}\,(0.5f)^{0.5}] + 1.75 \tag{1.97}$$

(*ii*) An approximate and simpler expression for $\text{Re} < 10^5$ is given by Blasius

$$f = \frac{0.079}{\text{Re}^{0.25}} \tag{1.98}$$

(*iii*) Falkner gives for fully turbulent flow

$$f = \frac{0.0306}{\text{Re}^{1/7}} \tag{1.99}$$

1.49 PROPERTIES OF THE ATMOSPHERE

The bulk of the atmosphere is made up of oxygen and nitrogen. Besides these there are small quantities of other gases like argon, helium and hydrogen. The total weight of the atmosphere is estimated to be 5×10^{15} tons.

The atmosphere can be approximately divided into five regions as shown in Figure 1.10.

The limits of various regions shown in the figure are approximate and vary with latitude, time and season.

Troposphere: The troposphere is the region in which normal weather and clouds occur and extends upto an altitude of about 11 km

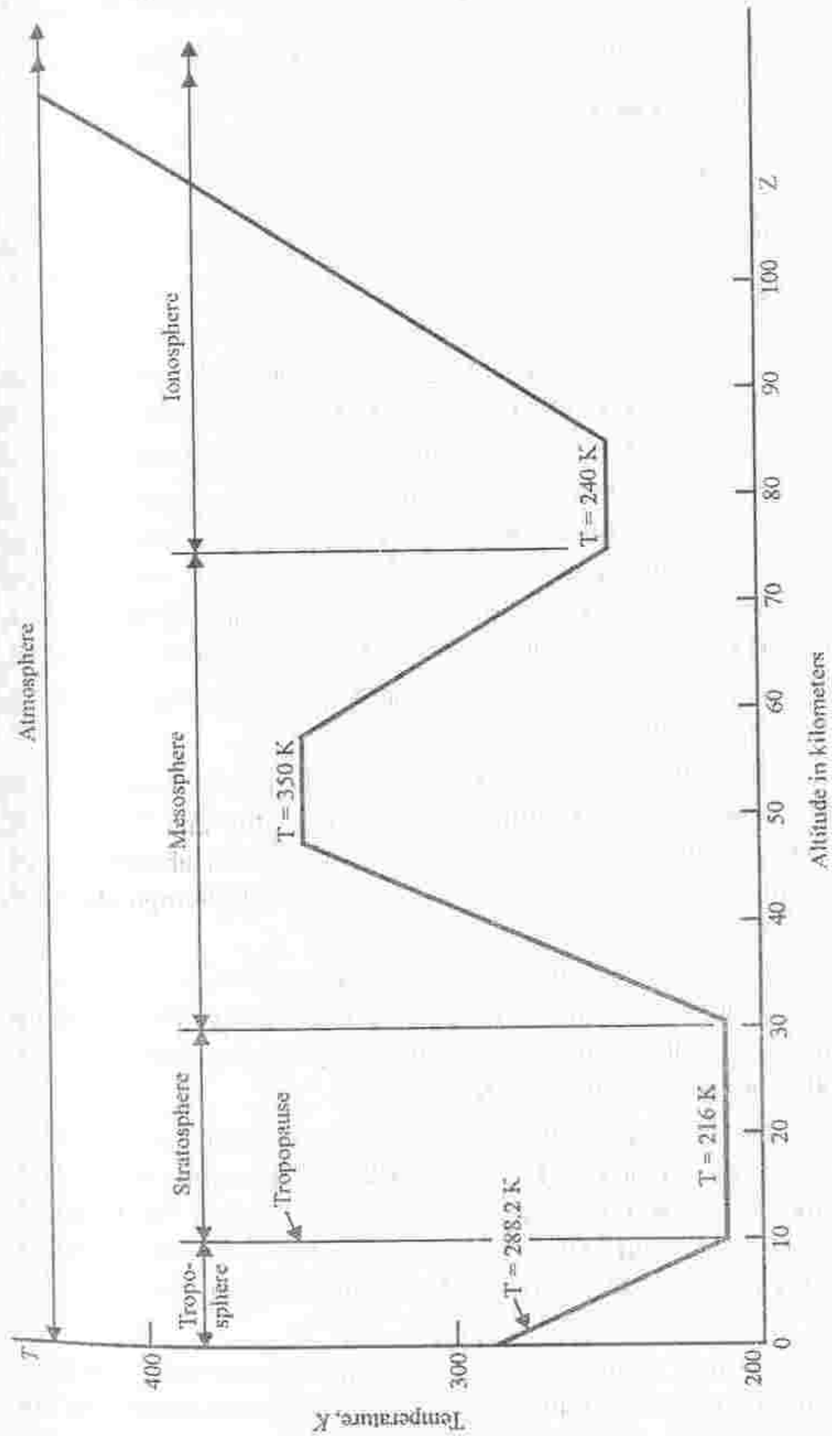

FIGURE 1.10 : Temperature variation in the atmosphere

from the mean sea level. This contains about 75 per cent weight of the atmosphere. The composition of the troposphere is given in Table 1.3.

TABLE 1.3: Volumetric composition of the troposphere

Gases	Approximate %
Oxygen	21.00
Nitrogen	78.00
Argon	0.94
Hydrogen	0.01
Carbon dioxide	0.03
Others	0.02

The pressure of the atmosphere always decreases with altitude. The temperature decreases linearly with altitude in the troposphere, the rate of decrease or "lapse rate" being 6.5°C per kilometre.

Stratosphere: The stratosphere is the region above the troposphere. This extends upto an altitude of 32 km and contains a little less than 25% of the weight of the atmosphere. The two regions are separated by the "tropopause" which is at an altitude of about 11,000 metres. The temperature in the stratosphere remains constant at 216.5 K (– 56.50°C) and the composition of the air in this region does not differ much from that in the troposphere.

Mesosphere: This region is sometimes considered as a part of the stratosphere and lies between the altitudes of 32 km and 76 km. This is characterized by the concentration of ozone which absorbs a large portion of the ultraviolet radiation from the sun. The temperature first rises to 350 K and then decreases to 240 K.

Ionosphere: The region beyond the mesosphere is called ionosphere which extends upto 640 km. This contains electrically conducting layers, the compositions of which change during the day and night. The temperature increases with altitude.

Exosphere (not shown in the figure): Beyond the ionosphere is a very low density region known as exosphere. This region merges with the interplanetary medium. There is no sharp boundary between the ionosphere and the exosphere. Both the ionosphere and the exosphere have extremely low weight compared to the troposphere and the stratosphere.

The location of various regions in the atmosphere and the properties of air in them vary with the geography of the place and time during the day and the year. This presents difficulties in assigning definite

properties to the atmosphere at various altitudes. Therefore, to overcome this difficulty a reference atmosphere has been postulated by the International Civil Aviation Organization (ICAO). This is referred to as the International standard atmosphere (ISA). The conditions at the sea level for this atmosphere are given below in Table 1.4.

TABLE 1.4: Properties of the International Standard atmosphere at sea level

Pressure	$p^0 = 1.0133$ bar $= 1.033$ kgf/cm^2
Temperature	$T^0 = 288.2$ K
Density	$\rho^0 = 1.225$ kg/m^3
Velocity of sound	$a^0 = 340.3$ m/s
Coefficient of viscosity	$\mu^0 = 1.789 \times 10^{-5}$ kg/ms
Kinematic viscosity	$\nu^0 = 1.461 \times 10^{-5}$ m^2/s

The properties of the atmosphere at other altitudes are calculated from their values at the sea level.

For an atmospheric column of height dZ and density ρ (Figure 1.11) we have

$$dp = -\rho g dZ \tag{1.100}$$

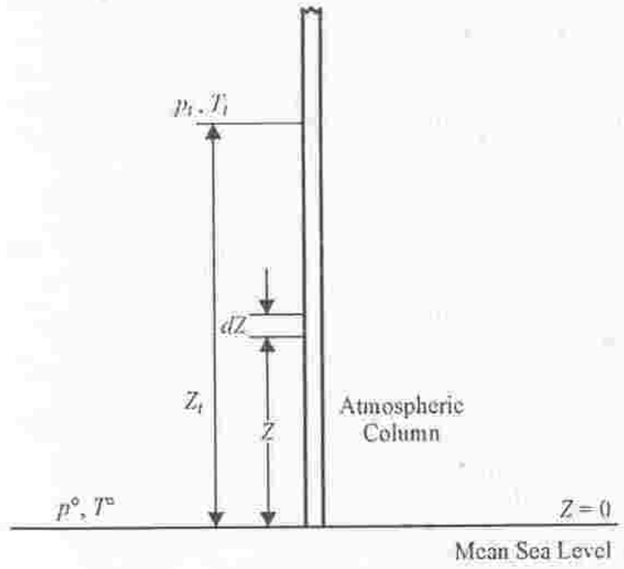

FIGURE 1.11 : Variation of pressure and temperature of the troposphere with altitude

The equation of state for an ideal gas is

$$\rho = \frac{p}{RT}$$

Therefore, assuming ideal gas and constancy of g with altitude Equation (1.100) yields

$$dp = -\frac{gp}{RT} dZ \tag{1.101}$$

Properties of the troposphere: In this region (from $Z = 0$ to $Z = 11{,}000$ m) the temperature is given by

$$T = T^0 - \alpha Z \tag{1.102}$$

Therefore, the temperature ratio is

$$T_r = \frac{T}{T^0} = 1 - \frac{\alpha Z}{T^0}$$

From Equations (1.101) and (1.102)

$$\frac{dp}{p} = -\frac{g}{R} \frac{dZ}{T^0 - \alpha Z} = -\frac{g}{R} \frac{dZ}{T} \tag{1.103}$$

Integration of Equation (1.103) between the sea-level ($Z = 0$) and the altitude $Z = Z$ yields

$$[\ln p]_{p^0}^{p} = \frac{g}{\alpha R} [\ln (T^0 - \alpha Z)]_0^Z$$

$$[\ln p]_{p^0}^{p} = \frac{g}{\alpha R} [\ln T]_{T^0}^{T}$$

$$\ln \frac{p}{p^0} = \ln \left(\frac{T}{T^0} \right)^{g/\alpha R}$$

$$p_r = \frac{p}{p^0} = \left(\frac{T}{T^0} \right)^{g/\alpha R} = \left(\frac{T^0 - \alpha Z}{T^0} \right)^{g/\alpha R} \tag{1.104}$$

Equation of state gives

$$\frac{\rho}{\rho^0} = \frac{p}{p^0} \frac{T^0}{T} \tag{1.105}$$

Equations (1.104) and (1.105) give

$$\rho_r = \frac{\rho}{\rho^0} = \left(\frac{T}{T^0} \right)^{(g - \alpha R)/\alpha R} \tag{1.106}$$

Viscosity is a complex function of temperature. Van Driest showed that it is possible to obtain a relation $\mu = f(T)$ by interpolation of Sutherland's theory. For air this is

$$\frac{\mu_0}{\mu} = \left(\frac{T}{T^0} \right)^{1.5} \times \frac{T^0 + 110}{T + 110} \tag{1.107 (a)}$$

This can be further expressed in the following empirical form:

$$\mu_r = \frac{\mu}{\mu^0} = \left(\frac{T}{T^0} \right)^{0.75} \tag{1.107 (b)}$$

At the tropopause ($Z = Z_t = 11{,}000$ m)

$$p = p_t = 0.227 \text{ bar}$$

$$T = T_t = 216.5 \text{ K}$$

$$\rho = \rho_t = 0.365 \text{ kg/m}^3$$

$$\mu = \mu_t = 1.42 \times 10^{-5} \text{ kg/ms}$$

Properties of the stratosphere: As stated before, in this region (from $Z = Z_t$ to $Z = 32{,}000$ m) the temperature remains constant at

$$T = T_t = 216.5 \text{ K}$$

Therefore, Equation (1.101) becomes

$$\frac{dp}{p} = -\frac{g}{RT_t} dZ$$

which on integration between $Z = Z_t$ and $Z = Z$ gives

$$\int_{p_t}^{p} \frac{dp}{p} = -\frac{g}{RT_t} \int_{Z_t}^{Z} dZ$$

$$\ln \frac{p}{p_t} = -\frac{g}{RT_t} (Z - Z_t)$$

$$p_r = \frac{p}{p_t} = \exp\left\{-\frac{g}{RT_t}(Z - Z_t)\right\} \tag{1.108}$$

Since $T_r = 1$

$$\mu_r = 1 \tag{1.109}$$

and

$$\rho_r = \frac{\rho}{\rho_t} = \frac{p}{p_t} \tag{1.110}$$

Approximate variations (decrease) of atmospheric pressure and density with altitude are depicted graphically in Figure 1.12.

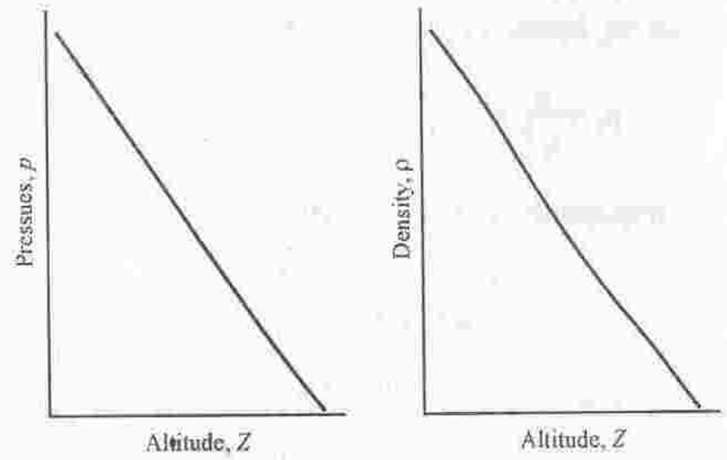

FIGURE 1.12 : Variation of pressure and density of the atmosphere with altitude

Aircrafts and space vehicles flying at very high altitudes experience negligible aerodynamic resistance (drag) on account of low density. This decreases the frictional heating of the aerospace vehicles significantly specially at high flight speeds. However, for aircrafts this advantage is off set by the considerable decrease in the lift on the wings, and the air flow rate in the engines for given cross-sectional areas. In contrast to this the performance of rocket engines is not affected by low density of air because they carry their own supply of oxidizers.

NOTATION FOR CHAPTER 1

a	local velocity of sound or a constant	$\overline{M}$	molecular weight
A	area or a constant	n	number of moles or degrees of freedom of a molecule
ΔA_c	minimum area below which assumption of a continuum is not valid	p	pressure
B	constant	q	heat transfer
b	constant	Q	mq
c	fluid velocity or specific heat or constant	r	radius
D	diameter	R	radius or gas constant
e	constant or specific energy	$\overline{R}$	universal gas constant
E	mc	Re	Reynolds number
f	friction factor	s	specific entropy
$f()$	function of	t	time
F	force	T	absolute temperature
H	intensity of magnetism	u	specific internal energy
$H = mh$	enthalpy	$U = mu$	
k	a constant	v	specific volume
K	bulk modulus	$V = mv$	volume
l	length parameter	ΔV_c	minimum volume below which assumption of continuum is not valid
L	length	w	specific work
L_0	length at $T = 0$	$W = mw$	work
L_T	length at $T = T$	x, y	distances
m	mass or mass flow rate or magnetic moment	Y	Young's modulus
M	Mach number	Z	altitude, compressibility factor or electric charge

GREEK SYMBOLS

α	lapse rate	σ	surface tension
β	coefficient of compressibility	τ	tension or shear stress
		μ	viscosity
$\gamma = c_p/c_v$	ratio of specific heats	ν	kinematic viscosity
ρ	density	ϵ	e.m.f.

SUBSCRIPTS

1	initial state	R	reversible
2	final state	s	adiabatic
c	critical values	t	tropopause
p	constant pressure	T	isothermal
fp	flow process	v	constant volume
nfp	non-flow process	w	wall
r	ratio	x, y, z	x, y and z directions

SUPERSCRIPT

—	molal values, average values	0	sea level conditions

SOLVED EXAMPLES

Example 1.1. Define internal energy and enthalpy. 3.0 kg/s of air is to be discharged through a smooth circular duct at a velocity of 10 m/s. The pressure and temperature of air in the pipe are 1.5 bar and 300 K respectively. Determine the enthalpy and internal energy of air and the diameter of the duct ($R = 0.287$ kJ/kg-K, $c_p = 1.005$ kJ/kg-K).

Solution. $c_v = c_p - R$

$$c_v = 1.005 - 0.287 = 0.718 \text{ kJ/kg-K}$$

Assuming the datum values of u and h as zero at $T = 0$

$$h = c_p T = 1.005 \times 300 = 301.5 \text{ kJ/kg} \quad \textbf{Ans.}$$

$$u = c_v T = 0.718 \times 300 = 215.4 \text{ kJ/kg} \quad \textbf{Ans.}$$

$$\rho = \frac{p}{RT} = \frac{1.5 \times 10^5}{287 \times 300} = 1.745 \text{ kg/m}^3$$

$$\rho \left(\frac{\pi}{4} D^2 \right) c = \dot{m}$$

$$1.745 \times 0.785 \times 10 D^2 = 3$$

$$D^2 = 0.219$$

$$D = 46.9 \text{ cm} \quad \textbf{Ans.}$$

Example 1.2. Explain the difference between flow and non-flow work.

Carbon dioxide expands isentropically through a nozzle from a pressure of 3.0 bar to 1.0 bar. If the initial temperature is 473 K determine the final temperature, the enthalpy drop and the change in the internal energy.

Take $\gamma = 1.24$, $R = 0.189$ kJ/kg-K.

Solution. $c_p = \dfrac{\gamma}{\gamma - 1} R$

$$c_p = \frac{1.24}{0.24} \times 0.189 = 0.975 \text{ kJ/kg-K}$$

$$c_v = \frac{c_p}{\gamma} = \frac{0.975}{1.24} = 0.785 \text{ kJ/kg-K}$$

$$\frac{T_2}{T_1} = \left(\frac{p_2}{p_1} \right)^{(\gamma-1)/\gamma} = \left(\frac{1}{3} \right)^{(1.24-1)/1.24} = 0.812$$

$$T_2 = 0.812 T_1$$

$$= 0.812 \times 473 = 383 \text{ K} \quad \textbf{Ans.}$$

$$\Delta h = c_p (T_1 - T_2)$$

$$= 0.975 (473 - 383) = 87.75 \text{ kJ/kg} \quad \textbf{Ans.}$$

$$\Delta u = c_v (T_1 - T_2)$$

$$= 0.785 \times 90 = 70.65 \text{ kJ/kg} \quad \textbf{Ans.}$$

Example 1.3. Show that the change of entropy in a polytropic process is given by

$$\Delta s = c_v \ln \frac{p_2}{p_1} + c_p \ln \frac{v_2}{v_1}$$

Superheated steam ($c_p = 2.15$ kJ/kg-K, $\gamma = 1.3$) expands polytropically ($n = 1.2$) from $p_1 = 10$ bar, $T_1 = 650$ K to a pressure of 3 bar. Determine the change of entropy.

Solution. $\dfrac{p_2}{p_1} = \dfrac{3}{10} = 0.3$

$$\frac{v_2}{v_1} = \left(\frac{p_1}{p_2} \right)^{1/n} = \left(\frac{10}{3} \right)^{1/1.2} = 2.72$$

$$c_v = \frac{1}{\gamma} c_p$$

$$= \frac{2.15}{1.3} = 1.655 \text{ kJ/kg-K}$$

$$\Delta s = c_v \ln \frac{p_2}{p_1} + c_p \ln \frac{v_2}{v_1}$$

$$= 1.655 \ln (0.3) + 2.15 \ln (2.72)$$

$$\Delta s = 0.24 \quad \textbf{Ans.}$$

Example 1.4. How is Fanning's coefficient of skin friction f defined? Show that the pressure loss in a pipe of length L metres and diameter D metres is

$$\Delta p = 4f \frac{L}{D} \frac{1}{2} \rho c^2$$

The pressure and temperature of air at the entry of a 100 metre long 50 cm diameter duct are 3 bar and 315 K. If the average velocity of air in the duct is 15 m/s and the friction factor 0.025 determine the pressure at the exit of the duct.

Solution. $\rho = \frac{p}{RT} = \frac{3 \times 10^5}{287 \times 315} = 3.32 \text{ kg/m}^3$

$$\Delta p = 4 \times 0.025 \times \frac{100}{0.5} \times \frac{1}{2} \times 3.32 \times 15^2$$

$$= 0.746 \times 10^5 \text{ N/m}^2$$

$$= 0.746 \text{ bar}$$

$$p_2 = p_1 - \Delta p$$

$$p_2 = 3 - 0.746$$

$$p_2 = 2.254 \text{ bar} \quad \textbf{Ans.}$$

Example 1.5. Define adiabatic bulk modulus of a gas. Show that for an ideal gas in an isothermal process the bulk modulus is equal to the pressure.

1 m^3 of a fluid at a pressure of 1 bar is compressed isothermally to a volume of 0.885 m^3 raising its pressure to 3600 bar. Determine its bulk modulus of elasticity.

Solution. $K_T = -v \frac{\Delta p}{\Delta v}$

$$= \frac{-1 \times (3600 - 1)}{(0.885 - 1)} = \frac{3599}{0.115}$$

$$= 3.12 \times 10^4 \text{ bar}$$

The above value can be obtained more accurately in the following manner:

$$-dp = K_T \frac{dv}{v}$$

By integration between initial and final conditions

$$p_2 - p_1 = K_T \ln \frac{v_1}{v_2}$$

$$K_T = \frac{p_2 - p_1}{\ln (v_1/v_2)}$$

$$= \frac{3599}{\ln (1/0.885)}$$

$$= 2.88 \times 10^4 \text{ bar} \quad \textbf{Ans.}$$

Example 1.6. If the condition of the standard atmosphere at the mean sea level is given by $p^0 = 1.0133$ bar, $T^0 = 288.2$ K and $\mu^0 = 1.79 \times 10^{-5}$ kg/ms determine pressure, temperature, density and viscosity at altitudes of 10,000 m and 15,000 m.

Solution. $\rho^0 = \frac{p^0}{RT^0} = \frac{1.0133 \times 10^5}{287 \times 288.2} = 1.227 \text{ kg/m}^3$

At $Z = 10{,}000$ m

The lapse rate α is 6.5°C per 1000 m.

Therefore, $T = T^0 - \alpha Z$

$$= 288.2 - 6.5 \times 10$$

$$= 223.2 \text{ K} \quad \textbf{Ans.}$$

$$p = \left(\frac{T}{T^0} \right)^{g/\alpha R} p^0$$

$$\frac{g}{\alpha R} = \frac{9.81}{0.0065 \times 287} = 5.25$$

$$p = \left(\frac{223.3}{288.2} \right)^{5.25} \times 1.0133$$

$$= (0.775)^{5.25} \times 1.0133$$

$$= 0.265 \text{ bar} \quad \textbf{Ans.}$$

$$\rho = \frac{p}{RT} = \frac{0.265 \times 10^5}{287 \times 223.3}$$

$$= 0.415 \text{ kg/m}^3$$

$$\mu = \mu^0 \left(\frac{T}{T^0} \right)^{0.75}$$

$$= 1.79 \times 10^{-5} (0.775)^{0.75}$$

$$= 1.48 \times 10^{-5} \text{ kg/ms}$$

At $Z = 15{,}000$ m.

This is in the stratosphere. Therefore,

$$T = T_t = 216.5 \text{ K} \quad \textbf{Ans.}$$

$$\mu = \mu_t = 1.42 \times 10^{-5} \text{ kg/ms}$$

$$p = p_t \exp\left\{-\frac{g}{RT_t}(Z - Z_t)\right\}$$

$$= 0.227 \exp\left\{-\frac{9.81 \times 4000}{287 \times 216.5}\right\}$$

$$= \frac{0.227}{\exp(0.635)} = \frac{0.227}{1.89}$$

$$p = 0.120 \text{ bar} \quad \textbf{Ans.}$$

$$\rho = \frac{p}{RT} = \frac{0.120 \times 10^5}{287 \times 216.5}$$

$$= 0.194 \text{ kg/m}^3 \quad \textbf{Ans.}$$

T_t and μ_t can also be calculated at $Z = 11{,}000$ metres.

QUESTIONS AND PROBLEMS

1.1 Explain briefly what is the difference between the control volume and system approaches. Define closed, open and isolated systems.

1.2 What is the difference between intensive property, extensive property and a specific quantity? Why work and heat are not properties?

1.3 What is a continuum? Under what conditions the assumption of a continuum is valid? How is it used to define pressure and density in a medium?

1.4 Define dynamic viscosity and kinematic viscosity; write down their formulas and units. What is the effect of viscosity on the flight of aircrafts?

1.5 What are Reynolds and Mach numbers? Write down their expressions. How would you vary their values?

1.6 Define the following terms:

streamlines, laminar flow, turbulent flow, one dimensional flow and incompressible flow.

1.7 (*a*) What is International standard atmosphere?

(*b*) What are ICAO, lapse rate and tropopause?

1.8 (*a*) Show graphically the variation of pressure, temperature and viscosity of air with altitude.

(*b*) Derive the following relations stating the assumptions:

$$p = p^0\left(1 - \frac{\alpha Z}{T^0}\right)^{g/\alpha R} \qquad \text{(for troposphere)}$$

$$\rho = \rho^0\left(\frac{T}{T^0}\right)^{(g-\alpha R)/\alpha R} \qquad \text{(for troposphere)}$$

$$p = p_t \exp\left\{-\frac{g}{RT_t}(Z - Z_t)\right\} \qquad \text{(for stratosphere)}$$

1.9 Ambient air at an altitude of 5000 m above sea level enters the engine of an aircraft flying at 450 kmph. If the air flow rate through the engine is 25 kg/s determine the diameter of the inlet to the engine. State the assumptions used.

Ans. $D = 58.82$ cm.

1.10 (*a*) Starting from the properties of air at the mean sea level determine temperature, pressure, density, kinematic viscosity and velocity of sound at altitudes of 2000, 7000 and 15000 metres.

(*b*) Determine the Mach numbers of aircrafts flying at 1080 km/hr at these altitudes.

Ans.

Z	$T(K)$	p (bar)	ρ (kg/m^3)	ν (m^2/s)	a (m/s)	M
2000	275.15	0.795	1.006	17.176×10^{-6}	332.6	0.902
7000	242.65	0.411	0.589	26.485×10^{-6}	312.4	0.960
15000	216.65	0.120	0.194	73.04×10^{-6}	295.2	1.016

1.11 An aircraft cruises at 220 m/s at altitudes of 1800, 5500 and 12000 metres. Determine its Mach number at these altitudes.

Ans. 0.660, 0.690, 0.745.

1.12 Air is conveyed from a compressor station to a quarry through a 30 cm diameter pipe line over a distance of 1.0 km. The rate

of flow is 5 kg/s and the Fanning's friction factor can be assumed to have a constant value of 0.008. The condition of air at the station is $p_1 = 3.0$ bar, $T_1 = 300$ K. Determine the pressure drop in the line assuming incompressible flow. What would be diameter of the pipeline if this loss is to be reduced to half?

Ans. (0.766 bar, 34.46 cm).

1.13 The Reynolds number of air-flow in a duct is 8000. Calculate the value of Fanning's friction factor.

Ans. 0.002.

1.14 (*a*) How is the International Standard atmosphere defined?

(*b*) Starting from values at mean sea level determine dynamic and kinematic viscosities of air at an altitude of 2500 metres. What is the velocity of sound at this altitude?

Ans. $\left(\mu = 17.12 \times 10^{-6} \frac{\text{Ns}}{\text{m}^2},\ \nu = 17.94 \times 10^{-4} \frac{\text{m}^2}{\text{s}};\ a = 330.6 \text{ m/s} \right)$

1.15 (*a*) Show that the pressure variation in the stratosphere is given by

$$p = p^0 \left(1 - \frac{\alpha Z_t}{T^0} \right)^{g/\alpha R} \times e^{\frac{-g\,(Z - Z_t)}{R\,(T^0 - \alpha Z_t)}}$$

(*b*) Show graphically the variation of pressure and density of the atmosphere with altitude.

2

The Energy Equation

In this chapter the energy equation is derived in its various forms and the stagnation state and stagnation values are defined. Other important relations based on the adiabatic energy equation are also derived.

Figure 2.1 shows the flow of a fluid through the control volume. Various thermofluid dynamic parameters at entry and exit sections are shown with subscripts 1 and 2 respectively. For the sake of generality heat (Q) supplied or rejected and work (W) output or input are also shown.

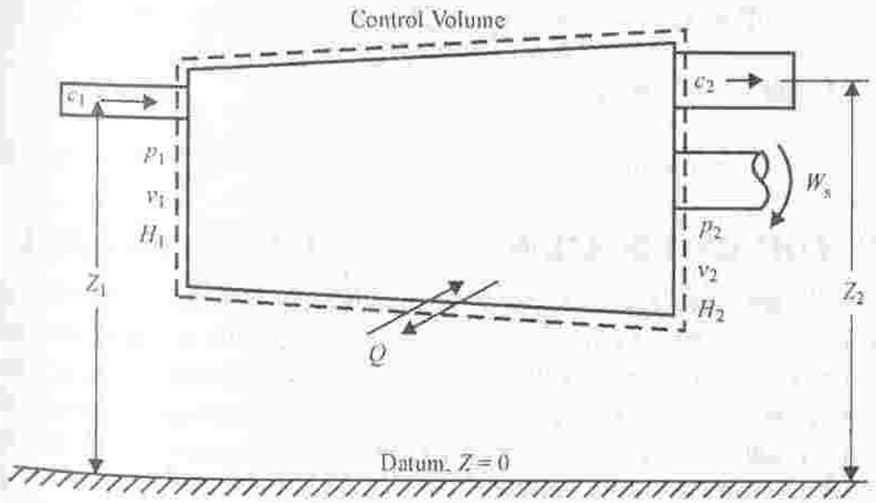

FIGURE 2.1 : Steady flow through a control volume (open system)

The energy Equation (1.8) $Q = W + (E_2 - E_1)$ in Chapter one, for a system was derived from the first law of thermodynamics. The energy terms (E) in Equation (1.8) may include gravitational potential energy, kinetic energy, internal energy, strain energy, magnetic energy, etc. As an example we may write

$$E = U + mgZ + \frac{1}{2} mc^2 \tag{2.1}$$

ignoring other forms of energy.

The differential form of Equation (2.1) is

$$dE = dU + mgdZ + md\left(\frac{1}{2} c^2\right) \tag{2.2}$$

Integrating Equation (2.2) between two given states

$$E_2 - E_1 = \int_1^2 dE = \int_1^2 dU + mg \int_1^2 dZ + \frac{1}{2} m \int_1^2 d(c^2)$$

$$E_2 - E_1 = (U_2 - U_1) + mg\,(Z_2 - Z_1) + \frac{1}{2} m\,(c_2^2 - c_1^2) \tag{2.3}$$

Equation (2.3) in (1.8) yields a more general form of the energy equation

$$Q = W + (U_2 - U_1) + mg\,(Z_2 - Z_1) + \frac{1}{2} m\,(c_2^2 - c_1^2) \quad (2.4\ (a))$$

In terms of specific values

$$q = w + (u_2 - u_1) + g\,(Z_2 - Z_1) + \frac{1}{2}\,(c_2^2 - c_1^2) \quad (2.4\ (b))$$

2.1 ENERGY EQUATION FOR A NON-FLOW PROCESS

As explained before in Section 1.42 (Chapter 1), processes like the expansion and compression of gases in a cylinder with a piston are non-flow processes in closed systems. The potential and kinetic energy terms for such processes are negligible compared to other quantities in the energy equation; and the work term W includes only shaft work. Therefore, Equation (2.4 (a)) reduces to

$$Q = W_s + (U_2 - U_1) \tag{2.5}$$

$$dQ = dW_s + dU$$

Assumption of perfect gas gives

$$dQ = pdV + mc_v\,dT \tag{2.6}$$

Equation (2.6) on integration yields

$$Q = \int_1^2 pdV + mc_v\,(T_2 - T_1) \tag{2.7}$$

The value of the integral $\int_1^2 pdV$ depends on the type of process e.g. p = constant, pV = constant, etc.

2.2 ENERGY EQUATION FOR A FLOW PROCESS

As stated before in Section 1.41 (Chapter 1) expansion of steam and gas in turbines and compression of air and gases in turbocompressors are examples of flow processes in open systems. In such processes the work term (W) includes the flow work also.

$$W = W_s + (p_2 V_2 - p_1 V_1) \tag{2.8}$$

Equation (2.4 (a)) and (2.8) give

$$Q = W_s + (p_2 V_2 - p_1 V_1) + (U_2 - U_1) + mg\,(Z_2 - Z_1) + \frac{1}{2} m\,(c_2^2 - c_1^2)$$

$$Q = W_s + (U_2 + p_2 V_2) - (U_1 + p_1 V_1) + mg\,(Z_2 - Z_1) + \frac{1}{2} m\,(c_2^2 - c_1^2)$$

putting $U + pV = H$

$$Q = W_s + (H_2 - H_1) + mg\,(Z_2 - Z_1) + \frac{1}{2} m\,(c_2^2 - c_1^2)$$

$$H_1 + mgZ_1 + \frac{1}{2} mc_1^2 + Q = H_2 + mgZ_2 + \frac{1}{2} mc_2^2 + W_s \quad (2.9\ (a))$$

In terms of specific values

$$h_1 + gZ_1 + \frac{1}{2} c_1^2 + q = h_2 + gZ_2 + \frac{1}{2} c_2^2 + w_s \quad (2.9\ (b))$$

Equations (2.9 (a)) and (2.9 (b)) are the steady flow energy Equations (SFEE). Generally in flow problems of gases and vapours the magnitude of $g\,(Z_2 - Z_1)$ is negligible compared to other quantities. Therefore,

$$h_1 + \frac{1}{2} c_1^2 + q = h_2 + \frac{1}{2} c_2^2 + w_s \tag{2.10}$$

2.3 THE ADIABATIC ENERGY EQUATION

In some engineering problems the heat transfer (q) during the process is negligibly small and can be ignored. Expansion of gases and vapours in turbines are examples of such processes. For such processes Equations (2.9 (b)) and (2.10) reduce to

$$h_1 + gZ_1 + \frac{1}{2}c_1^2 = h_2 + gZ_2 + \frac{1}{2}c_2^2 + w_s \tag{2.11}$$

$$h_1 + \frac{1}{2}c_1^2 = h_2 + \frac{1}{2}c_2^2 + w_s \tag{2.12}$$

2.3.1 Work in flow process

If the difference in the kinetic energy terms in Equation (2.12) is negligible, it reduces to

$$w_s = h_1 - h_2 = -\int_1^2 dh \tag{2.13}$$

For a perfect gas Equation (2.13) gives

$$w_s = -c_p \int_1^2 dT$$

$$w_s = c_p (T_1 - T_2) \tag{2.14}$$

For a reversible process Equation (2.13) can be written as

$$w_s = -\int_1^2 \frac{dp}{\rho} = -\int_1^2 v\,dp \tag{2.15}$$

2.3.2 Adiabatic energy transformation

Equations (2.11) and (2.12) are adiabatic energy Equations valid for processes involving both energy transfer (on account of shaft work) and energy transformation.

Some adiabatic processes involve only energy transformation, e.g., expansion of gases in nozzles and their compression in diffusers. In these processes shaft work is absent and Equations (2.11) and (2.12) are modified to

$$h_1 + gZ_1 + \frac{1}{2}c_1^2 = h_2 + gZ_2 + \frac{1}{2}c_2^2 \tag{2.16}$$

$$h_1 + \frac{1}{2}c_1^2 = h_2 + \frac{1}{2}c_2^2 \tag{2.17}$$

(when change in elevation is ignored).

2.3.3 Stagnation enthalpy

Figure 2.2 shows the deceleration of a gas stream at velocity c, pressure p and temperature T to almost zero velocity ($c \simeq 0$) in an infinitely large settling chamber.

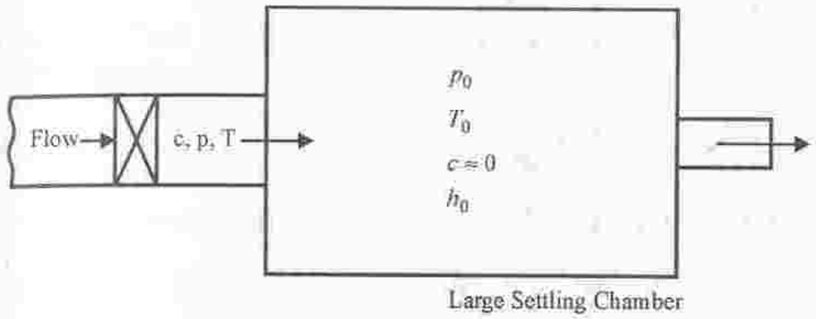

FIGURE 2.2 : Deceleration of a gas to stagnation state

Stagnation enthalpy of a gas or a vapour is its enthalpy when it is adiabatically decelerated to zero velocity at zero elevation. Putting $h_1 = h$, $Z_1 = Z$ and $c_1 = c$ for the initial state and $h_2 = h_0$, $Z_2 = 0$, $c_2 = 0$ for the final state in Equation (2.16) the value of the stagnation enthalpy (h_0) is obtained.

$$h_0 = h + gZ + \frac{1}{2}c^2 \tag{2.18}$$

But as mentioned before the magnitude of gZ compared to other quantities is generally negligible.

Therefore, $$h_0 = h + \frac{1}{2}c^2 \tag{2.19}$$

For an adiabatic energy transformation process stagnation enthalpy remains constant. Therefore, by differentiation Equation (2.19) gives

$$dh + c\,dc = 0 \tag{2.20}$$

2.3.4 Stagnation temperature

Stagnation temperature is the temperature of the gas when it is adiabatically decelerated to zero velocity at zero elevation.

For a perfect gas, this is defined through stagnation enthalpy. Equation (2.19) for a perfect gas gives

$$c_p T_0 = c_p T + \frac{1}{2} c^2$$

$$T_0 = T + \frac{c^2}{2c_p} \tag{2.21}$$

The quantity $c^2/2c_p$ is known as the velocity temperature (T_c) corresponding to the velocity c.

$$T_0 = T + T_c \tag{2.22}$$

$$T_c = \frac{c^2}{2c_p} \tag{2.23}$$

From Equation (2.21)

$$\frac{T_0}{T} = 1 + \frac{c^2}{2c_p T}$$

$$\frac{T_0}{T} = 1 + \frac{c^2}{2\gamma RT/(\gamma - 1)}$$

But $\gamma RT = a^2$ and $\frac{c^2}{a^2} = M^2$

Therefore, $\frac{T_0}{T} = 1 + \frac{\gamma - 1}{2} \frac{c^2}{a^2}$

$$\frac{T_0}{T} = 1 + \frac{\gamma - 1}{2} M^2. \tag{2.24}$$

2.4 STAGNATION VELOCITY OF SOUND

For a given value of the stagnation temperature Equation (1.78) gives the velocity of sound for a perfect gas

$$a_0 = \sqrt{\gamma RT_0} \tag{2.25}$$

By substituting $R = \frac{\gamma - 1}{\gamma} c_p$

$$a_0 = \sqrt{(\gamma - 1)\, c_p\, T_0}$$

$$a_0 = \sqrt{(\gamma - 1)\, h_0}. \tag{2.26}$$

2.5 STAGNATION PRESSURE

Stagnation pressure is the pressure of a fluid which is attained when it is decelerated to zero velocity at zero elevation in a reversible adiabatic (isentropic) process. For given values of static pressure and temperature its value can be derived from the stagnation temperature.

$$\frac{p_0}{p} = \left(\frac{T_0}{T} \right)^{\gamma/(\gamma-1)} = \left(1 + \frac{\gamma - 1}{2} M^2 \right)^{\gamma/(\gamma-1)} \tag{2.27}$$

2.6 STAGNATION DENSITY

For given values of stagnation pressure and temperature of an ideal gas the stagnation density is given by

$$\rho_0 = \frac{p_0}{RT_0} \tag{2.28}$$

From isentropic relations

$$\frac{\rho_0}{\rho} = \left(\frac{p_0}{p} \right)^{1/\gamma} \tag{2.29}$$

$$\frac{\rho_0}{\rho} = \left(\frac{T_0}{T} \right)^{1/(\gamma-1)} = \left(1 + \frac{\gamma - 1}{2} M^2 \right)^{1/(\gamma-1)} \tag{2.30}$$

2.7 STAGNATION STATE

Figure 2.3 depicts the deceleration of a gas in both the isentropic and

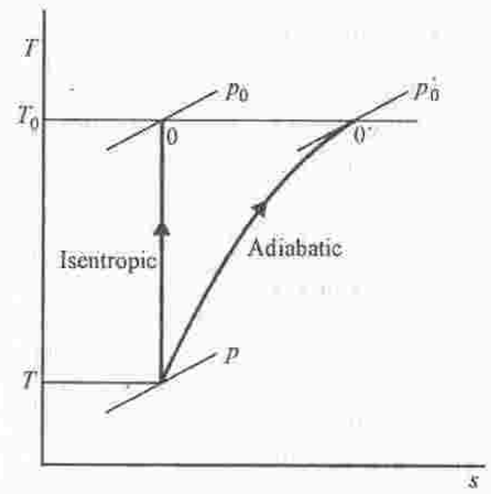

FIGURE 2.3 : Deceleration of a gas to stagnation conditions

adiabatic processes. It is observed that during the adiabatic deceleration the gas experience decrease in stagnation pressure and increase in entropy.

The state of a fluid attained by isentropically decelerating it to zero velocity at zero elevation is referred to as the stagnation state. This is fully defind by stagnation enthalpy/stagnation temperature and the stagnation pressure. The stagnation state in Figure 2.3 is represented by point O.

It should be remembered here that the deceleration process needs to be isentropic only for defining stagnation pressure and stagnation state. This condition is not necessary for defining stagnation enthalpy or stagnation temperature. This is because quantities (h_0, T_0) have been derived from the energy Equation for adiabatic flow.

2.8 VARIOUS REGIONS OF FLOW

Here the adiabatic energy equation for a perfect gas is derived in terms of velocities (c) and (a). This is then graphically discussed by differentiating various regions of flow on the c-a plot.

Equation (2.19) is

$$h + \frac{1}{2}c^2 = h_0 = \text{constant} \tag{2.19}$$

$$h = c_p T = \frac{\gamma}{\gamma - 1} RT$$

But $\gamma RT = a^2$ and $RT = \frac{p}{\rho}$

Therefore, $$h = \frac{a^2}{\gamma - 1} = \frac{\gamma}{\gamma - 1}\frac{p}{\rho} \tag{2.31}$$

Using Equations (2.31) in (2.19) gives

$$\frac{a^2}{\gamma - 1} + \frac{1}{2}c^2 = \text{constant} \tag{2.32}$$

At $T = 0$, $h = 0$ and $c = c_{max}$.

Therefore, from Equation (2.19)

$$\text{constant} = h_0 = \frac{1}{2}c_{max}^2 \tag{2.33}$$

At $c = 0$, $a = a_0$.

Therefore, from Equation (2.32)

$$\text{constant} = h_0 = \frac{a_0^2}{\gamma - 1} \tag{2.34}$$

Equations (2.32), (2.33) and (2.34) yield

$$\frac{a^2}{\gamma - 1} + \frac{1}{2}c^2 = \frac{1}{2}c_{max}^2 = \frac{a_0^2}{\gamma - 1} = h_0 \tag{2.35}$$

Equations (2.35) is yet another form of the adiabatic energy equation. This expresses the total energy of a fluid in a number of ways.

By plotting Equation (2.35) on (c) and (a) co-ordinates a steady flow ellipse is obtained. This is shown in Figure 2.4. Five regions of flow are quite distinct on this ellipse.

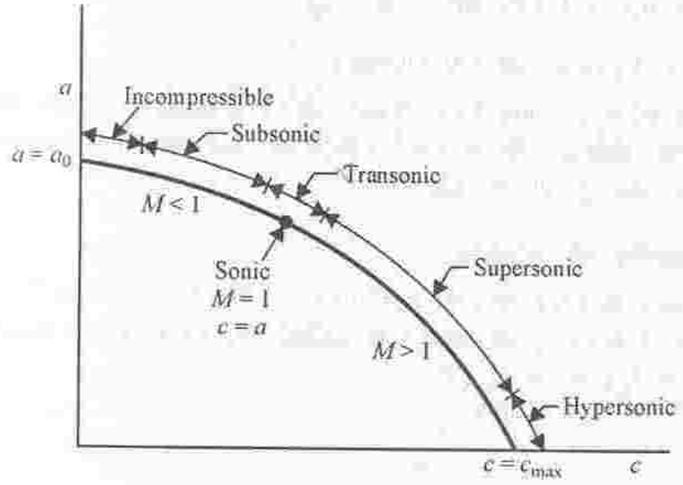

FIGURE 2.4 : Various regions of flow

(*i*) The region of flow close to the a-axis is the incompressible flow region. Here fluid velocity (c) is much smaller than the velocity of sound (a) *i.e.*, the Mach number is very low.

(*ii*) The subsonic flow region is on the right of the incompressible flow region upto a Mach number value of a little less than unity. The Mach number in this region is always less than unity.

(*iii*) A small region extending on both sides of the sonic point ($M = 1$) has Mach numbers, which are either slightly lower or higher than unity. This region is called transonic region.

(*iv*) The supersonic region is on the right of the transonic region; the Mach number in this region is always greater than unity.

(*v*) The region close to the c-axis is called hypersonic region; in this region Mach number is very high and the flow velocity is considerably greater than the velocity of sound.

2.9 REFERENCE VELOCITIES

In compressible flow analyses it is often convenient to express fluid velocities in non-dimensional forms. This is done by dividing the flow velocity by some reference or standard velocity. The reference velocities which can be used are:

(*i*) local velocity of sound, a

(*ii*) stagnation velocity of sound, a_0

(*iii*) maximum velocity of fluid, c_{max}

(*iv*) critical velocity of fluid/sound, $c^* = a^*$

Some of these quantities have been mentioned before. The selection of the above reference velocities for non-dimensionalization depends on the given problem.

2.9.1 Velocity of sound

As mentioned in Section 1.45 in Chapter 1 the ratio of the fluid velocity and the local velocity of sound is called the local Mach number. This is given by Equation (1.79).

$$M = \frac{c}{a} = \frac{c}{\sqrt{\gamma RT}} \tag{1.79}$$

This non-dimensional number is named after Ernst Mach, a German physicist. Stagnation velocity of sound (a_0) is given by Equations (2.25) and (2.26); its value is constant in an adiabatic flow for a given stagnation temperature.

2.9.2 Maximum fluid velocity

The adiabatic energy Equation (2.19) has two components of the total energy: the ethalpy h and the kinetic energy $\frac{1}{2}c^2$. If kinetic energy is absent the total energy is entirely represented by the stagnation enthalpy h_0. The other extreme condition which can be conceived is when the entire energy is made up of kinetic energy only, *i.e.*, $h = 0$ and

$c = c_{max}$. The fluid velocity (c_{max}) corresponding to this condition is the maximum velocity that would be achieved by the fluid when it is accelerated to absolute zero temperature ($T = 0$, $h = 0$) in an imaginary adiabatic expansion process. For this condition Equation (2.19) gives

$$c_{max} = \sqrt{2h_0} \tag{2.36}$$

For a perfect gas

$$c_{max} = \sqrt{2c_p T_0} \tag{2.37}$$

$$= \sqrt{\frac{2\gamma}{\gamma - 1} RT_0} \tag{2.38}$$

Equations (2.25) and (2.38) yield

$$\frac{c_{max}}{a_0} = \sqrt{\frac{2}{\gamma - 1}} = 2.24 \text{ (for } \gamma = 1.4) \tag{2.39}$$

2.9.3 Critical velocity of sound

The critical velocity of a fluid is its velocity at a Mach number of unity.

$$M_{critical} = \frac{c^*}{a^*} = 1 \tag{2.40}$$

$$c^* = a^* = \sqrt{\gamma RT^*}$$

Equation (2.19) for adiabatic expansion from the stagnation temperature to the critical temperature is

$$h_0 = h^* + \frac{1}{2}c^{*2}$$

For a perfect gas

$$T_0 = T^* + \frac{c^{*2}}{2c_p}$$

$$c^* = \sqrt{2c_p (T_0 - T^*)} \tag{2.41}$$

Equation (2.24) for the critical Mach number ($M = 1$, $T = T^*$) gives

$$\frac{T_0}{T^*} = \frac{\gamma + 1}{2} = 1.2 \text{ (for } \gamma = 1.4) \tag{2.42}$$

Equations (2.41) and (2.42) after some manipulation give

$$c^* = a^* = \sqrt{\frac{2\gamma}{\gamma+1} RT_0} \tag{2.43}$$

Equations (2.25) and (2.43) give

$$\frac{c^*}{a_0} = \frac{a^*}{a_0} = \sqrt{\frac{2}{\gamma+1}} = 0.913 \text{ (for } \gamma = 1.4) \tag{2.44}$$

Equations (2.24) and (2.42) yield

$$\frac{T^*}{T} = \frac{2}{\gamma+1} + \frac{\gamma-1}{\gamma+1} M^2 \tag{2.45}$$

Equations (2.39) and (2.44) give

$$\frac{c_{\max}}{a^*} = \frac{c_{\max}}{c^*} = \sqrt{\frac{\gamma+1}{\gamma-1}} = 2.45 \text{ (for } \gamma = 1.4) \tag{2.46}$$

Equations (2.35) and (2.46) yield

$$\frac{a^2}{\gamma-1} + \frac{1}{2} c^2 = \frac{1}{2} c_{\max}^2 = \frac{1}{2} a^{*2} \frac{\gamma+1}{\gamma-1} \tag{2.47}$$

2.9.4 Mach number M^*

A second kind of Mach number M^* can be defined by non-dimensionalizing the fluid velocity by the critical fluid velocity or the sound velocity.

$$M^* = \frac{c}{c^*} = \frac{c}{a^*} \tag{2.48}$$

$$M^{*2} = \frac{c^2}{a^{*2}} = \frac{c^2}{a^2} \cdot \frac{a^2}{a^{*2}} = \frac{a^2}{a^{*2}} M^2 \tag{2.49}$$

Sometimes it is more convenient to use M^* instead of M because

(*i*) at high fluid velocities M approaches infinity

(*ii*) M is not proportional to the fluid velocity alone.

It should be pointed out here that M^* does not mean $M = 1$. This is only another type of Mach number defined by Equations (2.48) and (2.49). Equations (2.47) is

$$c^2 + \frac{2a^2}{\gamma-1} = \frac{\gamma+1}{\gamma-1} a^{*2}$$

$$\frac{c^2}{a^{*2}} + \frac{2}{\gamma-1} \frac{a^2}{a^{*2}} = \frac{\gamma+1}{\gamma-1} \tag{2.50}$$

Using Equations (2.48) and (2.49) in (2.50)

$$M^{*2} + \frac{2}{\gamma-1} \frac{M^{*2}}{M^2} = \frac{\gamma+1}{\gamma-1} \tag{2.51}$$

$$M^{*2} \left(1 + \frac{2}{\gamma-1} \frac{1}{M^2}\right) = \frac{\gamma+1}{\gamma-1}$$

$$M^{*2} \left(\frac{2}{\gamma-1}\right) \left(\frac{\gamma-1}{2} + \frac{1}{M^2}\right) = \frac{\gamma+1}{\gamma-1}$$

$$M^{*2} = \frac{½ (\gamma+1) M^2}{1 + ½ (\gamma-1) M^2} \tag{2.52}$$

Equation (2.52) gives an important relation between M^* and M. In this equation

$$M^* = 0 \quad \text{at} \quad M = 0$$

$$M^* = 1 \quad \text{at} \quad M = 1$$

Equation (2.51) gives

$$\frac{2}{\gamma-1} \frac{M^{*2}}{M^2} = \frac{\gamma+1}{\gamma-1} - M^{*2}$$

$$\frac{M^{*2}}{M^2} = \frac{\gamma+1}{2} - \frac{\gamma-1}{2} M^{*2}$$

$$M^2 = \frac{\{2/(\gamma+1)\} M^{*2}}{1 - \{(\gamma-1)/(\gamma+1)\} M^{*2}} \tag{2.53}$$

In Equation (2.53)

at $M = \infty$

$$1 - \frac{\gamma-1}{\gamma+1} M^{*2} = 0$$

$$M^*_{\max} = \frac{c_{\max}}{c^*} = \sqrt{\frac{\gamma+1}{\gamma-1}} = 2.45 \text{ (for } \gamma = 1.4) \tag{2.54}$$

Table 2.1 gives the comparison of M and M^*

TABLE 2.1: Comparison of M and M^*

$M = 0$	$M^* = 0$
$M < 1$	$M^* < 1$
$M = 1$	$M^* = 1$
$M > 1$	$M^* > 1$
$M = \infty$	$M^* = \sqrt{\frac{\gamma+1}{\gamma-1}}$

2.9.5 Crocco Number

A non-dimensional fluid velocity can be defined by using the maximum fluid velocity c_{max}. This is known as Crocco number (C_r) named after Crocco.

$$C_r = \frac{c}{c_{max}} \tag{2.55}$$

$$C_r = \frac{c}{c^*}\,\frac{c^*}{c_{max}}$$

Substituting for $\frac{c}{c^*}$ and $\frac{c^*}{c_{max}}$ from Equations (2.48) and (2.46) respectively, we get

$$C_r = M^* \sqrt{\frac{\gamma-1}{\gamma+1}} \tag{2.56}$$

Equations (2.52) and (2.56) relate C_r and M

$$C_r = \sqrt{\frac{½\,(\gamma-1)\,M^2}{1 + ½\,(\gamma-1)\,M^4}} \tag{2.57}$$

$$M = \sqrt{\frac{2C_r^2}{(\gamma-1)\;(1-C_r^2)}} \tag{2.58}$$

Substituting for M^2 from Equation (2.58) in (2.24)

$$\frac{T_0}{T} = \frac{1}{1-C_r^2} \tag{2.59}$$

2.10 BERNOULLI EQUATION

The adiabatic energy Equation (2.20) is

$$dh + c\,dc = 0$$

For isentropic flow this can be written as

$$\frac{dp}{\rho} + c\,dc = 0 \tag{2.60}$$

If the flow is assumed incompressible

$$\rho \approx \text{constant}$$

Then Equation (2.60) on integration yields

$$\frac{1}{\rho}\int dp + \frac{1}{2}\int d(c^2) = \text{constant}$$

$$\frac{p}{\rho} + \frac{1}{2}c^2 = \text{constant} \tag{2.61}$$

As stated before when the flow is isentropically decelerated to zero velocity, the resultant pressure is the stagnation pressure. Therefore, when $c = 0$

$$p = p_0$$

$$\rho = \rho_0$$

Thus constant (in Equation (2.61) $= \frac{p_0}{\rho_0}$.

Therefore, $$\frac{p}{\rho} + \frac{1}{2}c^2 = \frac{p_0}{\rho_0}$$

In incompressible flow since

$$\rho_0 \approx \rho = \text{constant}$$

$$p + \frac{1}{2}\rho c^2 = p_0 \tag{2.62}$$

This is the well known Bernoulli equation. Though it has been derived from the adiabatic energy equation it should be remembered that it is valid only when the flow is isentropic and incompressible. These conditions do not govern the adiabatic energy equation. The adiabatic energy Equation (2.19) can also be expressed in terms of pressures.

Assuming perfect gas

$$h_0 = c_p T_0 = \frac{\gamma}{\gamma - 1} RT_0$$

$$RT_0 = \frac{p_0}{\rho_0}$$

$$h_0 = \frac{\gamma}{\gamma - 1} \frac{p_0}{\rho_0} \tag{2.63}$$

Substitution of Equations (2.31) and (2.63) in (2.19) gives

$$\frac{\gamma}{\gamma - 1} \frac{p}{\rho} + \frac{1}{2} c^2 = \frac{\gamma}{\gamma - 1} \frac{p_0}{\rho_0} \tag{2.64}$$

A similar equation for isentropic flow is also derived here. Equation (2.29) for isentropic flow gives

$$\rho = \rho_0 \left(\frac{p}{p_0} \right)^{1/\gamma}$$

$$\frac{p}{\rho} = \frac{p}{\rho_0} \cdot \frac{p_0}{p_0} \left(\frac{p_0}{p} \right)^{1/\gamma}$$

$$\frac{p}{\rho} = \frac{p_0}{\rho_0} \left(\frac{p}{p_0} \right)^{(\gamma-1)/\gamma} \tag{2.65}$$

Substituting from Equation (2.65) in (2.64)

$$\frac{\gamma}{\gamma - 1} \frac{p_0}{\rho_0} \left(\frac{p}{p_0} \right)^{(\gamma-1)/\gamma} + \frac{1}{2} c^2 = \frac{\gamma}{\gamma - 1} \frac{p_0}{\rho_0} \tag{2.66}$$

This is the equivalent of Bernoulli Equation for isentropic compressible flow.

2.11 EFFECT OF MACH NUMBER ON COMPRESSIBILITY

If the flow is assumed incompressible, the value of the pressure coefficient (sometimes referred to as compressibility factor) obtained by Bernoulli Equation is unity

$$\frac{p_0 - p}{\frac{1}{2} \rho c^2} = 1 \tag{2.67}$$

For compressible flow the value of the pressure coefficient deviates from unity; the magnitude of deviation increases with the Mach number of the flow.

For isentropic compressible flow the ratio of the stagnation and static pressures is given by

$$\frac{p_0}{p} = \left(\frac{T_0}{T} \right)^{\gamma/(\gamma-1)} = \left(1 + \frac{\gamma - 1}{2} M^2 \right)^{\gamma/(\gamma-1)}$$

This can be expanded by the following series:

$$(1 + x)^n = 1 + nx + \frac{n(n-1)}{2!} x^2 + \frac{n(n-1)(n-2)}{3!} x^3 + \ldots \tag{2.68}$$

Here $x = \frac{\gamma - 1}{2} M^2$ and $n = \frac{\gamma}{\gamma - 1}$

Therefore, $\frac{p_0}{p} = 1 + \frac{\gamma}{2} M^2 + \frac{\gamma}{8} M^4 + \frac{\gamma(2 - \gamma)}{48} M^6 + \ldots$

$$\frac{p_0 - p}{p \left(\frac{\gamma}{2} M^2 \right)} = 1 + \frac{M^2}{4} + \frac{2 - \gamma}{24} M^4 + \ldots \tag{2.69}$$

But $p = \rho RT$ and

$$\frac{\gamma}{2} M^2 = \frac{\gamma}{2} \frac{c^2}{a^2} = \frac{c^2}{2RT} \tag{2.70}$$

Therefore, $p \left(\frac{\gamma}{2} M^2 \right) = (\rho RT) \left(\frac{c^2}{2RT} \right) = \frac{1}{2} \rho c^2$ (2.71)

Equations (2.69) and (2.71) give

$$\frac{p_0 - p}{\frac{1}{2} \rho c^2} = 1 + \frac{M^2}{4} + \frac{2 - \gamma}{24} M^4 + \ldots \tag{2.72}$$

For $\gamma = 1.4$

$$\frac{p_0 - p}{\frac{1}{2} \rho c^2} = 1 + \frac{M^2}{4} + \frac{M^4}{40} + \ldots \tag{2.73}$$

Equation (2.73) gives the percentage deviation of the pressure coefficient from its incompressible flow value with the Mach number.

Table 2.2 gives the error or deviation due to the assumption of incompressibility.

TABLE 2.2: Effect of compressibility

M	Percentage deviation
0.1	0.3
0.2	1.0
0.3	2.3
0.4	4.1
0.5	6.4
0.6	9.3
0.7	12.9
0.8	17.0
0.9	22.0
1.0	27.5

NOTATION FOR CHAPTER 2

a	local velocity of sound	n	index in binomial expansion
c	fluid velocity		
c_p	specific heat at constant pressure	p	pressure
		$Q = mq$	heat transfer
C_r	Crocco number	R	gas constant
$E = me$	energy	T	absolute temperature
$H = mh$	enthalpy	$U = mu$	internal energy
$\dot{m}$	mass flow rate	$V = mv$	volume
M	Mach number	$W = mw$	work
$M^* = \frac{c}{a^*}$		Z	elevation

GREEK SYMBOLS

$\gamma = c_p/c_v$		ρ	density

SUBSCRIPTS

0	stagnation values	2	final state
1	initial state	s	shaft work

SUPERSCRIPT

*	Critical value (corresponding to $M = 1$)

SOLVED EXAMPLES

Example 2.1. For adiabatic flow of a perfect gas show that

(*a*) $$\frac{T}{T_0} = \left(1 - \frac{\gamma - 1}{\gamma + 1} M^{*2}\right)$$

(*b*) $$\left(\frac{c}{a_0}\right)^2 = \frac{M^2}{1 + \frac{\gamma - 1}{2} M^2}$$

(*c*) Compute these values for $\gamma = 1.4$ and $M = 2.0$; what is the value of M^*?

Solution. $$\left(\frac{c}{a_0}\right)^2 = \frac{4}{1 + 0.2 \times 4} = \frac{4}{1.8} = 2.22$$

$$M^{*2} = \frac{½ (\gamma + 1) M^2}{1 + ½ (\gamma - 1) M^2} = \frac{1.2 \times 4}{1.8} = \frac{8}{3} = 2.67$$

$$M^* = 1.634 \quad \textbf{Ans.}$$

$$\frac{T}{T_0} = \left(1 - \frac{1.4 - 1}{1.4 + 1} \times 2.67\right) = 1 - 0.445$$

$$\frac{T}{T_0} = 0.555 \quad \textbf{Ans.}$$

Example 2.2. Define stagnation enthalpy and stagnation temperature; do these quantities define the stagnation state?

Argon is stored in a reservior at 300 K; determine stagnation enthalpy and velocity of sound in it. $\gamma = 1.658$, and the molecular weight of argon is 39.94.

Solution. $$R = \frac{\bar{R}}{W} = \frac{1.986}{39.94} \times 4.2 \times 1000 = 208.85 \text{ J/kg K}$$

$$a_0 = \sqrt{1.66 \times 208.85 \times 300} = \sqrt{10.4 \times 10^4}$$

$$a_0 = 322.5 \text{ m/s} \quad \textbf{Ans.}$$

$$c_p = \frac{\gamma}{\gamma - 1} R = \frac{1.66}{0.66} \times 208.15 = 525 \text{ J/kg K}$$

$$h_0 = c_p T_0 = 0.525 \times 300 = 157.5 \text{ kJ/kg K} \quad \textbf{Ans.}$$

Example 2.3. Derive the energy equation

$$\frac{a^2}{\gamma-1}+\frac{1}{2}c^2=\frac{1}{2}c_{max}^2=\frac{a_0^2}{\gamma-1}=h_0$$

stating the assumptions used.

An air jet ($\gamma=1.4$, $R=287$ J/kg K) at 400 K has sonic velocity. Determine:

(*i*) velocity of sound at 400 K,

(*ii*) velocity of sound at the stagnation conditions,

(*iii*) maximum velocity of the jet,

(*iv*) stagnation enthalpy,

(*v*) Crocco number.

Solution. (*i*) $c=a=\sqrt{\gamma RT}=\sqrt{1.4\times287\times400}=400$ m/s **Ans.**

(*ii*) $$\frac{a_0^2}{\gamma-1}=\frac{a^2}{2}\left(\frac{\gamma+1}{\gamma-1}\right)=\frac{1}{2}\left(\frac{2.4}{0.4}\right)400^2$$

$$2.5a_0^2=3\,(400)^2$$

$$a_0=\sqrt{1.2}\times400=438.18\text{ m/s}\quad\textbf{Ans.}$$

(*iii*) $$\frac{a^2}{\gamma-1}+\frac{a^2}{2}=\frac{a^2}{2}\left(\frac{\gamma+1}{\gamma-1}\right)=\frac{400^2}{2}\left(\frac{2.4}{0.4}\right)=3\times400^2$$

$$\frac{1}{2}c_{max}^2=3\times400^2$$

$$c_{max}^2=6\times400^2$$

$$c_{max}=979.8\text{ m/s}\quad\textbf{Ans.}$$

(*iv*) $$h_0=\frac{1}{2}c_{max}^2=3\times400^2\text{ Nm/kg}$$

$$h_0=48\times10^4\text{ J/kg}$$

$$h_0=480\text{ kJ/kg}\quad\textbf{Ans.}$$

(*v*) $$C_r=\frac{c}{c_{max}}=\frac{a}{c_{max}}=\frac{400}{979.8}=0.4082.$$

Example 2.4. Assuming perfect gas derive the energy equation of adiabatic flow:

$$\frac{\gamma}{\gamma-1}\frac{p}{\rho}+\frac{1}{2}c^2=\frac{\gamma}{\gamma-1}\frac{p_0}{\rho_0}$$

An air stream at $p=1.0$ bar, $T=400$ K and $c=400$ m/s is brought to rest (*i*) adiabatically (*ii*) isentropically. Determine the stagnation pressure and temperature in the two cases.

Solution. $$T_0=T+\frac{c^2}{2c_p}=400+\frac{400\times400}{2\times1005}$$

$$T_0=400+79.5+479.5\text{ K}$$

(for both isentropic and adiabatic processes)

For isentropic flow

$$\frac{p_0}{p}=\left(\frac{T_0}{T}\right)^{\gamma/(\gamma-1)}=\left(\frac{479.5}{400}\right)^{3.5}=(1.193)^{3.5}=1.85$$

$$p_0=1.85\times1.0=1.85\text{ bar}\quad\textbf{Ans.}$$

For adiabatic flow the value of the stagnation pressure would depend on the efficiency of the deceleration process. Therefore, with the given data the stagnation pressure cannot be determined.

Example 2.5. The pressure, temperature and Mach number at the entry of a flow passage are 2.45 bar, 26.5°C and 1.4 respectively. If the exit Mach number is 2.5 determine for adiabatic flow of a perfect gas ($\gamma=1.3$, $R=0.469$ kJ/kg K):

(*i*) stagnation temperature,

(*ii*) temperature and velocity of gas at exit, and

(*iii*) the flow rate per square metre of the inlet cross-section.

Solution. For adiabatic flow

$$T_{01}=T_{02}=T_0$$

$$\frac{T_{01}}{T_1}=1+\frac{\gamma-1}{2}M_1^2$$

$$\frac{T_{01}}{T_1}=1+\frac{1.3-1}{2}(1.4)^2=1.295$$

$$T_1=273+26.5$$

$$T_1=299.5\text{ K}$$

$$T_{01}=1.295\times299.5=388\text{ K}\quad\textbf{Ans.}$$

$$\rho_1=\frac{p_1}{RT_1}=\frac{2.45\times10^5}{469\times299.5}=1.745\text{ kg/m}^3$$

$$\frac{\dot{m}}{A_1} = \rho_1 c_1$$

$$a_1 = \sqrt{\gamma R T_1}$$

$$c_1 = M_1 a_1 = 1.4\sqrt{1.3 \times 469 \times 299.5}$$

$$c_1 = 1.4 \times 427.3 = 598.25 \text{ m/s}$$

$$\frac{\dot{m}}{A_1} = 1.745 \times 598.25 = 1043.95 \text{ kg/s-m}^2$$

$$\frac{T_{02}}{T_2} = 1 + \frac{\gamma - 1}{2} M_2^2 = 1 + \frac{0.3}{2}(2.5)^2 = 1.938$$

$$T_2 = \frac{T_2}{T_{02}} \times \frac{T_{01}}{T_1} \times T_1$$

$$T_2 = \frac{1.295}{1.938} \times 299.5$$

$$T_2 = 201 \text{ K} \quad \textbf{Ans.}$$

$$a_2 = \sqrt{1.3 \times 469 \times 201}$$

$$a_2 = 350 \text{ m/s}$$

$$c_2 = M_2 a_2$$

$$c_2 = 2.5 \times 350.0$$

$$c_2 = 875 \text{ m/s} \quad \textbf{Ans.}$$

Example 2.6. Air ($\gamma = 1.4$, $R = 287.43$ J/kg K) enters a straight axisymmetric duct at 300 K, 3.45 bar and 150 m/s and leaves it at 277 K, 2.058 bar and 260 m/s. The area of cross-section at entry is 500 cm^2. Assuming adiabatic flow determine:

(*i*) stagnation temperature,

(*ii*) maximum velocity,

(*iii*) mass flow rate, and

(*iv*) area of cross-section at exit.

Solution. (*i*) $c_p = \frac{\gamma}{\gamma - 1} R$

$$= \frac{1.4}{0.4} \times 287.43$$

$$= 1006 \text{ J/kg-K}$$

$$T_{01} = T_1 + \frac{c_1^2}{2c_p} = 300 + \frac{150 \times 150}{2 \times 1006}$$

$$T_{01} = 300 + 11.15 = 311.15 \text{ K} \quad \textbf{Ans.}$$

Since the flow is adiabatic the stagnation temperature must remain constant. This can be seen by calculating its value at exit section.

$$T_{02} = T_2 + \frac{c_2^2}{2c_p} = 277 + \frac{260 \times 260}{2 \times 1006}$$

$$= 277 + 33.7 = 310.7 \text{ K}$$

(*ii*) $c_{max} = \sqrt{2c_p T_0}$

$$= \sqrt{2 \times 1006 \times 311.15}$$

$$= 790 \text{ m/s} \quad \textbf{Ans.}$$

(*iii*) $\rho_1 = \frac{p_1}{RT_1} = \frac{3.45 \times 10^5}{287.43 \times 300} = 4.0 \text{ kg/m}^3$

$$\rho_2 = \frac{p_2}{RT_2} = \frac{2.058 \times 10^5}{287.43 \times 277} = 2.59 \text{ kg/m}^3$$

$$\dot{m} = \rho_1 A_1 c_1 = \rho_2 A_2 c_2$$

$$\dot{m} = 4.0 \times 0.05 \times 150$$

$$\dot{m} = 30 \text{ kg/s} \quad \textbf{Ans.}$$

$$A_2 = \frac{\rho_1 c_1}{\rho_2 c_2} A_1$$

$$A_2 = \frac{4 \times 150}{2.59 \times 260} \times 500$$

$$A_2 = 445 \text{ cm}^2 \quad \textbf{Ans.}$$

Example 2.7. An aircraft flies at 800 km/hr at an altitude of 10,000 metres ($T = 223.15$ K, $p = 0.264$ bar). The air is reversibly compressed in an inlet diffuser. If the Mach number at the exit of the diffuser is 0.36 determine (*a*) entry Mach number and (*b*) velocity, pressure and temperature of air at the diffuser exit.

Solution. Let subscripts *i* and *e* refer to conditions at entry and exit of the diffuser respectively.

(*a*) $p_i = 0.264$ bar, $T_i = 223.15$ K

$$c_i = 800 \times 1000/3600 = 222.22 \text{ m/s}$$

$$T_0 = T_i + \frac{c_i^2}{2c_p} = 223.15 + \frac{222.22^2}{2 \times 1000} = 247.84 \text{ K}$$

$$M_i = \frac{c_i}{\sqrt{\gamma RT_i}} = \frac{222.22}{\sqrt{1.4 \times 287 \times 223.15}} = 0.74 \quad \textbf{Ans.}$$

(*b*) From isentropic flow tables for $\gamma = 1.4$ at

$M_i = 0.74$, $p_i/p_0 = 0.695$

$M_e = 0.36$, $p_e/p_0 = 0.914$, $T_e/T_0 = 0.975$

$p_0 = 0.264/0.695 = 0.379$ bar

$p_e = 0.914 \times 0.379 = 0.346$ bar **Ans.**

$T_e = 0.975 \times 247.84 = 241.6$ K **Ans.**

$a_e = \sqrt{1.4 \times 287 \times 241.6} = 311.57$ m/s

$c_e = M_e a_e = 0.36 \times 311.57 = 112.17$ m/s **Ans.**

Example 2.8. Air ($c_p = 1.05$ kJ/kg K, $\gamma = 1.38$) at $p_1 = 3 \times 10^5$ N/m^2 and $T_1 = 500$ K flows with a velocity of 200 m/s in a 30 cm diameter duct. Calculate:

(*a*) mass flow rate,

(*b*) stagnation temperature,

(*c*) Mach number, and

(*d*) stagnation pressure values assuming the flow as compressible and incompressible.

Solution. $R = c_p - c_v$

$$R = 1.05 - \frac{1.05}{1.38} = 0.289 \text{ kJ/kg K}$$

$$\rho_1 = \frac{p_1}{RT_1} = \frac{3 \times 10^5}{289 \times 500} = 2.076 \text{ kg/m}^3$$

a) Mass flow rate

$$\dot{m} = \rho_1 A_1 c_1$$

$$\dot{m} = 2.076 \left(\frac{\pi}{4} \times 0.3^2 \right) \times 200$$

$$\dot{m} = 29.348 \text{ kg/s} \quad \textbf{Ans.}$$

(*b*) Stagnation temperature

$$T_0 = T_1 + \frac{c_1^2}{2c_p}$$

$$T_0 = 500 + \frac{200 \times 200}{2 \times 1050}$$

$$T_0 = 519.047 \text{ K} \quad \textbf{Ans.}$$

(*c*) Mach number

$$M_1 = \frac{c_1}{\sqrt{\gamma RT_1}} = \frac{200}{\sqrt{1.38 \times 289 \times 500}} = 0.4478 \quad \textbf{Ans.}$$

(*d*) Stagnation pressure:

For compressible flow

$$\frac{p_0}{p_1} = \left(\frac{T_0}{T} \right)^{\gamma/(\gamma-1)} = \left(\frac{519.047}{500} \right)^{1.38/0.38} = 1.145$$

$$p_0 = 1.145 \times 3 \times 10^5 = 3.435 \times 10^5 \text{ N/m}^2 \quad \textbf{Ans.}$$

For incompressible flow

$$p_0 = p_1 + \frac{1}{2} \rho_1 c_1^2$$

$$p_0 = 3 \times 10^5 + \frac{1}{2} \times 2.076 \times 200^2$$

$$p_0 = 3.415 \times 10^5 \text{ N/m}^2 \quad \textbf{Ans.}$$

QUESTIONS AND PROBLEMS

2.1 Define the following terms; write down their formulas and units where applicable:

Stagnation pressure, stagnation temperature,stagnation velocity of sound, Mach number, critical and maximum velocities, transonic and hypersonic flows.

2.2 Derive the following relations stating the assumptions used:

(*a*) $h_0 = h + \frac{1}{2} c^2$

(*b*) $p_0 = p + \frac{1}{2}\rho c^2$

(*c*) $a_0^2 = (\gamma - 1)\, h_0$

(*d*) $\frac{T_0}{T} = 1 + \frac{\gamma - 1}{2} M^2$

(*e*) $\frac{T^*}{T} = \frac{2}{\gamma + 1} + \frac{\gamma - 1}{\gamma + 1} M^2$

2.3 What is the advantage of using M^* instead of M in some cases? Show that

(*a*) $M^* = \left(\frac{T}{T^*}\right)^{1/2} M$

(*b*) $M^*_{max} = \left(\frac{\gamma + 1}{\gamma - 1}\right)^{1/2}$.

2.4 (*a*) What is the difference between the Bernoulli Equation and the steady flow energy equation?

(*b*) Derive the following energy equation

$$\frac{\gamma}{\gamma - 1}\frac{p_0}{\rho_0}\left(\frac{p}{p_0}\right)^{(\gamma-1)/\gamma} + \frac{1}{2}c^2 = \frac{\gamma}{\gamma - 1}\frac{p_0}{\rho_0}$$

2.5 (*a*) What is the effect of Mach number on the compressibility? Prove for $\gamma = 1.4$

$$\frac{p_0 - p}{\frac{1}{2}\rho c^2} = 1 + \frac{1}{4}M^2 + \frac{1}{40}M^4 + \ldots$$

(*b*) Show that for sonic flow the deviation between the compressible and incompressible flow values of the pressure coefficient of a perfect gas ($\gamma = 1.4$) is about 27.5 per cent.

2.6 (*a*) What is velocity temperature? Determine the velocity of air ($\gamma = 1.4$, $c_p = 1.005$ kJ/kg K) corresponding to a velocity temperature of 1°C.

(*b*) Determine the Mach number of an aircraft at which the velocity temperature of air at the entry of the engine equals the static temperature.

Ans. (*a*) 44.8 m/s, (*b*) $M = 2.235$.

2.7 Steam at a section of a pipe has pressure = 10 bar, temperature = 600 K, velocity = 120 m/s, datum head = 10 m.

(*a*) Taking $c_p = 2.150$ kJ/kg K, $c_v = 1.615$ kJ/kg K, determine Mach number, stagnation pressure and temperature.

(*b*) Compare the stagnation pressure value with that obtained from the Bernoulli Equation and comment on the difference.

(*c*) Are the effects of Mach number and datum significant in this case?

Ans. $M = 0.1835$, $p_0 = 10.225$ bar, $T_0 = 603.348$ K.

2.8 The conditions of an air stream at entry to a duct are

$$p_1 = 1.0 \text{ bar}, \; T_1 = 300 \text{ K}, \; M_1 = 1.3$$

If the Mach number at exit of the duct is 0.6 determine for adiabatic flow the temperature and velocity of air at the duct exit.

Ans. $T_2 = 374.69$ K, $c_2 = 232.8$ m/s.

2.9 An aircraft is flying at an altitude of 12,000 meters ($T = 216.65$ K, $p = 0.193$ bar) at a Mach number of 0.82. The cross-sectional area of the inlet diffuser before the L.P. compressor stage is 0.5 m^2. Determine:

(*a*) the mass of air entering the compressor per second,

(*b*) the speed of the aircraft and

(*c*) the stagnation pressure and temperature of air at the diffuser entry.

Ans. (*a*) 37.5 kg/s, (*b*) 871 km/hr, (*c*) 0.30 bar, 246 K.

2.10 The jet of a gas at 593 K ($\gamma = 1.3$, $R = 469$ J/kg-K) has a Mach number of 1.2. Determine for local and stagnation conditions velocity of sound and enthalpy.

What is the maximum attainable velocity of this jet?

Ans. $a = 601.29$ m/s, $h = 1205$ kJ/kg, $a_0 = 663.2$ m/s

$h_0 = 1466$ kJ/kg, $c_{max} = 1712.38$ m/s.

2.11 In a settling chamber air is at $p_0 = 5$ bar, $T_0 = 500$ K. Determine the values of h_0, a_0, c_{max}, T^*, c^* and a^*.

Which type of flow has been assumed in the calculations?

Ans. $h_0 = 502.5$ kJ/kg, $a_0 = 448.218$ m/s, $c_{max} = 1002.49$ m/s, $T^* = 416.67$ K, $c^* = a^* = 409.16$ m/s.

2.12 (*a*) For steady adiabatic flow obtain the following relation:

$$\frac{dT}{T} + \frac{\gamma - 1}{2} M^2 \frac{dc^2}{c^2} = 0$$

(*b*) Derive

$$\frac{dT}{T} = \frac{dc^2}{c^2} - \frac{dM^2}{M^2}$$

$$\frac{dc^2}{c^2} = \frac{2}{2 + (\gamma - 1) M^2} \frac{dM^2}{M^2}.$$

3

Rate Equations for a Control Volume

As pointed out at the beginning of Chapter 1, laws of conservation of mass, momentum, energy and entropy govern the Equations of compressible flows. These conservation laws are well explained for a system. Here the rate Equations based on these laws for flow through a control volume will be developed and discussed. The difference between the concepts "control volume" and the "system" has already been explained in Chapter 1.

3.1 CONTINUITY EQUATION (CONSERVATION OF MASS)

Continuity Equation for both steady and unsteady flow is derived on the basis of the conservation of mass; this states that mass can neither be created nor destroyed.

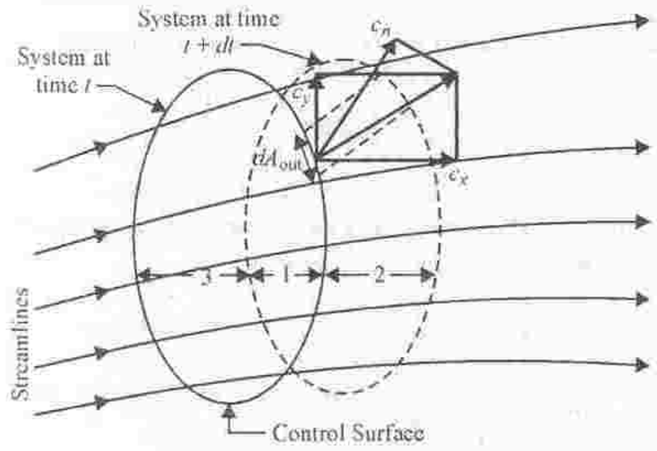

FIGURE 3.1 : Flow of fluid through a control volume

Figure 3.1 shows a system at time t and $t + dt$. The two positions of the system contain three regions 1, 2 and 3.

Applying the law of conservation of mass to the above system

$$m_{1t} + m_{3t} = m_{1\,(t+dt)} + m_{2\,(t+dt)}$$

$$\frac{m_{1\,(t+dt)} - m_{1t}}{dt} = \frac{m_{3t}}{dt} - \frac{m_{2\,(t+dt)}}{dt} \tag{3.1}$$

$$\lim_{dt \to 0} \frac{m_{1\,(t+dt)} - m_{1t}}{dt} = \frac{\partial}{\partial t}(m_{cv}) \tag{3.2}$$

This is the rate of change of mass with time within the control volume

$$\frac{m_{3t}}{dt} = \frac{\Sigma\, dm_{3t}}{dt} = \int_{\text{in}} d\dot{m} \text{ (inflow of mass-flux)} \tag{3.3}$$

$$\frac{m_{2\,(t+dt)}}{dt} = \frac{\Sigma\, dm_{2\,(t+dt)}}{dt} = \int_{\text{out}} d\dot{m} \text{ (outflow of mass-flux)} \tag{3.4}$$

Substituting Equations (3.2), (3.3) and (3.4) in (3.1) gives

$$\frac{\partial}{\partial t}(m_{cv}) = \int_{\text{in}} d\dot{m} - \int_{\text{out}} d\dot{m} \tag{3.5}$$

Equation (3.5) mathematically demonstrates an obvious fact, that the rate of change of mass within the control volume is equal to the difference of rates of flows of the incoming and outgoing masses.

Equation (3.5) can also be expressed in another useful form

$$\frac{\partial}{\partial t}(m_{cv}) = \frac{\partial}{\partial t}\int_{cv} \rho\, dV = \int_{cv} \frac{\partial \rho}{\partial t}\, dV \tag{3.6}$$

Here ρdV is the elemental mass in the control volume corresponding to the infinitesimal volume dV.

$$\int_{\text{in}} d\dot{m} = \int_{\text{in}} \rho c_n\, dA \tag{3.7}$$

$$\int_{\text{out}} d\dot{m} = \int_{\text{out}} \rho c_n\, dA \tag{3.8}$$

Substituting Equations (3.6), (3.7) and (3.80 in (3.5) yields

$$\int_{cv} \frac{\partial \rho}{\partial t}\, dV = \int_{\text{in}} \rho c_n\, dA - \int_{\text{out}} \rho c_n\, dA \tag{3.9}$$

The integrals on the right hand side of Equation (3.9) represent the integral of quantities at entry and exit.

$$\int_{\text{in}} \rho c_n\, dA = \int \rho_1\, c_{n1}\, dA_1$$

$$\int_{\text{out}} \rho c_n\, dA = \int \rho_2\, c_{n2}\, dA_2$$

In vector notation Equation (3.9) is written as

$$\int_{cv} \frac{\partial \rho}{\partial t}\, dV = -\oint_{cs} \rho \mathbf{c}\, d\mathbf{A} \tag{3.10}$$

The integral $\oint_{cs}$ represents the surface integral over the entire control surface.

For steady compressible or incompressible flows

$$\frac{\partial \rho}{\partial t} = 0$$

Therefore, Equation (3.9) gives

$$\int_{\text{in}} \rho c_n\, dA = \int_{\text{out}} \rho c_n\, dA \tag{3.11}$$

In one-dimensional steady flow

$$\int \rho c_n\, dA = \rho c \int dA = \rho c A \tag{3.12}$$

If the entry and exit sections are designated as 1 and 2 respectively, substituting Equations (3.12) in (3.11) yields

$$\dot{m} = \rho_1 c_1 A_1 = \rho_2 c_2 A_2 = \text{constant} \tag{3.13}$$

This is the couninuity equation for one-dimensional steady flow.

3.2 MOMENTUM EQUATION (Conservation of Momentum)

Here the momentum flux through the control volume is considered.

Newton's second law of motion states that the rate of change of momentum in a given direction is produced by the algebraic sum of the forces acting on the control surface in that direction. Referring again to Figure 3.1 and considering x-direction

$$\Sigma F_x = \frac{d}{dt}(mc_x) \tag{3.14}$$

The momentum in the final state of the system under consideration is

$$(mc_x)_{1\,(t+dt)} + (mc_x)_{2\,(t+dt)}$$

The momentum in the initial state is

$$(mc_x)_{1t} + (mc_x)_{3t}$$

Therefore, the rate of change of momentum

$$\frac{d}{dt}(mc_x) = \lim_{dt \to 0} \frac{(mc_x)_{1\,(t+dt)} + (mc_x)_{2\,(t+dt)} - (mc_x)_{1t} - (mc_x)_{3t}}{dt} \tag{3.15}$$

Now $$\lim_{dt \to 0} \frac{(mc_x)_{1\,(t+dt)} - (mc_x)_{1t}}{dt} = \frac{\partial}{\partial t}(mc_x)_{cv} \tag{3.16}$$

$$\frac{(mc_x)_{2\,(t+dt)}}{dt} = \Sigma \frac{c_x\, dm_{2\,(t+dt)}}{dt} = \int_{\text{out}} c_x\, d\dot{m} \tag{3.17}$$

= outflow of momentum flux

Similarly $$\frac{(mc_x)_{3t}}{dt} = \Sigma \frac{c_x\, dm_{3t}}{dt} = \int_{\text{in}} c_x\, d\dot{m} \tag{3.18}$$

= inflow of momentum flux

Substituting Equations (3.16), (3.17) and (3.18) in (3.15) and (3.14) gives

$$\Sigma F_x = \frac{\partial}{\partial t}(mc_x)_{cv} + \int_{\text{out}} c_x\, d\dot{m} - \int_{\text{in}} c_x\, d\dot{m} \tag{3.19}$$

Equation (3.19) states that the algebraic sum of forces acting on the control surface in a given direction equals the rate of change of momentum within the control volume plus the excess of the outgoing momentum flux over the incoming momentum flux.

Equation (3.19) can also be expressed in the following form. As in Section 3.1 the elemental mass in the control volume is ρdV and the elemental entry and exit areas of the control surface are dA_{in} and dA_{out} respectively.

Therefore, $$\frac{\partial}{\partial t}(mc_x)_{cv} = \frac{\partial}{\partial t}\int_{cv} \rho c_x\, dV = \int_{cv} \frac{\partial}{\partial t}(\rho c_x)\, dV \tag{3.20}$$

$$\int_{\text{out}} c_x\, d\dot{m} = \int c_x\, \rho c_n\, dA_{\text{out}} = \int_{\text{out}} \rho c_x\, c_n\, dA \tag{3.21}$$

Similarly $$\int_{\text{in}} c_x\, d\dot{m} = \int c_x\, \rho c_n\, dA_{\text{in}} = \int_{\text{in}} \rho c_x\, c_n\, dA \tag{3.22}$$

Substitution of Equations (3.20), (3.21) and (3.22) in (3.19) yields

$$\Sigma F_x = \int_{cv} \frac{\partial}{\partial t}(\rho c_x)\, dV + \int_{\text{out}} \rho c_x\, c_n\, dA - \int_{\text{in}} \rho c_x\, c_n\, dA \tag{3.23}$$

Similar expressions for y- and z-directions are

$$\Sigma F_y = \int_{cv} \frac{\partial}{\partial t}(\rho c_y)\, dV + \int_{\text{out}} \rho c_y\, c_n\, dA - \int_{\text{in}} \rho c_y\, c_n\, dA \tag{3.24}$$

$$\Sigma F_z = \int_{cv} \frac{\partial}{\partial t}(\rho c_z)\, dV + \int_{\text{out}} \rho c_z\, c_n\, dA - \int_{\text{in}} \rho c_z\, c_n\, dA \tag{3.25}$$

In vector notation Equations (3.23), (3.24) and (3.25) can be expressed by a single general expression

$$\Sigma \mathbf{F} = \frac{\partial}{\partial t}\int_{cv} \rho \mathbf{c}\, dV + \oint_{cs} \rho\, (\mathbf{c} d\mathbf{A})\, \mathbf{c} \tag{3.26}$$

The term $\Sigma \mathbf{F}$ includes (*i*) body forces like the inertia, gravitational and the electro-magnetic forces, and (*ii*) the surface forces like friction, pressure and surface tension forces.

For steady flow $\dfrac{\partial}{\partial t}\displaystyle\int_{cv} \rho c\, dV = 0$

Therefore, $$\Sigma \mathbf{F} = \oint \rho\, (\mathbf{c} d\mathbf{A})\, \mathbf{c} \tag{3.27}$$

For steady one-dimensional flow

$$\Sigma F = \rho_2 A_2 c_2^2 - \rho_1 A_1 c_1^2 \tag{3.28}$$

3.3 MOMENT OF MOMENTUM EQUATION

In some practical applications, for example in turbomachines often the quantity of interest is the moment of momentum.

Therefore, in this section the momentum equation derived earlier is used to develop the moment of momentum equation. This can be developed by giving a mathematical form to the following statement:

The algebraic sum of torques is equal to the rate of change of the moment of momentum with respect to time. Thus

$$\Sigma \mathbf{F} \times \mathbf{r} = \frac{d}{dt}(\Sigma m \mathbf{c} \times \mathbf{r}) \tag{3.29}$$

The equivalent of Equation (3.26) can also be written by introducing the radius vector **r**.

$$\Sigma \mathbf{F} \times \mathbf{r} = \frac{\partial}{\partial t} \int_{cv} \rho\, (\mathbf{c} \times \mathbf{r})\, dV + \oint_{cs} \rho\, (\mathbf{c} d\mathbf{A})\, \mathbf{c} \times \mathbf{r} \tag{3.30}$$

As an example, considering the tangential direction for turbomachine applications Equation (3.30) can be written as

$$\Sigma F_t\, r = \frac{\partial}{\partial t} \int_{cv} (\rho r c_t)\, dV + \int_{\text{out}} \rho r c_n\, c_t\, dA - \int_{\text{in}} \rho r c_n\, c_t\, dA \tag{3.31}$$

3.4 ENERGY EQUATION (CONSERVATION OF ENERGY)

In Chapter 2 energy Equation was discussed for steady flow; the rate of flow of the fluid was assumed constant with time. In this section the flow is considered as unsteady.

The energy Equation (1.8) in its differential form is

$$dQ = dE + dW$$

$$\frac{dQ}{dt} = \frac{dE}{dt} + \frac{dW}{dt} \tag{3.32}$$

The change is energy dE/dt is equal to the time rate of change of energy within the control volume plus the outgoing energy flux minus the incoming energy flu. Thus

$$\frac{dE}{dt} = \left(\frac{\partial E}{\partial t}\right)_{cv} + \int_{\text{out}} e\, d\dot{m} - \int_{\text{in}} e\, d\dot{m} \tag{3.33}$$

The work term in Equation (3.32) includes the flow work and the shaft work.

$$\frac{dW}{dt} = \int_{\text{out}} pv\, d\dot{m} - \int_{\text{in}} pv\, d\dot{m} + \frac{dW_s}{dt} \tag{3.34}$$

Substituting from Equations (3.33) and (3.34) in (3.32) and rearranging

$$\frac{dQ}{dt} = \left(\frac{\partial E}{\partial t}\right)_{cv} + \int_{\text{out}} (e + pv)\, d\dot{m} - \int_{\text{in}} (e + pv)\, d\dot{m} + \frac{dW_s}{dt} \tag{3.35}$$

As shown in Equation (2.1) the energy term is given by

$$e = u + \frac{1}{2}c^2 + gZ$$

Therefore, $e + pv = (u + pv) + \frac{1}{2}c^2 + gZ$

$$e + pv = h + \frac{1}{2}c^2 + gZ \tag{3.36}$$

Substituting Equation (3.36) in (3.35) we get

$$\frac{dQ}{dt} = \left(\frac{\partial E}{\partial t}\right)_{cv} + \int_{\text{out}} \left(h + \frac{1}{2}c^2 + gZ\right) d\dot{m} - \int_{\text{in}} \left(h + \frac{1}{2}c^2 + gZ\right) d\dot{m} + \frac{dW_s}{dt} \tag{3.37}$$

In short, Equation (3.37) can be written in vector notation as

$$\frac{dQ}{dt} = \frac{\partial}{\partial t} \int_{cv} (\rho e)\, dV + \oint_{cs} \left(h + \frac{1}{2}c^2 + gZ\right) \rho \mathbf{c} d\mathbf{A} + \frac{dW_s}{dt} \tag{3.38}$$

For steady flow

$$\left(\frac{\partial E}{\partial t}\right)_{cv} = 0$$

$$\frac{dQ}{dt} = \int_{\text{out}} \left(h + \frac{1}{2}c^2 + gZ\right) d\dot{m} - \int_{\text{in}} \left(h + \frac{1}{2}c^2 + gZ\right) d\dot{m} + \frac{dW_s}{dt} \tag{3.39}$$

For adiabatic flow $\frac{dQ}{dt} = 0$

$$\frac{dW_s}{dt} = \int_{\text{in}} \left(h + \frac{1}{2}c^2 + gZ \right) d\dot{m} - \int_{\text{out}} \left(h + \frac{1}{2}c^2 + gZ \right) d\dot{m}$$

For one-dimensional and steady adiabatic flow

$$\frac{dW_s}{dt} = \dot{m} \left\{ \left(h_1 + \frac{1}{2}c_1^2 + gZ_1 \right) - \left(h_2 + \frac{1}{2}c_2^2 + gZ_2 \right) \right\}$$

For gases $Z_1 - Z_2 \simeq 0$. Putting $h + \frac{1}{2}c^2 = h_0$

$$\frac{dW_s}{dt} = \dot{m}\,(h_{01} - h_{02}) \tag{3.40}$$

If shaft work is absent

$$h_{01} = h_{02}$$

These results have already been obtained for steady flow in Chapter 2.

3.5 ENTROPY EQUATION

In Chapter 1 Equation (1.41) gives the entropy change in any steady irreversible process as

$$\frac{dQ}{T} < dS$$

$$\frac{1}{T}\frac{dQ}{dt} < \frac{dS}{dt} \tag{3.41}$$

For unsteady flow through a control volume the rate of change in entropy dS/dt is equal to the rate of change of entropy within the control volume plus the excess of outgoing entropy flux over the incoming entropy flux. Therefore,

$$\frac{1}{T}\frac{dQ}{dt} < \frac{\partial}{\partial t}\int_{\text{cv}} dS + \int_{\text{out}} dS - \int_{\text{in}} dS$$

$$\frac{1}{T}\frac{dQ}{dt} < \frac{\partial}{\partial t}\int_{\text{cv}} \rho s\, dV + \int_{\text{out}} \rho s c\, dA - \int_{\text{in}} \rho s c\, dA$$

In vector notation this can be written as

$$\frac{1}{T}\frac{dQ}{dt} < \frac{\partial}{\partial t}\int_{\text{cv}} \rho s\, dV + \oint_{\text{cs}} \rho s\, \mathbf{c}\, d\mathbf{A} \tag{3.42}$$

For steady flow

$$\frac{\partial}{\partial t}\int_{\text{cv}} \rho s\, dV = 0$$

Therefore,

$$\frac{1}{T}\frac{dQ}{dt} < \oint_{\text{cs}} \rho s \mathbf{c}\, d\mathbf{A} \tag{3.43}$$

For steady one-dimensional flow

$$\frac{1}{T}\frac{dQ}{dt} < \dot{m}\,(s_2 - s_1) \tag{3.44}$$

For adiabatic flow

$$\frac{1}{T}\frac{dQ}{dt} = 0$$

$$s_2 > s_1$$

Notation for Chapter 3

area	A	
area vector	$\mathbf{A}$	
fluid velocity	c	
velocity vector	$\mathbf{c}$	
energy	$E = me$	
force or thrust	F	
force vector	$\mathbf{F}$	
enthaply	h	
mass flow rate	$\dot{m}$	
pressure	p	
power	P	
	Q	heat transfer
	r	radius
	$\mathbf{r}$	radius vector
	$S = ms$	entropy
	t	time
	v	specific volume
	V	volume
	W	work
	α	angle
	ρ	density
	τ	torque
	ω	rotational speed

Subscripts

stagnation values	0	
entry conditions	1	
exit conditions	2	
control surface	cs	
	n	normal direction
	t	at time t, tangential
	$t + dt$	at time $t + dt$
	x, y, z	directions along the Cartesian coordinates

SOLVED EXAMPELS

Example 3.1. The cross-section of the exit section of a control surface enclosing an aircraft propeller is 9 m^2. The mean values of air velocities at the entry an exit of the control surface are 133 m/s and 170 m/s respectively. Taking the density of air as 1.25 kg/m^3 determine the thrust acting on the propeller.

Assume incompressible and steady flow.

Solution. The control surface is shown in Figure 3.2

From continuity Equation

$$\rho\, c_1\, A_1 = \rho\, c_2\, A_2$$

$$A_1 = \frac{c_2 A_2}{c_1} = \frac{170}{133} \times 9 = 11.503 \text{ m}^2$$

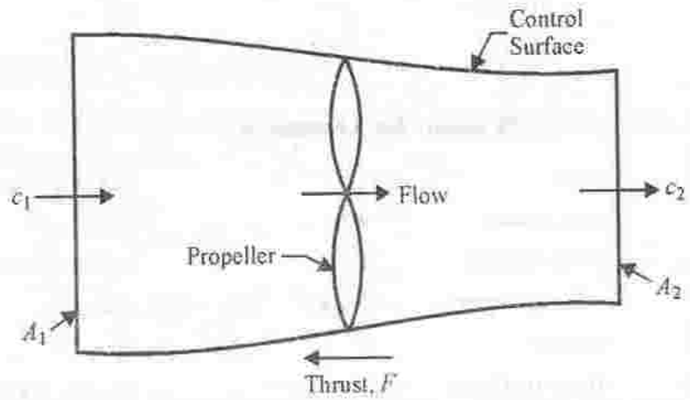

FIGURE 3.2 : Control surface containing a propeller

For steady and incompressible flow, using Equation (3.28),

$$F = \rho\, A_2\, c_2^2 - \rho A_1\, c_1^2$$

$$F = \frac{1.25}{1000}(9 \times 170^2 - 11.503 \times 133^2)$$

$$F = 70.78 \text{ kN}$$ **Ans.**

Example 3.2. Gas enters a radially tipped rotor of an inward flow turbine and leaves it with negligible tangential component. The absolute velocity vector of 285 m/s at entry is inclined at 30 degrees to the tangential direction. The radius of the rotor at entry is 25 cm, and the

flow rate of the gas 5 kg/s. For steady flow calculate the torque exerted and the power transferred.

Solution. The velocity vectors at the entry and exit of the rotor are shown in Figure 3.3.

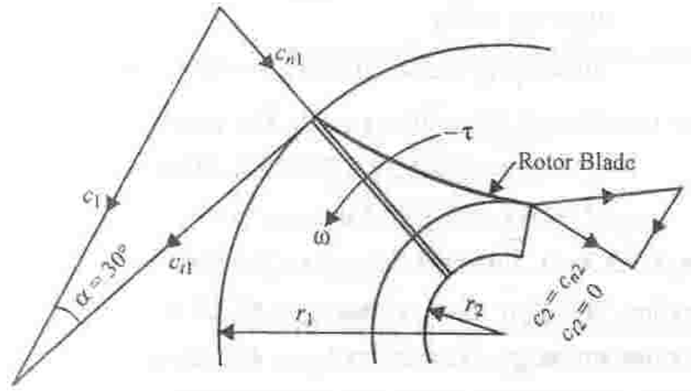

FIGURE 3.3 : Velocity vectors at the entry and exit of an inward-flow radial turbine

For steady flow Equation (3.31) is

$$\text{Torque } \tau = F_t\, r = \int_{\text{out}} \rho r c_n\, c_t\, dA - \int_{\text{in}} \rho r\, c_n\, c_t\, dA$$

For one-dimensional flow

$$\int_{\text{out}} \rho\, r\, c_n\, c_t\, dA = \rho_2\, r_2\, c_{n2}\, c_{t2}\, A_2$$

In the given problem $c_{t2} = 0$, therefore,

$$\int_{\text{out}} \rho r\, c_n\, c_t\, dA = 0$$

The torque exerted on the fluid is

$$\tau = -\int_{\text{in}} \rho\, r\, c_n\, c_t\, dA = -(\rho_1\, c_{n1}\, A_1)\, r_1\, c_{t1}$$

$$\rho_1\, c_{n1}\, A_1 = \dot{m} = \text{gas flow rate}$$

$$\tau = -\dot{m} r_1\, c_{t1}$$

The torque exerted on the rotor is equal and opposite to the torque exerted on the fluid. Therefore,

$$-\tau = \dot{m} r_1\, c_{t1}$$

$$c_{t1} = c_1 \cos \alpha_1$$

$$c_{t1} = 285 \cos 30 = 246.817 \text{ m/s}$$

$$-\tau = 5 \times 0.25 \times 246.817 = 308.521 \text{ mN}$$ **Ans.**

The tangential velocity of the rotor is given by

$$u_1 = c_{t1} = \omega r_1$$

$$\omega = u_1 / r_1 = 246.817/0.25 = 987.268 \text{ rad/s}$$

Power transferred from the gas to the rotor is

$$P = \tau\omega = 308.521 \times 987.268/1000$$

$$P = 304.593 \text{ kW}$$ **Ans.**

Example 3.3. A turbomachine has the following data:

Stagnation enthalpy flux at entry = 15 kJ/s

Stagnation enthalpy flux at exit = 115 kJ/s

Heat rejected = 5 kJ/s

Calculate the power supplied to or generated by the turbomachine. Identify the turbomachine as a compressor or turbine.

Solution. Assume the flow to be steady and one-dimensional. Therefore, Equation (3.39) gives

$$\dot{Q} = \int_{\text{out}} h_0 \, d\dot{m} - \int_{\text{in}} h_0 \, d\dot{m} + P$$

Substituting the values in the above expression we get,

$$-5 = 115 - 15 + P$$

$$P = -105 \text{ kJ/s} = -105 \text{ kW}$$

This is the rate of energy supplied to the gas by the turbomachine; hence the turbomachine is a compressor. This requires a power supply of 105 kW.

QUESTIONS AND PROBLEMS

3.1 Develop the following relations for a control volume from first principles:

(*a*) $$\frac{d}{dt}(mc_x) = \frac{\partial}{\partial t}(mc_x)_{cv} + \int_{\text{out}} c_x \, d\dot{m} - \int_{\text{in}} c_x \, d\dot{m}$$

(*b*) $$\frac{d}{dt}(\Sigma mc_t r) = \frac{\partial}{\partial t}\int_{cv} \rho r c_t \, dV + \int_{\text{out}} \rho r c_x c_t \, dA - \int_{\text{in}} \rho r c_x c_t \, dA$$

(*c*) $$\frac{dE}{dt} = \left(\frac{\partial E}{\partial t}\right)_{cv} + \int_{\text{out}} e \, d\dot{m} - \int_{\text{in}} e \, d\dot{m}$$

(*d*) $$\frac{dS}{dt} = \frac{\partial}{\partial t}\int_{cv} \rho s \, dV + \int_{\text{out}} \rho s c \, dA - \int_{\text{in}} \rho s c \, dA$$

3.2 Derive the unsteady flow continuity Equation for a control volume

$$\int_{cv} \frac{\partial \rho}{\partial t} dV = \int_{\text{in}} \rho c_n \, dA - \int_{\text{out}} \rho c_n \, dA$$

Hence show that for one-dimensional steady flow

$$\rho A c = \text{constant}.$$

3.3 A turbojet engine takes in 40 kg/s of air and consumes 1.0 kg/s of fuel. Air enters the engine at a velocity of 300 m/s. Exhaust gases leave the engine with a velocity of 500 m/s. If the pressure at both the entry and exit sections is the same determine the thrust produced.

Ans. F = 8.5 kN.

3.4 An axial flow fan has the following data:

mass flow rate = 8 kg/s,

mean diameter of the rotor = 60 cm.

Absolute velocity vectors at entry and exit of the rotor are 50 m/s and 70.71 m/s respectively. They are inclined in the same direction to the tangential components at entry and exit at angles of 45 and 30 degrees respectively.

For steady flow calculate the torque applied by the rotor on the flow. If the rotational speed of the rotor is 335 rad/s calculate the power required to drive the fan.

Ans. $\tau = 62.114$ mN, $P = 20.808$ kW.

3.5 A turbomachine has the following data:

Entry : gas temperature = 800 K,

: gas velocity = 75 m/s

Exit : gas temperature = 500 K

: gas velocity = 116 m/s.

Heat losses = 50 kJ/s.

Calculate the power supplied to or generated by the turbomachine for a flow rate of 50 kg/s. The specific heat of the gas at constant pressure is 1.05 kJ/kg K.

Ans. $P = 15{,}504.225$ kW.

3.6 The stagnation enthalpy fluxes entering and leaving the control volume containing a turbine stage are 25 and 10 kJ/s respectively. The heat loss is 2.5 kJ/s. Determine the power developed by the turbine.

Ans. $P = 12.5$ kW.

4

Isentropic Flow with Variable Area

A steady one-dimensional isentropic flow in variable area passages is considered in this chapter.

As stated before if the flow parameters do not vary with time it is referred to as steady flow. Along with this condition if the flow parameters do not vary in directions normal to the flow direction it is said to be one-dimensional. A truly one-dimensional flow would occur in a stream tube where the effects of boundary layer and heat conduction are absent. In many cases one-dimensional flow is assumed to simplify a complex problem and to obtain quickly a rough idea of the variations in various flow parameters along the direction of flow. For more accurate assessment of these variations in the flow field two-and three-dimensional analyses are employed which are tedious.

The problem can be further simplified at the cost of accuracy by making the assumption of isentropic flow. This is justified when the process is such that the heat transfer is negligible and there are no other irreversibilities due to fluid friction etc. The processes occurring in real systems obviously deviate from the idealized one-dimensional isentropic process; in a large number of applications it is used as a standard reference process for comparing the actual processes with it.

This chapter deals with the variation of flow parameters due to area change in expansion and compression processes. Shaft work is absent throughout the analysis.

4.1 COMPARISON OF ISENTROPIC AND ADIABATIC PROCESSES

Figure 4.1 (*a*) shows isentropic and adiabatic expansions of a perfect

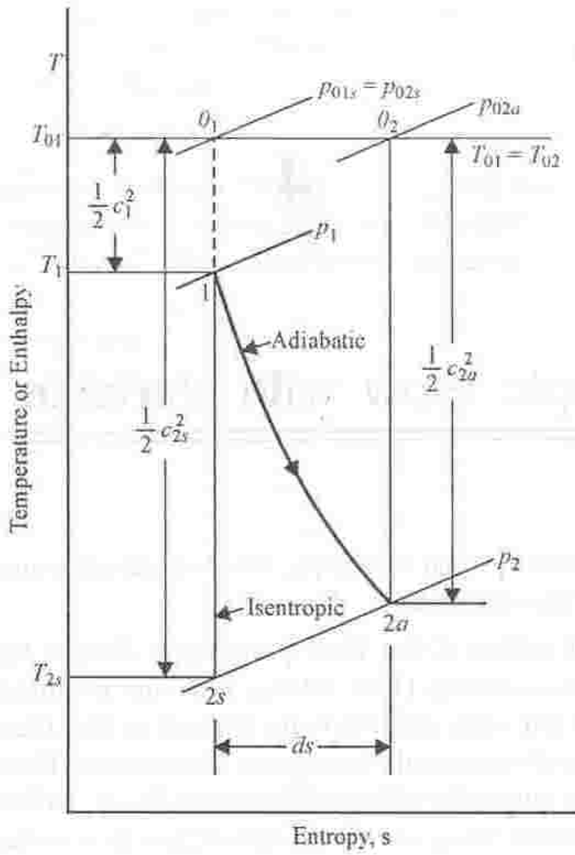

FIGURE 4.1 (*a*) : Temperature-entropy diagram for expansion processes (Shaft work = 0)

gas between the two states 1 and 2. the initial stagnation pressure is p_{01s} and the kinetic energy $\frac{1}{2}c_1^2$; the stagnation and static temperatures are T_{01} and T_1. The final temperature and the kinetic energy in the isentropic process are T_{2s}, and $\frac{1}{2}c_{2s}^2$.

In the adiabatic process for the same initial state the final state is defined by point $2a$. There is an increase in entropy ds and the final stagnation pressure p_{02a} is lower than its initial value p_{01s}. The final kinetic energy is also lower than its corresponding isentropic value.

The stagnation temperature remains unaltered in both isentropic and adiabatic processes.

From the equation of state for a perfect gas

$$v_{2s} = \frac{RT_{2s}}{p_2}$$

$$v_{2a} = \frac{RT_{2a}}{p_2}$$

But $T_{2a} > T_{2s}$

Therefore,

$$v_{2a} > v_{2s}.$$

This is shown on the p-v co-ordinates in Figure 4.1 (*b*).

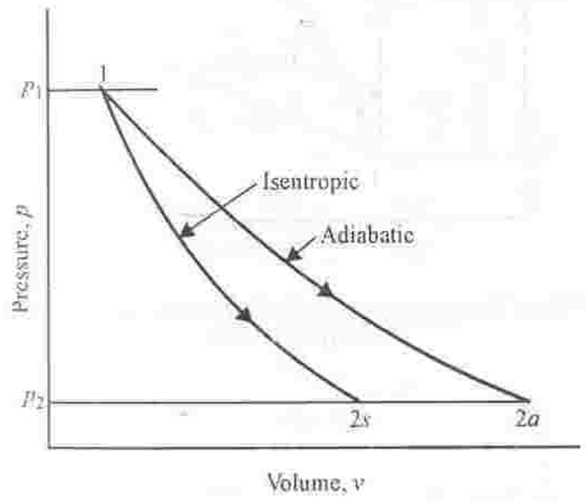

FIGURE 4.1 (*b*) : *p-v* diagram for expansion processes (Shaft work = 0)

The isentropic and adiabatic compression processes between pressures p_1 and p_2 on T-s and p-v co-ordinates are shown in Figures 4.2 (*a*) and (*b*). Here also

$$T_{2a} > T_{2s}$$

$$v_{2a} > v_{2s}$$

$$p_{02a} < p_{01s}$$

$$\frac{1}{2}c_{2a}^2 < \frac{1}{2}c^2 2s.$$

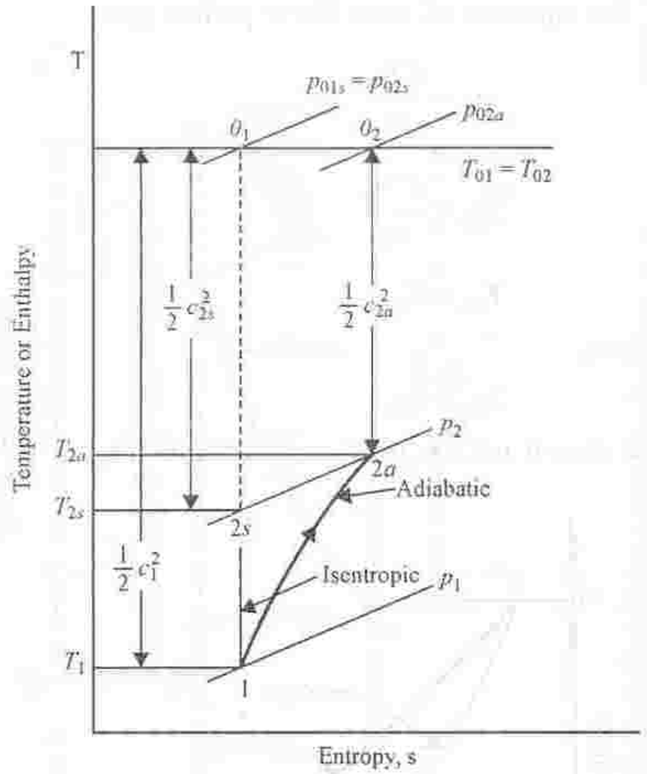

FIGURE 4.2 (*a*) : Temperature-entropy diagram for compression processes (Shaft work = 0)

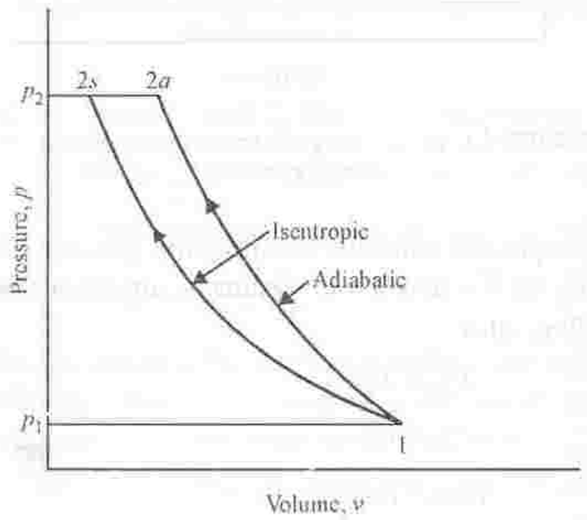

FIGURE 4.2 (*b*) : p-v diagram for compression processes (Shaft work = 0)

4.2 MACH NUMBER VARIATION

The isentropic energy Equation (2.60) gives

$$dp = -\rho c\, dc \tag{4.1}$$

From continuity equation mass flow rate is given by

$$\dot{m} = \rho A c = \text{constant}$$

Taking logs and differentiating

$$\ln \rho + \ln A + \ln c = \text{constant}$$

$$\frac{d\rho}{\rho} + \frac{dA}{A} + \frac{dc}{c} = 0$$

$$dc = -c\left(\frac{d\rho}{\rho} + \frac{dA}{A}\right) \tag{4.2}$$

Equations (4.1) and (4.2) yield

$$dp = \rho c^2 \left(\frac{d\rho}{\rho} + \frac{dA}{A}\right)$$

$$\frac{dA}{A} = \frac{dp}{\rho c^2}\left(1 - \frac{d\rho}{dp}c^2\right) \tag{4.3}$$

For an isentropic process from Equation (1.78)

$$\frac{dp}{d\rho} = \left(\frac{\partial p}{\partial \rho}\right)_s = a^2 \tag{4.4}$$

Equations (4.3) and (4.4) give

$$\frac{dA}{A} = \frac{dp}{\rho c^2}\left(1 - \frac{c^2}{a^2}\right) = \frac{dp}{\rho c^2}(1 - M^2) \tag{4.5}$$

Equation (4.5) can now be considered for both accelerating and decelerating passages for various values of Mach number.

4.2.1 Expansion in Nozzles

Gases and vapours are expanded in nozzles by providing a pressure ratio across them. It is shown here with the aid of Equation (4.5), that the shape of the passage depends on the local Mach number. Since the purpose of a nozzle is to accelerate the flow by providing a pressure drop, dp in Equation (4.5) is always negative. Following three possible conditions are considered for Equation (4.5):

(*a*) For $M < 1$, $dA = -ve$.

This shows that for nozzles the area decreases in the range $M = 0$ to $M = 1$ giving a convergent passage.

(*b*) For $M = 1$ (sonic velocity)

$$dA = 0$$

which implies that there is no change of passage area at the point where the Mach numbers is unity. This section is referred to as the throat of the passage.

(*c*) For $M > 1$, $dA = +ve$

This shows that for $M > 1$ the area of the nozzle increases continuously giving a divergent passage.

4.2.2 Compression in Diffusers

Diffusers are employed to obtain pressure rise in flowing gases for a given value of the initial kinetic energy. The static pressure rise is at the cost of the deceleration of flow in the diffuser passage. Here dp in Equation (4.5) is always positive. Equation (4.5) is now considered for such a case for three possible values of the Mach number.

(*a*) For $M < 1$, $dA = +ve$.

This shows that for subsonic diffusers ($M = 0$ to $M = 1$) the area increases with Mach number giving a divergent passage.

(*b*) For $M = 1$, $dA = 0$;

There is no change in the passage area.

(*c*) For $M > 1$, $dA = -ve$;

The area of the diffuser passage decreases with Mach number giving a convergent passage.

The passages for expansion and compression of gases in nozzles and diffusers are shown in Figure 4.3 and 4.4 respectively. It may be noted that while a continuous acceleration of a real flow from subsonic

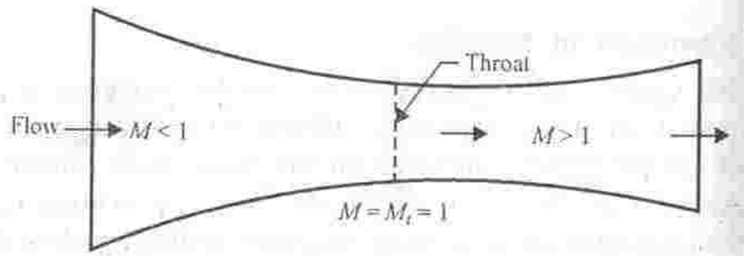

FIGURE 4.3 : Isentropic flow of a gas in a nozzle (decreasing pressure)

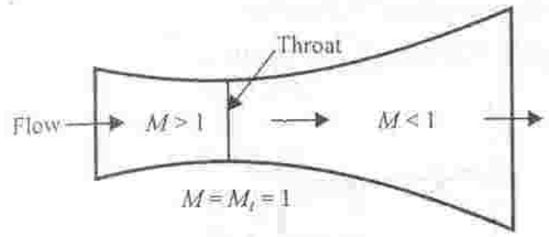

FIGURE 4.4 : Isentropic flow of a gas in a diffuser (increasing pressure)

to supersonic Mach numbers is possible the converse of this *i.e.*, continuous deceleration of a real flow from supersonic to subsonic Mach numbers is impossible. It will be seen in Sections 4.7.2 and 6.15 that a real supersonic flow decelerates to a subsonic flow only through a shock wave. The results obtained in this section on the basis of Equation (4.5) are summarized in Table 4.1.

TABLE 4.1: Variation of flow parameters in isentropic flow

Mach number	Nozzles			Diffusers		
	A	*p*	*c*	*A*	*p*	*c*
$M < 1$ (Subsonic flow)	decreases	decreases	increases	increases	increases	decreases
$M = 1$ (Sonic flow)	A^*	p^*	$c^* = a^*$	A^*	p^*	$c^* = a^*$
$M > 1$ (Supersonic flow)	increases	decreases	increases	decreases	increases	decreases

4.3 STAGNATION AND CRITICAL STATES

In Chapter 2, Equation (2.24) was derived for adiabatic flow. This holds for isentropic flow also. The stagnation state was defined for the isentropic process. The pressure and density ratios are given by Equations (2.27) and (2.30). The relevant equations are repeated below for convenience. Thus for isentropic flow

$$\frac{T_0}{T} = 1 + \frac{\gamma - 1}{2} M^2 \tag{2.24}$$

$$\frac{p_0}{p} = \left(1 + \frac{\gamma - 1}{2} M^2 \right)^{\gamma/(\gamma-1)} \tag{2.27}$$

$$\frac{\rho_0}{\rho} = \left(1 + \frac{\gamma - 1}{2} M^2 \right)^{1/(\gamma-1)} \tag{2.30}$$

Stagnation temperature (T_0) and pressure (p_0) fully define the stagnation state. Figure 4.5 shows the isentropic expansion of a gas to its

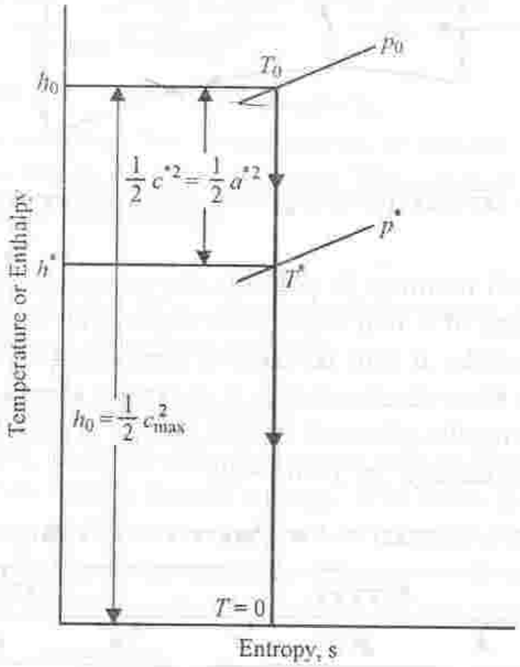

FIGURE 4.5 : Critical and Maximum velocities

maximum velocity c_{max}, through the critical velocity $c^* = a^*$. As in adiabatic flow, the critical point ($M = 1$) is an important landmark in isentropic flow also. But it should be remembered that for the same stagnation conditions (p_0, T_0) the critical points ($M = 1$) for adiabatic and isentropic flows are different. This is shown in Figure 4.6.

For the sake of comparison the two processes are considered for the same initial stagnation pressure and temperature. The exit temperature (T_e) is also assumed same. By Equation (2.42) of Chapter 2 the critical temperature ratio is same *i.e.*,

$$\frac{T_0}{T^*} = \frac{\gamma+1}{2} \tag{2.42}$$

The critical velocities are also same

$$c_s^* = c_a^* = a_s^* = a_a^* = \sqrt{\gamma R T^*} \tag{4.6}$$

But for the above mentioned conditions the pressures at the critical point and the exit for adiabatic flow are different; the same is true for the stagnation pressures.

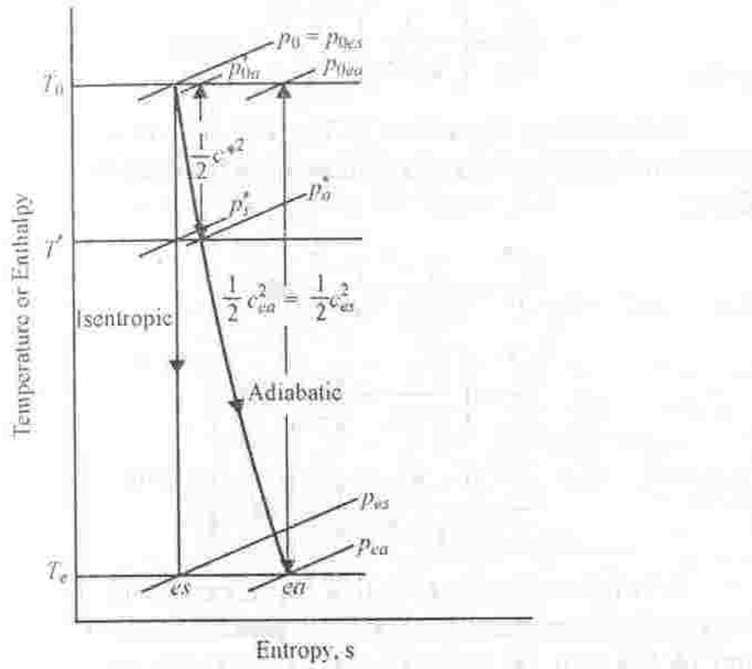

FIGURE 4.6 : Comparison of adiabatic and isentropic expansion processes

For the critical point

$$p_s^* > p_a^*$$

$$p_{0s}^* > p_{0a}^*$$

For the exit

$$p_{es} > p_{ea}$$

$$p_{0es} > p_{0ea}$$

For isentropic flow

$$p_0 = p_{0s}^* = p_{0es}$$

For the critical state in isentropic flow by putting $M = 1$ in Equations (2.24), (2.27) and (2.30),

$$\frac{T^*}{T_0} = \frac{2}{\gamma+1} = 0.833 \qquad (\text{for } \gamma = 1.4) \tag{4.7}$$

$$\frac{p^*}{p_0} = \left(\frac{2}{\gamma+1}\right)^{\gamma/(\gamma-1)} = 0.528 \qquad (\text{for } \gamma = 1.4) \tag{4.8}$$

$$\frac{\rho^*}{\rho_0} = \left(\frac{2}{\gamma+1}\right)^{1/(\gamma-1)} = 0.634 \qquad (\text{for } \gamma = 1.4) \tag{4.9}$$

Substituting Equations (4.7), (4.8) and (4.9) in Equations (2.24), (2.27) and (2.30) yields the following important relations for isentropic flow:

$$\frac{T^*}{T} = \frac{2}{\gamma+1} + \frac{\gamma-1}{\gamma+1} M^2 \tag{4.10}$$

$$\frac{p^*}{p} = \left(\frac{2}{\gamma+1} + \frac{\gamma-1}{\gamma+1} M^2\right)^{\gamma/(\gamma-1)} \tag{4.11}$$

$$\frac{\rho^*}{\rho} = \left(\frac{2}{\gamma+1} + \frac{\gamma-1}{\gamma+1} M^2\right)^{1/(\gamma-1)} \tag{4.12}$$

It is interesting to note that Equations (2.45) and (4.10) are same because both are based on energy equation. In contrast Equations (4.11) and (4.12) will be different for an adiabatic process.

4.4 AREA RATIO AS FUNCTION OF MACH NUMBER

Like temperature, pressure and density ratios, area ratio at a given section of a passage is also a useful quantity. Here the ratio of the area (A) at the given Mach number (M) and the reference area (A^*) at sonic conditions ($M = M_t = 1$) is expressed as a function of the local Mach number (M).

From continuity Equation

$$\rho A c = \rho^* A^* c^*$$

$$\frac{A}{A^*} = \frac{\rho^*}{\rho}\frac{c^*}{c} \tag{4.13}$$

From Equation (2.52)

$$\frac{c^*}{c} = \frac{a^*}{c} = \frac{1}{M^*} = \left(\frac{1 + \frac{\gamma-1}{2} M^2}{\frac{\gamma+1}{2} M^2}\right)^{1/2}$$

$$\frac{c^*}{c} = \frac{1}{M}\left(\frac{2}{\gamma+1} + \frac{\gamma-1}{\gamma+1} M^2\right)^{1/2} \tag{4.14}$$

Substituting Equations (4.12) and (4.14) in (4.13) gives

$$\frac{A}{A^*} = \frac{1}{M}\left(\frac{2}{\gamma+1} + \frac{\gamma-1}{\gamma+1} M^2\right)^{(\gamma+1)/2(\gamma-1)} \tag{4.15}$$

The variation of area ratio for subsonic and supersonic isentropic acceleration and deceleration is shown in Figure 4.7.

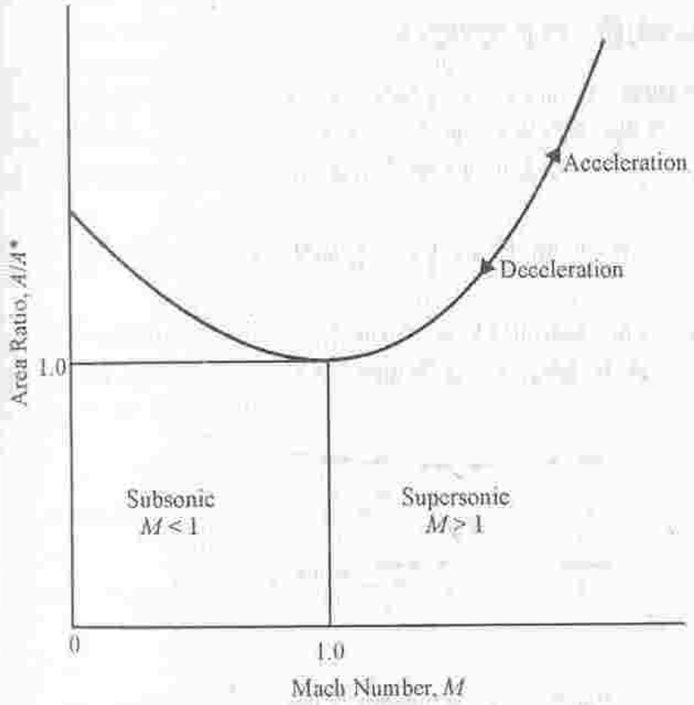

FIGURE 4.7 : Variation of area ratio with Mach number

In many compressible flow calculations the function $\frac{A}{A^*}\frac{p}{p_0}$ occurs frequently. This can also be obtained as a function of Mach number from Equations (2.27) and (4.15)

$$\frac{A}{A^*}\frac{p}{p_0} = \frac{1}{M}\left(\frac{2}{\gamma+1} + \frac{\gamma-1}{\gamma+1} M^2\right)^{(\gamma+1)/2(\gamma-1)} \times \left(1 + \frac{\gamma-1}{2} M^2\right)^{-\gamma/(\gamma-1)}$$

This on simplification and rearrangement yields

$$\frac{A}{A^*}\frac{p}{p_0}=\frac{\frac{1}{M}\left(\frac{2}{\gamma+1}\right)^{(\gamma+1)/2(\gamma-1)}}{\left(1+\frac{\gamma-1}{2}M^2\right)^{1/2}} \tag{4.16}$$

4.5 IMPULSE FUNCTION

The quantities pA and ρAc^2 occur frequently in some compressible flow problems. Since the units of both these quantities are the units of force they are conveniently expressed together as an important gas dynamic parameter.

This is referred to as the impulse function (F) or the wall force function.

One dimensional flow through a control surface (a symmetrical straight duct) is shown in Figure 4.8. The thrust or wall force ex-

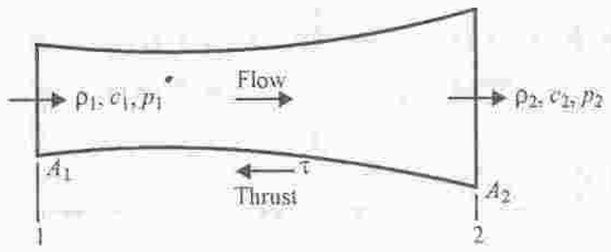

FIGURE 4.8 : Directions of flow and thrust in a duct

perienced by the duct in the direction shown is a result of changes in pressure and Mach number between the cross-sections 1 and 2. By momentum equation the thrust (τ) is given by

$$\tau=(p_2A_2+\rho_2A_2c_2^2)-(p_1A_1+\rho_1A_1c_1^2) \tag{4.17}$$

For a perfect gas

$$\rho c^2=\frac{p}{RT}c^2=\gamma p\frac{c^2}{\gamma RT}=\gamma pM^2 \tag{4.18}$$

The impulse function is $F=pA+\rho Ac^2$ (4.19)

Equations (4.18) and (4.19) give

$$F=pA+\gamma pAM^2$$

$$F=pA(1+\gamma M^2) \tag{4.20}$$

Substituting Equation (4.20) in (4.17) yields

$$\tau=F_2-F_1$$

$$\tau=p_2A_2(1+\gamma M_2^2)-p_1A_1(1+\gamma M_1^2) \tag{4.21}$$

This Equation demonstrates that the use of impulse function is very convenient in obtaining the thrust exerted by the flowing fluids. The thrust exerted by the fluid due to its flow between two sections of a duct can be obtained by the change of the impulse function between these sections. Equations (4.17) to (4.21) are independent of the type of process. However, for obtaining a relation between the non-dimensional impulse function and the Mach number the flow is assumed isentropic.

At $M=1$, $F=F^*$ and Equation (4.20) reduces to

$$F^*=p^*A^*(1+\gamma) \tag{4.22}$$

Equations (4.20) and (4.22) yield the expression for the non-dimensional impulse function

$$\frac{F}{F^*}=\frac{p}{p^*}\frac{A}{A^*}\frac{1+\gamma M^2}{1+\gamma} \tag{4.23}$$

Substituting from Equations (4.11) and (4.15) for $\frac{p}{p^*}$ and $\frac{A}{A^*}$ in Equation (4.23)

$$\frac{F}{F^*}=\left(\frac{2}{\gamma+1}+\frac{\gamma-1}{\gamma+1}M^2\right)^{-\gamma/(\gamma-1)}$$

$$\times\frac{1}{M}\left(\frac{2}{\gamma+1}+\frac{\gamma-1}{\gamma+1}M^2\right)^{(\gamma+1)/2(\gamma-1)}\times\frac{1+\gamma M^2}{1+\gamma}$$

$$\frac{F}{F^*}=\frac{1}{M}\left(\frac{2}{\gamma+1}+\frac{\gamma-1}{\gamma+1}M^2\right)^{-1/2}\times\frac{1+\gamma M^2}{1+\gamma}$$

On simplifying and rearranging the above relation reduces to

$$\frac{F}{F^*}=\frac{1+\gamma M^2}{M\sqrt{2(1+\gamma)\left(1+\frac{\gamma-1}{2}M^2\right)}} \tag{4.24}$$

Another non-dimensional expression for the impulse function may be obtained as follows:

$$\frac{F}{p_0 A^*} = \frac{pA\,(1+\gamma M^2)}{p_0 A^*} \tag{4.25}$$

Substituting for $\frac{pA}{p_0 A^*}$ from Equation (4.16)

$$\frac{F}{p_0 A^*} = \left(\frac{2}{\gamma+1}\right)^{(\gamma+1)/2\,(\gamma-1)} \frac{1+\gamma M^2}{M\sqrt{1+\frac{\gamma-1}{2}M^2}} \tag{4.26}$$

4.6 MASS FLOW RATE

From continuity equation the mass flow rate is

$$\dot{m} = \rho A c$$

For isentropic flow

$$\frac{p_0}{\rho_0^\gamma} = \frac{p}{\rho^\gamma}$$

$$\rho = \rho_0 \left(\frac{p}{p_0}\right)^{1/\gamma} \tag{4.27}$$

Equation (2.21) for a constant stagnation temperature process, gives

$$c^2 = 2c_p\,(T_0 - T)$$

$$c^2 = 2\frac{\gamma}{\gamma-1} RT_0 \left(1 - \frac{T}{T_0}\right)$$

$$c = \sqrt{2\frac{\gamma}{\gamma-1} RT_0 \left\{1 - \left(\frac{p}{p_0}\right)^{(\gamma-1)/\gamma}\right\}} \tag{4.28}$$

4.6.1 Non-dimensional mass flow rate in terms of pressure ratio

Substituting from Equations (4.27) and (4.28) into the continuity equation

$$\dot{m} = A\rho_0 \left(\frac{p}{p_0}\right)^{1/\gamma} \sqrt{2\frac{\gamma}{\gamma-1} RT_0 \left\{1 - \left(\frac{p}{p_0}\right)^{(\gamma-1)/\gamma}\right\}}$$

Now $\rho_0 = \frac{p_0}{RT_0}$

Therefore, $\dot{m} = \frac{Ap_0}{\sqrt{RT_0}} \sqrt{2\frac{\gamma}{\gamma-1}\left(\frac{p}{p_0}\right)^{2/\gamma} \left\{1 - \left(\frac{p}{p_0}\right)^{(\gamma-1)/\gamma}\right\}}$

The mass flow density is given by

$$\frac{\dot{m}}{A} = \frac{p_0}{\sqrt{RT_0}} \sqrt{2\frac{\gamma}{\gamma-1}\left\{\left(\frac{p}{p_0}\right)^{2/\gamma} - \left(\frac{p}{p_0}\right)^{(\gamma+1)/\gamma}\right\}} \tag{4.29}$$

This expression can be reduced to the conventional non-dimensional form by rearranging the terms.

$$\frac{\dot{m}\sqrt{T_0}}{Ap_0}\sqrt{\frac{R}{\gamma}} = \sqrt{\frac{2}{\gamma-1}\left\{\left(\frac{p}{p_0}\right)^{2/\gamma} - \left(\frac{p}{p_0}\right)^{(\gamma+1)/\gamma}\right\}} \tag{4.30}$$

The value of pressure ratio for maximum mass flow rate can be obtained by differentiating the variable quantity on the right hand side and equating the expression to zero.

Let $q = \frac{p}{p_0}$

$$\frac{d}{dq}\{q^{2/\gamma} - q^{(\gamma+1)/\gamma}\} = 0$$

$$q_{max} = \left(\frac{p}{p_0}\right)_{max} = \left(\frac{2}{\gamma+1}\right)^{\gamma/(\gamma-1)}$$

It may be noted that this expression is same as Equation (4.8) derived earlier. Therefore, for maximum mass flow conditions

$$\left(\frac{p}{p_0}\right)_{max} = \frac{p^*}{p_0} = \left(\frac{2}{\gamma+1}\right)^{\gamma/(\gamma-1)} \tag{4.31}$$

$$A = A^*$$

$$\frac{\dot{m}_{max}\sqrt{T_0}}{A^* p_0}\sqrt{\frac{R}{\gamma}} = \sqrt{\frac{2}{\gamma-1}\left\{\left(\frac{2}{\gamma+1}\right)^{2/(\gamma-1)} - \left(\frac{2}{\gamma+1}\right)^{(\gamma+1)/(\gamma-1)}\right\}} \tag{4.32}$$

This expression can also be expressed in a slightly different form.

$$\frac{\dot{m}_{max}\sqrt{T_0}}{A^* p_0}\sqrt{\frac{R}{\gamma}} = \left(\frac{2}{\gamma+1}\right)^{(\gamma+1)/2(\gamma-1)} \times \sqrt{\frac{2}{\gamma-1}\left\{\left(\frac{2}{\gamma+1}\right)^{(1-\gamma)/(\gamma-1)} - 1\right\}}$$

$$\frac{\dot{m}_{max}\sqrt{T_0}}{A^* p_0}\sqrt{\frac{R}{\gamma}} = \left(\frac{2}{\gamma+1}\right)^{(\gamma+1)/2(\gamma-1)} \sqrt{\frac{2}{\gamma-1}\left(\frac{\gamma+1}{2}-1\right)}$$

$$\frac{\dot{m}_{max}\sqrt{T_0}}{A^* p_0}\sqrt{\frac{R}{\gamma}} = \left(\frac{2}{\gamma+1}\right)^{(\gamma+1)/2(\gamma-1)} \tag{4.33}$$

4.6.2 Mass flow rate in terms of area ratio

The continuity equation can be written as

$$\dot{m} = \rho A c = \rho^* A^* c^*$$

$$\frac{\dot{m}}{A} = \rho c = \rho^* c^* \frac{A^*}{A} \tag{4.34}$$

Now $$\rho^* = \frac{p^*}{RT^*}$$

$$c^* = a^* = \sqrt{\gamma RT}$$

Therefore, $$\frac{\dot{m}}{A} = \frac{p^*}{RT^*}\sqrt{\gamma RT^*}\frac{A^*}{A}$$

$$\frac{\dot{m}}{A} = \frac{p^*}{\sqrt{T^*}}\sqrt{\frac{\gamma}{R}}\frac{A^*}{A} \tag{4.35}$$

Substituting from Equations (4.7) and (4.8) for T^* and p^*

$$\frac{\dot{m}}{A} = \left(\frac{2}{\gamma+1}\right)^{\gamma/(\gamma-1)}\sqrt{\frac{\gamma+1}{2}}\frac{p_0}{\sqrt{T_0}}\sqrt{\frac{\gamma}{R}}\frac{A^*}{A}$$

The non-dimensional form of the mass flow parameter is obtained by simplifying and rearranging

$$\frac{\dot{m}\sqrt{T_0}}{Ap_0}\sqrt{\frac{R}{\gamma}} = \left(\frac{2}{\gamma+1}\right)^{(\gamma+1)/2(\gamma-1)}\frac{A^*}{A} \tag{4.36}$$

The value of the maximum mass flow parameter similar to Equation (4.33) can be obtained simply by making $A^*/A = 1$ in Equation (4.36).

4.6.3 Mass flow rate in terms of Mach Number

Since A/A^* is a unique function of Mach number in an isentropic flow, its value from Equation (4.15) can be substituted in Equation (4.36). Therefore,

$$\frac{\dot{m}\sqrt{T_0}}{Ap_0}\sqrt{\frac{R}{\gamma}} = \left(\frac{2}{\gamma+1}\right)^{(\gamma+1)/2(\gamma-1)} \frac{M}{\left(\frac{2}{\gamma+1}+\frac{\gamma-1}{\gamma+1}M^2\right)^{(\gamma+1)/2(\gamma-1)}}$$

This on rearranging yields the value of the mass flow parameter in terms of the local Mach number.

$$\frac{\dot{m}\sqrt{T_0}}{Ap_0}\sqrt{\frac{R}{\gamma}} = \frac{M}{\left(1+\frac{\gamma-1}{2}M^2\right)^{(\gamma+1)/2(\gamma-1)}} \tag{4.37}$$

This relation can also be obtained from Equation (4.30) as shown here. From Equation (4.30)

$$\frac{\dot{m}\sqrt{T_0}}{Ap_0}\sqrt{\frac{R}{\gamma}} = \left(\frac{p_0}{p}\right)^{-(\gamma+1)/2\gamma}\sqrt{\frac{2}{\gamma-1}\left\{\left(\frac{p_0}{p}\right)^{(\gamma-1)/\gamma} - 1\right\}}$$

Substituting for p_0/p from the following expressions

$$\frac{p_0}{p} = \left(1+\frac{\gamma-1}{2}M^2\right)^{\gamma/(\gamma-1)}$$

$$\left(\frac{p_0}{p}\right)^{(\gamma-1)/\gamma} - 1 = \frac{\gamma-1}{2}M^2$$

Expression of Equation (4.37) is again obtained

$$\frac{\dot{m}\sqrt{T_0}}{Ap_0}\sqrt{\frac{R}{\gamma}} = \left(1+\frac{\gamma-1}{2}M^2\right)^{-\frac{\gamma+1}{2\gamma}\frac{\gamma}{\gamma-1}}\sqrt{\frac{2}{\gamma-1}\frac{\gamma-1}{2}M^2}$$

$$\frac{\dot{m}\sqrt{T_0}}{Ap_0}\sqrt{\frac{R}{\gamma}} = \frac{M}{\left(1+\frac{\gamma-1}{2}M^2\right)^{(\gamma+1)/2(\gamma-1)}}$$

For maximum mass flow conditions

$$A = A^* \text{ and } M = 1$$

$$\frac{\dot{m}_{max}\sqrt{T_0}}{A^*p_0}\sqrt{\frac{R}{\gamma}} = \frac{1}{\left(1+\frac{\gamma-1}{2}\times 1\right)^{(\gamma+1)/2(\gamma-1)}}$$

$$\frac{\dot{m}_{max}\sqrt{T_0}}{A^*p_0}\sqrt{\frac{R}{\gamma}} = \left(\frac{2}{\gamma+1}\right)^{(\gamma+1)/2(\gamma-1)} \tag{4.33}$$

4.6.4 Numerical value of the non-dimensional maximum mass flow parameter

Equations (4.30), (4.36) and (4.37) show that for a given gas (given values of R and γ) mass flow per unit area at a given Mach number is directly proportional to the initial stagnation pressure and inversely proportional to the square root of the stagnation temperature.

The value of the maximum mass flow parameter is fixed by the properties of the gas *i.e.*, R and γ. Therefore, for the same gas various combinations of p_0 and T_0 can be determined to give maximum mass flow density from the following expression:

$$\frac{\dot{m}_{max}\sqrt{T_0}}{A^*p_0} = \sqrt{\frac{\gamma}{R}}\left(\frac{2}{\gamma+1}\right)^{(\gamma+1)/2(\gamma-1)} \tag{4.38}$$

The above expression has a fixed value for each gas. Its values for air in various units will now be determined.

SI units: For air, $R = 287$ Nm/kg K and $\gamma = 1.4$

Therefore, $$\frac{\dot{m}_{max}\sqrt{T_0}}{A^*p_0} = \left(\frac{1.4}{287}\right)^{1/2}\left(\frac{2}{2.4}\right)^{2.4/2\times0.4}$$

$$\frac{\dot{m}_{max}\sqrt{T_0}}{A^*p_0} = 0.0404 \tag{4.39}$$

where $\dot{m}_{max}$ is in kg/s

T_0 is in K

A^* is in m^2

p_0 is in N/m^2

MKS units: For air, $R = 29.3$ kgf-m/kg K and $\gamma = 1.4$.

Therefore, $$\frac{\dot{m}_{max}\sqrt{T_0}}{A^*p_0} = \left(\frac{1.4\times9.81}{29.3}\right)^{1/2}\left(\frac{2}{2.4}\right)^{2.4/2\times0.4}$$

$$\frac{\dot{m}_{max}\sqrt{T_0}}{A^*p_0} = 0.397 \tag{4.40 (a)}$$

where $\dot{m}_{max}$ is in kg/s

T_0 is in K

A^* is in m^2

p_0 is in kgf/m^2

In FPS system of units Equation (4.40 (*a*)) is given by

$$\frac{\dot{m}_{max}\sqrt{T_0}}{A^*p_0} = 0.532 \tag{4.40 (b)}$$

This is also known as Fliegner's formula; he developed this expression empirically much earlier than its theoretical derivation. Fliegner verified this by experiments with very close agreement.

4.7 FLOW THROUGH NOZZLES

Flow through nozzles occurs in a variety of engineering applications.

Convergent nozzles are used for subsonic and sonic flows. They can also be used as flow measuring and flow regulating devices.

Convergent-divergent nozzles are used for supersonic flows. It is comparatively difficult to obtain convergent-divergent passages in compressors and turbine blade rows.

Some of the flow characteristics of these nozzles are discussed here.

Besides isentropic flow a brief reference to flow with irreversibilities (shock waves) is also made.

4.7.1 Convergent Nozzles

Figure 4.9 shows the flow from an infinite reservoir to an exhaust chamber through a convergent nozzle. The stagnation conditions (p_0, T_0, etc.) in the reservoir are kept constant while the back pressure *i.e.*, the exhaust chamber pressure can be varied.

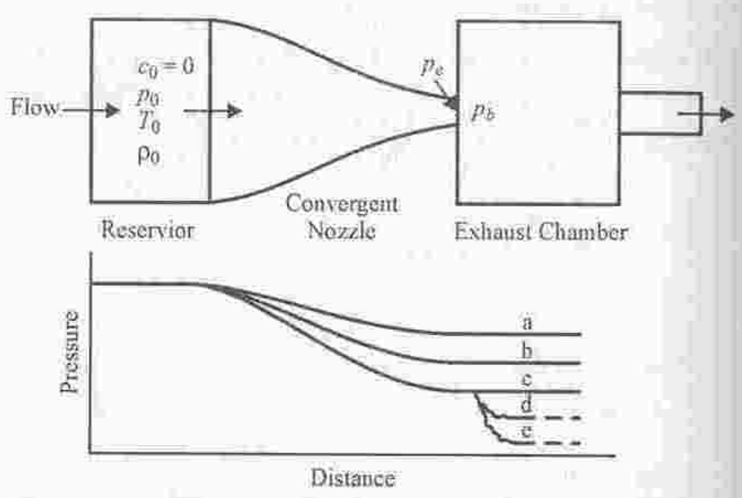

FIGURE 4.9 : Isentropic flow through a convergent nozzle

The pressure distributions along the nozzle for various values of the pressure ratio (p_e/p_0) across the nozzle are shown in curves *a*, *b*, *c*, *d* and *e*. Curves *a* and *b* correspond to values of the pressure ratio more than the critical. Curve *c* corresponds to the critical pressure ratio: $p_b/p_0 = 0.528$ (for $\gamma = 1.4$). For these curves the pressure p_e at the exit of the nozzle is same as the pressure in the exhaust chamber.

The nozzle exit pressure does not decrease when the exhaust chamber pressure is further reduced below the critical value. This condition is depicted by the curves *d* and *e*; here the nozzle exit pressure is still p_e^* but $p_b < p_e^*$. The change of pressure from p_e to p_b takes place outside the nozzle exit through an expansion wave.

Figure 4.10 shows the variation of the nozzle pressure ratio (p_e/p_0) and the mass flow parameter against the pressure ratio p_b/p_0 for $\gamma = 1.4$. Points corresponding to the curves *a*, *b*, *c*, *d* and *e* of Figure 4.9 have also been shown on these curves. The maximum

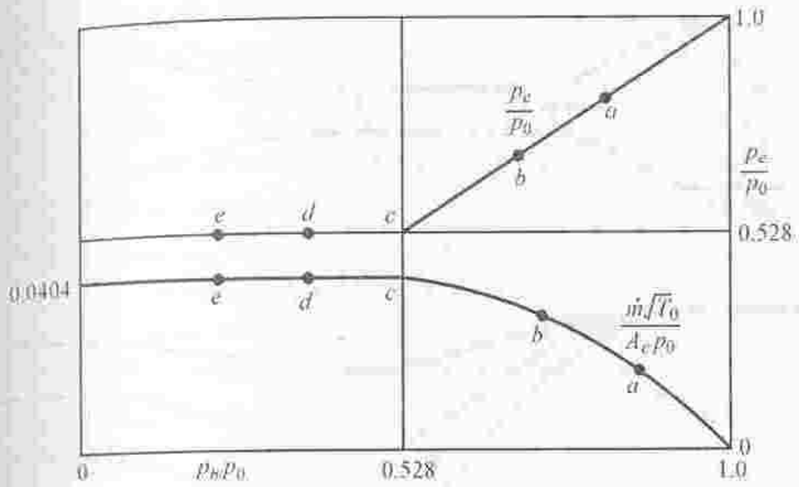

FIGURE 4.10 : Variation of pressure ratio and the mass flow parameter for a convergent nozzle ($\gamma = 1.4$)

mass flow occurs at point *c* after which both the mass flow parameter and the nozzle pressure ratio cease to vary. The numerical values in the figure are for $\gamma = 1.4$.

4.7.2 Convergent-divergent nozzles

Figure 4.11 shows the flow from an infinite reservoir through a convergent-divergent nozzle to an exhaust chamber. The experiment reported in Section 4.7.1 is repeated here. Though the main subject here is isentropic flow, it will be observed that flow through a convergent-divergent nozzle is not isentropic under all conditions. The static pressure distributions for various values of the pressure ratio p_b/p_0 are shown in curves *a*, *b*, *c*, ..., *h*, *i* and *j*

In curves *a* and *b* the pressure ratio p_e/p_0 across the nozzle is such that the flow is accelerating only upto the throat; the diverging part acts as a diffuser through which the pressure rises to the back pressure p_b. In curve *c* critical conditions ($p_t = p^*$; $M_t = 1$) are reached at the throat but the back pressure is such that the diverging part still acts as a diffuser.

Curve *h* corresponds to the design value of the back pressure. All other curves are for off-design conditions. Here the flow is supersonic in the entire divergent part of the nozzle. The flow in the curves *a*, *b*, *c*, *h*, *i* and *j* is isentropic but non-isentropic in other curves.

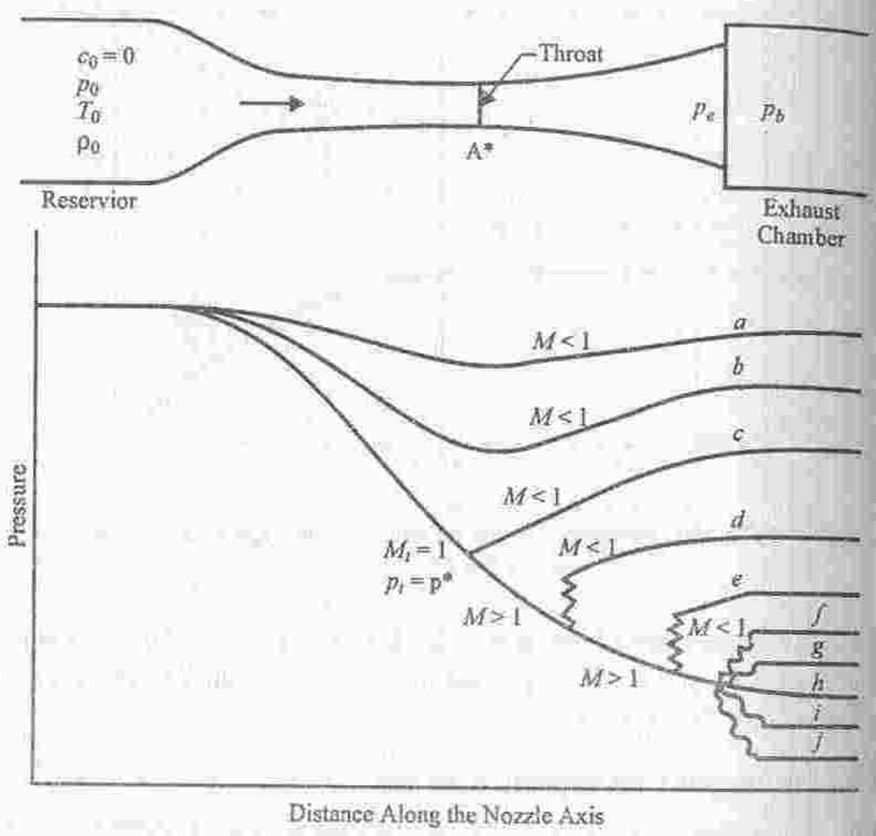

FIGURE 4.11 : Flow through a convergent-divergent nozzle

After the conditions of curve *c*, when the back pressure is further lowered expansion takes place to supersonic velocity beyond the throat to a point where a discontinuity in the flow occurs; this is on account of the "off design" value of the back pressure and the supersonic flow as in curves *d* and *e*. In these cases at some point the minimum pressure reached in supersonic expansion has to rise to the back pressure. But from the discussion of Equation (4.5) it is known that for the deceleration of supersonic flow the passage should be convergent. Therefore, the existing shape of the nozzle downstream of this point is incompatible with the required process; as a result of this the flow readjusts itself to the shape of the passage by suddenly becoming subsonic. This satisfies Equation (4.5). The pressure, temperature and density suddenly rise to values which are compatible with the subsonic flow immediately downstream of the supersonic flow region. Such a sudden change of supersonic flow to subsonic occurs through a plane of discontinuity between the supersonic and subsonic flow regions. This plane of discontinuity is called a shock wave which will be discussed in detail in Chapter 6. The flow through the shock wave is no longer isentropic.

When the back pressure is lowered further the shock wave moves downstream till it reaches the exit as in curves *f* and *g*; here the back pressure is still higher than the design value. The nozzle exit pressure p_e rises to the back pressure p_b through a shock wave outside the nozzle exit section as shown in curves *f* and *g*.

Curves *i* and *j* correspond to back pressure lower than the nozzle exit pressure. The conditions in the nozzle remain unchanged and the adjustment of the nozzle exit pressure to the exhaust chamber pressure occurs through an expansion wave outside the nozzle.

Figure 4.12 shows the variation of the throat pressure ratio with the pressure ratio p_b/p_0. It may be seen that after choking conditions ($M_t = 1$, $p_t = p^*$) are reached (point *c*) at the throat, further variation of the back pressure does not affect the throat pressure.

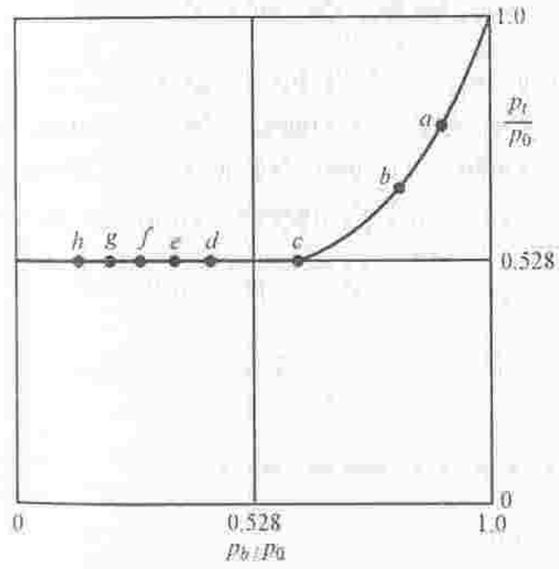

FIGURE 4.12 : Variation of throat pressure ratio in a convergent-divergent nozzle ($\gamma = 1.4$)

Figure 4.13 shows the variation of the nozzle pressure ratio (p_e/p_0) with p_b/p_0. In curves *a*, *b*, *c*, *d*, *e* and *h* (Figure 4.11) p_e is identical with p_b. This is shown by the points *a*, *b*, *c*, *d*, *e* and *h* on the line inclined at 45 degrees. At point *f* and beyond *i.e.*, at *g*, *i* and *j* there is no variation in p_e with further reduction in p_b.

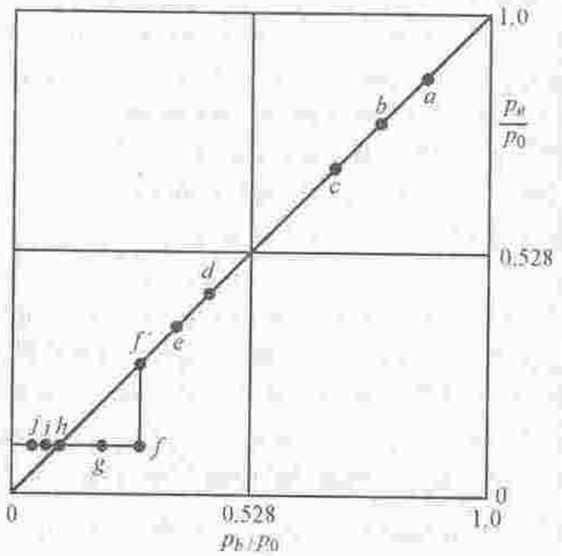

FIGURE 4.13 : Variation of exit pressure ratio in a convergent-divergent nozzle ($\gamma = 1.4$)

Variation of the mass flow parameter $\dot{m}\sqrt{T_0}/A^* p_0$ with the pressure ratio p_b/p_0 is shown in Figure 4.14. The maximum mass flow conditions are reached (at point c) when the throat pressure ratio achieves critical value ($p_t = p^*$); there is no further increase in the mass flow with decrease in the back pressure after this point. This condition is called "choking".

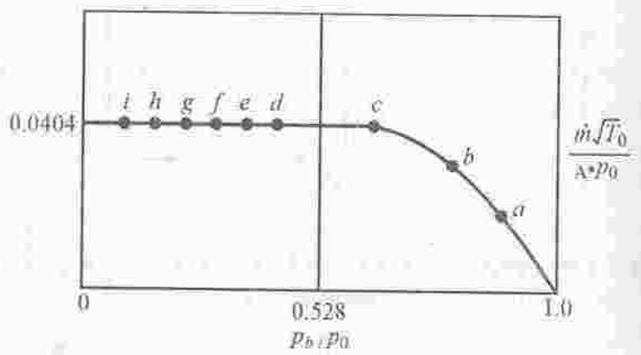

FIGURE 4.14 : Variation of the mass flow parameter in a convergent-divergent nozzle ($\gamma = 1.4$)

4.8 FLOW THROUGH DIFFUSERS

Diffusion of flow, *i.e.*, deceleration of the flow with rise in pressure

is a common feature of the flow machines and systems. Figure 4.15 shows both reversible and irreversible diffusion of supersonic flow. In the isentropic diffusion there is a continuous rise in static pressure.

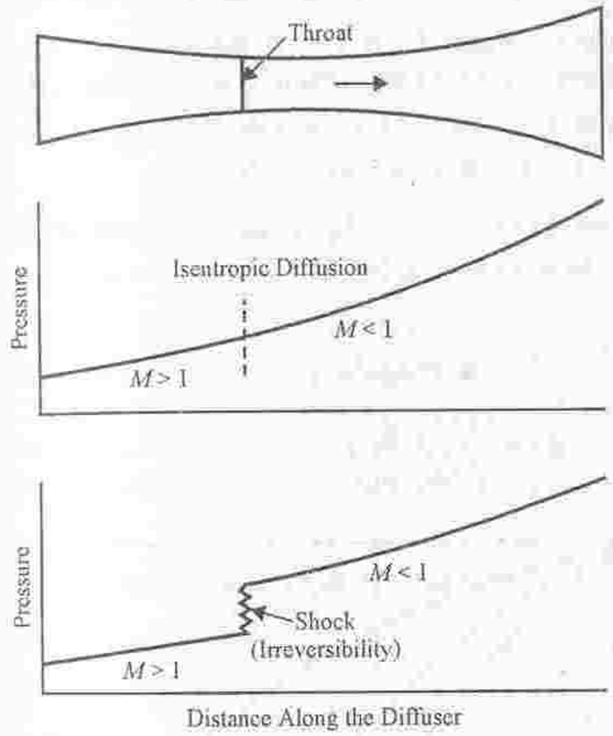

FIGURE 4.15 : Reversible and irreversible flows through a diffuser

As shown in Section 4.2 the supersonic part of the diffuser is convergent and the subsonic divergent.

In many applications diffusion occurs through a shock wave (irreversible diffusion). The pressure rise across the shock wave is sudden and is governed by the upstream supersonic Mach number. The flow before and after the shock may still be isentropic. Since the Mach number is minimum at the throat it is profitable to have the shock at this section. This will be further discussed in Chapter 6.

4.9 USE OF GAS TABLES

Some quantities derived in this chapter are functions of only M and γ. Therefore, it is possible to compute their values for various values of the Mach number M and γ. Thus gas tables for steady isentropic flow can be computed for T/T_0, p/p_0, ρ/ρ_0, M^*, A/A^*, $Ap/A^* p_0$ and

F/F^* from Equations (2.24), (2.27), (2.30), (2.52), (4.15), (4.16) and (4.24) respectively. These tables are given in Appendix A.3. Such tables are very useful in compressible flow calculations.

In an isentropic flow with constant stagnation state p_0, T_0, ρ_0, A^* etc. remain constant. Therefore, if the values of some parameters (p_1, T_1 etc.) are known at the initial Mach number (M_1) their values (p_2, T_2 etc.) at any other Mach number (M_2) can be determined with the help of the gas tables as shown here.

From gas table p/p_0, T/T_0, ρ/ρ_0, A/A^* and F/F^* are known at both the Mach numbers M_1 and M_2.

Therefore, $$p_2 = \frac{(p/p_0)_{M2}}{(p/p_0)_{M1}} p_1 \tag{4.41}$$

$$T_2 = \frac{(T/T_0)_{M2}}{(T/T_0)_{M1}} T_1 \tag{4.42}$$

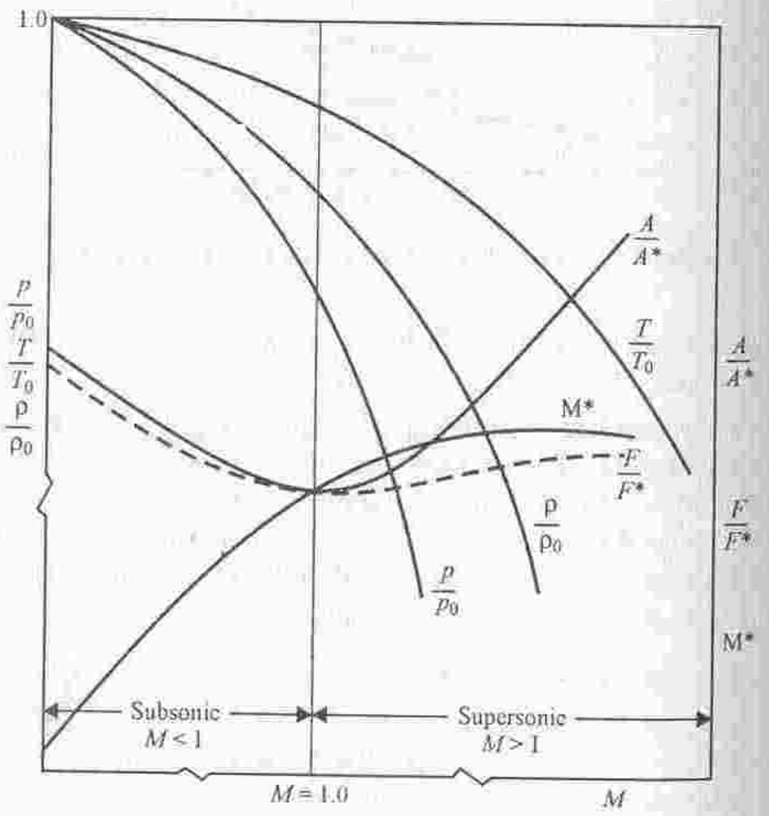

FIGURE 4.16 : Variation of some gas dynamic parameters in isentropic flow

$$\rho_2 = \frac{(\rho/\rho_0)_{M2}}{(\rho/\rho_0)_{M1}} \rho_1 \tag{4.43}$$

$$A_2 = \frac{(A/A^*)_{M2}}{(A/A^*)_{M1}} A_1 \tag{4.44}$$

$$F_2 = \frac{(F/F^*)_{M2}}{(F/F^*)_{M1}} F_1 \tag{4.45}$$

Mach number of the flow at a state can also be found from gas tables through known values of the parameters such as p/p_0, T/T_0 or A/A^*.

Gas tables can be presented graphically in the form of gas charts as shown in Figure 4.16. They present a complete picture of the variation of various parameters and help in their quick estimation. This is specially useful as a first attempt at an approximate calculation in a lengthy problem.

NOTATION FOR CHAPTER 4

a	local velocity of sound	$\dot{m}$	mass flow rate
A	area of cross section	p	pressure
c	fluid velocity	$q = p/p_0$	pressure ratio
c_p	specific heat at constant pressure	R	gas constant
F	impulse function	s	entropy
M	local Mach number	T	temperature

GREEK SYMBOLS

$\gamma =$	c_p/c_v	$\tau =$	thrust

SUBSCRIPTS

0	stagnation values	max	corresponding to maximum mass flow rate
1	initial values		
2	final values	M	corresponding to Mach number M
a	actual		
b	back pressure	s	isentropic
e	exit	t	throat or test section

SUPERSCRIPT

*	corresponding to $M = 1$

SOLVED EXAMPLES

Example 4.1. Air flowing in a duct has a velocity of 300 m/s, pressure 1.0 bar and temperature 290 K. Taking $\gamma = 1.4$ and $R = 287$ J/kg-K determine:

(*i*) stagnation pressure and temperature,

(*ii*) velocity of sound in the dynamic and stagnation conditions,

(*iii*) stagnation pressure assuming constant density.

Solution. (*i*) $c_p = \dfrac{\gamma}{\gamma - 1} R$

$$c_p = \frac{1.4}{0.4} \times 287 = 1005 \text{ J/kg–K}$$

$$T_0 = T + \frac{c^2}{2c_p}$$

$$T_0 = 290 + \frac{300 \times 300}{2 \times 1005} = 290 + 44.7$$

$$= 334.7 \text{ K} \quad \textbf{Ans.}$$

For isentropic flow

$$\frac{p_0}{p} = \left(\frac{T_0}{T} \right)^{\gamma/(\gamma-1)}$$

$$= \left(\frac{334.7}{290} \right)^{3.5} = (1.158)^{3.5} = 1.67$$

$$p_0 = 1.67p = 1.67 \times 1$$

$$p_0 = 1.67 \text{ bar} \quad \textbf{Ans.}$$

(*ii*) $a = \sqrt{\gamma RT}$

$$= \sqrt{1.4 \times 287 \times 290}$$

$$= 342 \text{ m/s} \quad \textbf{Ans.}$$

$$a_0 = \sqrt{\gamma RT_0} = \sqrt{1.4 \times 287 \times 334.7}$$

$$a_0 = 366.7 \text{ m/s} \quad \textbf{Ans.}$$

(*iii*) $\rho = \dfrac{p}{RT}$

$$\rho = \frac{1 \times 10^5}{287 \times 290} = 1.2 \text{ kg/m}^3$$

For incompressible reversible flow

$$p_0 = p + \frac{1}{2} \rho c^2$$

$$= 10^5 + 0.5 \times 1.2 \times 300^2$$

$$= 1.54 \times 10^5 \text{ N/m}^2$$

$$= 1.54 \text{ bar} \quad \textbf{Ans.}$$

Example 4.2. A conical diffuser has entry and exit diameters of 15 cm and 30 cm respectively. The pressure, temperature and velocity of air at entry are 0.69 bar, 340 K and 180 m/s respectively. Determine:

(*a*) the exit pressure,

(*b*) the exit velocity and

(*c*) the force exerted on the diffuser walls.

Assume isentropic flow, $\gamma = 1.4$, $c_p = 1.00$ kJ kg-K.

Solution. (See Figure 4.8)

$$A_1 = \frac{\pi}{4} d_1^2 = 0.785 \times 15^2 = 176.8 \text{ cm}^2$$

$$A_2 = \frac{\pi}{4} d_2^2 = 0.785 \times 30^2 = 706 \text{ cm}^2$$

$$T_{01} = T_1 + \frac{c_1^2}{2c_p} = 340 + \frac{180 \times 180}{2 \times 1000} = 340 + 16.2$$

$$= 356.2 \text{ K}$$

$$\frac{T_1}{T_{01}} = \frac{340}{356.2} = 0.952$$

From isentropic flow tables at this temperature ratio

$$M_1 = 0.5, \quad \frac{p_1}{p_{01}} = 0.843, \quad \left(\frac{A}{A^*} \right)_1 = 1.34, \quad \left(\frac{F}{F^*} \right)_1 = 1.203$$

$$\frac{p_1}{p_{01}} = \frac{0.69}{p_{01}} = 0.843$$

$$p_{01} = p_{02} = \frac{0.69}{0.843} = 0.818 \text{ bar}$$

$$\frac{A_1}{A_1^*} = \frac{176.8}{A_1^*} = 1.34$$

$$A_1^* = A_2^* = 176.8/1.34 = 132 \text{ cm}^2$$

$$p_1^* = 0.528 p_{01}$$

$$p_1^* = p_2^* = 0.528 \times 0.818 = 0.432 \text{ bar}$$

$$F_1^* = F_2^* = p_1^* A_1^* (1 + \gamma)$$

$$F_1^* = 0.432 \times 10^5 \times 0.0132 \, (1 + 1.4)$$

$$F_1^* = F_2^* = 1370 \text{ N}$$

$$\frac{A_2}{A_2^*} = \frac{706}{132} = 5.37$$

From isentropic tables at this area ratio

$$M_2 = 0.107, \quad \frac{p_2}{p_{02}} = 0.992, \quad \frac{F_2}{F_2^*} = 4.30.$$

(*a*) $$p_2 = 0.992 \times p_{02} = 0.992 \times 0.818$$

$$p_2 = 0.810 \text{ bar} \quad \textbf{Ans.}$$

(*b*) $$A_2 c_2 = A_1 c_1$$

$$c_2 = \frac{A_1}{A_2} c_1$$

$$c_2 = \frac{176.8}{706} \times 180$$

$$c_2 = 45 \text{ m/s}$$

(*c*) The force exerted on the diffuser walls is equal to the thrust of the flow in the backward direction; this is equal to the change in the impulse function.

$$\tau = F_2 - F_1$$

$$= 4.3 F_2^* - 1.203 F_1^*$$

$$= 3.097 \times F_1^*$$

$$= 3.097 \times 1370$$

$$\tau = 4243 \text{ N} \quad \textbf{Ans.}$$

Example 4.3. A nozzle in a wind tunnel gives a test-section Mach number of 2.0 Air enters the nozzle from a large reservoir at 0.69 bar and 310 K. The cross-sectional area of the throat is 1000 cm^2. Determine the following quantities for the tunnel for one dimensional isentropic flow:

(*i*) pressures, temperatures and velocities at the throat and test sections,

(*ii*) area of cross-section of the test section,

(*iii*) mass flow rate,

(*iv*) power required to drive the compressor.

Solution. $p_0 = 0.69$ bar, $T_0 = 310$ K, $A^* = 1000 \text{ cm}^2$

$$\rho_0 = \frac{p_0}{RT_0}$$

$$\rho_0 = \frac{0.69 \times 10^5}{287 \times 310} = 0.775 \text{ kg/m}^3$$

$$a_0 = \sqrt{\gamma RT_0}$$

$$a_0 = \sqrt{1.4 \times 287 \times 310} = 353 \text{ m/s}$$

From gas tables at $M = 1$ (throat section)

$$\frac{p^*}{p_0} = 0.528; \quad p^* = 0.528 \times 0.69 = 0.365 \text{ bar} \quad \textbf{Ans.}$$

$$\frac{T^*}{T_0} = 0.834; \quad T^* = 0.834 \times 310 = 258 \text{ K} \quad \textbf{Ans.}$$

$$\frac{\rho^*}{\rho_0} = 0.632; \quad \rho^* = 0.632 \times 0.775 = 0.49 \text{ kg/m}^3 \quad \textbf{Ans.}$$

$$a^* = \sqrt{\gamma RT^*}$$

$$a^* = \sqrt{1.4 \times 287 \times 258} = 323 \text{ m/s}$$

$$c^* = a^* = 323 \text{ m/s} \quad \textbf{Ans.}$$

From gas tables at $M_t = 2.0$ (test section)

$$\frac{p}{p_0} = 0.128;\ p = 0.128 \times 0.69 = 0.0885 \text{ bar} \quad \textbf{Ans.}$$

$$\frac{T}{T_0} = 0.555;\ T = 0.555 \times 310 = 175 \text{ K} \quad \textbf{Ans.}$$

$$\frac{A}{A^*} = 1.687;\ A = 1.687 \times 1000 = 1687 \text{ cm}^2 \quad \textbf{Ans.}$$

$$a_t = \sqrt{\gamma R T_t}$$

$$a_t = \sqrt{1.4 \times 287 \times 173} = 264 \text{ m/s}$$

$$M_t = \frac{c_t}{a_t} = \frac{c_t}{264} = 2$$

$$c_t = 528 \text{ m/s} \quad \textbf{Ans.}$$

Mass flow rate

$$\dot{m} = \rho^* A^* c^*$$
$$= 0.49 \times 0.1 \times 323$$
$$= 15.9 \text{ kg/s} \quad \textbf{Ans.}$$

Assuming reversible flow, compressor work $W_c = \dot{m} c_p \times$ temperature drop

$$W_c = 15.9 \times 1005 \times (310 - 173) \text{ J/s}$$
$$= 15.9 \times 1.005 \times 137 \text{ kJ/s}$$
$$= 2182 \text{ kW} \quad \textbf{Ans.}$$

Example 4.4. Air is discharged from a reservoir at $p_0 = 6.91$ bar and $t_0 = 325^\circ$C through a nozzle to an exit pressure of 0.98 bar. If the flow rate is 3600 kg/hr determine for isentropic flow:

(*i*) throat area, pressure and velocity,

(*ii*) exit area, Mach number, and

(*iii*) maximum velocity.

Solution. $\frac{p_0}{p} = 7;\ T_0 = 273 + 325 = 598 \text{ K};\ \dot{m} = 1.0 \text{ kg/s}$

$$\rho_0 = \frac{p_0}{RT_0} = \frac{6.91 \times 10^5}{287 \times 598}$$

$$\rho_0 = 4.04 \text{ kg/m}^3$$

From isentropic gas tables

at $$\frac{p}{p_0} = \frac{1}{7} = 0.142$$

$$M = 1.93,\ M^* = 1.6,\ \frac{T}{T_0} = 0.573$$

$$\frac{A}{A^*} = 1.593$$

(*i*) at $M = 1$, $\frac{T^*}{T_0} = 0.834,\ \frac{p^*}{p_0} = 0.528,\ \frac{\rho^*}{\rho_0} = 0.634$

$$p^* = 0.528 \times 6.91 = 3.65 \text{ bar} \quad \textbf{Ans.}$$

$$T^* = 0.834 \times 598 = 500 \text{ K}$$

$$\rho^* = 0.834 \times 4.04 = 2.56 \text{ kg/m}^3$$

$$a^* = \sqrt{\gamma R T^*}$$
$$= \sqrt{1.4 \times 287 \times 500} = 448.2$$

$$c^* = a^* = 448.2 \text{ m/s} \quad \textbf{Ans.}$$

$$\rho^* A^* c^* = \dot{m}$$

$$A^* = \frac{1 \times 10^4}{2.56 \times 448.2} = 8.68 \text{ cm}^2 \quad \textbf{Ans.}$$

(*ii*) At exit

$$M = 1.93 \quad \textbf{Ans.}$$

This can be verified by another calculation.

$$M^* = \frac{c}{c^*} = 1.6$$

$$c = 1.6 \times 448.2 = 717 \text{ m/s}$$

$$T = 0.573,\ T_0 = 0.573 \times 598 = 344 \text{ K}$$

$$a = \sqrt{1.4 \times 287 \times 344} = 371.8 \text{ m/s}$$

$$M = \frac{c}{a} = \frac{717}{371.8} = 1.93$$

$$\frac{A}{A^*} = 1.593$$

$$A = 1.593 \times 8.68 = 13.85 \text{ cm}^2 \quad \textbf{Ans.}$$

(*iii*) $$c_{max} = \sqrt{\frac{2\gamma}{\gamma - 1} RT_0}$$

$$= \sqrt{\frac{2 \times 1.4}{0.4} \times 287 \times 598}$$

$$= 1096 \text{ m/s} \quad \textbf{Ans.}$$

c_{max} is also given by

$$c_{max} = \sqrt{\frac{\gamma + 1}{\gamma - 1}}\, a^*$$

$$= \sqrt{\frac{1.4 + 1}{0.4}} \times 448.2$$

$$= 1097.8 \text{ m/s} \quad \textbf{Ans.}$$

Example 4.5. Superheated steam is supplied to a supersonic nozzle at the design flow rate of 1.0 kg/s (per cm^2 of the throat area). If the stagnation temperature of steam is 800 K determine the stagnation pressure of the steam required for this flow rate. Take $R = 0.477$ kJ/kg K, $\gamma = 1.278$ for steam. Assume isentropic flow.

Solution. Since the flow is supersonic the value of the flow rate given is its maximum value. For isentropic flow we have

$$\frac{\dot{m}_{max} \sqrt{T_0}}{A^* p_0} \sqrt{\frac{R}{\gamma}} = \left(\frac{2}{\gamma + 1} \right)^{(\gamma+1)/2(\gamma-1)}$$

$$\frac{\dot{m}_{max}}{A^*} = 1.0 \frac{\text{kg}}{\text{s cm}^2} = 10{,}000 \frac{\text{kg}}{\text{s m}^2}$$

$$\left(\frac{2}{\gamma + 1} \right)^{(\gamma+1)/2(\gamma-1)} = \left(\frac{2}{1.278 + 1} \right)^{2.278/2 \times .278}$$

$$= (0.87796)^{4.097} = 0.5867$$

Therefore,

$$10{,}000 \frac{\sqrt{800}}{p_0} \times \sqrt{\frac{477}{1.278}} = 0.5867$$

$$p_0 = \frac{\sqrt{8}}{0.03036} \times 10^5 \text{ N/m}^2$$

$$p_0 = 93.163 \text{ bar} \quad \textbf{Ans.}$$

Example 4.6. A supersonic wind tunnel settling chamber expands air or Freon-21 through a nozzle from a pressure of 10 bar to 4 bar in the test section. Calculate the stagnation temperature to be maintained in the settling chamber to obtain a velocity of 500 m/s in the test section for,

(*a*) Air, $c_p = 1.025$ kJ/kg K, $c_v = 0.735$ kJ/kg K

(*b*) Freon $-$ 21, $c_p = 0.785$ kJ/kg K, $c_v = 0.675$ kJ/kg K

What is the test section Mach number is each case?

Solution. From energy equation $h_0 = h + \frac{1}{2} c^2$

$$T_0 = T + \frac{c^2}{2c_p}$$

Assuming isentropic flow, $$\frac{T}{T_0} = \left(\frac{p}{p_0} \right)^{(\gamma-1)/\gamma}$$

$$T_0 = \frac{c^2}{2c_p \left\{ 1 - \left(\frac{p}{p_0} \right)^{(\gamma-1)/\gamma} \right\}}$$

(*a*) For air $\gamma = \frac{c_p}{c_v} = \frac{1.025}{0.735} = 1.394$, $\frac{\gamma - 1}{\gamma} = 0.283$

$$T_0 = \frac{500 \times 500}{2 \times 1025 \, (1 - 0.4^{0.283})} = 533.89 \text{ K} \quad \textbf{Ans.}$$

$$1 + \frac{\gamma - 1}{2} M^2 = \left(\frac{p_0}{p} \right)^{(\gamma-1)/\gamma}$$

$$1 + \frac{0.394}{2} M^2 = 2.5^{0.283}$$

$$M = \sqrt{1.5025} = 1.225 \quad \textbf{Ans.}$$

(*b*) For Freon-21 $\gamma = \frac{0.785}{0.675} = 1.163$, $\frac{\gamma - 1}{\gamma} = 0.14$

$$T_0 = \frac{500 \times 500}{2 \times 785\,(1 - 0.4^{0.14})} = 1322.508 \text{ K} \quad \textbf{Ans.}$$

$$1 + \frac{1.163 - 1}{2} M^2 = 2.5^{0.14}$$

$$M = \sqrt{1.6794} = 1.296 \quad \textbf{Ans.}$$

Example 4.7. A reservoir whose temperature can be varied in a wide range of temperature receives air at a constant pressure of 1.5 bar. The air is expanded isentropically in a nozzle to an exit pressure of 1.015 bar. Determine (without using Gas tables) the values of the temperature to be maintained in the reservoir to produce the following velocities at the nozzle exit:

(*a*) 100 m/s (*b*) 250 m/s

What are the values of Mach numbers in the two cases?

Solution. Following values are taken for air:

$$\gamma = 1.4,\ R = 287 \text{ J/kg K},\ c_p = 1005 \text{ J/kg K} = \text{constant}$$

From energy equation

$$h_0 = h + \frac{1}{2}c^2 \text{ or } \frac{T_0}{T} = 1 + \frac{c^2}{2c_p T} = \left(\frac{p_0}{p}\right)^{(\gamma-1)/\gamma}$$

(*a*) For $c = 100$ m/s

$$\frac{T_0}{T} = 1 + \frac{100 \times 100}{2 \times 1005T} = \left(\frac{1.5}{1.015}\right)^{(1.4-1)/1.4} = 1.118$$

$$\frac{4.975}{T} = 0.118,\ T = 42.16 \text{ K}$$

$$T_0 = 1.118 \times 42.16 = 47.13 \text{ K} \quad \textbf{Ans.}$$

$$a = \sqrt{\gamma RT} = \sqrt{1.4 \times 287 \times 42.16} = 130.15 \text{ m/s}$$

$$M = \frac{c}{a} = \frac{100}{130.15} = 0.768 \quad \textbf{Ans.}$$

The temperatures in this case are impractically low.

(*b*) For $c = 250$ m/s

$$\frac{T_0}{T} = 1 + \frac{250 \times 250}{2 \times 1005T} = 1 + \frac{31.095}{T}$$

$$1 + \frac{31.095}{T} = 1.118,\ T = 263.517 \text{ K}$$

$$T_0 = 1.118 \times 263.517 = 294.612 \text{ K} \quad \textbf{Ans.}$$

$$a = \sqrt{1.4 \times 287 \times 263.517} = 325.394 \text{ m/s}$$

$$M = \frac{c}{a} = \frac{250}{325.394} = 0.768$$

Mach number is same in the two cases because the pressure ratio is same.

QUESTIONS AND PROBLEMS

4.1 Derive the following relations for one dimensional isentropic flow:

(*i*) $\dfrac{dA}{A} = \dfrac{dp}{\rho c^2}(1 - M^2)$

(*ii*) $\dfrac{p^*}{p} = \left(\dfrac{2}{\gamma+1} + \dfrac{\gamma-1}{\gamma+1} M^2\right)^{\gamma/(\gamma-1)}$

(*iii*) $\dfrac{A}{A^*} = \dfrac{1}{M}\left(\dfrac{2}{\gamma+1} + \dfrac{\gamma-1}{\gamma+1} M^2\right)^{(\gamma+1)/2\,(\gamma-1)}$

(*iv*) $\dfrac{F}{p_0 A^*} = \left(\dfrac{2}{\gamma+1}\right)^{(\gamma+1)/2\,(\gamma-1)} \dfrac{1 + \gamma M^2}{M\left(1 + \dfrac{\gamma-1}{2} M^2\right)^{1/2}}$

(*v*) $\dfrac{F^*}{p_0 A^*} = (\gamma + 1)\left(\dfrac{2}{\gamma+1}\right)^{\frac{\gamma}{\gamma-1}}$

4.2 Prove that the mass flow parameter is given by the following expressions:

(*i*) $\dfrac{\dot{m}\sqrt{T_0}}{A p_0} = \sqrt{\dfrac{2\gamma}{R(\gamma-1)}\left\{\left(\dfrac{p}{p_0}\right)^{2/\gamma} - \left(\dfrac{p}{p_0}\right)^{(\gamma+1)/\gamma}\right\}}$

(*ii*) $\dfrac{\dot{m}\sqrt{T_0}}{A p_0} = \left(\dfrac{\gamma}{R}\right)^{1/2}\left(\dfrac{2}{\gamma+1}\right)^{(\gamma+1)/2\,(\gamma-1)} \dfrac{A^*}{A}$

(*iii*) $\dfrac{\dot{m}\sqrt{T_0}}{A^* p_0} = \left(\dfrac{\gamma}{R}\right)^{1/2} \dfrac{M}{\left(1 + \dfrac{\gamma-1}{2} M^2\right)^{(\gamma+1)/2\,(\gamma-1)}}$

Show that its maximum value is given by

$$\frac{\dot{m}_{max}\sqrt{T_0}}{A^* p_0} = \left(\frac{\gamma}{R}\right)^{1/2}\left(\frac{2}{\gamma+1}\right)^{(\gamma+1)/2(\gamma-1)} = 0.0404$$

when $\dot{m}_{max}$ is in kg/s

T_0 is in K

A^* is in m^2

p_0 is in N/m^2

$\gamma = 1.4$, $R = 287$ J/kg K.

4.3 Describe the behaviour of flow in a convergent-divergent nozzle when it is operated at (*i*) design pressure ratio; (*ii*) pressure ratio higher than the design value; and (*iii*) pressure ratio lower than the design value.

4.4 Explain briefly what is meant by impulse function. Derive

$$\frac{F}{F^*} = \frac{1+\gamma M^2}{M}\left\{2(1+\gamma)\left(1+\frac{\gamma-1}{2}M^2\right)\right\}^{-1/2}$$

4.5 Following quantities are given at the entry and exit of a passage:

Entry: $p_1 = 2.07$ bar, $T_1 = 300$ K, $M_1 = 1.4$

Exit: $M_2 = 2.5$

Assuming isentropic flow of an ideal gas ($\gamma = 1.3$, $R = 0.52$ kJ/kg-K) determine:

(*a*) velocity of sound (a_0) at stagnation conditions,

(*b*) the maximum velocity (c_{max}),

(*c*) the Mach numbers M_1^* and M_2^*,

(*d*) temperature and pressure at exit.

Ans. $a_0 = 512$ m/s, $c_{max} = 1322.5$ m/s, $M_1^* = 1.32$, $M_2^* = 1.93$

$T_2 = 200$ K, $p_2 = 0.362$ bar.

4.6 For one-dimensional isentropic flow of air ($\gamma = 1.4$) at $M = 3.5$ determine the following quantities by calculations and compare them with values given in the gas tables:

$$M^*, \frac{T}{T_0}, \frac{p^*}{p_0}, \frac{\rho}{\rho_0}, \frac{A}{A^*}, \frac{F}{F^*} \text{ and } \frac{Ap}{A^* p_0}.$$

4.7 The Mach number and pressure at the entry of a subsonic diffuser are 0.9 and 4.165 bar. Determine the area ratio required and the pressure rise if the Mach number at the exit of diffuser is 0.20. Assume isentropic diffusion of air.

Ans. $A_2/A_1 = 2.94$, 2.685 bar.

4.8 The entry conditions of air for a nozzle are $p_1 = 1.392$ bar, $T_1 = 333$ K, $M_1 = 0.40$. If the exit pressure is 1.039 bar determine the exit Mach number and the maximum specific mass flow $\dot{m}_{max}/A^*$.

Ans. $M_2 = 0.785$: $\dot{m}_{max}/A^* = 340$ kg/s m^2

4.9 The pressure, velocity and temperature of air ($\gamma = 1.4$, $c_p = 1.0$ kJ/kg K) at the entry of a nozzle are 2 bar, 145 m/s and 330 K; the exit pressure is 1.5 bar.

(*a*) what is the shape of the nozzle?

(*b*) Determine for isentropic flow

(*i*) the Mach numbers at entry and exit

(*ii*) the flow rate and maximum possible flow rate

Ans. $M_1 = 0.399$, $M_2 = 0.762$, $\dot{m}/A_2 = 465$ kg/s m^2,

$\dot{m}_{max}/A^* = 485$ kg/s m^2

4.10 A gas is isentropically expanded from $p = 10$ bar and $t = 525°C$ in a nozzle to a pressure of 7.6 bar. If the rate of flow of the gas is 1.5 kg/s determine: (*a*) pressure, temperature and velocity at the nozzle throat and exit; (*b*) maximum possible velocity attainable by the gas and (*c*) the type of the nozzle and its throat area. Take $\gamma = 1.3$ and $R = 0.464$ kJ/kg K.

Ans. I(*a*) The nozzle is convergent type; the throat and exit are same; $p = 7.6$ bar $t = 475.52°C$, $c = 443.48$ m/s (*b*) $c_{max} = 1791.37$ m/s, (*c*) $A = 15.44$ cm^2.

4.11 A supersonic nozzle expands air from $p_0 = 25$ bar and $T_0 = 1050$ K to an exit pressure of 4.35 bar; the exit area of the nozzle is 100 cm^2. Determine: (*a*) throat area; (*b*) pressure and temperature at the throat; (*c*) temperature at exit; (*d*) exit velocity as fraction of the maximum attainable velocity; and (*e*) mass flow rate.

Ans. (*a*) 69.5 cm^2 (*b*) $p^* = 13.2$ bar, $T^* = 875.7$ K (*c*) 637.35 K (*d*) 0.63 (*e*) 21.66 kg/s.

4.12 A Freon-turbine has to use a maximum flow rate of 5 kg/s of freon employing a ring of convergent nozzles of total exit area of cross-section of 100 cm^2. The pressure in the nozzle entry space is 2.0×10^5 N/m^2. Taking $c_p = 0.845$ kJ/kg K, $\gamma = 1.2$ calculate:

(*a*) stagnation temperature,

(*b*) static pressure and temperature at the nozzle exit, and

(*c*) Mach number at the nozzle exit.

State the assumptions used.

Ans. (*a*) $T_0 = 476.98$ K (*b*) $p = 1.129$ bar, $T = 433.62$ K (*c*) $M = 1$.

4.13 Ambient air ($p_0 = 1.013$ bar, $T_0 = 288$ K) is sucked by a blower through a convergent nozzle (throat diameter = 10 cm). If the air velocity at the throat reaches the sonic value, determine:

(*a*) pressure and temperature at the throat,

(*b*) mass flow rate through the nozzle, and

(*c*) maximum mass flow rate.

Ans. $p = 0.534$ bar, $T = 240.19$ K, 1.890 kg/s.

4.14 A reservoir of infinite size maintains air with a density of 1.12 kg/m^3; the velocity of sound in the reservoir is measured as 500 m/s. Determine:

(*a*) the value of maximum mass flow rate through a nozzle of 1 cm diameter throat,

(*b*) pressure and temperature at the throat for this flow rate.

Ans. (*a*) 0.0254 kg/s, (*b*) 1.056 bar, 518.3 K.

4.15 Show graphically the variation of area ratio (A/A^*), temperature ratio (T/T^*) Mach number (M^*) and mass flow rate ($\dot{m}/\dot{m}_{max}$) with pressure ratio (p_0/p) in isentropic flow in a convergent-divergent nozzle. Mark the points where these quantities have a value of 1.0.

4.16 Explain how does a shock wave develop in the diverging section of a supersonic nozzle? How does this wave move towards the exit?

4.17 Show isentropic and adiabatic expansion and compression processes in nozzles and diffusers on enthalpy-entropy co-ordinates. Indicate the initial and final values of static and stagnation pressures and temperatures.

4.18 A convergent nozzle has an exit area of cross-section of 1000 cm^2. Air expands isentropically through the nozzle from constant inlet conditions ($p_0 = 5$ bar, $T_0 = 500$ K) to (*a*) $M = 1$, (*b*) $M = 0.80$.

Determine for the above two cases the exit velocity and the mass flow rate. Show graphically (in one figure) the variation of pressure along the nozzle in the two cases.

Ans. (*a*) $c = 409.32$ m/s, $\dot{m} = 90.295$ kg/s

(*b*) $c = 337$ m/s, $\dot{m} = 87.05$ kg/s.

4.19 The area of cross-section at the entry of a diffuser is 0.25 m^2, Mach number 1.6 and temperature of air 350 K. If the exit Mach number is 0.80 calculate the velocity and temperature of air, and the area of cross-section at exit for isentropic flow. Draw the sketch of the diffuser indicating the directions of the flow and the thrust.

Ans. $c_2 = 347.28$ m/s, $T_2 = 469$ K, $A_2 = 0.207$ m^2.

4.20 Determine the thrust developed by a rocket nozzle from the following data:

Thrust chamber pressure	400 bar
Nozzle throat cross-section	5 cm^2
Ratio of specific heats of gases	1.2
Mach number at the nozzle exit	5.0

State the assumptions used.

Ans. 39.238 kN.

4.21 (*a*) Prove that the maximum value of the thrust function for $M > 1$ is given by

$$F_{max} = \gamma (\gamma^2 - 1)^{-1/2} \times F^*$$

(*b*) Calculate the maximum value of the thrust function from the following data:

$$\gamma = 1.3,\ p_0 = 100 \text{ bar},\ A^* = 10 \text{ cm}^2$$

Ans. 19.653 kN.

4.22 A convergent-divergent steam nozzle has an area ratio $A/A^* = 1.436$. Calculate (without using gas tables) the Mach number and pressure ratio (p/p_0) for isentropic flow taking $\gamma = 1.3$.

Recalculate the above values in the subsonic section of the nozzle for the same area ratio.

Ans. $M = 1.76,\ 0.46$

$p/p_0 = 0.191,\ 0.873.$

5

Wave Motion

Wave motion in a medium is the movement of a disturbance relative to the medium. The effect of changes at a given point in the medium is communicated to other points through wave motion. Since the molecules in a solid medium are closer to each other compared to liquids and gases a disturbance is communicated (through an elastic wave) to other parts in a comparatively much shorter time. The special phenomenon of the wave propagation in compressible fluid media (gases and vapours) is largely responsible for the marked departure in the nature of analyses between compressible and incompressible flow problems.

Various types of waves in closed passages that may be considered are:

(*a*) Infinitesimal pressure waves (sound waves)

(*b*) Non-steep pressure waves with finite amplitude

(*c*) Steep pressure waves (shock wave)

(*d*) Expansion waves.

A wave which is at a lower pressure than the fluid into which it is moving is called an expansion (rarefaction) wave. Conversely a wave which is at a higher pressure than the fluid is referred to as a compression wave.

5.1 WAVE PROPAGATION IN AN ELASTIC SOLID MEDIUM

Wave action only in gases will be discussed in this chapter. However, for a better understanding of some aspects of the wave phenomenon

a brief article on wave propagation in an elastic solid medium is considered here.

Figure 5.1 shows a solid rod of uniform area of cross-section A. Compressive stress f (N/cm^2) is generated due to the sudden action of

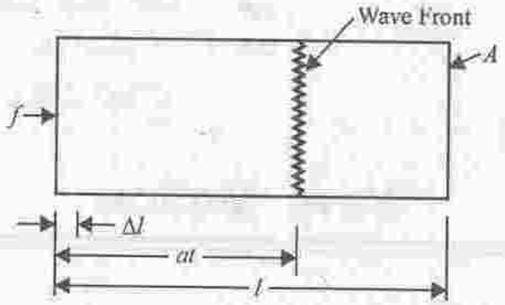

FIGURE 5.1 : Wave propagation in an elastic solid medium

a force at one end of the rigid rod. The distance travelled by the wave front with a velocity a in time t is (at). The change in the length of the portion of the rod through which the wave has travelled is Δl. Therefore,

$$\text{Strain} \quad = \frac{\Delta l}{at} \tag{5.1}$$

Modulus of elasticity of the rod is

$$E = \frac{\text{stress}}{\text{strain}} = \frac{f}{\Delta l / at} \tag{5.2}$$

The particle velocity of the medium (particles of the rod material)

$$c = \frac{\Delta l}{t} \tag{5.3}$$

Equations (5.2) and (5.3) yield

$$c = \frac{f}{E/a} \tag{5.4}$$

Applying momentum equation to the above system.

Impulsive force = change of momentum

$$fAt = \rho A\,(at)\,c$$

$$c = \frac{f}{\rho a} \tag{5.5}$$

By comparison of Equations (5.4) and (5.5), we get

$$\frac{f}{E/a} = \frac{f}{\rho a}$$

$$E = \rho a^2$$

$$a = \sqrt{\frac{E}{\rho}} \tag{5.6}$$

5.2 PROPAGATION OF INFINITESIMAL WAVES (SOUND WAVES)

In this section propagation of sound waves in gases is considered.

A sound wave is an infinitesimal pressure wave. The changes across such a wave are small and the speed of the process corresponding to these changes is fast. Therefore, if there is no heat transfer in the system under consideration the changes across an infinitesimal pressure wave can be assumed as reversible adiabatic or isentropic. The velocity of sound in a gas depends on its bulk modulus of elasticity (K) or the rate of change of pressure with density $(\partial p/\partial \rho)$.

The propagation of an infinitesimal pressure wave into the stagnant gas in a constant area duct is shown in Figure 5.2. The wave moves

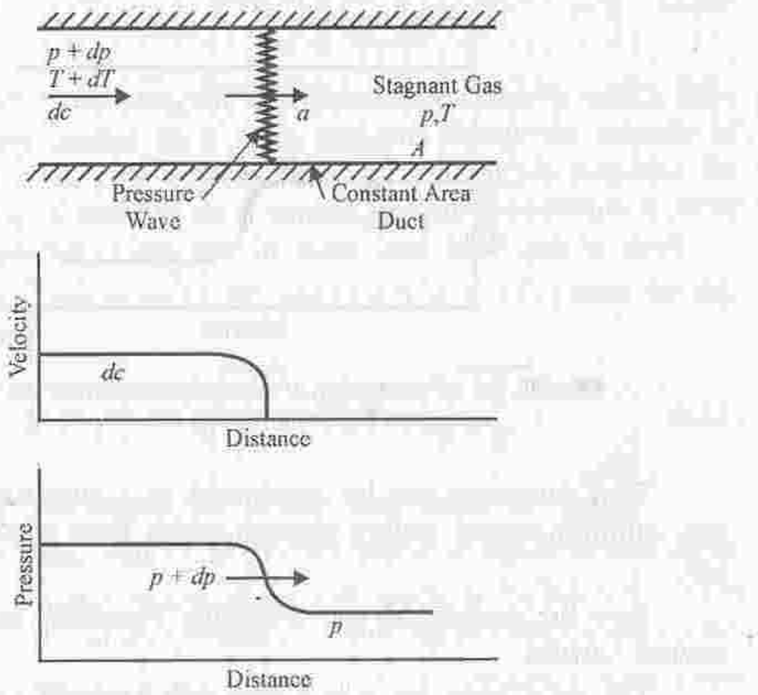

FIGURE 5.2 : Propagation of an infinitesimal wave in a constant area duct (observer at rest)

with a velocity a towards the right into the stagnant gas which is at pressure p and temperature T. The pressure and temperature of the gas that has been traversed by the wave are raised to $p+dp$ and $T+dT$ respectively and a velocity dc is imparted to the gas. This is the pattern of the process that will be observed by an observer at rest.

The pattern shown in Figure 5.3 will be observed when the observer moves with the wave. In this case the stagnant gas at pressure p on the right appears to flow towards the left with a velocity a. When the flow has passed through the wave to the left its pressure is raised to $(p+dp)$ and the velocity lowered to $(a-dc)$.

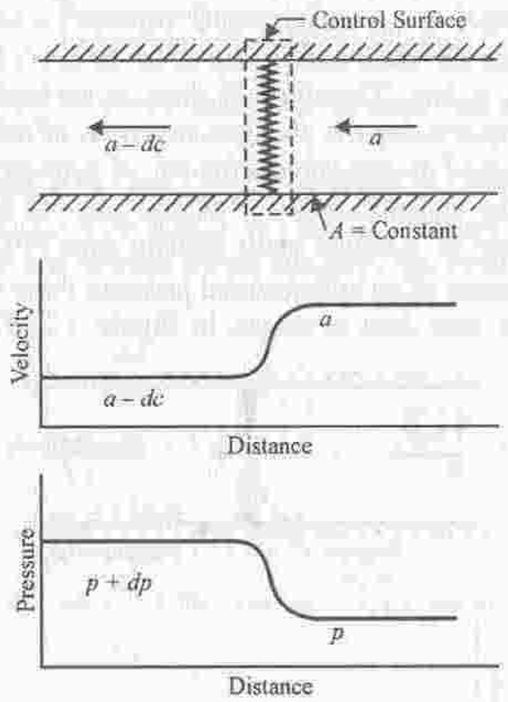

FIGURE 5.3 : Propagation of an infinitesimal wave in a constant area duct (observer moving with the wave)

Thus the wave can be considered as a stationary wave contained within a control surface through which flow occurs from right to left.

Now the momentum and continuity equations are written for the control surface.

The shear force for such a flow will be small and therefore, can be ignored.

Momentum equation for this process gives

$$A\,[p-(p+dp)] = \dot{m}\,[(a-dc)-a]$$

$$A\,dp = \dot{m}\,dc \tag{5.7}$$

From continuity equation

$$\dot{m} = \rho A a \tag{5.8}$$

Equations (5.7) and (5.8) yield

$$dp = \rho a\,dc \tag{5.9}$$

From continuity equation for the two sides of the wave

$$\dot{m} = \rho A a = (\rho + d\rho)\;(a-dc)\,A$$

$$\rho\,dc = a\,d\rho \tag{5.10}$$

Substituting from Equation (5.10) in (5.9)

$$a^2 = \frac{dp}{d\rho} \tag{5.11}$$

Since the process has been assumed isentropic Equation (5.11) can be written as

$$a = \left(\sqrt{\frac{\partial p}{\partial \rho}}\right)_s \tag{5.12}$$

Equation (5.12) shows that in compressible fluids in which there is a large density change for a given pressure change the velocity of sound is much lower compared to incompressible fluids (liquids); for example, velocity of sound in air at normal ambient temperature is about 340 m/s compared to 1700 m/s in water and 5000 m/s in steel.

Substituting Equations (1.58) and (1.62) in (5.12) yields the following relations:

$$a = \sqrt{\frac{K}{\rho}} = \sqrt{\frac{\gamma p}{\rho}} = \sqrt{\gamma RT} = \sqrt{\gamma \frac{\overline{R}}{W}\,T} \tag{5.13}$$

Following conclusions are drawn from Equation (5.13):

(*a*) In a given fluid, velocity of sound is higher at higher temperatures.

(*b*) Fluids with higher values of the bulk modulus (or lower values of the coefficients of compressibility) have higher velocities of sound.

(*c*) With little change in the values of γ for commonly used gases velocity of sound at a given temperature is higher for lower

molecular weight gases and vice-versa. Hydrogen, with a very low molecular weight has a high speed of sound of about 1400 m/s; while the velocity of sound in some freons which have higher molecular weights, is only about 150 m/s.

The above figures suggest that Mach number plays an important role in the design and working of machines using higher molecular weight fluids. In contrast to this Mach number has negligible effect on machines using low molecular weight gases like hydrogen; this is because the fluid or gas velocities are very small compared to velocity of sound at the prevailing temperatures.

5.2.1 Mach Number

As stated earlier Mach number (M) of a moving object like an aircraft or a missile is the ratio of its velocity and the velocity of sound in the medium (at a given state) into which it is moving. The Mach number of a flowing fluid is the ratio of its velocity and the velocity of sound at the prevailing temperature.

Definition of Mach number can also be obtained from

$$M^2 = \frac{\text{inertia force}}{\text{elastic force}}$$

Inertia force $= \rho A c^2$

Elastic force $= KA$

Substituting for K from Equation (5.13)

Elastic force $= \rho A a^2$ (5.14)

Therefore, $$M^2 = \frac{\rho A c^2}{\rho A a^2}$$

$$M^2 = \left(\frac{c}{a}\right)^2 \quad (5.15)$$

5.2.2 Mach Angle

Figures 5.4 ((*a*), (*b*), (*c*) and (*d*)) show the movement of a source of disturbance (S) at a velocity u in a fluid from right to the left. Point S represents the present position, while 1, 2 and 3 show its positions before 1, 2 and 3 seconds respectively. The disturbance travels distances of a, $2a$ and $3a$ metres in 1, 2 and 3 seconds respectively.

In an incompressible flow model (as shown in Figure 5.4 (*a*)) velocity u of the source of disturbance is negligibly small compared

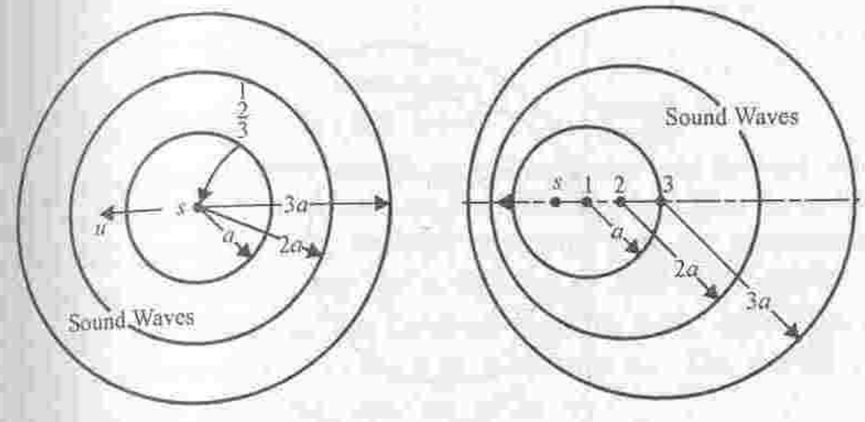

(*a*) Incompressible flow ($u/a = 0$, $M = 0$)

(*b*) Subsonic flow ($a/2u$, $M = 0.5$)

FIGURE 5.4

to the velocity of sound a. Infinitesimal spherical waves (sound waves) are generated which travel at a velocity a in all the directions; here the displacement of the point S during the time considered (3 sec.) is insignificantly small compared to the distance travelled by the pressure waves.

Wave propagation in subsonic flow at ($M = u/a = 0.5$) is shown in Figure 5.4 (*b*); here the source of disturbance travels at half the velocity of the wave (disturbance). Spherical sound waves generated at $t = 3$, 2 and 1 secs. before the present position S are shown. It is observed that the wave fronts move ahead of the point source and the intensity is not symmetrical.

In Figure 5.4 (*c*) the point source travels with the same velocity as that of the wave; the velocity of the point source is sonic ($M = 1$). Under this condition the wave fronts always exist at the present position of the point source and cannot move ahead of it. Therefore, the region downstream of the point source, *i.e.*, the zone lying on the left of the wave front is a zone of silence because the waves do not reach this zone. The zone on the right of the wave front is traversed by the waves and is therefore a zone of action.

Figure 5.4 (*d*) shows a supersonic flow model. As an example the point source is assumed to be moving at twice the velocity of sound ($M = u/a = 2$). The waves generated at positions 3, 2, 1 and S are shown. The point source is always ahead of the wave fronts. Tangents drawn from the point S on the spheres define a conical surface referred to as 'Mach cone'.

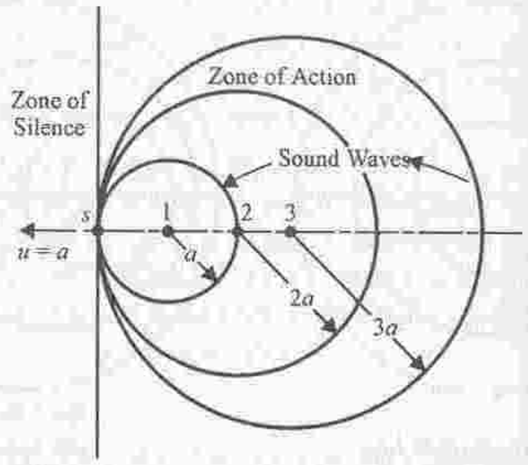

FIGURE 5.4 (*c*) : Sonic flow ($a = u,\ M = 1.0$)

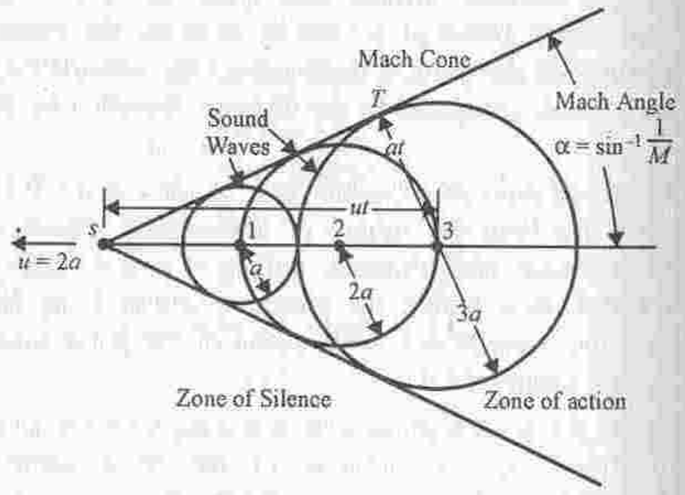

FIGURE 5.4 (*d*) : Supersonic flow $\left(a = \frac{1}{2}u,\ M = 2.0\right)$

All the waves are confined to the region within the Mach cone; therefore, this is referred to as the zone of action. The waves do not reach the region outside the Mach cone; therefore, this zone is known as the zone of silence.

The semi-angle of the cone is known as the Mach angle; this is given by

$$\alpha = \sin^{-1}\frac{3T}{3S} = \sin^{-1}\frac{at}{ut} = \sin^{-1}\frac{1}{u/a}$$

$$\alpha = \sin^{-1}\left(\frac{1}{M}\right). \tag{5.16}$$

5.2.3 Equation of a sound wave

In this section equation of motion for a sound wave is derived. Continuity and momentum equations for three dimensional flow have been derived in Chapter 10. Here the flow is assumed as one-dimensional, inviscid and the body forces are considered as negligibly small.

Figure 5.5 shows an infinitesimal pressure wave (sound wave) moving into the stagnant gas ($c_\infty = 0$) of density ρ_∞. The density and velocity changes along the wave are given by

$$\rho = \rho_\infty + \Delta\rho \tag{5.17}$$

$$c = c_\infty + c' = c' \tag{5.18}$$

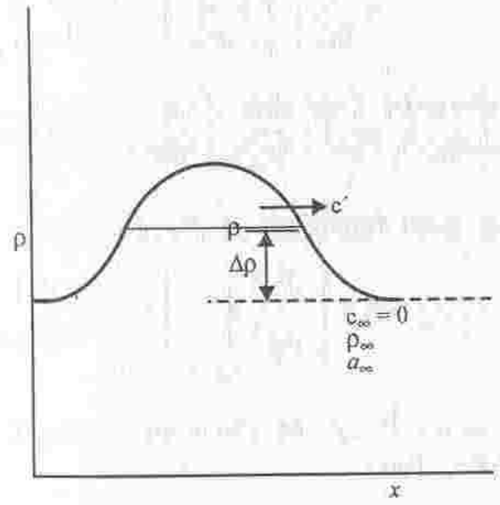

FIGURE 5.5 : Changes across a sound wave

The fluid through which the wave has passed moves with a small velocity c'. Momentum equation for this flow is

$$\frac{1}{\rho}\frac{\partial p}{\partial x} + c\frac{\partial c}{\partial x} + \frac{\partial c}{\partial t} = 0 \tag{5.19}$$

$$\frac{1}{\rho}\left(\frac{\partial p}{\partial x}\right)_s = \frac{1}{\rho}\left(\frac{\partial p}{\partial \rho}\right)_s\left(\frac{\partial \rho}{\partial x}\right)_s \tag{5.20}$$

Expansion of $\left(\frac{\partial p}{\partial \rho}\right)_s$ in Taylor's series gives

$$\left(\frac{\partial p}{\partial \rho}\right)_s = \left(\frac{\partial p}{\partial \rho}\right)_{s,\infty} + \Delta\rho \left(\frac{\partial^2 p}{\partial \rho^2}\right)_{s,\infty} + \ldots$$

But $$\left(\frac{\partial p}{\partial \rho}\right)_{s,\infty} = a_\infty^2$$

Therefore, $$\left(\frac{\partial p}{\partial \rho}\right)_s = a_\infty^2 + \Delta\rho \left(\frac{\partial^2 p}{\partial \rho^2}\right)_{s,\infty} \tag{5.21}$$

$$\frac{1}{\rho}\left(\frac{\partial \rho}{\partial x}\right)_s = \frac{1}{\rho_\infty + \Delta\rho}\left(\frac{\partial}{\partial x}\Delta\rho\right)_s$$

$$= \frac{1}{\rho_\infty}\left(1 + \frac{\Delta\rho}{\rho_\infty}\right)^{-1}\left(\frac{\partial \Delta\rho}{\partial x}\right)_s$$

$$\frac{1}{\rho}\left(\frac{\partial \rho}{\partial x}\right)_s = \left(1 - \frac{\Delta\rho}{\rho_\infty}\right)\left[\frac{\partial}{\partial x}\left(\frac{\Delta\rho}{\rho_\infty}\right)\right] = 0 \tag{5.22}$$

Substituting from Equations (5.21) and (5.22) in (5.20)

$$\frac{1}{\rho}\left(\frac{\partial p}{\partial x}\right)_s = \left[a_\infty^2 + \Delta\rho\left(\frac{\partial^2 p}{\partial \rho^2}\right)_{s,\infty}\right]\left(1 - \frac{\Delta\rho}{\rho_\infty}\right)\frac{\partial}{\partial x}\left(\frac{\Delta\rho}{\rho_\infty}\right)$$

For small values of $\Delta\rho$ the above equation can be written in the following simplified form:

$$\frac{1}{\rho}\left(\frac{\partial p}{\partial x}\right)_s = a_\infty^2 \frac{\partial}{\partial x}\left(\frac{\Delta\rho}{\rho_\infty}\right) \tag{5.23}$$

Substituting from Equations (5.18) and (5.23) in (5.19)

$$a_\infty^2 \frac{\partial}{\partial x}\left(\frac{\Delta\rho}{\rho_\infty}\right) + c'\frac{\partial c'}{\partial x} + \frac{\partial c'}{\partial t} = 0$$

For small values of c', $c'\dfrac{\partial c'}{\partial x} = 0$, therefore,

$$a_\infty^2 \frac{\partial}{\partial x}\left(\frac{\Delta\rho}{\rho_\infty}\right) + \frac{\partial c'}{\partial t} = 0 \tag{5.24}$$

Continuity equation gives

$$\frac{\partial \rho}{\partial t} + c\frac{\partial \rho}{\partial x} + \rho\frac{\partial c}{\partial x} = 0$$

Substituting from Equations (5.17) and (5.18) in the above equation

$$\frac{\partial}{\partial t}(\rho_\infty + \Delta\rho) - c'\frac{\partial}{\partial x}(\rho_\infty + \Delta\rho) + (\rho_\infty + \Delta\rho)\frac{\partial c'}{\partial x} = 0$$

Noting that $\partial\rho_\infty/\partial t = 0$, $\partial\rho_\infty/\partial x = 0$ and $\Delta\rho$ and c' are small quantities, the above equation reduces to

$$\frac{\partial}{\partial t}(\Delta\rho) + \rho_\infty\frac{\partial c'}{\partial x} = 0$$

$$\frac{\partial}{\partial t}\left(\frac{\Delta\rho}{\rho_\infty}\right) + \frac{\partial c'}{\partial x} = 0 \tag{5.25}$$

Since Equations (5.24) and (5.25) have been derived assuming isentropic flow with infinitesimal changes, they are valid for the sound waves.

Differentiating Equations (5.24) and (5.25) with respect to x and t respectively

$$a_\infty^2\frac{\partial^2}{\partial x^2}\left(\frac{\Delta\rho}{\rho_\infty}\right) + \frac{\partial^2 c'}{\partial x\,\partial t} = 0$$

$$\frac{\partial^2}{\partial t^2}\left(\frac{\Delta\rho}{\rho_\infty}\right) + \frac{\partial^2 c'}{\partial t\,\partial x} = 0$$

By subtraction of the above equations and noting that

$$\frac{\partial^2 c'}{\partial x\,\partial t} = \frac{\partial^2 c'}{\partial t\,\partial x}$$

we have $$a_\infty^2\frac{\partial^2}{\partial x^2}\left(\frac{\Delta\rho}{\rho_\infty}\right) - \frac{\partial^2}{\partial t^2}\left(\frac{\Delta\rho}{\rho_\infty}\right) = 0 \tag{5.26}$$

Differentiating Equations (5.24) and (5.25) with respect to t and x respectively we have

$$\frac{\partial^2}{\partial t\,\partial x}\left(\frac{\Delta\rho}{\rho_\infty}\right) + \frac{1}{a_\infty^2}\frac{\partial^2 c'}{\partial t^2} = 0$$

$$\frac{\partial^2}{\partial x\ \partial t}\left(\frac{\Delta\rho}{\rho_\infty}\right)+\frac{\partial^2 c'}{\partial x^2}=0$$

By subtraction of the above equations and noting that

$$\frac{\partial^2}{\partial t\ \partial x}\left(\frac{\Delta\rho}{\rho_\infty}\right)=\frac{\partial^2}{\partial x\ \partial t}\left(\frac{\Delta\rho}{\rho_\infty}\right)$$

we have

$$a_\infty^2\frac{\partial^2 c'}{\partial x^2}-\frac{\partial^2 c'}{\partial t^2}=0 \tag{5.27}$$

Equations (5.26) and (5.27) show that changes in both velocity and density follow a wave pattern defined by these equations.

A general solution of the wave Equation (5.26) can be written as

$$\frac{\Delta\rho}{\rho_\infty}=f_1(x-a_\infty t)+f_2(x+a_\infty t) \tag{5.28}$$

This is shown graphically in Figure 5.6.

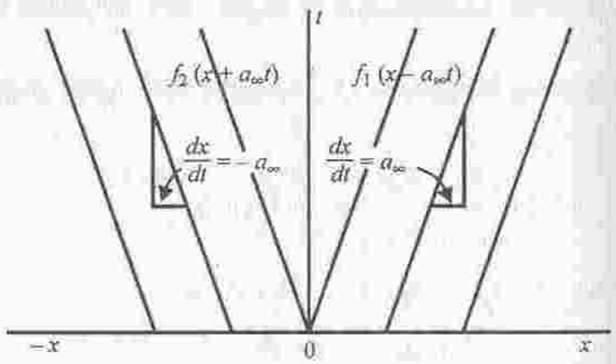

FIGURE 5.6 : Rightward and leftward characteristics

The rightward running lines represent the first part of the solution

$$f_1(x-a_\infty t)=\text{constant} \tag{5.29}$$

$$\frac{dx}{dt}=a_\infty \tag{5.30}$$

The leftward running lines represent the other part of the solution

$$f_2(x+a_\infty t)=\text{constant} \tag{5.31}$$

$$\frac{dx}{dt}=-a_\infty. \tag{5.32}$$

5.3 NON-STEEP FINITE PRESSURE WAVES

Till now only infinitesimal pressure waves have been considered. As stated before the changes across these waves are isentropic and small in magnitude. Such waves can be generated by an impulse imparted by the sudden movement of a piston in a cylinder as shown in Figure 5.7 (*c*). If such impulses are continuously generated by the piston in a few steps before it achieves a steady speed there will be a finite change in pressure and other quantities. This finite change is made up of a number of infinitesimal isentropic changes as shown in Figure 5.7 (*b*); therefore, the overall change across the wave is finite but still remains isentropic. Since the changes across the wave are continuous it is a non-steep finite wave. Such a wave is considered here. This is moving towards the right into the stagnant gas ($c = 0$) at pressure (p_1) and temperature (T_1). The flat top of this wave corresponds to the steady speed of the piston. The passage of the wave into the fluid sets it into motion with a velocity c and raises its pressure to p as

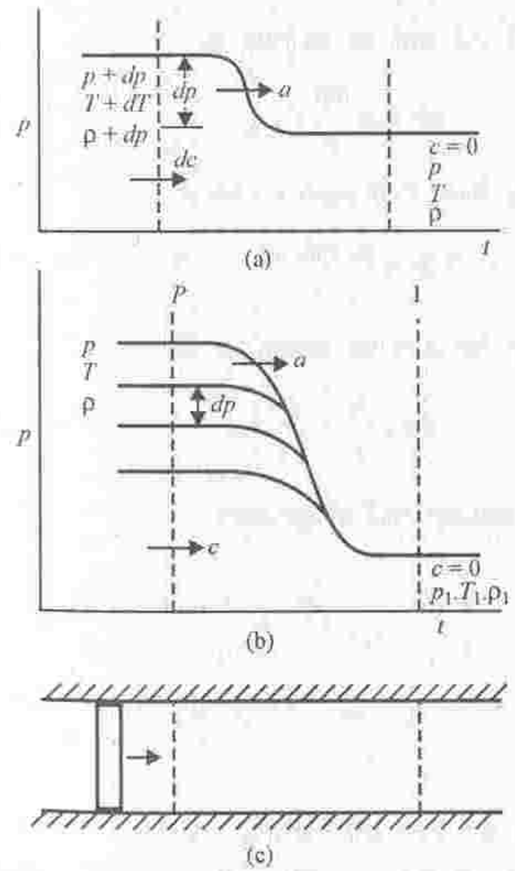

FIGURE 5.7 : Development of a non-steep finite compression wave

at section P in Figure 5.7. The properties at points P and 1 can be related through isentropic relations:

$$\frac{a}{a_1}=\left(\frac{T}{T_1}\right)^{1/2}=\left(\frac{p}{p_1}\right)^{(\gamma-1)/2\gamma} \tag{5.33}$$

$$p=\text{constant}\,\rho^{\gamma}$$

$$\ln p=\ln\text{constant}+\gamma\ln\rho$$

By differentiation

$$\frac{dp}{p}=\gamma\frac{d\rho}{\rho}$$

$$\frac{dp}{d\rho}=\frac{\gamma p}{\rho}=a^2$$

$$\frac{d\rho}{\rho}=\frac{1}{\gamma}\frac{dp}{p} \tag{5.34}$$

Equation (5.10) can be written as

$$dc=a\frac{d\rho}{\rho}$$

Substituting from Equation (5.34)

$$dc=\frac{a}{\gamma}\frac{dp}{p}$$

Substituting for a from Equation (5.33)

$$dc=\frac{a_1}{\gamma}\left(\frac{p}{p_1}\right)^{(\gamma-1)/2\gamma}\frac{dp}{p}$$

After rearranging and integrating

$$\int_0^c dc=\frac{a_1}{\gamma p_1^{(\gamma-1)/2\gamma}}\int_{p_1}^{p} p^{-(\gamma+1)/2\gamma}\,dp$$

$$c=\frac{2a_1}{\gamma-1}\left[\left(\frac{p}{p_1}\right)^{(\gamma-1)/2\gamma}-1\right]. \tag{5.35}$$

5.3.1 Velocity of the non-steep wave

Equation (5.35) gives the velocity of the gas (at section P) that is induced after the passage of the finite non-steep pressure wave. The local velocity of sound, from Equation (5.33) is given by

$$a=a_1\left(\frac{p}{p_1}\right)^{(\gamma-1)/2\gamma} \tag{5.36}$$

Therefore, the velocity of the wave propagation is

$$c_w=c+a$$

$$c_w=\frac{2a_1}{\gamma-1}\left[\left(\frac{p}{p_1}\right)^{(\gamma-1)/2\gamma}-1\right]+a_1\left(\frac{p}{p_1}\right)^{(\gamma-1)/2\gamma}$$

$$c_w=\left[\frac{\gamma+1}{\gamma-1}\left(\frac{p}{p_1}\right)^{(\gamma-1)/2\gamma}-\frac{2}{\gamma-1}\right]a_1 \tag{5.38 (a)}$$

A wave Mach number can be defined by

$$M_w=\frac{c_w}{a_1}=\frac{\gamma+1}{\gamma-1}\left(\frac{p}{p_1}\right)^{(\gamma-1)/2\gamma}-\frac{2}{\gamma-1} \tag{5.38 (b)}$$

If $p=p_1+\Delta p$

$$\left(\frac{p}{p_1}\right)^{(\gamma-1)/2\gamma}=\left(1+\frac{\Delta p}{p_1}\right)^{(\gamma-1)/2\gamma}$$

For small values of Δp, by binomial expansion

$$\left(\frac{p}{p_1}\right)^{(\gamma-1)/2\gamma}=1+\frac{\gamma-1}{2\gamma}\frac{\Delta p}{p_1}$$

Substituting the above equation in (5.38 (a)), we get

$$c_w=\left[\frac{\gamma+1}{\gamma-1}+\frac{\gamma+1}{2\gamma}\frac{\Delta p}{p_1}-\frac{2}{\gamma-1}\right]a_1$$

$$c_w=\left(1+\frac{\gamma+1}{2\gamma}\frac{\Delta p}{p_1}\right)a_1 \tag{5.38 (c)}$$

When the finite wave approaches the infinitesimal wave

$$\frac{\Delta p}{p_1}\to 0$$

and the above expression yields $c_w=a_1$.

5.3.2 Mach number of the flow induced by the non-steep wave

The Mach number of the gas through which the wave has passed is given by

$$M = \frac{c}{a}$$

Substituting from Equations (5.35) and (5.36)

$$M = \frac{2a_1}{\gamma - 1}\left[\left(\frac{p}{p_1}\right)^{(\gamma-1)/2\gamma} - 1\right] \Big/ a_1\left(\frac{p}{p_1}\right)^{(\gamma-1)/2\gamma}$$

$$M = \frac{2}{\gamma - 1}\left[1 - \left(\frac{p_1}{p}\right)^{(\gamma-1)/2\gamma}\right] \tag{5.39}$$

Figure 5.8 shows the generation and propagation of compression waves in a cylinder. The space-time diagram for the waves along with the trajectories of the piston and the fluid particles is shown.

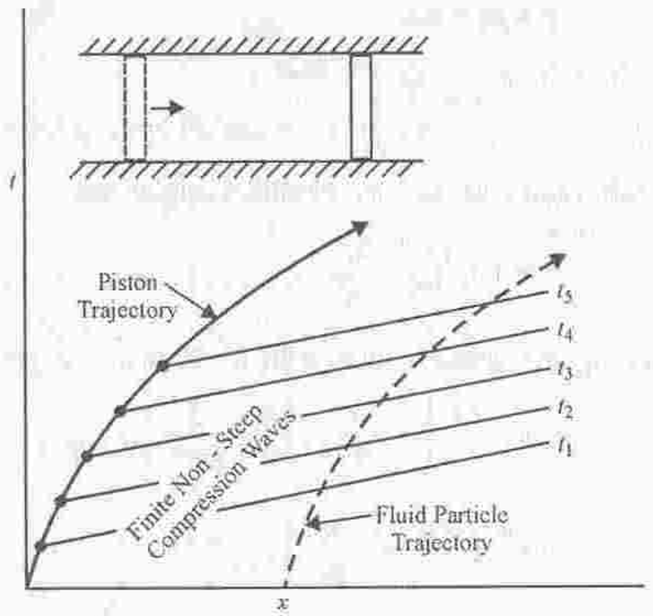

FIGURE 5.8 : Compression waves in the direction of motion of the piston

Due to the continuous passage of waves through the fluid its pressure and temperature are raised. Therefore, the local velocity of sound for a wave generated at $t = t_5$ will be much higher (on account of the

higher gas temperature) compared to a wave generated at an earlier stage say at $t = t_1$. Besides this with the continuous passage of pressure waves through the fluid its velocity is also progressively increasing. Therefore, the waves generated in the later stages propagate at higher velocities of sound relative to the fluid which itself is moving faster than before. But the velocity of wave propagation is given by

$$c_w = c + a$$

Therefore, the propagation velocity of each subsequent wave is greater than that of the preceding wave; this fact can be observed as the decreasing slope of the subsequent waves on the time-space diagram.

5.4 STEEP FINITE PRESSURE WAVES

In this section a special case of the finite pressure waves is discussed. In the preceding section it was explained that the impulsive motion of the piston in a number of steps generated pressure waves which move at higher velocities than the preceding waves. Thus the faster moving waves tend to overtake the slower waves generated earlier.

Figure 5.9 shows a condition when a number of compression waves merge into one "finite pressure steep wave". This is due to the above phenomenon of faster waves overtaking the slower waves ahead,and is best explained on a time-space diagram (Figure 5.9).

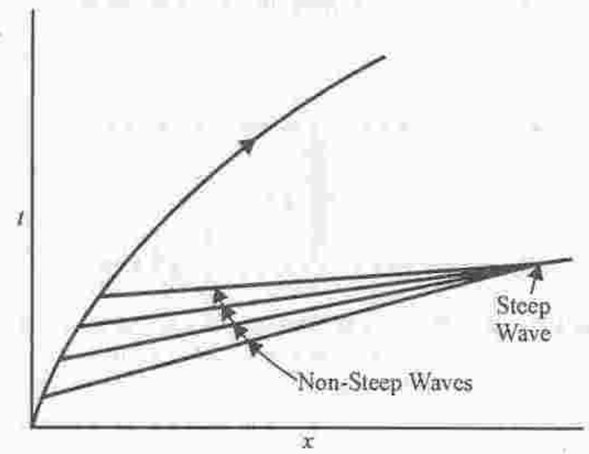

FIGURE 5.9 : Development of a finite pressure steep wave (shock wave)

In contrast to the infinitesimal and non-steep compression waves the change in the pressure and other properties of the flow across a steep compression wave is abrupt; therefore, it is referred to as a "shock

wave''. A detailed analysis of the shock waves will be covered in the latter chapters.

5.4.1 Velocity of the steep wave

Figures 5.10 (*a*), (*b*) show the propagation of a steep compression wave into stagnant gas in a constant area duct; the quantities upstream of the wave are c_2, p_2, T_2, ρ_2 etc. and those in the stagnant gas are $c_1 = 0$, p_1, T_1 and ρ_1. The velocity of propagation of the wave is c_{sw}.

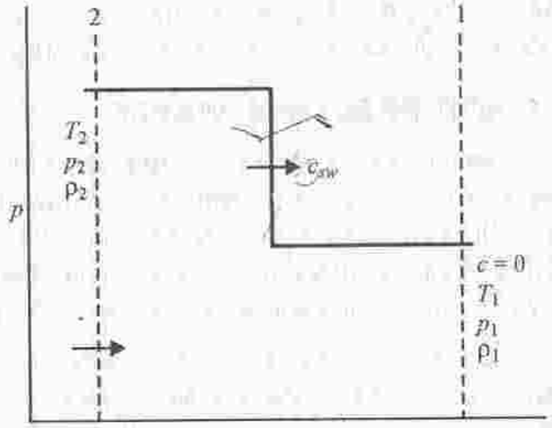

FIGURE 5.10 (*a*) : Propagation of a steep compression or shock wave in stagnant gas (observer at rest)

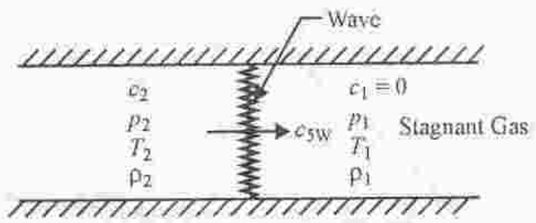

FIGURE 5.10 (*b*) : Propagation of a steep compression or shock wave in stagnant gas (observer at rest)

In Figure 5.10 (*c*) the gas is assumed to be moving towards the left at a velocity $c_1 = c_{sw}$. This gives zero velocity to the wave and a velocity $(c_{sw} - c_2)$ to the flow on the left of the stationary steep compression wave.

Continuity equation for this flow model (Figure 5.10 (*c*)) gives

$$\dot{m} = \rho_1 c_{sw} A = \rho_2 (c_{sw} - c_2) A$$

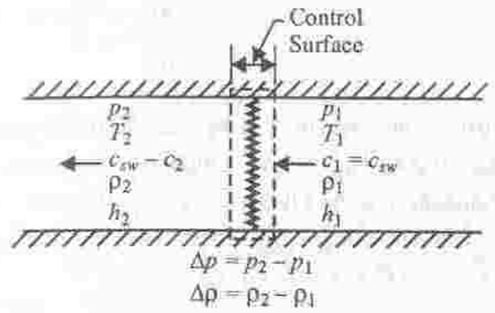

FIGURE 5.10 (*c*) : Flow through a steep compression or shock wave (observer moving with the wave)

$$\frac{\rho_1}{\rho_2} = \frac{c_{sw} - c_2}{c_{sw}} = 1 - \frac{c_2}{c_{sw}} \tag{5.40}$$

$$c_2 = \left(\frac{\rho_2 - \rho_1}{\rho_2} \right) c_{sw} \tag{5.41}$$

Momentum equation for the control volume gives

$$(p_1 - p_2) A = \dot{m} [(c_{sw} - c_2) - c_{sw}]$$

$$p_2 - p_1 = \rho_1 c_{sw} c_2$$

Substituting for c_2 from Equation (5.41), we get

$$p_2 - p_1 = \rho_1 c_{sw}^2 \left(\frac{\rho_2 - \rho_1}{\rho_2} \right)$$

This gives the velocity of the steep wave as

$$c_{sw} = \sqrt{\frac{\rho_2}{\rho_1} \left(\frac{p_2 - p_1}{\rho_2 - \rho_1} \right)} \tag{5.42}$$

$$c_{sw} = \sqrt{\frac{\rho_2}{\rho_1} \frac{\Delta p}{\Delta \rho}} \tag{5.43}$$

Equation (5.42) can also be written as

$$c_{sw} = \sqrt{\frac{p_1}{\rho_1} \frac{(p_2/p_1) - 1}{1 - (\rho_1/\rho_2)}} = \sqrt{RT_1 \frac{(p_2/p_1) - 1}{1 - (\rho_1/\rho_2)}} \tag{5.44}$$

$$c_{sw}^2 \left(1 - \frac{\rho_1}{\rho_2} \right) = \frac{p_1}{\rho_1} \left(\frac{p_2}{p_1} - 1 \right)$$

$$\frac{\rho_1}{\rho_2} = 1 - \frac{1}{c_{sw}^2}\frac{p_1}{\rho_1}\left(\frac{p_2}{p_1} - 1\right) \tag{5.45}$$

Unlike the infinitesimal and non-steep finite compression waves the changes across the steep wave may or may not be adiabatic. If heat transfer is considered negligible or absent the flow process can be assumed as adiabatic. Therefore, from energy equation for adiabatic flow across the wave (Figure 5.10 (*c*))

$$h_1 + \frac{1}{2}c_{sw}^2 = h_2 + \frac{1}{2}(c_{sw} - c_2)^2 \tag{5.46}$$

But $$h = \frac{\gamma}{\gamma - 1}\frac{p}{\rho} \quad \text{(Equation 2.31)}$$

Therefore, substituting from Equation (2.31) for h and from (5.40) for $(c_{sw} - c_2)$ into Equation (5.46)

$$\frac{\gamma}{\gamma - 1}\frac{p_1}{\rho_1} + \frac{1}{2}c_{sw}^2 = \frac{\gamma}{\gamma - 1}\frac{p_2}{\rho_2} + \frac{1}{2}c_{sw}^2\left(\frac{\rho_1}{\rho_2}\right)^2$$

Expressing the first term on the right hand side in the above equation in terms of density and pressure ratios we get

$$\frac{2\gamma}{\gamma - 1}\frac{p_1}{\rho_1} + c_{sw}^2 = \frac{2\gamma}{\gamma - 1}\left(\frac{p_2}{p_1}\right)\left(\frac{\rho_1}{\rho_2}\right)\frac{p_1}{\rho_1} + c_{sw}^2\left(\frac{\rho_1}{\rho_2}\right)^2 \tag{5.47}$$

Substituting for ρ_1/ρ_2 from Equation (5.45) in (5.47) yields

$$\frac{2\gamma}{\gamma - 1}\frac{p_1}{\rho_1} + c_{sw}^2 = \frac{2\gamma}{\gamma - 1}\left(\frac{p_2}{p_1}\right)\left\{1 - \frac{1}{c_{sw}^2}\frac{p_1}{\rho_1}\left(\frac{p_2}{p_1} - 1\right)\right\}\frac{p_1}{\rho_1} + \left\{1 - \frac{1}{c_{sw}^2}\frac{p_1}{\rho_1}\left(\frac{p_2}{p_1} - 1\right)\right\}^2 c_{sw}^2$$

Opening the brackets, simplifying and collecting the terms containing c_{sw}^2

$$\frac{1}{c_{sw}^2}\left(\frac{p_1}{\rho_1}\right)\left(\frac{p_2}{p_1} - 1\right)\left(1 + \frac{p_2}{p_1}\cdot\frac{\gamma + 1}{\gamma - 1}\right) = \frac{2p_2}{p_1}\left(\frac{1}{\gamma - 1}\right) - \frac{2}{\gamma - 1}$$

$$= \frac{2}{\gamma - 1}\left(\frac{p_2}{p_1} - 1\right)$$

The above equation on further simplification and rearrangement yields

$$c_{sw}^2 = \frac{\gamma - 1}{2}\frac{p_1}{\rho_1} + \frac{\gamma + 1}{2}\frac{p_1}{\rho_1}\frac{p_2}{p_1} \tag{5.48}$$

This equation gives the velocity of the steep wave in terms of the initial properties (p_1, ρ_1 etc.) and the amplitude ($p_2 - p_1$) of the wave or the pressure ratio across it.

If $$p_2 = p_1 + \Delta p$$

$$\frac{p_2}{p_1} = 1 + \frac{\Delta p}{p_1}$$

Substituting the above value in Equation (5.48)

$$c_{sw}^2 = \frac{\gamma - 1}{2}\frac{p_1}{\rho_1} + \frac{\gamma + 1}{2}\frac{p_1}{\rho_1}\left(1 + \frac{\Delta p}{p_1}\right)$$

$$c_{sw}^2 = \gamma\frac{p_1}{\rho_1} + \left(\frac{\gamma + 1}{2}\right)\frac{\Delta p}{\rho_1}$$

When the finite pressure wave approaches the infinitesimal wave ($\Delta p \to 0$) the above equation yields

$$c_{sw}^2 = \gamma\frac{p_1}{\rho_1} = a_1^2$$

which has been derived earlier for the sound wave.

5.4.2 Mach number of the flow induced by a steep wave

An expression for the Mach number of the flow ($M_2 = c_2/a_2$) through which the wave has passed can be derived from the relations so far developed.

Comparison of Equations (5.40) and (5.45) gives

$$\frac{\rho_1}{\rho_2} = 1 - \frac{c_2}{c_{sw}} = 1 - \frac{1}{c_{sw}^2}\frac{p_1}{\rho_1}\left(\frac{p_2}{p_1} - 1\right)$$

Now $$\frac{p_1}{\rho_1} = RT_1 = \frac{a_1^2}{\gamma}$$

Therefore, $$\frac{c_2}{c_{sw}} = \frac{a_1^2}{c_{sw}^2}\,\frac{1}{\gamma}\left(\frac{p_2}{p_1} - 1\right)$$

which after rearrangement gives

$$\frac{c_2}{a_1} = \frac{a_1}{c_{sw}}\,\frac{1}{\gamma}\left(\frac{p_2}{p_1} - 1\right) \tag{5.49}$$

Equation (5.48) can also be rewritten as

$$c_{sw}^2 = \frac{\gamma-1}{2}\,\frac{a_1^2}{\gamma} + \frac{\gamma+1}{2}\,\frac{a_1^2}{\gamma}\,\frac{p_2}{p_1}$$

$$\frac{c_{sw}}{a_1} = \sqrt{\frac{\gamma-1}{2\gamma} + \frac{\gamma+1}{2\gamma}\,\frac{p_2}{p_1}} \tag{5.50 (a)}$$

The velocity ratio given by Equation (5.50 (*a*)) may be referred to as the Mach number (M_{sw}) of the steep wave.

This relation also gives the upstream Mach number ($M_1 = c_1/a_1$) of the flow occurring through the steep pressure wave (considered stationary as shown in Figure 5.10 (*c*)) for a pressure ratio of p_2/p_1. Equation (5.50 (*a*)) will be identified later as Equation (6.26) for flow through a normal shock in Chapter 6.

Putting $p_2 = p_1 + \Delta p$

$$\frac{\gamma-1}{2\gamma} + \frac{\gamma+1}{2\gamma}\,\frac{p_2}{p_1} = 1 + \frac{\gamma+1}{2\gamma}\,\frac{\Delta p}{p_1}$$

Substitution of this value in Equation (5.50 (*a*)) gives

$$c_{sw} = \left(1 + \frac{\gamma+1}{2\gamma}\,\frac{\Delta p}{p_1}\right)^{1/2} a_1 \tag{5.50 (b)}$$

Comparison of Equations (5.38 (*c*)) and (5.50 (*b*)) shows that the non-steep wave moves faster than the steep wave.

Equations (5.49) and (5.50 (*a*)) yield

$$\frac{c_2}{a_1} = \frac{(p_2/p_1 - 1)}{\gamma\sqrt{\dfrac{\gamma-1}{2\gamma} + \dfrac{\gamma+1}{2\gamma}\,\dfrac{p_2}{p_1}}} \tag{5.51}$$

Now $$\left(\frac{a_2}{a_1}\right) = \left(\frac{T_2}{T_1}\right)^{1/2} = \left(\frac{p_2}{p_1}\,\frac{\rho_1}{\rho_2}\right)^{1/2}$$

Substituting for $\dfrac{\rho_1}{\rho_2}$ from Equation (5.40) in the above expression

$$\frac{a_2}{a_1} = \left(\frac{p_2}{p_1}\right)^{1/2}\left(1 - \frac{c_2}{c_{sw}}\right)^{1/2}$$

$$\frac{a_2}{a_1} = \left(\frac{p_2}{p_1}\right)^{1/2}\left(1 - \frac{c_2}{a_1}\,\frac{a_1}{c_{sw}}\right)^{1/2} \tag{5.52}$$

Substituting for c_2/a_1 and a_1/c_{sw} from Equations (5.51) and (5.50 (*a*)) respectively

$$\frac{a_2}{a_1} = \left(\frac{p_2}{p_1}\right)^{1/2}\left[1 - \frac{p_2/p_1 - 1}{\dfrac{\gamma-1}{2} + \dfrac{\gamma+1}{2}\,\dfrac{p_2}{p_1}}\right]^{1/2}$$

The above expression on simplification gives

$$\frac{a_2}{a_1} = \left(\frac{p_2}{p_1}\right)^{1/2}\left[\frac{\dfrac{\gamma+1}{\gamma-1} + \dfrac{p_2}{p_1}}{1 + \dfrac{\gamma+1}{\gamma-1}\,\dfrac{p_2}{p_1}}\right]^{1/2} \tag{5.53}$$

Division of Equation (5.51) by (5.53) gives

$$M_2 = \frac{c_2}{a_2}$$

$$= \frac{(p_2/p_1 - 1)}{\left[\gamma\left(\dfrac{\gamma-1}{2}\right)\left(1 + \dfrac{\gamma+1}{\gamma-1}\,\dfrac{p_2}{p_1}\right)\right]^{1/2}}\,\frac{\left(1 + \dfrac{\gamma+1}{\gamma-1}\,\dfrac{p_2}{p_1}\right)^{1/2}}{\left[\dfrac{p_2}{p_1}\left(\dfrac{\gamma+1}{\gamma-1} + \dfrac{p_2}{p_1}\right)\right]^{1/2}}$$

$$= \frac{(p_2/p_1 - 1)}{\left[\gamma\left(\dfrac{\gamma-1}{2}\right)\dfrac{p_2}{p_1}\left(\dfrac{\gamma+1}{\gamma-1} + \dfrac{p_2}{p_1}\right)\right]^{1/2}} \tag{5.54}$$

Calculations show that both the Equations (5.39) and (5.54) for the Mach numbers of the flows induced by the non-steep and the steep waves respectively give almost the same values; these are shown in Figure 5.11 against the pressure ratios across the waves.

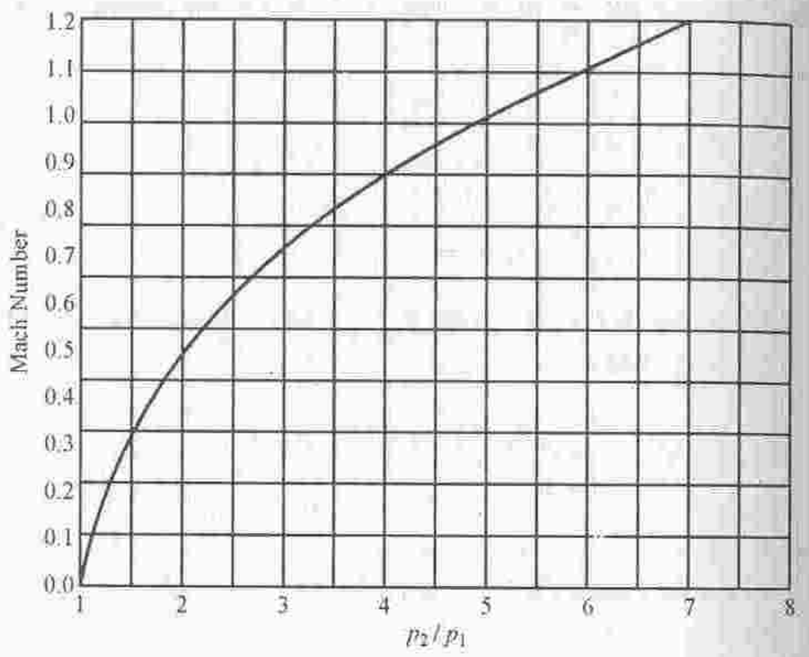

FIGURE 5.11 : Mach number of the flow induced by steep and non-steep waves ($\gamma = 1.4$)

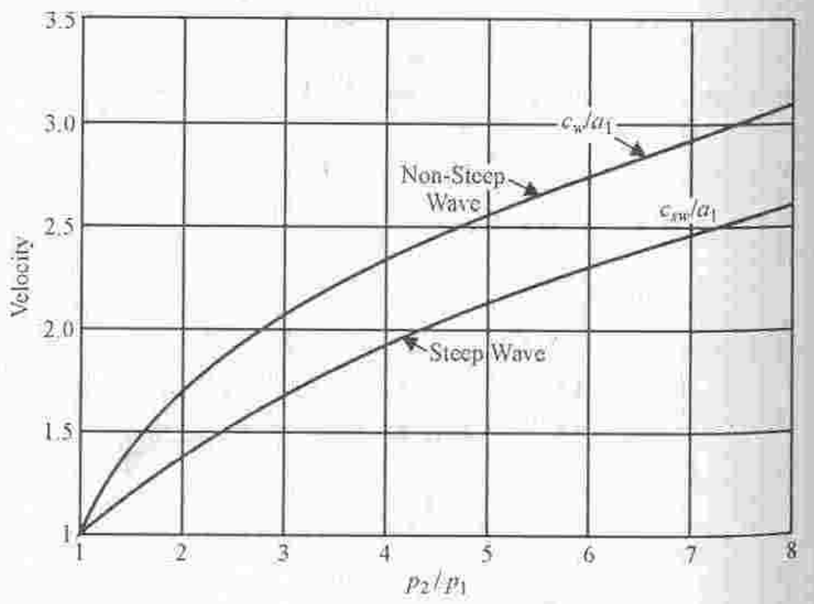

FIGURE 5.12 : Non-dimensional velocities of the non-steep and steep waves ($\gamma = 1.4$)

Figure 5.12 shows the non-dimensional velocities of the finite pressure waves given by the Equations (5.38 (*b*)) and (5.50). It is observed that the non-steep isentropic wave always moves faster than the steep pressure wave.

5.5 EXPANSION WAVES

An expansion (or rarefaction) wave is one which reduces the pressure of the fluid through which it is propagating. A sudden outward motion of the piston in a cylinder generates an expansion wave; expansion waves are also generated in a gas duct downstream of a valve which is suddenly closed as shown in Figure 5.15.

5.5.1 Infinitesimal Expansion Waves

An infinitesimal expansion wave is shown in Figure 5.13 (*a*) (compare it with the infinitesimal compression wave shown in Figure 5.7 (*a*)). This wave is moving towards the right at the velocity of sound into

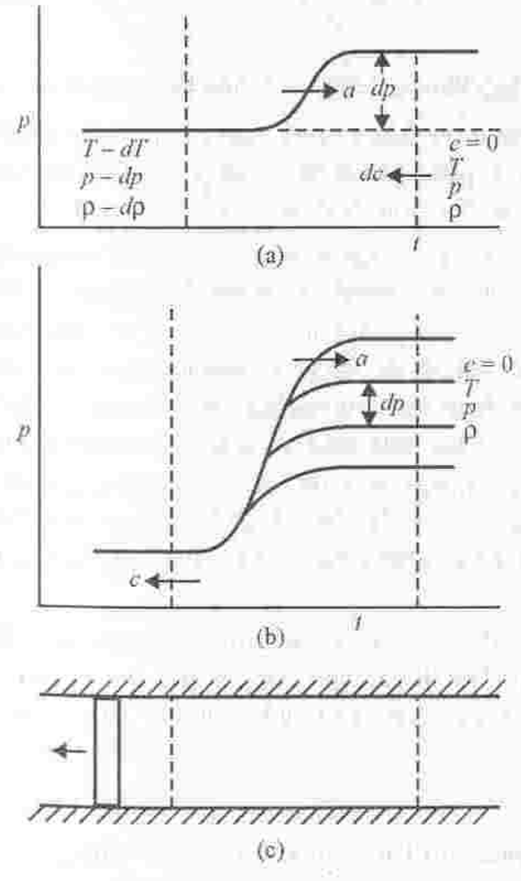

FIGURE 5.13 : Development of a non-steep finite expansion wave

the stagnant gas ($c = 0$) at a pressure and temperature of p and T respectively. The wave reduces the pressure and temperature of the gas by dp and dT respectively and induces a small leftward velocity dc. Thus the directions of the expansion wave propagation and the flow are opposite in contrast to the flow pattern discussed for the compression waves.

Equation (5.10) for an infinitesimal expansion wave can be written as

$$\frac{d\rho}{\rho} = -\frac{dc}{a} \tag{5.55}$$

Substituting for $d\rho$ from Equation (5.11)

$$\frac{dp}{\rho a^2} = -\frac{dc}{a}$$

$$dc = -\frac{dp}{a\rho} \tag{5.56}$$

5.5.2 Finite Amplitude Expansion Waves

In Section 5.3 the development of non-steep finite amplitude compression waves was explained. Here a flow model which is opposite of that considered in Section 5.3 will be discussed.

The piston moves to the left in a series of impulsive accelerations before achieving steady speed as shown in Figure 5.13 (*c*). This sends a series of right running expansion waves in the duct as shown in Figure 5.13 (*b*). The local velocity of sound ($a \propto \sqrt{T}$) in the fluid corresponding to the first wave is higher on account of the higher pressure and temperature of the gas into which it is moving, compared to the subsequent waves which will be moving in the gas at lower temperatures. This is because of the fact that the gas pressure and temperature continuously decrease after it has been traversed by a series of expansion waves.

The leftward motion of the piston induces a fluid velocity c towards the left. The local velocity of the waves with respect to the fluid is a. Therefore, the resultant velocity of the wave propagation towards the right is

$$c_w = a - c$$

With the motion of the piston, the gas velocity c towards the left is increasing, and the value of a is decreasing as explained before. As

a result the velocities of waves generated subsequently are progressively decreasing; in other words the slopes (dt/dx) of the waves are becoming steeper:

$$\left(\frac{dt}{dx}\right)_{IV} > \left(\frac{dt}{dx}\right)_{III}$$

This proves that the paths of these waves are diverging (as shown on the time-space diagram in Figure 5.14) in contrast to the path of

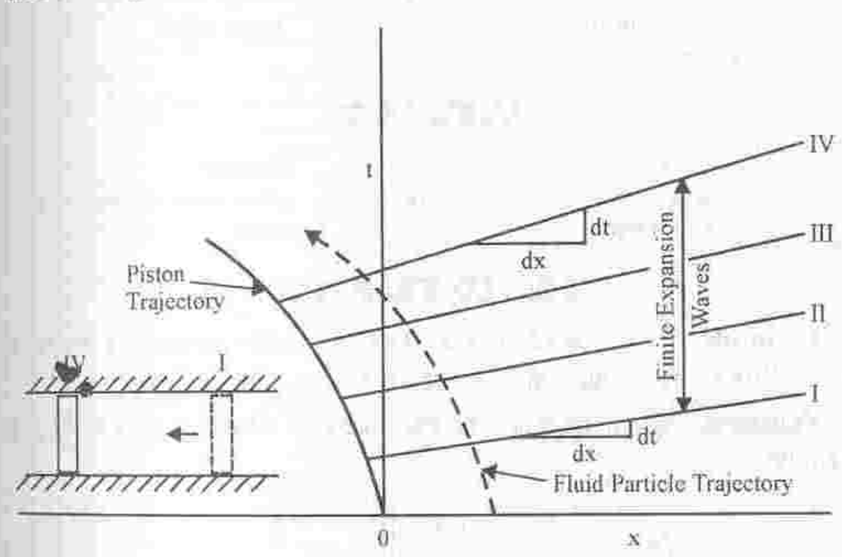

FIGURE 5.14 : Expansion waves in the direction opposite to the motion of the piston

the compression waves as shown in Figure 5.9; and the coalescence of a number of expansion waves into a steep expansion shock is not possible. This will be further discussed in the chapter on shocks.

Figure 5.13 (*b*) shows a finite amplitude non-steep expansion wave moving rightwards. The overall change of properties across this is made up of a number of infinitesimal isentropic changes (as in the infinitesimal wave). Therefore, the changes across a finite expansion wave are continuous and isentropic.

Since for the expansion waves the value of p/p_1 in Equation (5.35) is less than unity the fluid velocity will be negative.

NOTATION FOR CHAPTER 5

A	area of cross-section	$\dot{m}$	mass flow rate
a	velocity of sound	p	pressure

c	fluid or particle velocity	Δp	change in pressure
c'	perturbation velocity	R	gas constant
E	modulus of ealsticity of the solid medium	$\overline{R}$	universal gas constant
		t	time
f	stress	T	absolute temperature
f_1, f_2	functions	W	molecular weight
h	enthalpy	x	distance
K	bulk modulus of elasticity of the gas	$\gamma = c_p/c_v$	
		ρ	density
l	length	$\Delta\rho$	change in density
Δl	change in length	α	Mach angle
M	Mach number		

SUBSCRIPTS

1	initial state	s	isentropic
2	final state	sw	steep wave or shock wave
∞	undisturbed fluid	w	wave

SOLVED EXAMPLES

Example 5.1. Calculate the pressure ratio across an expansion wave moving into stagnant air for inducing sonic flow.

Solution. Mach number of the induced flow is given by Equation (5.39)

$$M = \frac{2}{\gamma - 1}\left[1 - \left(\frac{p_1}{p_2}\right)^{(\gamma-1)/2\gamma}\right]$$

In this case the directions of the wave propagation and the induced flow are opposite to each other. Therefore, $M = -c/a = -1$. The initial and final pressures in the fluid are p_1 and p_2 respectively. After the passage of the wave fluid pressure is reduced from p_1 to p_2.

$$-1 = \frac{2}{1.4 - 1}\left[1 - \left(\frac{p_1}{p_2}\right)^{(1.4-1)/2\times 1.4}\right]$$

$$\frac{p_1}{p_2} = 1.2^7 = 3.583$$

The pressure ratio across the wave is

$$p_2/p_1 = 1/3.583 = 0.279 \quad \textbf{Ans.}$$

Example 5.2. A long pipe conveys hot air ($p = 1.5$ bar, $T = 400$ K) at a Mach number of 0.4. Regulating valves are provided both at entry

and exit. Determine the pressure ratios across the waves and their velocities when:

(*a*) the entry valve is closed suddenly

(*b*) the exit valve is closed suddenly.

Assume constant area frictionless flow.

Solution. Refer to Figures 5.15 and 5.16.

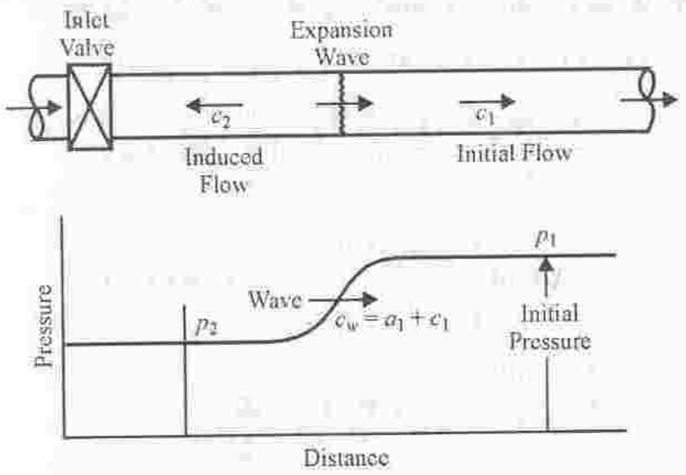

FIGURE 5.15 : Development of a finite expansion wave due to the closure of the inlet valve

(*a*) Closure of the entry valve:

$$a_1 = 20.1\sqrt{400} = 402 \text{ m/s}$$

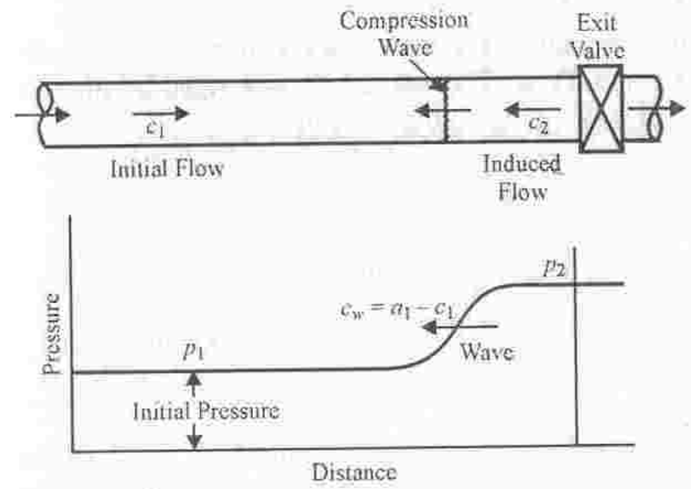

FIGURE 5.16 : Development of a finite compression wave due to the closure of the exit valve

$$c_1 = 0.4a_1 = 0.4 \times 402 = 160.8 \text{ m/s}$$

The induced flow velocity is given by

$$c_2 = \frac{2a_1}{\gamma - 1}\left[\left(\frac{p_2}{p_1}\right)^{0.143} - 1\right]$$

For the flow to stop, the velocity (c_2) induced by the rarefaction wave is equal and opposite to the initial velocity (c_1) *i.e.*,

$c_1 + c_2 = 0$, therefore,

$$\frac{2 \times 402}{0.4}\left[\left(\frac{p_2}{p_1}\right)^{0.143} - 1\right] + 160.8 = 0$$

$$2010\left[\left(\frac{p_2}{p_1}\right)^{0.143} - 1\right] + 160.8 = 0$$

$$\left(\frac{p_2}{p_1}\right)^{0.143} = 1 - 0.08 = 0.92$$

$$\frac{p_2}{p_1} = (0.92)^{1/0.143} = 0.558 \quad \textbf{Ans.}$$

$$c_w = c_1 + a_1$$

$$= 160.8 + 402 = 562.8 \text{ m/s}$$

(*b*) Closure of the exit valve:

In this case the compression wave moves against the direction of the initial flow. The velocity (c_2) induced by the wave is equal and opposite to the initial velocity (c_1)

$$-\frac{2a_1}{\gamma - 1}\left\{\left(\frac{p_2}{p_1}\right)^{0.143} - 1\right\} + c_1 = 0$$

$$-\left(\frac{p_2}{p_1}\right)^{0.143} + 1 + 0.08 = 0$$

$$\frac{p_2}{p_1} = (1.08)^7 = 1.714 \quad \textbf{Ans.}$$

$$c_w = a_1 - c_1$$

$$= 402 - 160.8$$

$$= 241.2 \text{ m/s} \quad \textbf{Ans.}$$

Example 5.3. A finite amplitude expansion wave with a pressure ratio of 1/1.35 across it traverses stagnant air at a pressure of 1.2 bar and temperature 300 K in a duct. Determine:

(*a*) velocity of the air in the duct,

(*b*) pressure and temperature of air, and

(*c*) velocity of the wave.

Solution. $c_2 = \frac{2a_1}{\gamma - 1}[p_r^{(\gamma-1)/2\gamma} - 1]$

$$a_1 = 20.1\sqrt{300}$$

$$= 348 \text{ m/s}$$

$$\frac{\gamma - 1}{2\gamma} = \frac{1.4 - 1}{2 \times 1.4} = 0.1428 \approx 0.143$$

$$c_2 = \frac{2 \times 348}{0.4}(1.35^{-0.143} - 1)$$

$$= 1740 \times \left(-\frac{0.0438}{1.0438}\right)$$

$$= -73 \text{ m/s}$$

$$a_2 = a_1\left(\frac{p_2}{p_1}\right)^{0.143} = \frac{348}{1.0438} = 333 \text{ m/s}$$

$$c_w = a_2 - c_2 = 333 - 73 = 260 \text{ m/s}$$

$$p_2 = \frac{1.2}{1.35} = 0.892 \text{ bar} \quad \textbf{Ans.}$$

$$\frac{T_2}{T_1} = \left(\frac{p_2}{p_1}\right)^{(\gamma-1)/\gamma} = \left(\frac{1}{1.35}\right)^{0.286} = \frac{1}{1.09}$$

$$T_2 = \frac{300}{1.09} = 276 \text{ K} \quad \textbf{Ans.}$$

Example 5.4. If the pressure wave in Example 5.3 is a compression wave determine for a pressure ratio of 1.35.

(*a*) velocity of air in the duct,

(*b*) pressure and temperature of air in the duct, and

(*c*) velocity of the wave.

Solution. $$c_2 = \frac{2a_1}{\gamma - 1}\left\{\left(\frac{p_2}{p_1}\right)^{(\gamma-1)/2\gamma} - 1\right\}$$

$$= \frac{2 \times 348}{0.4} = (1.0438 - 1) = 76.2 \text{ m/s}$$

$$a_2 = a_1\left(\frac{p_2}{p_1}\right)^{(\gamma-1)/\gamma} = 348 \times 1.0438 = 363 \text{ m/s}$$

$$c_w = c_2 + a_2$$

$$= 76.2 + 363 = 439.2 \text{ m/s} \quad \textbf{Ans.}$$

$$p_2 = 1.2 \times 1.35 = 1.62 \text{ bar} \quad \textbf{Ans.}$$

$$\frac{T_2}{T_1} = \left(\frac{p_2}{p_1}\right)^{(\gamma-1)/\gamma} = 1.35^{0.286} = 1.09$$

$$T_2 = 1.09 \times 300 = 327 \text{ K} \quad \textbf{Ans.}$$

Example 5.5. Derive the following relations for the non-steep finite pressure waves:

(*i*) $c = \pm \dfrac{2}{\gamma - 1}(a - a_1)$

(*ii*) $c_w = a_1 \pm \dfrac{\gamma + 1}{2} c$

where a_1 and ρ_1 refer to the stagnant fluid into which the wave is moving.

Solution. The flow through a non-steep compression or expansion wave is isentropic. Therefore,

$$\left(\frac{a}{a_1}\right) = \left(\frac{T}{T_1}\right)^{1/2} = \left(\frac{\rho}{\rho_1}\right)^{(\gamma-1)/2} = \left(\frac{p}{p_1}\right)^{(\gamma-1)/2\gamma} \tag{1}$$

(*i*) The fluid velocity as given by Equation (5.35) is

$$c = \frac{2a_1}{\gamma - 1}\left\{\left(\frac{p}{p_1}\right)^{(\gamma-1)/2\gamma} - 1\right\}$$

Substituting from Equation (1)

$$c = \frac{2a_1}{\gamma - 1}\left(\frac{a}{a_1} - 1\right)$$

To represent the fluid velocity for both compression and expansion waves the above expression can be written in a general form as

$$c = \pm \frac{2}{\gamma - 1}(a - a_1) \tag{2}$$

(*ii*) By rearrangement Equation (2) may be written as

$$a = a_1 \pm \frac{\gamma - 1}{2} c \tag{3}$$

The velocity of the wave is given by

$$c_w = a \pm c$$

Substituting from Equation (3) for the velocity (*a*)

$$c_w = a_1 \pm \frac{\gamma - 1}{2} c \pm c$$

$$c_w = a_1 \pm \frac{\gamma + 1}{2} c.$$

Example 5.6. Compare the final values of the pressure in a duct generated by sudden closure of the exit valve with:

(*a*) Hydrogen, $\gamma = 1.4$, $R = 4125$ J/kg K

(*b*) Air, $\gamma = 1.4$, $R = 287$ J/kg K

(*c*) Freon, $\gamma = 1.2$, $R = 135$ J/kg K

The initial flow conditions in each case are:

pressure 10 bar,

temperature 400 K,

velocity 100 m/s.

Solution. (*a*) Hydrogen

$$a_1 = \sqrt{\gamma R T_1}$$

$$a_1 = \sqrt{1.4 \times 4125 \times 400} = 1519.80 \text{ m/s}$$

$$\frac{\gamma - 1}{2\gamma} = \frac{1.4 - 1}{2 \times 1.4} = 0.1428$$

For initial and final pressures p_1 and p_2 Equation (5.35), gives

$$\frac{2a_1}{\gamma-1}\left[\left(\frac{p_2}{p_1}\right)^{(\gamma-1)/2\gamma}-1\right]=c_1$$

$$\left(\frac{p_2}{p_1}\right)^{(\gamma-1)/2\gamma}=1+\frac{\gamma-1}{2a_1}c_1$$

$$\left(\frac{p_2}{p_1}\right)^{0.1428}=1+\frac{0.4\times100}{2\times1519.80}=1.013$$

$$\frac{p_2}{p_1}=1.0946,\ p_2=10.946\text{ bar}\quad\textbf{Ans.}$$

(*b*) Air $a_1=\sqrt{1.4\times287\times400}=400.89$ m/s

$$\frac{\gamma-1}{2\gamma}=0.1428$$

$$\left(\frac{p_2}{p_1}\right)^{0.1428}=1+\frac{0.4\times100}{2\times400.89}=1.0498$$

$$\frac{p_2}{p_1}=1.405,\ p_2=10\times1.405=14.05\text{ bar}\quad\textbf{Ans.}$$

(*c*) Freon $a_1=\sqrt{1.2\times135\times400}=254.56$ m/s

$$\frac{\gamma-1}{2\gamma}=\frac{1.2-1}{2\times1.2}=0.0833$$

$$\left(\frac{p_2}{p_1}\right)^{0.0833}=1+\frac{0.2\times100}{2\times254.56}=1.0392$$

$$\frac{p_2}{p_1}=1.586,\ p_2=10\times1.586=15.86\text{ bar}\quad\textbf{Ans.}$$

It is observed that the pressure rise on account of the passage of the compression wave is least in hydrogen and maximum in freon. This is on account of the large difference in the velocity of sound in these gases.

Example 5.7. Two separate ducts of constant area contain stagnant air ($\gamma=1.4$) and ethane ($\gamma=1.25$) respectively. Compression waves of pressure ratio = 1.5 are propagated in these ducts. Determine for non-

steep and steep waves the wave Mach numbers and the Mach numbers of the flow induced by these waves in each case.

Solution. (*a*) Non-steep waves

Equations (5.38 (*a*)) and (5.39) give the Mach numbers of the wave and the induced flow:

$$M_w=\frac{c_w}{a_1}=\frac{\gamma+1}{\gamma-1}\left(\frac{p_2}{p_1}\right)^{(\gamma-1)/2\gamma}-\frac{2}{\gamma-1}$$

$$M=\frac{2}{\gamma-1}\left\{1-\left(\frac{p_1}{p_2}\right)^{(\gamma-1)/2\gamma}\right\}$$

(*i*) Air ($\gamma=1.4$),

$$\frac{\gamma-1}{2\gamma}=\frac{1}{7}$$

$$M_w=\frac{1.4+1}{1.4-1}(1.5)^{1/7}-\frac{2}{1.4-1}=1.357\quad\textbf{Ans.}$$

$$M=\frac{2}{1.4-1}\left\{1-\left(\frac{1}{1.5}\right)^{1/7}\right\}=0.281\quad\textbf{Ans.}$$

(*ii*) Ethane ($\gamma=1.25$),

$$\frac{\gamma-1}{2\gamma}=\frac{1}{10}=0.1$$

$$M_w=\frac{1.25+1}{1.25-1}(1.5)^{0.1}-\frac{2}{1.25-1}=1.372\quad\textbf{Ans.}$$

$$M=\frac{2}{1.25-1}\left\{1-\left(\frac{1}{1.5}\right)^{0.1}\right\}=0.318\quad\textbf{Ans.}$$

(*b*) Steep Waves

Equations (5.50) and (5.54) give the Mach numbers of the wave and the induced flow

$$M_w=\left\{\frac{\gamma-1}{2\gamma}+\frac{\gamma+1}{2\gamma}\frac{p_2}{p_1}\right\}^{1/2}$$

$$M=\frac{p_2/p_1-1}{\left\{\gamma\left(\frac{\gamma-1}{2}\right)\frac{p_2}{p_1}\left(\frac{\gamma+1}{\gamma-1}+\frac{p_2}{p_1}\right)\right\}^{1/2}}$$

(*i*) Air $M_w = \left(\frac{1.4-1}{2\times 1.4} + \frac{1.4+1}{2\times 1.4} \times 1.5 \right)^{1/2} = 1.195$ **Ans.**

$$M = \frac{1.5-1}{\left\{ 1.4 \left(\frac{1.4-1}{2} \right) \times 1.5 \times \left(\frac{1.4+1}{1.4-1} + 1.5 \right) \right\}^{1/2}} = 0.281 \quad \textbf{Ans.}$$

(*ii*) Ethane $M_w = \left(\frac{1.25-1}{2\times 1.25} + \frac{1.25+1}{2\times 1.25} \times 1.5 \right)^{1/2} = 1.204$ **Ans.**

$$M = \frac{1.5-1}{\left\{ 1.25 \left(\frac{1.25-1}{2} \right) \times 1.5 \times \left(\frac{1.25+1}{1.25-1} + 1.5 \right) \right\}^{1/2}} = 0.318 \quad \textbf{Ans.}$$

Example 5.8. (*a*) Prove that the ratio of the velocities of sound across the steep wave in a constant area duct is given by

$$\frac{a_2^2}{a_1^2} = \left(\frac{p_2}{p_1} \right) \left(1 - \frac{p_2/p_1 - 1}{\frac{\gamma-1}{2} + \frac{\gamma+1}{2} \frac{p_2}{p_1}} \right)$$

(*b*) From the above relation obtain the following relations for pressure and density ratios:

$$\frac{p_2}{p_1} = \frac{\frac{\gamma+1}{\gamma-1} \frac{\rho_2}{\rho_1} - 1}{\frac{\gamma+1}{\gamma-1} - \frac{\rho_2}{\rho_1}}$$

$$\frac{\rho_2}{\rho_1} = \frac{1 + \frac{\gamma+1}{\gamma-1} \frac{p_2}{p_1}}{\frac{\gamma+1}{\gamma-1} + \frac{p_2}{p_1}}$$

Solution. (*a*) The required expression has been derived in Section 5.4.2 as Equation (5.53).

(*b*) Writing velocities of sound in terms of temperatures we get

$$\frac{a_2^2}{a_1^2} = \frac{\gamma R T_2}{\gamma R T_1} = \frac{p_2}{p_1} \left(1 - \frac{p_2/p_1 - 1}{\frac{\gamma-1}{2} + \frac{\gamma+1}{2} \frac{p_2}{p_1}} \right)$$

$$\frac{p_1}{T_1} \frac{T_2}{p_2} = \frac{\frac{\gamma+1}{2} \left(1 + \frac{p_2}{p_1} \right) - \frac{p_2}{p_1}}{\frac{\gamma-1}{2} + \frac{\gamma+1}{2} \frac{p_2}{p_1}}$$

$$\frac{\rho_1}{\rho_2} = \frac{\frac{\gamma+1}{2} + \frac{\gamma-1}{2} \frac{p_2}{p_1}}{\frac{\gamma-1}{2} \left(1 + \frac{\gamma+1}{\gamma-1} \frac{p_2}{p_1} \right)}$$

The above expression on rearrangement yields

$$\frac{\rho_2}{\rho_1} = \frac{1 + \frac{\gamma+1}{\gamma-1} \frac{p_2}{p_1}}{\frac{\gamma+1}{\gamma-1} + \frac{p_2}{p_1}} \quad \textbf{Ans.}$$

$$\frac{\rho_2}{\rho_1} \frac{\gamma+1}{\gamma-1} + \frac{\rho_2}{\rho_1} \frac{p_2}{p_1} = 1 + \frac{\gamma+1}{\gamma-1} \frac{p_2}{p_1}$$

$$\frac{p_2}{p_1} \left(\frac{\gamma+1}{\gamma-1} - \frac{\rho_2}{\rho_1} \right) = \frac{\rho_2}{\rho_1} \frac{\gamma+1}{\gamma-1} - 1$$

$$\frac{p_2}{p_1} = \frac{\frac{\gamma+1}{\gamma-1} \frac{\rho_2}{\rho_1} - 1}{\frac{\gamma+1}{\gamma-1} - \frac{\rho_2}{\rho_1}} \quad \textbf{Ans.}$$

QUESTIONS AND PROBLEMS

5.1 What is the chief difference between steep and non-steep compression waves? How are they formed? Why is it not possible to generate a steep rarefaction wave?

5.2 Derive the following relations for infinitesimal waves in elastic solids and fluids:

(*a*) $E = \rho a^2$

(*b*) $K = \rho a^2$

(*c*) $a^2 = \left(\frac{\partial p}{\partial \rho}\right)_s = \frac{\gamma p}{\rho} = \gamma RT.$

5.3 Develop the following relations for a sound wave:

(*a*) $\frac{\partial^2 p}{\partial t^2} - a_\infty^2 \frac{\partial^2 p}{\partial x^2} = 0$

(*b*) $\frac{\partial^2 \rho}{\partial t^2} - a_\infty^2 \frac{\partial^2 \rho}{\partial x^2} = 0$

(*c*) $\frac{\partial^2 c}{\partial t^2} - a_\infty^2 \frac{\partial^2 c}{\partial x^2} = 0$

State the assumptions used.

5.4 Give two practical examples of each where the following waves occur:

(*a*) Infinitesimal pressure wave,

(*b*) Finite non-steep compression wave,

(*c*) Finite non-steep expansion wave, and

(*d*) Steep compression waves.

5.5 (*a*) If the Mach number of a steep pressure wave with respect to the stagnant gas is M_x show that the pressure ratio across this wave is given by

$$\frac{p_2}{p_1} = \frac{2\gamma}{\gamma+1} M_x^2 - \frac{\gamma-1}{\gamma+1}$$

(*b*) The pressure ratio across a steep wave is 3.5. If the initial pressure and temperature of the gas at rest are 1.38 bar and 310 K respectively, determine the velocity of the wave and the Mach number of the flow induced by the wave.

Take $\gamma = 1.3$, $c_p = 2.26$ kJ/kg K.

Ans. (821.54 m/s, 0.905).

5.6 (*a*) Show that the Mach number of the flow in a gas which has been traversed by an isentropic finite amplitude pressure wave (pressure ratio p_r) is given by

$$M = \frac{2}{\gamma-1}\{1 - p_r^{(\gamma-1)/2\gamma}\}$$

(*b*) Show that for inducing sonic velocity in a gas ($\gamma = 1.4$) the pressure ratio required for a compression wave is 4.77.

5.7 Describe with the aid of sketches the development of a finite amplitude rarefaction wave. Show the directions of flow and the wave propagation.

5.8 An emergency governor shuts off the flow in a steam pipe carrying steam at a pressure of 98 bar and temperature 800 K. The initial velocity of steam in the pipe is 85 m/s. Determine the amplitude and the velocity of the pressure waves generated. Take $\gamma = 1.28$, $R = 480$ J/kg K.

Ans. 16.29 bar, 798 m/s (upstream of the valve), 13.96 bar, 607 m/s (downstream of the valve).

5.9 For a steep compression wave derive expressions for:

(*a*) The Mach number (M_2) of the flow induced when the wave passes through stagnant gas.

(*b*) The Mach number (M_{sw}) of the wave with respect to the stagnant gas.

(*c*) Show that for air their values are:

$$M_2 = \frac{p_2/p_1}{\left[0.28\frac{p_2}{p_1}\left(6+\frac{p_2}{p_1}\right)\right]^{1/2}}$$

$$M_{sw} = \sqrt{\frac{1}{7}\left(1+6\frac{p_2}{p_1}\right)}$$

(*d*) Determine the pressure ratio across a steep wave which will induce sonic flow. (4.83).

(*e*) Determine the pressure ratio across the wave when its Mach number is unity. Comment on the value so determined.

5.10 Determine the final values of the pressure downstream of the duct in Exercise (5.6). State the assumptions used.

Ans. (*a*) 9.11 bar, (*b*) 7.0 bar, (*c*) 6.18 bar.

5.11 Steam at $p_1 = 15$ bar, $T_1 = 500$ K flows in a constant area pipe-line at 100 m/s. If a valve in the pipe-line is suddenly closed calculate

the pressure and temperature reached upstream and downstream of the valve. For steam take $\gamma = 1.348$, $R = 566$ J/kg K.

Ans. Upstream: $p = 18.530$ bar, $T = 528.5$ K,
downstream: $p = 12.03$ bar, $T = 472$ K.

5.12 The density ratio across a steep pressure wave moving into stagnant air in a constant area duct is 2.0. Calculate (*a*) the pressure and temperature ratios across the wave and (*b*) the wave Mach number and the Mach number of the induced flow.

Ans. (*a*) 2.75, 1.375 (*b*) 1.581, 0.672.

5.13 In an experiment the density of water is increased by 130 kg/m^3 by applying a pressure of 36×10^7 N/m^2. Determine the velocity of the infinitesimal pressure waves in water.

Ans. $a = 1664.4$ m/s.

5.14 Calculate the values of the pressure ratios required across the compression and expansion waves to produce a Mach number of 0.5 in stagnant air.

Ans. 2.09, 0.513.

6

Flow With Normal Shock Waves

Wave motion in general has been discussed in the previous chapter. A shock wave is a special kind of wave referred to as a steep finite pressure wave. The changes in the flow properties across such a wave are abrupt. The normal shock wave is perpendicular to the one dimensional flow.

In some situations shocks are undesirable because they interfere with the normal flow behaviour. For example in turbomachines if the areas and profiles of flow passages are incorrectly designed shock may occur on account of supersonic flow developed due to local accelerations.

These shocks may be normal or inclined to the direction of local flow; they may cause boundary layer separation and deviation of flow from its designed direction. It will be shown later that there is a loss in stagnation pressure and increase in entropy across a shock wave. Thus the efficiencies of machines experiencing shock waves are considerably low.

Other undesirable forms of the shock waves are the sonic boom created by supersonic aircrafts and the blast waves generated by an explosion. These wave have a damaging effect on human life and buildings.

Some useful applications of the shock waves are in the shock tubes and supersonic compressors. A strong moving shock wave is utilized to accelerate the flow to a high Mach number in a shock tube where flow behaviour at high Mach numbers can be studied.

On account of abrupt changes of pressure, density etc., across shock waves, they are profitably used in supersonic compressors to obtain considerably high pressure ratios in one stage; in such compressors the pressure ratio developed per stage may be as high as 10.0.

6.1 DEVELOPMENT OF A SHOCK WAVE

Though the development of a shock wave (steep finite pressure wave) has been described in the previous chapter, events leading to a shock wave will be summarized here.

It was pointed out in Section 4.7.2 that for some off-design values of the pressure ratio in a convergent-divergent nozzle the variation in the fluid properties is sudden and the flow changes from supersonic to subsonic at some sections in the divergent portion; this is due to the formation of "finite wave fronts" or shock waves at these sections. The thickness of such waves is of the order of 10^{-3} mm which is comparable with the mean free path of the gas molecules.

Figure 6.1 (*a*) shows a constant area duct which initially contains a gas at rest. Pressure pulses (infinitesimal pressure waves) are transmitted through the gas to the right by the rightward movement of the piston in instantaneous impulses. The growth of one such wave at time t_1, t_2, t_3, ... is shown in Figure 6.1 (*b*); the waves travel towards the

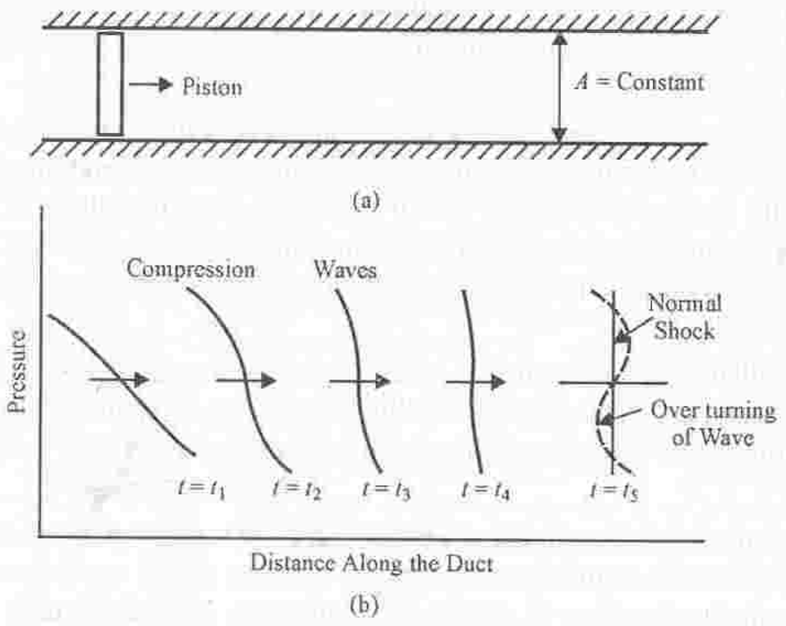

FIGURE 6.1 : Development of a normal shock wave

right with the speed of sound (corresponding to the prevailing temperature) relative to the gas. The portion of the gas which has been traversed by the pressure waves is set in motion. The gas nearer the piston moves at a higher velocity than the gas in the downstream region.

Similarly the pressure of the gas in the regions closer to the piston is higher than in the regions downstream. On account of this, isentropic expansion of the higher pressure gas on the upstream side occurs continuously towards the lower pressure regions downstream. Thus pressure and temperature gradients along the duct length are established. On account of the higher temperature the speed of sound is higher in the upstream regions. Therefore, the pressure waves in the upstream region travel at higher velocities on account of higher gas velocity and speed of sound. Thus the upstream waves are continuously overtaking those in the downstream region.

On account of the above phenomena the weak pressure wave generated at time $t = t_1$ grows stronger and steeper as it moves further towards the right. This is due to the other waves overtaking the wave under consideration and consequently strengthening it. If this continuous growth continues, at some stage (as at time t_5) it will overturn; this wave form is not possible on account of the impossibility of three different values of pressure occurring simultaneously. Therefore, the extreme form of the wave is vertical. This vertical wave front of finite amplitude is the shock wave across which the changes in pressure, temperature, density, velocity and Mach number are abrupt.

6.2 RAREFACTION WAVE

In this section the possibility of a "rarefaction shock" is discussed. The development of a finite amplitude rarefaction or expansion wave has been explained in Section 5.5.2.

Figure 6.2 shows the wave forms at time $t = t_1, t_2, \ldots$ of a wave generated at time by the leftward movement of a piston in the duct. Here also as in the previous case, a series of rarefaction waves are generated by the movement of the piston in instantaneous impulses. Once a wave has traversed the gas its pressure and temperature are lowered. Therefore, the subsequent waves will travel at lower velocities on account of lower temperatures. The wave velocities are further reduced because the fluid motion is occurring against the direction of wave propagation. As a result of the cumulative effect of the above phenomena the waves generated later lag behind the waves which were generated earlier. Therefore, in contrast to the compression waves, here

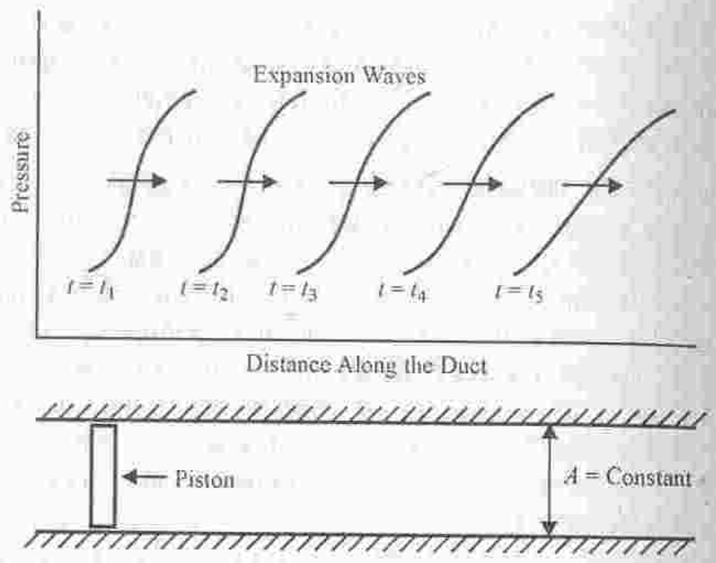

FIGURE 6.2 : Development of expansion waves

the subsequent waves cannot strengthen the earlier wave by coalescence. On the contrary, wave becomes weaker (flatter) as it moves further. Due to this spreading out of rarefaction waves with time a steep wave front or a "rarefaction shock" cannot develop. Hence rarefaction shocks are not possible.

6.3 THE GOVERNING EQUATIONS

Figure 6.3 shows a normal shock wave in a constant area frictionless duct; the shock wave is considered to be contained in a control volume. Continuity, momentum, energy and the state equations govern the flow through the shock. Figure 6.4 shows the conditions of the flow upstream and downstream of a shock wave on an enthalpy-entropy diagram. It must be noted that the state of the gas before and after the shock lies on both the curves which satisfy the aforementioned four equations.

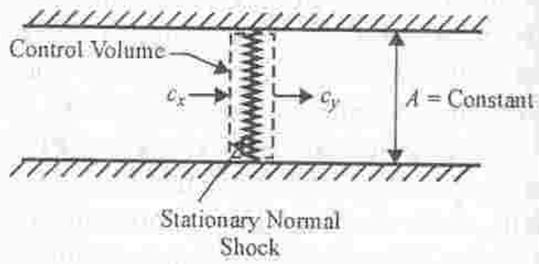

FIGURE 6.3 : Flow through a normal shock in a constant area duct

Continuity equation for the shock waves gives the flow rate as

$$\dot{m} = \rho_x A_x c_x = \rho_y A_y c_y$$

Since $$A_x = A_y = A = \text{constant}$$

$$\frac{\dot{m}}{A} = \rho_x c_x = \rho_y c_y \tag{6.1}$$

If heat transfer is assumed negligible, in the absence of shaft work application of the adiabatic energy equation for the control volume containing the shock gives

$$h_{0x} = h_{0y} = h_0 = \text{constant}$$

$$T_{0x} = T_{0y} = T_0 = \text{constant}$$

$$h_x + \frac{1}{2} c_x^2 = h_y + \frac{1}{2} c_y^2 \tag{6.2}$$

Momentum equation gives

$$(p_x - p_y) A = \dot{m} (c_y - c_x)$$

$$p_x - p_y = \frac{\dot{m}}{A} (c_y - c_x) \tag{6.3}$$

Equations (6.1) and (6.3) give

$$p_x + \rho_x c_x^2 = p_y + \rho_y c_y^2 \tag{6.4}$$

Definition of impulse function in Equation (6.4) gives

$$F_x = F_y = \text{constant} \tag{6.5}$$

The equation of state gives

$$h = f(s, \rho)$$

$$s = f(p, \rho) \tag{6.6}$$

These equations will now be used to define two important curves known as Fanno and Rayleigh lines.

6.3.1 Fanno Line

Fanno line describes an adiabatic flow process in a constant area duct with friction. The stagnation enthalpy and the flow rate per unit area remain constant. On account of friction the process is irreversible. The process is governed by the Equations of continuity, energy and state.

Equations (6.1), (6.2) and (6.6) are rewritten in the following form:

$$\rho_y = \left(\frac{\dot{m}}{A} \right) \frac{1}{c_y} \tag{6.7}$$

$$h_y = h_0 - \frac{1}{2} c_y^2 \tag{6.8}$$

$$s_y = f(p_y, \rho_y) \tag{6.9}$$

Equations (6.7), (6.8) and (6.9) for different values of c_y define the Fanno line on the enthalpy-entropy diagram shown in Figure 6.4. The constant pressure lines have also been shown for studying changes in pressure in a given Fanno process.

Now an infinitesimal Fanno process is considered in the vicinity of the maximum entropy point F. The changes being small the process may be considered as reversible ($\Delta s = 0$) near point F. For this process we have

$$h + \frac{1}{2} c^2 = \text{constant}$$

$$dh = -c\,dc \text{ (energy equation)} \tag{6.10}$$

Equation (6.1) gives

$$\rho c = \text{constant}$$

$$\rho \,.\, dc + c \,.\, d\rho = 0$$

$$dc = -\frac{c}{\rho} d\rho \text{ (continuity equation)} \tag{6.11}$$

For an isentropic process,

$$dh = \frac{1}{\rho} dp \tag{6.12}$$

Substituting Equations (6.11) and (6.12) in (6.10) gives

$$c^2 = a^2 = \frac{dp}{d\rho} = \left(\frac{\partial p}{\partial \rho} \right)_s \tag{6.13}$$

Equation (6.13) demonstrates that the gas velocity at the maximum entropy point (F) on the Fanno line is sonic ($M = 1$). It can also be shown that the upper branch of this curve represents subsonic flow and the lower branch supersonic flow. This will again be discussed in Chapter 8.

6.3.2 Rayleigh Line

Rayleigh line describes a frictionless flow process in a constant area duct with heat transfer. Here also the flow rate per unit area remains constant. The process is governed by the equations of continuity, momentum and state. Equations (6.1), (6.4), (6.6) for this process are

$$\rho_y = \left(\frac{\dot{m}}{A} \right) \frac{1}{c_y} \tag{6.7}$$

$$p_y = (p_x + \rho_x c_x^2) - \rho_y c_y^2 \tag{6.14}$$

$$s_y = f(\rho_y, p_y) \tag{6.15}$$

Equations (6.7), (6.14) and (6.15) for different values of c_y define the Rayleigh line on the enthalpy-entropy diagram shown in Figure 6.4. The maximum entropy point on this curve is R. An infinitesimal process is now considered in the vicinity of this point.

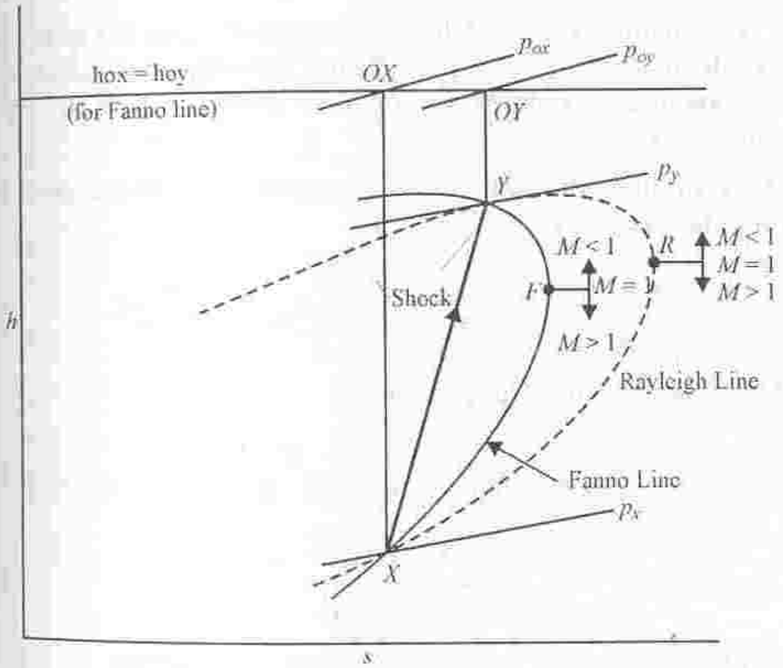

FIGURE 6.4 : Normal shock on Fanno and Rayleigh curves

The momentum Equation gives

$$p + \rho c^2 = \text{constant}$$

$$dp + c^2\, d\rho + 2\rho c\, dc = 0 \tag{6.16}$$

Substituting from Equation (6.11) in (6.16) and simplifying

$$c^2 = \frac{dp}{d\rho}$$

Since the changes are small during the process in the vicinity of point R it can be considered as isentropic ($\Delta s = 0$). Therefore,

$$c^2 = a^2 = \left(\frac{\partial p}{\partial \rho}\right)_s \tag{6.17}$$

This demonstrates that the gas velocity at the maximum entropy point on the Rayleigh line is sonic ($M = 1$). The upper branch of this curve represents subsonic flow and the lower branch supersonic flow. This will be proved in Chapter 9.

Since the shock occurs from supersonic to subsonic flow it is shown from X to Y on Fanno and Rayleigh lines in Figure 6.4.

6.4 PRANDTL-MEYER RELATION

In this section fundamental relation between the gas velocities before and after the normal shock and the critical velocity of sound is derived. This is known as Prandtl-Meyer relation which is the basis of other Equations for shock waves.

Applying the adiabatic energy Equation (2.47) to the flow before and after the shock wave we get

$$\frac{a_x^2}{\gamma - 1} + \frac{1}{2}c_x^2 = \frac{a_y^2}{\gamma - 1} + \frac{1}{2}c_y^2 = \frac{1}{2}\frac{\gamma + 1}{\gamma - 1}a^{*2} \tag{2.47}$$

First part of this equation gives

$$a_x^2 = \frac{\gamma + 1}{2}a^{*2} - \frac{\gamma - 1}{2}c_x^2$$

$$\frac{a_x^2}{c_x} = \frac{\gamma + 1}{2}\frac{a^{*2}}{c_x} - \frac{\gamma - 1}{2}c_x \tag{6.18}$$

Similarly the other part of Equation (2.47) gives

$$\frac{a_y^2}{c_y} = \frac{\gamma + 1}{2}\frac{a^{*2}}{c_y} - \frac{\gamma - 1}{2}c_y \tag{6.19}$$

Equation (6.3) gives

$$(p_x - p_y)\frac{A}{\dot{m}} = c_y - c_x$$

Substituting for $A/\dot{m}$ from Equation (6.1)

$$\frac{p_x}{\rho_x c_x} - \frac{p_y}{\rho_y c_y} = c_y - c_x$$

$$\frac{1}{c_x}\frac{\gamma p_x}{\rho_x} - \frac{1}{c_y}\frac{\gamma p_y}{\rho_y} = \gamma(c_y - c_x)$$

But $$\frac{\gamma p_x}{\rho_x} = a_x^2 \text{ and } \frac{\gamma p_y}{\rho_y} = a_y^2$$

Therefore, $$\frac{a_x^2}{c_x} - \frac{a_y^2}{c_y} = \gamma(c_y - c_x) \tag{6.20}$$

Introduction of Equations (6.18) and (6.19) in (6.20) gives

$$\frac{\gamma + 1}{2}\frac{a^{*2}}{c_x} - \frac{\gamma - 1}{2}c_x - \frac{\gamma + 1}{2}\frac{a^{*2}}{c_y} + \frac{\gamma - 1}{2}c_y = \gamma(c_y - c_x)$$

$$\frac{\gamma + 1}{2}a^{*2}\left(\frac{1}{c_x} - \frac{1}{c_y}\right) + \frac{\gamma - 1}{2}(c_y - c_x) = \gamma(c_y - c_x)$$

$$\frac{\gamma + 1}{2}a^{*2}\left(\frac{c_y - c_x}{c_x c_y}\right) + \frac{\gamma - 1}{2}(c_y - c_x) = \gamma(c_y - c_x)$$

$$\frac{\gamma + 1}{2}a^{*2} + \frac{\gamma - 1}{2}c_x c_y = \gamma c_x c_y$$

This expression on simplification and rearrangement yields

$$c_x \cdot c_y = a^{*2} \text{ (Prandtl-Meyer relation)} \tag{6.21}$$

$$\frac{c_x}{a^*} \cdot \frac{c_y}{a^*} = 1$$

Now $$T_x^* = \frac{2}{\gamma + 1}T_{0x} = T_y^* = \frac{2}{\gamma + 1}T_{0y}$$

$$a_x^* = \sqrt{\gamma R T_x^*},\ a_y^* = \sqrt{\gamma R T_y^*}$$

Therefore, $$a^* = a_x^* = a_y^*$$

$$\frac{c_x}{a_x^*} \cdot \frac{c_y}{a_y^*} = 1$$

But $$\frac{c_x}{a_x^*} = M_x^* \text{ and } \frac{c_y}{a_y^*} M_y^*$$

Therefore, $M_x^* \cdot M_y^* = 1$ (6.22)

This is another useful form of the Prandtl-Meyer relation.

6.5 MACH NUMBER DOWNSTREAM OF THE NORMAL SHOCK WAVE

Generally the upstream Mach number (M_x) in a given problem is known and it is desired to determine the Mach number (M_y) downstream of the shock wave.

It will be seen in this section that the only independent parameter required for a given gas (of $\gamma = c_p/c_v$) to determine the downstream Mach number is the upstream Mach number.

Equation (2.43) for adiabatic flow of a perfect gas gives

$$a^{*2} = \frac{2\gamma}{\gamma+1} RT_0 \tag{2.43}$$

Equations (6.21) and (2.43) give

$$c_x \cdot c_y = \frac{2\gamma}{\gamma+1} RT_0 \tag{6.23}$$

But $$c_x = M_x a_x = M_x \sqrt{\gamma RT_x}$$

$$c_y = M_y a_y = M_y \sqrt{\gamma RT_y}$$

Substituting these values in Equation (6.23)

$$M_x \sqrt{\gamma RT_x} \cdot M_y \sqrt{\gamma RT_y} = \frac{2\gamma}{\gamma+1} RT_0$$

Rearranging and squaring both sides

$$M_x^2 \cdot M_y^2 = \left(\frac{2}{\gamma+1}\right)^2 \frac{T_0}{T_x} \frac{T_0}{T_y}$$

Substituting the values of T_0/T_x and T_0/T_y for adiabatic flow

$$M_x^2 \cdot M_y^2 = \left(\frac{2}{\gamma+1}\right)^2 \left(1+\frac{\gamma-1}{2} M_x^2\right)\left(1+\frac{\gamma-1}{2} M_y^2\right)$$

This is a convernient form to solve for M_y^2. After some algebraic steps it gives

$$M_y^2 = \frac{4 + 2(\gamma-1) M_x^2}{(\gamma+1)^2 M_x^2 - 2(\gamma-1)\left(1+\frac{\gamma-1}{2} M_x^2\right)}$$

This on rearrangement and further simplification yields a simple relation as follows.

$$M_y^2 = \frac{\frac{2}{\gamma-1} + M_x^2}{\frac{2\gamma}{\gamma-1} M_x^2 - 1} \tag{6.24}$$

6.6 STATIC PRESSURE RATIO ACROSS THE SHOCK

Equations (6.4) and (6.5) give

$$F_x = F_y$$

$$p_x + \rho_x c_x^2 = p_y + \rho_y c_y^2$$

Equation (4.18) gives

$$\rho_x c_x^2 = \gamma p_x M_x^2$$

$$\rho_y c_y^2 = \gamma p_y M_y^2$$

Therefore,

$$p_x + \gamma p_x M_x^2 = p_y + \gamma p_y M_y^2$$

$$\frac{p_y}{p_x} = \frac{1+\gamma M_x^2}{1+\gamma M_y^2} \tag{6.25}$$

Substituting from Equation (6.24) for M_y^2 in Equation (6.25)

$$\frac{p_y}{p_x} = \frac{1+\gamma M_x^2}{1+\frac{\frac{2\gamma}{\gamma-1}+\gamma M_x^2}{\frac{2\gamma}{\gamma-1} M_x^2 - 1}}$$

$$\frac{p_y}{p_x} = \frac{(1+\gamma M_x^2)\left(\frac{2\gamma}{\gamma-1}M_x^2 - 1\right)}{\frac{2\gamma}{\gamma-1}M_x^2 - 1 + \frac{2\gamma}{\gamma-1} + \gamma M_x^2}$$

Simplifying and rearranging the denominator

$$\frac{p_y}{p_x} = \frac{(1+\gamma M_x^2)\left(\frac{2\gamma}{\gamma-1}M_x^2 - 1\right)}{\frac{\gamma+1}{\gamma-1} + \frac{\gamma+1}{\gamma-1}\gamma M_x^2}$$

$$\frac{p_y}{p_x} = \frac{\gamma-1}{\gamma+1}\left(\frac{2\gamma}{\gamma-1}M_x^2 - 1\right)$$

$$\frac{p_y}{p_x} = \frac{2\gamma}{\gamma+1}M_x^2 - \frac{\gamma-1}{\gamma+1} \tag{6.276}$$

This expression shows that for a shock ($M_x > 1$) there is always a pressure rise across it. Values of the pressure ratio (p_y/p_x) corresponding to $M_x < 1$ are absured.

For $M_x = 1$, $\frac{p_y}{p_x} = 1$; for $M_x = \infty$, $\frac{p_y}{p_x} = \infty$.

6.7 TEMPERATURE RATIO ACROSS THE SHOCK

From Equation (2.24) upstream and downstream of the stock we get

$$\frac{T_{0x}}{T_x} = 1 + \frac{\gamma-1}{2}M_x^2$$

$$\frac{T_{0y}}{T_y} = 1 + \frac{\gamma-1}{2}M_y^2$$

From the adiabatic energy equation for a perfect gas

$$T_{0x} = T_{0y} = T_0$$

Therefore, $\frac{T_y}{T_x} = \frac{T_{0x}}{T_x}\frac{T_y}{T_{0y}}$

$$\frac{T_y}{T_x} = \frac{1+\frac{\gamma-1}{2}M_x^2}{1+\frac{\gamma-1}{2}M_y^2} \tag{6.27}$$

Substituting from Equation (6.24) for M_y^2 in (6.27)

$$\frac{T_y}{T_x} = \frac{1+\frac{\gamma-1}{2}M_x^2}{1+\frac{\gamma-1}{2}M_x^2}$$

$$\frac{T_y}{T_x} = \frac{\left(1+\frac{\gamma-1}{2}M_x^2\right)\left(\frac{2\gamma}{\gamma-1}M_x^2 - 1\right)}{\frac{2\gamma}{\gamma-1}M_x^2 - 1 + 1 + \frac{\gamma-1}{2}M_x^2}$$

$$\frac{T_y}{T_x} = \frac{\left(1+\frac{\gamma-1}{2}M_x^2\right)\left(\frac{2\gamma}{\gamma-1}M_x^2 - 1\right)}{\frac{1}{2}\frac{(\gamma+1)^2}{(\gamma-1)}M_x^2} \tag{6.28}$$

Since $\frac{a_y}{a_x} = \sqrt{\frac{T_y}{T_x}}$

Therefore, $\frac{a_y}{a_x} = \frac{\sqrt{2(\gamma-1)\left(1+\frac{\gamma-1}{2}M_x^2\right)\left(\frac{2\gamma}{\gamma-1}M_x^2 - 1\right)}}{(\gamma+1)M_x}$

(6.29)

6.8 DENSITY RATIO ACROSS THE SHOCK (THE RANKINE-HUGONIOT EQUATIONS)

Equation of state for a perfect gas gives

$$\frac{\rho_y}{\rho_x} = \frac{p_y}{p_x}\frac{T_x}{T_y} \tag{6.30}$$

Substituting for the pressure ratio and temperature ratio from Equations (6.26) and (6.28).

$$\frac{\rho_y}{\rho_x}=\left(\frac{2\gamma}{\gamma+1}M_x^2-\frac{\gamma-1}{\gamma+1}\right)\frac{\frac{1}{2}\frac{(\gamma+1)^2}{\gamma-1}M_x^2}{\left(1+\frac{\gamma-1}{2}M_x^2\right)\left(\frac{2\gamma}{\gamma-1}M_x^2-1\right)}$$

$$\frac{\rho_y}{\rho_x}=\frac{\frac{\gamma+1}{2}\left(\frac{2\gamma}{\gamma-1}M_x^2-1\right)M_x^2}{\left(1+\frac{\gamma-1}{2}M_x^2\right)\left(\frac{2\gamma}{\gamma-1}M_x^2-1\right)}$$

$$\frac{\rho_y}{\rho_x}=\frac{\left(\frac{\gamma+1}{2}\right)M_x^2}{1+\frac{\gamma-1}{2}M_x^2} \tag{6.31}$$

The equation of continuity for constant flow rate through the shock gives

$$\frac{c_y}{c_x}=\frac{\rho_x}{\rho_y}$$

$$\frac{c_y}{c_x}=\frac{1+\frac{\gamma-1}{2}M_x^2}{\frac{\gamma+1}{2}M_x^2} \tag{6.32}$$

Another expression for the density ratio across the shock can be derived in terms of the pressure ratio alone. This is useful for comparing the density ratios in isentropic process and a shock for given values of the pressure ratio.

Equation (6.26) can be written as

$$\frac{2\gamma}{\gamma+1}M_x^2=\frac{p_y}{p_x}+\frac{\gamma-1}{\gamma+1}$$

$$M_x^2=\frac{\gamma+1}{2\gamma}\frac{p_y}{p_x}+\frac{\gamma-1}{2\gamma} \tag{6.33}$$

Substituting for M_x^2 from Equation (6.33) in (6.28)

$$\frac{T_y}{T_x}=\frac{\left[1+\frac{\gamma-1}{2}\left(\frac{\gamma+1}{2\gamma}\frac{p_y}{p_x}+\frac{\gamma-1}{2\gamma}\right)\right]\left[\frac{2\gamma}{\gamma-1}\left(\frac{\gamma+1}{2\gamma}\frac{p_y}{p_x}+\frac{\gamma-1}{2\gamma}\right)-1\right]}{\frac{(\gamma+1)^2}{2(\gamma-1)}\left(\frac{\gamma+1}{2\gamma}\frac{p_y}{p_x}+\frac{\gamma-1}{2\gamma}\right)}$$

After simplifying and rearranging the numerator and denominator

$$\frac{T_y}{T_x}=\frac{\frac{(\gamma+1)^3}{4\gamma(\gamma-1)}\frac{p_y}{p_x}\left(1+\frac{\gamma-1}{\gamma+1}\frac{p_y}{p_x}\right)}{\frac{(\gamma+1)^3}{4\gamma(\gamma-1)}\left(\frac{p_y}{p_x}+\frac{\gamma-1}{\gamma+1}\right)}$$

$$\frac{T_y}{T_x}=\frac{\frac{p_y}{p_x}\left(1+\frac{\gamma-1}{\gamma+1}\frac{p_y}{p_x}\right)}{\frac{p_y}{p_x}+\frac{\gamma-1}{\gamma+1}} \tag{6.34}$$

$$\frac{p_y}{p_x}\frac{T_x}{T_y}=\frac{\frac{p_y}{p_x}+\frac{\gamma-1}{\gamma+1}}{1+\frac{\gamma-1}{\gamma+1}\frac{p_y}{p_x}}$$

This expression along with Equation (6.30) after rearrangement of terms gives

$$\frac{\rho_y}{\rho_x}=\frac{1+\frac{\gamma+1}{\gamma-1}\frac{p_y}{p_x}}{\frac{\gamma+1}{\gamma-1}+\frac{p_y}{p_x}} \tag{6.35}$$

Equation (6.35) on rearrangement gives pressure ratio in terms of the density ratio.

$$\frac{p_y}{p_x} = \frac{\dfrac{\gamma+1}{\gamma-1}\dfrac{\rho_y}{\rho_x} - 1}{\dfrac{\gamma+1}{\gamma-1} - \dfrac{\rho_y}{\rho_x}} \tag{6.36}$$

Equations (6.35) and (6.36) are known as the Rankine-Hugoniot Equations. The pressure-density relations for an isentropic process is given by

$$\frac{p_y}{p_x} = \left(\frac{\rho_y}{\rho_x}\right)^{\gamma} \tag{6.37}$$

The suffixes x and y have been retained in Equation (6.37) but in this case they do not refer to the shock wave.

Equations (6.36) and (6.37) have been compared in Figure 6.5. It may be observed that for a given density change the pressure ratio

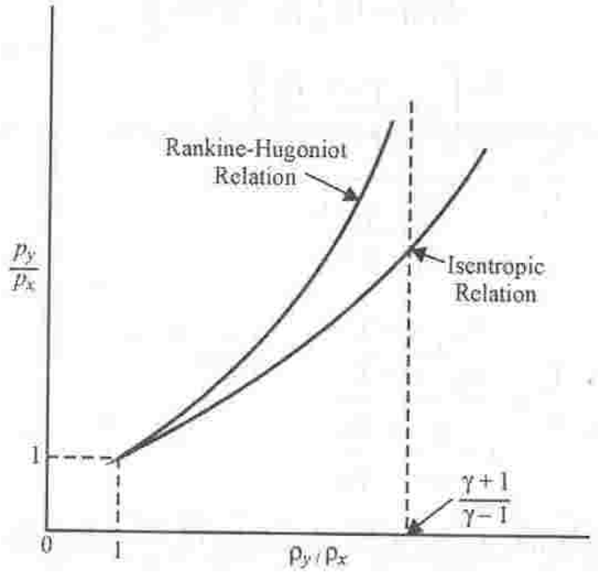

FIGURE 6.5 : Comparison of the Rankine-Hugoniot and isentropic relations

across the shock is greater than its corresponding isentropic value. But at lower Mach numbers the difference is negligible and the flow through the shock wave can be considered nearly isentropic.

6.9 STAGNATION PRESSURE RATIO ACROSS THE SHOCK

As pointed out earlier a shock wave is an irreversibility across which

there is a stagnation pressure loss and increase in entropy. The stagnation pressure ratio is a function of the upstream Mach number M_x.

The required expression is derived here

$$\frac{p_{0y}}{p_{0x}} = \frac{p_{0y}}{p_y}\frac{p_y}{p_x}\frac{p_x}{p_{0x}} \tag{6.38}$$

$$\frac{p_{0y}}{p_y} = \left(1 + \frac{\gamma-1}{2}M_y^2\right)^{\gamma/(\gamma-1)}$$

Substituting for M_y^2 from Equation (6.24)

$$\frac{p_{0y}}{p_y} = \left\{1 + \frac{\dfrac{\gamma-1}{2}M_x^2 + 1}{\dfrac{2\gamma}{\gamma-1}M_x^2 - 1}\right\}^{\gamma/(\gamma-1)}$$

$$\frac{p_{0y}}{p_y} = \left\{\frac{\dfrac{\gamma+1}{2}M_x^2}{\dfrac{2\gamma}{\gamma+1}M_x^2 - \dfrac{\gamma-1}{\gamma+1}}\right\}^{\gamma/(\gamma-1)} \tag{6.39}$$

p_y/p_x is given by Equation (6.26)

$$\frac{p_x}{p_{0x}} = \left(1 + \frac{\gamma-1}{2}M_x^2\right)^{-\gamma/(\gamma-1)} \tag{6.40}$$

Substituting from Equations (6.39), (6.26) and (6.40) in (6.38)

$$\frac{p_{0y}}{p_{0x}} = \left\{\frac{\dfrac{\gamma+1}{2}M_x^2}{\dfrac{2\gamma}{\gamma+1}M_x^2 - \dfrac{\gamma-1}{\gamma+1}}\right\}^{\gamma/(\gamma-1)} \times \left(\frac{2\gamma}{\gamma+1}M_x^2 - \frac{\gamma-1}{\gamma+1}\right) \times \left(1 + \frac{\gamma-1}{2}M_x^2\right)^{-\gamma/(\gamma-1)}$$

$$\frac{p_{0y}}{p_{0x}} = \left\{\frac{\dfrac{\gamma+1}{2}M_x^2}{1 + \dfrac{\gamma-1}{2}M_x^2}\right\}^{\gamma/(\gamma-1)} \times \left(\frac{2\gamma}{\gamma+1}M_x^2 - \frac{\gamma-1}{\gamma+1}\right)^{-1/(\gamma-1)} \tag{6.41}$$

6.10 CHANGE IN ENTROPY ACROSS THE SHOCK

Change of entropy across the shock is given by Equation (1.49)

$$\Delta s = s_y - s_x = c_p \ln \frac{T_y}{T_x} - R \ln \frac{p_y}{p_x}$$

$$\Delta s = c_p \ln \frac{T_y}{T_x} - c_p \left(\frac{\gamma - 1}{\gamma} \right) \ln \frac{p_y}{p_x}$$

$$\Delta s = c_p \ln \frac{T_y / T_x}{(p_y / p_x)^{(\gamma-1)/\gamma}} \tag{6.42}$$

$$\frac{T_y}{T_x} = \frac{1 + \dfrac{\gamma - 1}{2} M_x^2}{1 + \dfrac{\gamma - 1}{2} M_y^2} \cdot \frac{T_{0y}}{T_{0x}} \tag{6.43}$$

$$\frac{p_y}{p_x} = \left\{ \frac{1 + \dfrac{\gamma - 1}{2} M_x^2}{1 + \dfrac{\gamma - 1}{2} M_y^2} \right\}^{\gamma/(\gamma-1)} \frac{p_{0y}}{p_{0x}}$$

$$\left(\frac{p_y}{p_x} \right)^{(\gamma-1)/\gamma} = \frac{1 + \dfrac{\gamma - 1}{2} M_x^2}{1 + \dfrac{\gamma - 1}{2} M_y^2} \left(\frac{p_{0y}}{p_{0x}} \right)^{(\gamma-1)/\gamma} \tag{6.44}$$

By combining Equations (6.43) and (6.44)

$$\frac{T_y / T_x}{(p_y / p_x)^{(\gamma-1)/\gamma}} = \frac{T_{0y} / T_{0x}}{(p_{0y} / p_{0x})^{(\gamma-1)/\gamma}}$$

But $T_{0y}/T_{0x} = 1$, therefore,

$$\frac{T_y / T_x}{(p_y / p_x)^{(\gamma-1)/\gamma}} = \left(\frac{p_{0y}}{p_{0x}} \right)^{-(\gamma-1)/\gamma} \tag{6.45}$$

Substituting Equation (6.45) in (6.42) we get

$$\Delta s = c_p \ln \left(\frac{p_{0y}}{p_{0x}} \right)^{-(\gamma-1)/\gamma}$$

$$\Delta s = -c_p \left(\frac{\gamma - 1}{\gamma} \right) \ln \left(\frac{p_{0y}}{p_{0x}} \right) \tag{6.46}$$

$$\Delta s = -R \ln \left(\frac{p_{0y}}{p_{0x}} \right) \tag{6.47}$$

$$\frac{p_{0y}}{p_{0x}} = e^{-\Delta s / R} \tag{6.48}$$

Substituting from Equation (6.41) in (6.47)

$$\frac{\Delta s}{R} = -\frac{\gamma}{\gamma - 1} \ln \frac{\dfrac{\gamma + 1}{2} M_x^2}{1 + \dfrac{\gamma - 1}{2} M_x^2} + \frac{1}{\gamma - 1} \ln \left(\frac{2\gamma}{\gamma + 1} M_x^2 - \frac{\gamma - 1}{\gamma + 1} \right)$$

$$\frac{\Delta s}{R} = \frac{\gamma}{\gamma - 1} \ln \left(\frac{2}{(\gamma + 1) M_x^2} + \frac{\gamma - 1}{\gamma + 1} \right) + \frac{1}{\gamma - 1} \ln \left(\frac{2\gamma}{\gamma + 1} M_x^2 - \frac{\gamma - 1}{\gamma + 1} \right) \tag{6.49}$$

6.11 IMPOSSIBILITY OF A SHOCK IN SUBSONIC FLOW

Equation (6.49) for a given value of γ is plotted in Figure 6.6.

Perfect gases of engineering applications have γ between 1.0 and 1.67; for this range $\Delta s/R$ always has positive values for values of the upstream Mach number M_x greater than unity.

At $M_x = 1$, Equation (6.49) gives

$$\left(\frac{\Delta s}{R} \right)_{Mx=1} = \frac{\gamma}{\gamma - 1} \ln \frac{\gamma + 1}{\gamma + 1} + \frac{1}{\gamma - 1} \ln \frac{\gamma + 1}{\gamma + 1}$$

$$\left(\frac{\Delta s}{R} \right)_{Mx=1} = 0 \tag{6.50}$$

For the sake of explanation Equation (6.49) has also been plotted for values of M_x less than unity; this branch of curve represents a decrease in the entropy, which by the second law of thermodynamics is impossible.

Therefore, shock waves cannot develop in a subsonic flow.

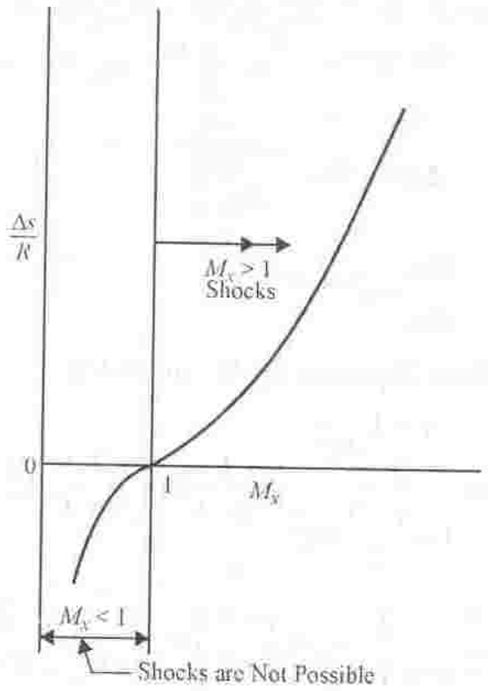

FIGURE 6.6 : Change of entropy across a normal shock wave

This fact is also corroborated by Equations (6.48). For a decrease in entropy this equation gives

$$\frac{p_{0y}}{p_{0x}} > 1$$

which implies that there is an increase in the stagnation pressure; but this is not possible is an adiabatic flow under consideration.

6.12 STRENGTH OF A SHOCK WAVE

A parameter which defines the strength of a shock wave is often used in shock wave analyses. This is given by

$$\xi = \frac{p_y - p_x}{p_x} = \frac{p_y}{p_x} - 1 \tag{6.51}$$

Substituting for p_y/p_x from Equation (6.26)

$$\xi = \frac{2\gamma}{\gamma+1} M_x^2 - \frac{\gamma-1}{\gamma+1} - 1$$

$$\xi = \frac{2\gamma}{\gamma+1} (M_x^2 - 1) \tag{6.52}$$

This shock strength is expressed in another form using the Rankine-Hugoniot relation given by Equation (6.36)

$$\xi = \frac{\dfrac{\gamma+1}{\gamma-1}\dfrac{\rho_y}{\rho_x} - 1}{\dfrac{\gamma+1}{\gamma-1} - \dfrac{\rho_y}{\rho_x}} - 1$$

On simplification and rearrangement the above expression reduces to

$$\xi = \frac{\dfrac{2\gamma}{\gamma-1}\left(\dfrac{\rho_y}{\rho_x} - 1\right)}{\dfrac{2}{\gamma-1} - \left(\dfrac{\rho_y}{\rho_x} - 1\right)} \tag{6.53}$$

For weak shocks *i.e.*, for small values of the density ratio (ρ_y/ρ_x), following approximate relation holds:

$$\xi \propto \left(\frac{\rho_y}{\rho_x} - 1\right) \tag{6.54}$$

For shocks of any strength Equation (6.52) gives

$$\xi \propto (M_x^2 - 1) \tag{6.55}$$

6.12.1 Shocks of Vanishing Strength

Shock waves for which ξ is almost zero are referred to as shocks of vanishing strength. For such shocks

$$M_x \approx 1$$

$$\frac{\rho_y}{\rho_x} \approx 1$$

These conditions in Equations (6.26), (6.28), (6.41) and (6.49) lead to

$$\frac{p_y}{p_x} \approx 1$$

$$\frac{T_y}{T_x} \approx 1$$

$$\frac{p_{0y}}{p_{0x}} \approx 1$$

$$\frac{\Delta s}{R} \approx 0.$$

6.12.2 Strong Shocks

Since shock strength is proportional to $(M_x^2 - 1)$, strong shocks are a result of very high values of the upstream Mach number. The maximum values of quantities in Equations (6.24), (6.26), (6.28), (6.36) and (6.41) are given below:

$$\lim_{M_x \to \infty} M_y = \sqrt{\frac{\gamma - 1}{2\gamma}} \tag{6.56}$$

$$\lim_{M_x \to \infty} \left(\frac{p_y}{p_x} \right) = \infty \tag{6.57}$$

$$\lim_{M_x \to \infty} \left(\frac{T_y}{T_x} \right) = \infty \tag{6.58}$$

$$\lim_{M_x \to \infty} \left(\frac{\rho_y}{\rho_x} \right) = \frac{\gamma + 1}{\gamma - 1} \tag{6.59}$$

$$\lim_{M_x \to \infty} \left(\frac{p_{0y}}{p_{0x}} \right) = 0 \tag{6.60}$$

6.13 DETERMINATION OF MACH NUMBER OF SUPERSONIC FLOWS

A pitot tube along with a wall tapping can be used to determine the Mach number of a supersonic stream. The introduction of the pitot tube produces a curved shock a little distance upstream of its mouth as shown in Figure 6.7. Therefore, the pitot tube measures the stagnation pressure (p_{0y}) downstream of the shock wave. The static pressure tapping located upstream of the shock measures p_x. Figure 6.7 shows the locations of the wall tapping, shock wave and the pitot tube.

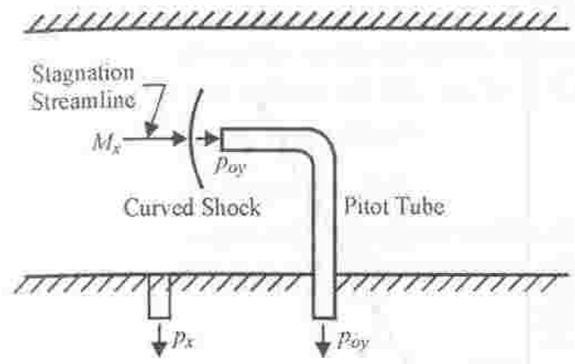

FIGURE 6.7 : Pitot-tube in supersonic flow

Now a relation between p_{0y}/p_x and the upstream Mach number is derived under the following assumptions:

(*a*) The shock wave is normal at the stagnation streamline, this can be ensured if the pitot tube is placed parallel to the flow. In this condition the shock wave is symmetrical on both sides of the stagnation streamline.

(*b*) Gas is brought to rest at the mouth of the tube isentropically.

Now $$\frac{p_{0y}}{p_x} = \frac{p_{0y}}{p_y} \frac{p_y}{p_x}$$

Substituting for p_{0y}/p_y and p_y/p_x from Equations (6.39) and (6.26) respectively, we get

$$\frac{p_{0y}}{p_x} = \left(\frac{\frac{\gamma+1}{2} M_x^2}{\frac{2\gamma}{\gamma+1} M_x^2 - \frac{\gamma-1}{\gamma+1}} \right)^{\gamma/(\gamma-1)} \times \left(\frac{2\gamma}{\gamma+1} M_x^2 - \frac{\gamma-1}{\gamma+1} \right)$$

On simplifying this gives

$$\frac{p_{0y}}{p_x} = \frac{\left(\frac{\gamma+1}{2} M_x^2 \right)^{\gamma/(\gamma-1)}}{\left(\frac{2\gamma}{\gamma+1} M_x^2 - \frac{\gamma-1}{\gamma+1} \right)^{1/(\gamma-1)}} \tag{6.61}$$

Equation (6.61) shows that for a given gas p_{0y}/p_x is a function of only the Mach number. This is graphically shown in Figure 6.8.

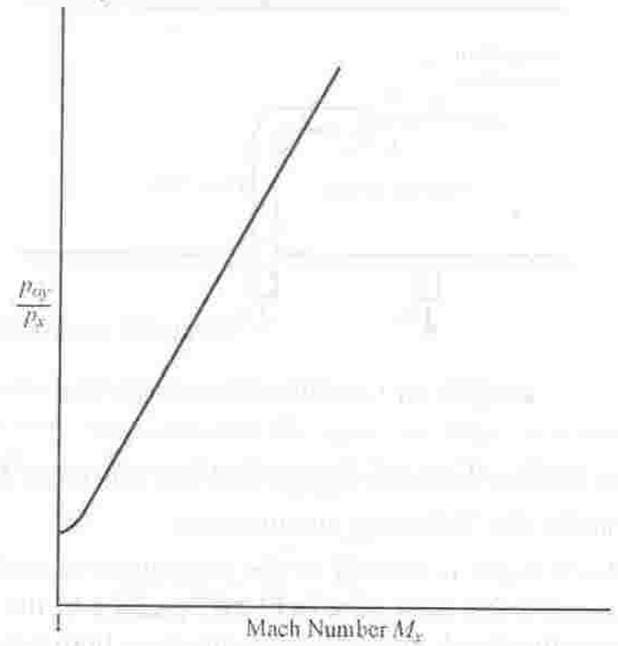

FIGURE 6.8 : Mach number from pitot tube measurement

This plot can be conveniently used to read off M_x for a measured value of p_{0y}/p_x in supersonic flows.

It should be noted that Equation (6.61) has been derived for a normal stock; therefore, it can be used only for supersonic flow. For subsonic flow the two pressures are related by the isentropic relation.

$$\frac{p_0}{p} = \left(1 + \frac{\gamma - 1}{2} M^2\right)^{\gamma/(\gamma-1)}$$

This can be used to determine the Mach number of subsonic flow. In this case the Mach number should not be close to unity because supersonic flow can be generated due to local acceleration of a high Mach number subsonic flow.

6.14 TABLES AND CHARTS FOR NORMAL SHOCK WAVES

It is observed that most of the relations derived here for the normal shock waves are unique functions of the upstream Mach number. Therefore, their values for various gases can be computed in a wide range of Mach numbers and tabulated. Such tables reduce the calculations and make the solutions of problems very simple.

Equations (6.24), (6.26), (6.28), (6.29), (6.31), (6.32), (6.41) and (6.61) are used to prepare tables for normal shock waves in perfect gases. These Equations give the values of M_y, p_y/p_x, T_y/T_x, a_y/a_x, ρ_y/ρ_x, c_y/c_x, p_{0y}/p_{0x} and p_{0y}/p_x respectively.

Such tables are given in Appendix A4.

Gas charts can also be constructed from these tables. A chart showing the plots of various quantities for normal shocks is shown in Figure 6.9.

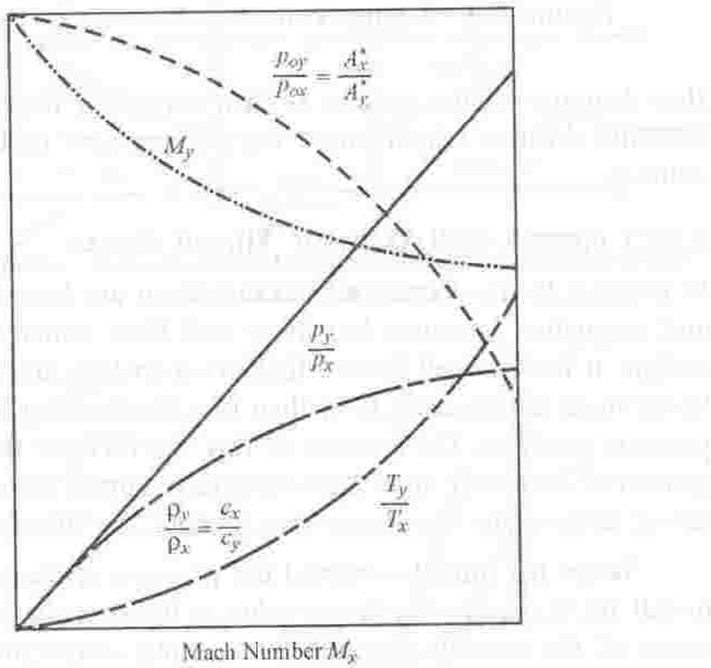

FIGURE 6.9 : Variation of parameters for flow through normal shock waves

6.15 SUPERSONIC WIND TUNNELS

Normal shocks have applications in supersonic wind tunnels where the diffusion of the supersonic flow after the test section takes place through a shock wave. Such a wind tunnel is shown in Figure 6.10. The details and the working of such tunnels are given in Chapter 11. This consists of a nozzle, test section and the diffuser.

In an ideal flow through the tunnel at designed running conditions there is no shock anywhere in the tunnel. The ideal flow is reversibly accelerated in the nozzle to supersonic Mach number; thus the model can be tested at supersonic velocity in the test section. The supersonic

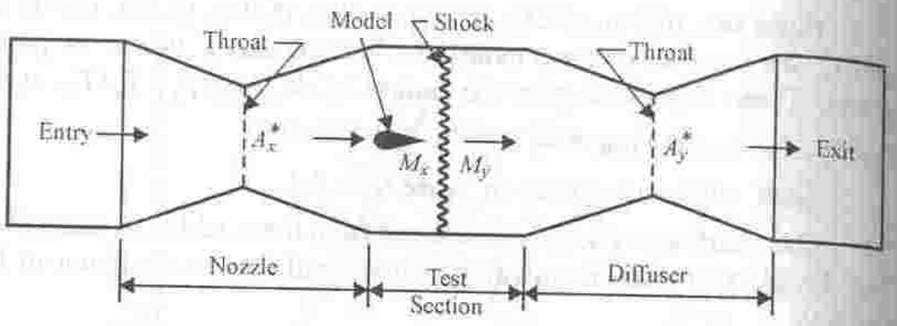

FIGURE 6.10 : Supersonic wind tunnel with shock in the test section

flow leaving the test section is then reversibly decelerated in the supersonic diffuser which raises the gas pressure to the back pressure value.

6.15.1 Nozzle and Diffuser Throat Areas

In contrast to the above flow model, there are boundary layer growth and stagnation pressure loss in a real flow which affect the tunnel design. It is also well known that the boundary layer growth is much lesser in an accelerating flow than in a decelerating flow with adverse pressure gradient. On account of this the diffuser throat has a larger growth of boundary layer than the nozzle throat; therefore, the diffuser throat dimensions are larger than that of the nozzle throat.

When the tunnel is started the pressure at the nozzle exit begins to fall till it reaches the deign value at the running conditions. On account of the variable pressure ratio acting across the nozzle a shock wave moves in the downstream direction in the diverging portion of the nozzle as explained in Section 4.7.2. As a result of the appearance of the shock wave there will be a stagnation pressure loss across it and a change in the critical areas. The stagnation pressure loss is governed by Equation (6.41) and the critical areas by Equation (4.39). For $\gamma = 1.4$.

$$\frac{\dot{m}\sqrt{T_{0x}}}{A_x^* p_{0x}} = \frac{\dot{m}\sqrt{T_{0y}}}{A_y^* p_{0y}} = 0.0404$$

For constant flow rate and adiabatic conditions in the tunnel

$$\dot{m} = \text{constant}$$

$$T_{0x} = T_{0y} = T_0 = \text{constant}$$

Therefore, $A_x^* p_{0x} = A_y^* p_{0y}$

$$\frac{A_y^*}{A_x^*} = \frac{p_{0x}}{p_{0y}} > 1 \tag{6.62}$$

Equation (6.62) shows that in the presence of shock the diffuser throat area is always larger than the nozzle throat area.

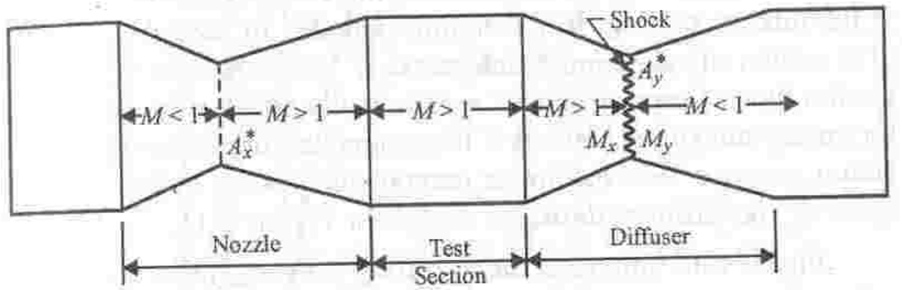

FIGURE 6.11 : Supersonic wind tunnel with shock at the diffuser throat (steady running condition)

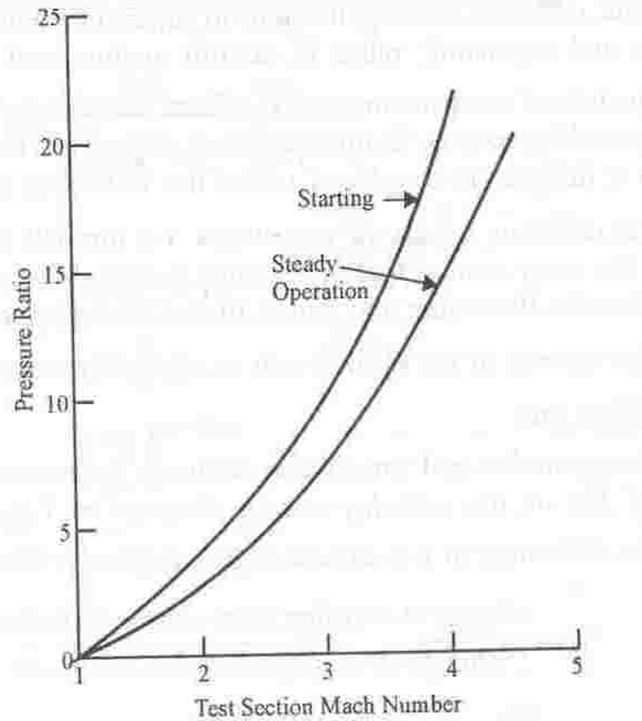

FIGURE 6.12 : Comparison of pressure ratios during starting and steady operation

If the required power is supplied to account for the stagnation pressure loss and correct value of the diffuser to nozzle throal area ratio is used, the shock will move to the test section as shown in Figure 6.10. It could be kept downstream of the model in test section. But the Mach number M_x is maximum in the test section. Therefore, the stagnation pressure loss (as given by Equation (6.41)) will be maximum for this position of the shock wave. Therefore, this is not the best location of the shock wave though this condition will have to be always encountered at the time of starting. It is therefore desirable to keep the shock wave at a section of minimum Mach number. The minimum Mach number section downstream of the test section is the diffuser throat. Therefore, for steady running conditions it is economical (on account of low stagnation pressure loss and lower compressor power) to keep the shock wave at he diffuser throat as shown in Figure 6.11.

Figure 6.12 compares the operating pressure ratios with those required for starting at various values of the test section Mach number for a given gas.

6.15.2 Diffuser Efficiency

Supersonic diffusers have applications in supersonic wind tunnels, compressors and supersonic inlets of aircraft engines and missiles.

The role of a supersonic shock diffuser has already been discussed in the preceding section. In this section an expression for the efficiency of such a diffuser is developed under the following assumptions:

(*a*) The diffusion occurs in two stages: (*i*) through a normal shock at the entry section and (*ii*) through isentropic deceleration of the subsonic flow after the shock in the diverging passage.

(*b*) The velocity at the diffuser exit is negligibly small, *i.e.*, $p_{02} \approx p_2$.

(*c*) Perfect gas.

The reversible and irreversible diffusion processes are shown by 1-2*s* and 1-2 on the enthalpy-entropy diagram in Figure 6.13.

The efficiency of the diffuser is defined in the following manner:

$$\eta_D = \frac{\text{change of enthalpy in reversible diffusion}}{\text{change of enthalpy in actual diffusion}}$$

$$\eta_D = \frac{h_{2s} - h_1}{h_2 - h_1} \tag{6.63}$$

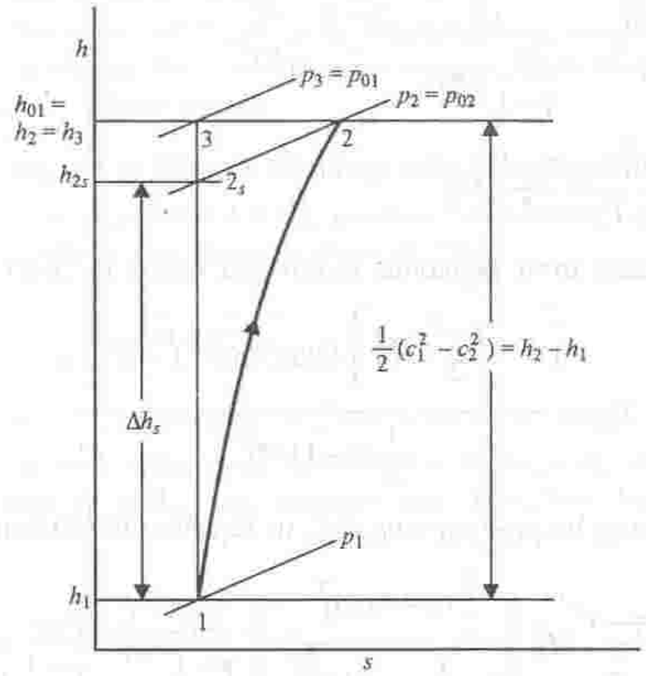

FIGURE 6.13 : Diffusion process in a supersonic diffuser

$$\eta_D = \frac{\Delta h_s}{\frac{1}{2}(c_1^2 - c_2^2)} \approx \frac{\Delta h_s}{\frac{1}{2}c_1^2} \tag{6.64}$$

$$\eta_D = \frac{c_p (T_{2s} - T_1)}{\frac{1}{2}c_1^2} = \frac{T_1\left(\frac{T_{2s}}{T_1} - 1\right)}{c_1^2/2c_p}$$

$$\eta_D = \frac{\left(\frac{p_2}{p_1}\right)^{(\gamma-1)/\gamma} - 1}{c_1^2/2c_p T_1} \tag{6.65}$$

$$\frac{p_2}{p_1} = \frac{p_{01}}{p_1}\frac{p_2}{p_{01}} = \frac{p_{01}}{p_1}\frac{p_{02}}{p_{01}}$$

$$\frac{p_2}{p_1} = \left(1 + \frac{\gamma - 1}{2} M_1^2\right)^{\gamma/(\gamma-1)} \times \frac{p_{02}}{p_{01}} \tag{6.66}$$

$$\frac{c_1^2}{2c_p T_1} = \frac{c_1^2}{\frac{2}{\gamma-1}\gamma R T_1} = \frac{\gamma-1}{2}\frac{c_1^2}{\gamma R T_1}$$

$$\frac{c_1^2}{2c_p T_1} = \frac{\gamma-1}{2} M_1^2 \tag{6.67}$$

Substituting from Equations (6.66) and (6.67) in (6.65)

$$\eta_D = \frac{\left(1+\frac{\gamma-1}{2}M_1^2\right)(p_{02}/p_{01})^{(\gamma-1)/\gamma} - 1}{\frac{1}{2}(\gamma-1)M_1^2} \tag{6.68}$$

Substituting for $p_{02}/p_{01} = p_{0y}/p_{0x}$ in Equation (6.68) from (6.41)

$$\eta_D = \frac{\left(1+\frac{\gamma-1}{2}M_1^2\right)\frac{\frac{1}{2}(\gamma+1)M_1^2}{1+\frac{1}{2}(\gamma-1)M_1^2} \times \left(\frac{2\gamma}{\gamma+1}M_1^2 - \frac{\gamma-1}{\gamma+1}\right)^{-1/\gamma} - 1}{\frac{\gamma-1}{2}M_1^2}$$

$$\eta_D = \frac{\frac{\gamma+1}{\gamma-1}}{\left(\frac{2\gamma}{\gamma+1}M_1^2 - \frac{\gamma-1}{\gamma+1}\right)^{1/\gamma}} - \left(\frac{2}{\gamma-1}\right)\frac{1}{M_1^2} \tag{6.69}$$

Equations (6.68) and (6.69) show that the efficiency of the normal shock diffuser is only a function of the entry Mach number.

6.16 MOVING NORMAL SHOCK WAVES

Till now the flow of gas only through stationary normal shock waves has been discussed. In this section moving normal shocks are considered: this may deal with a shock wave moving either into stagnant gas or a gas already in motion. In Section 5.4 steep finite waves (shock waves) moving into stagnant gas were considered; the concepts developed in that section would be useful here.

Propagating steep waves of finite amplitude or shock waves occur in a variety of applications like shock tubes, supersonic gas ducts, partial admission turbines, comprex and pulse jet engines.

Moving shock waves have useful applications in the study of high temperature chemistry and high speed aerodynamics. The destructive effects of blast waves due to explosions are also understood by the studies of moving shock waves.

6.16.1 Velocity of a Shock Moving into Stagnant Gas

In Section 6.6 an expression for the pressure ratio across a stationary shock through which gas flows is derived. This is

$$\frac{p_y}{p_x} = \frac{2\gamma}{\gamma+1}M_x^2 - \frac{\gamma-1}{\gamma+1} \tag{6.26}$$

In Figure 6.3 if the shock is given a leftward velocity of c_x an observer at rest will observe the shock wave propagating leftward at a Mach number $M_x = M_{sh}$ into stagnant gas. Therefore, from Equation (6.26)

$$M_{sh}^2 = \frac{\gamma+1}{2\gamma}\frac{p_y}{p_x} + \frac{\gamma-1}{2\gamma} \tag{6.70}$$

This is the Mach number of shock wave moving into the stagnant gas and can be identified as the same expression given in Equation (5.50).

6.16.2 Other Relations for a Moving Shock

Figure 6.14 shows a normal shock wave propagating into stagnant gas on the right. Let the shock wave velocity be c_{sh}. Other quantities on the two sides of the moving shock are also shown in Figure 6.14.

Now stationary shock relations derived in earlier sections can be used for a moving shock if it is transformed into a stationary shock. This is done by giving leftward velocity ($c_x = c_{sh}$) to the stationary coor-

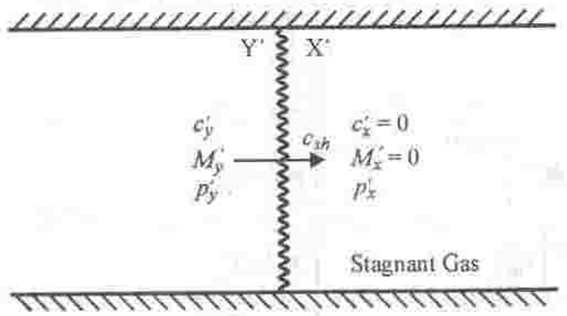

FIGURE 6.14 : Normal shock wave propagating into stagnant gas

dinates containing the flow pattern of Figure 6.14. In other words the velocities of the shock and the gas on the two sides of the shock have a component of leftward velocity c_x superimposed on their original velocities. As a result of this, following velocities are obtained in the new (moving) coordinate system shown in Figure 6.15:

$$c_x' + c_x = c_x \text{ (gas velocity on the right)}$$

$$c_x - c_x = 0 \text{ (shock wave velocity)}$$

$$c_y = c_x - c_y' \text{ (gas velocity on the left)}$$

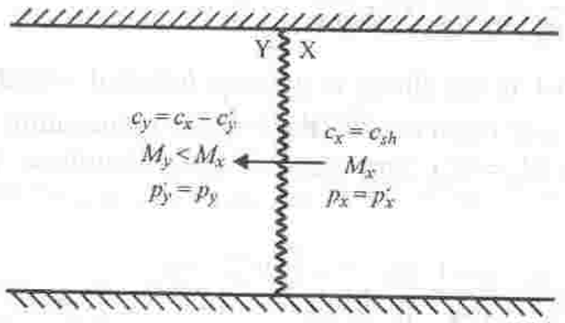

FIGURE 6.15 : Flow of gas through a stationary shock wave (moving coordinate system)

It may be mentioned here that by this transformation, only stagnation values (p_0, T_0 etc.) on the two sides of the shock are affected; static values (p, T etc.) remain unaffected. Various values on the two sides of the shock are given in Table 6.1.

TABLE 6.1: Comparison of the moving and stationary shock parameters

On left of the shock	On right of the shock
(*a*) Normal moving shock (Figure 6.14)	
c_y'	$c_x' = 0$
$M_y' = c_y'/a_y'$	$M_x' = 0$
p_y'	p_x'
T_y'	T_x'
$p_{0y}' = p_y' \left(1 + \frac{\gamma-1}{2} M_y'^2\right)^{\gamma/(\gamma-1)}$	$p_{0x}' = p_x'$
$T_{0y}' = \left(1 + \frac{\gamma-1}{2} M_y'^2\right) T_{0y}'$	$T_{0x}' = T_x'$
$a_y' = \sqrt{\gamma R T_y'}$	$a_x' = \sqrt{\gamma R T_x'}$

(*b*) Normal stationary shock (Figure 6.15)	
$c_y = c_x - c_y'$	$c_x = c_{sh}$
$M_y = \frac{c_y}{a_y} = \frac{c_x - c_y'}{a_y}$	$M_x = \frac{c_x}{a_x}$
$p_y = p_y'$	$p_x = p_x'$
$T_y = T_y'$	$T_x = T_x'$
$p_{0y} = p_y \left(1 + \frac{\gamma-1}{2} M_y^2\right)^{\gamma/(\gamma-1)}$	$p_{0x} = p_x \left(1 + \frac{\gamma-1}{2} M_x^2\right)^{\gamma/(\gamma-1)}$
$T_{0y} = T_y \left(1 + \frac{\gamma-1}{2} M_y^2\right)$	$T_{0x} = T_x \left(1 + \frac{\gamma-1}{2} M_x^2\right)$
$a_y = a_y'$	$a_x = a_x'$

Comparison of Figures 6.14 and 6.15 with 5.10 (*b*) and 5.10 (*c*) respectively shows the similarity between the two analyses.

As in Section 6.7 the stagnation temperature across a stationary shock remains constant.

$$T_{0y} = T_{0x}$$

$$T_y + \frac{c_y^2}{2c_p} = T_x + \frac{c_x^2}{2c_p}$$

$$T_y - T_x = \frac{1}{2c_p}(c_x^2 - c_y^2) \tag{6.71}$$

The stagnation temperature across the moving shock does not remain constant.

$$\Delta T_0' = T_{0y}' - T_{0x}'$$

$$\Delta T_0' = \left(T_y' + \frac{c_y'^2}{2c_p}\right) - \left(T_x' + \frac{c_x'^2}{2c_p}\right)$$

$$\Delta T_0' = (T_y' - T_x') + \frac{1}{2c_p}(c_y'^2 - c_x'^2)$$

$$\Delta T_0' = (T_y - T_x) + \frac{1}{2c_p}(c_y'^2 - c_x'^2) \tag{6.72}$$

For the normal shock moving into stagnant gas

$$c_x' = 0$$

$$c_y = c_x - c_y'$$

$$c_y' = c_x - c_y$$

Therefore, Equation (6.72) yields

$$\Delta T_0' = (T_y - T_x) + \frac{1}{2c_p}(c_x - c_y)^2 \tag{6.73}$$

Equation (6.71) in (6.73) gives

$$\Delta T_0' = \frac{1}{2c_p}(c_x^2 - c_y^2) + \frac{1}{2c_p}(c_x - c_y)^2$$

$$\Delta T_0' = \frac{c_x (c_x - c_y)}{c_p} \tag{6.74}$$

NOTATION FOR CHAPTER 6

A	area of cross-section	p	pressure
a	velocity of sound	R	gas constant
c	velocity of gas	s	entropy
c_p	specific heat at constant pressure	Δs	increase in entropy
		T	temperature
F	impulse function	ΔT	temperature rise across the shock
$f(\ )$	function of		
h	enthalpy	γ	c_p/c_v
Δh	increase in enthalpy	ρ	density
M	Mach number	ξ	shock strength
$\dot{m}$	mass flow rate	η	efficiency

SUBSCRIPTS

0	stagnation	D	diffuser
1	entry, initial	s	isentropic
2	exit, final	sh	shock wave
*	critical values	x	upstream of shock
		y	downstream of shock

SUPERSCRIPT

' Moving shock

SOLVED EXAMPLES

Example 6.1. The state of a gas ($\gamma = 1.3$, $R = 0.469$ kJ/kg K) upstream of a normal shock wave is given by the following data:

$$M_x = 2.5,\ p_x = 2 \text{ bar},\ T_x = 275 \text{ K}$$

Calculate the Mach number, pressure, temperature and velocity of the gas downstream of the shock; check the calculated values with those given in the gas tables.

Solution. Substituting the values of M_x and γ

(*i*) $$M_y^2 = \frac{\frac{2}{1.3-1} + 2.5^2}{\frac{2 \times 1.3}{1.3-1} \times 2.5^2 - 1} = \frac{12.92}{53.19} = 0.243$$

$$M_y = 0.4928 \quad \textbf{Ans.}$$

(*ii*) $$\frac{p_y}{p_x} = \frac{2 \times 1.3}{1.3+1} \times 2.5^2 - \frac{1.3-1}{1.3+1}$$

$$\frac{p_y}{p_x} = 7.065 - 0.130 = 6.935$$

$$p_y = 6.935 \times 2 = 13.870 \text{ bar} \quad \textbf{Ans.}$$

(*iii*) $$\frac{T_y}{T_x} = \frac{\left(1 + \frac{0.3}{2} \times 6.25\right) \times 53.19}{\frac{1}{2}\frac{2.3^2}{0.3} \times 6.25} = \frac{1.937 \times 53.19}{55.104}$$

$$\frac{T_y}{T_x} = 1.869$$

$$T_y = 1.869 \times 275 = 513.975 \text{ K} \quad \textbf{Ans.}$$

(*iv*) $$\frac{c_y}{c_x} = \frac{3}{1.3+1} \times \frac{1}{6.25} + \frac{0.3}{2.3} = 0.269$$

$$c_y = 0.269 c_x = 0.269 M_x a_x$$

$$c_y = 0.269 M_x \sqrt{\gamma R T_x}$$

$$c_y = 0.269 \times 2.5 \sqrt{1.3 \times 469 \times 275}$$

$$c_y = 275.375 \text{ m/s} \quad \textbf{Ans.}$$

Alternatively, $c_y = M_y \sqrt{\gamma R T_y}$

$$c_y = 0.4928 \sqrt{1.4 \times 469 \times 513.975}$$

$$c_y = 275.16 \text{ m/s}.$$

Example 6.2. (*a*) Derive the Rankine-Hugoniot relation for a normal shock wave

$$\frac{p_y}{p_x} = \frac{\dfrac{\gamma+1}{\gamma-1}\dfrac{\rho_y}{\rho_x} - 1}{\dfrac{\gamma+1}{\gamma-1} + \dfrac{\rho_y}{\rho_x}}$$

(*b*) A gas ($\gamma = 1.4$, $R = 0.287$ kJ/kg K) at a Mach number of 1.8, $p = 0.8$ bar and $T = 373$ K passes through a normal shock. Determine its density after the shock. Compare this value in an isentropic compression through the same pressure ratio.

Solution. $\rho_x = \dfrac{p_x}{RT_x} = \dfrac{0.8 \times 10^5}{287 \times 373} = 0.747 \text{ kg/m}^3$

From normal shock tables for $\gamma = 1.4$ at $M_x = 1.8$

$$\frac{p_y}{p_x} = 3.613, \quad \frac{T_y}{T_x} = 1.532$$

$$\frac{\rho_y}{\rho_x} = \frac{p_y}{p_x}\frac{T_x}{T_y}$$

$$\frac{\rho_y}{\rho_x} = \frac{3.613}{1.532} = 2.358$$

$$\rho_y = 2.358 \times 0.747 = 1.762 \text{ kg/m}^3 \quad \textbf{Ans.}$$

Alternatively the value of p_y/p_x can be substituted in the Rankine-Hugoniots' equation to determine the density ratio $\dfrac{\rho_y}{\rho_x}$.

For isentropic flow

$$\frac{\rho_y}{\rho_x} = \left(\frac{p_y}{p_x}\right)^{1/\gamma}$$

$$\frac{\rho_y}{\rho_x} = (3.613)^{1/1.4} = 2.5$$

$$\rho_y = 2.5 \times 0.747 = 1.867 \text{ kg/m}^3$$

It is noted that the final density in the isentropic process is greater than in the shock process. This is depicted in Figure 6.5.

Example 6.3. The ratio of the exit to entry area in a subsonic diffuser is 4.0. The Mach number of a jet of air approaching the diffuser at $p_0 = 1.013$ bar, $T = 290$ K is 2.2. There is a standing normal shock wave just outside the diffuser entry. The flow in the diffuser is isentropic. Determine at the exit of the diffuser.

(*a*) Mach number,

(*b*) temperature, and

(*c*) pressure

What is the stagnation pressure loss between the initial and final states of the flow?

Solution. Refer to Figure 6.16.

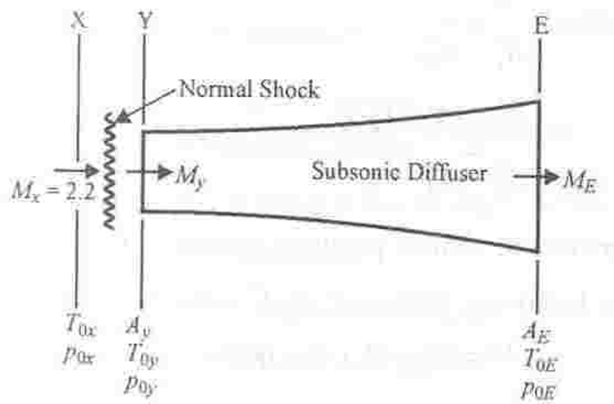

FIGURE 6.16 : Normal shock at the diffuser entry (Example 6.3)

The given data is

$$p_{0x} = 1.013 \text{ bar}, \; T_x = 290 \text{ K}, \; M_x = 2.2, \; A_E = 4A_y$$

From Isentropic tables for $\gamma = 1.4$

at $M = M_x = 2.2$

$$\frac{p}{p_0} = \frac{p_x}{p_{0x}} = 0.0935, \quad \frac{T}{T_0} = \frac{T_x}{T_{0x}} = 0.508$$

$$p_x = 0.0935 \times 1.013 = 0.0947 \text{ bar}$$

$$T_{0x} = \frac{290}{0.508} = 570.87 \text{ K}$$

From normal shock tables for $\gamma = 1.4$ at $M_x = 2.2$

$$M_y = 0.547,\ \frac{p_y}{p_x} = 5.48,\ \frac{T_y}{T_x} = 1.857,\ \frac{p_{0y}}{p_{0x}} = 0.628$$

$$T_y = 1.857 \times 290 = 538.53 \text{ K}$$

$$p_y = 5.48 \times 0.0947 = 0.519 \text{ bar}$$

From Isentropic tables at $M = M_y = 0.547$

$$\left(\frac{A}{A^*}\right)_y = 1.26$$

Now $A_y^* = A_E^*$

Therefore, $\frac{A_y}{A_y^*} = \frac{A_y}{A_E^*}$

$$\frac{A_E}{A_E^*} = \frac{A_y}{A_E^*}\frac{A_E}{A_y} = 1.26 \times 4 = 5.04$$

Parameters at various points in the flow are shown in Figure 6.16.

From Isentropic tables at $A/A^* = A_E/A^* = 5.04$

$$M = M_E = 0.116 \quad \textbf{Ans.}$$

$$\frac{T}{T_0} = \frac{T_E}{T_{0E}} = 0.997$$

$$T_{0x} = T_{0y} = T_{0E} = 570.87 \text{ K}$$

$$T_E = 0.997 \times 570.87 = 569.15 \text{ K} \quad \textbf{Ans.}$$

The continuity equation between sections Y and E gives

$$\rho_y c_y A_y = \rho_E c_E A_E$$

$$\frac{p_y}{RT_y} M_y \sqrt{\gamma RT_y}\, A_y = \frac{p_E}{RT_E} M_E \sqrt{\gamma RT_E}\, A_E$$

$$\frac{p_y M_y A_y}{\sqrt{T_y}} = \frac{p_E M_E A_E}{\sqrt{T_E}}$$

$$\frac{p_E}{p_y} = \frac{M_y}{M_E}\frac{A_y}{A_E}\sqrt{\frac{T_E}{T_y}}$$

$$\frac{p_E}{p_y} = \frac{0.547}{0.116} \times \frac{1}{4} \times \sqrt{\frac{569.15}{538.53}} = 1.212$$

$$p_E = 1.212 \times 0.519 = 0.629 \text{ bar} \quad \textbf{Ans.}$$

$$p_{0y} = 0.628 p_{0x} = 0.628 \times 1.013$$

$$p_{0y} = 0.636 \text{ bar} = 636 \text{ mbar}$$

$$p_{0x} = 1013 \text{ mbar}$$

Stagnation pressure loss = 1013 – 636

$$p_0 = 377 \text{ mbar} \quad \textbf{Ans.}$$

Alternatively, from Isentropic tables for $\gamma = 1.4$ at $M_y = 0.547$

$p_y/p_{0y} = 0.816$, therefore,

$$p_{0E} = p_{0y} = \frac{p_y}{0.816} = \frac{0.519}{0.816} = 0.636 \text{ bar}$$

From Isentropic tables for $\gamma = 1.4$ at $M_E = 0.116$

$p_E/p_{0E} = 0.990$, therefore,

$$p_E = 0.990 \times p_{0E} = 0.990 \times p_{0y}$$

$$p_E = 0.990 \times 0.636 = 0.629 \text{ bar.}$$

Example 6.4. A normal shock occurs in the diverging section of a convergent-divergent air nozzle. The throat area is $\frac{1}{3}\times$ (exit area) and the static pressure at exit is 0.4 times the stagnation pressure at the entry. The flow is throughout isentropic except through the shock. Determine:

(*a*) the Mach numbers M_x and M_y,

(*b*) the static pressure, and

(*c*) the area of cross-section of the nozzle at the section of the nozzle where the normal shock occurs.

Solution. The flow through the nozzle is shown in Figure 6.17. Following relations may be noted:

$$A_1^* = A_t = A_t^* = A_x^*$$

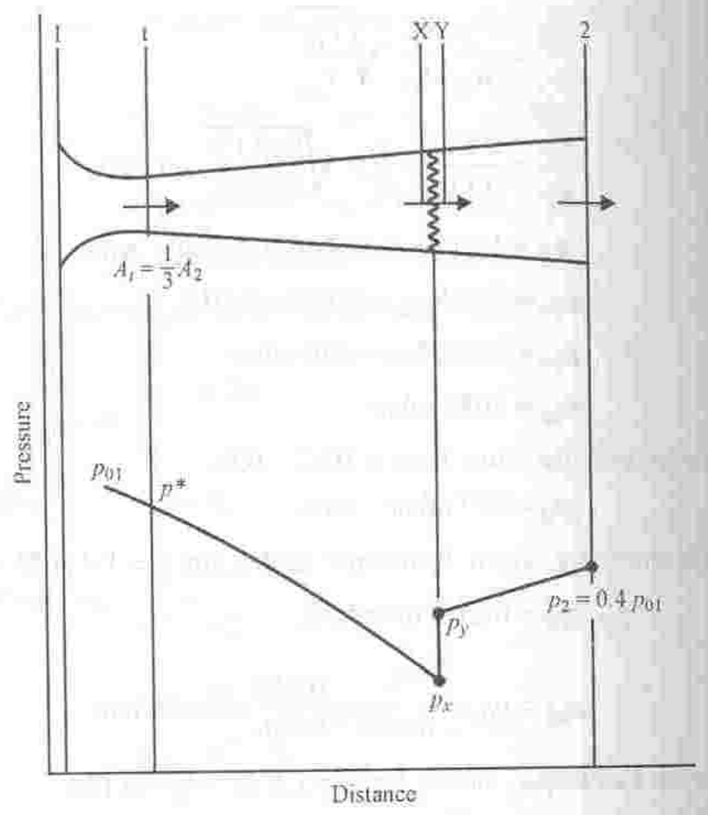

FIGURE 6.17 : Normal shock in a convergent-divergent nozzle (Example 6.4)

$$A_y^* = A_2^*$$

$$\frac{\dot{m}\sqrt{T_0}}{A^* p_0} = \text{constant}$$

For constant $\dot{m}$ and T_0,

$$A^* p_0 = \text{constant}$$

Therefore, between the entry and exit sections

$$A_1^* p_{01} = A_2^* p_{02}$$

$$p_{01} = p_{0t} = p_{0x}$$

$$p_{0y} = p_{02}$$

$$\frac{A_1^*}{A_2^*} = \frac{p_{02}}{p_{01}}$$

$$\frac{A_1}{A_2^*} = \frac{A_1}{A_1^*}\frac{A_1^*}{A_2^*} = \frac{A_1}{A_1^*}\frac{p_{02}}{p_{01}}$$

Similarly $$\frac{A_t}{A_2^*} = \frac{A_t}{A_t^*}\frac{p_{02}}{p_{0t}} = \frac{p_{02}}{p_{01}}$$

Now $$\frac{A_2}{A_t} = \frac{A_2}{A_2^*}\frac{A_2^*}{A_t} = \frac{A_2}{A_2^*}\frac{p_{01}}{p_{02}} = 3$$

Substituting for p_{01}

$$\frac{A_2}{A_2^*}\frac{p_2}{0.4}\frac{1}{p_{02}} = 3$$

$$\frac{A_2 p_2}{A_2^* p_{02}} = 1.2$$

From Isentropic tables at $\dfrac{Ap}{A^* p_0} = 1.2$

$$M = M_2 = 0.472 \text{ and } \frac{p}{p_0} = \frac{p_2}{p_{02}} = 0.859$$

$$p_{02} = \frac{p_2}{0.859} = \frac{0.4 p_{01}}{0.859} = 0.466 p_{01}$$

$$\frac{p_{0y}}{p_{0x}} = \frac{p_{02}}{p_{01}} = 0.466$$

(*a*) From normal shock tables at $\dfrac{p_{0y}}{p_{0x}} = 0.466$

$$\left.\begin{aligned} M_x &= 2.58 \\ M_y &= 0.506 \end{aligned}\right\} \quad \textbf{Ans.}$$

$$\frac{p_{0y}}{p_x} = 9.115$$

(*b*) From Isentropic tables at $M = M_x = 2.58$

$$\frac{A}{A^*} = 2.842$$

$$\frac{A_x}{A_x^*} = \frac{A_x}{A_t} = \frac{A}{A^*} = 2.842$$

Therefore, shock occurs in the diverging portion where

$$A_x = 2.842 A_t \quad \textbf{Ans.}$$

(*c*) $$p_x = \frac{p_{0y}}{9.115} = \frac{p_{02}}{9.115} = \frac{0.466 p_{01}}{9.115}$$

$$p_x = 0.051 p_{01} \quad \textbf{Ans.}$$

The same value can also be obtained by taking the value of p/p_0 direct from the isentropic tables at $M = 2.58$.

Example 6.5. The velocity of a normal shock wave moving into stagnant air ($p = 1.0$ bar, $t = 17°C$) is 500 m/s. If the area of cross-section of the duct is constant determine (*a*) pressure (*b*) temperature (*c*) velocity of air (*d*) stagnation temperature and (*e*) the Mach number imparted upstream of the wave front.

Solution. Refer to Figures 6.14 and 6.15. The shock is first considered in the moving co-ordinate system; here the shock is stationary and the stagnant air on the right of the wave appears to be flowing through the wave towards the left (Figure 6.15)

$$T_x = 273 + 17 = 290 \text{ K}, \; p_x = 1.0 \text{ bar}$$

$$c_x = 500 \text{ m/s}$$

$$a_x = \sqrt{\gamma R T_x}$$

$$a_x = \sqrt{1.4 \times 287 \times 290} = 341.35 \text{ m/s}$$

$$M_x = \frac{c_x}{a_x} = \frac{500}{341.35} = 1.465$$

From normal shock tables at $M_x = 1.465$

$$M_y = 0.715, \; \frac{p_y}{p_x} = 2.335, \; \frac{T_y}{T_x} = 1.297$$

(*a*) $$p_y = 2.335 p_x = 2.335 \times 1 = 2.335 \text{ bar}$$

$$p_y' = p_y = 2.335 \text{ bar} \quad \textbf{Ans.}$$

$$T_y = 1.297 \times T_x = 1.297 \times 290 = 376.13 \text{ K}$$

(*b*) $$T_y = T_y' = 376.13 \text{ K} \quad \textbf{Ans.}$$

$$a_y = \sqrt{\gamma R T_y} = \sqrt{1.4 \times 287 \times 376.13} = 388.75 \text{ m/s}$$

$$c_y = M_y \, . \, a_y = 0.715 \times 388.75 = 277.95 \text{ m/s}$$

$$c_y = c_x - c_y'$$

$$c_y' = c_x - c_y = 500 - 277.95$$

(*c*) $$c_y' = 222.05 \text{ m/s} \quad \textbf{Ans.}$$

(*d*) Now the shock is considered as moving (Figure 6.14)

$$M_y' = \frac{c_y'}{a_y} = \frac{222.05}{388.75} = 0.571 \quad \textbf{Ans.}$$

(*e*) From Isentropic tables at $M = M_y' = 0.571$

$$\frac{T}{T_0} = \frac{T_y'}{T_{0y'}} = 0.939$$

$$T_{0y'} = \frac{T_y'}{0.939} = \frac{376.13}{0.939} = 400.56 \text{ K} \quad \textbf{Ans.}$$

Example 6.6. The following data refers to a supersonic wind tunnel:

Nozzle throat area $= 200 \text{ cm}^2$

Test section cross-section $= 337.5 \text{ cm}^2$

Working fluid: air ($\gamma = 1.4$, $c_p = 0.287$ kJ/kg K)

Determine the test section Mach number and the diffuser throat area if a normal shock is located in the test section.

Solution. Refer to Figure 6.10. The cross-sectional area of the test section $A = 337.5 \text{ cm}^2$. Nozzle throat area $A^* = 200 \text{ cm}^2$

$$\frac{A}{A^*} = \frac{337.5}{200} = 1.6875$$

From Isentropic tables for $\gamma = 1.4$ at $\frac{A}{A^*} = 1.6875$

the test section Mach number is

$$M = M_x = 2.0 \quad \textbf{Ans.}$$

For normal shock in the test section

$$\frac{\dot{m}\sqrt{T_{0x}}}{A_x^* p_{0x}} = \frac{\dot{m}\sqrt{T_{0y}}}{A_y^* p_{0y}}$$

But at $\dot{m} = \text{constant}$ and $T_{0x} = T_{0y}$

$$A_x^* p_{0x} = A_y^* p_{0y}$$

$$A_y^* = \left(\frac{p_{0x}}{p_{0y}}\right) A_x^*$$

From normal shock tables at $M_x = 2.0$

$$\frac{p_{0y}}{p_{0x}} = 0.721$$

Therefore, the diffuser throat area

$$A_y^* = \frac{200}{0.721} = 277.39 \text{ cm}^2 \quad \textbf{Ans.}$$

Alternatively,

From shock tables for $\gamma = 1.4$ at $M_x = 2.0$, $M_y = 0.577$.

From Isentropic tables for $\gamma = 1.4$ at $M = 0.577$

$$\left(\frac{A}{A^*}\right)_y = \frac{A_y}{A_y^*} = 1.217$$

Now the test-section cross-section

$$A_y = 337.5 \text{ cm}^2$$

Therefore, the diffuser throat cross-section is

$$A_y^* = \frac{A_y}{1.217} = \frac{337.5}{1.217} = 277.32 \text{ cm}^2.$$

Example 6.7. A supersonic diffuser for air ($\gamma = 1.4$) has an area ratio of 0.416 with an inlet Mach number of 2.4 (design value). Determine the exit Mach number and the design value of the pressure ratio across the diffuser for isentropic flow. At an off-design value of the inlet Mach number (2.7) a normal shock occurs inside the diffuser. Determine the upstream Mach number and area ratio at the section where the shock occurs, diffuser efficiency and the pressure ratio across the diffuser. Depict graphically the static pressure distribution at off design.

Solution. Refer to Figure 6.18.

Design values: $\frac{A_2}{A_1} = 0.416 = \frac{A_2/A_2^*}{A_1/A_1^*}$

From isentropic gas tables for $\gamma = 1.4$ at $M_1 = 2.4$

$$A_1/A_1^* = 2.403, \quad p_1/p_0 = 0.0684$$

Therefore, $A_2/A_2^* = 0.416 \times 2.403 = 0.9996 \approx 1$

From isentropic gas tables at this area ratio = 1

$$M_2 = 1 \text{ and } p_2/p_0 = 0.528$$

The pressure ratio across the diffuser is given by

$$\frac{p_2}{p_1} = \frac{p_2/p_0}{p_1/p_0} = \frac{0.528}{0.0684} = 7.7193$$

Therefore, for design values,

$$M_2 = 1 \quad \textbf{Ans.} \qquad p_2/p_1 = 7.7193 \quad \textbf{Ans.}$$

Off design values:

From Isentropic gas tables for $\gamma = 1.4$

at $M_1 = 2.7, \ \frac{p_1}{p_{01}} = 0.043, \ \frac{T_1}{T_{01}} = 0.407, \ \frac{A_1}{A_1^*} = \frac{A_1}{A_x^*} = 3.183$

at $M_2 = 1.0, \ \frac{p_2}{p_{02}} = 0.528, \ \frac{A_2}{A_2^*} = \frac{A_2}{A_y^*} = 1.0$

Now, $p_{01} = p_{0x}$ and $p_{02} = p_{0y}$, therefore,

$$\frac{p_{0y}}{p_{0x}} = \frac{p_{02}}{p_{01}} = \frac{A_2^*}{A_1^*} = \frac{A_1/3.183}{A_2/1.0} = \frac{1}{3.183 A_2/A_1}$$

Substituting $A_2/A_1 = 0.416$ (design value)

$$\frac{p_{0y}}{p_{0x}} = \frac{1}{3.183 \times 0.416} = 0.7552$$

From normal shock tables ($\gamma = 1.4$)

at $p_{0y}/p_{0x} = 0.7552$

$$M_x = 1.92, \ M_y = 0.592, \ A_x/A_x^* = 1.58$$

$$M_x = 1.92 \quad \textbf{Ans.}$$

$$\frac{A_x}{A_1} = \frac{A_x/A_x^*}{A_1/A_1^*} = \frac{1.58}{3.183} = 0.496 \quad \textbf{Ans.}$$

The diffuser efficiency at off-design with shock is given by

$$\eta_D = \frac{\dfrac{T_{01}}{T_1}\left(\dfrac{p_{0y}}{p_{0x}}\right)^{(\gamma-1)/\gamma} - 1}{\dfrac{\gamma-1}{2} M_1^2}$$

$$\eta_D = \frac{\dfrac{1}{0.407}(0.7552)^{0.286} - 1}{\dfrac{1.4-1}{2} \times 2.7^2}.$$

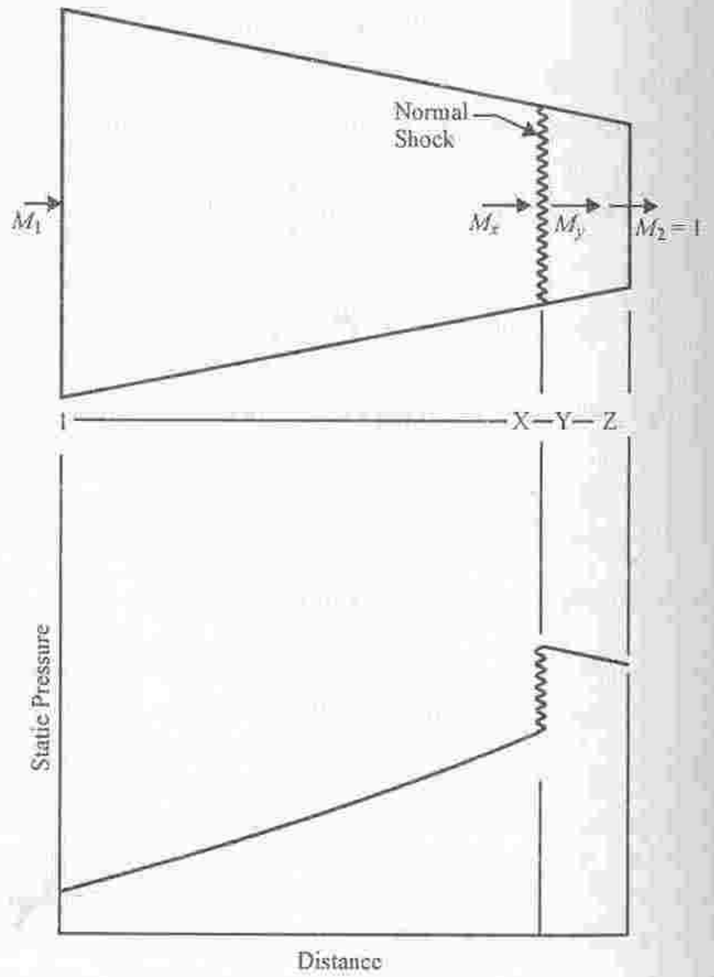

FIGURE 6.18 : Static pressure distribution in a supersonic diffuser with normal shock (Example 6.7)

$$\eta_D = 0.8694 \quad \textbf{Ans.}$$

The static pressure distribution through the diffuser is shown in Figure 6.18.

QUESTIONS AND PROBLEMS

6.1 (*a*) Explain how strong compression and expansion waves are formed in a compressible fluid.

(*b*) Under what conditions a compression wave changes into a shock wave?

(*c*) Why are expansion shocks impossible?

6.2 (*a*) Write down the four basic Equations which satisfy the state points before and after a normal shock wave.

(*b*) Using the above Equations prove that at the maximum entropy point on the enthalpy-entropy diagrams the Mach number is unity.

6.3 Starting from the energy Equation for flow through a normal shock obtain the following relations:

$$c_x c_y = a^{*2}$$

$$M_x^* M_y^* = 1$$

6.4 Derive the following relations for flow through a normal shock:

(*a*) $M_y^2 = \dfrac{[2/(\gamma-1)] + M_x^2}{[2\gamma/(\gamma-1)] M_x^2 - 1}$

(*b*) $\dfrac{p_y}{p_x} = \dfrac{2\gamma}{\gamma+1} M_x^2 - \dfrac{\gamma-1}{\gamma+1}$

(*c*) $\dfrac{T_y}{T_x} = \dfrac{[1 + [(\gamma-1)/2] M_x^2]\ [[2\gamma/(\gamma-1)] M_x^2 - 1]}{\dfrac{1}{2}[(\gamma+1)^2/(\gamma-1)] M_x^2}$

(*d*) $\dfrac{c_y}{c_x} = \left(\dfrac{2}{\gamma+1}\right)\dfrac{1}{M_y^2} + \dfrac{\gamma-1}{\gamma+1}.$

6.5 (*a*) Show that the stagnation pressure ratio and the change in entropy across a normal shock are given by

$$\frac{p_{0y}}{p_{0x}} = \left\{ \frac{\frac{\gamma+1}{2} M_x^2}{1 + \frac{\gamma-1}{2} M_x^2} \right\}^{\gamma/(\gamma-1)} \times \left(\frac{2\gamma}{\gamma+1} M_x^2 - \frac{\gamma-1}{\gamma+1} \right)^{-1/(\gamma-1)}$$

$$\Delta s = c_p \ln \left(\frac{p_{0y}}{p_{0x}} \right)^{-(\gamma-1)/\gamma} = R \ln \left(\frac{p_{0x}}{p_{0y}} \right)$$

(*b*) If a diffuser achieves compression of air through a normal shock wave at an initial Mach number of 1.5 determine (*i*) its efficiency (*ii*) stagnation pressure loss and (*iii*) the increase in entropy.

Ans. (*i*) 93.1%, (*ii*) 7.0%, (*iii*) 0.02 kJ/kg K.

6.6 A jet of air at 275 K and 0.69 bar has an initial Mach number of 2.0. If it passes through a normal shock wave determine (*a*) Mach number (*b*) pressure (*c*) temperature (*d*) density (*e*) speed of sound and (*f*) jet velocity downstream of the shock.

Ans. (*a*) 0.577, (*b*) 3.105 bar, (*c*) 463.93 K, (*d*) 2.332 kg/m^3, (*e*) 431.75 m/s, (*f*) 249.1 m/s.

6.7 An aircraft flies at a Mach number of 1.2 at an altitude of 16000 metres ($p = 103$ mbar, $T = 216.65$ K). The compression in its engine is partly achieved by a normal shock wave standing at the entry of its diffuser. Determine immediately downstream of the shock:

(*a*) Mach number,

(*b*) temperature of the air,

(*c*) pressure of the air, and

(*d*) stagnation pressure loss across the shock.

Ans. (*a*) 0.842, (*b*) 244.38 K, (*c*) 155.84 mbar, (*d*) 2 m bar.

6.8 Explain why the throat area of the diffuser in a supersonic wind tunnel is larger than the nozzle throat area. Why is it desirable to locate the shock wave at the diffuser throat during the operation of the tunnel?

6.9 Determine the test section Mach numbers and diffuser throat areas in Example 6.6 for gases with

(*a*) $\gamma = 1.3$, (*b*) $\gamma = 1.67$.

Ans. (*a*) $M_x = 1.945$, $A_y^* = 273.97$ cm^2,

(*b*) $M_x = 2.15$, $A_y^* = 283.68$ cm^2.

6.10 Solve Example 6.5 with

(*a*) $\gamma = 1.3$, $R = 0.49$ kJ/kg K, (*b*) $\gamma = 1.67$, $R = 0.208$ kJ/kg K.

Ans. For $\gamma = 1.3$: $p_y' = 1.391$ bar, $T_y' = 313.2$ K, $c_y' = 122.71$ m/s, $M_y' = 0.275$ and $T_{0y}' = 317$ K. For $\gamma = 1.67$; $p_y' = 2.871$ bar, $T_y' = 458.2$ K, $c_y' = 223.93$ m/s, $M_y' = 0.561$ and $T_{0y}' = 505.7$ K.

6.11 The stagnation pressure and temperature of air at the entry of a nozzle are 5 bar and 500 K respectively. The exit Mach number is 2.0 where a normal shock occurs. Calculate the following quantities before and after the shock: Static and stagnation pressures and temperatures, air velocities and Mach numbers. What are the values of stagnation pressure loss and increase in entropy across the shock?

Ans. $p_x = 0.64$ bar, $T_x = 277.5$ K, $p_{0x} = 5$ bar

$T_{0x} = 500$ K, $c_x = 667.83$ m/s, $M_x = 2.0$

$p_y = 2.88$ bar, $T_y = 468.14$ K, $p_{0y} = 3.605$ bar

$T_{0y} = 500$ K, $c_y = 250.24$ m/s, $M_y = 0.577$

$\Delta p_0 = 1.395$ bar, $\Delta s = 0.09388$ kJ/kg K.

6.12 A Mach-2 aircraft engine employes a subsonic inlet diffuser of area ratio 3. A normal shock is formed just upstream of the diffuser inlet. The free-stream conditions upstream of the diffuser are: $p = 0.10$ bar, $T = 300$ K. Determine:

(*a*) Mach number, pressure and temperature at the diffuser exit.

(*b*) Diffuser efficiency including the shock.

Assume Isentropic flow in the diffuser downstream of the shock.

Ans. (*a*) $M = 0.16$, $p = 0.554$ bar, $T = 537.8$ K

(*b*) $\eta_D = 0.800$.

6.13 (*a*) Derive the following relations for normal shock waves:

(*i*) $M_y\,(\text{minimum}) = \sqrt{\frac{\gamma-1}{2\gamma}}$

(*ii*) $(\rho_y/\rho_x)_{\max} = \frac{\gamma+1}{\gamma-1}$

(*iii*) $\dfrac{A_y^*}{A_x^*} = e^{\Delta s/R}$

(*b*) Depict graphically the variation of the following quantities with the Mach number upstream of the normal shock:

$$M_y,\ A_y^*/A_x^*,\ p_y/p_x,\ \rho_y/\rho_x,\ \frac{c_x}{c_y}.$$

6.14 A supersonic nozzle is provided with a constant diameter circular duct at its exit. The duct diameter is same as the nozzle exit diameter. Nozzle exit cross-section is three times that of its throat. The entry conditions of the gas ($\gamma = 1.4$, $R = 0.287$ kJ/kg K) are $p_0 = 10$ bar, $T_0 = 600$ K. Calculate the static pressure, Mach number and the velocity of the gas in the duct:

(*a*) when the nozzle operates at its design condition,

(*b*) when a normal shock occurs at its exit, and

(*c*) when a normal shock occurs at a section in the diverging part where the area ratio $A/A^* = 2.0$

Ans. (*a*) $p = 0.471$ bar, $M = 2.64$, $c = 837.05$ m/s

(*b*) $p = 3.7515$ bar, $M = 0.5$, $c = 239.33$ m/s

(*c*) $p = 5.834$ bar, $M = 0.328$, $c = 159.3$ m/s.

6.15 A nozzle is designed for superheated steam ($\gamma = 1.3$) with a pressure ratio $p/p_0 = 0.185$; this operates at an off-design condition with a pressure ratio of 0.754. Determine the area ratio (A/A^*) at the section where the normal shock occurs. What are the values of design and off-design Mach numbers at the nozzle exit?

Ans. $A/A^* = 1.254$; $M_2 = 1.78$ (design); $M_2 = 0.52$ (off-design).

6.16 Determine the pressure ratio and exit Mach number for a normal shock at the area ratio $A/A^* = 1.305$ in the nozzle of Problem 6.15. What is the maximum value of the Mach number occurring in the nozzle?

Ans. $p_2/p_{01} = 0.725$, $M_2 = 0.54$, $M_{max} = 1.64$.

7

Flow With Oblique Shock Waves

When the direction of flow is inclined at an oblique angle to the shock wave it is known as "oblique shock wave". Normal shock wave discussed in Chapter 6 is a special case of oblique shock wave in which the wave angle (σ) is 90 degrees. The oblique shock is also referred to as a two dimensional plane shock wave. A shock of conical shape is oblique but not plane.

A stronger oblique shock wave is nearer to a normal shock wave and has a larger wave angle (approaching 90 degrees); whereas weak oblique shock waves have smaller wave angles and are closer to the Mach waves. There are large changes in flow parameters across strong oblique shocks.

Oblique shocks are found to occur at the exit of turbine blade passages (Figure 7.1) with supersonic flow. Their presence alters the direction of the jet at the exit of the blades.

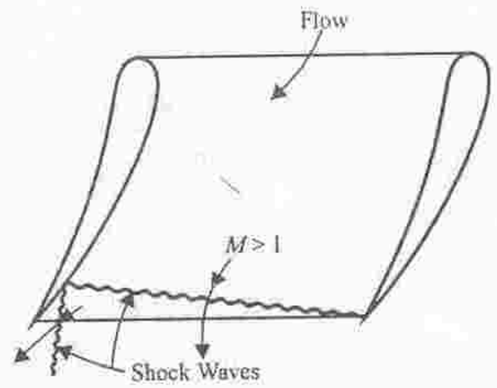

FIGURE 7.1 : Oblique shock waves in a turbine blade passage

Interferograms of supersonic flow fields over wedges of small and large angles show the presence of attached shocks on thinner wedges and detached shocks upstream of the thick wedges and blunt bodies (aerofoils with thick leading edges). These are shown in Figures 7.2 (*a*), (*b*), (*c*) and (*d*).

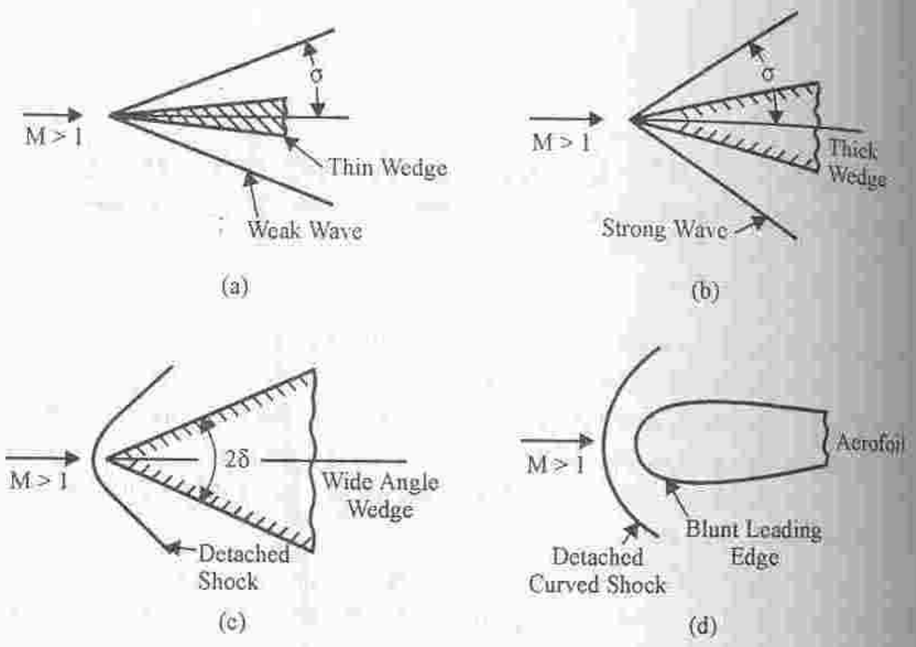

FIGURE 7.2 : Examples of oblique shock waves

The diffusion in the Oswatitsch diffuser is through conical shock waves as shown in Figure 7.3. Oblique and curved shocks are also formed at the entry of supersonic diffusers of aircraft engines. Figure 7.4 shows attached and detached shocks of this type.

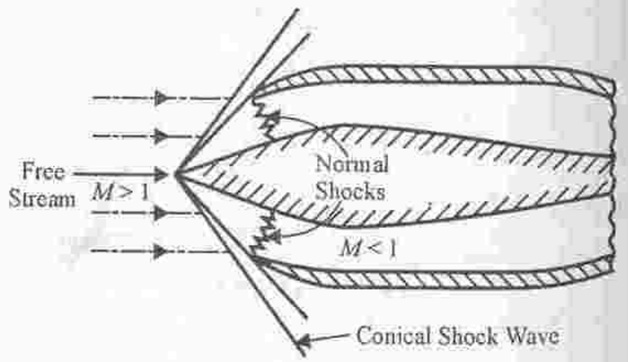

FIGURE 7.3 : Conical shock waves on Oswatitsch type diffuser

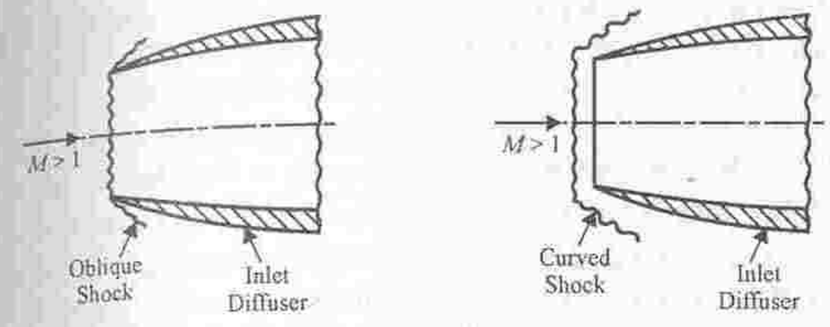

FIGURE 7.4 : Oblique shock waves at supersonic inlets

The drag due to shock on an aerodynamic body is greater for a larger wave angle; this is on account of greater turning of a supersonic jet in the presence of a thick leading edge. Therefore, in order to reduce this drag the nose in such a case must be made slimmer. The shock waves on such bodies are curved instead of straight oblique as shown in Figures 7.2 (*c*) and (*d*).

7.1 NATURE OF FLOW THROUGH OBLIQUE SHOCK WAVES

An oblique shock is formed when a supersonic flow is deflected inwards (anticlockwise direction). Figure 7.5 (*b*) shows a supersonic flow stream over a concave corner of a curved wall. This produces an oblique shock

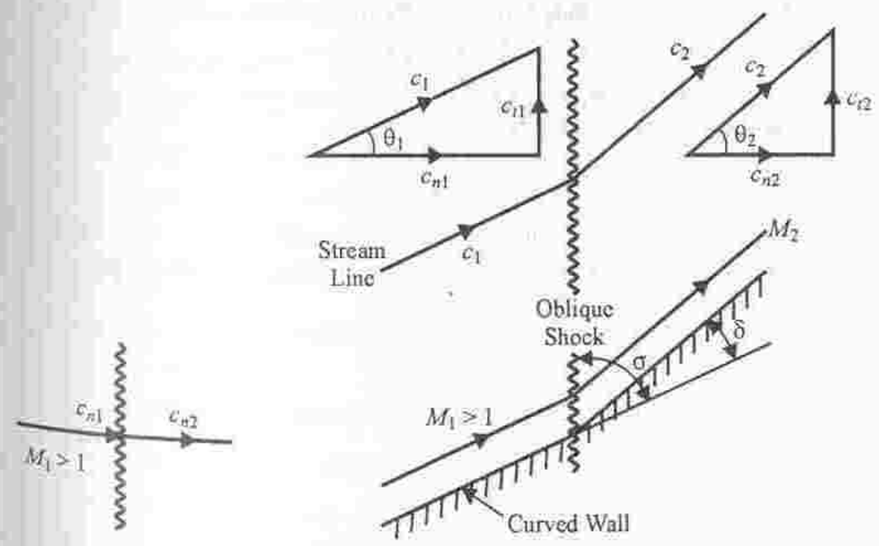

(*a*) Flow through normal shock (*b*) Flow through oblique shock

FIGURE 7.5 : Transformation of a normal shock pattern into an oblique shock

wave at the corner. The flow is parallel to the walls before and after the shock. The angle which the oblique shock wave makes with the initial direction of flow is called the wave angle σ; for a given gas this is a function of the upstream Mach number M_1 and the deviation angle δ. The downstream Mach number M_2 is less than its upstream value. But unlike normal shocks this may or may not be less than unity.

Figures 7.5 (*a*) and (*b*) explain the development of an oblique shock wave, and the nature of flow through it; here the flow through a normal shock is transformed into an oblique shock. The velocities upstream and downstream of a normal shock wave (Figure 7.5 (*a*)) are c_{n1} and c_{n2} respectively. Now the normal shock pattern of Figure 7.5 (*a*) is transformed into a coordinate system which is moving downwards at a velocity c_t; this imparts upward velocity components of c_t to the flows both upstream and downstream of the shock wave. This pattern is shown in Figure 7.5 (*b*).

The velocity triangles obtained in this new flow pattern are shown on each side of the shock wave in Figure 7.5 (*b*). The resultant velocity vectors c_1 and c_2 are inclined to the normal direction at angles θ_1 and θ_2 respectively. For the upstream side of the shock

$$\tan \theta_1 = \frac{c_{t1}}{c_{n1}} \tag{7.1}$$

The direction and magnitude of the tangential velocity components is same on both the sides of the shock wave.

This is possible since there is no pressure gradient along the shock wave in the tangential direction.

$$c_t = c_{t1} = c_{t2} \tag{7.2}$$

As explained in Chapter 6 there is a reduction in the magnitude of the normal component of velocity and Mach number downstream of the shock.

$$c_{n2} < c_{n1} \tag{7.3}$$

From the velocity triangle downstream of the shock

$$\tan \theta_2 = \frac{c_{t2}}{c_{n2}} \tag{7.4}$$

Equations (7.1) to (7.4) yield,

$$\tan \theta_2 > \tan \theta_1 \tag{7.5}$$

which shows that the flow deviates anticlockwise after passing through the shock wave. The angle of deviation or deflection is

$$\delta = \theta_2 - \theta_1 \tag{7.6}$$

From the velocity triangles

$$c_1^2 = c_{n1}^2 + c_t^2$$

$$c_2^2 = c_{n2}^2 + c_t^2$$

Since $c_{n2} < c_{n1}$

$$c_2 < c_1$$

Also since $T_2 > T_1$ due to compression

$$\frac{c_2}{\sqrt{\gamma RT_2}} < \frac{c_1}{\sqrt{\gamma RT_1}}$$

$$M_2 < M_1$$

Now an ideal supersonic flow similar to the above pattern is considered along a concave corner as shown in the lower part of Figure 7.5 (*b*); the inclined walls are parallel to the velocity vectors c_1 and c_2. Here an initially supersonic flow at Mach number M_1 is deflected anticlockwise through an angle δ by the curved wall. The oblique shock wave occurs at the corner due to the turning of the supersonic flow; the wave angle is σ and the downstream Mach number M_2.

7.2 FUNDAMENTAL RELATIONS

In this section some fundamental relations for the oblique shock waves are derived; they form the basis of various equations relating the flow parameters on the two sides of the shock. Following assumptions are used:

(*a*) perfect gas,
(*b*) steady, adiabatic and frictionless flow through a stationary oblique shock wave,
(*c*) absence of external work, and
(*d*) absence of body forces.

Figure 7.6 shows an initially supersonic flow through a control volume containing the oblique shock wave. The velocity triangles of Figure 7.5 (*b*) have been redrawn in Figure 7.7.

Oblique shock relations are governed by the equation of continuity, momentum equations in the tangential and normal directions, the energy equation and the equation of state. These equations will be written for the flow through the control volume shown in Figure 7.6.

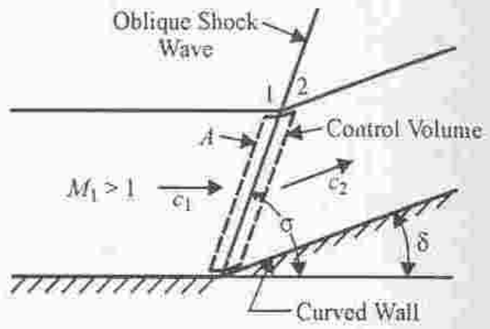

FIGURE 7.6 : Flow through an oblique shock

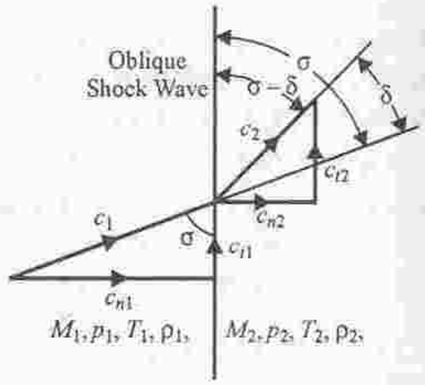

FIGURE 7.7 : Velocity triangles upstream and downstream of an oblique shock

Continuity equation gives

$$\dot{m} = \rho_1 A\, c_{n1} = \rho_2 A\, c_{n2} \tag{7.7}$$

The area A perpendicular to the normal velocity components is same on the two sides of the shock.

$$\rho_1 c_{n1} = \rho_2 c_{n2} \tag{7.8}$$

Momentum equation in the tangential direction is

$$\dot{m}\, c_{t1} = \dot{m}\, c_{t2}$$

$$c_{t1} = c_{t2} = c_t$$

This is same as Equation (7.2).

Momentum equation in the normal direction is

$$\dot{m}\, c_{n1} - \dot{m}\, c_{n2} = (p_2 - p_1) A$$

Substituting from Equation (7.7)

$$\rho_1 A\, c_{n1}^2 - \rho_2 A\, c_{n2}^2 = A\,(p_2 - p_1)$$

$$\rho_1 c_{n1}^2 - \rho_2 c_{n2}^2 = p_2 - p_1 \tag{7.9}$$

Energy equation gives

$$h_0 = h_{01} = h_{02} = \text{constant}$$

$$h_1 + \frac{1}{2} c_1^2 = h_2 + \frac{1}{2} c_2^2$$

$$h_2 - h_1 = \frac{1}{2}(c_1^2 - c_2^2)$$

$$c_p (T_2 - T_1) = \frac{1}{2}(c_1^2 - c_2^2) \tag{7.10}$$

Velocity triangles upstream and downstream of the shock give

$$c_1^2 - c_2^2 = (c_{n1}^2 + c_t^2) - (c_{n2}^2 + c_t^2)$$

$$c_1^2 - c_2^2 = c_{n1}^2 - c_{n2}^2 \tag{7.11}$$

Equation of state gives

$$h = c_p T = \frac{\gamma}{\gamma - 1} RT = \frac{a^2}{\gamma - 1} = \frac{\gamma}{\gamma - 1} \frac{p}{\rho} \tag{7.12}$$

Substituting from Equations (7.11) and (7.12) in (7.10)

$$\frac{\gamma}{\gamma - 1}\left(\frac{p_2}{\rho_2} - \frac{p_1}{\rho_1}\right) = \frac{1}{2}(c_{n1}^2 - c_{n2}^2) \tag{7.13}$$

Equation (7.12) in terms of stagnation values can be written as

$$h_0 = c_p T_0 = \frac{\gamma}{\gamma - 1} RT_0 = \frac{\gamma}{\gamma - 1} \frac{p_0}{\rho_0} = \frac{a_0^2}{\gamma - 1} \tag{7.14 (a)}$$

In Chapter 2 Equation (2.47) is

$$h_0 = \frac{a_0^2}{\gamma - 1} = \frac{1}{2} \frac{\gamma + 1}{\gamma - 1} a^{*2} \tag{2.47}$$

Equations (2.47) and (7.14 (*a*)) give

$$h_0 = \frac{\gamma}{\gamma-1}\frac{p_0}{\rho_0} = \frac{a_0^2}{\gamma-1} = \frac{1}{2}\frac{\gamma+1}{\gamma-1}a^{*2} \qquad (7.14\ (b))$$

Equations (7.13), (7.14 (*a*)) and (7.14 (*b*)) are different forms of the energy equation.

7.3 PRANDTL'S EQUATION

Here a relation similar to Equation (6.22) will be derived for oblique shocks.

Substituting Equation (7.2) in (7.13) gives

$$\frac{\gamma}{\gamma-1}\left(\frac{p_2}{\rho_2}-\frac{p_1}{\rho_1}\right) = \frac{1}{2}(c_{n1}^2 + c_{t1}^2) - \frac{1}{2}(c_{n2}^2 + c_{t2}^2)$$

This on rearrangement gives

$$\frac{\gamma}{\gamma-1}\frac{p_1}{\rho_1} + \frac{1}{2}(c_{n1}^2 + c_{t1}^2) = \frac{\gamma}{\gamma-1}\frac{p_2}{\rho_2} + \frac{1}{2}(c_{n2}^2 + c_{t2}^2)$$

Using velocity triangles and Equation (7.12) on both sides of the above equation we get

$$\frac{\gamma}{\gamma-1}\frac{p_1}{\rho_1} + \frac{1}{2}(c_{n1}^2 + c_{t1}^2) = h_1 + \frac{1}{2}c_t^2 = h_0 \qquad (7.15)$$

From Equations (7.14 (*b*)) and (7.15) we get

$$\frac{\gamma}{\gamma-1}\frac{p_1}{\rho_1} + \frac{1}{2}(c_{n1}^2 + c_{t1}^2) = \frac{1}{2}\frac{\gamma+1}{\gamma-1}a^{*2}$$

$$p_1 = \frac{\gamma-1}{2\gamma}\rho_1\left\{\frac{\gamma+1}{\gamma-1}a^{*2} - (c_{n1}^2 + c_{t1}^2)\right\}$$

$$p_1 = \rho_1\left\{\frac{\gamma+1}{2\gamma}a^{*2} - \frac{\gamma-1}{2\gamma}(c_{n1}^2 + c_{t1}^2)\right\} \qquad (7.16)$$

Similarly $$\frac{\gamma}{\gamma-1}\frac{p_2}{\rho_2} + \frac{1}{2}(c_{n2}^2 + c_{t2}^2) = \frac{1}{2}\frac{\gamma+1}{\gamma-1}a^{*2} \qquad (7.17)$$

$$p_2 = \rho_2\left\{\frac{\gamma+1}{2\gamma}a^{*2} - \frac{\gamma-1}{2\gamma}(c_{n2}^2 + c_{t2}^2)\right\} \qquad (7.18)$$

Substituting Equations (7.16) and (7.18) in (7.9) gives

$$\rho_1 c_{n1}^2 - \rho_2 c_{n2}^2 = \frac{\gamma+1}{2\gamma}a^{*2}(\rho_2-\rho_1) + \frac{\gamma-1}{2\gamma}\{\rho_1(c_{n1}^2 + c_{t1}^2) - \rho_2(c_{n2}^2 + c_{t2}^2)\}$$

Using $c_{t1} = c_{t2} = c_t$ and rearranging we get

$$\frac{\gamma+1}{2\gamma}(\rho_2-\rho_1)a^{*2} = \left(1-\frac{\gamma-1}{2\gamma}\right)(\rho_1 c_{n1}^2 - \rho_2 c_{n2}^2) + \frac{\gamma-1}{2\gamma}(\rho_2-\rho_1)c_t^2$$

$$\frac{\gamma+1}{2\gamma}(\rho_2-\rho_1)a^{*2} = \frac{\gamma+1}{2\gamma}(\rho_1 c_{n1}^2 - \rho_2 c_{n2}^2) + \frac{\gamma-1}{2\gamma}(\rho_2-\rho_1)c_t^2$$

$$a^{*2} = \frac{\gamma-1}{\gamma+1}c_t^2 + \frac{\rho_1 c_{n1}^2 - \rho_2 c_{n2}^2}{\rho_2-\rho_1}$$

$$a^{*2} - \frac{\gamma-1}{\gamma+1}c_t^2 = \frac{c_{n1}c_{n2}}{\rho_2-\rho_1}\left(\rho_1\frac{c_{n1}}{c_{n2}} - \rho_2\frac{c_{n2}}{c_{n1}}\right)$$

However, from Equation (7.8), $\frac{c_{n1}}{c_{n2}} = \frac{\rho_2}{\rho_1}$

Therefore, $$a^{*2} - \frac{\gamma-1}{\gamma+1}c_t^2 = c_{n1}c_{n2} \qquad (7.19)$$

This is known as Prandtl's equation for oblique shocks. This reduces to Equation (6.22) for normal shocks by making the following substitutions:

$c_t = 0$

$c_{n1} = c_1 = c_x$

$c_{n2} = c_2 = c_y$ (see Figure 7.5)

7.4 RANKINE-HUGONIOT EQUATION

The relations derived earlier are used here to relate pressure ratio p_2/p_1 to the density ratio ρ_2/ρ_1 across the oblique shock.

Equation (7.9) is rewritten as

$$p_2 - p_1 = \rho_1 c_{n1}^2\left(1 - \frac{\rho_2}{\rho_1}\frac{c_{n2}^2}{c_{n1}^2}\right)$$

Substituting from Equation (7.8) for c_{n2}^2/c_{n1}^2

$$p_2 - p_1 = \rho_1 c_{n1}^2 \left(1 - \frac{\rho_1}{\rho_2}\right) = (\rho_2 - \rho_1)\frac{\rho_1}{\rho_2} c_{n1}^2$$

$$c_{n1}^2 = \frac{p_2 - p_1}{\rho_2 - \rho_1}\frac{\rho_2}{\rho_1} \tag{7.20}$$

Substituting Equation (7.8) in (7.20) we get

$$c_{n2}^2 = \frac{p_2 - p_1}{\rho_2 - \rho_1}\frac{\rho_1}{\rho_2} \tag{7.21}$$

Substituting from Equations (7.20) and (7.21) in (7.13)

$$\frac{\gamma}{\gamma - 1}\left(\frac{p_2}{\rho_2} - \frac{p_1}{\rho_1}\right) = \frac{1}{2}\left(\frac{p_2 - p_1}{\rho_2 - \rho_1}\right)\left(\frac{\rho_2}{\rho_1} - \frac{\rho_1}{\rho_2}\right)$$

$$= \frac{1}{2}\frac{(p_2 - p_1)\ (\rho_2 + \rho_1)}{\rho_1 \rho_2}$$

On rearranging, we get

$$2\gamma(\rho_1 p_2 - \rho_2 p_1) = (\gamma - 1)\ (p_2 - p_1)\ (\rho_2 + \rho_1) \tag{7.22}$$

$$p_2\{2\gamma\rho_1 - (\gamma - 1)\ (\rho_2 + \rho_1)\} = p_1(2\gamma\rho_2 - (\gamma - 1)\ (\rho_2 + \rho_1)\}$$

After simplifying and rearranging, we get

$$p_2\{(\gamma - 1)\rho_2 - (\gamma + 1)\rho_1\} = p_1\{(\gamma - 1)\rho_1 - (\gamma + 1)\rho_2\}$$

$$\frac{p_2}{p_1} = \frac{(\gamma - 1)\rho_1 - (\gamma + 1)\rho_2}{(\gamma - 1)\rho_2 - (\gamma + 1)\rho_1}$$

$$\frac{p_2}{p_1} = \frac{\frac{\gamma + 1}{\gamma - 1}\frac{\rho_2}{\rho_1} - 1}{\frac{\gamma + 1}{\gamma - 1} - \frac{\rho_2}{\rho_1}} \tag{7.23}$$

Equation (7.22) can also be written by collecting the coefficients for ρ_2 and ρ_1 separately

$$\rho_2\{-2\gamma p_1 - (\gamma - 1)\ (p_2 - p_1)\} = \rho_1\{(\gamma - 1)\ (p_2 - p_1) - 2\gamma p_2\}$$

After simplifying and rearranging, we get

$$\frac{\rho_2}{\rho_1} = \frac{(\gamma + 1)\ p_2 + (\gamma - 1)\ p_1}{(\gamma + 1)\ p_1 + (\gamma - 1)\ p_2}$$

$$\frac{\rho_2}{\rho_1} = \frac{\frac{\gamma + 1}{\gamma - 1}\frac{p_2}{p_1} + 1}{\frac{\gamma + 1}{\gamma - 1} + \frac{p_2}{p_1}} \tag{7.24}$$

Equations (7.23) and (7.24) are the Rankine-Hugoniot equations and are identical to Equations (6.36) and (6.35) respectively; this was expected because the parameters in these equations are static quantities which are not affected by the moving coordinate system adopted to transform a normal shock into an oblique shock.

Combination of Equations (7.20) and (7.21) gives

$$c_{n1}^2\, c_{n2}^2 = \left(\frac{p_2 - p_1}{\rho_2 - \rho_1}\right)^2 \tag{7.25}$$

Substituting Equation (7.25) in (7.19) yields

$$a^{*2} - \frac{\gamma - 1}{\gamma + 1} c_t^2 = \frac{p_2 - p_1}{\rho_2 - \rho_1} \tag{7.26}$$

These relations will be used later.

7.5 VARIATION OF FLOW PARAMETERS

From Figure 7.7 and the various equations developed it is observed that a large number of dependent and independent variables on the two sides of the oblique shock wave are involved. In a given problem some of these parameters are known while others are to be determined.

A simple way to look at this rather complicated problem is to consider that a supersonic stream of gas at Mach number M_1 and a given state (p_1, T_1, etc.) is deflected by an angle δ which generates an oblique shock at a wave angle σ. Therefore, in such a problem dependent and independent variables may be written as

$$\sigma, p_2, T_2, \rho_2, a_2, c_2, M_2, p_{02}, s_2 = f(M_1, \delta, p_1, T_1, \rho_1, a_1, c_1, p_{01}, s_1) \tag{7.27}$$

But only a few of the above properties (in Equation (7.27)) need be known because the remaining can be calculated from the known quantities. For example

$$\left.\begin{aligned} \rho &= f(p,\ T) \\ a &= f(T) \\ M &= f(c,\ T) \\ p_0 &= f(p,\ M) \\ &\text{etc.} \end{aligned}\right\} \qquad (7.28)$$

Substituting Equations (7.28) in (7.27) we get

$$\sigma,\ p_2,\ T_2,\ c_2,\ s_2 = f(\delta,\ p_1,\ T_1,\ c_1,\ s_1) \qquad (7.29)$$

The initial properties p_1, T_1 and s_1 are fixed by the initial state of the gas. Besides this, various properties are generally determined as ratios or differences. In compressible flows the use of Mach numbers instead of velocities is preferred. In view of this Equation (7.29) is rewritten as

$$\sigma,\ \frac{p_2}{p_1},\ \frac{\rho_2}{\rho_1},\ M_2,\ \Delta s = f(\delta,\ M_1, \text{initial state}) \qquad (7.30)$$

It will be observed in the subsequent analyses that M_2 and Δs can also be determined from the wave angle, and pressure and density ratios.

Therefore, for a given initial state Equation (7.30) can be slightly modified

$$\sigma,\ \frac{p_2}{p_1},\ \frac{\rho_2}{\rho_1} = f(\delta,\ M_1) \qquad (7.31)$$

The variables in Equation (7.31) can be rearranged by taking any one of the following sets of parameters as independent variables:

(*a*) $\sigma,\ \delta$

(*b*) M_1, δ (as in Equation (7.30))

(*c*) $M_1,\ \sigma$

Since the relations in terms of M_1 and σ are comparatively more straight-forward, Equation (7.31) will be henceforth considered in the following form:

$$\delta,\ \frac{p_2}{p_1},\ \frac{\rho_2}{\rho_1} = f(M_1,\ \sigma) \qquad (7.32)$$

The first attempt in the following sections is to develop relations for the deflection, pressure ratio and the density ratio. Then other parameters are derived from the following:

$$\frac{T_2}{T_1} = f\left(\frac{p_2}{p_1},\ \frac{\rho_2}{\rho_1}\right) \qquad (7.33\ (a))$$

$$\frac{p_{02}}{p_{01}} = f\left(\frac{p_2}{p_1},\ \frac{\rho_2}{\rho_1}\right) \qquad (7.33\ (b))$$

$$\Delta s = f\left(\frac{p_{02}}{p_{01}}\right) \qquad (7.33\ (c))$$

$$M_2^2 = f\left(\frac{\rho_2}{\rho_1},\ \delta\right) \qquad (7.33\ (d))$$

7.5.1 Trigonometrical Relations

Following relations are obtained from the velocity triangles upstream and downstream of the oblique shock (Figure 7.7)

$$c_{n1} = c_1 \sin\sigma \qquad (7.34)$$

$$c_{t1} = c_t = c_1 \cos\sigma \qquad (7.35)$$

$$c_{n2} = c_2 \sin(\sigma - \delta) \qquad (7.36)$$

$$c_{t2} = c_t = c_2 \cos(\sigma - \delta) \qquad (7.37)$$

Equations (7.35) and (7.37) give

$$c_t = c_1 \cos\sigma = c_2 \cos(\sigma - \delta)$$

$$\frac{c_1}{c_2} = \frac{\cos(\sigma - \delta)}{\cos\sigma} \qquad (7.38)$$

Substituting Equations (7.34) and (7.36) in (7.8), we get

$$\rho_1 c_1 \sin\sigma = \rho_2 c_2 \sin(\sigma - \delta)$$

$$\frac{\rho_2}{\rho_1} = \frac{c_1}{c_2}\,\frac{\sin\sigma}{\sin(\sigma - \delta)} \qquad (7.39)$$

Combining Equations (7.38) and (7.39) we get

$$\frac{\rho_2}{\rho_1} = \frac{\tan\sigma}{\tan(\sigma - \delta)} \qquad (7.40)$$

Equation (7.9) gives

$$p_2 - p_1 = \rho_1 c_{n1}^2 \left(1 - \frac{\rho_2}{\rho_1}\frac{c_{n2}^2}{c_{n1}^2}\right)$$

$$p_2 - p_1 = \rho_1 c_1^2 \sin^2\sigma \left(1 - \frac{\rho_1}{\rho_2}\right)$$

Now $\rho_1 c_1^2 = \gamma p_1 M_1^2$

Therefore, $p_2 - p_1 = \gamma p_1 M_1^2 \sin^2\sigma \left(1 - \frac{\rho_1}{\rho_2}\right)$

$$\frac{p_2}{p_1} = 1 + \gamma M_1^2 \sin^2\sigma \left(1 - \frac{\rho_1}{\rho_2}\right) \tag{7.41}$$

In a similar manner from Equation (7.9) we get

$$p_1 - p_2 = \rho_2 c_{n2}^2 \left(1 - \frac{\rho_1 c_{n1}^2}{\rho_2 c_{n2}^2}\right)$$

$$p_1 - p_2 = \rho_2 c_2^2 \sin^2(\sigma - \delta) \left(1 - \frac{\rho_2}{\rho_1}\right)$$

$$p_1 - p_2 = \gamma p_2 M_2^2 \sin^2(\sigma - \delta) \left(1 - \frac{\rho_2}{\rho_1}\right)$$

$$\frac{p_1}{p_2} = 1 + \gamma M_2^2 \sin^2(\sigma - \delta) \left(1 - \frac{\rho_2}{\rho_1}\right) \tag{7.42}$$

7.5.2 Density Ratio

Substitution from Rankine-Hugoniot Equation (7.23) for p_2/p_1 in Equation (7.41) gives

$$\frac{\frac{(\gamma+1)\rho_2}{(\gamma-1)\rho_1} - 1}{\frac{(\gamma+1)}{(\gamma-1)} - \frac{\rho_2}{\rho_1}} - 1 = \gamma M_1^2 \sin^2\sigma \left(1 - \frac{\rho_1}{\rho_2}\right)$$

$$\frac{2\gamma}{\gamma-1}\left(\frac{\rho_2}{\rho_1} - 1\right) = \gamma M_1^2 \sin^2\sigma \frac{\rho_1}{\rho_2}\left(\frac{\rho_2}{\rho_1} - 1\right)\left(\frac{\gamma+1}{\gamma-1} - \frac{\rho_2}{\rho_1}\right)$$

$$\frac{2}{M_1^2 \sin^2\sigma\,(\gamma+1)} + \frac{\gamma-1}{\gamma+1} = \frac{\rho_1}{\rho_2}$$

$$\frac{\rho_2}{\rho_1} = \frac{(\gamma+1) M_1^2 \sin^2\sigma}{2 + (\gamma-1) M_1^2 \sin^2\sigma} \tag{7.43}$$

7.5.3 Pressure Ratio

Substituting for ρ_1/ρ_2 from Equations (7.43) in (7.41) we get

$$\frac{p_2}{p_1} = 1 + \gamma M_1^2 \sin^2\sigma \left\{1 - \frac{2 + (\gamma-1) M_1^2 \sin^2\sigma}{(\gamma+1) M_1^2 \sin^2\sigma}\right\}$$

After simplifying and rearranging

$$\frac{p_2}{p_1} = 1 + \frac{2\gamma}{\gamma+1}\,(M_1^2 \sin^2\sigma - 1)$$

$$\frac{p_2}{p_1} = \frac{2\gamma}{\gamma+1} M_1^2 \sin^2\sigma - \frac{\gamma-1}{\gamma+1} \tag{7.44}$$

7.5.4 Temperature Ratio

From the equation of state

$$\frac{T_2}{T_1} = \frac{(p_2/p_1)}{(\rho_2/\rho_1)}$$

Substituting from Equations (7.44) and (7.43) respectively

$$\frac{T_2}{T_1} = \left(\frac{2\gamma}{\gamma+1} M_1^2 \sin^2\sigma - \frac{\gamma-1}{\gamma+1}\right)\left(\frac{2 + (\gamma-1) M_1^2 \sin^2\sigma}{(\gamma+1) M_1^2 \sin^2\sigma}\right)$$

$$\frac{T_2}{T_1} = \frac{[2\gamma M_1^2 \sin^2\sigma - (\gamma-1)]\;[2 + (\gamma-1) M_1^2 \sin^2\sigma]}{(\gamma+1)^2 M_1^2 \sin^2\sigma} \tag{7.45}$$

7.5.5 Stagnation pressure ratio

$$\frac{p_{01}}{p_1} = \left(\frac{T_{01}}{T_1}\right)^{\gamma/(\gamma-1)}$$

$$\frac{p_{02}}{p_2} = \left(\frac{T_{02}}{T_1}\right)^{\gamma/(\gamma-1)}$$

$$T_{01} = T_{02}$$

$$\frac{p_{02}}{p_{01}} = \left(\frac{T_{02}}{T_{01}} \cdot \frac{T_1}{T_2}\right)^{\gamma/(\gamma-1)} \times \frac{p_2}{p_1} = \left(\frac{T_1}{T_2}\right)^{\gamma/(\gamma-1)} \times \frac{p_2}{p_1}$$

$$\frac{p_{02}}{p_{01}} = \left(\frac{\rho_2}{\rho_1}\right)^{\gamma/(\gamma-1)} \Big/ \left(\frac{p_2}{p_1}\right)^{1/(\gamma-1)}$$

Substituting from Equations (7.43) and (7.44) respectively

$$\frac{p_{02}}{p_{01}} = \left[\frac{(\gamma+1) M_1^2 \sin^2\sigma}{(\gamma-1) M_1^2 \sin^2\sigma + 2}\right]^{\gamma/(\gamma-1)} \left[\frac{\gamma+1}{2\gamma M_1^2 \sin^2\sigma - (\gamma-1)}\right]^{1/(\gamma-1)} \tag{7.46}$$

7.5.6 Change of Entropy

$$\frac{s_2 - s_1}{R} = \frac{\Delta s}{R} = -\ln\frac{p_{02}}{p_{01}}$$

Substitution from Equation (7.46) gives

$$\frac{\Delta s}{R} = \frac{\gamma}{\gamma-1}\ln\left[\frac{(\gamma-1) M_1^2 \sin^2\sigma + 2}{(\gamma+1) M_1^2 \sin^2\sigma}\right] + \frac{1}{\gamma-1}\ln\left[\frac{2\gamma M_1^2 \sin^2\sigma - (\gamma-1)}{\gamma+1}\right] \tag{7.47}$$

7.5.7 Deflection Angle

From Equations (7.40) and (7.43) we get

$$\frac{\rho_2}{\rho_1} = \frac{\tan\sigma}{\tan(\sigma-\delta)} = \frac{(\gamma+1) M_1^2 \sin^2\sigma}{2 + (\gamma-1) M_1^2 \sin^2\sigma}$$

$$\frac{(\gamma+1) M_1^2 \sin^2\sigma}{2 + (\gamma-1) M_1^2 \sin^2\sigma} = \frac{\sin\sigma(\cos\sigma\ \cos\delta + \sin\sigma\ \sin\delta)}{\cos\sigma(\sin\sigma\ \cos\delta - \cos\sigma\ \sin\delta)}$$

After cross multiplication, simplification and rearrangement we get

$$\sin\delta\,[2M_1^2 \sin^4\sigma - (\gamma+1) M_1^2 \sin^2\sigma - 2\sin^2\sigma]$$
$$= \cos\delta\,[2\sin\sigma\ \cos\sigma - 2M_1^2 \sin^3\sigma\ \cos\sigma]$$
$$\tan\delta \sin^2\sigma\,[2M_1^2 \sin^2\sigma - (\gamma+1) M_1^2 - 2]$$
$$= 2\sin\sigma\ \cos\sigma\,[1 - M_1^2 \sin^2\sigma]$$

$$\tan\delta = 2\cot\sigma \frac{1 - M_1^2 \sin^2\sigma}{2M_1^2 \sin^2\sigma - \gamma M_1^2 - M_1^2 - 2}$$

$$\tan\delta = 2\cot\sigma \frac{M_1^2 \sin^2\sigma - 1}{2 + \gamma M_1^2 + M_1^2(1 - 2\sin^2\sigma)} \tag{7.48}$$

$$\tan\delta = \frac{M_1^2 \sin 2\sigma - 2\cot\sigma}{2 + M_1^2(\gamma + \cos 2\sigma)} \tag{7.49}$$

7.5.8 Downstream Mach Number

Equation (7.42) can be rewritten in the following form:

$$\left(\frac{p_1}{p_2} - 1\right) = \gamma M_2^2 \sin^2(\sigma-\delta)\left(1 - \frac{\rho_2}{\rho_1}\right) \tag{7.42 (a)}$$

From Equation (7.44)

$$\frac{p_1}{p_2} - 1 = \frac{2\gamma(1 - M_1^2 \sin^2\sigma)}{2\gamma M_1^2 \sin^2\sigma - (\gamma-1)} \tag{7.50}$$

From Equation (7.43)

$$1 - \frac{\rho_2}{\rho_1} = \frac{2(1 - M_1^2 \sin^2\sigma)}{2 + (\gamma-1) M_1^2 \sin^2\sigma} \tag{7.51}$$

Substituting Equations (7.50) and (7.51) in (7.42 (*a*)) yields

$$\frac{2\gamma(1 - M_1^2 \sin^2\sigma)}{2\gamma M_1^2 \sin^2\sigma - (\gamma-1)} = \frac{2\gamma M_2^2 \sin^2(\sigma-\delta)\ (1 - M_1^2 \sin^2\sigma)}{2 + (\gamma-1) M_1^2 \sin^2\sigma}$$

After rearrangement the above expression gives

$$M_2^2 = \frac{2 + (\gamma-1) M_1^2 \sin^2\sigma}{[2\gamma M_1^2 \sin^2\sigma - (\gamma-1)] \sin^2(\sigma-\delta)} \tag{7.52}$$

This expression is not yet explicit in terms of M_1 and σ. However, in a numerical example the value of $\sin^2(\sigma - \delta)$ can be determined from Equations (7.48) or (7.49) for use in Equation (7.52) to obtain the value of the downstream Mach number M_2.

To obtain an explicit relation of the form $M_2 = f(M_1, \sigma)$, Equation (7.48) can be used to eliminate δ in Equation (7.52). After laborious trigonometric and algebraic work, simplification and convenient factorization the following relation is obtained:

$$M_2^2 = \frac{(\gamma+1)^2 M_1^4 \sin^2\sigma - 4(\gamma M_1^2 \sin^2\sigma + 1)(M_1^2 \sin^2\sigma - 1)}{[2\gamma M_1^2 \sin^2\sigma - (\gamma - 1)][2 + (\gamma - 1) M_1^2 \sin^2\sigma]} \quad (7.53)$$

It can be seen that Equation (7.52) though implicit is more convenient to use.

7.6 OBLIQUE SHOCK RELATIONS FROM THE NORMAL SHOCK EQUATIONS

Equations (7.43) to (7.52) for the flow parameters across the oblique shocks can also be easily derived from the corresponding relations developed for normal shocks in Chapter 6.

Following relations connect up the property equations for the normal and oblique shocks:

$$M_x = \frac{c_x}{a_x} = \frac{c_{n1}}{a_1} = \frac{c_1}{a_1}\sin\sigma$$

$$M_x = M_1 \sin\sigma \quad (7.54)$$

$$M_y = \frac{c_y}{a_y} = \frac{c_{n2}}{a_2} = \frac{c_2}{a_2}\sin(\sigma - \delta)$$

$$M_y = M_2 \sin(\sigma - \delta) \quad (7.55)$$

Substitutions from Equations (7.54) and (7.55) in the normal shock Equations (6.31), (6.26), (6.28), (6.41), (6.49) and (6.24) give the corresponding relations for oblique shocks in Equations (7.43), (7.44), (7.45), (7.46), (7.47) and (7.52) respectively.

It must also be noted that for normal shocks the wave angle by definition is 90°.

$$\sigma_{\text{normal shock}} = \frac{\pi}{2} \quad (7.56)$$

Therefore, substitution from Equation (7.56) in Equations (7.48) and (7.49) gives

$$\delta_{\text{normal shock}} = 0 \quad (7.57)$$

7.7 MACH WAVES

From Equation (7.54)

$$\sin\sigma = \frac{M_x}{M_1} \quad (7.54)$$

For an infinitesimal shock wave the initial Mach number based on the normal velocity component is nearly unity. Therefore,

$$M_x = \frac{c_{n1}}{a_1} \approx 1 \quad (7.58)$$

The changes in the flow properties across such a wave are negligible; such a wave is known as a Mach wave. The inclination of this wave to the initial direction of flow is, from Equations (7.54) and (7.58), given by

$$\sin\sigma = \frac{1}{M_1}$$

For the sake of generality writing $M_1 = M$

$$\sigma = \sin^{-1}\frac{1}{M}$$

This particular value of the wave angle is termed as the Mach angle (α). Thus

$$\alpha = \sigma_{\text{Mach wave}} = \sin^{-1}\frac{1}{M} \quad (7.59)$$

This has already been discussed in greater detail in Section 5.2.2 where Equation (7.59) is derived as Equation (5.16).

When this value of σ is substituted in Equation (7.48) the value of the deflection obtained is zero *i.e.*,

$$\delta_{\text{Mach wave}} = 0 \quad (7.60)$$

Substituting from Equation (7.59) in Equations (7.43), (7.44), (7.45), (7.46), (7.47) and (7.52) we get

$$\frac{\rho_2}{\rho_1} = 1,\ \frac{p_2}{p_1} = 1,\ \frac{T_2}{T_1} = 1,\ \frac{p_{02}}{p_{01}} = 1$$

$$\frac{\Delta s}{R} = 0 \text{ and } M_2 = M_1 = M$$

Besides these results following relations are also true for a Mach wave:

$$c_{n1} = c_{n2} = c_n$$

$$c_t = 0$$

Therefore, Equation (7.25) yields

$$c_n^4 = \left(\frac{p_2 - p_1}{\rho_2 - \rho_1}\right)^2 = \left(\frac{\Delta p}{\Delta \rho}\right)^2 \tag{7.61}$$

Equation (7.26) gives

$$\frac{p_2 - p_1}{\rho_2 - \rho_1} = \frac{\Delta p}{\Delta \rho} = a^{*2} = \left(\frac{\partial p}{\partial \rho}\right)_s \tag{7.62}$$

Equations (7.61) and (7.62) give

$$\left.\begin{aligned} c_n &= a \\ \frac{c_n}{a} &= M_x = 1 \end{aligned}\right\} \tag{7.63}$$

From the above equations it is seen that a Mach wave is not a discontinuity in the flow, and flow through this wave is isentropic. Therefore, they can exist anywhere in a supersonic field.

7.8 GAS TABLES FOR OBLIQUE SHOCKS

Various equations derived for the properties of flow through oblique shocks are not generally used for calculations; instead the Equations (7.43-7.53) can be used to prepare tables for various property ratios. It is observed that calculations are much simpler with the use of such tables. But unlike normal shock tables the corresponding tables for oblique shocks have to be very large in size on account of the two basic independent variables—M_1, δ or σ.

Some tables give the values of the initial Mach number (M_1) at various values of the wave angle (σ) and the deflection (δ) as shown in Appendix A.5. In most of the calculations for oblique shocks these are the basic variables from which other properties can be calculated.

Tables in Appendix A.6 show the use of the normal shock tables for oblique shock calculations. For example computation of M_1, δ and

M_2 for a given value of the wave angle at $M_x = 1.5$ is shown in the following:

$$M_1 = \frac{M_x}{\sin \sigma} = \frac{1.5}{\sin 30} = 3.0$$

$$\tan \delta = \frac{M_1^2 \sin 2\sigma - 2 \cot \sigma}{2 + M_1^2 (\gamma + \cos 2\sigma)} = \frac{9 \times \sin 60 - 2 \cot 30}{2 + 9\,(1.4 + \cos 60)}$$

$$\tan \delta = \frac{4.330}{19.10} = 0.2267$$

$$\delta = 12.77^\circ$$

From normal shock tables at $M_x = 1.5$, $M_y = 0.701$

$$M_2 = \frac{M_y}{\sin (\sigma - \delta)} = \frac{0.701}{\sin (30 - 12.77)}$$

$$M_2 = \frac{0.701}{\sin 17.23} = \frac{0.701}{0.296} = 2.368$$

Other property ratios like p_2/p_1, T_2/T_1 etc. can be directly obtained from the conventional normal shock tables at $M_x = 1.5$.

7.9 CHARTS FOR OBLIQUE SHOCKS

Various property ratios for flow through oblique shocks can also be presented graphically in the form of charts; such charts can be drawn on a convenient scale from the corresponding tables or equations. To cite some examples following charts are discussed.

7.9.1 Wave Angle

Figure 7.8 shows variation of the wave angle with the initial Mach number at different values of the deflection angle; the curves are drawn using Equation (7.49).

It is observed that this family of curves are bound between the normal shock line ($\sigma = \pi/2$, $\delta = 0$) and the Mach wave line $\left(\sigma = \sin^{-1}\frac{1}{M_1},\ \delta = 0\right)$. For a given value of the Mach number and deflection there are two values for the wave angle; the values on the upper branches of the curves represent strong shock waves while those on the lower branches represent the weak shocks as shown in Figure 7.8.

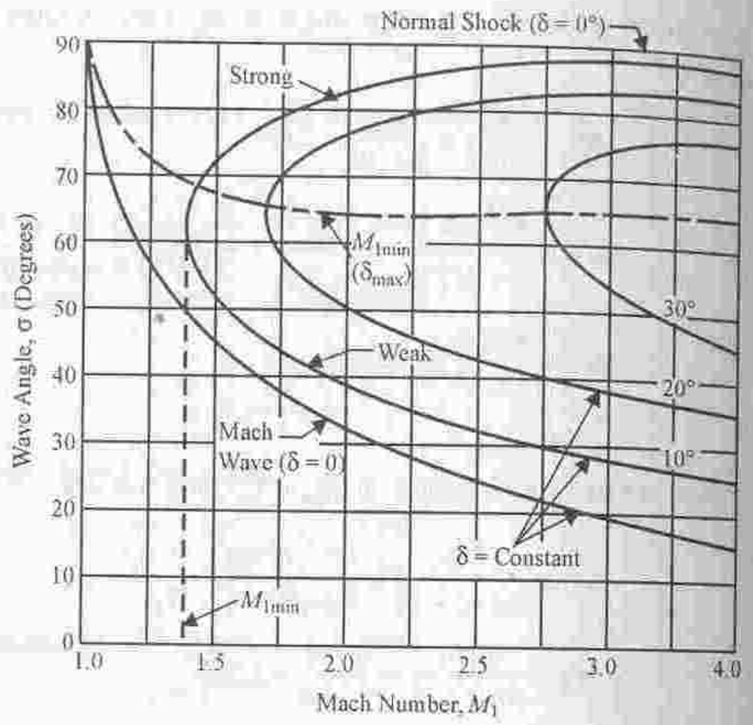

FIGURE 7.8 : Variation of the wave angle (Equation (7.49))

The limits for the strong and weak shocks are the normal shock waves and the Mach waves respectively. Therefore, the fact that the stronger waves are near the normal shock and the weaker waves nearer the Mach waves is quite understandable.

The value of the Mach number at the extreme left hand side of the δ = constant curve gives the minimum value of the Mach number ($M_{1\,min}$) for which there would be an attached shock at the corner as shown in Figures 7.16 (*a*) and (*b*) (page 249); below this value the shock will be detached as shown in Figure 7.16 (*c*). At this value ($M_{1\,min}$) of the Mach number the wedge angle (δ) is the maximum for which there will be an attached shock; if the wedge angle at this Mach number is larger than this (δ_{max}) the shock will be detached.

7.9.2 Pressure Ratio

Figure 7.9 shows plots of pressure ratio against the Mach number for different values of δ. Here again the lower branches of the δ = constant curves represent weak oblique shocks whereas the upper branches represent strong shocks. As would be expected the pressure ratio across

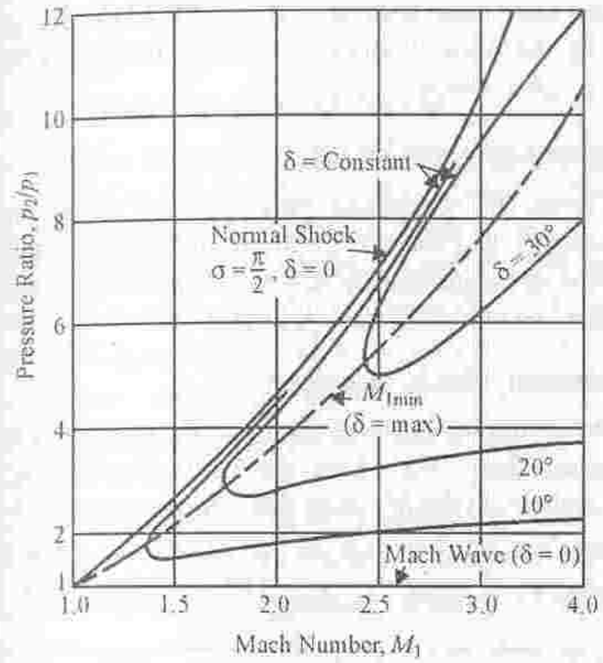

FIGURE 7.9 : Variation of the static pressure ratio (Equation (7.44))

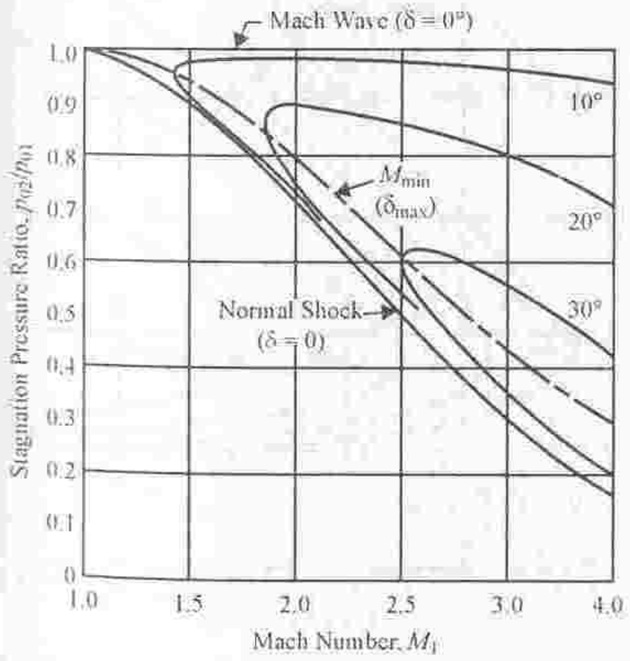

FIGURE 7.10 : Variation of the stagnation pressure loss (Equation (7.46))

weak shocks is lower than its corresponding value for the strong shocks. There is no pressure difference across the Mach wave; pressure ratio is maximum for the normal shock wave. The minimum Mach number or δ_{max} line is also shown.

7.9.3 Stagnation pressure loss

Figure 7.10 shows the stagnation pressure ratio as a function of the initial Mach number and the wedge angle. It is observed that the maximum stagnation pressure loss is across the normal shock waves, and there is no loss across the Mach waves.

7.9.4 Downstream Mach Number

Figure 7.11 shows the variation of the downstream Mach number along some δ = constant lines. The Mach wave line ($\delta = 0$) is a straight line inclined at 45 degrees to the M_1-axis; there is no change of Mach number along this line. The downstream Mach number is mostly supersonic along the upper branches of the curve, representing weak shocks. The

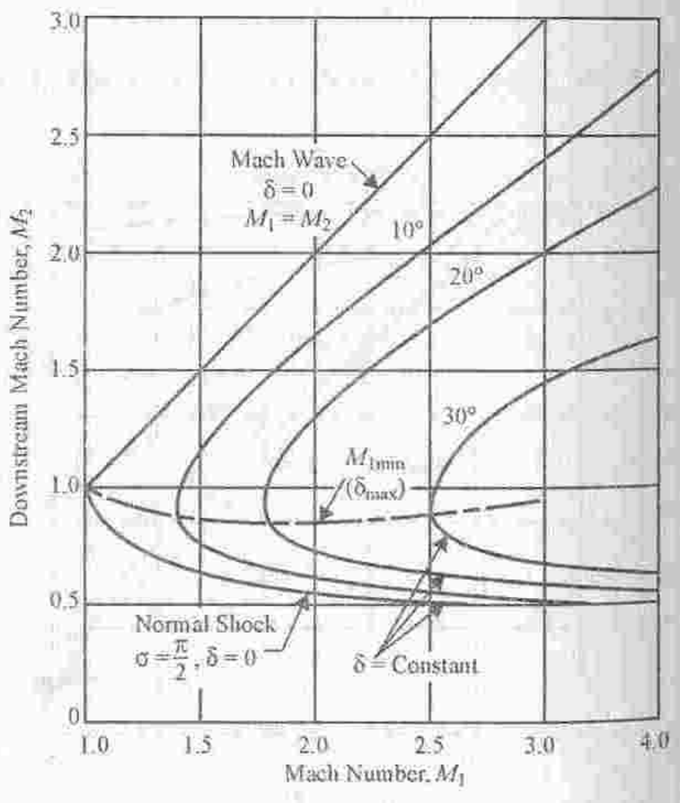

FIGURE 7.11 : Variation of the downstream Mach number (Equation (7.52))

Mach number along the lower branches representing strong waves is always subsonic, being minimum along the normal shock line as shown in the figure.

7.10 THE SHOCK POLAR DIAGRAM

It is observed from the oblique shock tables and charts (Figures 7.8 and 7.11) that for a given value of the upstream Mach number (or velocity) there are a number of sets of values of the downstream Mach number M_2 (or velocity c_2) and the wave angle σ. Figures in 7.12 show the upstream and downstream velocity triangles of Figure 7.7 for three pairs of values of c_2 and σ. The velocity vector c_1 (OQ) is kept constant and parallel to the x-axis while the velocity vector c_2 (OP) is rotated in the direction shown by the arrow. The triangle ONQ in each case is a right-angled triangle.

In this section an equation to describe the locus of the end point (P) of the vector c_2 for a given value of the initial Mach number (M_1) is derived. This equation is expressed in terms of the Cartesian com-

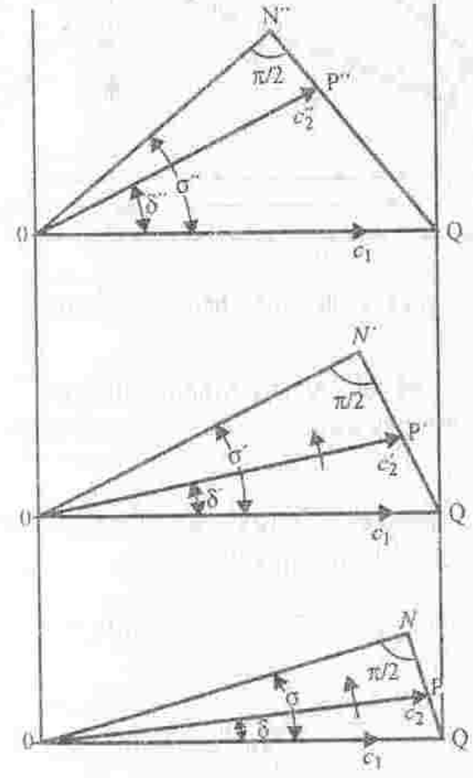

FIGURE 7.12 : Upstream and downstream velocity triangles for different pairs of c_2 and σ

ponents u_2 and v_2 of the vector c_2; these components are later expressed in the non-dimensional form u_2^* and v_2^*.

In Figure 7.13 velocity triangles shown in Figure 7.7 are redrawn with the velocity vector c_1 along the u-axis. This is easily done by rotating Figure 7.7 clockwise by an angle of $\left(\frac{\pi}{2} - \sigma\right)$ and combining the two velocity triangles such that c_1 and c_2 have the same origin O.

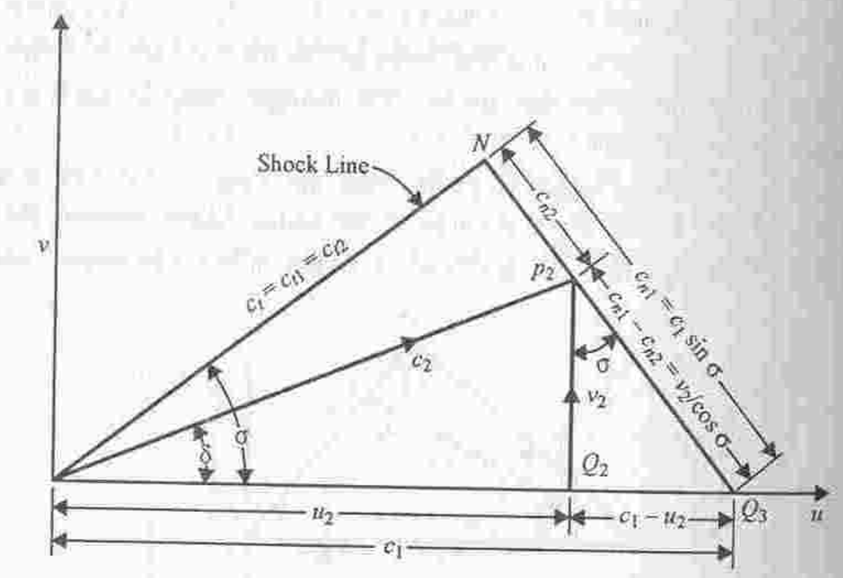

FIGURE 7.13 : Velocity triangles in the hodograph plane ($u - v$ coordinates)

The normal and tangential directions of Figure 7.7 are represented here by NQ_3 and ON respectively subtending an angle of $\pi/2$ between them.

Following geometrical relations are obtained from Figure 7.13:

$$c_{n1} = c_1 \sin\sigma \tag{7.34}$$

$$c_t = c_{t1} = c_{t2} = c_1 \cos\sigma \tag{7.35}$$

$$c_{n2} = c_{n1} - \frac{v_2}{\cos\sigma}$$

$$c_{n2} = c_1 \sin\sigma - \frac{v_2}{\cos\sigma} \tag{7.64}$$

$$\tan\sigma = \frac{c_1 - u_2}{v_2} \tag{7.65}$$

Substituting from Equations (7.34), (7.35) and (7.64) in (7.19) we get

$$c_1 \sin\sigma \left(c_1 \sin\sigma - \frac{v_2}{\cos\sigma} \right) = a^{*2} - \frac{\gamma - 1}{\gamma + 1} c_1^2 \cos^2\sigma \tag{7.66}$$

Following trigonometrical relations are also obtained from Figure 7.13:

$$\sin^2\sigma = \frac{\tan^2\sigma}{1 + \tan^2\sigma} = \frac{(c_1 - u_2)^2}{v_2^2 + (c_1 - u_2)^2} \tag{7.67}$$

$$\cos^2\sigma = \frac{1}{1 + \tan^2\sigma} = \frac{v_2^2}{v_2^2 + (c_1 - u_2)^2} \tag{7.68}$$

From Equation (7.66)

$$c_1^2 \sin^2\sigma - c_1 v_2 \tan\sigma = a^{*2} - \frac{\gamma - 1}{\gamma + 1} c_1^2 \cos^2\sigma$$

Substituting from Equations (7.67), (7.65) and (7.68) in the above relation

$$\frac{c_1^2 (c_1 - u_2)^2}{v_2^2 + (c_1 - u_2)^2} - c_1 (c_1 - u_2) = a^{*2} - \frac{\gamma - 1}{\gamma + 1} \frac{c_1^2 v_2^2}{v_2^2 + (c_1 - u_2)^2}$$

Collecting terms containing v_2^2 on one side and simplifying,

$$\left\{ a^{*2} - \frac{\gamma - 1}{\gamma + 1} c_1^2 + c_1^2 - c_1 u_2 \right\} v_2^2$$

$$= (c_1 - u_2)^2 \{ c_1^2 - c_1 (c_1 - u_2) - a^{*2} \}$$

$$\left(a^{*2} + \frac{2}{\gamma + 1} c_1^2 - c_1 u_2 \right) v_2^2 = (c_1 - u_2)^2 \ (c_1 u_2 - a^{*2}) \tag{7.69}$$

Various velocities in the above equation are non-dimensionalized by using the following non-dimensional velocities or Mach numbers:

$$M_1^* = \frac{c_1}{a^*},\ v_2^* = \frac{v_2}{a^*},\ u_2^* = \frac{u_2}{a^*}$$

Equation (7.69) is rewritten after dividing both sides by a^{*4},

$$\left\{1+\frac{2}{\gamma+1}\left(\frac{c_1}{a^*}\right)^2-\frac{c_1}{a^*}\frac{u_2}{a^*}\right\}\left(\frac{v_2}{a^*}\right)^2$$

$$=\left(\frac{c_1}{a^*}-\frac{u_2}{a^*}\right)^2\left(\frac{c_1}{a^*}\frac{u_2}{a^*}-1\right)$$

After introducing the aforementioned Mach numbers

$$\left(1+\frac{2}{\gamma+1}M_1^{*2}-M_1^*u_2^*\right)v_2^*=(M_1^*-u_2^*)^2\ (M_1^*u_2^*-1)$$

$$v_2^*=\frac{(M_1^*-u_2^*)^2\ (M_1^*u_2^*-1)}{1+\frac{2}{\gamma+1}M_1^{*2}-M_1^*u_2^*} \tag{7.70}$$

It is seen that in Equation (7.70) v_2^* is a function of only M_1^* and u_2^*; thus

$$v_2^*=f(M_1^*,\ u_2^*) \tag{7.71}$$

When Equation (7.70) is plotted in the $u_2^*-v_2^*$ plane for a given value of M_1^*, it gives a strophoid curve which is symmetrical about the u_2^*-axis; this curve is known as a shock polar diagram and is helpful in studying the characteristics of flow through oblique shocks.

A typical shock polar diagram in the $u_2^*-v_2^*$ plane is shown in Figure 7.14. Velocity triangles of Figures 7.12 and 7.13 are also shown here for two pairs of σ and c_2 at a given value of the initial Mach number M_1^*. There is only one shock polar for a specified value of M_1^* and an infinite number of pairs of σ and c_2. The shock polar is the locus of the end point (P, P', P'' etc.) of the velocity vector c_2. The tangential direction (ON, ON') along the shock wave is also shown for each pair of σ and c_2.

Some aspects of the shock polar diagram are further explained in Figure 7.15. Various rays (OR, OP_3, OM, OD etc.) drawn on the shock polar from the origin represent flows through oblique shocks corresponding to different values of the deflection angle (δ). For instance the ray OP_3 cuts the shock polar at P_1, P_2 and P_3.

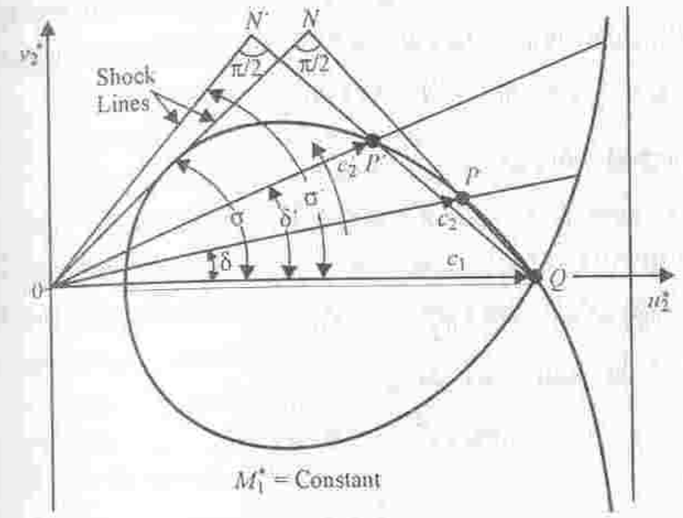

FIGURE 7.14 : A typical shock polar diagram in the hodograph plane ($u_2^*-v_2^*$ plane)

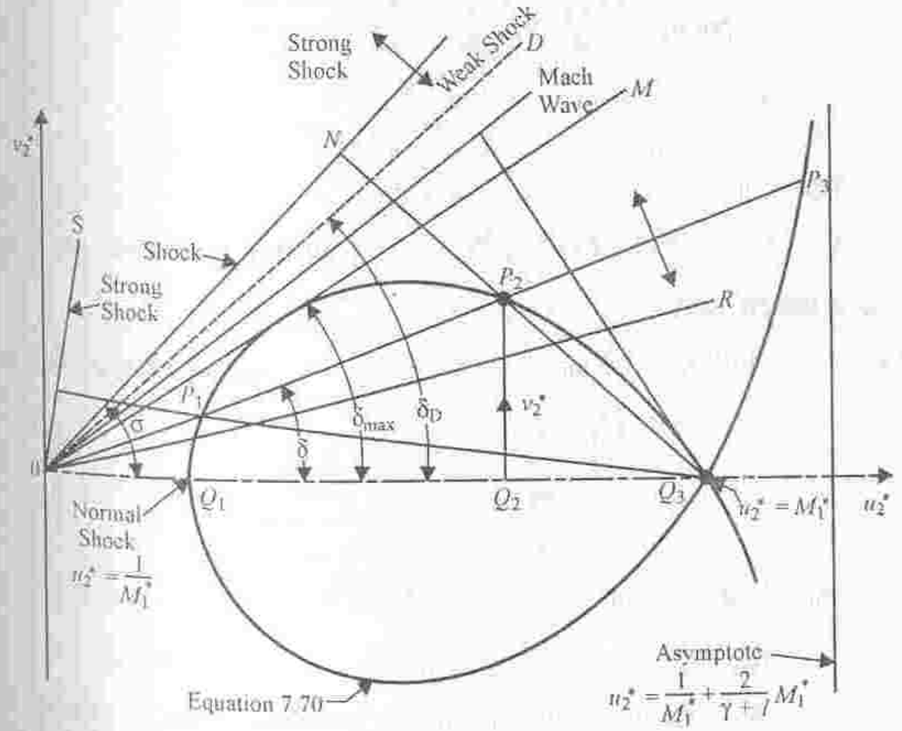

FIGURE 7.15 : Various solutions of the shock polar Equation (7.70)

Points P_1 and P_2 correspond to the strong and weak shock wave solutions of Equation (7.70); but point P_3 does not represent any solution because it gives an impossible condition $u_2^* > M_1^*$.

7.10.1 Normal Shock

When a ray coincides with u_2^*-axis ($v_2^* = 0$) the shock polar equation given by Equation (7.70) gives two solutions at points Q_1 and Q_3.

$$(M_1^* - u_2^*)^2 \; (M_1^* \, u_2^* - 1) = 0$$

One of the solutions (at Q_1) gives

$$M_1^* \, u_2^* - 1 = 0$$

$$u_2^* = \frac{1}{M_1^*} \tag{7.72}$$

$$u_2^* \, M_1^* = 1$$

$$u_2 \, c_1 = a^{*2}$$

At this point,

$$c_1 = c_{n1} = c_x$$

$$u_2 = c_2 = c_{n2} = c_y$$

Therefore, $$c_x \, c_y = a^{*2} \tag{6.21}$$

The above relation is the Prandtl's equation for normal shocks.

7.10.2 Mach Wave

The other solution of Equation (7.70) at $v_2^* = 0$ is at point Q_3 for which

$$M_1^* - u_2^* = 0$$

$$u_2^* = M_1^*$$

$$u_2 = c_1$$

But for this point $u_2 = c_2$, therefore,

$$c_2 = c_1$$

This condition at $\delta = 0$ can only be satisfied by an infinitesimal or a Mach wave; this wave is perpendicular to the tangent drawn on the shock polar at Q_3.

7.10.3 Strong and Weak Shocks

Between the points Q_3 and Q_1 there are two more solutions at points P_2 and P_1. Velocity vector diagrams (like Figure 7.13) drawn through these points give the weak and strong shock lines ON and OS respectively. It is observed that like other figures in this section the strong shock is nearer the normal shock whereas the weak shock is close to the Mach wave.

7.10.4 Maximum Deflection and Detached Shocks

When the ray OP_3 is rotated in the anticlockwise direction to a position where it becomes tangent to the shock polar the deflection angle has its maximum value for which there is a shock at the corner of the concave wall. Ray OM represents this condition ($\delta = \delta_{max}$). A further leftward shift of the ray beyond OM will give a detached shock as by the ray OD; here $\delta_D > \delta_{max}$. Effect of the deflection or the wedge angle on the shock position is shown in Figures 7.16 (*a*), (*b*) and (*c*).

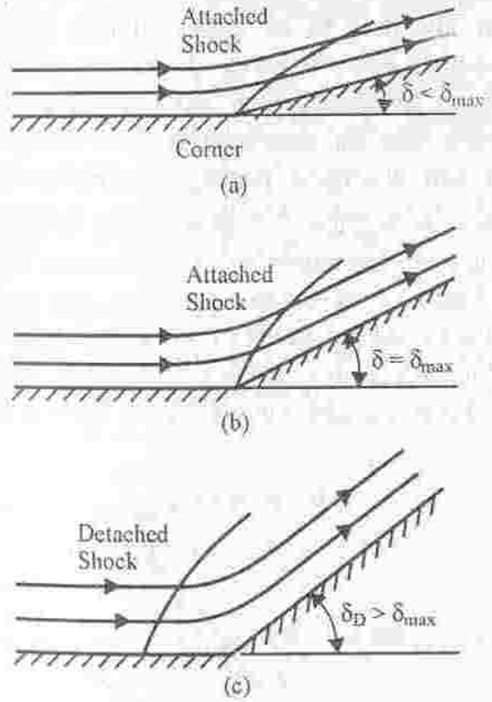

FIGURE 7.16 : Attached and detached shocks at the wall corner

7.10.5 Equation of the Asymptote

As pointed out earlier point P_3 on the outer branch of the shock polar

does not represent any meaningful solution of Equation (7.70). It is noticed that the Mach number u_2^* at this point is greater than the initial Mach number M_1^* which is impossible in a compression shock. This branch of the shock polar assumes an asymptotic form as shown in the figure. The equation for the asymptote is obtained by putting $v_2^* = \infty$ in Equation (7.70). This gives

$$1 + \frac{2}{\gamma + 1} M_1^{*2} - M_1^* u_2^* = 0$$

$$u_2^* = \frac{1}{M_1^*} + \frac{2}{\gamma + 1} M_1^* \tag{7.73}$$

7.11 EXPANSION OF SUPERSONIC FLOW

In the earlier sections of this chapter compression of supersonic flow over the corner of a concave wall through oblique compression shock waves has been discussed; the turning of the wall was inwards or anticlockwise. From this it is to be expected that if the wall is turned away from the flow (in the clockwise direction) an initially supersonic flow will experience acceleration or expansion. In Section 4.2 it has already been proved that for decelerating and accelerating supersonic flows convergent and divergent passages respectively are required.

It was shown in Section 7.7 that Mach waves or infinitesimal waves could be drawn anywhere in a supersonic flow field. Figure 7.17 (*a*) shows Mach waves emanating from the concave corners of a wall curving inwards. As the Mach number is progressively decreasing the direction of Mach waves is changing according to $\sin \alpha = 1/M$. Thus they converge to form an oblique shock as shown in the figure.

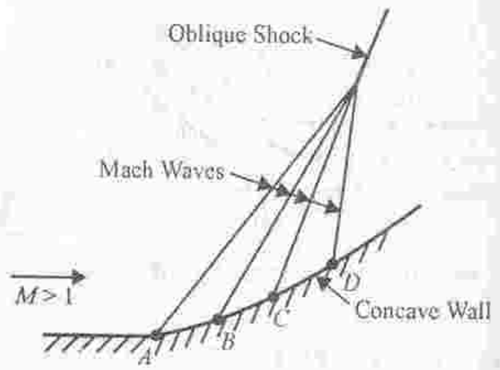

FIGURE 7.17 (*a*) : Formation of an oblique shock from infinitesimal waves

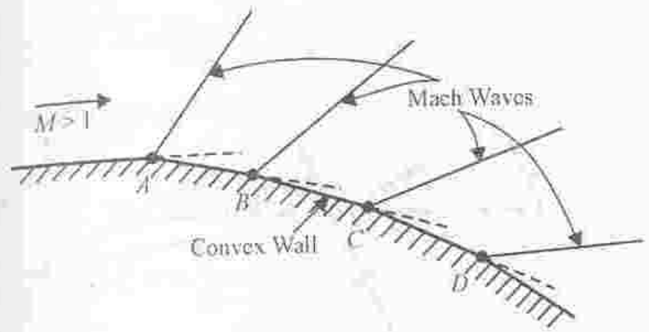

FIGURE 7.17 (*b*) : Infinitesimal expansion waves

In contrast to this, Figure 7.17 (*b*) shows supersonic flow over an outward curving wall with convex corners. The Mach lines emanating from these corners are diverging on account of the progressive increase of Mach numbers; therefore, these Mach waves cannot form a shock wave. Thus in the absence of other irreversibilities supersonic flow over a convex wall can be assumed as isentropic because of the presence of Mach waves only.

Smoothly converging and diverging passages for supersonic flows can be looked upon as made up of an infinite number of infinitesimal corners shown in Figures 7.17 (*a*) and (*b*).

A supersonic flow over a convex corner actually occurs through a fan of Mach waves shown in Figure 7.19.

7.11.1 Governing Equations

Supersonic flow over a convex wall ACB is shown in Figure 7.18; the wall has an infinitesimal outward (negative) turning of $d\delta$. The Mach wave angle α is a function of the initial Mach number. The upstream and downstream velocity triangles relative to the wave are shown in the figure. The resultant velocity vectors $c_1 = c$ and $c_2 = c + dc$ are parallel to the walls AC and CB respectively; the normal and tangential components of these vectors are also shown.

For an infinitesimal change across the Mach wave the magnitude of the velocity vector OP increases from c to $c + dc$ (OQ). Since there is no tangential pressure gradient

$$c_{t1} = c_{t2} = c_t$$

The upstream velocity triangle can be combined with that on the downstream as shown in the figure; ONP and ONQ are the upstream and downstream velocity triangles.

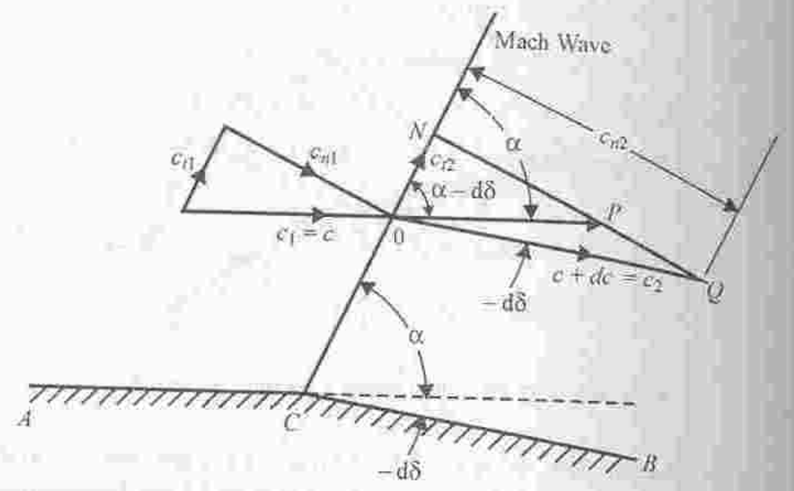

FIGURE 7.18 : Supersonic flow over an infinitesimal convex corner of a wall

It is interesting to note the correspondence between the combined velocity triangles in Figures 7.13 and 7.18. The main differences in the two figures are easily understandable if it is remembered that the flow is decelerated in Figure 7.13 whereas Figure 7.18 represents accelerating flow. All the assumptions of Section 7.2 are also valid for Figure 7.18 except for the fact that the flow here is isentropic on account of the presence of only Mach waves in the flow field.

This isentropically accelerating flow over the convex wall is known as Prandtl-Meyer flow.

From the velocity triangles of Figure 7.18

$$c_t = c \cos \alpha = (c + dc) \cos (\alpha - d\delta)$$

$$c \cos \alpha = (c + dc)\ (\cos \alpha \cos d\delta + \sin \alpha \sin d\delta)$$

For small values of $d\delta$

$$\sin d\delta \approx d\delta \text{ and } \cos d\delta \approx 1$$

Therefore, $c \cos \alpha = (c + dc)\ (\cos \alpha + d\delta \sin \alpha)$

$$c \cos \alpha = c \cos \alpha + c\, d\delta \sin \alpha + dc \cos \alpha + dc\, d\delta \sin \alpha$$

Neglecting the last term as a product of two small quantities

$$c\, d\delta \sin \alpha + dc \cos \alpha = 0$$

$$\frac{dc}{c} = -d\delta \tan \alpha \tag{7.74}$$

$$\tan \alpha = \frac{\sin \alpha}{\sqrt{1 - \sin^2 \alpha}}$$

$$\tan \alpha = \frac{1/M}{\sqrt{1 - 1/M^2}} = \frac{1}{\sqrt{M^2 - 1}} \tag{7.75}$$

From the definition of Mach number

$$c = Ma$$

$$c = \text{constant } M \sqrt{T}$$

$$\ln c = \ln (\text{constant}) + \ln M + \frac{1}{2} \ln T$$

On differentiation this gives

$$\frac{dc}{c} = \frac{dM}{M} + \frac{1}{2} \frac{dT}{T} \tag{7.76}$$

From energy equation

$$\frac{T_0}{T} = 1 + \frac{\gamma - 1}{2} M^2$$

Again by logarithmic differentiation

$$\frac{dT}{T} = \frac{-(\gamma - 1)\, M}{1 + \dfrac{\gamma - 1}{2} M^2} dM$$

Combining Equations (7.76) and (7.77) we get

$$\frac{dc}{c} = \frac{dM}{M} - \frac{\{(\gamma - 1)/2\}\, M^2}{1 + \{(\gamma - 1)/2\}\, M^2} \frac{dM}{M}$$

$$\frac{dc}{c} = \frac{1}{1 + \{(\gamma - 1)/2\}\, M^2} \frac{dM}{M} \tag{7.78}$$

Substituting from Equations (7.75) and (7.78) in (7.74), we get

$$-d\delta = \frac{1}{\tan \alpha} \frac{dc}{c}$$

$$-d\delta = \frac{\sqrt{M^2 - 1}}{1 + \{(\gamma - 1)/2\}\, M^2} \frac{dM}{M} \tag{7.79}$$

The above relation is the differential equation for the Prandtl-Meyer flow.

7.11.2 Prandtl-Meyer Function

Equation (7.79) on integration yields

$$-\delta = \int \frac{\sqrt{M^2-1}}{1+\{(\gamma-1)/2\}\,M^2}\,\frac{dM}{M} + \text{constant} \tag{7.80}$$

The integral on the right hand side is known as the "Prandtl-Meyer function" usually denoted by

$$\omega(M) = \int \frac{\sqrt{M^2-1}}{1+\{(\gamma-1)/2\}\,M^2}\,\frac{dM}{M} \tag{7.81}$$

The integral in Equation (7.81) has been solved in Appendix A.1. This gives

$$\omega(M) = \sqrt{\frac{\gamma+1}{\gamma-1}}\,\tan^{-1}\sqrt{\frac{\gamma-1}{\gamma+1}(M^2-1)} - \tan^{-1}\sqrt{M^2-1} \tag{7.82}$$

Substituting from Equation (7.81) in (7.80) we get

$$-\delta = \omega(M) + \text{constant} \tag{7.83}$$

The value of the constant in Equation (7.83) can be determined for given values of δ and $\omega(M)$.

Figure 7.19 shows an initially sonic flow turning over a corner through a deflection angle of $-\delta$. The Mach lines in the sonic region have $\alpha = 90^\circ$ and $\delta = 0^\circ$; the flow after the turning has a Mach number M and the corresponding Mach angle α as shown in the figure. For these conditions Equations (7.82) and (7.83) give

$$\omega(M) = 0$$

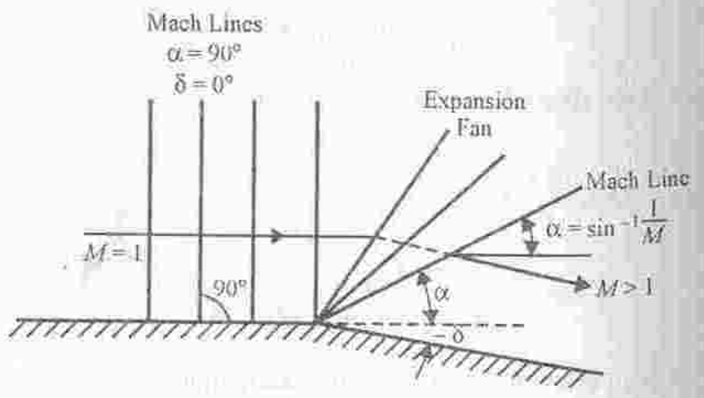

FIGURE 7.19 : Passage of an initially sonic flow over a convex corner

$$\text{constant} = 0$$

Using the above values as reference, Equation (7.83) can be written as

$$-\delta = \omega(M) \tag{7.84}$$

Equation (7.84) gives the value of the deflection angle δ by which an initially sonic flow is turned away from its original direction to accelerate it to a Mach number M. The negative sign indicates the outward or the clockwise direction in Figure 7.19. This angle is also known as the Prandtl-Meyer angle.

The curved wall has been shown below the flow in Figure 7.19. If this wall forms the upper boundary of the flow it will be deflected in the anticlockwise direction and the value of the Prandtl-Meyer angle will be positive. Therefore, to generalize, Equation (7.84) is written as

$$\mp\delta = \omega(M)$$

From Equation (7.82) the value of the Prandtl-Meyer angle is given by

$$\mp\delta = \omega(M) = \sqrt{\frac{\gamma+1}{\gamma-1}}\,\tan^{-1}\sqrt{\frac{\gamma-1}{\gamma+1}(M^2-1)} - \tan^{-1}\sqrt{M^2-1} \tag{7.85}$$

Equation (7.85) can be used to prepare tables giving values of $\omega(M)$ at various values of the Mach number for a given value of γ; for supersonic flow calculations tables giving the values of Mach number as a function of the Prandtl-Meyer angle are also useful. Figure 7.20

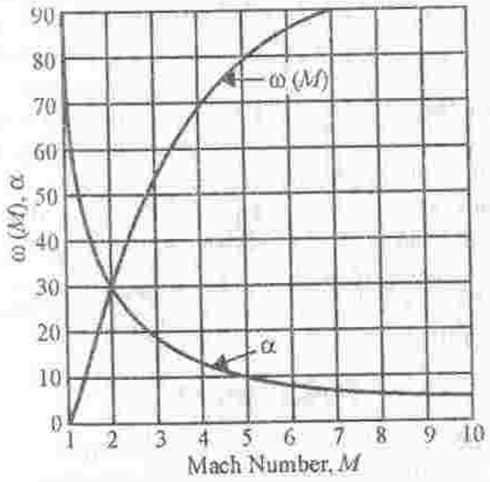

FIGURE 7.20 : Variation of Prandtl-Meyer function and Mach angle

shows the variations of the Mach angle and the Prandtl-Meyer angle with the Mach number.

7.11.3 Maximum Prandtl-Meyer Angle

It is useful to know the value of the Prandtl-Meyer angle for very large values of the Mach number. At $M = \infty$ Equation (7.85) gives

$$\omega\,(M)_{max} = \left(\sqrt{\frac{\gamma+1}{\gamma-1}} - 1 \right) \frac{\pi}{2} \tag{7.86}$$

For $\gamma = 1.4$

$$\omega\,(M)_{max} = 0.725\pi = 130.5^{o} \tag{7.87}$$

Equation (7.87) shows that in contrast to subsonic flows supersonic flows can be deflected through large angles.

NOTATION FOR CHAPTER 7

a	velocity of sound	$u_2^* = \frac{u_2}{a^*}$	dimensionless velocity u_2 (Figures 7.14 and 7.15)
A	area of cross-section		
c	gas velocity		
c_p	specific heat at constant pressure	$v_2^* = \frac{v_2}{a^*}$	dimensionless velocity v_2 (Figures 7.14 and 7.15)
h	enthalpy		
$\dot{m}$	mass flow rate	$\alpha = \sin^{-1}\frac{1}{M}$	Mach angle
M	Mach number		
$M_1^* = \frac{c_1}{a^*}$	dimensionless velocity c_1	θ	angle between the resultant velocity vector and the normal direction
p	pressure	σ	wave angle
Δp	pressure difference	δ	deflection, deviation or half wedge angle
R	gas constant		
s	entropy	ρ	density
Δs	change of entropy	$\Delta\rho$	change in density
T	temperature in Kelvins	$\omega\,(M)$	Prandtl-Meyer function
u, v	components of the absolute velocity in the x and y directions (Figure 7.13)	$\gamma = \frac{c_p}{c_v}$	specific heat ratio

SUBSCRIPTS

0	stagnation value	n	normal
1	initial, upstream of oblique shock	s	isentropic
		t	tangential or along the shock

2	final, downstream of the oblique shock	x	upstream of the normal shock
max	maximum		
min	minimum	y	downstream of the normal shock

SUPERSCRIPT

*	corresponding to $M = 1$, based on a^*

SOLVED EXAMPLES

Example 7.1. Air approaches a symmetrical wedge ($\delta = 15^{o}$) at a Mach number of 2.0. Determine for the strong and weak waves (*a*) wave angle, (*b*) pressure ratio, (*c*) density ratio, (*d*) temperature ratio and (*e*) downstream Mach number.

Verify these values using Gas tables for normal shocks.

Solution. Refer to Figure 7.7.

From Equation (7.48)

$$\tan\delta = 2\cot\sigma \frac{M_1^2\sin^2\sigma - 1}{2 + \gamma M_1^2 + M_1^2\,(1 - 2\sin^2\sigma)}$$

Here $\delta = 15^{o}$ and $M_1 = 2.0$

$$\tan 15^{o} = \frac{4\sin^2\sigma - 1}{2 + 1.4\times 4 + 4\,(1 - 2\sin^2\sigma)} 2\cot\sigma$$

$$0.1339 = \frac{4\sin^2\sigma - 1}{11.6 - 8\sin^2\sigma}\cot\sigma \tag{A}$$

The right hand side for $\sigma = 80^{o}$, 79^{o}, 80.3^{o} and 79.8^{o} gives 0.132, 0.142, 0.128 and 0.134 respectively. This iteration which is quite tedious gives $\sigma = 79.8^{o}$.

This angle being closer to 90^{o} is obviously the angle of the strong shock wave

(*a*) $\sigma_{strong} = 79.8^{o}$ **Ans.**

(*b*) $\frac{p_2}{p_1} = \frac{2\gamma}{\gamma+1} M_1^2\sin^2\sigma - \frac{\gamma-1}{\gamma+1}$

$$\frac{p_2}{p_1} = \frac{2 \times 1.4}{2.4} \times 4 \sin^2 79.8 - \frac{0.4}{2.4}$$

$$\frac{p_2}{p_1} = 4.353 \quad \textbf{Ans.}$$

(*c*) $\sigma - \delta = 79.8^\circ - 15^\circ = 64.8^\circ$

$$\frac{\rho_2}{\rho_1} = \frac{\tan \sigma}{\tan (\sigma - \delta)} = \frac{\tan 79.8}{\tan 64.8}$$

$$\frac{\rho_2}{\rho_1} = 2.615 \quad \textbf{Ans.}$$

(*d*) $$\frac{T_2}{T_1} = \frac{p_2/p_1}{\rho_2/\rho_1} = \frac{4.353}{2.615}$$

$$\frac{T_2}{T_1} = 1.665 \quad \textbf{Ans.}$$

(*e*) From Equation (7.42 (*a*))

$$\gamma M_2^2 \sin^2 (\sigma - \delta) = \frac{1 - p_1/p_2}{\rho_2/\rho_1 - 1}$$

$$1.4 M_2^2 \sin^2 64.8 = \frac{1 - \dfrac{1}{4.353}}{2.615 - 1} = 0.4774$$

$$1.4 \times 0.8187 M_2^2 = 0.4774$$

$$M_2 = 0.645 \quad \textbf{Ans.}$$

We proceed in a similar manner for the weak shock wave.

(*a*) Equation (A) can again be solved by iteration for weak shock wave angles much lesser than 90°. This gives

$$\sigma_{weak} = 45.3^\circ \quad \textbf{Ans.}$$

(*b*) $$\frac{p_2}{p_1} = \frac{2 \times 1.4}{2.4} \times 4 \sin^2 45.3 - \frac{0.4}{2.4}$$

$$\frac{p_2}{p_1} = 2.191 \quad \textbf{Ans.}$$

(*c*) $\sigma - \delta = 45.3 - 15 = 30.3^\circ$

$$\frac{\rho_2}{\rho_1} \frac{\tan 45.3}{\tan 30.3} = 1.729 \quad \textbf{Ans.}$$

(*d*) $$\frac{T_2}{T_1} = \frac{2.191}{1.729} = 1.267 \quad \textbf{Ans.}$$

(*e*) $$M_2^2 = \frac{1 - \dfrac{p_1}{p_2}}{\dfrac{\rho_2}{\rho_1} - 1} \times \frac{1}{\gamma \sin^2 (\sigma - \delta)}$$

$$M_2^2 = \frac{1 - \dfrac{1}{2.191}}{1.729 - 1} \times \frac{1}{1.4 \sin^2 30.3}$$

$$M_2 = 1.448 \quad \textbf{Ans.}$$

For using gas tables for normal shocks, first the value of M_x is determined. For strong shock waves,

$$M_x = M_1 \sin \sigma$$

$$M_x = 2 \sin 79.8 = 1.968 \approx 1.97$$

From normal shock tables for $\gamma = 1.4$ at $M_x = 1.97$

$$M_y = 0.582, \quad \frac{p_y}{p_x} = 4.35, \quad \frac{T_y}{T_x} = 1.66 \quad \textbf{Ans.}$$

$$M_2 = \frac{M_y}{\sin 64.8} = \frac{0.582}{0.904} = 0.644 \quad \textbf{Ans.}$$

$$\frac{p_2}{p_1} = \frac{p_y}{p_x} = 4.35 \quad \textbf{Ans.}$$

$$\frac{T_2}{T_1} = \frac{T_y}{T_x} = 1.66 \quad \textbf{Ans.}$$

$$\frac{\rho_2}{\rho_1} = \frac{4.35}{1.66} = 2.62 \quad \textbf{Ans.}$$

For weak shock wave

$$M_x = 2 \sin 45.3 = 1.42$$

From normal shock tables for $\gamma = 1.4$ at $M_x = 1.42$,

$$M_y = 0.731, \quad \frac{p_y}{p_x} = 2.186, \quad \frac{T_y}{T_x} = 1.267$$

$$M_2 = \frac{M_y}{\sin 30.3} = \frac{0.731}{\sin 30.3} = 1.448 \quad \textbf{Ans.}$$

$$\frac{p_2}{p_1} = \frac{p_y}{p_x} = 2.186 \quad \textbf{Ans.}$$

$$\frac{T_2}{T_1} = \frac{T_y}{T_x} = 1.267 \quad \textbf{Ans.}$$

$$\frac{\rho_2}{\rho_1} = \frac{2.186}{1.267} = 1.725 \quad \textbf{Ans.}$$

From this example it is observed that calculations are much easier with the aid of gas tables for normal shocks.

Example 7.2. A gas ($\gamma = 1.3$) at $p_1 = 345$ mbar, $T_1 = 350$ K and $M_1 = 1.5$ is to be isentropically expanded to 138 mbar. Determine (*a*) the deflection angle, (*b*) final Mach number and (*c*) the temperature of the gas.

Solution. From isentropic gas tables for $\gamma = 1.3$ at $M_1 = 1.5$

$$\frac{p_1}{p_{01}} = 0.284, \quad \frac{T_1}{T_{01}} = 0.748$$

$$\frac{p_2}{p_{02}} = \frac{p_2}{p_1} \times \frac{p_1}{p_{01}} = \frac{138}{345} \times 0.284 = 0.1136$$

From isentropic tables at $\dfrac{p_2}{p_{02}} = 0.1136$

$$M_2 = 2.08, \quad \frac{T_2}{T_{02}} = 0.606$$

(*a*) From tables for Prandtl-Meyer function for $\gamma = 1.3$ at

$M_1 = 1.50$ $\qquad$ $\omega(M_1) = 12.693^\circ$

$M_2 = 2.08$ $\qquad$ $\omega(M_2) = 31.120^\circ$

Therefore, the deflection required is

$$\delta = \omega(M_1) - \omega(M_2)$$

$$\delta = 12.693 - 31.120 = -18.427^\circ \quad \textbf{Ans.}$$

(*b*) $M_2 = 2.08$ **Ans.**

(*c*) $$T_2 = \frac{T_2}{T_{02}} \times \frac{T_{01}}{T_1} \times T_1$$

$$T_2 = \frac{0.606}{0.748} \times 350$$

$$T_2 = 283.56 \text{ K} \quad \textbf{Ans.}$$

Example 7.3. A jet of air at a Mach number of 2.5 is deflected inwards at the corner of a curved wall. The wave angle at the corner is 60°. Determine the deflection angle of the wall, pressure and temperature ratios and final Mach number.

Solution. $$\tan\delta = 2\cot\sigma \frac{M_1^2 \sin^2\sigma - 1}{2 + \gamma M_1^2 + M_1^2(1 - 2\sin^2\sigma)}$$

$$\tan\delta = 2\cot 60 \frac{6.25 \sin^2 60 - 1}{2 + 1.4 \times 6.25 + 6.25(1 - 2\sin^2 60)}$$

$$\tan\delta = 4.258/7.625 = 0.5584$$

$$\delta = 29.18^\circ \quad \textbf{Ans.}$$

$$M_x = M_1 \sin\sigma = 2.5 \sin 60 = 2.165$$

From normal shock tables for $\gamma = 1.4$ at $M_x = 2.165$

$$p_y/p_x = p_2/p_1 = 5.276 \quad \textbf{Ans.}$$

$$T_y/T_x = T_2/T_1 = 1.825 \quad \textbf{Ans.}$$

$$M_y = 0.553$$

$$\sigma - \delta = 60.00 - 29.18 = 30.82$$

$$M_2 = \frac{M_y}{\sin(\sigma - \delta)} = \frac{0.553}{\sin 30.82} = \frac{0.553}{0.512}$$

$$M_2 = 1.08 \quad \textbf{Ans.}$$

QUESTIONS AND PROBLEMS

7.1 Describe two practical situations where oblique shock waves are produced. How are strong and weak shocks generated and how do they affect the flow?

7.2 Derive the energy equation for flow through an oblique shock:

$$h_0 = \frac{a_0^2}{\gamma - 1} = \frac{1}{2}\,\frac{\gamma + 1}{\gamma - 1}\,a^{*2}$$

State the assumptions used. Why is it same for the normal and oblique shocks?

7.3 Starting from the general energy equation for flow through an oblique shock obtain the Prandtl's equation:

$$a^{*2} - \frac{\gamma - 1}{\gamma + 1}\,c_t^2 = c_{n1}\,c_{n2}$$

Deduce from this the corresponding relations for the normal shock and an infinitesimal pressure wave.

7.4 Derive the Rankine-Hugoniot relation for an oblique shock

$$\frac{\rho_2}{\rho_1} = \left(\frac{\gamma + 1}{\gamma - 1}\,\frac{p_2}{p_1} + 1\right) \Big/ \left(\frac{\gamma + 1}{\gamma - 1} + \frac{p_2}{p_1}\right)$$

Compare graphically the variation of density ratio with the initial Mach number in isentropic flow and flow with oblique shock.

7.5 Using the normal shock relations obtain the explicit expressions for the following quantities in terms of the initial Mach number and the wave angle, for oblique shocks:

$$\frac{\rho_2}{\rho_1},\ \frac{p_2}{p_1},\ \frac{T_2}{T_1},\ \frac{p_{02}}{p_{01}} \text{ and } M_2$$

7.6 Show graphically the variations of the following quantities for flow through an oblique shock, with the initial Mach number at two different values of the wedge angle:

$$\sigma,\ \frac{p_2}{p_1},\ \frac{p_{02}}{p_{01}},\ \frac{\Delta s}{R} \text{ and } M_2$$

7.7 (*a*) What is a shock polar?

(*b*) Derive the shock polar equation

$$v_2^* = \frac{(M_1^* - u_2^*)^2\,(M_1^*\,u_2^* - 1)}{1 + \dfrac{2}{\gamma + 1}\,M_1^{*2} - M_1^*\,u_2^*}$$

(*c*) Sketch shock polar diagrams at two values of the initial Mach number. Show the positions of the strong and weak oblique shocks, the normal shock and the infinitesimal wave on the diagrams.

7.8 Sketch the Mach waves in a flow field over a convex corner of a curved wall. The initial flow is sonic and the final Mach number is 2.0. Draw Mach waves indicating the Mach angles at

$$M = 1,\ 1.2,\ 1.5,\ 1.8 \text{ and } 2.0$$

7.9 (*a*) Explain what is Prandtl-Meyer angle?

(*b*) Starting from the flow geometry show that the value of the Prandtl-Meyer angle is

$$\omega(M) = \int \frac{\sqrt{M^2 - 1}}{2M^2\left(1 + \dfrac{\gamma - 1}{2}\,M^2\right)}\,dM^2$$

(*c*) Obtain the value of the above integral and show that the maximum Prandtl-Meyer angle is

$$\left(\sqrt{\frac{\gamma + 1}{\gamma - 1}} - 1\right)\frac{\pi}{2} = 130.5^\circ \quad (\text{for } \gamma = 1.4)$$

7.10 Solve Example 7.1 for an initial Mach number of 2.5.

Ans.

Wave	σ	p_2/p_1	T_2/T_1	ρ_2/ρ_1	M_2
Strong	83°	6.980	2.096	3.330	0.555
Weak	37°	2.448	1.316	1.859	1.800

7.11 Solve Example 7.2 for air ($\gamma = 1.4$).

Ans. $M_2 = 2.100$, $\delta = -17.192^\circ$, $T_2 = 269.74$ K.

7.12 An air stream at a Mach number of 2.0 is isentropically deflected by 10° in the clockwise direction. If the initial pressure and

temperature are 98 kN/m^2 and 97°C determine the final state of air after expansion.

Ans. ($p_2 = 52.45$ kN/m^2, $t = 36.3$°C, $\rho_2 = 0.591$ kg/m^3).

7.13 An oblique shock wave at an angle of 35 degrees occurs at the leading edge of a symmetrical wedge. Air has a Mach number of 2.0, and pressure and temperature of 10 bar and 310 K respectively upstream of this wave. Determine the wedge angle, and the pressure, temperature and Mach number downstream of the wave.

Ans. (11.5°, 13.7 bar, 340.07 K and 1.79).

7.14 A supersonic stream of air at $M = 3.0$ is deflected inwards by 15 degrees. This generates strong and weak oblique shock waves. Calculate the following quantities for these waves:

Wave angle, downstream Mach number, temperature ratio, static and stagnation pressure ratios.

Ans.

Wave	σ	M_2	p_2/p_1	T_2/T_1	p_{02}/p_{01}
Strong	84.5°	0.51	10.194	2.65	0.334
Weak	32.25°	2.25	2.80	1.40	0.895

7.15 (*a*) Sketch (in the same diagram) strong and weak oblique shock waves indicating the normal, tangential and the absolute velocity vectors upstream and downstream of the waves.

(*b*) Prove that the downstream Mach number (M_2) is lesser than the upstream Mach number (M_1) for an oblique shock wave.

(*c*) Sketch a detached shock wave. How is it formed?

8

Flow in Constant Area Ducts with Friction

Flow in a constant area duct with friction in the absence of work and heat transfer is known as Fanno flow; such a flow has already been discussed in Section 6.3.1. It was proved by Equation (6.13) that at the maximum entropy point F on the Fanno line (Figure 6.4) the gas had sonic velocity.

Fanno flow occurs in a number of practical situations; flow processes occurring in gas ducts of aircraft engines, airconditioning systems and many industrial plants can be represented by Fanno flow. Here the flow parameters vary chiefly due to the duct wall friction.

Steam pipe lines in power plants and other industrial applications are well insulated to minimize heat losses. Therefore, the flow through them can be assumed adiabatic. The effect of wall friction on the fluid parameters is considerably significant in long pipes and ducts.

8.1 THE FANNO CURVES

In this section an equation representing the locus of the state points occurring in a Fanno flow is derived under the following assumptions:

(*a*) perfect gas,
(*b*) constant area duct,
(*c*) one-dimensional steady frictional flow, and
(*d*) absence of heat and work transfer, and body forces.

Equation of continuity is

$$\dot{m} = \rho A c$$

The mass flow density is defined by

$$G = \frac{\dot{m}}{A} = \rho c \tag{8.1}$$

$$c = \frac{G}{\rho} \tag{8.1 (a)}$$

The energy equation is

$$h + \frac{1}{2} c^2 = h_0$$

$$h + \frac{1}{2} \frac{G^2}{\rho^2} = h_0$$

$$h = h_0 - \frac{1}{2} \frac{G^2}{\rho^2} \tag{8.2}$$

Equation of state can be written as

$$\rho = f(s, h) \tag{8.3}$$

Combination of Equations (8.2) and (8.3) yields the equation of the Fanno line.

$$h = h_0 - \frac{1}{2} \frac{G^2}{[f(s, h)]^2} \tag{8.4}$$

With the aid of Equation (8.2) or (8.4) for given values of h_0 and G a curve in the (h-s) plane as shown in Figure 8.1 is obtained. The curve consists of two branches AF and BF above and below the sonic point F ($M = 1$, $c = c^* = a^*$). It is seen that at all points along the curve AF the gas velocity is lower than the sonic velocity and the process occurs in the direction AF; the processes in the direction FA are not possible because they lead to decrease in entropy which violates the second law of thermodynamic. Thus in a subsonic region friction causes irreversible acceleration of the flow with pressure drop. But the maximum velocity obtainable is sonic at point F. Further acceleration of the flow beyond F towards B cannot occur because of the impossibility of decrease in entropy.

All points along the curve BF have gas velocities greater than the sonic and the processes occur in the direction BF; the processes in the direction FB being impossible as explained before. Thus in a supersonic region wall friction causes irreversible deceleration of the

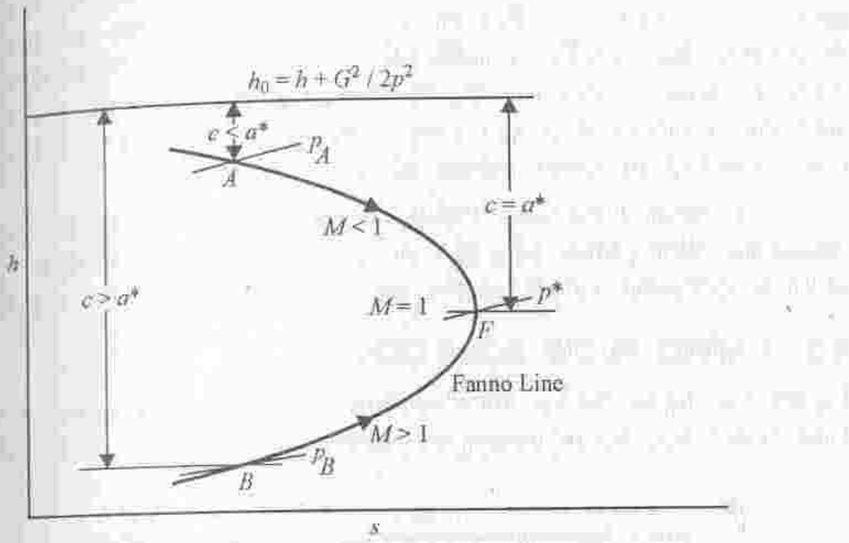

FIGURE 8.1 : A Fanno line or curve

flow with increase in pressure. The minimum velocity obtainable is sonic at point F.

From the above it is seen that the upper and lower branches of the Fanno line represent subsonic and supersonic flows respectively and for given initial conditions the final state in a process always lies towards the sonic state.

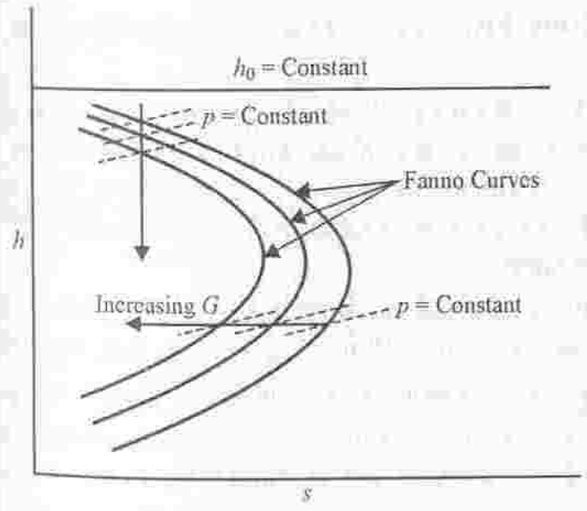

FIGURE 8.2 : Fanno curves for various values of the mass flow density

Figure 8.2 shows three Fanno curves for different values of the mass flow density (G). For the sake of comparison the stagnation enthalpy has also been kept constant for the three curves. Constant pressure lines in various regions of the flow are also shown. It is seen that the subsonic branches of these curves at higher values of G lie below those corresponding to lower values of G.

For instance the three Fanno curves shown in Figure 8.2 may represent the state points of a gas along a duct fed by a subsonic nozzle at three different values of the pressure ratio across the nozzle.

8.2 FANNO FLOW EQUATIONS

Figure 8.3 shows the variation of flow properties along a duct in Fanno flow processes. An infinitesimal element of the flow (control volume)

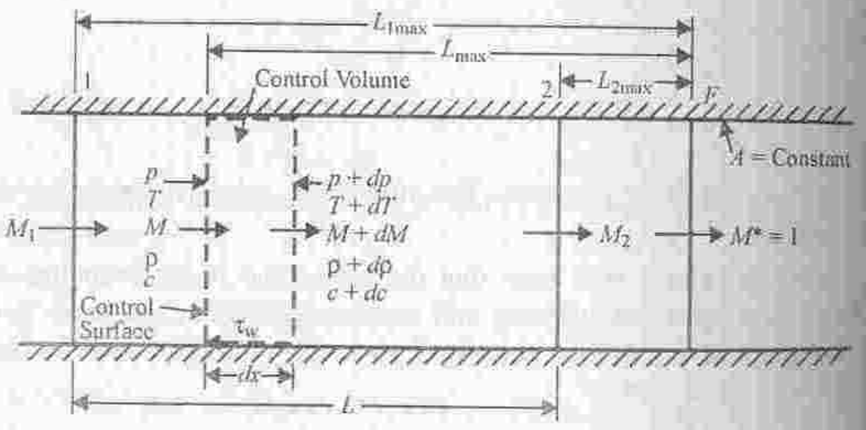

FIGURE 8.3 : Variation of flow properties in Fanno flow

at a distance x from Section 1 is shown. The changes between Sections 1 and 2, 1 and F and 2 and F are finite whereas across the control volume they are infinitesimal as shown in the figure. The sonic section at F is only shown as a reference section and need not be actually reached in a process.

The changes in flow properties in the above processes on the enthalpy-entropy diagram are shown in Figure 8.4; the states at p_1, p, $p+dp$ and p_2 are shown on the subsonic branch only. The same can be shown for the supersonic flow also on the lower branch. The stagnation pressure corresponding to the various states are also shown.

An equivalent isentropic expansion process (1 to I) is also shown for comparison. The corresponding value of the final pressure at

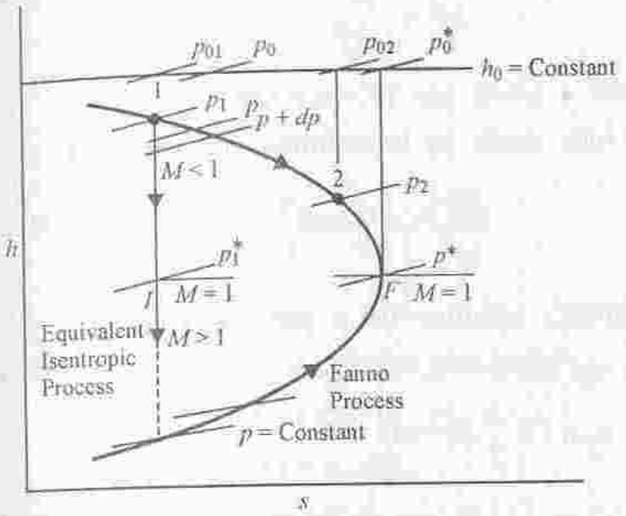

FIGURE 8.4 : Finite and infinitesimal Fanno processes

$M=1$ is $p_1^* > p^*$ as shown in the figure. It may be again noted that while the isentropic process can be extended from I to B, this is impossible in a Fanno process as explained before.

Form Equation (8.1)

$$\ln G = \ln \rho + \ln c$$

Since G is constant for a given process the above expression on differentiation gives

$$\frac{d\rho}{\rho} + \frac{dc}{c} = 0$$

$$\frac{d\rho}{\rho} = -\frac{dc}{c} = -\frac{1}{2}\frac{dc^2}{c^2} \tag{8.5}$$

The equation of state is

$$p = \rho RT$$

This on logarithmic differentiation gives

$$\frac{dp}{p} = \frac{d\rho}{\rho} + \frac{dT}{T} \tag{8.6}$$

Mach number is given by

$$M = \frac{c}{a} = \frac{c}{\sqrt{\gamma RT}}$$

$$M^2 = \frac{c^2}{\gamma RT}$$

But for a given gas $\gamma R = \text{constant}$.

Therefore, again by logarithmic differentiation

$$\frac{dM^2}{M^2} = \frac{dc^2}{c^2} - \frac{dT}{T} \tag{8.7}$$

The energy equation for a perfect gas is

$$dh + c\,dc = 0$$

$$c_p\,dT + \frac{1}{2}\,dc^2 = 0$$

Now $$c_p = \frac{\gamma}{\gamma - 1}\,R.$$

Therefore, $$\frac{\gamma}{\gamma - 1}\,RT\frac{dT}{T} + \frac{1}{2}\,dc^2 = 0$$

$$a^2\frac{dT}{T} + \frac{\gamma - 1}{2}\,dc^2 = 0$$

$$\frac{c^2}{M^2}\,\frac{dT}{T} + \frac{\gamma - 1}{2}\,dc^2 = 0$$

$$\frac{dT}{T} + \frac{\gamma - 1}{2}\,M^2\frac{dc^2}{c^2} = 0 \tag{8.8}$$

The non-dimensional friction factor (Fanning's coefficient of skin friction) as defined by Equation (1.81) is

$$f = \frac{\text{wall shear stress}}{\text{dynamic head}} = \frac{\tau_w}{\frac{1}{2}\rho c^2}$$

$$\tau_w = f\,\frac{1}{2}\rho c^2 \tag{8.9}$$

The wetted area of the duct within the elemental control surface is given by

$$dA_w = \text{Perimeter} \times \text{length} \tag{8.10}$$

$$dA_w = P\,dx$$

The hydraulic mean diameter of the duct is given by

$$D = \frac{4A}{P}$$

$$P = \frac{4A}{D}$$

Substituting this value in Equation (8.10)

$$dA_w = \frac{4A}{D}\,dx \tag{8.11}$$

Momentum equation for the control surface (Figure 8.3) gives

$$m\,[(c + dc) - c] = pA - (p + dp)\,A - \tau_w\,dA_w$$

$$\dot{m}\,dc = -A\,dp - \tau_w\,dA_w \tag{8.12}$$

Substitution from Equations (8.9) and (8.11) in (8.12) gives

$$\frac{\dot{m}}{A}\,dc = -dp - \frac{1}{2}\rho c^2\left(4f\frac{dx}{D}\right) \tag{8.13}$$

Now $\rho c^2 = \gamma p M^2$ and

$$\frac{\dot{m}}{A}\,dc = \frac{\rho A c}{A}\,dc = \rho c\,dc = \rho c^2\frac{dc}{c} = \frac{\gamma p M^2}{2}\,\frac{dc^2}{c^2}$$

Therefore, Equation (8.13) gives

$$\frac{dp}{p} + \frac{\gamma M^2}{2}\,\frac{dc^2}{c^2} + \frac{\gamma M^2}{2}\left(4f\frac{dx}{D}\right) = 0 \tag{8.14}$$

The relation between the stagnation and static pressures is given by

$$\frac{p_0}{p} = \left(1 + \frac{\gamma - 1}{2}\,M^2\right)^{\gamma/(\gamma - 1)}$$

$$\ln p_0 = \ln p + \frac{\gamma}{\gamma - 1}\ln\left(1 + \frac{\gamma - 1}{2}\,M^2\right)$$

Differentiation gives

$$\frac{dp_0}{p_0} = \frac{dp}{p} + \frac{\gamma}{\gamma - 1}\cdot\frac{d\left(1 + \frac{\gamma - 1}{2}\,M^2\right)}{1 + \frac{\gamma - 1}{2}\,M^2}$$

$$\frac{dp_0}{p_0}=\frac{dp}{p}+\frac{\gamma M^2}{2\left(1+\frac{\gamma-1}{2}M^2\right)}\frac{dM^2}{M^2} \tag{8.15}$$

Definition of impulse function gives

$$F=pA+\rho Ac^2=pA+\gamma pA\,M^2$$

$$F=(1+\gamma M^2)\,pA$$

By logarithmic differentiation

$$\frac{dF}{F}=\frac{d(1+\gamma M^2)}{1+\gamma M^2}+\frac{dp}{p}$$

$$\frac{dF}{F}=\frac{\gamma M^2}{1+\gamma M^2}\frac{dM^2}{M^2}+\frac{dp}{p} \tag{8.16}$$

8.3 SOLUTION OF FANNO FLOW EQUATIONS

In this section the differential flow parameters

$$\frac{dc^2}{c^2},\ \frac{d\rho}{\rho},\ \frac{dp}{p},\ \frac{dT}{T},\ \frac{dp_0}{p_0},\ \frac{dF}{F}\ \text{and}\ 4f\frac{dx}{D}$$

will be expressed as functions of γ and M^2 only.

Substituting for dT/T in Equation (8.7) from (8.8)

$$\frac{dM^2}{M^2}=\frac{dc^2}{c^2}+\frac{\gamma-1}{2}M^2\frac{dc^2}{c^2}=\left(1+\frac{\gamma-1}{2}M^2\right)\frac{dc^2}{c^2}$$

$$2\frac{dc}{c}=\frac{dc^2}{c^2}=\frac{1}{1+\frac{\gamma-1}{2}M^2}\frac{dM^2}{M^2} \tag{8.17}$$

Equation (8.17) in (8.5) gives

$$\frac{d\rho}{\rho}=-\frac{1}{2\left(1+\frac{\gamma-1}{2}M^2\right)}\frac{dM^2}{M^2} \tag{8.18}$$

Substituting Equation (8.17) in (8.8) gives

$$\frac{dT}{T}=-\frac{\gamma-1}{2}M^2\frac{1}{1+\frac{\gamma-1}{2}M^2}\frac{dM^2}{M^2}$$

$$\frac{dT}{T}=-\frac{\gamma-1}{2\left(1+\frac{\gamma-1}{2}M^2\right)}dM^2 \tag{8.19}$$

Substituting Equations (8.18) and (8.19) in (8.6) gives

$$\frac{dp}{p}=-\frac{1}{2\left(1+\frac{\gamma-1}{2}M^2\right)}\frac{dM^2}{M^2}-\frac{(\gamma-1)M^2}{2\left(1+\frac{\gamma-1}{2}M^2\right)}\frac{dM^2}{M^2}$$

$$\frac{dp}{p}=-\frac{1+(\gamma-1)M^2}{2\left(1+\frac{\gamma-1}{2}M^2\right)}\frac{dM^2}{M^2} \tag{8.20}$$

Substituting Equation (8.20) in (8.15) yields

$$\frac{dp_0}{p_0}=-\frac{1+(\gamma-1)M^2}{2\left(1+\frac{\gamma-1}{2}M^2\right)}\frac{dM^2}{M^2}+\frac{\gamma M^2}{2\left(1+\frac{\gamma-1}{2}M^2\right)}\frac{dM^2}{M^2}$$

$$\frac{dp_0}{p_0}=-\frac{1-M^2}{2\left(1+\frac{\gamma-1}{2}M^2\right)}\frac{dM^2}{M^2} \tag{8.21}$$

Substituting Equation (8.20) in (8.16) gives

$$\frac{dF}{F}=\frac{\gamma M^2}{1+\gamma M^2}\frac{dM^2}{M^2}-\frac{1+(\gamma-1)M^2}{2\left(1+\frac{\gamma-1}{2}M^2\right)}\frac{dM^2}{M^2}$$

On simplification it yields

$$\frac{dF}{F}=-\frac{1-M^2}{2(1+\gamma M^2)\left(1+\frac{\gamma-1}{2}M^2\right)}\frac{dM^2}{M^2} \tag{8.22}$$

Substituting for dp/p and dc^2/c^2 from Equations (8.20) and (8.17) respectively in (8.14)

$$\frac{\gamma M^2}{2}\left(4f\frac{dx}{D}\right)=\left[\frac{1+(\gamma-1)M^2}{2\left(1+\frac{\gamma-1}{2}M^2\right)}-\frac{\gamma M^2}{2}\frac{1}{1+\frac{\gamma-1}{2}M^2}\right]\frac{dM^2}{M^2}$$

On simplification and rearrangement it gives the following expressions:

$$4f\frac{dx}{D}=\frac{1-M^2}{\gamma M^2\left(1+\frac{\gamma-1}{2}M^2\right)}\frac{dM^2}{M^2} \tag{8.23}$$

$$\frac{dM^2}{M^2}=\frac{\gamma M^2\left(1+\frac{\gamma-1}{2}M^2\right)}{1-M^2}4f\frac{dx}{D} \tag{8.24}$$

Equation (8.24) represents the variation of the Mach number with the friction factor and the duct length or with the parameter $4f\,dx/D$. The dependence of other flow properties on this parameter can be shown by obtaining another set of Equations in terms of $4f\,dx/D$. This is done by substituting for dM^2/M^2 in Equations (8.17), (8.18), (8.19), (8.20), (8.21) and (8.22) from Equation (8.24). The resulting Equations after this procedure are

$$\frac{1}{2}\frac{dc^2}{c^2}=\frac{dc}{c}=\frac{\gamma M^2}{2(1-M^2)}4f\frac{dx}{D} \tag{8.25}$$

$$\frac{d\rho}{\rho}=-\frac{\gamma M^2}{2(1-M^2)}4f\frac{dx}{D} \tag{8.26}$$

$$\frac{dT}{T}=-\frac{\gamma(\gamma-1)M^2}{2(1-M^2)}4f\frac{dx}{D} \tag{8.27}$$

$$\frac{dp}{p}=-\frac{\gamma M^2[1+(\gamma-1)M^2]}{2(1-M^2)}4f\frac{dx}{D} \tag{8.28}$$

$$\frac{dp_0}{p_0}=-\frac{\gamma M^2}{2}4f\frac{dx}{D} \tag{8.29}$$

$$\frac{dF}{F}=-\frac{\gamma M^2}{2(1+\gamma M^2)}4f\frac{dx}{D} \tag{8.30}$$

However, for the purpose of integration Equations (8.17) to (8.22) have been used in the next section.

8.4 VARIATION OF FLOW PROPERTIES

In this section the flow properties have been expressed in explicit form after integration of Equations (8.17) to (8.22). Flow properties at $M=M^*=1$ are used as reference values for non-dimensionalizing various properties at any section of the duct. Various integrals mentioned here have been solved in Appendix A.2.

8.4.1 Velocity

Equation (8.17) is

$$\frac{dc}{c}=\frac{1}{2M^2\left(1+\frac{\gamma-1}{2}M^2\right)}dM^2$$

Integrating between $M=1$ and $M=M$,

$$\int_{c^*}^{c}\frac{dc}{c}=\int_{1}^{M}\frac{dM^2}{2M^2\left(1+\frac{\gamma-1}{2}M^2\right)}$$

$$\ln\frac{c}{c^*}=\ln M\left[\frac{\gamma+1}{2\left(1+\frac{\gamma-1}{2}M^2\right)}\right]^{1/2}$$

$$\frac{c}{c^*}=M\left[\frac{\gamma+1}{2\left(1+\frac{\gamma-1}{2}M^2\right)}\right]^{1/2} \tag{8.31}$$

Applying this equation for sections 1 and 2 of the duct (Figure 8.3)

$$\frac{c_2}{c_1}=\frac{M_2}{M_1}\left(\frac{1+\frac{\gamma-1}{2}M_1^2}{1+\frac{\gamma-1}{2}M_2^2}\right)^{1/2} \tag{8.32}$$

8.4.2 Density

$$\rho c=\rho^* c^*$$

$$\frac{\rho}{\rho^*} = \frac{c^*}{c}$$

From Equation (8.31)

$$\frac{\rho}{\rho^*} = \frac{1}{M}\left\{\frac{2\left(1+\frac{\gamma-1}{2}M^2\right)}{\gamma+1}\right\}^{1/2} \tag{8.33}$$

$$\frac{\rho_2}{\rho_1} = \frac{c_1}{c_2}$$

From Equation (8.32)

$$\frac{\rho_2}{\rho_1} = \frac{M_1}{M_2}\left\{\frac{1+\frac{\gamma-1}{2}M_2^2}{1+\frac{\gamma-1}{2}M_1^2}\right\}^{1/2} \tag{8.34}$$

8.4.3 Temperature

From Equation (8.19)

$$\int_{T^*}^{T}\frac{dT}{T} = -\int_{1}^{M}\frac{\gamma-1}{2\left(1+\frac{\gamma-1}{2}M^2\right)}dM^2$$

$$\ln\frac{T}{T^*} = \ln\frac{\gamma+1}{2\left(1+\frac{\gamma-1}{2}M^2\right)}$$

$$\frac{T}{T^*} = \frac{\gamma+1}{2\left(1+\frac{\gamma-1}{2}M^2\right)} \tag{8.35}$$

Applying this equation for sections 1 and 2

$$\frac{T_2}{T_1} = \frac{1+\frac{\gamma-1}{2}M_1^2}{1+\frac{\gamma-1}{2}M_2^2} \tag{8.36}$$

8.4.4 Pressure

From Equation (8.20)

$$\int_{p^*}^{p}\frac{dp}{p} = -\int_{1}^{M}\frac{1+(\gamma-1)M^2}{2M^2+(\gamma-1)M^2}dM^2$$

$$\ln\frac{p}{p^*} = \ln\frac{1}{M}\left[\frac{\gamma+1}{2\left(1+\frac{\gamma-1}{2}M^2\right)}\right]^{1/2}$$

$$\frac{p}{p^*} = \frac{1}{M}\left[\frac{\gamma+1}{2\left(1+\frac{\gamma-1}{2}M^2\right)}\right]^{1/2} \tag{8.37}$$

$$\frac{p_2}{p_1} = \frac{M_1}{M_2}\left\{\frac{1+\frac{\gamma-1}{2}M_1^2}{1+\frac{\gamma-1}{2}M_2^2}\right\}^{1/2} \tag{8.38}$$

8.4.5 Stagnation pressure

From Equation (8.21)

$$\int_{p_0}^{p_0^*}\frac{dp_0}{p_0} = -\frac{1}{2}\int_{1}^{M^*}\frac{1-M^2}{M^2\left(1+\frac{\gamma-1}{2}M^2\right)}dM^2$$

$$\ln\frac{p_0}{p_0^*} = \ln\frac{1}{M}\left[\frac{2\left(1+\frac{\gamma-1}{2}M^2\right)}{\gamma+1}\right]^{(\gamma+1)/2(\gamma-1)}$$

$$\frac{p_0}{p_0^*} = \frac{1}{M}\left[\frac{2\left(1+\frac{\gamma-1}{2}M^2\right)}{\gamma+1}\right]^{(\gamma+1)/2(\gamma-1)} \tag{8.39}$$

$$\frac{p_{02}}{p_{01}} = \frac{M_1}{M_2}\left[\frac{1+\frac{\gamma-1}{2}M_2^2}{1+\frac{\gamma-1}{2}M_1^2}\right]^{(\gamma+1)/2(\gamma-1)} \tag{8.40}$$

8.4.6 Impulse function

From Equation (8.22)

$$\int_{F^*}^{F}\frac{dF}{F} = -\int_{1}^{M}\frac{1-M^2}{2M^2(1+\gamma M^2)\left(1+\frac{\gamma-1}{2}M^2\right)}dM^2$$

$$\ln\frac{F}{F^*} = \ln\frac{1+\gamma M^2}{M\left[2(\gamma+1)\left(1+\frac{\gamma-1}{2}M^2\right)\right]^{1/2}}$$

$$\frac{F}{F^*} = \frac{1+\gamma M^2}{M\left[2(\gamma+1)\left(1+\frac{\gamma-1}{2}M^2\right)\right]^{1/2}} \tag{8.41}$$

$$\frac{F_2}{F_1} = \frac{1+\gamma M_2^2}{1+\gamma M_1^2}\frac{M_1}{M_2}\left[\frac{1+\frac{\gamma-1}{2}M_1^2}{1+\frac{\gamma-1}{2}M_2^2}\right]^{1/2} \tag{8.42}$$

8.4.7 Change of entropy

From Equation (6.47) the change of entropy is given by

$$\frac{s-s^*}{R} = -\ln\frac{p_0}{p_0^*} \tag{8.43}$$

Substituting from Equation (8.39)

$$\frac{s-s^*}{R} = -\ln\frac{1}{M}\left[\frac{2\left(1+\frac{\gamma-1}{2}M^2\right)}{\gamma+1}\right]^{(\gamma+1)/2(\gamma-1)} \tag{8.44}$$

Similarly $\dfrac{s_2-s_1}{R} = \ln\dfrac{p_{01}}{p_{02}}$

Substituting from Equation (8.40) on the right hand side of the above equation

$$\frac{s_2-s_1}{R} = \ln\frac{M_2}{M_1}\left[\frac{1+\frac{\gamma-1}{2}M_1^2}{1+\frac{\gamma-1}{2}M_2^2}\right]^{(\gamma+1)/2(\gamma-1)} \tag{8.45}$$

8.5 VARIATION OF MACH NUMBER WITH DUCT LENGTH

At a given Mach number (M) on either the subsonic or supersonic branch of the Fanno line (Figure 8.4) there is a specific value of the duct length (L_{max}) downstream of this section ($M = M$) which will change this Mach number to unity. For a given gas and the duct this length is an explicit function of the Mach number. Since no continuous process is possible beyond $M = 1$ on the Fanno line this is the maximum value of the duct length. This can be clearly seen from Figures 8.3 and 8.4. This length (L_{max}) can be determined from Equation (8.23) by using a constant value of the friction factor over the length. For this purpose a mean coefficient of friction is defined by

$$\bar{f} = \frac{1}{L_{max}}\int_0^{L_{max}} f\,dx \tag{8.46}$$

It is seen from Figures 8.3 and 8.4 that the limits of integration of Equation (8.23) are

from $x = 0$ to $x = L_{max}$, and

from $M = M$ to $M = M^* = 1$

Therefore, $\displaystyle\int_0^{L_{max}} 4f\frac{dx}{D} = \int_M^1 \frac{1-M^2}{\gamma M^4\left(1+\frac{\gamma-1}{2}M^2\right)}dM^2$ (8.47)

Equations (8.46) and (8.47) yield

$$\left(4\bar{f}\frac{L_{max}}{D}\right)_M = \frac{1-M^2}{\gamma M^2} + \frac{\gamma+1}{2\gamma}\ln\frac{(\gamma+1)M^2}{2\left(1+\frac{\gamma-1}{2}M^2\right)} \tag{8.48}$$

This equation gives $4\bar{f}L_{max}/D = 0$ for $M = 1$.

The distance (L) beween the two sections of the duct where the Mach numbers are M_1 and M_2 is given by

$$4\bar{f}\frac{L}{D} = 4\bar{f}\frac{L_{1\max}}{D} - 4\bar{f}\frac{L_{2\max}}{D} \tag{8.49}$$

Equation (8.49) can also be written as

$$4\bar{f}\frac{L}{D} = \left(4\bar{f}\frac{L_{\max}}{D}\right)_{M_1} - \left(4\bar{f}\frac{L_{\max}}{D}\right)_{M_2} \tag{8.50}$$

Using Equation (8.48) for Mach numbers M_1 and M_2 respectively in Equation (8.50) and simplifying

$$4\bar{f}\frac{L}{D} = \frac{M_2^2 - M_1^2}{\gamma M_1^2 M_2^2} + \frac{\gamma+1}{2\gamma}\ln\frac{M_1^2}{M_2^2}\,\frac{1+\frac{\gamma-1}{2}M_2^2}{1+\frac{\gamma-1}{2}M_1^2} \tag{8.51}$$

8.6 TABLES FOR FANNO FLOW

The use of Equations (8.31), (8.33), (8.35), (8.37), (8.39), (8.41), (8.44) and (8.48) for the determination of the properties c, ρ, T, p, p_0, F, s and $4\bar{f}L_{\max}/D$ involves long and tedious calculations. As pointed out in other chapters it is more convenient to use these expressions to prepare tables for Fanno flow; such tables for a number of values of γ can then be used to solve the problems in a comparatively much shorter time. A short extract from such a table for $\gamma = 1.4$ is given in Appendix A.7. For generality various properties are expressed in the non-dimensional form.

8.7 CHARTS FOR FANNO FLOW

Quick and approximate solutions of Fanno flow problems can also be obtained by Fanno flow charts shown in Figures 8.5 and 8.6. Such charts can be prepared by plotting various property ratios from Fanno flow gas tables. The observations from these charts are summarized in Table 8.1. While interpreting various equations (indicated in this table) graphically, following facts must be kept in mind:

For supersonic flows the quantities dM^2 and $(1-M^2)$ are negative whereas for subsonic flows these quantities are positive.

The direction of all changes is towards the sonic point ($M=1$) as shown in Figures 8.5 and 8.6.

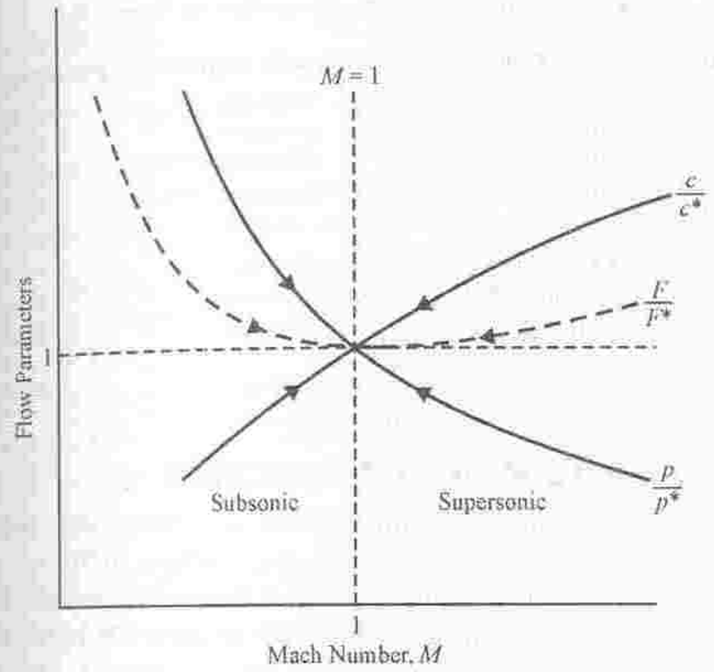

FIGURE 8.5 : Variation of flow parameters in Fanno flow

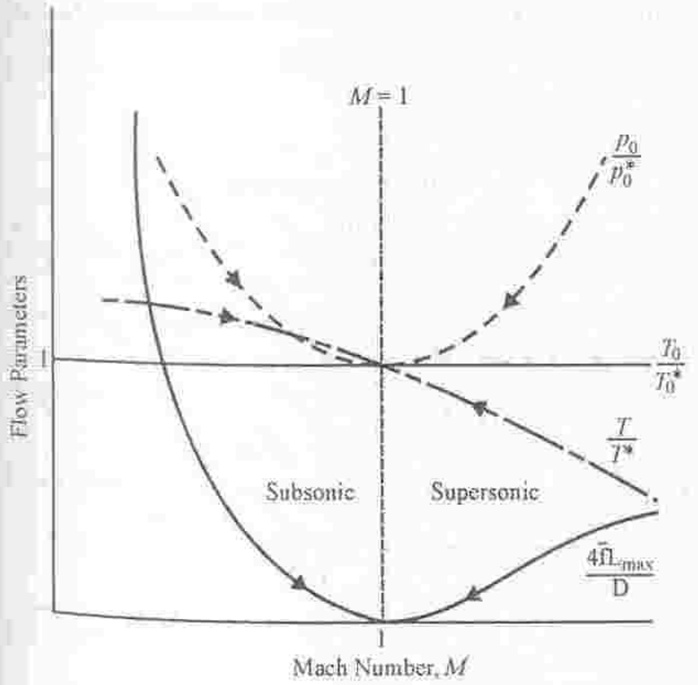

FIGURE 8.6 : Variation of flow parameters in Fanno flow

TABLE 8.1: Variation of flow parameters in Fanno flow

Properties	Equations	Subsonic region	Supersonic region
M	—	increases	decreases
c	8.17, 8.25, 8.31	increases	decreases
ρ	8.18, 8.26, 8.33	decreases	increases
T	8.19, 8.27, 8.35	decreases	increases
T_0	—	constant	constant
p	8.20, 8.28, 8.37	decreases	increases
p_0	8.21, 8.29, 8.39	decreases	decreases
F	9.22, 8.30, 8.41	decreases	decreases
$4\bar{f}\frac{L_{max}}{D}$	8.48	decreases	decreases

8.8 ISOTHERMAL FLOW WITH FRICTION

In this section isothermal flow in constant area ducts with friction is considered. Such a flow occurs in long ducts where sufficient time is available for the heat transfer to occur and therefore temperature may remain constant. On account of constant temperature the friction factor may be assumed constant along the duct. The analysis of such a flow is comparatively simpler.

Natural gas pipe lines are several kilometers long between the pumping stations. On account of this there is considerable surface area

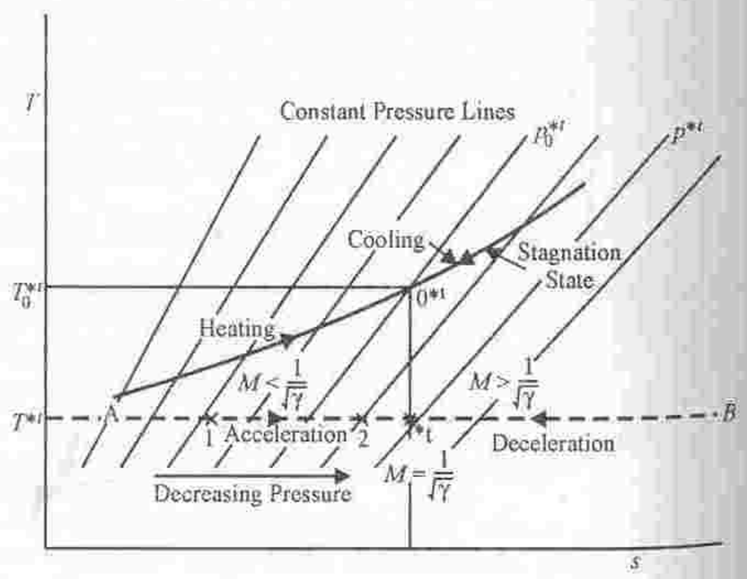

FIGURE 8.7 : Isothermal flow with friction

and time available for heat transfer to take place. Therefore, the flow here is closer to isothermal than adiabatic.

Isothermal flow processes are represented by straight horizontal lines on the temperature-entropy diagram like $A\text{-}^*t$ and $B\text{-}^*t$ in Figure 8.7. It will be shown later that in these processes the limiting state occurs at $M = 1/\sqrt{\gamma}$ and all processes approach this Mach number.

On account of the heat transfer required for maintaining constant temperature the stagnation temperature line is curved. Constant pressure lines are also shown in Figure 8.7; the pressure of the gas decreases in the acceleration process $A\text{-}^*t$; therefore, to maintain constant temperature in the process heat is supplied (from the surroundings) resulting in entropy increase. In the constant temperature deceleration process $B\text{-}^*t$ there is increase in pressure and decrease in entropy due to cooling.

8.8.1 Fundamental Equations

Following assumptions are used to derive Equations for isothermal flow:

(*a*) Perfect gas,
(*b*) Constant area duct,
(*c*) Absence of body forces, and
(*d*) One dimensional frictional flow at constant temperature.

In contrast to the adiabatic flow here

$$dT = 0$$
$$h_{01} \neq h_{02}$$
$$T_{01} \neq T_{02}$$

The equations of continuity, state and momentum will again be used here. The energy Equation will be used by way of defining the relationship between the static and stagnation temperatures. Expressions defining the Mach number, and the stagnation pressure remain the same as in adiabatic flow. For isothermal flow Equations (8.6) and (8.7) are

$$\frac{dp}{p} = \frac{d\rho}{\rho} \tag{8.52}$$

$$\frac{dM^2}{M^2} = \frac{dc^2}{c^2} \tag{8.53}$$

Equations (8.5) and (8.52) give

$$\frac{dp}{p} = \frac{d\rho}{\rho} = -\frac{dc}{c} = -\frac{1}{2}\frac{dc^2}{c^2} \tag{8.54}$$

Momentum Equation (8.14) gives

$$\frac{dp}{p} = -\frac{\gamma M^2}{2}\left(\frac{dc^2}{c^2} + 4f\frac{dx}{D}\right) \tag{8.55}$$

Substituting for dc^2/c^2 from Equation (8.54) into (8.55)

$$\frac{dp}{p} = \gamma M^2 \frac{dp}{p} - \frac{\gamma M^2}{2} 4f\frac{dx}{D}$$

On rearrangement this gives

$$\frac{dp}{p} = \frac{-\gamma M^2}{2(1-\gamma M^2)} 4f\frac{dx}{D} \tag{8.56}$$

Combination of Equations (8.53), (8.54) and (8.56) yields

$$\frac{dp}{p} = \frac{d\rho}{\rho} = -\frac{dc}{c} = -\frac{dc^2}{2c^2} = -\frac{dM^2}{2M^2} = -\frac{\gamma M^2}{2(1-\gamma M^2)} 4\bar{f}\frac{dx}{D} \tag{8.57}$$

Definition of stagnation temperature gives

$$\frac{T_0}{T} = 1 + \frac{\gamma - 1}{2} M^2$$

This on logarithmic differentiation gives

$$\frac{dT_0}{T_0} = \frac{(\gamma - 1) M^2}{2\left(1 + \frac{\gamma - 1}{2} M^2\right)} \frac{dM^2}{M^2} \tag{8.58}$$

8.8.2 Direction of Isothermal Processes

In Equation (8.57) the friction factor is always positive. Therefore, the direction of a process (sign of the variables dp, $d\rho$ etc.) depends on the sign of the factor $(1-\gamma M^2)$. This gives two regimes of the processes.

(*a*) When $1-\gamma M^2 =$ positive

This gives $\gamma M^2 < 1$

$$M < \frac{1}{\sqrt{\gamma}} \tag{8.59}$$

In this regime the processes are along A-$^*t$ as shown by Equation (8.57) and Figure 8.7. The limiting value of the Mach number is

$$M^{*t} = \frac{1}{\sqrt{\gamma}} \tag{8.60}$$

and occurs at point $^*t$ as shown in Figure 8.7; other flow parameters at this point are p^{*t}, ρ^{*t}, c^{*t}, F^{*t}, p_0^{*t}, T_0^{*t} and s^{*t}.

(*b*) When $1-\gamma M^2 =$ negative

This gives $\gamma M^2 > 1$

$$M > \frac{1}{\sqrt{\gamma}} \tag{8.61}$$

In this regime the processes are along B-$^*t$ as shown in Figure 8.7 and Equation (8.57).

8.8.3 Variation of Flow Properties

Equations (8.57) will now be integrated to express various flow properties in explicit form. As before these quantities are expressed as ratios by using the values at the limiting point $^*t$.

Static pressure:

$$\int_p^{p^{*t}} \frac{dp}{p} = -\frac{1}{2}\int_M^{M^{*t}} \frac{dM^2}{M^2}$$

$$M^{*t} = \frac{1}{\sqrt{\gamma}}$$

$$[\ln p]_p^{p^{*t}} = -\frac{1}{2}\,[\ln M^2]_M^{1/\sqrt{\gamma}}$$

This on simplifying gives

$$\frac{p}{p^{*t}} = \frac{1}{\sqrt{\gamma}M} \tag{8.62}$$

Using Equation (8.62) between sections 1 and 2

$$\frac{p_1}{p_2} = \frac{M_2}{M_1} \tag{8.63}$$

Velocity and density: Similarly, proceeding as before,

$$\frac{c^{*t}}{c} = \frac{\rho}{\rho^{*t}} = \frac{1}{\sqrt{\gamma}M} \tag{8.64}$$

$$\frac{c_2}{c_1}=\frac{\rho_1}{\rho_2}=\frac{M_2}{M_1} \tag{8.65}$$

It will be noticed here that such relations for p_0, T_0 and F are obtained in a straight forward way than through Equations (8.15), (8.58) and (8.16) respectively.

Stagnation pressure: Substituting from Equation (8.57) for dp/p in (8.15),

$$\frac{dp_0}{p_0}=-\frac{1}{2}\frac{dM^2}{M^2}+\frac{\gamma M^2}{2\left(1+\dfrac{\gamma-1}{2}M^2\right)}\frac{dM^2}{M^2}$$

This on simplification and rearrangement gives

$$\frac{dp_0}{p_0}=\left(\frac{\gamma+1}{2}M^2-1\right)\frac{dM^2}{M^2} \tag{8.66}$$

Stagnation pressure is given by

$$p_0=p\left(1+\frac{\gamma-1}{2}M^2\right)^{\gamma/(\gamma-1)}$$

At the limiting state point ${}^*t\,(M^2=1/\gamma)$

$$p_0^{*t}=p^{*t}\left(1+\frac{\gamma-1}{2}\frac{1}{\gamma}\right)^{\gamma/(\gamma-1)}=p^{*t}\left(\frac{3\gamma-1}{2\gamma}\right)^{\gamma/(\gamma-1)}$$

Therefore, by division

$$\frac{p_0}{p_0^{*t}}=\frac{p}{p^{*t}}\left[\frac{2\gamma}{3\gamma-1}\left(1+\frac{\gamma-1}{2}M^2\right)\right]^{\gamma/(\gamma-1)} \tag{8.67 (a)}$$

Combination of Equations (8.62) and (8.67 (*a*)) gives

$$\frac{p_0}{p_0^{*t}}=\frac{1}{\sqrt{\gamma}M}\left[\frac{2\gamma}{3\gamma-1}\left(1+\frac{\gamma-1}{2}M^2\right)\right]^{\gamma/(\gamma-1)} \tag{8.67 (b)}$$

$$\frac{p_{01}}{p_{02}}=\frac{M_2}{M_1}\left[\frac{1+\dfrac{\gamma-1}{2}M_1^2}{1+\dfrac{\gamma-1}{2}M_2^2}\right]^{\gamma/(\gamma-1)} \tag{8.68}$$

Stagnation temperature:

$$T_0=T\left(1+\frac{\gamma-1}{2}M^2\right)$$

$$T_0^{*t}=T^{*t}\left(1+\frac{\gamma-1}{2}\frac{1}{\gamma}\right)=\frac{3\gamma-1}{2\gamma}T^{*t}$$

$$T=T^{*t}=\text{constant}$$

$$\frac{T_0}{T^{*t}}=\frac{2\gamma}{3\gamma-1}\left(1+\frac{\gamma-1}{2}M^2\right) \tag{8.69}$$

$$\frac{T_{01}}{T_{02}}=\frac{1+\dfrac{\gamma-1}{2}M_1^2}{1+\dfrac{\gamma-1}{2}M_2^2} \tag{8.70}$$

Change of entropy: From Equation (6.42) change of entropy is given by

$$s_2-s_1=c_p\ln\frac{T_2/T_1}{(p_2/p_1)^{(\gamma-1)/\gamma}}$$

$$T_2/T_1=1$$

$$s_2-s_1=-c_p\ln\left(\frac{p_2}{p_1}\right)^{(\gamma-1)/\gamma}$$

$$s_2-s_1=R\ln\left(\frac{p_1}{p_2}\right) \tag{8.71}$$

Combination of Equations (8.63) and (8.71) gives

$$s_2-s_1=R\ln\left(\frac{M_2}{M_1}\right) \tag{8.72 (a)}$$

$$\frac{s-s^{*t}}{R}=\ln(\sqrt{\gamma}M) \tag{8.72 (b)}$$

Length of the duct: From Equation (8.57)

$$\frac{\gamma M^2}{2(1-\gamma M^2)}4f\frac{dx}{D}=\frac{dM^2}{2M^2}$$

$$4f\frac{dx}{D}=\frac{1-\gamma M^2}{\gamma M^4}dM^2 \tag{8.73}$$

The limits of integration for this equation are

from $x=0$ to $x=L_{max}$ and

from $M=M$ to $M=M^{*t}=\dfrac{1}{\sqrt{\gamma}}$

L_{max} is the length of the duct which will be required to achieve the limiting state $^{*}t\,(M=1/\sqrt{\gamma})$; as pointed out earlier this state is used only as a reference point and may not actually occur in a process.

On integration between the above limits Equation (8.73) gives

$$\int_0^{L_{max}} 4f\frac{dx}{d}=\frac{1}{\gamma}\int_{M^2}^{1/\gamma}\frac{dM^2}{M^4}-\int_{M^2}^{1/\gamma}\frac{dM^2}{M^2}$$

This on simplifying and rearrangement yields

$$\left(4\bar{f}\frac{L_{max}}{D}\right)_M=\frac{1-\gamma M^2}{\gamma M^2}+\ln\gamma M^2 \tag{8.74}$$

The distance between the two sections 1 and 2 of the duct is given by

$$4\bar{f}\frac{L}{D}=\left(4\bar{f}\frac{L_{max}}{D}\right)_{M_1}-\left(4\bar{f}\frac{L_{max}}{D}\right)_{M_2}$$

Using Equation (8.74) for Mach numbers M_1 and M_2 respectively in the above expression and simplifying,

$$4\bar{f}\frac{L}{D}=\frac{1}{\gamma}\left(\frac{1}{M_1^2}-\frac{1}{M_2^2}\right)+\ln\frac{M_1^2}{M_2^2} \tag{8.75 (a)}$$

Equation (8.63) in (8.75 (*a*)) gives another useful relation:

$$4\bar{f}\frac{L}{D}=\frac{1}{\gamma M_1^2}\left(1-\frac{p_2^2}{p_1^2}\right)+\ln\frac{p_2^2}{p_1^2} \tag{8.75 (b)}$$

Impulse function: Impulse function is given by

$$F=p\,(1+\gamma M^2)\,A$$

Its value at the limiting state point is

$$F^{*t}=p^{*t}\left(1+\gamma\frac{1}{\gamma}\right)A$$

$$F^{*t}=2A\,p^{*t}$$

Therefore,

$$\frac{F}{F^{*t}}=\frac{p}{2p^{*t}}(1+\gamma M^2)$$

$$\frac{F}{F^{*t}}=\frac{1+\gamma M^2}{2\sqrt{\gamma}M} \tag{8.76}$$

$$\frac{F_1}{F_2}=\frac{M_2}{M_1}\frac{1+\gamma M_1^2}{1+\gamma M_2^2} \tag{8.77}$$

Chart for Isothermal flow: Variation of various flow parameters in an isothermal frictional flow are shown graphically in Figures 8.8 and 8.9. Table 8.2 summarizes these variations with the aid of the Equations developed in the earlier sections.

As discussed in Section 8.8.2 the direction of change in a flow property depends on whether the Mach number is less than or greater than the limiting value $M^{*t}=1/\sqrt{\gamma}$. It should be further noted that

for $$M<\frac{1}{\sqrt{\gamma}},\ dM^2=+\text{ve}$$

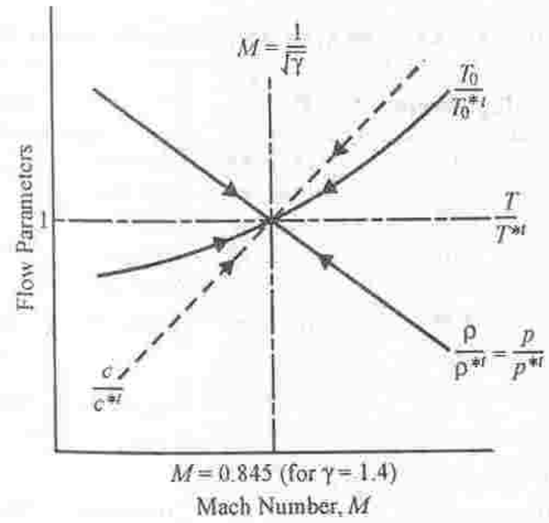

FIGURE 8.8 : Variation of flow parameters in isothermal flow with friction

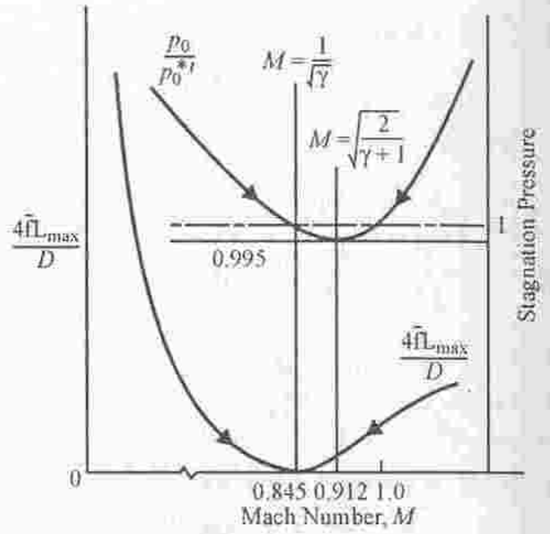

FIGURE 8.9 : Variation of stagnation pressure and duct length in isothermal flow with friction ($\gamma = 1.4$)

for $$M > \frac{1}{\sqrt{\gamma}},\ dM^2 = -\text{ve}$$

The variation of the stagnation pressure depends, besides the aforementioned factor, on the factor $\sqrt{\frac{2}{\gamma+1}}$ also; this is observed in Equation (8.66). For $M < 1/\sqrt{\gamma}$ the Mach number is always less than $\sqrt{2/(\gamma+1)}$ therefore, the stagnation pressure always decreases in this regime.

TABLE 8.2: Variation of flow parameters in isothermal frictional flow

Properties	Equations	$M < \frac{1}{\sqrt{\gamma}}$	$M > \frac{1}{\sqrt{\gamma}}$
M	—	increases	decreases
p	8.57	decreases	increases
ρ	8.57	decreases	increases
c	8.57	increases	decreases
T_0	8.58	increases	decreases
$4fL_{max}/D$	8.74	decreases	decreases
p_0	8.66	decreases	decreases for $M > \sqrt{\frac{2}{\gamma+1}}$
			increases for $M < \sqrt{\frac{2}{\gamma+1}}$

But for $M > 1/\sqrt{\gamma}$ it will decrease only when the Mach number is greater than $\sqrt{2/(\gamma+1)}$. The stagnation pressure increases between Mach numbers $1/\sqrt{\gamma}$ and $\sqrt{2/(\gamma+1)}$.

With reference to Figure 8.9 it must be noted that at $M = 1/\sqrt{\gamma}$ Equation (8.67 (*b*)) gives $p_0/p_0^{*f} = 1$ whereas at $M = \sqrt{2/(\gamma+1)}$ the value obtained is 0.995. To illustrate this point the difference between these values is shown magnified in Figure 8.9. This peculiar mode of variation of stagnation pressure with Mach number is further illustrated in Figure 8.10.

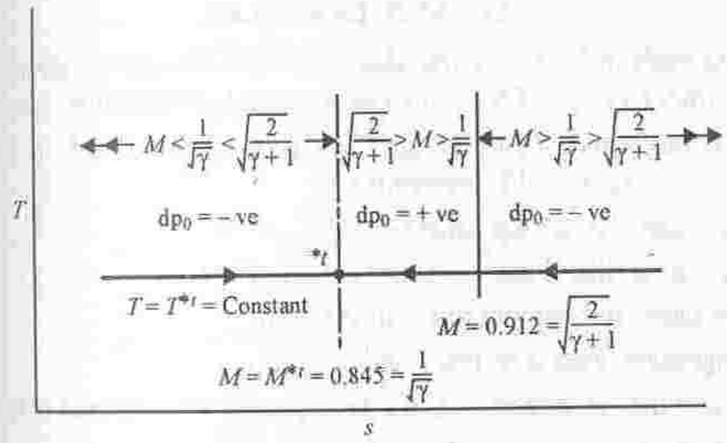

FIGURE 8.10 : Variation of stagnation pressure with Mach number in isothermal flow with friction ($\gamma = 1.4$)

NOTATION FOR CHAPTER 8

A	area	L	duct length
a	velocity of sound	$\dot{m}$	mass flow rate
c	fluid velocity	M	Mach number
d	hydraulic mean diameter	p	pressure
D	diameter of a circular duct	P	perimeter
		R	gas constant
f	Fanning's coefficient of skin friction	s	entropy
		T	temperature
F	impulse function	x	distance along the duct
G	mass flow density or mass velocity	$\gamma = c_p/c_v$	ratio of specific heats
		ρ	density
h	enthalpy	τ	wall shear stress

SUBSCRIPTS

0	stagnation values	max	maximum
1	initial state	w	wall
2	final state	x	upstream of normal shock
I	isentropic	y	downstream of normal shock

SUPERSCRIPT

*	corresponding to $M=1$	—	mean value
$^*_t$	corresponding to $M=\frac{1}{\sqrt{\gamma}}$	1	limiting values at $M=\sqrt{\frac{2}{\gamma+1}}$

SOLVED EXAMPLES

Example 8.1. A circular duct passes 8.25 kg/s of air at an exit Mach number of 0.5. The entry pressure and temperature are 3.45 bar and 38°C respectively and the coefficient of friction 0.005. If the Mach number at entry is 0.15, determine

(*a*) the diameter of the duct,
(*b*) length of the duct,
(*c*) pressure and temperature at the exit,
(*d*) stagnation pressure loss, and
(*e*) verify the exit Mach number through exit velocity and temperature.

Solution. $T_1 = 273 + 38 = 311$ K

(*a*)
$$\rho_1 = \frac{p_1}{RT_1} = \frac{3.45\times10^5}{287\times311} = 3.865 \text{ kg/m}^3$$
$$a_1 = \sqrt{\gamma RT_1}$$
$$a_1 = \sqrt{1.4\times287\times311} = 353.496 \text{ m/s}$$
$$c_1 = M_1 a_1 = 0.15\times353.496 = 53.02 \text{ m/s}$$
$$\rho_1 A c_1 = \dot{m}$$
$$A = \frac{\dot{m}}{\rho_1 c_1} = \frac{8.25}{3.865\times53.02} = 0.0403 \text{ m}^2$$
$$\frac{\pi}{4}D^2 = 403 \text{ cm}^2$$
$$D = 22.66 \text{ cm} \quad \textbf{Ans.}$$

From isentropic tables for $\gamma = 1.4$ at $M_1 = 0.15$
$$p_1/p_{01} = 0.984$$

$$p_{01} = \frac{p_1}{0.984} = \frac{3.45}{0.984} = 3.506 \text{ bar}$$

TABLE 8.3: From Fanno tables for $\gamma = 1.4$

M	p/p^*	T/T^*	p_0/p_0^*	c/c^*	$4\bar{f}L_{max}/D$
$M_1 = 0.15$	7.319	1.1945	3.928	0.164	28.354
$M_2 = 0.50$	2.138	1.143	1.340	0.534	1.069

(*b*)
$$\frac{4\bar{f}L}{D} = \left(4\bar{f}\frac{L_{max}}{D}\right)_{M_1} - \left(4\bar{f}\frac{L_{max}}{D}\right)_{M_2}$$
$$\frac{4\bar{f}L}{D} = 28.354 - 1.069 = 27.285$$
$$L = 27.285\times0.2266/4\times0.005$$
$$L = 309 \text{ metres} \quad \textbf{Ans.}$$

(*c*)
$$p_2 = \frac{(p/p^*)_2}{(p/p^*)_1}p_1 = \frac{2.138}{7.319}\times3.45$$
$$p_2 = 1.008 \text{ bar} \quad \textbf{Ans.}$$
$$T_2 = \frac{1.143}{1.1945}\times311 = 297.59 \text{ K} \quad \textbf{Ans.}$$

(*d*)
$$p_{02} = \frac{p_{02}/p_{02}^*}{p_{01}/p_{01}^*}p_{01}$$
$$= \frac{1.34}{3.928}\times3.506 = 1.196 \text{ bar}$$
$$p_{01} - p_{02} = 3.506 - 1.196 = 2.31 \text{ bar} \quad \textbf{Ans.}$$

(*e*)
$$c_2 = \frac{(c/c^*)_2}{(c/c^*)_1}c_1 = \frac{0.534}{0.164}\times53.02 = 172.638 \text{ m/s}$$
$$a_2 = \sqrt{\gamma RT_2} = \sqrt{1.4\times287\times297.59} = 345.79 \text{ m/s}$$
$$M_2 = c_2/a_2 = 172.638/345.79$$
$$M_2 = 0.499 \text{ (verified)}$$

Example 8.2. Air at $p_0 = 10$ bar, $T_0 = 400$ K is supplied to a 50 mm diameter pipe. The friction factor for the pipe surface is 0.002.

If the Mach number changes from 3.0 at the entry to 1.0 at the exit determine

(*a*) the length of the pipe and

(*b*) the mass flow rate.

Solution. (*a*) From Fanno flow tables for $\gamma = 1.4$ at

$M_1 = 3, \qquad 4\bar{f}L_{max}/D = 0.522$

$M_2 = 1, \qquad 4\bar{f}L_{max}/D = 0$

Therefore, $\dfrac{4\bar{f}L}{D} = 0.522 - 0 = 0.522$

$$L = \frac{0.522D}{4\bar{f}}$$

$$L = 0.522 \times 0.05/4 \times 0.002$$

$$L = 3.263 \text{ m} \quad \textbf{Ans.}$$

(*b*) From Isentropic tables for $\gamma = 1.4$, at $M_1 = 3.0$

$$T/T_0 = 0.357, \; p/p_0 = 0.0272, \; A/A^* = 4.235$$

$$A = \frac{\pi}{4} D^2 = 0.785 \times 0.05^2 = 0.00196 \text{ m}^2$$

$$A^* = A/4.235 = 0.00196/4.235 = 0.000463 \text{ m}^2$$

The flow rate can be found by the following method:

$$p_1 = 0.0272 \times 10 = 0.272 \text{ bar}$$

$$T_1 = 0.357 \times 400 = 142.8 \text{ K}$$

$$\rho_1 = p_1/RT_1$$

$$\rho_1 = \frac{0.272 \times 10^5}{287 \times 142.8} = 0.664 \text{ kg/m}^3$$

$$a_1 = \sqrt{\gamma RT_1}$$

$$a_1 = \sqrt{1.4 \times 287 \times 142.8} = 239.54 \text{ m/s}$$

$$c_1 = M_1 a_1 = 3 \times 239.54 = 718.6 \text{ m/s}$$

$$\dot{m} = \rho_1 A c_1$$

$$\dot{m} = 0.664 \times 0.00196 \times 718.6$$

$$\dot{m} = 0.935 \text{ kg/s} \quad \textbf{Ans.}$$

Since the flow is choked following formula for the maximum flow can be used for isentropic flow:

$$\dot{m}\sqrt{T_0}/A^* p_0 = 0.0404$$

$$\dot{m} = 0.0404 \times 0.000463 \times 10 \times 10^5/\sqrt{400}$$

$$\dot{m} = 0.935 \text{ kg/s} \quad \textbf{Ans.}$$

Example 8.3. A gas ($\gamma = 1.3$, $R = 0.287$ kJ/kg K) at $p_1 = 1.0$ bar, $T_1 = 400$ K enters a 30 cm diameter duct at a Mach number of 2.0. A normal shock occurs at a Mach number of 1.5 and the exit Mach number is 1.0. If the mean value of the friction factor is 0.003 determine:

(*a*) lengths of the duct upstream and downstream of the shock wave,

(*b*) mass flow rate of the gas and

(*c*) change of entropy upstream of the shock, across the shock and downstream of the shock.

Solution. Refer to Figures 8.11 and 8.12.

From isentropic tables for $\gamma = 1.3$ at $M_1 = 2.0$

$$p_1/p_{01} = 0.131, \; T_1/T_{01} = 0.625$$

$$p_{01} = 1.0/0.131 = 7.633 \text{ bar}$$

$$T_{01} = 400/0.625 = 640 \text{ K}$$

$$A = \frac{\pi}{4} D^2 = 0.785 \; (0.3)^2 = 0.0706 \text{ m}^2$$

From normal shock tables for $\gamma = 1.3$ at

$$M_x = 1.5$$

$$M_y = 0.69 \approx 0.7, \; p_y/p_x = 2.413, \; T_y/T_x = 1.247$$

$$p_{0y}/p_{0x} = 0.926$$

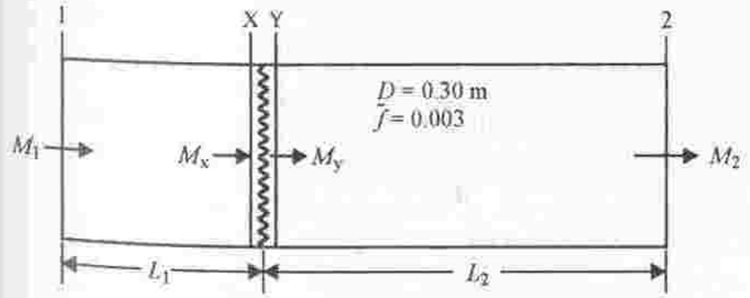

FIGURE 8.11 : Frictional flow in constant area duct with normal shock (Example 8.3)

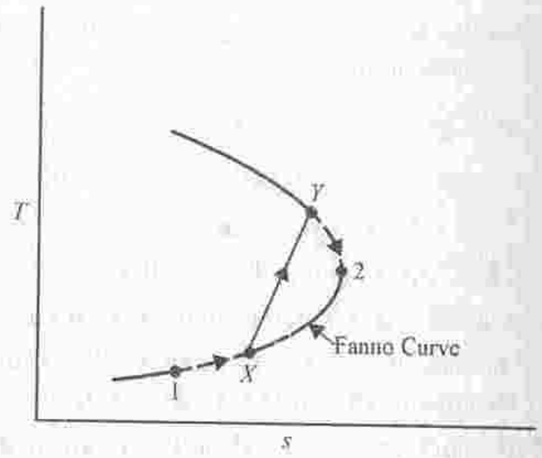

FIGURE 8.12 : *T-s* diagram for Fanno flow with normal shock (Example 8.3)

TABLE 8.4: From Fanno tables for $\gamma = 1.3$

M	p/p^*	T/T^*	p_0/p_0^*	$4\bar{f}L_{max}/D$
2.0	0.424	0.719	1.773	0.357
1.5	0.618	0.860	1.189	0.156
0.7	1.479	1.071	1.097	0.231

(*a*) *Lengths of the duct upstream and downstream of the shock*

$$\frac{4\bar{f}L_1}{D} = \left(\frac{4\bar{f}L_{\max}}{D}\right)_{M_1} - \left(\frac{4\bar{f}L_{\max}}{D}\right)_{M_x} = 0.357 - 0.156$$

$$\frac{4\bar{f}L_1}{D} = 0.201$$

$$L_1 = 0.201 \times 0.3/4 \times 0.003$$

$$L_1 = 5.025 \text{ m} \quad \textbf{Ans.}$$

$$\frac{4\bar{f}L_2}{D} = 0.231 - 0 = 0.231$$

$$L_2 = 0.231 \times 0.3/4 \times 0.003$$

$$L_2 = 5.775 \text{ m} \quad \textbf{Ans.}$$

(*b*) *Mass flow rate*

$$T_x = \frac{(T/T^*)_x}{(T/T^*)_1} T_1$$

$$T_x = \frac{0.86}{0.719} \times 400 = 478.45 \text{ K}$$

$$T_y = 1.247 \times 478.45 = 596.63 \text{ K}$$

$$T_2 = \frac{(T/T^*)_2}{(T/T^*)_y} T_y$$

$$T_2 = \frac{1}{1.071} \times 596.63 = 557 \text{ K}$$

Similarly pressure p_2 is calculated

$$p_x = \frac{0.618}{0.424} \times 1 = 1.457 \text{ bar}$$

$$p_y = 2.413 \times 1.457 = 3.517 \text{ bar}$$

$$p_2 = \frac{1}{1.479} \times 3.517 = 2.378 \text{ bar}$$

$$\rho_2 = \frac{p_2}{RT_2} = \frac{2.378 \times 10^5}{287 \times 557} = 1.488 \text{ kg/m}^3$$

$$a_2 = \sqrt{\gamma RT_2} = \sqrt{1.3 \times 287 \times 557} = 455.87 \text{ m/s}$$

$$c_2 = M_2 a_2 = 1 \times 455.87 = 455.87 \text{ m/s}$$

$$\dot{m} = \rho_2 A c_2$$

$$\dot{m} = 1.488 \times 0.0706 \times 455.87$$

$$\dot{m} = 47.89 \text{ kg/s} \quad \textbf{Ans.}$$

(*c*) *Change of entropy*

$$\frac{p_{01}}{p_{0x}} = \frac{(p_0/p_0^*)_1}{(p_0/p_0^*)_x} = \frac{1.773}{1.189} = 1.491$$

$$\frac{(\Delta s)_{1-x}}{R} = \ln \frac{p_{01}}{p_{0x}} = \ln 1.491 = 0.399 \quad \textbf{Ans.}$$

$$\frac{(\Delta s)_{x-y}}{R} = \ln \frac{p_{0x}}{p_{0y}} = \ln \frac{1}{0.926} = 0.077 \quad \textbf{Ans.}$$

$$\frac{p_{02}}{p_{0y}} = \frac{(p_0/p_0^*)_2}{(p_0/p_0^*)_y} = \frac{1}{1.097}$$

$$\frac{(\Delta s)_{y-2}}{R} = \ln \frac{p_{0y}}{p_{02}} = \ln 1.097 = 0.0925 \quad \textbf{Ans.}$$

Example 8.4. Air enters a long circular duct ($d = 12.5$ cm, $\bar{f} = 0.0045$) at a Mach number 0.5, pressure 3.0 bar and temperature 312 K. If the flow is isothermal throughout the duct determine (*a*) the length of the duct required to change the Mach number to 0.7, (*b*) pressure and temperature of air at $M = 0.7$, (*c*) the length of the duct required to attain limiting Mach number, and (*d*) state of air at the limiting Mach number.

Compare these values with those obtained in adiabatic flow.

Solution. (*a*) $$\left(\frac{4\bar{f}L_{max}}{D}\right)_{M_1=0.5} = \frac{1-\gamma M_1^2}{\gamma M_1^2} + \ln \gamma M_1^2$$

$$= \frac{1-1.4\times0.25}{1.4\times0.25} + \ln 1.4\times0.25 = 0.807$$

$$\left(\frac{4\bar{f}L_{max}}{D}\right)_{M_2} = \frac{1-1.4\times0.49}{1.4\times0.49} + \ln 1.4\times0.49 = 0.0808$$

$$\frac{4\bar{f}L}{D} = 0.807 - 0.0808 = 0.7262$$

$$L = 0.7262\times0.125/4\times0.0045$$

$$L = 5.043 \text{ m} \quad \textbf{Ans.}$$

(*b*) $$\frac{p_2}{p_1} = \frac{M_1}{M_2} = \frac{0.5}{0.7}$$

$$p_2 = \frac{5}{7}\times3.0 = 2.143 \text{ bar} \quad \textbf{Ans.}$$

$$T_2 = T_1 = 312 \text{ K}$$

(*c*) $$\left(\frac{4\bar{f}L_{max}}{D}\right)_{M_1} = 0.807$$

The duct length required to change to Mach number M^{*t} to $M^t = \sqrt{\frac{1}{\gamma}}$ is

$$L_{max} = 0.807D/4\bar{f}$$

$$L_{max} = 0.807\times0.125/4\times0.0045$$

$$L_{max} = 5.604 \text{ m} \quad \textbf{Ans.}$$

(*d*) $$p^{*t} = \sqrt{\gamma}Mp$$

$$p^{*t} = \sqrt{1.4}\times0.5\times3 = 1.775 \text{ bar} \quad \textbf{Ans.}$$

$$T^{*t} = T_1 = 312 \text{ K} \quad \textbf{Ans.}$$

$$M^{*t} = \frac{1}{\sqrt{\gamma}} = \frac{1}{\sqrt{1.4}} = 0.845 \quad \textbf{Ans.}$$

The values for adiabatic flow can easily be calculated using Fanno flow gas tables for $\gamma = 1.4$. These are compared with the isothermal values in Table 8.5.

TABLE 8.5: Comparison of isothermal and adiabatic flows

Process	L Metre	p_2 bar	T_2 K	L_{max} metre	p^1 bar	T^1 K
Isothermal	5.04 $M = 0.5$	2.143 $M = 0.7$	312	5.604 $M^{*1} = 8.45$	1.775	312
Adiabatic	5.98 $M = 0.5$	2.095 $M = 0.7$	298.35	7.424	1.403 $M^* = 1$	272.96

Example 8.5. A convergent-divergent nozzle is provided with a pipe of constant cross-section at its exit; the exit diameter of the nozzle and that of the pipe is 40 cm. The mean coefficient of friction for the pipe is 0.0025. Stagnation pressure and temperature of air at the nozzle entry are 12 bar and 600 K. The flow is isentropic in the nozzle and adiabatic in the pipe. The Mach numbers at the entry and exit of the pipe are 1.8 and 1.0 respectively. Determine:

(*a*) the length of the pipe,

(*b*) diameter of the nozzle throat, and

(*c*) pressure and temperature at the pipe exit.

Depict graphically the static and stagnation pressure variation from the nozzle entry to the pipe exit.

Solution. Refer to Figure 8.13

From isentropic flow gas tables ($\gamma = 1.4$) at $M_1 = 1.8$

$$\frac{p_1}{p_{01}} = 0.174, \quad \frac{T_1}{T_{01}} = 0.607, \quad \frac{A_1}{A_1^*} = 1.439$$

$$p_{01} = 12 \text{ bar}, \quad T_{01} = 600 \text{ K}, \quad A_1 = \frac{\pi}{4}D_1^2 = \frac{\pi}{4}\times0.16 = 0.1257 \text{ m}^2$$

$$p_1 = 0.174\times12 = 2.088 \text{ bar}$$

$$T_1 = 0.607 \times 600 = 364.2 \text{ K}$$

$$A_1^* = \frac{0.1257}{1.439} = 0.8735 \text{ m}^2$$

Therefore, nozzle throat diameter is given by

$$\frac{\pi}{4} D^{*2} = 873.5 \text{ cm}^2$$

$$D^* = 33.35 \text{ cm} \quad \textbf{Ans.}$$

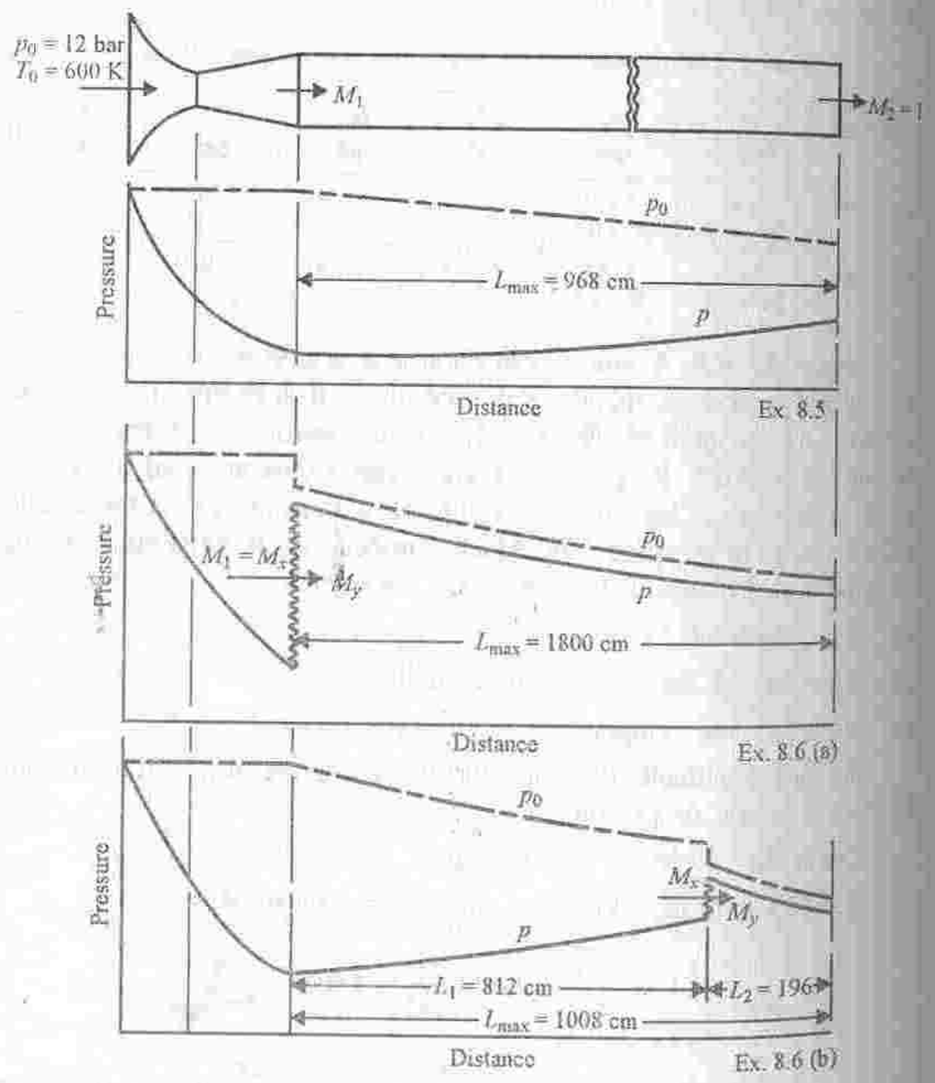

FIGURE 8.13 : Variation of static and stagnation pressures in a convergent-divergent nozzle with a duct (Examples 8.5, 8.6 (*a*) and 8.6 (*b*))

From Fanno table ($\gamma = 1.4$) at $M_1 = 1.8$

$$\frac{p_1}{p^*} = 0.474, \quad \frac{T_1}{T^*} = 0.728, \quad 4\bar{f}\frac{L_{max}}{D} = 0.242$$

$$4\bar{f}\frac{L_{max}}{D} = 4 \times \frac{0.0025}{40} L_{max} = 0.242$$

(*a*) $L_{max} = 968$ cm **Ans.**

Since the flow is sonic at the pipe exit this is the length of the pipe; the pressure and temperature are p^* and T^* respectively.

$$p^* = \frac{p_1}{0.474} = \frac{2.088}{0.474} = 4.405 \text{ bar} \quad \textbf{Ans.}$$

$$T^* = \frac{T_1}{0.728} = \frac{364.2}{0.728} = 500.275 \text{ K} \quad \textbf{Ans.}$$

Example 8.6. Determine the length of the pipe of Example 8.5, pressure and temperature at the pipe-exit and location of the shock with

(*a*) a normal, shock at the nozzle exit,

(*b*) a normal shock at $M_x = 1.22$ in the pipe.

Solution. Refer to Figure 8.13.

(*a*) Normal shock at nozzle exit

From normal shock tables ($\gamma = 1.4$) at $M_x = 1.8$

$$M_y = 0.616, \quad \frac{p_y}{p_x} = 3.613, \quad \frac{T_y}{T_x} = 1.532$$

$$p_y = 3.613 p_x = 3.613 p_1 = 3.613 \times 2.089 = 7.544 \text{ bar}$$

$$T_y = 1.532 T_x = 1.532 T_1 = 1.532 \times 364.2 = 557.954 \text{ K}$$

From Fanno tables ($\gamma = 1.4$) at $M_y = 0.616$

$$\frac{p}{p^*} = \frac{p_y}{p^*} = 1.725, \quad \frac{T_y}{T^*} = 1.116, \quad 4\bar{f}\frac{L_{max}}{D} = 0.450$$

$$L_{max} = \frac{0.450 \times 40}{4 \times 0.0025} = 1800 \text{ cm} \quad \textbf{Ans.}$$

The pressure and temperature at pipe exit are:

$$p^* = \frac{p_y}{1.725} = \frac{7.544}{1.725} = 4.375 \text{ bar} \quad \textbf{Ans.}$$

$$T^* = \frac{T_y}{1.116} = \frac{557.954}{1.116} = 499.950 \text{ K} \quad \textbf{Ans.}$$

It should be noted that except for small calculation errors these values are same as in Example 8.5; this is because of the same Fanno line.

(*b*) Normal shock at $M_x = 1.22$.

Let this shock be at distance L_1 and L_2 from the entry and exit of the pipe. From Fanno tables ($\gamma = 1.4$) at $M_x = 1.22$

$$\frac{p_x}{p^*} = 0.788, \quad \frac{T_x}{T^*} = 0.925, \quad 4\bar{f}\frac{L_{\max}}{D} = 0.039$$

$$\frac{p_x}{p_1} = \frac{p_x/p^*}{p_1/p^*} = \frac{0.788}{0.474} = 1.6625$$

$$p_x = 1.6625 \times 2.088 = 3.471 \text{ bar}$$

$$\frac{T_x}{T_1} = \frac{T_x/T^*}{T_1/T^*} = \frac{0.925}{0.728} = 1.2706$$

$$T_x = 1.2706 \times 364.2 = 462.752$$

From normal shock tables ($\gamma = 1.4$) at $M_x = 1.22$

$$M_y = 0.83, \quad \frac{p_y}{p_x} = 1.57, \quad \frac{T_y}{T_x} = 1.141$$

$$p_y = 1.57 p_x = 1.57 \times 3.471 = 5.449 \text{ bar}$$

$$T_y = 1.141 T_x = 1.141 \times 462.752 = 528 \text{ K}$$

Between nozzle exit and upstream section X of the normal shock

$$4\bar{f}\frac{L_1}{D} = \left(4\bar{f}\frac{L_{\max}}{D}\right)_{M_1} - \left(4\bar{f}\frac{L_{\max}}{D}\right)_{M_x}$$

$$4 \times 0.0025 \frac{L_1}{40} = 0.242 - 0.039 = 0.203$$

$$L_1 = 812 \text{ cm} \quad \textbf{Ans.}$$

From Fanno tables ($\gamma = 1.4$) at $M_y = 0.83$,

$$\frac{p_y}{p^*} = 1.2375, \quad \frac{T_y}{T^*} = 1.055, \quad 4\bar{f}\frac{L_{\max}}{D} = 0.049$$

Here $L_{\max} = L_2$ because the final state is sonic. Therefore,

$$L_2 = \frac{0.049 \times 40}{4 \times 0.0025} = 196 \text{ cm}$$

The total pipe length $L = L_1 + L_2$

$$L = 812 + 196 = 1008 \text{ cm} \quad \textbf{Ans.}$$

The final state of air at the pipe exit is given by

$$p^* = \frac{p_y}{1.2375} = \frac{5.449}{1.2375} = 4.403 \text{ bar} \quad \textbf{Ans.}$$

$$T^* = \frac{T_y}{1.055} = \frac{528}{1.055} = 500.473 \text{ K} \quad \textbf{Ans.}$$

Example 8.7. A convergent-divergent nozzle supplies air to a constant diameter duct. The nozzle diameters at the throat and exit are 10 cm and 20 cm respectively. Duct diameter is also 20 cm. The stagnation pressure at the nozzle entry is 10 bar and that at station – 1, $2.4D$ downstream of the nozzle-exit section-E is 0.4 bar. The flow at the duct exit section-2 is sonic. For a friction factor of 0.003 determine:

(*a*) Mach numbers at stations E and 1

(*b*) static pressures at stations E and 2, and

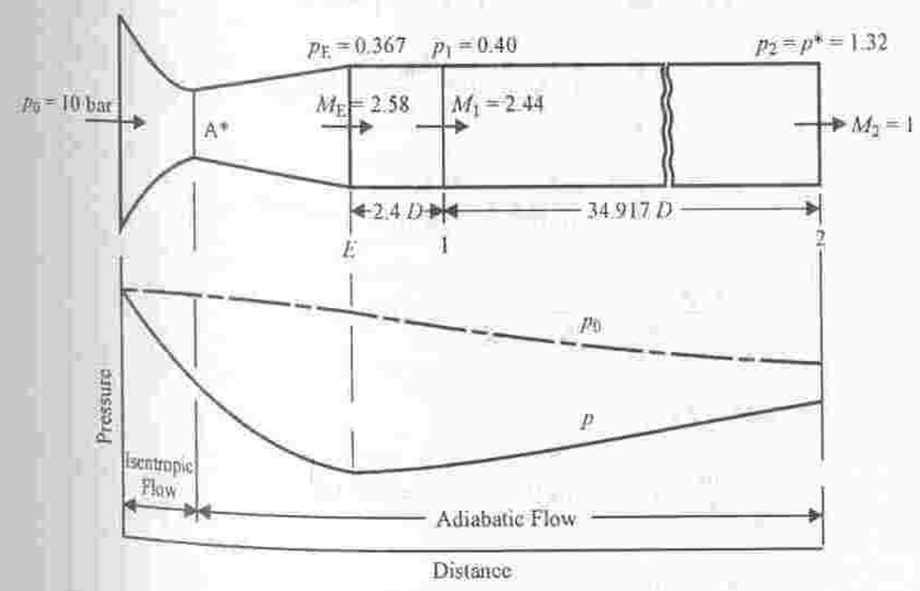

FIGURE 8.14 : Variation of static and stagnation pressures for adiabatic flow in the nozzle (divergent portion) and a duct (Example 8.7)

(*c*) total duct length from the nozzle exit.

Assume isentropic flow upto nozzle throat and adiabatic further downstream upto the duct exit.

Solution. Refer to Figure 8.14.

Area ratio $$\frac{A_1}{A^*} = \left(\frac{D_1}{D^*}\right)^2 = \left(\frac{20}{10}\right)^2 = 4$$

Pressure ratio $$\frac{p_1}{p_{01}} = \frac{0.40}{10} = 0.04$$

Therefore, for station 1

$$\frac{A_1 p_1}{A^* p_{01}} = 4 \times 0.04 = 0.16$$

Mach number for adiabatic flow corresponding to

$$\frac{A_1 p_1}{A^* p_{01}} = 0.16 \text{ is}$$

$$M_1 = 2.44 \quad \textbf{Ans.}$$

From Fanno tables ($\gamma = 1.4$) at $M_1 = 2.44$,

$$\frac{p_1}{p^*} = 0.303, \; 4\bar{f}\frac{L_{\max}}{D} = 0.419$$

$$p^* = \frac{p_1}{0.303} = \frac{0.40}{0.303} = 1.32 \text{ bar}$$

$$\left(\frac{L_{\max}}{D}\right)_{M_1} = \frac{0.419}{4 \times 0.003} = 34.917$$

At station E,

$$\left(\frac{L_{\max}}{D}\right)_{M_E} = 34.917 + 2.4 = 37.317$$

$$\left(4\bar{f}\frac{L_{\max}}{D}\right)_{M_E} = 4 \times 0.003 \times 37.317 = 0.4478$$

From Fanno tables ($\gamma = 1.4$) at $4\bar{f}\frac{L_{\max}}{D} = 0.448$ the Mach number is

$$M_E = 2.58 \quad \textbf{Ans.}$$

The pressure ratio $\frac{p_E}{p^*} = 0.278$

$$p_E = 0.278 p^* = 0.278 \times 1.32 = 0.367 \text{ bar} \quad \textbf{Ans.}$$

For isentropic flow the Mach number obtained at the nozzle exit for the pressure ratio $p_E/p_0 = 0.367/10 = 0.0367$ is $= 2.80$.

QUESTIONS AND PROBLEMS

8.1 Give three examples of Fanno flow in thermal systems; give reasons justifying Fanno flow in each of these cases.

8.2 Derive an equation describing a Fanno curve. Show three Fanno curves on the temperature-entropy coordinates at three mass flow densities.

8.3 Show that the upper and lower branches of a Fanno curve represent subsonic and supersonic flows respectively. Prove that at the maximum entropy point Mach number is unity and all processes approach this point.

How would the state of a gas in a flow change from the supersonic to subsonic branch?

8.4 Derive the following equations for Fanno flow:

(*a*) $$\frac{c}{c^*} = \frac{\rho^*}{\rho} = \left[\frac{(\gamma+1)M^2}{2+(\gamma-1)M^2}\right]^{1/2}$$

(*b*) $$\frac{p}{p^*} = \frac{1}{M}\left(\frac{T}{T^*}\right)^{1/2} = \frac{1}{M}\left[\frac{(\gamma+1)}{2+(\gamma-1)M^2}\right]^{1/2}$$

(*c*) $$\frac{p_0}{p_0^*} = \left(\frac{1}{M}\right)^{2\gamma/(\gamma-1)}\left(\frac{p^*}{p}\right)^{(\gamma+1)/(\gamma-1)}$$

$$= \frac{1}{M}\left[\frac{2+(\gamma-1)M^2}{\gamma+1}\right]^{(\gamma+1)/2(\gamma-1)}$$

(*d*) $$\frac{F}{F^*} = \frac{1+\gamma M^2}{M\left[(\gamma+1)\left\{2+(\gamma-1)M^2\right\}\right]^{1/2}}$$

(*e*) $$s^* - s = R \ln \frac{1}{M}\left[\frac{2+(\gamma-1)M^2}{\gamma+1}\right]^{(\gamma+1)/2(\gamma-1)}$$

(*f*) $$\left(\frac{4\bar{f}L_{max}}{D}\right)_M = \frac{1-M^2}{\gamma M^2} + \frac{\gamma+1}{2\gamma}\ln\frac{(\gamma+1)M^2}{2+(\gamma-1)M^2}$$

8.5 The friction factor for a 25 mm diameter 11.5 m long pipe is 0.004. The conditions of air at entry are

$$p_1 = 2.0 \text{ bar},\ T_1 = 301 \text{ K},\ M_1 = 0.25$$

Determine the mass flow rate, and the pressure, temperature and the Mach number at exit.

($\dot{m} = 0.098$ kg/s, $p_2 = 1.002$ bar, $T_2 = 290.8$ K, $M_2 = 0.49$).

8.6 Repeat Example 8.4 for a gas having $\gamma = 1.3$ and $R = 0.469$ kJ/kg K. The values calculated are given in Table 8.6.

TABLE 8.6: Comparison of isothermal and adiabatic flows

Process	L Metre	p_2 bar	T_2 K	L_{max} metre	p^1 bar	T^1 K
Isothermal	5.79 $M = 0.5$	2.143 $M = 0.7$	312	6.618 $M^{*t} = 0.877$	1.71	312
Adiabatic	6.535 $M = 0.5$	2.107 $M = 0.7$	301.58	8.139 $M^* = 1$	1.425	281.58

8.7 A long pipe of 25.4 mm diameter has a mean coefficient of friction of 0.003. Air enters the pipe at a Mach number of 2.5, stagnation temperature 310 K and static pressure 0.507 bar. Determine for a section at which the Mach number reaches 1.2,

(*a*) static pressure and temperature,

(*b*) stagnation pressure and temperature,

(*c*) velocity of air,

(*d*) distance of this section from the inlet, and

(*e*) mass flow rate of air.

[(*a*) 1.396 bar, 240.676 K, (*b*) 3.386 bar, 310 K, (*c*) 373.16 m/s, (*d*) 84.2 cm, (*e*) 0.382 kg/s].

8.8 A circular duct of 13.4 cm diameter is fed with air by a supersonic nozzle. The stagnation pressure at the nozzle entry and static pressures at sections 5 D and 33 D downstream are 7.00, 0.245 and 0.50 bar respectively. The nozzle throat diameter is 6.46 cm. Determine (*a*) Mach numbers at the two sections downstream of the nozzle (*b*) the mean value of the skin friction between the two sections. Assume isentropic flow upto the nozzle throat and adiabatic in the rest.

($M_{5D} = 2.52$, $M_{33D} = 1.54$, $f = 0.00255$).

8.9 Air at a pressure of 685 mbar and temperature 310 K enters a 60 cm diameter duct at a Mach number of 3.0. The flow passes through a normal shock wave at a section L_1 metres downstream of the entry where the Mach number is 2.5. The Mach number at the exit (at a distance L_2 metres downstream of the shock) is 0.8. The mean coefficient of skin friction is 0.005. Determine:

(*a*) the length L_1 and L_2,

(*b*) state of air at exit, and

(*c*) mass flow rate through the duct.

($L_1 = 2.7$ m, $L_2 = 27.5$ m, $p_2 = 4.05$ bar, $T_2 = 770$ K, $\dot{m} = 230.5$ kg/s).

8.10 Derive the following relations for isothermal frictional flow in constant area ducts at $M = M^{*t} = 1/\sqrt{\gamma}$:

(*a*) $p^{*t} = \sqrt{\gamma} M p$

(*b*) $c^{*t} = c/\sqrt{\gamma} M$

(*c*) $\rho^{*t} = \sqrt{\gamma} M \rho$

(*d*) $$(p/p_0)^{*t} = \left(\frac{2\gamma}{3\gamma-1}\right)^{\gamma/(\gamma-1)}$$

(*e*) $F^{*t} = 2Ap^{*t}$

(*f*) $$s - s^{*t} = c_p\left(\frac{\gamma-1}{\gamma}\right)\ln(\sqrt{\gamma}M)$$

8.11 Using the formulas for isothermal frictional flow in constant area ducts obtain the following limiting values at $M = 1$:

(*a*) $$\frac{p^*}{p^{*t}} = \frac{\rho^*}{\rho^{*t}} = \frac{c^{*t}}{c^*} = \frac{1}{\sqrt{\gamma}}$$

(*b*) $$\frac{p_0^*}{p_0^{*t}} = \frac{1}{\sqrt{\gamma}}\left[\frac{\gamma(\gamma+1)}{3\gamma-1}\right]^{\gamma/(\gamma-1)}$$

(*c*) $$\frac{T_0^*}{T_0^{*t}} = \frac{\gamma(\gamma+1)}{3\gamma-1}$$

(*d*) $$\left(\frac{4\bar{f}L_{max}}{D}\right)^* = \frac{1-\gamma}{\gamma} + \ln\gamma$$

(*e*) $$\frac{F^*}{F^{*t}} = \frac{1+\gamma}{2\sqrt{\gamma}}$$

(*f*) $$\frac{s^* - s^{*t}}{R} = \frac{1}{2}\ln\gamma$$

(*g*) At $M = M^1 = \sqrt{\dfrac{2}{\gamma+1}}$

$$\frac{p_0^1}{p_0^{*t}} = \sqrt{\frac{\gamma+1}{2\gamma}}\left[\frac{4\gamma^2}{(3\gamma-1)(\gamma+1)}\right]^{\gamma/(\gamma-1)}$$

8.12 (*a*) Depict graphically the variation of L_{max}/D with Mach number varying between a very small subsonic value to a very large supersonic value.

(*b*) For a mean friction factor of 0.0025 in a duct with initially supersonic flow prove that the maximum duct length (for $\gamma = 1.4$) is 82.15 diameters.

9

Flow in Constant Area Ducts with Heat Transfer

A frictionless flow process in a constant area duct with heat transfer is referred to as Rayleigh flow. Flows in many thermal systems can be closely approximated to this process. For example, under some conditions heat transfer processes in heat exchangers and combustion chambers can be considered by ignoring frictional effects; here the changes in flow parameters on account of wall friction are negligible compared to those due to heat transfer. Therefore, such processes can be represented by Rayleigh process without sacrificing much accuracy. Besides this the analysis of many complicated problems is considerably simplified by using the Rayleigh flow model.

9.1 THE RAYLEIGH LINE

The frictionless flow process with heat transfer in a constant area duct is described by a curve known as Rayleigh line (Figure 9.1); this defines the locus of all state points during the Rayleigh process and satisfies the equations of state, continuity and momentum. Following assumptions are used in the analysis of Rayleigh process:

(*a*) perfect gas,
(*b*) constant area duct,
(*c*) one-dimensional, steady frictionless flow, and
(*d*) absence of body forces.

Section 6.3.2 briefly dealt with the Rayleigh line. It was shown by Equation (6.17) that the velocity at the maximum entropy point was sonic.

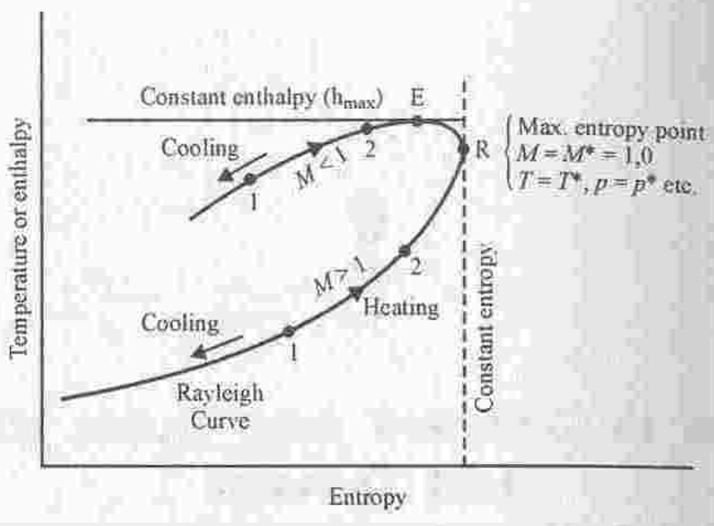

FIGURE 9.1 : A Rayleigh line or curve

The mass flow density is given by (8.1),

$$G = \frac{\dot{m}}{A} = \rho c$$

$$c = \frac{G}{\rho}$$

The momentum equation for frictionless flow gives

$$p + \rho c^2 = \text{constant}$$

$$p + \frac{G^2}{\rho} = \text{constant} \tag{9.1}$$

$$p + G^2 v = \text{constant} \tag{9.2}$$

Equation (9.2) represents a straight line on the p-v plane as shown in Figures 9.3 and 9.4. The gradient of this line is $-G^2$. p and ρ in Equation (9.1) can be expressed by the following equations of state:

$$p = p\,(h,\ s) \tag{9.3}$$

$$\rho = \rho\,(h,\ s) \tag{9.4}$$

Substituting Equations (9.3) and (9.4) in (9.1) gives

$$p\,(h,\ s) + \frac{G^2}{\rho\,(h,\ s)} = \text{constant} \tag{9.5}$$

Equation (9.5) represents the Rayleigh line on the h-s plane shown in Figures 9.1 and 9.2. The heat transfer causing heating or cooling of the gas changes its stagnation temperature. In a heating process the entropy must increase; therefore, the state of the gas moves towards the right on the Rayleigh line approaching the maximum entropy point R. Heating processes beyond this point are impossible because they lead to decrease in entropy. Therefore, the limit of the heating processes on both the subsonic and supersonic branches of the Rayleigh line is the maximum entropy point R.

The direction of cooling processes is away from the limiting point R leading to decrease in entropy, which conforms with the second law of thermodynamics.

Figure 9.2 shows the Rayleigh line along with the constant pressure, and stagnation temperature lines. Constant entropy and constant enthalpy, lines at point R and E respectively are also shown. The stagnation temperature lines for the subsonic and supersonic branches meet at $M = M^* = 1$. Since no further heating beyond this state ($M = 1$) is possible the stagnation temperature at this point has the maximum value;

$$T_0 = T_0^* = T_{0\,\max}$$

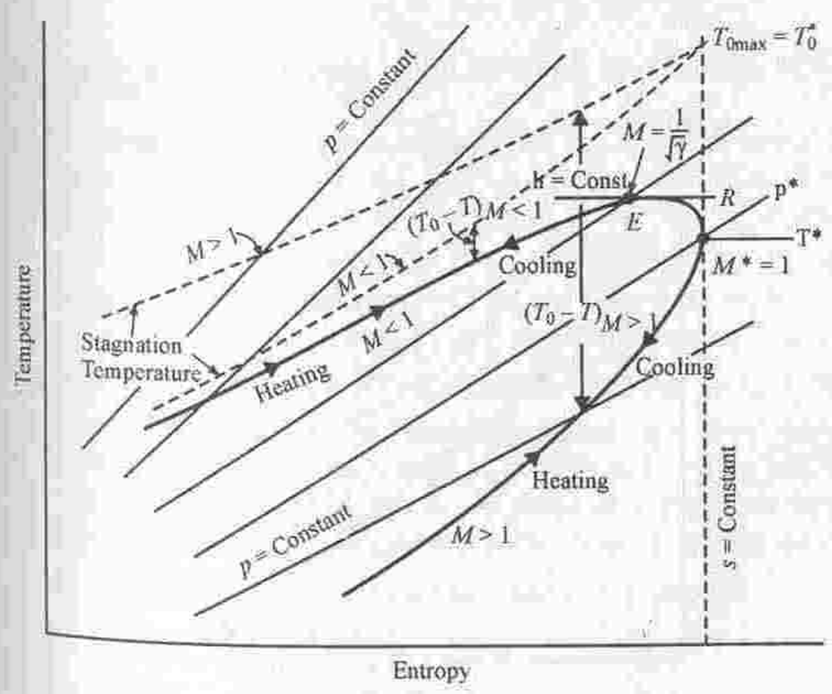

FIGURE 9.2 : Various flow parameters on Rayleigh line

The temperature differences $(T_0 - T)$ for higher $(M > 1)$ and lower $(M < 1)$ gas velocities are also shown. This depicts graphically the fact that the lower branch of the Rayleigh line represents supersonic flow and the upper branch the subsonic flow.

Subsonic flow is accelerated by heat addition (dT_0 = positive); the maximum obtainable velocity is sonic at point R (Figures 9.1 and 9.2). The static enthalpy or temperature also rise upto the maximum enthalpy point E beyond which further heat addition leads to decrease in the enthalpy. This is due to the fact that beyond point E the decrease in enthalpy due to pressure drop is greater than the increase by heat addition.

The value of the Mach number at this point is derived in Section 9.1.3.

9.1.1 Slope of the Rayleigh Line

Equations (9.2) for two state points along the Rayleigh line gives

$$p_1 + G^2 v_1 = p_2 + G^2 v_2$$

$$\frac{p_1 - p_2}{v_1 - v_2} = -G^2 = -\left(\frac{\dot{m}}{A}\right)^2 \tag{9.6}$$

For generalizing Equation (9.6), using differential quantities

$$\left(\frac{dp}{dv}\right)_R = -G^2 = \tan\theta = -(\rho c)^2 = -\rho^2 a^2 M^2 \tag{9.7}$$

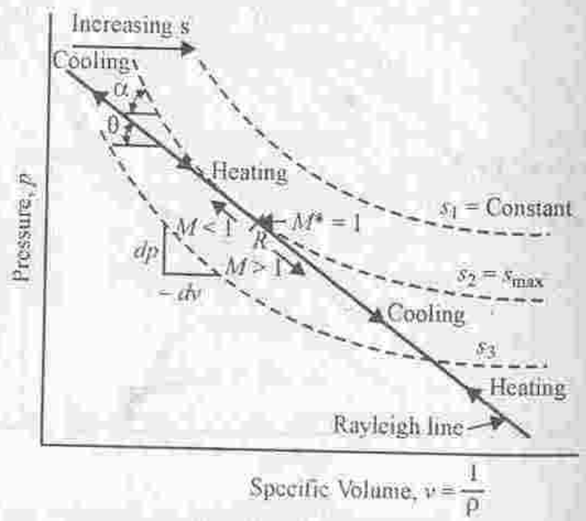

FIGURE 9.3 : Constant entropy lines and a Rayleigh line on p-v plane

The slope (θ) of the Rayleigh line is shown in Figures 9.3 and 9.4.

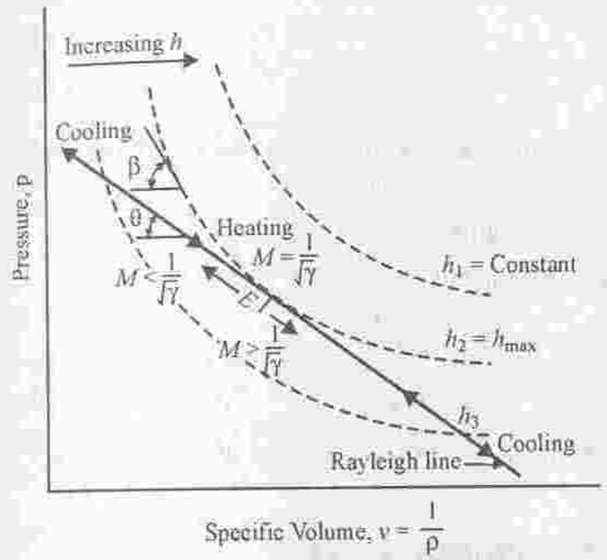

FIGURE 9.4 : Constant enthalpy lines and a Rayleigh line on p-v plane

9.1.2 Constant Entropy Lines

Constant entropy lines in the h-s or T-s plane are straight vertical lines as shown in Figures 9.1 and 9.2. Such a line passing through point R is tangential to the Rayleigh line as shown in the figures; therefore, this is the maximum entropy line (s_{max} = constant) for the given Rayleigh line. Three constant entropy lines are shown on the p-v plane in Figure 9.3. One of them $s_2 = s_{max}$ is the maximum entropy line which is tangential to the Rayleigh line at the limiting state point R where the flow is sonic $(M = M^* = 1)$. The subsonic and supersonic branches of the Rayleigh line and the directions of heating and cooling processes are also shown here. As stated before, the states of a gas move towards this limiting point during heating and away from it during cooling.

The slope of the constant entropy lines is given by

$$\tan\alpha = \frac{dp}{dv} = \frac{dp}{d\left(\frac{1}{\rho}\right)} = -\rho^2 \frac{dp}{d\rho}$$

But at constant entropy

$$\frac{dp}{d\rho} = \left(\frac{\partial p}{\partial \rho}\right)_s = a^2$$

Therefore, $$\tan \alpha = \frac{dp}{dv} = -\rho^2 a^2 \tag{9.8}$$

At the limiting state point R the slopes of the Rayleigh and the constant entropy line are same:

$$\tan \theta = \tan \alpha$$

Therefore, Equations (9.7) and (9.8) give

$$\rho^2 a^2 M^2 = \rho^2 a^2$$

$$M = M^* = 1 \tag{9.9}$$

This shows that the velocity of gas at the maximum entropy point is sonic.

9.1.3 Constant Enthalpy Lines

Figure 9.4 shows three constant enthalpy lines on the p-v plane. These lines on the h-s plane are straight horizontal lines as shown in Figures 9.1 and 9.2; one of the h = constant lines is tangential to the given Rayleigh line at E. This is the maximum enthalpy or h_{max} = constant line. It will be shown here that the Mach number at point E (which is not the limiting state point) is $1/\sqrt{\gamma}$. The directions of heating and cooling processes are still the same as stated before in Section 9.1.2.

For a perfect gas at constant enthalpy (or T = constant)

$$pv = RT = \text{constant}$$

Therefore, the slope of the constant enthalpy line is

$$\tan \beta = \left(\frac{dp}{dv}\right)_h = -\frac{p}{v} = -p\rho$$

The velocity of sound is given by

$$a^2 = \frac{\gamma p}{\rho}$$

$$p = \frac{\rho}{\gamma} a^2$$

Therefore, $$\tan \beta = \left(\frac{dp}{dv}\right)_h = -\rho^2 \frac{a^2}{\gamma} \tag{9.10}$$

At the maximum enthalpy point E the slopes of the Rayleigh line and the constant enthalpy line are same.

$$\tan \theta = \tan \beta$$

Therefore, comparing Equations (9.7) and (9.10)

$$\rho^2 a^2 M^2 = \rho^2 \frac{a^2}{\gamma}$$

$$M = M^{*t} = \frac{1}{\sqrt{\gamma}} \tag{9.11}$$

As stated earlier this value of the Mach number puts a limit on the increase in the static enthalpy or temperature. In a subsonic heating process the temperature of a gas increases upto this point and decreases beyond this point till the limiting value of the Mach number is attained.

9.2 FUNDAMENTAL EQUATIONS

Figure 9.5 shows Rayleigh flow through a control volume. The flow parameters in a finite process at entry and exit of the control volume

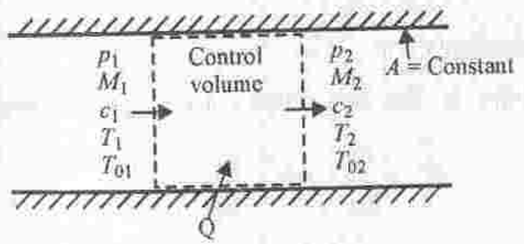

FIGURE 9.5 : Rayleigh flow through a control volume

are also shown. The changes in the flow parameters occur due to the heat transfer Q. The initial and final state points during the process are shown on the Rayleigh line in Figure 9.1. For generality they have been shown for both subsonic and supersonic heating processes. During cooling the processes will occur from state 2 to 1.

Following fundamental equations will be used to determine the variation of flow parameters in Rayleigh flows:

9.2.1 Continuity

$$\dot{m} = \rho_1 A c_1 = \rho_2 A c_2$$

$$\frac{c_1}{c_2} = \frac{\rho_2}{\rho_1} \tag{9.12}$$

9.2.2 Momentum

Equation (9.1) for the control surface can be written as

$$(p_1 - p_2)\,A = \dot{m}\,(c_2 - c_1)$$

$$(p_1 - p_2)\,A = \rho_2 A c_2^2 - \rho_1 A c_1^2$$

$$p_1 - p_2 = \rho_2 c_2^2 - \rho_1 c_1^2 \tag{9.13}$$

Now $\rho_2 c_2^2 = \gamma M_2^2 p_2$ and $\rho_1 c_1^2 = \gamma M_1^2 p_1$

Therefore, $p_1 - p_2 = \gamma M_2^2 p_2 - \gamma M_1^2 p_1$

$$(1 + \gamma M_1^2)\,p_1 = (1 + \gamma M_2^2)\,p_2 \tag{9.14}$$

9.2.3 State

$$p_1 = \rho_1 RT_1,\ p_2 = \rho_2 RT_2$$

$$\frac{p_2}{p_1} = \frac{\rho_2}{\rho_1}\,\frac{T_2}{T_1} \tag{9.15}$$

9.2.4 Mach Number

The Mach numbers at the two states are

$$M_1 = \frac{c_1}{a_1},\ M_2 = \frac{c_2}{a_2}$$

Now $a_1 = \sqrt{\gamma RT_1},\ a_2 = \sqrt{\gamma RT_2}$

Therefore, $$\frac{M_2}{M_1} = \frac{c_2}{c_1}\left(\frac{T_1}{T_2}\right)^{1/2} \tag{9.16}$$

9.2.5 Energy

The heat transfer during the process is given by

$$Q = c_p\,(T_{02} - T_{01})$$

Like other parameters it is convenient to express the heat transfer also in the non-dimensional form.

$$\frac{Q}{c_p T_1} = \frac{T_{01}}{T_1}\left(\frac{T_{02}}{T_{01}} - 1\right) \tag{9.17}$$

9.3 RAYLEIGH FLOW RELATIONS

In this section various flow parameters are expressed in explicit form in terms of the specific heat ratio and the initial and final Mach numbers. All parameters are expressed in the non-dimensional form.

9.3.1 Pressure

Equation (9.14) gives

$$\frac{p_2}{p_1} = \frac{1 + \gamma M_1^2}{1 + \gamma M_2^2} \tag{9.18}$$

9.3.2 Impluse Function

The impulse function is given by

$$F = (1 + \gamma M^2)\,p$$

Therefore, $$\frac{F_2}{F_1} = \frac{1 + \gamma M_2^2}{1 + \gamma M_1^2}\,\frac{p_2}{p_1}$$

Substituting from Equation (9.18),

$$\frac{F_2}{F_1} = 1 \tag{9.19}$$

9.3.3 Stagnation Pressure

By definition stagnation pressure is

$$p_0 = p\left(1 + \frac{\gamma - 1}{2} M^2\right)^{\gamma/(\gamma-1)}$$

$$\frac{p_{02}}{p_{01}} = \frac{p_2}{p_1}\left(\frac{1 + \frac{\gamma - 1}{2} M_2^2}{1 + \frac{\gamma - 1}{2} M_1^2}\right)^{\gamma/(\gamma-1)} \tag{9.20}$$

Combining Equations (9.18) and (9.20)

$$\frac{p_{02}}{p_{01}} = \left(\frac{1 + \gamma M_1^2}{1 + \gamma M_2^2}\right)\left(\frac{1 + \frac{\gamma - 1}{2} M_2^2}{1 + \frac{\gamma - 1}{2} M_1^2}\right)^{\gamma/(\gamma-1)} \tag{9.21}$$

9.3.4 Temperature

Equations (9.12) and (9.16) give

$$\frac{\rho_2}{\rho_1}=\frac{c_1}{c_2}=\frac{M_1}{M_2}\left(\frac{T_1}{T_2}\right)^{1/2} \tag{9.22}$$

Substituting from Equations (9.22) and (9.15),

$$\frac{p_2}{p_1}=\frac{M_1}{M_2}\left(\frac{T_1}{T_2}\right)^{1/2}$$

$$\frac{T_2}{T_1}=\left(\frac{p_2}{p_1}\frac{M_2}{M_1}\right)^2 \tag{9.23}$$

Combining Equations (9.18) and (9.23),

$$\frac{T_2}{T_1}=\frac{M_2^2\,(1+\gamma M_1^2)^2}{M_1^2\,(1+\gamma M_2^2)^2} \tag{9.24}$$

9.3.5 Stagnation temperature

By definition stagnation temperature is given by

$$T_0=T\left(1+\frac{\gamma-1}{2}M^2\right)$$

$$\frac{T_{02}}{T_{01}}=\frac{T_2}{T_1}\,\frac{1+\{(\gamma-1)/2\}\,M_2^2}{1+\{(\gamma-1)/2\}\,M_1^2} \tag{9.25}$$

Combining Equations (9.24) and (9.25)

$$\frac{T_{02}}{T_{01}}=\frac{M_2^2}{M_1^2}\left(\frac{1+\gamma M_1^2}{1+\gamma M_2^2}\right)^2\,\frac{1+\{(\gamma-1)/2\}\,M_2^2}{1+\{(\gamma-1)/2\}\,M_1^2} \tag{9.26}$$

9.3.6 Density and Velocity

Substituting Equation (9.24) in (9.22) we get

$$\frac{\rho_2}{\rho_1}=\frac{c_1}{c_2}=\frac{M_1^2\,(1+\gamma M_2^2)}{M_2^2\,(1+\gamma M_1^2)} \tag{9.27}$$

9.3.7 Change of entropy

It has been shown in earlier chapters that the change of entropy is given by

$$s_2-s_1=c_p\ln\left[\frac{T_2}{T_1}\Big/\left(\frac{p_2}{p_1}\right)^{(\gamma-1)/\gamma}\right]$$

Substituting from Equations (9.18) and (9.24) and rearranging

$$\frac{s_2-s_1}{c_p}=\ln\left[\frac{M_2^2}{M_1^2}\left(\frac{1+\gamma M_1^2}{1+\gamma M_2^2}\right)^2\left(\frac{1+\gamma M_2^2}{1+\gamma M_1^2}\right)^{(\gamma-1)/\gamma}\right]$$

This on simplification yields the following relations:

$$\frac{s_2-s_1}{c_p}=\ln\left[\frac{M_2^2}{M_1^2}\left(\frac{1+\gamma M_1^2}{1+\gamma M_2^2}\right)^{(\gamma+1)/\gamma}\right] \tag{9.28}$$

$$\frac{s_2-s_1}{R}=\ln\left[\left(\frac{M_2}{M_1}\right)^{2\gamma/(\gamma-1)}\left(\frac{1+\gamma M_1^2}{1+\gamma M_2^2}\right)^{(\gamma+1)/(\gamma-1)}\right] \tag{9.29}$$

9.3.8 Heat Transfer

Substituting for T_{02}/T_{01} from Equation (9.26) in (9.17),

$$\frac{Q}{c_p T_1}=\left(1+\frac{\gamma-1}{2}M_1^2\right)\left\{\frac{M_2^2\,(1+\gamma M_1^2)^2\left(1+\dfrac{\gamma-1}{2}M_2^2\right)}{M_1^2\,(1+\gamma M_2^2)^2\left(1+\dfrac{\gamma-1}{2}M_1^2\right)}-1\right\}$$

On opening the brackets, cancelling a large number of terms and simplifying, the above expression reduces to

$$\frac{Q}{c_p T_1}=\frac{1}{2M_1^2\,(1+\gamma M_2^2)^2}\,[2M_2^2+2\gamma M_1^4 M_2^2-2M_1^2-2\gamma M_1^2 M_2^4$$

$$+\gamma M_2^4-\gamma M_1^4-M_2^4+M_1^4]$$

$$\frac{Q}{c_p T_1}=\frac{1}{2M_1^2\,(1+\gamma M_2^2)^2}\,[2\,(M_2^2-M_1^2)-2\gamma M_1^2 M_2^2\,(M_2^2-M_1^2)$$

$$+\gamma\,(M_2^4-M_1^4)-(M_2^4-M_1^4)]$$

$$\frac{Q}{c_p T_1}=\frac{(M_2^2-M_1^2)\;[2-2\gamma M_1^2 M_2^2+(\gamma-1)\;(M_2^2+M_1^2)]}{2M_1^2\,(1+\gamma M_2^2)^2} \tag{9.30}$$

9.4 VARIATION OF FLOW PROPERTIES

The variation of various flow properties with the Mach number is studied here. Flow properties at $M = M^* = 1$ are used as reference values for non-dimensionalizing various properties at any section of the duct.

Property ratios in Equations (9.18), (9.19), (9.21), (9.24), (9.26), (9.27), (9.29) and (9.30) are expressed here as the non-dimensional quantities p/p^*, F/F^*, p_0/p_0^*, T/T^*, T_0/T_0^*, ρ/ρ^*, c^*/c, $(s^* - s)/R$ and $Q^*/c_p T_1$.

This is done by making the following substitutions in the above mentioned equations:

$$M_2 = 1,\ p_2 = p^*,\ F_2 = F^*,\ p_{02} = p_0^*,\ T_2 = T^*,\ T_{02} = T_0^*,$$

$$\rho_2 = \rho^*,\ c_2 = c^*,\ s_2 = s^* \text{ and } Q = Q^* \text{ and}$$

$$M_1 = M,\ p_1 = p,\ F_1 = F,\ p_{01} = p_0,\ T_1 = T,\ T_{01} = T_0,$$

$$\rho_1 = \rho,\ c_1 = c,\ s_1 = s.$$

Following expressions are obtained after the above procedure:

$$\frac{p}{p^*} = \frac{1+\gamma}{1+\gamma M^2} \tag{9.31}$$

$$\frac{F}{F^*} = 1 \tag{9.32}$$

$$\frac{p_0}{p_0^*} = \frac{1+\gamma}{1+\gamma M^2}\left[\frac{2\left(1+\frac{\gamma-1}{2}M^2\right)}{\gamma+1}\right]^{\gamma/(\gamma-1)} \tag{9.33}$$

$$\frac{T}{T^*} = \left(\frac{1+\gamma}{1+\gamma M^2}\right)^2 M^2 \tag{9.34}$$

$$\frac{T_0}{T_0^*} = \frac{2(1+\gamma)M^2}{(1+\gamma M^2)^2}\left(1+\frac{\gamma-1}{2}M^2\right) \tag{9.35}$$

$$\frac{\rho}{\rho^*} = \frac{c^*}{c} = \frac{1+\gamma M^2}{(1+\gamma)M^2} \tag{9.36}$$

$$\frac{s^* - s}{R} = \ln\left[\left(\frac{1}{M}\right)^{2\gamma/(\gamma-1)}\left(\frac{1+\gamma M^2}{1+\gamma}\right)^{(\gamma+1)/(\gamma-1)}\right] \tag{9.37}$$

$$\frac{Q^*}{c_p T_1} = \frac{(1-M^2)}{2M^2(1+\gamma)^2}\left[2-2\gamma M^2+(\gamma-1)\ (1+M^2)\right]$$

$$\frac{Q^*}{c_p T_1} = \frac{1-M^2}{2M^2(1+\gamma)^2}(1-\gamma M^2+\gamma-M^2)$$

$$\frac{Q^*}{c_p T_1} = \frac{(1-M^2)}{2M^2(1+\gamma)^2}(1+\gamma)\ (1-M^2)$$

$$\frac{Q^*}{c_p T_1} = \frac{(1-M^2)^2}{2(1+\gamma)M^2} \tag{9.38}$$

It may be pointed out here that the final sonic state ($M = 1$, $p = p^*$, $T = T^*$ etc.) may not be reached in a given process. However, since this is the limiting state for both subsonic and supersonic heating processes it is used besides non-dimensionalizing, to give a comparative idea of the magnitudes of various flow parameters.

9.5 MAXIMUM HEAT TRANSFER

Heat addition at subsonic and supersonic Mach numbers is shown in Figure 9.6. Due to the heating, entropy during the processes increases. Therefore, all heating processes in subsonic and supersonic flows shift the state of the gas towards the maximum entropy point ($s = s_{max}$, $M = 1$). This phenomenon imposes a limit on the heat addition in a flow process. The maximum possible heat transfer ($Q_{max} = Q^*$) occurs when the end state corresponds to $T_0/T_0^* = 1$.

The non-dimensional heat transfer quantity $Q/c_p T_1$ for both subsonic and supersonic branches is shown in Figure 9.6.

Equation (9.38) gives the value of the maximum possible heat transfer at a Mach number M.

$$Q_{max} = Q^* = \frac{(1-M^2)^2}{2(1+\gamma)M^2} c_p T_1 \tag{9.39}$$

Following limiting values are obtained from Equation (9.39):

(*a*) At $M = 0$

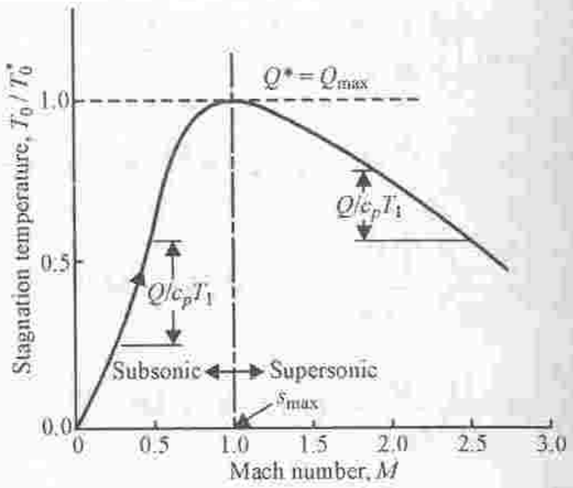

FIGURE 9.6 : Heating in subsonic and supersonic flows

$$Q_{max} = \infty$$

This corresponds to heating a gas at stagnation conditions.

(*b*) At $M = M$, the maximum heat transfer is given by Equation (9.38). The heat transfer required to change the Mach number from M_1 to M_2 is given by Equation (9.30). An alternate expression to denote the heat transfer is

$$Q = c_p (T_{02} - T_{01})$$

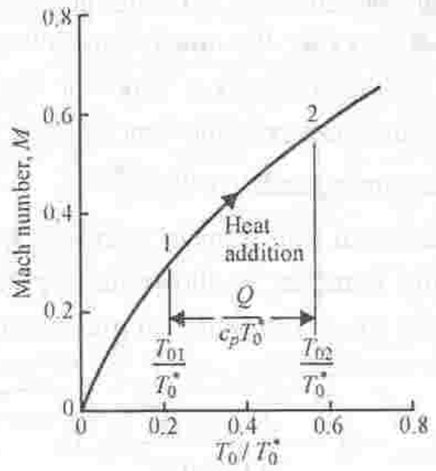

FIGURE 9.7 : Variation of Mach number with stagnation temperature due to heat transfer

$$\frac{Q}{c_p T_0^*} = \frac{T_{02}}{T_0^*} - \frac{T_{01}}{T_0^*} \tag{9.40}$$

This is graphically shown in Figure 9.7. Equation (9.40) is useful in that the quantities T_{02}/T_0^* and T_{01}/T_0^* are functions of the corresponding Mach numbers.

(*c*) At $M = 1$, no heat can be added without changing the initial conditions.

(*d*) At $M = \infty$

$$Q_{max} = \infty$$

This implies that a very large quantity of heat can be transferred for a large (infinite) change in Mach number.

9.6 TABLES FOR RAYLEIGH FLOW

Equations (9.31) to (9.38) are used to compile the various property ratios, change of entropy and the maximum heat transfer for various gases ($\gamma = 1.2$, 1.3, 1.4 etc.) in a wide range of Mach numbers. A typical gas table gives the ratios p/p^*, p_0/p_0^*, T/T^*, T_0/T_0^* and $c/c^* = \rho^*/\rho$ as functions of the Mach number. Such a table is given in Appendix A.8. Such tables are useful in solving numerical examples in a comparatively shorter time.

TABLE 9.1: Variation of flow properties in Rayleigh flow

Property	Heating		Cooling	
	Subsonic	Supersonic	Subsonic	Supersonic
M	increases	decreases	decreases	increases
p	decreases	increases	increases	decreases
F	constant	constant	constant	constant
p_0	decreases	decreases	increases	increases
c	increases	decreases	decreases	increases
ρ	decreases	increases	increases	decreases
T_0	increases	increases	decreases	decreases
T	1. increases for $M < \frac{1}{\sqrt{\gamma}}$ 2. decreases for $M > \frac{1}{\sqrt{\gamma}}$	increases	1. decreases for $M < \frac{1}{\sqrt{\gamma}}$ 2. increases for $M > \frac{1}{\sqrt{\gamma}}$	decreases
s	increases	increases	decreases	decreases

9.7 CHARTS FOR RAYLEIGH FLOW

The variations in various flow parameters are graphically depicted in Figures 9.8 and 9.9. Such charts for a given gas may be drawn with the aid of the tabulated values of the property ratios.

The observations from these charts are summarized in Table 9.1. They are also supported by Figures 9.1 and 9.2.

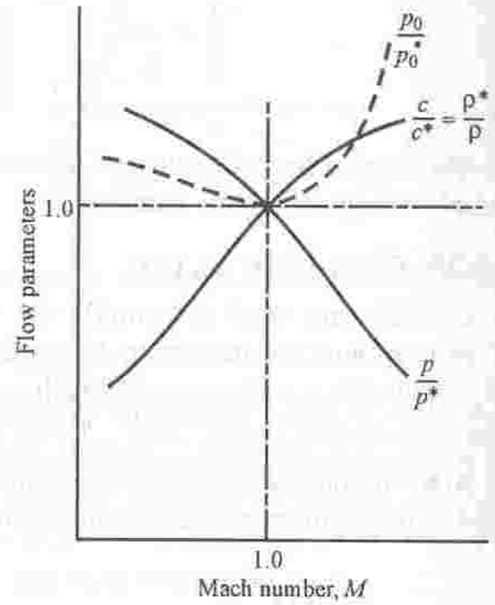

FIGURE 9.8 : Variation of flow parameters in Rayleigh flow

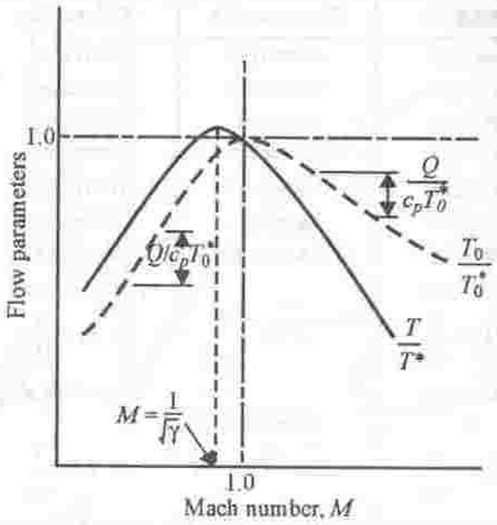

FIGURE 9.9 : Variation of flow parameters in Rayleigh flow

The directions of various changes given in Table 9.1 can also be obtained as in Section 8.3. For example, differential changes in various parameters can be expressed as functions of a chosen independent differential variable, say dT/T. Then the changes in other parameters dM, dp etc. can be derived from this.

NOTATION FOR CHAPTER 9

a	velocity of sound	Q	heat transfer per kg of gas
A	area of cross section	R	gas constant
c	gas velocity	s	entropy
c_p	specific heat at constant pressure	T	absolute temperature
F	impulse function	v	specific volume
$G = \rho c$	mass flow density or mass flux	α	slope of the constant entropy line
h	enthalpy	β	slope of the constant enthalpy line
$\dot{m}$	mass flow rate	θ	slope of the Rayleigh line
M	Mach number	ρ	gas density
p	pressure	γ	$= c_p/c_v$ specific heat ratio

SUBSCRIPTS AND SUPERSCRIPTS

o	stagnation values	$*$	corresponding to $M = 1$
1	initial state	h	at constant enthalpy
2	final state	max	maximum
$*_i$	at maximum temperature or enthalpy	R	Rayleigh line
		s	at constant entropy

SOLVED EXAMPLES

Example 9.1. The Mach number at the exit of a combustion chamber is 0.9. The ratio of stagnation temperatures at exit and entry is 3.74. If the pressure and temperature of the gas at exit are 2.5 bar and 1000°C respectively determine (*a*) Mach number, pressure and temperature of the gas at entry, (*b*) the heat supplied per kg of the gas and (*c*) the maximum heat that can be supplied.

Take $\gamma = 1.3$ and $c_p = 1.218$ kJ/kg K

Solution. $T_2 = 1000 + 273 = 1273$ K

From isentropic tables for $\gamma = 1.3$ at $M_2 = 0.9$

$$T_2/T_{02} = 0.892,$$

$$T_{02} = 1273/0.892 = 1427.13 \text{ K}$$

$$T_{01} = 1427.13/3.74 = 381.58 \text{ K}$$

From Rayleigh tables for $\gamma = 1.3$ at $M_2 = 0.9$

$$p/p^* = 1.12,\ T/T^* = 1.017,\ T_0/T_0^* = 0.991$$

$$\left(\frac{T_0}{T_0^*}\right)_1 = \frac{T_{01}}{T_{02}}\,\frac{T_{02}}{T_0^*} = \frac{0.991}{3.74} = 0.265$$

From Rayleigh tables for $\gamma = 1.3$ at

$$\left(\frac{T_0}{T_0^*}\right)_1 = 0.265$$

$$M_1 = 0.26,\ p/p^* = 2.114,\ T/T^* = 0.302$$

$M_1 = 0.26$ **Ans.**

$$p_1 = \frac{(p/p^*)_1}{(p/p^*)_2}\,p_2 = \frac{2.114}{1.12} \times 2.5$$

$p_1 = 4.718$ bar **Ans.**

$$T_1 = \frac{(T/T^*)_1}{(T/T^*)_2}\,T_2 = \frac{0.302}{1.017} \times 1273$$

$T_1 = 378$ K **Ans.**

(*b*) $$Q = c_p\,(T_{02} - T_{01})$$

$$= 1.218\ (1427.13 - 381.58)$$

$Q = 1273.48$ kJ/kg **Ans.**

(*c*) $$Q_{max} = c_p\,T_1\,\frac{(1 - M_1^2)^2}{2\,(1 + \gamma)\,M_1^2}$$

$$Q_{max} = \frac{1.218 \times 378\ (1 - 0.26^2)^2}{2 \times 2.3 \times 0.26^2}$$

$Q_{max} = 1287.18$ kJ/kg **Ans.**

Alternatively,

$$Q_{max} = c_p\,(T_0^* - T_{01})$$

$$T_0^* = \frac{T_{01}}{0.265} = \frac{T_{02}}{0.991}$$

$$T_0^* = \frac{381.58}{0.265} = \frac{1427.13}{0.991} = 1440\ \text{K}$$

$$Q_{max} = 1.218\ (1440 - 381.58)$$

$Q_{max} = 1289$ kJ/kg **Ans.**

Example 9.2. The conditions of a gas in a combuster at entry are:

$$p_1 = 0.343\ \text{bar},\ T_1 = 310\ \text{K},\ c_1 = 60\ \text{m/s}$$

Determine the Mach number, pressure, temperature and velocity at the exit if the increase in stagnation enthalpy of the gas between entry and exit is 1172.5 kJ/kg.

Take $c_p = 1.005$ kJ/kg K, $\gamma = 1.4$.

Solution. $$a_1 = \sqrt{1.4 \times 287 \times 310} = 353\ \text{m/s}$$

$$M_1 = c_1/a_1 = 60/353 = 0.17$$

From Isentropic tables for $\gamma = 1.4$

at $M_1 = 0.17,\ T_1/T_{01} = 0.9943$

$$T_{01} = T_1/0.9943 = 310/0.9943 = 311.78\ \text{K}$$

From Rayleigh tables for $\gamma = 1.4$ at $M_1 = 0.17$

$$p/p^* = 2.306,\ T/T^* = 0.154,\ T_0/T_0^* = 0.129$$

$$c/c^* = 0.0665$$

$$T_0^* = T_{01}/0.129 = 311.78/0.129 = 2416.89\ \text{K}$$

$$c_p\,(T_{02} - T_{01}) = \Delta h_0$$

$$T_{02} - T_{01} = 1172.5/1.005 = 1166.67\ \text{K}$$

$$T_{02} = 1166.67 + 311.78 = 1478.45\ \text{K}$$

$$T_{02}/T_0^* = 1478.45/2416.89 = 0.612$$

From Rayleigh tables for $\gamma = 1.4$ at

$$T_{02}/T_0^* = 0.612$$

$M_2 = 0.45$ **Ans.**

$$p/p^* = 1.87,\ T/T^* = 0.7075,\ c/c^* = 0.378$$

$$p_2 = \frac{1.87}{2.306} \times 0.343 = 0.278\ \text{bar}$$ **Ans.**

$$T_2 = \frac{0.7075}{0.154} \times 310 = 1424.18 \text{ K} \quad \textbf{Ans.}$$

$$c_2 = \frac{0.378}{0.0665} \times 60 = 341.05 \text{ m/s} \quad \textbf{Ans.}$$

Alternatively, $a_2 = \sqrt{1.4 \times 287 \times 1424.18} = 757.26$ m/s

$$c_2 = 0.45 \times 757.26 = 340.77 \text{ m/s} \quad \textbf{Ans.}$$

Example 9.3. A combustion chamber in a gas turbine plant receives air at 350 K, 0.55 bar and 75 m/s. The air-fuel ratio is 29 and the calorific value of the fuel is 41.87 MJ/kg. Taking $\gamma = 1.4$ and $R = 0.287$ kJ/kg K for the gas determine:

(*a*) the initial and final Mach numbers,

(*b*) final pressure, temperature and velocity of the gas,

(*c*) percent stagnation pressure loss in the combustion chamber, and

(*d*) the maximum stagnation temperature attainable.

Solution. (*a*) $a_1 = \sqrt{1.4 \times 287 \times 350} = 375$ m/s

$$M_1 = c_1/a_1 = 75/375 = 0.20 \quad \textbf{Ans.}$$

From Isentropic tables for $\gamma = 1.4$, at $M_1 = 0.2$, $p_1/p_{01} = 0.973$

$$T_1/T_{01} = 0.992$$

$$p_{01} = \frac{0.55}{0.975} = 0.565 \text{ bar}, \quad T_{01} = \frac{350}{0.992} = 352.82 \text{ K}$$

From Rayleigh tables for $\gamma = 1.4$ at $M_1 = 0.2$

$$\frac{p}{p^*} = 2.273, \quad \frac{p_0}{p_0^*} = 1.235, \quad \frac{T}{T^*} = 0.207 \cdot \frac{T_0}{T_0^*} = 0.174, \quad \frac{c}{c^*} = 0.091$$

Stagnation enthalpy rise due to the combustion of one kg of fuel is

$$\Delta h_0 = \frac{41870}{29 + 1} = 1395.67 \text{ kJ/kg of air fuel mixture}$$

$$c_p (T_{02} - T_{01}) = \Delta h_0$$

$$T_{02} = T_{01} + \frac{\Delta h_0}{c_p}$$

$$T_{02} = 352.82 + \frac{1395.67}{1.005} = 1741.55 \text{ K}$$

$$\frac{T_{02}}{T_0^*} = \frac{T_{02}}{T_{01}} \frac{T_{01}}{T_{01}^*} = \frac{1741.55}{352.82} \times 0.174 = 0.859$$

From Rayleigh tables for $\gamma = 1.4$ at $\frac{T_0}{T_0^*} = 0.859$

$$M_2 = 0.64 \quad \textbf{Ans.}$$

(*b*) $\frac{p}{p^*} = 1.525, \quad \frac{p_0}{p_0^*} = 1.061, \quad \frac{T}{T^*} = 0.953, \quad \frac{c}{c^*} = 0.625$

$$p_2 = \frac{(p/p^*)_2}{(p/p^*)_1} p_1 = \frac{1.525}{2.273} \times 0.55 = 0.369 \text{ bar} \quad \textbf{Ans.}$$

$$T_2 = \frac{(T/T^*)_2}{(T/T^*)_1} T_1 = \frac{0.953}{0.207} \times 350 = 1611.35 \text{ K} \quad \textbf{Ans.}$$

$$c_2 = \frac{(c/c^*)_2}{(c/c^*)_1} c_1$$

$$c_2 = \frac{0.625}{0.091} \times 75 = 515.11 \text{ m/s} \quad \textbf{Ans.}$$

$$p_{02} = \frac{(p_0/p_0^*)_2}{(p_0/p_0^*)_1} \times p_{01} = \frac{1.061}{1.235} \times 0.565 = 0.485 \text{ bar}$$

(*c*) Stagnation pressure loss

$$\Delta p_0 = p_{01} - p_{02}$$

$$\Delta p_0 = 0.565 - 0.485 = 0.080 \text{ bar}$$

$$\frac{\Delta p_0}{p_{01}} \times 100 = \frac{0.08}{0.565} \times 100 = 14.16$$

$$\Delta p_0 = 14.16\% \quad \textbf{Ans.}$$

(*d*) The maximum stagnation temperature for given inlet conditions exists at the sonic point.

$$T_{0\,\max} = T_{02}^* = T_{01}^* = T_0^*$$

$$T_0^* = \frac{352.82}{0.174} = 2027.7 \text{ K} \quad \textbf{Ans.}$$

or $$T_0^* = \frac{1741.55}{0.859} = 2027.4 \quad \textbf{Ans.}$$

Example 9.4. (*a*) What is the value of Mach number of air at the maximum enthalpy point in Rayleigh heating process? Depict static and stagnation values of pressure and temperature at this point and the sonic point on a Rayleigh line.

(*b*) If the conditions at sonic point are $p^* = 1$ bar, $T^* = 500$ K calculate pressure, temperature and velocity at the maximum enthalpy point. What is the change of entropy between these points?

Solution. (*a*) Let the maximum enthalpy point be E (Figure 9.2).

$$M_E = \frac{1}{\sqrt{\gamma}} = \frac{1}{\sqrt{1.4}} = 0.845 \quad \textbf{Ans.}$$

(*b*) From Rayleigh flow tables ($\gamma = 1.4$) at $M_E = 0.845$

$$p_E/p^* = 1.200, \; p_E = 1.200 \times 1 = 1.2 \text{ bar} \quad \textbf{Ans.}$$

$$T_E/T^* = 1.028, \; T_E = 1.028 \times 500 = 514 \text{ K} \quad \textbf{Ans.}$$

$$a_E = \sqrt{\gamma R T_E} = \sqrt{1.4 \times 287 \times 514} = 454.45 \text{ m/s}$$

Therefore, gas velocity at this point is

$$c_E = M_E \, a_E$$

$$c_E = 0.845 \times 454.45 = 384.01 \text{ m/s} \quad \textbf{Ans.}$$

Change of entropy is given by

$$s^* - s_E = c_p \ln \frac{T^*}{T_E} - R \ln \frac{p^*}{p_E}$$

$$s^* - s_E = 1.005 \ln \frac{1}{1.028} - 0.287 \ln \frac{1}{1.2}$$

$$s^* - s_E = 0.02455 \quad \textbf{Ans.}$$

QUESTIONS AND PROBLEMS

9.1 What is Rayleigh flow? Give two practical examples. Under what conditions the assumption of Rayleigh flow is not valid in a heat exchanger?

9.2 Obtain an equation representing the Rayleigh line. Draw Rayleigh lines on the h-s and p-v planes for two different values of the mass flux.

Show that the slope of the Rayleigh line on the p-v plane is

$$\left(\frac{dp}{dv}\right)_R = -\rho^2 c^2$$

9.3 Prove that the Mach numbers at the maximum enthalpy and maximum entropy points on the Rayleigh line are $1/\sqrt{\gamma}$ and 1.0 respectively. Show the h = constant and s = constant lines at these points on the Rayleigh line on the h-s and p-v planes.

9.4 Draw a Rayleigh line on T-s plane. Show the following on this line:

(*a*) Stagnation temperature lines for both subsonic and supersonic flows,

(*b*) maximum stagnation temperature point,

(*c*) constant static and stagnation pressure lines.

9.5 Develop the following relations for Rayleigh flow:

(*a*) $F_1 = F_2 = F^* = \text{constant}$

(*b*) $$\frac{T_1}{T_2} = \left(\frac{M_1}{M_2}\right)^2 \left(\frac{1+\gamma M_2^2}{1+\gamma M_1^2}\right)^2$$

(*c*) $$\frac{c_1}{c_2} = \frac{\rho_2}{\rho_1} = \left(\frac{M_1}{M_2}\right)^2 \frac{1+\gamma M_2^2}{1+\gamma M_1^2}$$

(*d*) $$\frac{s_2 - s_1}{R} = \ln \frac{M_2}{M_1} \left(\frac{M_2}{M_1} \frac{1+\gamma M_1^2}{1+\gamma M_2^2}\right)^{(\gamma+1)/(\gamma-1)}$$

9.6 Prove that the dimensionless value of the heat transfer in a Rayleigh process from a Mach number M_1 to M_2 is

$$\frac{Q}{c_p T_1} = \frac{M_2^2 - M_1^2}{2M_1^2 (1+\gamma M_2^2)^2} [2 (1 - \gamma M_1^2 M_2^2) + (\gamma - 1) (M_2^2 + M_1^2)]$$

Hence, show that the maximum value of heat transfer at a Mach number M is

$$Q_{\max} = c_p T_1 \frac{(1-M^2)^2}{2(1+\gamma) M^2}.$$

9.7 Air at $p_1 = 3$ bar, $T_1 = 288$ K and $M_1 = 1.5$ is brought to sonic velocity in a frictionless constant area duct through which heat transfer can occur.

(*a*) Determine the final pressure and temperature, and the heat added during the process.

(*b*) What will be the Mach number, pressure and temperature of air if this heat is extracted from the air?

Ans. (*a*) $p_2 = 5.19$ bar, $T_2 = 382.47$ K

$Q = 42.05$ kJ/kg

(*b*) $M_2 = 1.88$, $p_2 = 2.09$ bar $T_2 = 219.92$ K.

9.8 The stagnation temperature of air in a combustion chamber is increased to 3.5 times its initial value. If the air at entry is at 5 bar, 105°C and a Mach number of 0.25 determine:

(*a*) the Mach number, pressure and temperature at the exit,

(*b*) stagnation pressure loss, and

(*c*) the heat supplied per kg of air.

Ans. (*a*) $M_2 = 0.68$, $p_2 = 3.3$ bar, $t_2 = 944°C$,

(*b*) $\Delta p_0 = 0.735$ bar, (*c*) 962.3 kJ/kg.

9.9 A gas at a pressure of 0.69 bar and temperature 278 K enters a combustion chamber at a velocity of 60 m/s. The heat supplied in the combustion chamber is 1405.6 kJ/kg. Determine the Mach number, pressure, temperature and velocity of the gas at the exit. (Take $\gamma = 1.4$ and $c_p = 1.004$ kJ/kg K for the gas).

Ans. $M_2 = 0.64$, $p_2 = 0.458$ bar

$T_2 = 1549.3$ K, $c_2 = 506$ m/s.

9.10 The conditions of a gas ($\gamma = 1.3$, $c_p = 1.22$ kJ/kg K) at the entry of a constant area duct are:

$M_1 = 0.28$, $T_{01} = 383$ K, $p_{01} = 4.965$ bar.

627 kJ/kg of heat is supplied to the gas. Determine at the exit section—Mach number, pressure and temperature of the gas. What is the stagnation pressure loss during heating?

Ans. $M_2 = 0.52$, $p_2 = 3.845$ bar, $T_2 = 866.3$ K, $\Delta p_0 = 0.395$ bar.

9.11 The data for a gas ($\gamma = 1.3$, $R = 466$ J/kg K) at the entry of a constant area duct are:

$p_1 = 0.345$ bar, $T_1 = 312$ K, $c_1 = 65.5$ m/s

If 4592 kJ/kg of heat is added to the gas in the duct between entry and exit sections, determine at the exit (*a*) pressure (*b*) temperature (*c*) Mach number and (*d*) velocity of the gas. (*e*) How much heat is required to accelerate the gas from the initial to sonic conditions? What are the pressure and temperature of the gas at sonic conditions?

Ans. (*a*) 0.242 bar (*b*) 2451.6 K (*c*) $M_2 = 0.6$ (*d*) 731.2 m/s (*e*) 5818.15 kJ/kg, $p^* = 0.1544$ bar, $T^* = 2773.3$ K.

9.12 The data for a combustion chamber employing a hydrocarbon fuel is given below:

Entry: Gas velocity = 152 m/s, pressure = 4 bar, temperature = 400 K.

Exit: Mach number = 0.8.

Take $\gamma = 1.3$ $c_p = 2.144$ kJ/kg K for the products of combustion.

Calorific value of the fuel burnt = 43 MJ/kg. Determine:

(*a*) Entry Mach number,

(*b*) pressure. temperature and velocity of the gas at exit,

(*c*) stagnation pressure loss and

(*d*) Air-fuel ratio required.

Ans. (*a*) $M_1 = 0.30$ (*b*) $p_2 = 2.437$ bar, $T_2 = 1056.544$ K, $c_2 = 658.975$ m/s (*c*) $\Delta p_0 = 0.613$ bar (*d*) 25.605 kg of air per kg of fuel.

PART-II

10

Multi-dimensional Flow

Some terms in general fluid flow were defined in Sections 1.34 to 1.40. After this the following chapters dealt with the various compressible flow problems assuming the flow as one-dimensional. Besides simplifying an otherwise difficult problem one-dimensional analysis in a number of practical cases provides quick answers without much sacrifice in accuracy. However, there are many situations where one-dimensional treatment gives only a rough idea about the flow pattern; in some cases it may even give a misleading picture of an actual flow situation.

This chapter presents a wider view of the flow field and introduces the reader with situations where one-dimensional flow analysis is inadequate. Due to the limited space only some aspects of three and two-dimensional flows have been considered here. The two widely used systems of coordinates—the Cartesian and the cylindrical systems have been employed for deriving various equations of flow.

Following assumptions have been used throughout this chapter:

(*a*) isentropic flow of a perfect gas,

(*b*) multi-dimensional flow,

(*c*) absence of shocks, and

(*d*) irrotational flow.

Navier-Stokes equations have not been derived in this book; these have been written here only for comparison with the corresponding inviscid flow equations. Their derivation is given in conventional books on Fluid mechanics.

10.1 CARTESIAN COORDINATE SYSTEM

Figure 10.1 shows the three velocity and vorticity components in the Cartesian coordinate system. The axes of reference are X, Y and Z. A

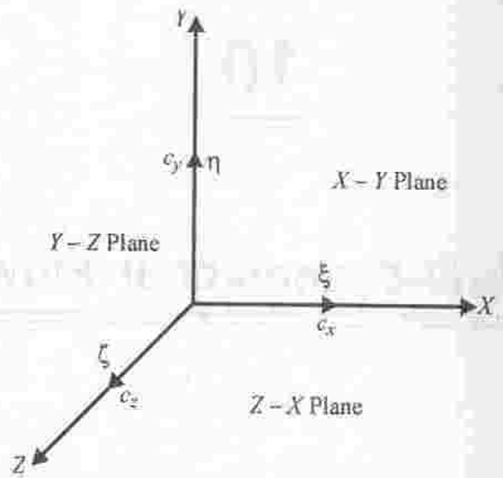

FIGURE 10.1 : Velocity and vorticity components in Cartesian coordinates

point in the flow field is determined by its coordinates x, y and z. Various flow parameters at this point are:

velocities c_x, c_y, and c_z

accelerations a_x, a_y, and a_z

vorticities ξ, η and ζ

pressure forces F_x, F_y and F_z

body forces X, Y and Z.

10.1.1 Continuity Equation

Equation of continuity is a mathematical statement of the law of conservation of mass. Figure 10.2 shows the flow of a fluid through an elemental cube in three dimensions. Quantities of flow entering and leaving the cube in the three directions are show in the figure.

The volume and mass of the fluid within the cube are $V = dx\ dy\ dz$ and $m = \rho V = \rho\ dx\ dy\ dz$ respectively. The law of conservation of mass for the cube taken as a system gives

$$d(\rho\ V) = 0$$

$$\rho\, dV + V\, d\rho = 0 \qquad (10.1)$$

The total change (dV) in volume during time dt is given by

$$dV = (dV)_x + (dV)_y + (dV)_z \qquad (10.2)$$

The quantities $(dV)_x$, $(dV)_y$ and $(dV)_z$ are the changes in the x, y and z directions. These are determined here with the aid of Figure 10.2.

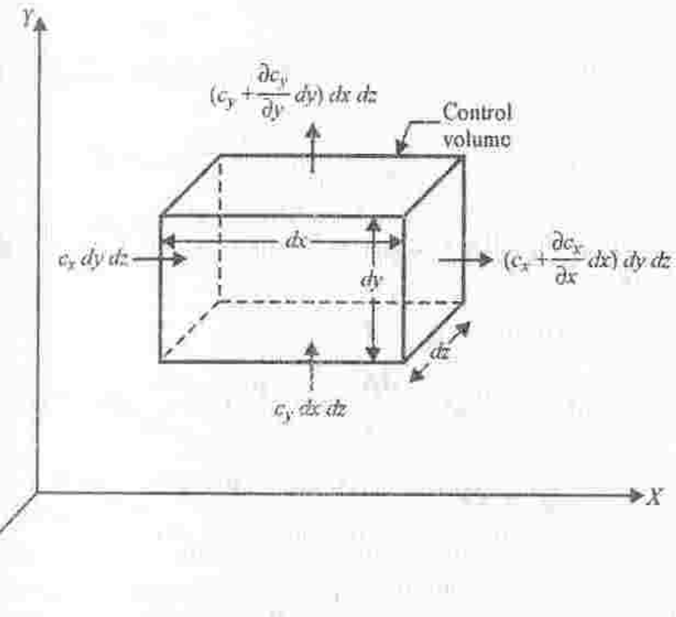

FIGURE 10.2 : Flow through an elemental cube (control volume)

$$(dV)_x = \left[\left(c_x + \frac{\partial c_x}{\partial x} dx \right) dy\ dz - c_x\, dy\ dz \right] dt$$

On simplification this gives

$$(dV)_x = \left(\frac{\partial c_x}{\partial x} \right) dx\ dy\ dz\ dt \qquad (10.3)$$

For the y-direction

$$(dV)_y = \left[\left(c_y + \frac{\partial c_y}{\partial y} dy \right) dx\ dz - c_y\, dx\ dz \right] dt$$

$$(dV)_y = \left(\frac{\partial c_y}{\partial y} \right) dx\ dy\ dz\ dt \qquad (10.4)$$

For the z-direction

$$(dV)_z = \left[\left(c_z + \frac{\partial c_z}{\partial z} dz \right) dx\ dy - c_z\, dx\ dy \right] dt$$

$$(dV)_z = \left(\frac{\partial c_z}{\partial z} \right) dx\ dy\ dz\ dt \tag{10.5}$$

Substituting Equations (10.3), (10.4) and (10.5) in (10.2) we get,

$$dV = \left(\frac{\partial c_x}{\partial x} + \frac{\partial c_y}{\partial y} + \frac{\partial c_z}{\partial z} \right) dx\ dy\ dz\ dt \tag{10.6}$$

The fluid density at a given point is a function of the coordinates x, y, z and t.

$$\rho = f(x, y, z, t)$$

$$d\rho = \frac{\partial \rho}{\partial x} dx + \frac{\partial \rho}{\partial y} dy + \frac{\partial \rho}{\partial z} dz + \frac{\partial \rho}{\partial t} dt$$

$$V\, d\rho = \left(\frac{\partial \rho}{\partial x} \frac{dx}{dt} + \frac{\partial \rho}{\partial y} \frac{dy}{dt} + \frac{\partial \rho}{\partial z} \frac{dz}{dt} + \frac{\partial \rho}{\partial t} \right) dx\ dy\ dz\ dt$$

Substituting $c_x = \frac{dx}{dt}$, $c_y = \frac{dy}{dt}$ and $c_z = \frac{dz}{dt}$

$$V\, d\rho = \left(c_x \frac{\partial \rho}{\partial x} + c_y \frac{\partial \rho}{\partial y} + c_z \frac{\partial \rho}{\partial z} + \frac{\partial \rho}{\partial t} \right) dx\ dy\ dz\ dt \tag{10.7}$$

Substituting Equations (10.6) and (10.7) in (10.1)

$$\rho \left(\frac{\partial c_x}{\partial x} + \frac{\partial c_y}{\partial y} + \frac{\partial c_z}{\partial z} \right) + c_x \frac{\partial \rho}{\partial x} + c_y \frac{\partial \rho}{\partial y} + c_z \frac{\partial \rho}{\partial z} + \frac{\partial \rho}{\partial t} = 0$$

Rearranging in pairs and writing as differential coefficients of products of two quantities,

$$\left(\rho \frac{\partial c_x}{\partial x} + c_x \frac{\partial \rho}{\partial x} \right) + \left(\rho \frac{\partial c_y}{\partial y} + c_y \frac{\partial \rho}{\partial y} \right) + \left(\rho \frac{\partial c_z}{\partial z} + c_z \frac{\partial \rho}{\partial z} \right) + \frac{\partial \rho}{\partial t} = 0$$

$$\frac{\partial}{\partial x}(\rho c_x) + \frac{\partial}{\partial y}(\rho c_y) + \frac{\partial}{\partial z}(\rho c_z) + \frac{\partial \rho}{\partial t} = 0 \tag{10.8}$$

This is the equation of continuity for three-dimensional unsteady compressible flow. This equation can also be obtained for a control volume by adopting the method used in Section 10.2.1. This is considered for the following conditions:

(*i*) **Steady flow:** In steady flow there is no change in flow parameters with time,

$$\frac{\partial}{\partial t}(\ ) = 0$$

This condition in Equation (10.8) yields

$$\frac{\partial}{\partial x}(\rho c_x) + \frac{\partial}{\partial y}(\rho c_y) + \frac{\partial}{\partial z}(\rho c_z) = 0 \tag{10.9}$$

(*ii*) **Incompressible flow:** As pointed out in chapter one the flow is said to be incompressible when the change in fluid density is negligible, *i.e.*,

$$\rho \approx \text{constant}$$

This condititon in Equation (10.9) gives

$$\frac{\partial c_x}{\partial x} + \frac{\partial c_y}{\partial y} + \frac{\partial c_z}{\partial z} = 0 \tag{10.10}$$

(*iii*) **Two-dimensional, steady incompressible flow:** In many flow patterns variations in the third dimension (here in the z-direction) are negligible or absent. Therefore,

$$\frac{\partial}{\partial z}(\ ) = 0$$

$$\frac{\partial c_x}{\partial x} + \frac{\partial c_y}{\partial y} = 0 \tag{10.11}$$

(*iv*) **One-dimensional steady flow:** In one-dimensional steady flow

$$\frac{\partial}{\partial y}(\ ) = 0,\ \frac{\partial}{\partial z}(\ ) = 0 \text{ and } \frac{\partial}{\partial t}(\ ) = 0,\ c = c_x$$

These conditions in Equation (10.8) give

$$\frac{\partial}{\partial x}(\rho c_x) = 0$$

$$\rho c_x = \rho c = \text{constant}$$

$$\rho A c = \text{constant} \tag{10.12}$$

This is the familiar and frequently used equation of continuity for one dimensional steady flow. The cross sectional area A is perpendicular to the velocity vector c.

10.1.2 Euler's Momentum Equations

The three momentum equations in the x, y and z directions are derived from the law of conservation of momentum.

Figures 10.3 and 10.4 show the elemental control volume at time t and $t + dt$ respectively in the frame of coordinates. The dimensions of the control volume are Δx, Δy and Δz. Pressure forces acting on the different faces of the control surface in the two positions are also shown.

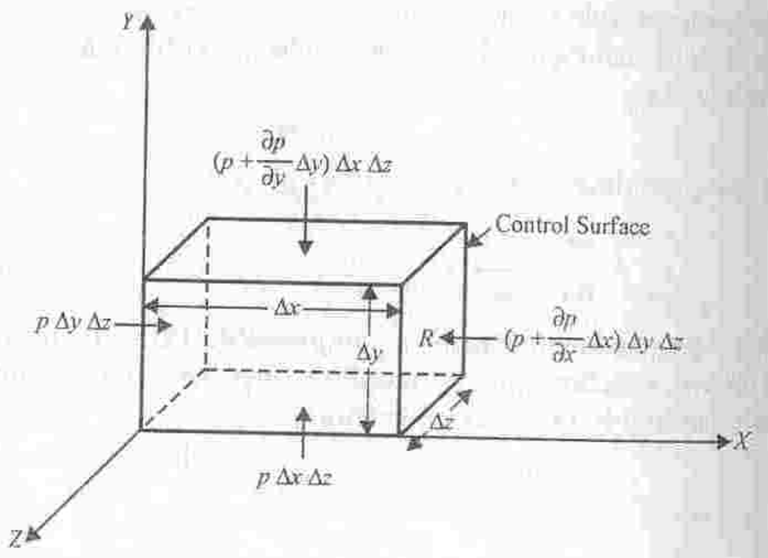

FIGURE 10.3 : Pressure forces on the control surface at time t

The elemental control volume has moved through distances dx, dy and dz in the frame of coordinates during the infinitesimal time interval dt. The changes in the pressure forces after time dt are shown in Figure 10.4.

The velocity vectors c_x, c_y and c_z are functions of x, y, z and t. Therefore,

$$c_x = f(x, y, z, t) \qquad (10.13\ (a))$$

$$c_y = f(x, y, z, t) \qquad (10.13\ (b))$$

$$c_z = f(x, y, z, t) \qquad (10.13\ (c))$$

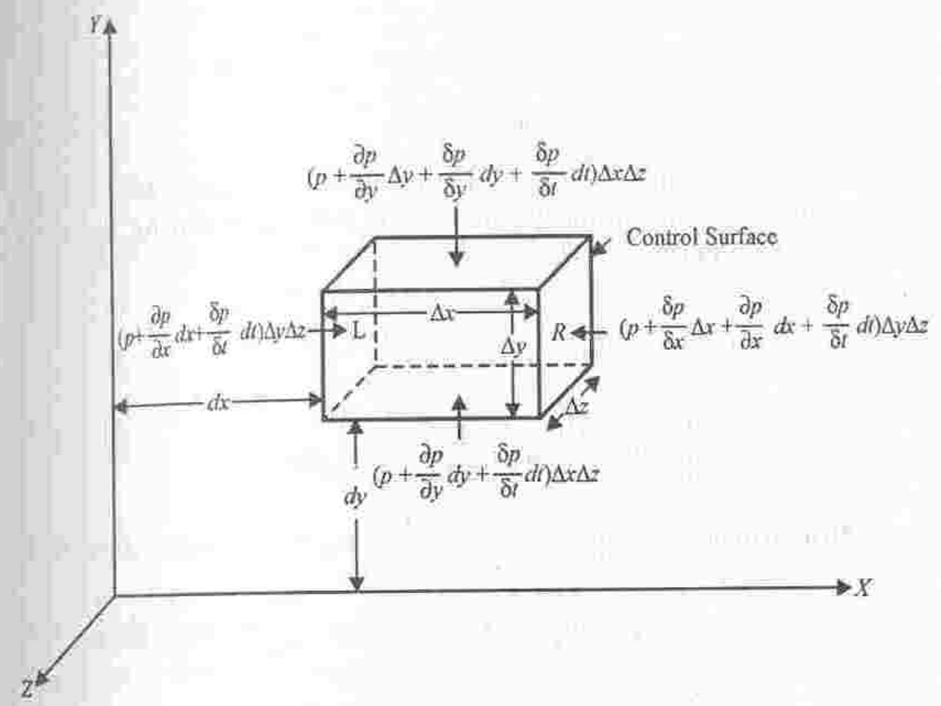

FIGURE 10.4 : Pressure forces on the control surface at time $t + dt$

The total change in the velocity vector c_x is given by

$$dc_x = \frac{\partial c_x}{\partial x}dx + \frac{\partial c_x}{\partial y}dy + \frac{\partial c_x}{\partial z}dz + \frac{\partial c_x}{\partial t}dt$$

$$\frac{dc_x}{dt} = \frac{\partial c_x}{\partial x}\frac{dx}{dt} + \frac{\partial c_x}{\partial y}\frac{dy}{dt} + \frac{\partial c_x}{\partial z}\frac{dz}{dt} + \frac{\partial c_x}{\partial t}$$

The differential operator d/dt is the material or substantial derivative; the symbol D/Dt is commonly used for this.

Therefore, $$\frac{D}{Dt} = c_x\frac{\partial}{\partial x} + c_y\frac{\partial}{\partial y} + c_z\frac{\partial}{\partial z} + \frac{\partial}{\partial t} \qquad (10.14)$$

$$\frac{Dc_x}{Dt} = a_x,\ \frac{Dc_y}{Dt} = a_y \text{ and } \frac{Dc_z}{Dt} = a_z \qquad (10.15)$$

Therefore, the accelerations in the three directions are given by

$$a_x = c_x\frac{\partial c_x}{\partial x} + c_y\frac{\partial c_x}{\partial y} + c_z\frac{\partial c_x}{\partial z} + \frac{\partial c_x}{\partial t} \qquad (10.16)$$

$$a_y = c_x \frac{\partial c_y}{\partial x} + c_y \frac{\partial c_y}{\partial y} + c_z \frac{\partial c_y}{\partial z} + \frac{\partial c_y}{\partial t} \tag{10.17}$$

$$a_z = c_x \frac{\partial c_z}{\partial x} + c_y \frac{\partial c_z}{\partial y} + c_z \frac{\partial c_z}{\partial z} + \frac{\partial c_z}{\partial t} \tag{10.18}$$

Considering the control surface in Figures 10.3 and 10.4 average pressure force acting on the left face L in x-direction during the infinitesimal time interval dt is

$$F_L = \frac{1}{2}\left(p + p + \frac{\partial p}{\partial x}dx + \frac{\partial p}{\partial t}dt\right)\Delta y\ \Delta z$$

$$F_L = \left(p + \frac{1}{2}\frac{\partial p}{\partial x}dx + \frac{1}{2}\frac{\partial p}{\partial t}dt\right)\Delta y\ \Delta z$$

Similarly average pressure force acting on the right face R is

$$F_R = \frac{1}{2}\left(p + \frac{\partial p}{\partial x}\Delta x + p + \frac{\partial p}{\partial x}\Delta x + \frac{\partial p}{\partial x}dx + \frac{\partial p}{\partial t}dt\right)\Delta y\ \Delta z$$

$$F_R = \left(p + \frac{\partial p}{\partial x}\Delta x + \frac{1}{2}\frac{\partial p}{\partial x}dx + \frac{1}{2}\frac{\partial p}{\partial t}dt\right)\Delta y\ \Delta z$$

Therefore, the net value of the average pressure force acting on the control surface in the positive x-direction is

$$F_x = F_L - F_R = -\frac{\partial p}{\partial x}\Delta x\ \Delta y\ \Delta z \tag{10.19}$$

The values of the forces in the y- and z-directions are also obtained by this procedure.

$$F_y = -\frac{\partial p}{\partial y}\Delta x\ \Delta y\ \Delta z \tag{10.20}$$

$$F_z = -\frac{\partial p}{\partial z}\Delta x\ \Delta y\ \Delta z \tag{10.21}$$

The body forces (gravitational, electromagnetic etc.) are proportional to the mass; these forces per unit mass in the three directions are, X, Y and Z. Therefore, by Newton's second law of motion in the x-direction

$$ma_x = mX + F_x$$

Substituting from Equation (10.19)

$$\rho\,\Delta x\ \Delta y\ \Delta z\, a_x = \rho\,\Delta x\ \Delta y\ \Delta z X - \frac{\partial p}{\partial x}\Delta x\ \Delta y\ \Delta z$$

$$a_x = X - \frac{1}{\rho}\frac{\partial p}{\partial x} \tag{10.22}$$

Following relations are obtained by a similar method.

$$ma_y = mY + F_y$$

$$a_y = Y - \frac{1}{\rho}\frac{\partial p}{\partial y} \tag{10.23}$$

$$ma_z = mZ + F_z$$

$$a_z = Z - \frac{1}{\rho}\frac{\partial p}{\partial z} \tag{10.24}$$

Substitution of Equations (10.16), (10.17), and (10.18) in (10.22), (10.23) and (10.24) respectively yields the three Euler's equations

$$c_x \frac{\partial c_x}{\partial x} + c_y \frac{\partial c_x}{\partial y} + c_z \frac{\partial c_x}{\partial z} + \frac{\partial c_x}{\partial t} = X - \frac{1}{\rho}\frac{\partial p}{\partial x} \tag{10.25}$$

$$c_x \frac{\partial c_y}{\partial x} + c_y \frac{\partial c_y}{\partial y} + c_z \frac{\partial c_y}{\partial z} + \frac{\partial c_y}{\partial t} = Y - \frac{1}{\rho}\frac{\partial p}{\partial y} \tag{10.26}$$

$$c_x \frac{\partial c_z}{\partial x} + c_y \frac{\partial c_z}{\partial y} + c_z \frac{\partial c_z}{\partial z} + \frac{\partial c_z}{\partial t} = Z - \frac{1}{\rho}\frac{\partial p}{\partial z} \tag{10.27}$$

Often to simplify the problems it is assumed that the flow is steady and body forces are absent; under these conditions the above equations become

$$c_x \frac{\partial c_x}{\partial x} + c_y \frac{\partial c_x}{\partial y} + c_z \frac{\partial c_x}{\partial z} = -\frac{1}{\rho}\frac{\partial p}{\partial x} \tag{10.28}$$

$$c_x \frac{\partial c_y}{\partial x} + c_y \frac{\partial c_y}{\partial y} + c_z \frac{\partial c_y}{\partial z} = -\frac{1}{\rho}\frac{\partial p}{\partial y} \tag{10.29}$$

$$c_x \frac{\partial c_z}{\partial x} + c_y \frac{\partial c_z}{\partial y} + c_z \frac{\partial c_z}{\partial z} = -\frac{1}{\rho}\frac{\partial p}{\partial z} \tag{10.30}$$

10.1.3 Circulation

Circulation is defined as the line integral of velocity around a closed contour in a flow field. Figure 10.5 shows a closed contour C in a flow field.

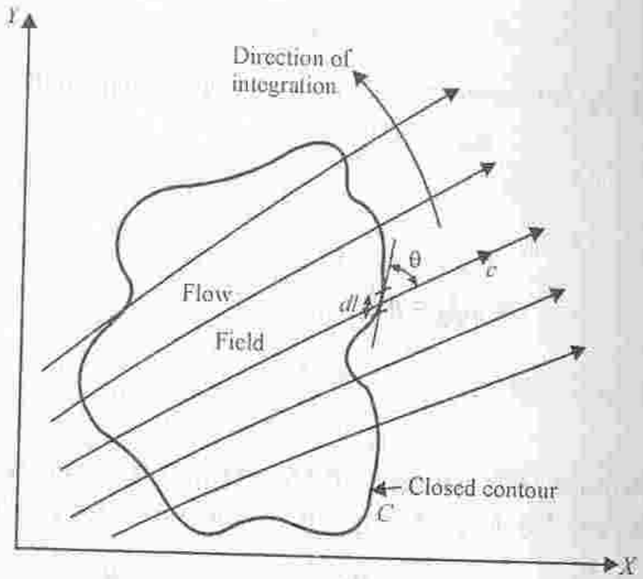

FIGURE 10.5 : Circulation around a closed contour

The velocity vector c at an elemental length dl of the curve is inclined at an angle θ to the curve. The line integral is $c \cos\theta \, dl$ and the circulation

$$\Gamma = \oint_C c \cos\theta \, dl \tag{10.31}$$

The symbol $\oint_C$ represents integration around the closed contour C; the integration is done in the anticlockwise (positive) direction.

When an elemental closed contour of area ΔA is considered in the flow field the circulation around it is $\Delta\Gamma$. The average rotation, and vorticity are then given by

$$\text{vorticity} = 2 \times \text{rotation} = \lim_{\Delta A \to 0} \frac{\Delta\Gamma}{\Delta A} \tag{10.32}$$

The basic derivation of Equation (10.32) can be found in books on fluid mechanics.

10.1.4 Vorticity Components

Figure 10.6 shows an elemental cube of sides Δx, Δy and Δz in a three-dimensional flow field. Various velocity vectors along its sides and the vorticity components ξ, η and ζ in the three planes are shown.

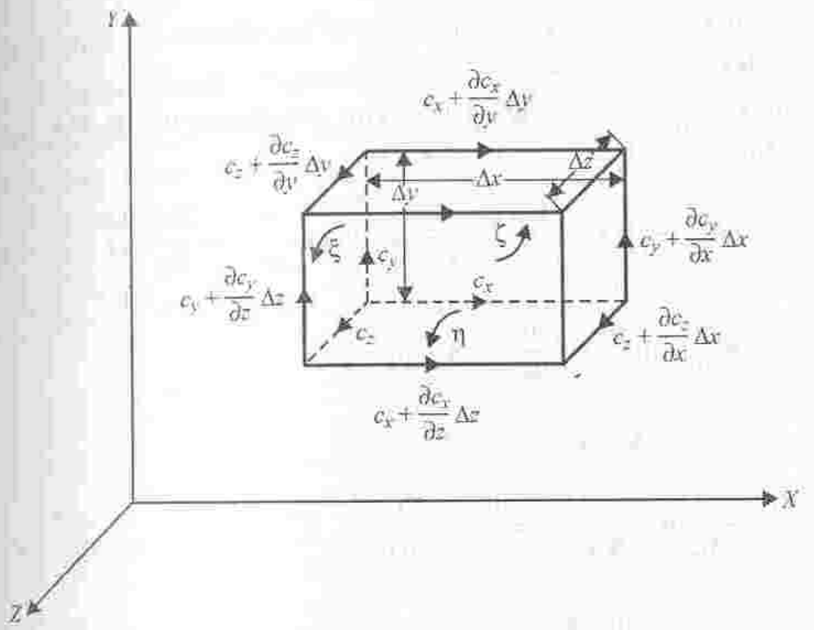

FIGURE 10.6 : Vorticity components ξ, η and ζ in Cartesian coordinates

Vorticity ξ and rotation ω_x: The circulation in the Y-Z plane (Figures 10.1 and 10.6) is given by

$$\Delta\Gamma_{yz} = c_y \Delta y + \left(c_z + \frac{\partial c_z}{\partial y}\Delta y \right) \Delta z - \left(c_y + \frac{\partial c_y}{\partial z}\Delta z \right) \Delta y - c_z \Delta z$$

After cancellation of some terms and rearrangement the above expression reduces to

$$\Delta\Gamma_{yz} = \left(\frac{\partial c_z}{\partial y} - \frac{\partial c_y}{\partial z} \right) \Delta y \, \Delta z$$

Now $\Delta A_{yz} = \Delta y \, \Delta z$, therefore,

$$\frac{\Delta\Gamma_{yz}}{\Delta A_{yz}} = \left(\frac{\Delta\Gamma}{\Delta A} \right)_{yz} = \frac{\partial c_z}{\partial y} - \frac{\partial c_y}{\partial z}$$

But $\lim_{\Delta A_{yz}\to 0}\left(\frac{\Delta\Gamma}{\Delta A}\right)_{yz} = \xi$, therefore,

$$\xi = 2\omega_x = \frac{\partial c_z}{\partial y} - \frac{\partial c_y}{\partial z} \tag{10.33}$$

Figure 10.6 shows the directions of circulation, vorticity and rotation in the three planes.

Vorticity η and rotation ω_y: The circulation in the Z-X plane is given by

$$\Delta\Gamma_{zx} = c_z\,\Delta z + \left(c_x + \frac{\partial c_x}{\partial z}\Delta z\right)\Delta x - \left(c_z + \frac{\partial c_z}{\partial x}\Delta x\right)\Delta z - c_x\,\Delta x$$

$$\Delta\Gamma_{zx} = \left(\frac{\partial c_x}{\partial z} - \frac{\partial c_z}{\partial x}\right)\Delta z\ \Delta x$$

$$\Delta A_{zx} = \Delta z\ \Delta x$$

$$\frac{\Delta\Gamma_{zx}}{\Delta A_{zx}} = \left(\frac{\Delta\Gamma}{\Delta A}\right)_{zx} = \frac{\partial c_x}{\partial z} - \frac{\partial c_z}{\partial x}$$

$$\lim_{\Delta A_{zx}\to 0}\left(\frac{\Delta\Gamma}{\Delta A}\right)_{zx} = \eta$$

$$\eta = 2\omega_y = \frac{\partial c_x}{\partial z} - \frac{\partial c_z}{\partial x} \tag{10.34}$$

Vorticity ζ and rotation ω_z: The circulation in the X-Y plane is

$$\Delta\Gamma_{xy} = c_x\,\Delta x + \left(c_y + \frac{\partial c_y}{\partial x}\Delta x\right)\Delta y - \left(c_x + \frac{\partial c_x}{\partial y}\Delta y\right)\Delta x - c_y\,\Delta y$$

$$\Delta\Gamma_{xy} = \left(\frac{\partial c_y}{\partial x} - \frac{\partial c_x}{\partial y}\right)\Delta x\ \Delta y$$

$$\Delta A_{xy} = \Delta x\ \Delta y$$

$$\frac{\Delta\Gamma_{xy}}{\Delta A_{xy}} = \left(\frac{\Delta\Gamma}{\Delta A}\right)_{xy} = \frac{\partial c_y}{\partial x} - \frac{\partial c_x}{\partial y}$$

$$\lim_{\Delta A_{xy}\to 0}\left(\frac{\Delta\Gamma}{\Delta A}\right)_{xy} = \zeta$$

$$\zeta = 2\omega_z = \frac{\partial c_y}{\partial x} - \frac{\partial c_x}{\partial y} \tag{10.35}$$

10.1.5 Navier-Stokes Equations

The momentum equations for three-dimensional unsteady, incompressible and viscous flow are given here for comparison with the corresponding equations for inviscid flow.

$$c_x\frac{\partial c_x}{\partial x} + c_y\frac{\partial c_x}{\partial y} + c_z\frac{\partial c_x}{\partial z} + \frac{\partial c_x}{\partial t}$$

$$= X - \frac{1}{\rho}\frac{\partial p}{\partial x} + \frac{\mu}{\rho}\left(\frac{\partial^2 c_x}{\partial x^2} + \frac{\partial^2 c_x}{\partial y^2} + \frac{\partial^2 c_x}{\partial z^2}\right) \tag{10.36}$$

$$c_x\frac{\partial c_y}{\partial x} + c_y\frac{\partial c_y}{\partial y} + c_z\frac{\partial c_y}{\partial z} + \frac{\partial c_y}{\partial t}$$

$$= Y - \frac{1}{\rho}\frac{\partial p}{\partial y} + \frac{\mu}{\rho}\left(\frac{\partial^2 c_y}{\partial x^2} + \frac{\partial^2 c_y}{\partial y^2} + \frac{\partial^2 c_y}{\partial z^2}\right) \tag{10.37}$$

$$c_x\frac{\partial c_z}{\partial x} + c_y\frac{\partial c_z}{\partial y} + c_z\frac{\partial c_z}{\partial z} + \frac{\partial c_z}{\partial t}$$

$$= Z - \frac{1}{\rho}\frac{\partial p}{\partial z} + \frac{\mu}{\rho}\left(\frac{\partial^2 c_z}{\partial x^2} + \frac{\partial^2 c_z}{\partial y^2} + \frac{\partial^2 c_z}{\partial z^2}\right) \tag{10.38}$$

10.2 CYLINDRICAL COORDINATE SYSTEM

Cartesian coordinate system is not convenient for dealing with problems of flow across bodies of revolution. A system employing, r, θ, x coordinates proves more convenient and useful in such cases: this is known as the cylindrical coordinate system. Here the coordinate x remains same as in the Cartesian system. In this system a point in the flow field is located by its radial, angular (tangential) and axial coordinates r, θ and x respectively.

An elemental control volume in cylindrical coordinate system is shown in Figure 10.7; its centre point has the coordinates r, θ and x. Its dimensions in the radial, tangential and axial directions are Δr, $r\,\Delta\theta$ and Δx respectively. Various flow parameters for the elemental control volume are:

velocities	$c_r,\ c_\theta,\ c_x$
accelerations	$a_r,\ a_\theta,\ a_x$
vorticities	$\xi,\ \eta,\ \zeta$
pressure forces	$F_r,\ F_\theta,\ F_x$
body forces	$X_r,\ X_\theta,\ X_x$

The pressure and density at the centre point are p and ρ respectively.

10.2.1 Continuity Equation

The law of conservation of mass is applied for the control volume shown in Figures 10.7 and 10.8. It is assumed that the outgoing mass from

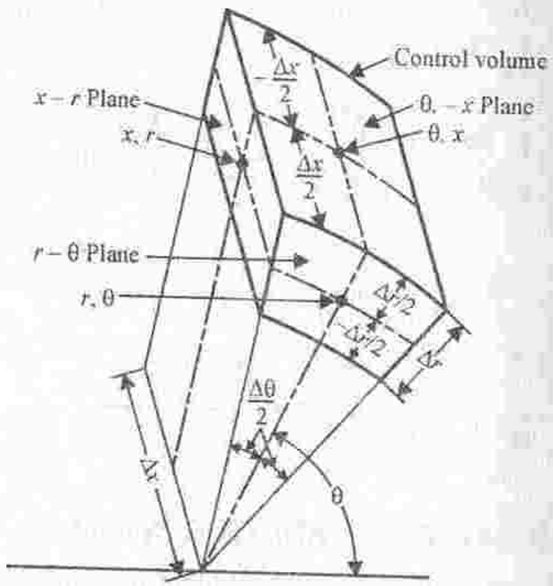

FIGURE 10.7 : An elemental control volume in cylindrical coordinates

the control volume is greater than the incoming mass, as a result the mass of the control volume decreases with time. Therefore, rate of decrease in mass of the control volume is

$$-\frac{\partial}{\partial t}(\rho r\ \Delta r\ \Delta\theta\ \Delta x) = -\Delta r\ \Delta\theta\ \Delta x\ \frac{\partial}{\partial t}(\rho r) \qquad (10.39)$$

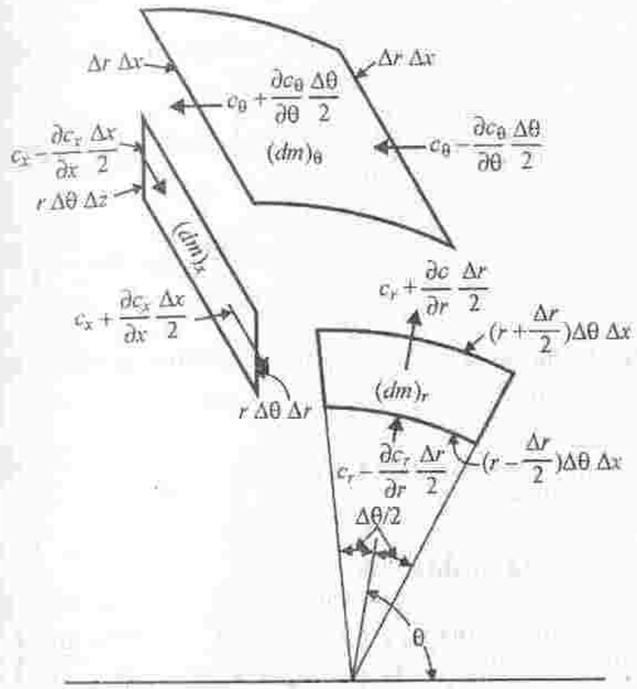

FIGURE 10.8 : Flow through an elemental control volume in cylindrical coordinates

The velocities and cross-sectional areas at various faces of the control volume are shown in Figure 10.8. Therefore, decrease in mass of the control volume due to flow in the r-direction

= (outgoing mass) – (incoming mass).

$$(dm)_r = \left(\rho + \frac{\partial\rho}{\partial r}\frac{\Delta r}{2}\right)\left(r + \frac{\Delta r}{2}\right)\Delta\theta\ \Delta x\left(c_r + \frac{\partial c_r}{\partial r}\frac{\Delta r}{2}\right)$$

$$-\left(\rho - \frac{\partial\rho}{\partial r}\frac{\Delta r}{2}\right)\left(r - \frac{\Delta r}{2}\right)\Delta\theta\ \Delta x\left(c_r - \frac{\partial c_r}{\partial r}\frac{\Delta r}{2}\right)$$

After cancelling some terms, neglecting products of small quantities and rearranging,

$$(dm)_r = \left[\, r\frac{\partial}{\partial r}(\rho c_r) + (\rho c_r)\frac{\partial r}{\partial r}\,\right]\Delta r\ \Delta\theta\ \Delta x$$

$$(dm)_r = \left[\frac{\partial}{\partial r} (\rho r c_r) \right] \Delta r \ \Delta\theta \ \Delta x \tag{10.40}$$

Decrease in the mass of control volume in the θ-direction is

$$(dm)_\theta = \left(\rho + \frac{\partial p}{\partial \theta} \frac{\Delta\theta}{2} \right) \Delta r \ \Delta x \left(c_\theta + \frac{\partial c_\theta}{\partial \theta} \frac{\Delta\theta}{2} \right)$$

$$- \left(\rho - \frac{\partial \rho}{\partial \theta} \frac{\Delta\theta}{2} \right) \Delta r \ \Delta x \left(c_\theta - \frac{\partial c_\theta}{\partial \theta} \frac{\Delta\theta}{2} \right)$$

On simplification and rearrangement the above expression reduces to

$$(dm)_\theta = \left[\frac{\partial}{\partial \theta} (\rho c_\theta) \right] \Delta r \ \Delta\theta \ \Delta x \tag{10.41}$$

Similarly for the x-direction,

$$(dm)_x = \left(\rho + \frac{\partial \rho}{\partial x} \frac{\Delta x}{2} \right) r \Delta\theta \ \Delta r \left(c_x + \frac{\partial c_x}{\partial x} \frac{\Delta x}{2} \right)$$

$$- \left(\rho - \frac{\partial \rho}{\partial x} \frac{\Delta x}{2} \right) r \Delta\theta \ \Delta r \left(c_x - \frac{\partial c_x}{\partial x} \frac{\Delta x}{2} \right)$$

After simplification and rearrangement it gives

$$(dm)_x = \left[\frac{\partial}{\partial x} (\rho c_x) \right] r \Delta r \ \Delta\theta \ \Delta x \tag{10.42}$$

The net rate of decrease in mass of the control volume, from Equations (10.40), (10.41) and (10.42) is

$$dm = (dm)_r + (dm)_\theta + (dm)_x$$

$$dm = \left[\frac{\partial}{\partial r} (\rho r c_r) + \frac{\partial}{\partial \theta} (\rho c_\theta) + r \frac{\partial}{\partial x} (\rho c_x) \right] \Delta r \ \Delta\theta \ \Delta x \tag{10.43}$$

According to the principle of conservation of mass Equations (10.39) and (10.43) must have identical values. Therefore,

$$\left[\frac{\partial}{\partial r} (\rho r c_r) + \frac{\partial}{\partial \theta} (\rho c_\theta) + r \frac{\partial}{\partial x} (\rho c_x) \right] \Delta r \ \Delta\theta \ \Delta x$$

$$= - \Delta r \ \Delta\theta \ \Delta x \frac{\partial}{\partial t} (\rho r)$$

This on rearrangement gives

$$\frac{\partial}{\partial r} (\rho r c_r) + \frac{1}{r} \frac{\partial}{\partial \theta} (\rho r c_\theta) + \frac{\partial}{\partial x} (\rho r c_x) + \frac{\partial}{\partial t} (\rho r) = 0 \tag{10.44}$$

This is the equation of continuity for three-dimensional, unsteady and compressible flow.

(*i*) *Steady flow:* For steady flow $\frac{\partial}{\partial t} (\rho r) = 0$ therefore, from Equation (10.44) we get

$$\frac{\partial}{\partial r} (\rho r c_r) + \frac{1}{r} \frac{\partial}{\partial \theta} (\rho r c_\theta) + \frac{\partial}{\partial x} (\rho r c_x) = 0 \tag{10.45}$$

(*ii*) *Incompressible flow:* If the flow is steady and incompressible,

$$\frac{\partial}{\partial t} (\rho r) = 0 \text{ and } \rho = \text{constant}$$

Therefore, Equation (10.44) yields

$$\frac{\partial}{\partial r} (r c_r) + \frac{1}{r} \frac{\partial}{\partial \theta} (r c_\theta) + \frac{\partial}{\partial x} (r c_x) = 0 \tag{10.46}$$

This is also expressed in the following form:

$$r \frac{\partial c_r}{\partial r} + c_r + \frac{\partial c_\theta}{\partial \theta} + r \frac{\partial c_x}{\partial x} = 0$$

$$\frac{\partial c_r}{\partial r} + \frac{c_r}{r} + \frac{1}{r} \frac{\partial c_\theta}{\partial \theta} + \frac{\partial c_x}{\partial x} = 0 \tag{10.47}$$

(*iii*) *Axisymmetric flow:* The flow is said to be axisymmetric when the variations in flow parameters are absent in the angular or tangential direction. For such a flow,

$$\frac{\partial}{\partial \theta} (\ ) = 0$$

This condition in Equation (10.45) gives

$$\frac{\partial}{\partial r} (\rho r c_r) + \frac{\partial}{\partial x} (\rho r c_x) = 0 \tag{10.48}$$

When the flow besides being axisymmetric is incompressible also,

$$\frac{\partial}{\partial r}(rc_r)+\frac{\partial}{\partial x}(rc_x)=0$$

$$\frac{\partial c_r}{\partial r}+\frac{c_r}{r}+\frac{\partial c_x}{\partial x}=0 \tag{10.49}$$

10.2.2 Radial Acceleration

The velocity components in cylindrical coordinates are given by the following relations:

$$c_r=\frac{dr}{dt} \tag{10.50}$$

$$\omega=\frac{d\theta}{dt} \tag{10.51}$$

$$c_\theta=r\omega=r\frac{d\theta}{dt} \tag{10.52}$$

$$c_x=\frac{dx}{dt} \tag{10.53}$$

Acceleration of a fluid particle is shown in Figure 10.9. The fluid particle moves from A to B during an infinitesimal time interval Δt.

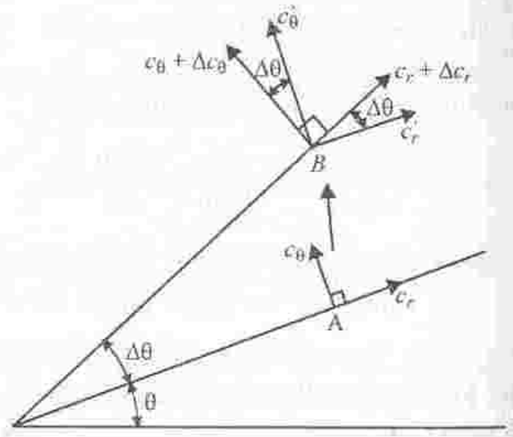

FIGURE 10.9 : Acceleration of a fluid particle in cylindrical coordinates

The velocity components at A are c_r, c_θ and c_x while at B these are $c_r+\Delta c_r$, $c_\theta+\Delta c_\theta$ and $c_x+\Delta c_x$. Since there is no change of direction

with time in the axial velocity component the acceleration in this direction is

$$a_x=\lim_{\Delta t\to 0}\frac{\Delta c_x}{\Delta t}=\frac{dc_x}{dt} \tag{10.54}$$

Acceleration in the r-direction is determined by the following method:

At point B the velocity component c_r' is parallel to the velocity vector c_r at A

$$c_r'=(c_r+\Delta c_r)\cos\Delta\theta-(c_\theta+\Delta c_\theta)\sin\Delta\theta$$

$$c_r'=c_r\cos\Delta\theta+\Delta c_r\cos\Delta\theta-c_\theta\sin\Delta\theta-\Delta c_\theta\sin\Delta\theta$$

For small values of $\Delta\theta$,

$$\cos\Delta\theta\approx 1,\ \sin\Delta\theta\approx\Delta\theta,$$

Therefore, $c_r'=c_r+\Delta c_r-c_\theta\,\Delta\theta-\Delta c_\theta\,\Delta\theta$

Neglecting $\Delta c_\theta\ \Delta\theta$,

$$c_r'-c_r=\Delta c_r-c_\theta\,\Delta\theta$$

Therefore, acceleration in the r-direction,

$$a_r=\lim_{\Delta t\to 0}\frac{c_r'-c_r}{\Delta t}=\lim_{\Delta t\to 0}\left(\frac{\Delta c_r}{\Delta t}-c_\theta\frac{\Delta\theta}{\Delta t}\right)$$

$$a_r=\frac{dc_r}{dt}-c_\theta\frac{d\theta}{dt} \tag{10.55}$$

Combination of Equations (10.52) and (10.55) gives

$$a_r=\frac{dc_r}{dt}-\frac{c_\theta^2}{r} \tag{10.56}$$

10.2.3 Tangential Acceleration

At point B the velocity component c_θ' is parallel to the tangential velocity vector c_θ at A.

$$c_\theta'=(c_r+\Delta c_r)\sin\Delta\theta+(c_\theta+\Delta c_\theta)\cos\Delta\theta$$

As stated before $\Delta\theta$ is small, therefore,

$$c_\theta'=c_r\,\Delta\theta+\Delta c_r\ \Delta\theta+c_\theta+\Delta c_\theta$$

Neglecting Δc_r, $\Delta\theta$,

$$c_\theta' - c_\theta = c_r \Delta\theta + \Delta c_\theta$$

Therefore, acceleration in the θ-direction,

$$a_\theta = \lim_{\Delta t \to 0} \frac{c_\theta' - c_\theta}{\Delta t} = \lim_{\Delta t \to 0} \left(c_r \frac{\Delta\theta}{\Delta t} + \frac{\Delta c_\theta}{\Delta t} \right)$$

$$a_\theta = c_r \frac{d\theta}{dt} + \frac{dc_\theta}{dt} \tag{10.57}$$

Combination of Equations (10.52) and (10.57) yields

$$a_\theta = \frac{c_r c_\theta}{r} + \frac{dc_\theta}{dt} \tag{10.58}$$

10.2.4 Momentum Equations

The velocity vectors c_r, c_θ and c_x are functions of r, θ, x and t. Therefore,

$$c_r = f(r, \theta, x, t) \tag{10.59 (a)}$$

$$c_\theta = f(r, \theta, x, t) \tag{10.59 (b)}$$

$$c_x = f(r, \theta, x, t) \tag{10.59 (c)}$$

From Equation (10.59 (*a*)),

$$dc_r = \frac{\partial c_r}{\partial r} dr + \frac{\partial c_r}{\partial \theta} d\theta + \frac{\partial c_r}{\partial x} dx + \frac{\partial c_r}{\partial t} dt$$

$$\frac{dc_r}{dt} = \frac{\partial c_r}{\partial r}\frac{dr}{dt} + \frac{\partial c_r}{\partial \theta}\frac{d\theta}{dt} + \frac{\partial c_r}{\partial x}\frac{dx}{dt} + \frac{\partial c_r}{\partial t}$$

Substituting from Equations (10.50), (10.52), (10.53) and (10.56) for dr/dt, $d\theta/dt$, dx/dt and dc_r/dt respectively,

$$a_r = c_r \frac{\partial c_r}{\partial r} + \frac{c_\theta}{r}\frac{\partial c_r}{\partial \theta} + c_x \frac{\partial c_r}{\partial x} + \frac{\partial c_r}{\partial t} - \frac{c_\theta^2}{r} \tag{10.60}$$

From Equation (10.59 (*b*)),

$$dc_\theta = \frac{\partial c_\theta}{\partial r} dr + \frac{\partial c_\theta}{\partial \theta} d\theta + \frac{\partial c_\theta}{\partial x} dx + \frac{\partial c_\theta}{\partial t} dt$$

$$\frac{dc_\theta}{dt} = \frac{\partial c_\theta}{\partial r}\frac{dr}{dt} + \frac{\partial c_\theta}{\partial \theta}\frac{d\theta}{dt} + \frac{\partial c_\theta}{\partial x}\frac{dx}{dt} + \frac{\partial c_\theta}{\partial t}$$

Substituting for dr/dt, $d\theta/dt$, dx/dt and dc_θ/dt from Equations (10.50), (10.52), (10.53), and (10.58) respectively,

$$a_\theta = c_r \frac{\partial c_\theta}{\partial r} + \frac{c_\theta}{r}\frac{\partial c_\theta}{\partial \theta} + c_x \frac{\partial c_\theta}{\partial x} + \frac{\partial c_\theta}{\partial t} + \frac{c_r c_\theta}{r} \tag{10.61}$$

From Equation (10.59 (*c*)),

$$dc_x = \frac{\partial c_x}{\partial r} dr + \frac{\partial c_x}{\partial \theta} d\theta + \frac{\partial c_x}{\partial x} dx + \frac{\partial c_x}{\partial t} dt$$

$$\frac{dc_x}{dt} = \frac{\partial c_x}{\partial r}\frac{dr}{dt} + \frac{\partial c_x}{\partial \theta}\frac{d\theta}{dt} + \frac{\partial c_x}{\partial x}\frac{dx}{dt} + \frac{\partial c_x}{\partial t}$$

Substituting for dr/dt, $d\theta/dt$, dx/dt and dc_x/dt from Equations (10.50), (10.52), (10.53) and (10.54) respectively

$$a_x = c_r \frac{\partial c_x}{\partial r} + \frac{c_\theta}{r}\frac{\partial c_x}{\partial \theta} + c_x \frac{\partial c_x}{\partial x} + \frac{\partial c_x}{\partial t} \tag{10.62}$$

Figure 10.10 shows the three faces of the elemental control surface separately; as shown in Figure 10.7 its dimensions in radial, tangential and axial directions are Δr, $r\Delta\theta$ and Δx respectively. For convenience in calculating the pressure forces the elemental surface in the $r - \theta$ plane is shown with parallel sides of length Δr. The elemental control surfaces

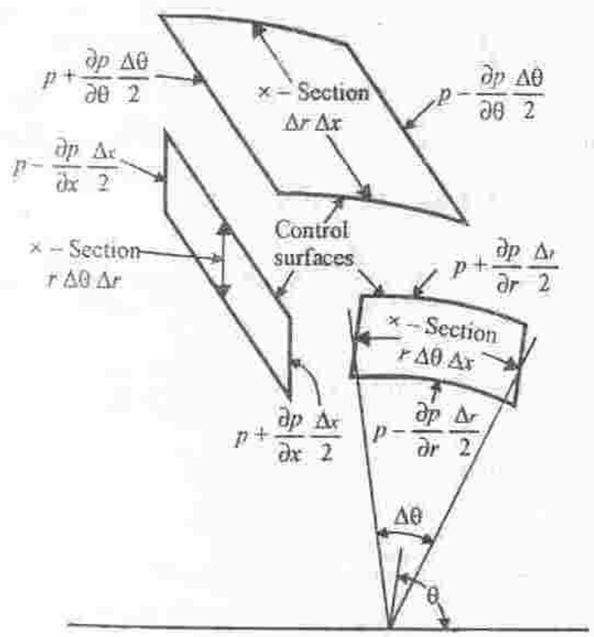

FIGURE 10.10: Pressure forces on the control surfaces in cylindrical coordinates

of Figure 10.7 have been shown separately in Figure 10.10 for convenience and clarity; the areas of cross-section (remaining constant) in the three directions are also shown.

The pressure at the centre point of the control volume is p; while the pressures acting on various faces of the control surface are shown in the figure.

The mass of the control volume is

$$m = \rho r\ \Delta\theta\ \Delta r\ \Delta x$$

The pressure force in the radial direction is

$$F_r = \left(p - \frac{\partial p}{\partial r}\ \frac{\Delta r}{2} \right) r\Delta\theta\ \Delta x - \left(p + \frac{\partial p}{\partial r}\ \frac{\Delta r}{2} \right) r\Delta\theta\ \Delta x$$

$$F_r = -r\Delta r\ \Delta\theta\ \Delta x \frac{\partial p}{\partial r} = -\frac{m}{\rho}\ \frac{\partial p}{\partial r} \qquad (10.63)$$

From Newton's second law of motion in the r-direction

$$ma_r = mX_r + F_r$$

Substituting from Equation (10.63),

$$a_r = X_r - \frac{1}{\rho}\ \frac{\partial p}{\partial r} \qquad (10.64)$$

Substituting Equation (10.60) in (10.64), we get

$$c_r \frac{\partial c_r}{\partial r} + \frac{c_\theta}{r}\ \frac{\partial c_r}{\partial \theta} + c_x \frac{\partial c_r}{\partial x} + \frac{\partial c_r}{\partial t} - \frac{c_\theta^2}{r} = X_r - \frac{1}{\rho}\ \frac{\partial p}{\partial r} \qquad (10.65)$$

The pressure force in the θ-direction is

$$F_\theta = \left(p - \frac{\partial p}{\partial \theta}\ \frac{\Delta\theta}{2} \right) \Delta r\ \Delta x - \left(p + \frac{\partial p}{\partial \theta}\ \frac{\Delta\theta}{2} \right) \Delta r\ \Delta x$$

$$F_\theta = -r\Delta r\ \Delta\theta\ \Delta x \frac{1}{r}\ \frac{\partial p}{\partial \theta} = -\frac{m}{\rho r}\ \frac{\partial p}{\partial \theta} \qquad (10.66)$$

$$ma_\theta = mX_\theta + F_\theta$$

$$a_\theta = X_\theta + \frac{1}{m} F_\theta$$

$$a_\theta = X_\theta - \frac{1}{\rho r}\ \frac{\partial p}{\partial \theta} \qquad (10.67)$$

Substituting from Equation (10.61)

$$c_r \frac{\partial c_\theta}{\partial r} + \frac{c_\theta}{r}\ \frac{\partial c_\theta}{\partial \theta} + c_x \frac{\partial c_\theta}{\partial x} + \frac{\partial c_\theta}{\partial t} + \frac{c_r c_\theta}{r} = X_\theta - \frac{1}{\rho r}\ \frac{\partial p}{\partial \theta} \qquad (10.68)$$

The pressure force in the x-direction is

$$F_x = \left(p - \frac{\partial p}{\partial x}\ \frac{\Delta x}{2} \right) r\Delta\theta\ \Delta r - \left(p + \frac{\partial p}{\partial x}\ \frac{\Delta x}{2} \right) r\Delta\theta\ \Delta r$$

$$F_x = -r\Delta\theta\ \Delta r\ \Delta x \frac{\partial p}{\partial x} = -\frac{m}{\rho}\ \frac{\partial p}{\partial x} \qquad (10.69)$$

$$ma_x = mX_x + F_x$$

$$a_x = X_x + \frac{1}{m} F_x$$

$$a_x = X_x - \frac{1}{\rho}\ \frac{\partial p}{\partial x} \qquad (10.70)$$

Substituting from Equation (10.62)

$$c_r \frac{\partial c_x}{\partial r} + \frac{c_\theta}{r}\ \frac{\partial c_x}{\partial \theta} + c_x \frac{\partial c_x}{\partial x} + \frac{\partial c_x}{\partial t} = X_x - \frac{1}{\rho}\ \frac{\partial p}{\partial x} \qquad (10.71)$$

Equations (10.65), (10.68) and (10.71) are the equations of motion in cylindrical coordinates for three-dimensional, unsteady and inviscid flow. Various simplifying assumptions are made depending on a given situation.

(*i*) **Steady flow:** If the body forces are assumed negligible and the flow is steady the equations of motion are reduced to the following form:

$$c_r \frac{\partial c_r}{\partial r} + \frac{c_\theta}{r}\ \frac{\partial c_r}{\partial \theta} + c_x \frac{\partial c_r}{\partial x} - \frac{c_\theta^2}{r} = -\frac{1}{\rho}\ \frac{\partial p}{\partial r} \qquad (10.72)$$

$$c_r \frac{\partial c_\theta}{\partial r} + \frac{c_\theta}{r}\ \frac{\partial c_\theta}{\partial \theta} + c_x \frac{\partial c_\theta}{\partial x} + \frac{c_r c_\theta}{r} = -\frac{1}{\rho r}\ \frac{\partial p}{\partial \theta} \qquad (10.73)$$

$$c_r \frac{\partial c_x}{\partial r} + \frac{c_\theta}{r}\ \frac{\partial c_x}{\partial \theta} + c_x \frac{\partial c_x}{\partial x} = -\frac{1}{\rho}\ \frac{\partial p}{\partial x} \qquad (10.74)$$

(*ii*) **Axisymmetric flow:** For three-dimensional, steady, inviscid and axisymmetric flow in the absence of body forces, by putting

$$\frac{\partial}{\partial \theta}\ (\ ) = 0$$

Equations (10.72), (10.73) and (10.74) give

$$c_r \frac{\partial c_r}{\partial r} + c_x \frac{\partial c_r}{\partial x} - \frac{c_\theta^2}{r} = -\frac{1}{\rho}\frac{\partial p}{\partial r} \tag{10.75}$$

$$c_r \frac{\partial c_\theta}{\partial r} + c_r \frac{\partial c_\theta}{\partial x} + \frac{c_r c_\theta}{r} = 0 \tag{10.76}$$

$$c_r \frac{\partial c_x}{\partial r} + c_x \frac{\partial c_x}{\partial x} = -\frac{1}{\rho}\frac{\partial p}{\partial x} \tag{10.77}$$

10.2.5 Vorticity Components

Figure 10.11 shows the three vorticity and velocity components in various planes within the elemental control surface. For convenience and clarity the three planes situated at the centre point with coordinates

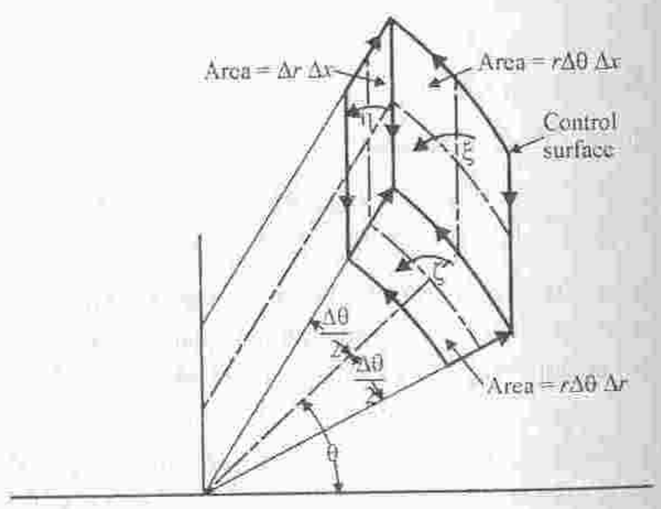

FIGURE 10.11 : Directions of the velocity and vorticity vectors in the three planes

r, θ and x are shown separated apart in Figure 10.12; the velocity components at this centre point are c_r, c_θ and c_x. Velocity components at each of the edges, in a given plane as derived from the values at the centre point are also shown in Figure 10.12.

The vorticity component in each of these planes is now determined from the line integral taken around the given plane. The direction of the vorticities and the areas of the planes containing them are shown in Figure 10.11.

Vorticity ξ and rotation ω_r: The circulation in the θ-x plane (Figure 10.12) is given by

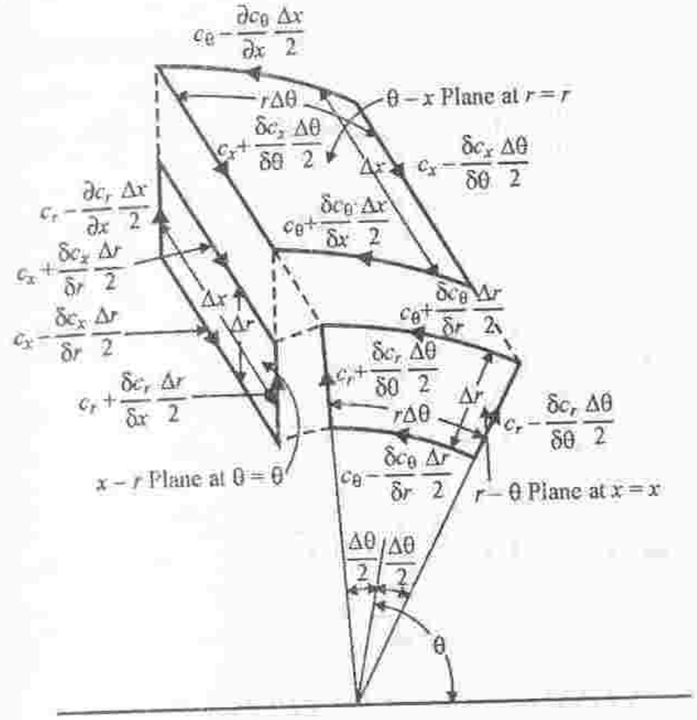

FIGURE 10.12 : Vorticity components ξ, η and ζ in cylindrical coordinates

$$\Delta\Gamma_{\theta x} = \left(c_\theta - \frac{\partial c_\theta}{\partial x}\frac{\Delta x}{2}\right) r\Delta\theta + \left(c_x + \frac{\partial c_x}{\partial\theta}\frac{\Delta\theta}{2}\right)\Delta x$$
$$-\left(c_\theta + \frac{\partial c_\theta}{\partial x}\frac{\Delta x}{2}\right) r\Delta\theta - \left(c_x - \frac{\partial c_x}{\partial\theta}\frac{\Delta\theta}{2}\right)\Delta x$$

$$\Delta\Gamma_{\theta x} = \left(\frac{1}{r}\frac{\partial c_x}{\partial\theta} - \frac{\partial c_\theta}{\partial x}\right) r\Delta\theta\ \Delta x$$

Now $\Delta A_{\theta x} = r\Delta\theta\ \Delta x$, therefore,

$$\frac{\Delta\Gamma_{\theta x}}{\Delta A_{\theta x}} = \left(\frac{\Delta\Gamma}{\Delta A}\right)_{\theta x} = \frac{1}{r}\frac{\partial c_x}{\partial\theta} - \frac{\partial c_\theta}{\partial x}$$

But $$\lim_{\Delta A_{\theta x}\to 0}\left(\frac{\Delta\Gamma}{\Delta A}\right)_{\theta x} = \xi,$$

Therefore,
$$\xi = \frac{1}{r}\frac{\partial c_x}{\partial\theta} - \frac{\partial c_\theta}{\partial x} \tag{10.78}$$

Vorticity η *and rotation* ω_θ*:* The circulation in the x-r plane is

$$\Delta\Gamma_{xr} = \left(c_r + \frac{\partial c_r}{\partial x}\frac{\Delta x}{2}\right)\Delta r - \left(c_x + \frac{\partial c_x}{\partial r}\frac{\Delta r}{2}\right)\Delta x - \left(c_r - \frac{\partial c_r}{\partial x}\frac{\Delta x}{2}\right)\Delta r + \left(c_x - \frac{\partial c_x}{\partial r}\frac{\Delta r}{2}\right)\Delta x$$

$$\Delta\Gamma_{xr} = \left(\frac{\partial c_r}{\partial x} - \frac{\partial c_x}{\partial r}\right)\Delta x\ \Delta r$$

$$\Delta A_{xr} = \Delta x\ \Delta r$$

$$\frac{\Delta\Gamma_{xr}}{\Delta A_{xr}} = \left(\frac{\Delta\Gamma}{\Delta A}\right)_{xr} = \frac{\partial c_r}{\partial x} - \frac{\partial c_x}{\partial r}$$

$$\lim_{\Delta A_{xr}\to 0}\left(\frac{\Delta\Gamma}{\Delta A}\right)_{xr} = \eta$$

$$\eta = \frac{\partial c_r}{\partial x} - \frac{\partial c_x}{\partial r} \tag{10.79}$$

Vorticity ζ *and rotation* ω_x*:* The circulation in the r-θ plane is

$$\Delta\Gamma_{r\theta} = \left(c_\theta + \frac{\partial c_\theta}{\partial r}\frac{\Delta r}{2}\right)\left(r + \frac{\Delta r}{2}\right)\Delta\theta - \left(c_r + \frac{\partial c_r}{\partial\theta}\frac{\Delta\theta}{2}\right)\Delta r - \left(c_\theta - \frac{\partial c_\theta}{\partial r}\frac{\Delta r}{2}\right)\left(r - \frac{\Delta r}{2}\right)\Delta\theta + \left(c_r - \frac{\partial c_r}{\partial\theta}\frac{\Delta\theta}{2}\right)\Delta r$$

$$\Delta\Gamma_{r\theta} = \left(\frac{\partial c_\theta}{\partial r} + \frac{c_\theta}{r} - \frac{1}{r}\frac{\partial c_r}{\partial\theta}\right) r\,\Delta\theta\ \Delta r$$

$$\Delta A_{r\theta} = r\,\Delta\theta\ \Delta r$$

$$\frac{\Delta\Gamma_{r\theta}}{\Delta A_{r\theta}} = \left(\frac{\Delta\Gamma}{\Delta A}\right)_{r\theta} = \frac{\partial c_\theta}{\partial r} + \frac{c_\theta}{r} - \frac{1}{r}\frac{\partial c_r}{\partial\theta}$$

$$\lim_{\Delta A_{r\theta}\to 0}\left(\frac{\Delta\Gamma}{\Delta A}\right)_{r\theta} = \zeta$$

$$\zeta = \frac{\partial c_\theta}{\partial r} - \frac{1}{r}\frac{\partial c_r}{\partial\theta} + \frac{c_\theta}{r} \tag{10.80}$$

10.2.6 Navier-Stokes Equations

Three-dimensional equations of motion for viscous incompressible flow in cylindrical coordinates are given in the following:

$$c_r\frac{\partial c_r}{\partial r} + \frac{c_\theta}{r}\frac{\partial c_r}{\partial\theta} + c_x\frac{\partial c_r}{\partial x} - \frac{c_\theta^2}{r} + \frac{\partial c_r}{\partial t} = X_r - \frac{1}{\rho}\frac{\partial p}{\partial r} + \frac{\mu}{\rho}\left(\frac{\partial^2 c_r}{\partial r^2} + \frac{1}{r}\frac{\partial c_r}{\partial r} - \frac{c_r}{r^2} + \frac{1}{r^2}\frac{\partial^2 c_r}{\partial\theta^2} - \frac{2}{r^2}\frac{\partial c_\theta}{\partial\theta} + \frac{\partial^2 c_r}{\partial x^2}\right) \tag{10.81}$$

$$c_r\frac{\partial c_\theta}{\partial r} + \frac{c_\theta}{r}\frac{\partial c_\theta}{\partial\theta} + c_x\frac{\partial c_\theta}{\partial x} + \frac{c_\theta c_r}{r} + \frac{\partial c_\theta}{\partial t} = X_\theta - \frac{1}{\rho r}\frac{\partial p}{\partial\theta} + \frac{\mu}{\rho}\left(\frac{\partial^2 c_\theta}{\partial r^2} + \frac{1}{r}\frac{\partial c_\theta}{\partial r} - \frac{c_\theta}{r^2} + \frac{1}{r^2}\frac{\partial^2 c_\theta}{\partial\theta^2} + \frac{2}{r^2}\frac{\partial c_r}{\partial\theta} + \frac{\partial^2 c_\theta}{\partial x^2}\right) \tag{10.82}$$

$$c_r\frac{\partial c_x}{\partial r} + \frac{c_\theta}{r}\frac{\partial c_x}{\partial\theta} + c_x\frac{\partial c_x}{\partial x} + \frac{\partial c_x}{\partial t} = X_x - \frac{1}{\rho}\frac{\partial p}{\partial x} + \frac{\mu}{\rho}\left(\frac{\partial^2 c_x}{\partial r^2} + \frac{1}{r}\frac{\partial c_x}{\partial r} + \frac{1}{r^2}\frac{\partial^2 c_x}{\partial\theta^2} + \frac{\partial^2 c_x}{\partial x^2}\right) \tag{10.83}$$

10.3 POTENTIAL FUNCTION

Flow fields under some conditions in a variety of situations are represented by ϕ = constant and ψ = constant lines; these lines are normal to each other and provide a convenient method for obtaining the velocity components.

Equations for the functions ϕ and ψ will be derived in the following sections:

10.3.1 Definition

The function ϕ is a point function; its definition is given here.

Figure 10.13 shows two points 1 and 2 in a two dimensional flow field; these are connected by three paths A, B and C. In order to define the function ϕ the flow is assumed irrotational; therefore, the circulation around any closed circuit in the flow field is zero.

The line integral around the circuit $1A\ 2B1$ is given by

$$\int_{A\,1}^{2} c\cos\theta\,dl + \int_{B\,2}^{1} c\cos\theta\,dl = 0$$

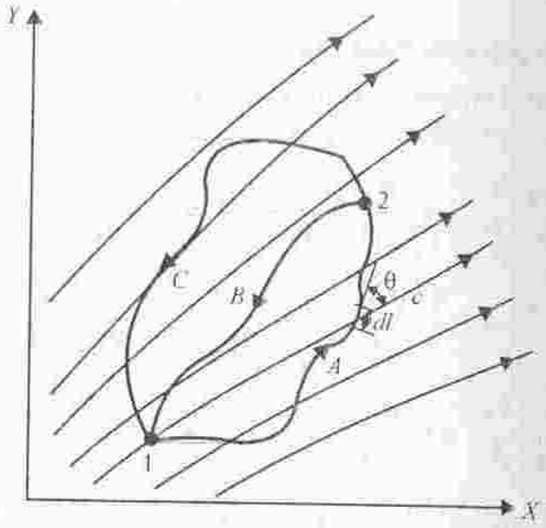

FIGURE 10.13 : Line integral through different paths

Similarly for irrotational flow

$$\int_{A}^{2}{}_{1} c\cos\theta\, dl + \int_{C}^{1}{}_{2} c\cos\theta\, dl = 0$$

By substraction the above two equations give

$$\int_{B}^{1}{}_{2} c\cos\theta\, dl = \int_{C}^{1}{}_{2} c\cos\theta\, dl \qquad (10.84)$$

It is seen from Equation (10.84) that the line integrals through paths B and C are same *i.e.*, they are independent of the path. This is the definition of a point function ϕ; hence the differential of this function is an exact differential:

$$d\phi = c\cos\theta\, dl$$

$$\frac{d\phi}{dl} = c\cos\theta = \text{velocity component along } l \qquad (10.85)$$

Therefore, the velocity potential function ϕ is a point function whose derivative in a given direction equals the velocity component in that direction. Thus

$$c_x = \phi_x = \frac{\partial\phi}{\partial x} \qquad (10.86)$$

$$c_y = \phi_y = \frac{\partial\phi}{\partial y} \qquad (10.87)$$

$$c_z = \phi_z = \frac{\partial\phi}{\partial z} \qquad (10.88)$$

Substituting Equations (10.87) and (10.88) in (10.33) for irrotational flow gives

$$\xi = \frac{\partial}{\partial y}\left(\frac{\partial\phi}{\partial z}\right) - \frac{\partial}{\partial z}\left(\frac{\partial\phi}{\partial y}\right) = 0$$

$$\frac{\partial^2\phi}{\partial y\,\partial z} = \frac{\partial^2\phi}{\partial z\,\partial y} \qquad (10.89)$$

Similarly making $\eta = 0$ and $\zeta = 0$

$$\frac{\partial^2\phi}{\partial z\,\partial x} = \frac{\partial^2\phi}{\partial x\,\partial z} \qquad (10.90)$$

$$\frac{\partial^2\phi}{\partial x\,\partial y} = \frac{\partial^2\phi}{\partial y\,\partial x} \qquad (10.91)$$

The above equations prove that ϕ is a continuous point function because the order of differentiation is immaterial.

10.3.2 Potential Function Equation in Cartesian Coordinates

Here the differential equation for three-dimensional flow is derived in terms of the potential function. Following assumptions are used:

(*a*) isentropic, steady and inviscid flow,
(*b*) irrotational flow,
(*c*) perfect gas and
(*d*) absence of body forces

Substituting Equations (10.86), (10.87) and (10.88) in (10.9) we get,

$$\frac{\partial}{\partial x}(\rho\phi_x) + \frac{\partial}{\partial y}(\rho\phi_y) + \frac{\partial}{\partial z}(\rho\phi_z) = 0$$

$$\rho\phi_{xx} + \phi_x\frac{\partial\rho}{\partial x} + \rho\phi_{yy} + \phi_y\frac{\partial\rho}{\partial y} + \rho\phi_{zz} + \phi_z\frac{\partial\rho}{\partial z} = 0$$

$$\rho\,(\phi_{xx} + \phi_{yy} + \phi_{zz}) + \phi_x\frac{\partial\rho}{\partial x} + \phi_y\frac{\partial\rho}{\partial y} + \phi_z\frac{\partial\rho}{\partial z} = 0 \qquad (10.92)$$

For three-dimensional flow,

$$c^2 = c_x^2 + c_y^2 + c_z^2$$

The momentum equation gives

$$dp = -\rho c\, dc = -\frac{1}{2}\rho d(c^2)$$

$$dp = -\frac{1}{2}\rho d(c_x^2 + c_y^2 + c_z^2) \tag{10.93}$$

For isentropic flow,

$$a^2 = \left(\frac{\partial p}{\partial \rho}\right)_s = \frac{dp}{d\rho}$$

$$d\rho = \frac{dp}{a^2} = -\frac{\rho}{2a^2} d(c_x^2 + c_y^2 + c_z^2)$$

$$d\rho = -\frac{\rho}{2a^2} d(\phi_x^2 + \phi_y^2 + \phi_z^2) \tag{10.94}$$

Equation (10.94) gives the following derivatives of the density in z-directions:

$$\frac{\partial \rho}{\partial x} = -\frac{\rho}{a^2}(\phi_x \phi_{xx} + \phi_y \phi_{xy} + \phi_z \phi_{xz}) \tag{10.95}$$

$$\frac{\partial \rho}{\partial y} = -\frac{\rho}{a^2}(\phi_x \phi_{yx} + \phi_y \phi_{yy} + \phi_z \phi_{yz}) \tag{10.96}$$

$$\frac{\partial \rho}{\partial z} = -\frac{\rho}{a^2}(\phi_x \phi_{zx} + \phi_y \phi_{zy} + \phi_z \phi_{zz}) \tag{10.97}$$

Substitution of Equations (10.95), (10.96) and (10.97) in (10.92) gives

$$\phi_{xx} + \phi_{yy} + \phi_{zz} - \frac{1}{a^2}(\phi_x^2 \phi_{xx} + \phi_x \phi_y \phi_{xy} + \phi_x \phi_z \phi_{xz}) - \frac{1}{a^2}(\phi_y \phi_x \phi_{yx} + \phi_y^2 \phi_{yy} + \phi_y \phi_z \phi_{yz}) - \frac{1}{a^2}(\phi_z \phi_x \phi_{zx} + \phi_z \phi_y \phi_{zy} + \phi_z^2 \phi_{zz}) = 0$$

Now $\phi_{xy} = \phi_{yx}$ (10.91)

$$\phi_{xz} = \phi_{zx} \tag{10.90}$$

$$\phi_{yz} = \phi_{zy} \tag{10.89}$$

Therefore, on rearrangement following final form of the potential flow equation is obtained:

$$\left(1 - \frac{\phi_x^2}{a^2}\right)\phi_{xx} + \left(1 - \frac{\phi_y^2}{a^2}\right)\phi_{yy} + \left(1 - \frac{\phi_z^2}{a^2}\right)\phi_{zz} - \frac{2\phi_x \phi_y \phi_{xy}}{a^2} - \frac{2\phi_y \phi_z \phi_{yz}}{a^2} - \frac{2\phi_z \phi_x \phi_{zx}}{a^2} = 0 \tag{10.98}$$

Incompressible flow: For incompressible flow the velocity of sound is much greater than the gas velocity components. Therefore, in Equation (10.98)

$$a^2 \approx \infty$$

$$\phi_{xx} + \phi_{yy} + \phi_{zz} = 0$$

$$\frac{\partial^2 \phi}{\partial x^2} + \frac{\partial^2 \phi}{\partial y^2} + \frac{\partial^2 \phi}{\partial z^2} = 0 \tag{10.99}$$

This is the Laplace's equation for three-dimensional incompressible flow.

10.3.3 Potential Function Equation in Cylindrical Coordinates

The velocity components in terms of the potential function in the cylindrical coordinate system are given by

$$c_r = \phi_r = \frac{\partial \phi}{\partial r} \tag{10.100}$$

$$c_\theta = \frac{1}{r}\phi_\theta = \frac{1}{r}\frac{\partial \phi}{\partial \theta} \tag{10.101}$$

$$c_x = \phi_x = \frac{\partial \phi}{\partial x} \tag{10.102}$$

Equations (10.78), (10.79) and (10.80) for irrotational flow give

$$\xi = 0$$

$$\eta = 0$$

$$\zeta = 0$$

Therefore, Equations (10.100), (10.101) and (10.102) with the above conditions give

$$\phi_{r\theta} = \phi_{\theta r} \qquad (10.103\ (a))$$

$$\phi_{rx} = \phi_{xr} \qquad (10.103\ (b))$$

$$\phi_{x\theta} = \phi_{\theta x} \qquad (10.103\ (c))$$

These equations again prove that the order of differentiation is immaterial and ϕ is a continuous point function.

The continuity equation given by Equation (10.45) for steady flow in cylindrical coordinates is

$$\frac{\partial}{\partial r}(\rho r c_r) + \frac{1}{r}\frac{\partial}{\partial \theta}(\rho r c_\theta) + \frac{\partial}{\partial x}(\rho r c_x) = 0$$

Substituting from Equations (10.100), (10.101) and (10.102) in the above equation,

$$\frac{\partial}{\partial r}(\rho r \phi_r) + \frac{1}{r}\frac{\partial}{\partial \theta}(\rho \phi_\theta) + \frac{\partial}{\partial x}(\rho r \phi_x) = 0$$

$$(\rho r)\,\phi_{rr} + r\phi_r \frac{\partial \rho}{\partial r} + \rho\phi_r + \frac{1}{r}\left(\rho\phi_{\theta\theta} + \phi_\theta \frac{\partial \rho}{\partial \theta}\right) + r\left(\rho\phi_{xx} + \phi_x \frac{\partial \rho}{\partial x}\right) = 0$$

This on rearrangement gives

$$\rho\left(r\phi_{rr} + \phi_r + \frac{\phi_{\theta\theta}}{r} + r\phi_{xx}\right) + r\phi_r \frac{\partial \rho}{\partial r} + \frac{\phi_\theta}{r}\frac{\partial \rho}{\partial \theta} + r\phi_x \frac{\partial \rho}{\partial x} = 0 \qquad (10.104)$$

Equation (10.94) in cylindrical coordinates gives

$$d\rho = -\frac{\rho}{2a^2}\, d\,(c_r^2 + c_\theta^2 + c_x^2)$$

$$d\rho = -\frac{\rho}{2a^2}\, d\left(\phi_r^2 + \frac{\phi_\theta^2}{r^2} + \phi_x^2\right) \qquad (10.105)$$

Equation (10.105) gives the following derivatives:

$$\frac{\partial \rho}{\partial r} = -\frac{\rho}{a^2}\left(\phi_r \phi_{rr} + \frac{\phi_\theta \phi_{r\theta}}{r^2} - \frac{\phi_\theta^2}{r^3} + \phi_x \phi_{rx}\right) \qquad (10.106)$$

$$\frac{\partial \rho}{\partial \theta} = -\frac{\rho}{a^2}\left(\phi_r \phi_{\theta r} + \frac{\phi_\theta \phi_{\theta\theta}}{r^2} + \phi_x \phi_{\theta x}\right) \qquad (10.107)$$

$$\frac{\partial \rho}{\partial x} = -\frac{\rho}{a^2}\left(\phi_r \phi_{xr} + \frac{\phi_\theta \phi_{x\theta}}{r^2} + \phi_x \phi_{xx}\right) \qquad (10.108)$$

Substituting from Equations (10.106), (10.107) and (10.108) in (10.104),

$$r\phi_{rr} + \phi_r + \frac{\phi_{\theta\theta}}{r} + r\phi_{xx}$$

$$-\frac{1}{a^2}\left(r\phi_r^2 \phi_{rr} + \frac{\phi_r \phi_\theta \phi_{r\theta}}{r} - \frac{\phi_r \phi_\theta^2}{r^2} + r\phi_r \phi_x \phi_{rx}\right)$$

$$-\frac{1}{a^2}\left(\frac{\phi_\theta \phi_r \phi_{\theta r}}{r} + \frac{\phi_\theta^2 \phi_{\theta\theta}}{r^3} + \frac{\phi_\theta \phi_x \phi_{\theta x}}{r}\right)$$

$$-\frac{1}{a^2}\left(r\phi_x \phi_r \phi_{xr} + \frac{\phi_x \phi_\theta \phi_{x\theta}}{r} + r\phi_x^2 \phi_{xx}\right) = 0$$

Making use of Equation (10.103) and rearranging,

$$\left(1 - \frac{\phi_r^2}{a^2}\right)\phi_{rr} + \left(1 - \frac{\phi_\theta^2}{r^2 a^2}\right)\frac{\phi_{\theta\theta}}{r^2} + \left(1 - \frac{\phi_x^2}{a^2}\right)\phi_{xx}$$

$$+\left(1 + \frac{\phi_\theta^2}{r^2 a^2}\right)\frac{\phi_r}{r} - \frac{2\phi_r \phi_\theta \phi_{r\theta}}{r^2 a^2} - \frac{2\phi_\theta \phi_x \phi_{\theta x}}{r^2 a^2} - \frac{2\phi_x \phi_r \phi_{xr}}{a^2} = 0 \qquad (10.109)$$

Incompresible flow: Using $a^2 \approx \infty$ in Equation (10.109)

$$\phi_{rr} + \frac{1}{r^2}\phi_{\theta\theta} + \phi_{xx} + \frac{1}{r}\phi_r = 0$$

$$\frac{\partial^2 \phi}{\partial r^2} + \frac{1}{r^2}\frac{\partial^2 \phi}{\partial \theta^2} + \frac{\partial^2 \phi}{\partial x^2} + \frac{1}{r}\frac{\partial \phi}{\partial r} = 0 \qquad (10.110)$$

Axisymmetric flow: Here the derivatives in the θ-direction are zero i.e.,

$$\frac{\partial}{\partial \theta}(\ ) = 0$$

Therefore, Equations (10.109) and (10.110) reduce to

$$\left(1-\frac{\phi_r^2}{a^2}\right)\phi_{rr}+\left(1-\frac{\phi_x^2}{a^2}\right)\phi_{xx}+\frac{\phi_r}{r}-\frac{2\phi_x\phi_r\phi_{xr}}{a^2}=0 \qquad (10.111)$$

$$\frac{\partial^2\phi}{\partial r^2}+\frac{\partial^2\phi}{\partial x^2}+\frac{1}{r}\frac{\partial\phi}{\partial r}=0 \qquad (10.112)$$

(for incompressible flow)

10.4 STREAM FUNCTION

Another point function known as the stream function (ψ) exists if the continuity equation for two-dimensional steady flow is satisfied. It is proved in the text books on Fluid Mechanics that constant ψ-lines are identical with streamlines and the change in stream function between two constant ψ-lines represents mass flow between these lines.

The stream function in Cartesian coordinates is defined by the following velocity components:

$$c_x=\frac{\rho_0}{\rho}\psi_y=\frac{\rho_0}{\rho}\frac{\partial\psi}{\partial y} \qquad (10.113)$$

$$c_y=-\frac{\rho_0}{\rho}\psi_x=-\frac{\rho_0}{\rho}\frac{\partial\psi}{\partial x} \qquad (10.114)$$

(ρ_0 in the above equations is constant).

The continuity equation for two-dimensional steady flow (from Equation (10.9)) is

$$\frac{\partial}{\partial x}(\rho c_x)+\frac{\partial}{\partial y}(\rho c_y)=0$$

Substituting Equations (10.113) and (10.114) in this equation gives

$$\rho_0\frac{\partial}{\partial x}\left(\frac{\partial\psi}{\partial y}\right)-\rho_0\frac{\partial}{\partial y}\left(\frac{\partial\psi}{\partial x}\right)=0$$

$$\frac{\partial^2\psi}{\partial x\,\partial y}=\frac{\partial^2\psi}{\partial y\,\partial x} \qquad (10.115)$$

This shows that the order of differentiation is immaterial and therefore ψ is a continuous point function.

10.4.1 Stream Function equation in Cartesian Coordinates

In this section equation of motion in terms of the stream function is derived for steady, two-dimensional and irrotational flow of a perfect gas.

Equation (10.35) for irrotational flow gives

$$\zeta=\frac{\partial c_y}{\partial x}-\frac{\partial c_x}{\partial y}=0$$

Substitution of Equations (10.113) and (10.114) in the above equation gives

$$\frac{\partial}{\partial x}\left(-\frac{\rho_0}{\rho}\frac{\partial\psi}{\partial x}\right)-\frac{\partial}{\partial y}\left(\frac{\rho_0}{\rho}\frac{\partial\psi}{\partial y}\right)=0$$

$$-\frac{1}{\rho}\frac{\partial^2\psi}{\partial x^2}+\frac{1}{\rho^2}\frac{\partial\psi}{\partial x}\frac{\partial\rho}{\partial x}-\frac{1}{\rho}\frac{\partial^2\psi}{\partial y^2}+\frac{1}{\rho^2}\frac{\partial\psi}{\partial y}\frac{\partial\rho}{\partial y}=0$$

In short form this can be expressed as

$$\rho(\psi_{xx}+\psi_{yy})=\left(\psi_x\frac{\partial\rho}{\partial x}+\psi_y\frac{\partial\rho}{\partial y}\right) \qquad (10.116)$$

The velocity vector in terms of its components is given by

$$c^2=c_x^2+c_y^2$$

$$c^2=\left(\frac{\rho_0}{\rho}\right)^2(\psi_x^2+\psi_y^2) \qquad (10.117)$$

The momentum equation gives

$$d\rho=-\frac{\rho}{2a^2}dc^2$$

$$d\rho=-\frac{\rho}{2a^2}d\left[\left(\frac{\rho_0}{\rho}\right)^2(\psi_x^2+\psi_y^2)\right] \qquad (10.118)$$

This gives the following partial derivatives of density:

$$\frac{\partial\rho}{\partial x}=-\frac{\rho}{a^2}\left[\left(\frac{\rho_0}{\rho}\right)^2(\psi_x\psi_{xx}+\psi_y\psi_{xy})-\left(\frac{\rho_0}{\rho}\right)^2\frac{1}{\rho}(\psi_x^2+\psi_y^2)\frac{\partial\rho}{\partial x}\right],$$

After rearrangement the above relation yields

$$\frac{\partial \rho}{\partial x} = \frac{-\frac{\rho}{a^2}\left(\frac{\rho_0}{\rho}\right)^2 (\psi_x \psi_{xx} + \psi_y \psi_{xy})}{1 - \frac{1}{a^2}\left(\frac{\rho_0}{\rho}\right)^2 (\psi_x^2 + \psi_y^2)} \tag{10.119}$$

Similarly the derivative in the y-direction is obtained as

$$\frac{\partial \rho}{\partial y} = \frac{-\frac{\rho}{a^2}\left(\frac{\rho_0}{\rho}\right)^2 (\psi_x \psi_{yx} + \psi_y \psi_{yy})}{1 - \frac{1}{a^2}\left(\frac{\rho_0}{\rho}\right)^2 (\psi_x^2 + \psi_y^2)} \tag{10.120}$$

Substitution of Equations (10.119) and (10.120) in (10.116) after rearrangement gives

$$(\psi_{xx} + \psi_{yy})\left[1 - \frac{1}{a^2}\left(\frac{\rho_0}{\rho}\right)^2 (\psi_x^2 + \psi_y^2)\right]$$

$$+ \frac{1}{a^2}\left(\frac{\rho_0}{\rho}\right)^2 (\psi_x^2 \psi_{xx} + \psi_x \psi_y \psi_{xy})$$

$$+ \frac{1}{a^2}\left(\frac{\rho_0}{\rho}\right)^2 (\psi_y \psi_x \psi_{yx} + \psi_y^2 \psi_{yy}) = 0$$

Noting that $\psi_{xy} = \psi_{yx}$ (Equation (10.115)) and simplifying,

$$\left[1 - \frac{1}{a^2}\left(\frac{\rho_0}{\rho}\right)^2 \psi_y^2\right]\psi_{xx} + \left[1 - \frac{1}{a^2}\left(\frac{\rho_0}{\rho}\right)^2 \psi_x^2\right]\psi_{yy}$$

$$+ \frac{2}{a^2}\left(\frac{\rho_0}{\rho}\right)^2 \psi_x \psi_y \psi_{xy} = 0 \tag{10.121}$$

Incompressible flow: In incompressible flow $a^2 = \infty$, therefore, Equation (10.121) yields

$$\psi_{xx} + \psi_{yy} = 0$$

$$\frac{\partial^2 \psi}{\partial x^2} + \frac{\partial^2 \psi}{\partial y^2} = 0 \tag{10.122}$$

10.4.2 Steam Function Equation in Cylindrical Coordinates

In order to satisfy the conditions for the stream function the flow is assumed axisymmetric, therefore, $\frac{\partial}{\partial \theta}(\ ) = 0$.

The two velocity components in terms of the stream function in the cylindrical coordinate system are given by

$$c_r = \frac{\rho_0}{\rho}\frac{1}{r}\psi_x = \frac{\rho_0}{\rho}\frac{1}{r}\frac{\partial \psi}{\partial x} \tag{10.123}$$

$$c_x = -\frac{\rho_0}{\rho}\frac{1}{r}\psi_r = -\frac{\rho_0}{\rho}\frac{1}{r}\frac{\partial \psi}{\partial r} \tag{10.124}$$

The continuity equation given by Equation (10.48) for steady and axisymmetric flow is

$$\frac{\partial}{\partial r}(\rho r c_r) + \frac{\partial}{\partial x}(\rho r c_x) = 0$$

Substituting Equations (10.123) and (10.124) in the above equation we get

$$\frac{\partial}{\partial r}\left(\frac{\partial \psi}{\partial x}\right) + \frac{\partial}{\partial x}\left(-\frac{\partial \psi}{\partial r}\right) = 0$$

$$\frac{\partial^2 \psi}{\partial r\, \partial x} = \frac{\partial^2 \psi}{\partial x\, \partial r} \tag{10.125}$$

Equation (10.125) shows that the order of differentiation is immaterial; therefore ψ is a continuous point function.

Equation (10.79) for irrotational flow gives

$$\eta = \frac{\partial c_r}{\partial x} - \frac{\partial c_x}{\partial r} = 0$$

Substituting Equations (10.123) and (10.124) in the above relation we get

$$\frac{\partial}{\partial x}\left(\frac{\rho_0}{\rho}\frac{1}{r}\frac{\partial \psi}{\partial x}\right) - \frac{\partial}{\partial r}\left(-\frac{\rho_0}{\rho}\frac{1}{r}\frac{\partial \psi}{\partial r}\right) = 0$$

$$\frac{\rho_0}{\rho}\frac{1}{r}\frac{\partial^2 \psi}{\partial x^2} - \frac{\rho_0}{\rho^2}\frac{1}{r}\frac{\partial \psi}{\partial x}\frac{\partial \rho}{\partial x} + \frac{\rho_0}{\rho}\frac{1}{r}\frac{\partial^2 \psi}{\partial r^2}$$

$$- \frac{\rho_0}{r\rho^2}\frac{\partial \psi}{\partial r}\frac{\partial \rho}{\partial r} - \frac{1}{r^2}\frac{\rho_0}{\rho}\frac{\partial \psi}{\partial r} = 0$$

Using short symbols and rearranging,

$$\psi_{xx}+\psi_{rr}-\frac{1}{r}\psi_r-\frac{1}{\rho}\left(\psi_x\frac{\partial\rho}{\partial x}+\psi_r\frac{\partial\rho}{\partial r}\right)=0 \qquad (10.126)$$

The velocity vector in terms of its components is given by

$$c^2=c_r^2+c_x^2$$

$$c^2=\left(\frac{\rho_0}{\rho}\right)^2\frac{1}{r^2}(\psi_x^2+\psi_r^2) \qquad (10.127)$$

The momentum equation gives

$$d\rho=-\frac{\rho}{2a^2}dc^2$$

Substitution of Equation (10.127) in the above equation gives

$$d\rho=-\frac{\rho}{2a^2}d\left[\left(\frac{\rho_0}{\rho}\right)^2\frac{1}{r^2}(\psi_x^2+\psi_r^2)\right] \qquad (10.128)$$

Following partial derivatives are obtained from Equation (10.128):

$$\frac{\partial\rho}{\partial r}=\frac{-\dfrac{\rho}{a^2r^2}\left(\dfrac{\rho_0}{\rho}\right)^2\left[(\psi_x\psi_{rx}+\psi_r\psi_{rr})-\dfrac{1}{r}(\psi_r^2+\psi_x^2)\right]}{1-\dfrac{1}{a^2r^2}\left(\dfrac{\rho_0}{\rho}\right)^2(\psi_r^2+\psi_x^2)} \qquad (10.129)$$

$$\frac{\partial\rho}{\partial x}=\frac{-\dfrac{\rho}{a^2r^2}\left(\dfrac{\rho_0}{\rho}\right)^2(\psi_x\psi_{xx}+\psi_r\psi_{xr})}{1-\dfrac{1}{a^2r^2}\left(\dfrac{\rho_0}{\rho}\right)^2(\psi_r^2+\psi_x^2)} \qquad (10.130)$$

Substituting Equations (10.129) and (10.130) in (10.126) we get

$$\left(\psi_{xx}+\psi_{rr}-\frac{1}{r}\psi_r\right)\left[1-\frac{1}{a^2r^2}\left(\frac{\rho_0}{\rho}\right)^2(\psi_r^2+\psi_x^2)\right]+\frac{1}{a^2r^2}\left(\frac{\rho_0}{\rho}\right)^2$$

$$\left[\psi_x^2\psi_{xx}+\psi_x\psi_r\psi_{xr}+\psi_r\psi_x\psi_{rx}+\psi_r^2\psi_{rr}-\frac{\psi_r}{r}(\psi_r^2+\psi_x^2)\right]=0$$

Making use of Equation (10.125), *i.e.*, $\psi_{rx}=\psi_{xr}$, the above expression on further simplification and rearrangement yields

$$\left[1-\frac{1}{a^2r^2}\left(\frac{\rho_0}{\rho}\right)^2\psi_x^2\right]\psi_{rr}+\left[1-\frac{1}{a^2r^2}\left(\frac{\rho_0}{\rho}\right)^2\psi_r^2\right]\psi_{xx}$$

$$-\frac{\psi_r}{r}+\frac{2}{a^2r^2}\left(\frac{\rho_0}{\rho}\right)^2\psi_r\psi_x\psi_{rx}=0 \qquad (10.131)$$

Incompressible flow: Taking $a^2\approx\infty$ in Equation (10.131)

$$\psi_{rr}+\psi_{xx}-\frac{1}{r}\psi_r=0$$

$$\frac{\partial^2\psi}{\partial r^2}+\frac{\partial^2\psi}{\partial x^2}-\frac{1}{r}\frac{\partial\psi}{\partial r}=0 \qquad (10.132)$$

NOTATION FOR CHAPTER 10

a	velocity of sound or acceleration	θ	angle or angular displacement
A	area of cross section	μ	coefficient of viscosity
c	gas velocity	ρ	density
F	pressure force	Γ	circulation
l	length along the curve	ϕ	potential function
m	mass or rate of mass flow	ψ	stream function
p	pressure	ω	angular velocity or rotation
r	radius	$\phi_x=$	$\partial\phi/\partial x$
t	time	$\phi_{xx}=$	$\partial^2\phi/\partial x^2$
V	volume	$\phi_{xy}=$	$\partial^2\phi/\partial x\,\partial y$
x, y, z	Cartesian coordinates	$\phi_y=$	$\partial\phi/\partial y$
X, Y, Z	body forces in the Cartesian coordinate system	$\phi_{yy}=$	$\partial^2\phi/\partial y^2$
		$\phi_{yx}=$	$\partial^2\phi/\partial y\,\partial x$
r, θ, x	cylindrical coordinates	$\psi_x=$	$\partial\psi/\partial x$
$X_r, X_\theta,$ X_x	body forces in the cylindrical coordinate system	$\psi_{xx}=$	$\partial^2\psi/\partial x^2$
		$\psi_{xy}=$	$\partial^2\psi/\partial x\,\partial y$
Δ	infinitesimal quantity	$\psi_y=$	$\partial\psi/\partial y$
ξ, η, ζ	vorticity components	$\psi_{yy}=$	$\partial^2\psi/\partial y^2$
		$\psi_{yx}=$	$\partial^2\psi/\partial y\,\partial x$

SUBSCRIPTS

0	stagnation value	r, θ, x	components along the cylindrical coordinates
x, y, z	components along the Cartesian coordinates	xr, $r\theta$, θx	planes in the cylindrical coordinate system
xy, yz, zx	planes in the Cartesian coordinate system		

QUESTIONS AND PROBLEMS

10.1 (*a*) Write down the Navier-Stokes equations of motion for three-dimensional, unsteady, compressible and viscous flow with body and pressure forces.

(*b*) Derive from the above the following equations for two-dimensional steady, inviscid and incompressible flow in the absence of body forces:

$$c_x \frac{\partial c_x}{\partial x} + c_y \frac{\partial c_x}{\partial y} = -\frac{1}{\rho}\frac{\partial p}{\partial x}$$

$$c_x \frac{\partial c_y}{\partial x} + c_y \frac{\partial c_y}{\partial y} = -\frac{1}{\rho}\frac{\partial p}{\partial y}$$

$$\frac{\partial^2 \phi}{\partial x^2} + \frac{\partial^2 \phi}{\partial y^2} = 0$$

$$\frac{\partial^2 \psi}{\partial x^2} + \frac{\partial^2 \psi}{\partial y^2} = 0.$$

10.2 Derive the following relations for one-dimensional unsteady flow:

(*a*) $\dfrac{\partial}{\partial s}(\rho c) + \dfrac{\partial \rho}{\partial t} = 0$

(*b*) $\dfrac{1}{\rho}\dfrac{\partial p_0}{\partial s} + \dfrac{\partial c}{\partial t} = 0$

(*c*) $\dfrac{\partial h_0}{\partial s} + \dfrac{\partial c}{\partial t} = 0$

(s is the distance along the streamline).

10.3 Show that the accelerations of a fluid particle in the radial and tangential directions are given by

$$a_r = \frac{dc_r}{dt} - \omega r \frac{d\theta}{dt}$$

$$a_\theta = \frac{2c_r c_\theta}{r} + r\frac{d^2\theta}{dt^2}.$$

10.4 What is axisymmetric flow? Derive the following relations for such a flow:

(*a*) $\dfrac{\partial c_r}{\partial r} + \dfrac{\partial c_x}{\partial x} + \dfrac{c_r}{r} = 0$

(*b*) $c_r \dfrac{\partial c_\theta}{\partial r} + c_x \dfrac{\partial c_\theta}{\partial x} + \dfrac{c_r c_\theta}{r} = 0$

(*c*) $\zeta = \dfrac{\partial c_\theta}{\partial r} + \dfrac{c_\theta}{r}$

(*d*) $c_r \dfrac{\partial c_r}{\partial r} + c_x \dfrac{\partial c_r}{\partial x} - \dfrac{c_\theta^2}{r} = -\dfrac{1}{\rho}\dfrac{\partial p}{\partial r} + \dfrac{\mu}{\rho}\left(\dfrac{\partial^2 c_r}{\partial r^2} + \dfrac{1}{r}\dfrac{\partial c_r}{\partial r} - \dfrac{c_r}{r^2} + \dfrac{\partial^2 c_r}{\partial x^2}\right)$

(*e*) $\dfrac{\partial^2 \phi}{\partial r^2} + \dfrac{\partial^2 \phi}{\partial x^2} + \dfrac{1}{r}\dfrac{\partial \phi}{\partial r} = 0$

(*f*) $\dfrac{\partial^2 \psi}{\partial r^2} + \dfrac{\partial^2 \psi}{\partial x^2} - \dfrac{1}{r}\dfrac{\partial \psi}{\partial r} = 0.$

10.5 (*a*) Define circulation and vorticity.

(*b*) Show that the line integral between two points in a flow field is independent of the path for irrotational flow.

10.6 (*a*) Explain what is meant by the velocity potential function ϕ.

(*b*) Obtain the following relations for the velocity potential:

$$\left.\begin{aligned} \phi_{xy} &= \phi_{yx} \\ \phi_{xz} &= \phi_{zx} \\ \phi_{yz} &= \phi_{zy} \end{aligned}\right\} \text{(in Cartesian coordinates)}$$

$$\left.\begin{aligned} \phi_{r\theta} &= \phi_{\theta r} \\ \phi_{rx} &= \phi_{xr} \\ \phi_{x\theta} &= \phi_{\theta x} \end{aligned}\right\} \text{(in cylindrical coordinates)}$$

10.7 Prove the following relations:

(*a*) $\dfrac{2a^2}{\gamma-1}+(\phi_x^2+\phi_y^2+\phi_z^2)=\text{constant}$

(*b*) $a^2=a_0^2-\dfrac{\gamma-1}{2}\left(\phi_r^2+\dfrac{1}{r^2}\phi_\theta^2+\phi_x^2\right)$

(*c*) $a^2=a_0-\dfrac{\gamma-1}{2}\left(\dfrac{\rho_0}{\rho}\right)^2(\psi_x^2+\psi_y^2)$

(*d*) $\dfrac{2a^2}{\gamma-1}+\dfrac{1}{r^2}\left(\dfrac{\rho_0}{\rho}\right)^2(\psi_r^2+\psi_x^2)=\text{constant}.$

10.8 Show for two dimensional plane flow in cylindrical (polar) coordinates

(*a*) $\dfrac{\partial c_r}{\partial r}+\dfrac{c_r}{r}+\dfrac{1}{r}\dfrac{\partial c_\theta}{\partial\theta}=0$

(*b*) $c_r\dfrac{\partial c_r}{\partial r}+\dfrac{c_\theta}{r}\dfrac{\partial c_r}{\partial\theta}-\dfrac{c_\theta^2}{r}=-\dfrac{1}{\rho}\dfrac{\partial p}{\partial r}$

(*c*) $c_r\dfrac{\partial c_\theta}{\partial r}+\dfrac{c_\theta}{r}\dfrac{\partial c_\theta}{\partial\theta}+\dfrac{c_r c_\theta}{r}=-\dfrac{1}{\rho r}\dfrac{\partial p}{\partial\theta}$

(*d*) $\dfrac{\partial^2\phi}{\partial r^2}+\dfrac{1}{r}\dfrac{\partial\phi}{\partial r}+\dfrac{1}{r^2}\dfrac{\partial^2\phi}{\partial\theta^2}=0$

(*e*) $\dfrac{\partial^2\psi}{\partial r^2}+\dfrac{1}{r}\dfrac{\partial\psi}{\partial r}+\dfrac{1}{r^2}\dfrac{\partial^2\psi}{\partial\theta^2}=0$

State the assumptions used.

10.9 (*a*) Sketch an elemental control surface in polar coordinates (r, θ) showing various velocities and vorticity components.

(*b*) Show that the vorticity components in these coordinates are

$$\xi=0$$

$$\eta=0$$

$$\zeta=\frac{1}{r}\frac{\partial}{\partial r}(rc_\theta)-\frac{\partial}{\partial\theta}\left(\frac{c_r}{r}\right).$$

10.10 (*a*) Explain what is meant by stream function ψ.

(*b*) Show ϕ = constant and ψ = constant lines in a converging-diverging passage.

(*c*) Prove that the difference between the values of the two ψ = constant lines represents the mass flow rate between these lines.

11

Methods of Measurement

Advances in gas dynamics have been accompanied by continuous development of instruments and measuring techniques. Qualitative and quantitative information in various compressible flow processes is obtained by the application of a variety of instruments and devices; they form an important discipline which is covered in separate volumes by specialists. Therefore, full justice to the treatment of such a vast subject cannot be done in a chapter like this. Here the reader is only introduced to the bare minimum material required on this subject. Other books on this subject are recommended for further studies in greater depth. This chapter only includes some of the fundamental methods of measurement.

In compressible flow problems the parameters which are generally required to be measured are static and stagnation pressures, temperature, velocity, direction of flow and the rate of flow. Besides these quantities flow visualization techniques in some situations are also useful in obtaining qualitative information about a given flow field. A variety of wind tunnels are used to test models under some prescribed conditions.

Experimental data is required to establish the validity of theoretical analyses developed and the assumptions used. A study and analysis of experimental data obtained for a process or the performance of a machine provides a useful basis for design methods. Better designs and more efficient machines have been developed on the basis of information collected by various measuring devices.

11.1 PRESSURE

Valuable information about a flow is obtained by measuring static and

stagnation pressures. Density of a medium can be determined through static pressure and temperature as

$$\rho = \frac{p}{RT}$$

The velocity of a gas stream is determined by measuring static and stagnation pressures. Stagnation pressure along with the stagnation temperature, as shown earlier fixes the maximum mass flow rate.

$$\frac{\dot{m}_{max}\sqrt{T_0}}{A^* p_0} = 0.0404 \text{ (for } \gamma = 1.4,\ R = 287 \text{ J/kg K)}$$

Difference of stagnation pressure at two points in a flow field gives a measure of losses.

Both static and stagnation pressure can be conveniently measured with high accuracy with the help of liquid manometers. Manometers and other devices for pressure measurement are described in Section 11.14.

11.1.1 Static Pressure

Static pressure of a fluid stream over a surface is the pressure transmitted by an orifice in the plane of the flow to a measuring device. Such an orifice is referred to as a static pressure hole. This hole must be small and drilled neatly away from any flow disturbances; it should be free from burrs and other imperfections. Different types of pressure tappings from static pressure holes are shown in Figure 11.1.

In many cases it is desired to determine the static pressure within the flow field away from the solid surface. This is measured by a static pressure tube as shown in Figure 11.2 (*a*). The leading end of this probe is closed and one or more static holes are drilled on its surface at a

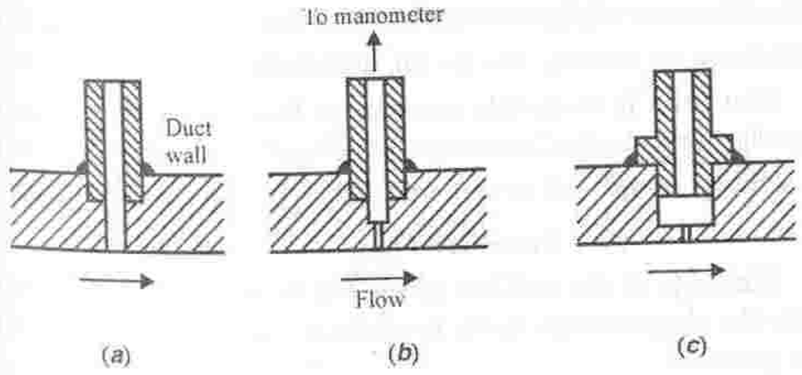

FIGURE 11.1 : Static pressure tappings

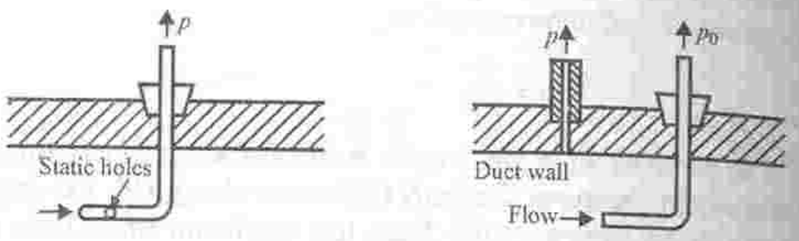

FIGURE 11.2 : Measurement of stagnation and static pressures

suitable section. To cause minimum disturbance in the flow the probe should be as small as possible. The probe will give correct value of the pressure when it is aligned parallel to the flow direction; in this position the static holes on the surface of the probe are in the plane of the flow. This probe is sufficiently accurate even if it deviates by ±5 degrees from the direction of flow.

The accuracy of the pressure measured through a static hole largely depends on the shape of the streamline passing over it. If the hole diameter is large the deflection of the streamline passing over it will be considerable; as a result of this the difference between the actual static pressure and the measured value will be large. Therefore, the static hole diameter should be as small as possible. But in this regard another important aspect cannot be overlooked; this is the response time aspect.

If the static hole is too small the response time will be too long. Therefore, in some applications if it is not necessary to keep the static hole too small a larger size can be used. In view of the above factors the sizes of the static holes are between 0.25 mm and 2.5 mm diameter.

11.1.2 Stagnation Pressure

This has already been defined in Section 2.5. Since stagnation pressure p_0 is a measure of the entropy level of the fluid, its change indicates an increase in entropy due to an irreversibility.

If a fluid is reversibly accelerated from an infinite reservoir the stagnation pressure (p_0) of the jet can be simply measured by recording the static pressure (p) in the reservoir.

$$p_{\text{reservoir}} = p_{0\,\text{jet}}$$

Similarly if the ambient air at rest is accelerated in a reversible nozzle the stagnation pressure throughout the flow is equal to the ambient pressure.

Besides measuring the reservoir static pressure, whenever possible stagnation pressure is also measured by a pitot tube or total pressure

tube (as it is sometimes called). This device was first used by Henry Pitot (hence the name) and is a very basic flow measuring device.

The pitot tube shown in Figure 11.2 (*b*) is a bent stainless steel tube designed and inserted into the flow field in such a way as to cause minimum disturbance in the flow. The deceleration of the flow to stagnation conditions at its open end is nearly reversible. Therefore, the pressure recorded by such a tube is the stagnation pressure. This gives fairly accurate results even if it deviates from the flow direction by about $\pm 20^0$.

11.1.3 Mean Values of the Static and Stagnation Pressures

Static pressure: If the value of the static pressure at a given section of a circular duct is required the static pressure probe (shown in Figure 11.2) is traversed at a number of points along the radius. The ''mass flow weighted'' mean value of the static pressure is then computed by the following method:

$$dA = 2\pi r\,dr \tag{11.1}$$

$$dq = 2\pi cr\,dr \tag{11.2}$$

$$d\dot{m} = 2\pi\rho cr\,dr \tag{11.3}$$

$$\bar{p} = \frac{\int_0^R p\,d\dot{m}}{\int_0^R d\dot{m}} = \frac{\int_0^R 2\pi\rho cpr\,dr}{\int_0^R 2\pi\rho cr\,dr} \tag{11.4}$$

If ρ and p do not vary along the radius the right hand side of Equations (11.4) reduces to p as in a truly one dimensional case.

Stagnation pressure: The mass flow weighted mean value of the stagnation pressure is given by

$$\bar{p}_0 = \bar{p} + \frac{1}{2}\rho\overline{c^2}$$

The dynamic head is given by

$$\frac{1}{2}\rho\overline{c^2} = \frac{\int_0^R \left(\frac{1}{2}\rho c^2\right) d\dot{m}}{\int_0^R d\dot{m}}$$

$$\frac{1}{2}\overline{\rho c^2} = \frac{\frac{1}{2}\int_0^R \rho^2 c^3 r\,dr}{\int_0^R \rho c r\,dr} \tag{11.5}$$

If ρ and c do not vary with the radius Equation (11.5) reduces to the familiar from $\frac{1}{2}\rho c^2$.

Equations (11.4) and (11.5) give the mass flow weighted mean value of the stagnation pressure

$$\bar{p}_0 = \frac{\int_0^R \rho c p r\,dr}{\int_0^R \rho c r\,dr} + \frac{\frac{1}{2}\int_0^R \rho^2 c^3 r\,dr}{\int_0^R \rho c r\,dr} \tag{11.6}$$

If ρ and p are nearly constant

$$\bar{p}_0 = p + \frac{\frac{1}{2}\rho\int_0^R c^3 r\,dr}{\int_0^R c r\,dr} \tag{11.7}$$

when ρ, p and c are all constant

$$\bar{p}_0 = p + \frac{1}{2}\rho c^2.$$

11.1.4 Types of Pressure Measuring Devices

Some pressure measuring devices are briefly described here. More technical details of these and many other devices can be found in literature on instruments and measurement systems.

Manometers: Steady pressures in lower ranges can be conveniently measured by liquid manometers. Their working principle is based on the deflection of a column of a suitable liquid e.g., water, alcohol or mercury. Very low pressures can be measured with high degree of accuracy. To amplify the deflection the simple vertical tube manometer

is tilted. For instance a small change in the vertical height of the liquid column can be magnified to 2, 5 and 10 times by inclining the tubes at 30, 11.6 and 5.8 degrees respectively to the horizontal.

Water and alcohol are used for lower pressures whilst mercury is used for higher pressures. For measuring still lower pressures micromanometers are used in which the reservoir (connected to the inclined tube) can be moved up and down by a micrometer. If the height of an average observer is 165 cm a deflection of 100 cm of the liquid column appears to be convenient for reading on a manometer as shown in Figure 11.3. Therefore, it can be easily used to measure gauge pressure of 1.3338 bar (with mercury) and 0.100 bar (with water).

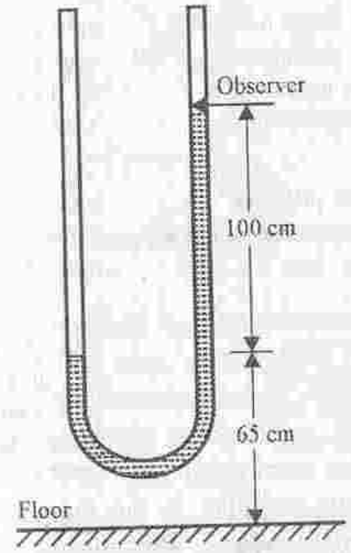

FIGURE 11.3 : A convenient range for a simple manometer

When manometers have to be used for very high pressures (using mercury) strength of the manometer glass tube and the sealing between the leads and the manometer require considerable attention. As an example the bursting pressures for two typical manometer tubes are given here:

bore 1 mm	40 bar
wall thickness 2 mm	
bore 6 mm	22 bar
wall thickness 4 mm	

Transparent protective shields may also have to be used for the safety of the users.

Other devices: Various types of pressure measuring devices and their ranges are given in Table 11.1. Manometers have been included in the low pressure devices though mercury manometers can be used for very high pressures particularly for calibration purposes.

TABLE 11.1: Types of pressure measuring devices and their ranges

Low pressures		
1.	Pirani gauges	10^{-5} – 1.3 mbar
2.	Mcleod gauges	10^{-4} – 0.1 mbar
3.	Diaphragm gauges	upto a minimum of 10^{-3} mbar
4.	Low pressure bourdon gauges	upto a minimum of 10 mbar
5.	Inclined tube water micromanometers	upto a minimum of 5×10^{-4} mbar
6.	Vertical tube water micro manometer	upto a minimum of 2.5×10^{-3} mbar
7.	Inclined tube water manometer	upto a minimum of 0.01 mbar
8.	Simple vertical tube manometer	0.1 mbar – 0.1 bar
9.	Vertical tube mercury manometer	1.334 mbar – 1.334 bar
Medium pressures		
10.	Strain gauge pressure pick ups	0.1 – 7.5 bar
11.	Variable inductance pressure transducers	0.05 – 35 bar
12.	Piezoelectric pressure pick ups	upto 350 bar
High pressures		
13.	Bourdon type (spiral tube)	upto 75 bar
14.	Capacitance type transducers	0.5 – 3600 bar
15.	Bourdon gauge (*C*-type tube)	upto 7000 bar
16.	Strain gauge pressure cells	7000 – 15000 bar

Bourdon tube gauges: This is the most widely used mechanical type pressure gauge or transducer. Pressure is exerted in a non-circular cross-section bourdon tube. One end of the tube is free to move. Due to the pressure inside the tube its cross-section tends to approach the circular shape; in doing so the free end of the bourdon tube moves. This movement is magnified in a variety of ways and can be used as a measure of the pressure. The bourdon tube is used as either *C*-type or the spiral type.

Electrical transducers: Pressure transducers are based upon either of the following effects:

(*a*) variation in resistance,
(*b*) variation in capacitance,
(*c*) variation in inductance,
(*d*) thermal effects, and
(*e*) Piezo-electric effect.

Some of the above electrical signals can be obtained by the deformation of a tube, membrane or bellows. In some pick ups electrical circuits using resistance potentiometers or strain gauges are used.

In thermal gauges (Pirani gauges) a thin wire forms one of the arms of the wheatstone bridge as shown in Figure 11.4; this is enclosed

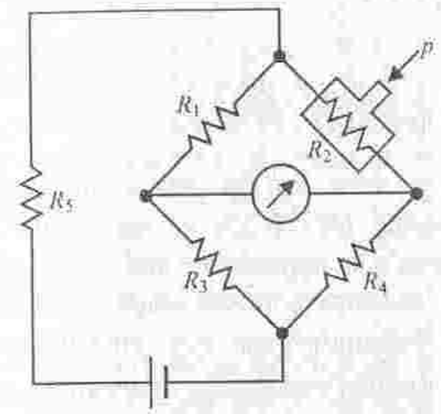

FIGURE 11.4 : Bridge circuit for a thermal pressure gauge

in a chamber which is exposed to the pressure to be measured. The wire is heated (like the hot wire anemometer) to a high temperature ($\approx 250^{\circ}$C) by adjusting the electric current through the resistance R5. At low pressures (high vacuum) the cooling of the wire is slower on account of lesser number of gas molecules around it.

For measuring fluctuating pressures (unsteady pressures) use of some form of an electrical transducer is unavoidable. They are very suitable for quick and automatic recording of a large number of pressure signals.

All transducers like bourdon tube pressure gauges require calibration. The dead weight gauge tester and mercury manometers are used for this purpose in a wide range.

11.2 TEMPERATURE

Temperature of the fluid is an important parameter in compressible flow problems. Besides the surface temperatures of aerodynamic bodies and flow passages other temperatures which are frequently used are the static and stagnation (total) temperature of the fluid.

Static temperature (T) is the temperature that would be measured by a device which moves with the fluid at its velocity. The stagnation

or the total temperature (T_0) is the temperature of the fluid at its stagnation state; this has been discussed earlier in Section 2.3.4. Various formulas relating these two temperatures are again reproduced here for further explanation.

$$T_0 = T + \frac{c^2}{2c_p} \tag{2.21}$$

$$\frac{T_0}{T} = 1 + \frac{\gamma - 1}{2} M^2 \tag{2.24}$$

Above relations show that the difference between these temperatures at low velocities ($M < 0.30$) is negligible. But at high fluid velocities this difference is appreciable and cannot be neglected. Therefore, their separate measurement becomes essential. The temperature (T_r) recorded by a thermometer or any other temperature probe introduced into the flow field is some value between the static and stagnation temperatures. The difference between the various temperatures is explained in the following:

(a) When a gas at high velocity flows over a temperature sensing device protruding over the wall of the flow passage shocks may develop; this interferes with the correct measurement of the temperature.

(b) As a gas flows over the temperature probe boundary layers surround the probe and separate it from the free stream. Some energy which is dissipated in the boundary layer reappears as heat and raises the temperature in the vicinity of the probe; this is besides the temperature rise that occurs due to the deceleration of flow near the probe.

(c) If the probe attains a temperature higher than the surroundings heat flows from it to the gas.

(d) Besides the aforementioned heat transfers there is outward transfer of heat from the probe through the stem of a thermometer or the connecting wires of a thermocouple. This makes the process non-adiabatic.

11.2.1 Correction Factor

In the above discussion it is observed that the actual temperature (T_r) recorded is neither static nor stagnation nor adiabatic wall temperature. In order to take into account all these factors a correction factor (K_T) is defined,

$$K_T = \frac{T_r - T}{T_0 - T}. \tag{11.8}$$

11.2.2 Recovery Factor

If the temperature of the gas is measured under such conditions that there is no heat transfer from the probe to the outside [as mentioned in (d) above] the value obtained is the adiabatic wall temperature (T_{aw}). The recovery factor relates this temperature to the static and stagnation temperatures,

$$R_f = \frac{T_{aw} - T}{T_0 - T} \tag{11.9}$$

The value of the recovery factor depends on the type of the probe, growth of the boundary layer and the Mach number. Following approximate values are generally used:

For subsonic flow $R_f = 0.89$

For supersonic flow $R_f = 0.86$

Equations (2.21) and (11.9) give

$$R_f = \frac{2c_p (T_{aw} - T)}{c^2} \tag{11.10}$$

$$\frac{T_{aw}}{T} = 1 + R_f \frac{c^2}{2c_p T}$$

$$\frac{T_{aw}}{T} = 1 + R_f \frac{\gamma - 1}{2} \frac{c^2}{\gamma RT}$$

$$\frac{T_{aw}}{T} = 1 + R_f \frac{\gamma - 1}{2} M^2 \tag{11.11}$$

Variation of various temperatures with Mach number is shown in Figure 11.5.

Temperature of a gas can also be obtained through the measurement of velocity of sound as

$$a^2 = \gamma RT$$

$$a_0^2 = \gamma RT_0$$

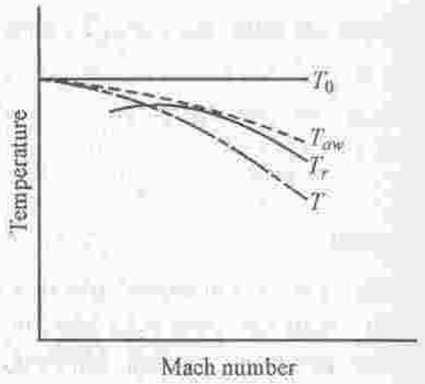

FIGURE 11.5 : Comparison of various temperatures

This can also be obtained from the values of pressure and density through the equation of state

$$T = \frac{p}{\rho R}$$

Some methods of direct measurement of temperature are given here.

11.2.3 Mercury in Glass Thermometers

These are the most commonly used devices for measuring temperature. Mercury is filled in a thick walled glass tube leaving some space above in the capillary for expansion of the mercury thread. This space is filled with an inert gas. These thermometers can measure temperatures upto about 550°C.

11.2.4 Vapour Pressure Thermometers

In this type a volatile liquid is filled in a metallic bulb which is connected to a sensitive pressure gauge. The vapour pressure of the liquid at the given temperature is employed for the measurement of temperature. Some of the liquids used are ethyl chloride and ethane.

11.2.5 Resistance Thermometers

It is well known that the electrical resistance of some materials changes with temperature. This is given by

$$R_T = R_0 (1 + C_1 T + C_2 T^2 + C_3 T^3 + \ldots + C_n T^n) \qquad (11.12)$$

This fact has been profitably used in the resistance thermometers. The most commonly used metals are copper, nickel and platinum. The

sensing element may be in the form of a flat grid pasted on the surface where temperature is required to be measured.

Figure 11.6 shows the wheatstone bridge for such a thermometer. The sensing element R_3 forms one of the arms of the bridge. R_4 is

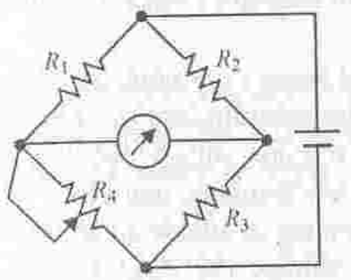

FIGURE 11.6 : Bridge circuit for a resistance thermometer

a variable resistance which is adjusted to obtain the null point. In a separate experiment a linear calibration curve between the variable resistance and the temperature is obtained. Platinum element in such a thermometer can be used from −270 to 1000°C.

11.2.6 Thermocouples

A thermocouple is formed by joining two wires of the dissimilar metals. If the two ends of the thermocouple are held at different temperatures T and T_0 an emf is generated; this is given by

$$V_a - V_b = \int_{T_0}^{T} (S_A^* - S_B^*)\, dT \qquad (11.13)$$

(here T_0 does not represent stagnation temperature).

Figure 11.7 shows two wires A and B of dissimilar metals in a conventional thermocouple circuit. The thermojunction is maintained at

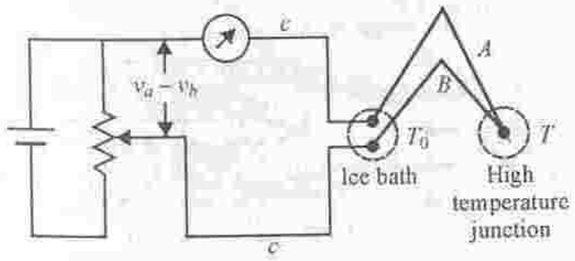

FIGURE 11.7 : Thermocouple circuit

the temperature (T) to be measured: while the other ends of the wires are maintained at a standard temperature T_0 (in this case $T_0 = 273$ K). It can be shown that the connecting wires C have no effect on the emf generated.

Thermocouples are ordinarily made from 0.50 to 2.5 mm diameter wires.

The emf generated being very small can be conveniently measured by a potentiometer as shown in the circuit or by a milli/micro voltmeter. Now the temperature-voltage curves for the commonly used thermocouple pairs are readily available and could be used for temperature measurements. If they are not available a calibration curve can be drawn by plotting the output voltage $(V_a - V_b)$ against the known values of the temperatures in a separate experiment.

Some of thermocouple pairs with their temperature ranges are given below:

TABLE 11.2: Range of various thermocouple pairs

	Thermocouple pair	Sensitivity	Range
1.	Copper-constantan	60μV/°C at 350°C	– 200 to 350°C
2.	Platinum-rhodium	—	—
3.	Iron-constantan	—	– 150 to 1000°C
4.	Chromel-alumel		– 200 to 1300°C
5.	Platinum-platinum rhodium	6μV/°C at 100°C	0 to 1500°C
6.	Rhodium iridium-rhodium	—	upto 2000°C

11.2.7 Stagnation Temperature Probe

To create near stagnation conditions of the gas at the temperature sensing element the thermojunction may be inserted into a total pressure tube. An advanced version of this arrangement is shown in Figure 11.8. A

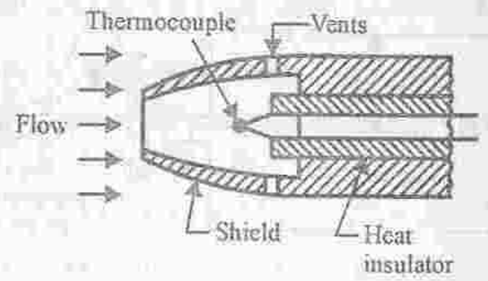

FIGURE 11.8 : Stagnation temperature probe

shield is provided to minimize the heat losses due to conduction and radiation. Conduction losses are further reduced by enclosing the thermocouple wires by heat insulators. Vents in the shield are provided to let in fresh sample of gas around the thermojunction. Such a probe nearly gives a recovery factor of unity.

11.3 DENSITY

Apart from other calculations in compressible flows density of the gas or air is also required for obtaining mass flow rate from the volume flow rate. If pressure and temperature of a gas are known its density can be determined from

$$\rho = \frac{p}{RT}$$

In the absence of temperature, magnitude of pressure and velocity of sound can also give the value of the gas density from

$$\rho = \frac{\gamma p}{a^2}$$

Velocity of sound is determined by the well established methods.

Variation of density in a flow field can also be determined by taking an interferogram of the flow field. This aspect is further explained in Section 11.10.

11.4 VELOCITY

Velocity measurement falls into three categories in terms of its range.

(*i*) Velocity measurement in incompressible flow;

(*ii*) Velocity measurement in compressible flow and

(*iii*) Velocity measurement in supersonic flow.

Depending on the range, accuracy desired and the practical situation any one of following basic principles can be employed:

(*a*) by using the dynamic effect of the fluid stream on a tiny wind mill (vane anemometer);

(*b*) by bringing the flow to rest in an infinitesimal stream tube (pitot-static tube);

(*c*) by measuring the cooling effect of the fluid stream on a heated element (hot-wire or a hot film);

(*d*) by using Doppler effect.

Some of these methods are described here.

11.4.1 Incompressible Flow

The stagnation pressure in an incompressible flow field is given by the Bernoulli equation

$$p_0 = p + \frac{1}{2}\rho c^2$$

$$\frac{1}{2}\rho c^2 = p_0 - p = \Delta p \tag{11.14}$$

Separate measurements of the stagnation and static pressure have already been described in Sections 11.1.1 to 11.1.3.

Figure 11.9 shows a combination of the pitot tube with an outer co-axial static pressure tube. The static pressure holes (generally seven)

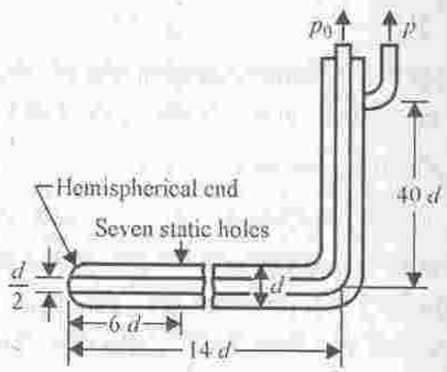

FIGURE 11.9 : Standard pitot-static tube

in the outer tube cannot be located too close to the probe end on account of the disturbed flow in this region and its effect on the static pressure measurement. Therefore, it is not possible to measure the static pressure at the mouth of the probe. Various proportions used in the pitot-static probe are shown in Figure 11.9. The velocity measuring probe, a pitot-static tube or a pitot tube with a separate static pressure tapping through the wall should create minimum disturbance in the flow. The effect of the stem on the static pressure measurement will be minimum only if the stem is far away from the static holes. This condition will require an impractically long head which makes its insertion into the flow field difficult.

In view of the above mentioned factors some effect of the probe end and the stem on the static pressure measurement is accepted: this plus the fact that the static pressure (p) is not recorded at the mouth of the probe is taken into account by a correction factor (K) for the pitot-static tube. This when introduced in Equation (11.14) gives

$$p_0 - p = \Delta p = K\left(\frac{1}{2}\rho c^2\right) \tag{11.15}$$

The value of K for a pitot-static tube is between 0.995 and 1.002. However, for most situations accuracy is little affected if it is taken as unity.

If the minimum reliable and readable value of the dynamic head recorded by the pitot-static probe is taken as 1 mm WG the minimum fluid velocity that can be measured accurately by this device is about 4 m/s.

11.4.2 Compressible Flow

Bernoulli equation for compressible flow is given in Chapter 2. This is

$$\frac{1}{2}c^2 + \frac{\gamma}{\gamma-1}\frac{p}{\rho} = \frac{\gamma}{\gamma-1}\frac{p_0}{\rho_0} \tag{2.64}$$

$$c = \sqrt{\frac{2\gamma}{\gamma-1}\left(\frac{p_0}{\rho_0} - \frac{p}{\rho}\right)} \tag{11.16}$$

This is applicable to all compressible flows including supersonic flow. But on account of the presence of shocks Equation (11.16) cannot be used for $M > 1$. Separate values for p and p_0 from the pitot-static tube are used in Equation (11.16) to calculate the gas velocity for $M < 1$.

Incompressible flow has already been defined in chapter one; this is further discussed in Section 2.11 (refer to Table 2.2). Table 11.3 gives a good idea about the velocity, manometer deflection (W.G) and the error caused due to incompressible flow assumption at two values of the Mach number.

TABLE 11.3: Limits for incompressible flow measurement in air ($\rho = 1.183$ kg/m^3, $a = 347.07$ m/s)

M	c (m/s)	Δh (mm W.G.)	$\Delta p/\frac{1}{2}\rho c^2$ (%)
0.2	70	300	1.0
0.3	106	680	2.3

These values ($M = 0.2$ or $M = 0.3$) can be treated as the limits for incompressible flow depending on the practical situation, and the accuracy required in measurement.

11.4.3 Supersonic Flow

The pitot tube can also be used for the measurement of gas velocity in supersonic flow. Section 6.13 deals with the normal shock upstream of a pitot tube. Static pressure (p_x) and temperature (T_x) in the flow upstream of the pitot probe and the shock are measured by the conventional methods. The pitot tube records the stagnation pressure (p_{0y}) downstream of the shock. Thus the Mach number (M_x) of the flow is determined from Equation (6.61). Alternatively, the value of M_x corresponding to the measured value of $\frac{p_{0y}}{p_x}$ is read directly from the normal shock gas tables.

The velocity of sound upstream of the shock is

$$a_x = \sqrt{\gamma R T_x}$$

Therefore, the gas velocity is given by

$$c_x = M_x a_x$$

In supersonic flows also the pitot tube is insensitive to slight misalignment relative to the flow direction. Thus the pitot tube can be set in supersonic flow merely by eye-judgement without loss of accuracy in the velocity measurement.

Wedge method: Supersonic flow over a symmetrical wedge is shown in Figure 11.10.

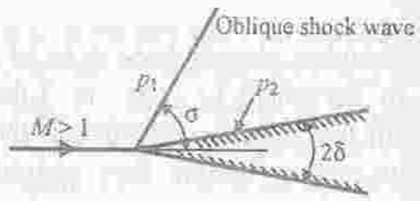

FIGURE 11.10 : Measurement of Mach number for supersonic flow by a wedge

It has been seen in Section 7.1 that when a supersonic flow passes over a symmetrical wedge (included angle 2δ) an oblique shock wave is formed. Thus the shock wave angle (σ) for a given gas, and the wedge angle can be used to obtain the free stream Mach number (M_1) either direct from the gas tables or the gas charts as shown in Figure 11.11.

Alternatively, the upstream pressure (p_1) and the pressure (p_2) on the wedge surface are measured. Then the value of the free stream Mach

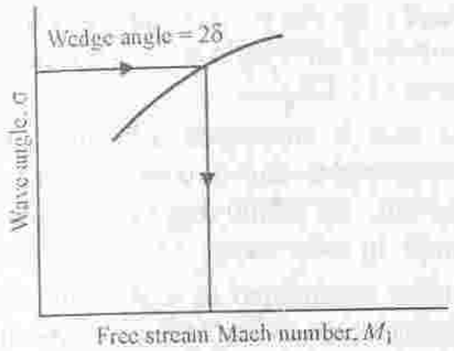

FIGURE 11.11 : Variation of wave angle with Mach number for a wedge with oblique shock

number (M_1) is determined from a plot of M_1 versus p_2/p_1 as shown in Figure 11.12.

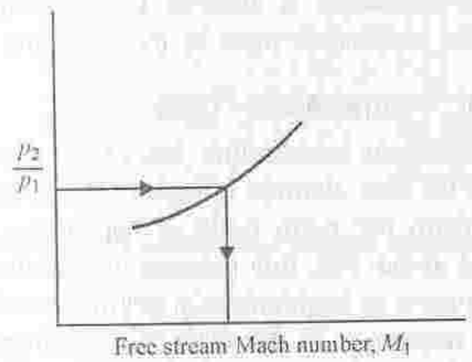

FIGURE 11.12 : Variation of pressure ratio with Mach number for a wedge with oblique shock

11.4.4 Vane Anemometer

It is a tiny windmill. The flat plate blades (generally eight) are small and light; they are mounted on a freely rotating shaft. The r.p.m. of the rotor shaft is a measure of the air velocity; this is generally transmitted to a pointer through a reduction gear (worm and worm-wheel arrangement). This method is particularly useful in measuring low velocities in small pipes and ducts. They can be calibrated by a standard pitot-static tube.

11.5 HOT-WIRE ANEMOMETER

A hot-wire anemometer consists of a tiny wire ($d \approx 0.005$ mm) held between two prongs; it is heated (hence the term hot-wire) to a given

temperature by passing an electric current through it. The dependence of its electrical resistance on temperature is given by an expression of the type of Equation (11.12).

When such a wire is introduced into the flow of a gas it cools down to a lower temperature due to convective heat transfer from the wire element to the gas. By employing suitable electrical circuitry the hot-wire can be used in two ways:

(*a*) The wire can be maintained at a constant temperature (T) and hence at constant value of the resistance R_T at all gas velocities. This is achieved by increasing the current through the wire element to balance the increased convective heat transfer from the wire at higher gas velocities, and vice versa.

This method is employed in the constant temperature hot-wire.

(*b*) The value of the heating current through the hot-wire is kept constant and its resistance is allowed to vary with the varying gas velocity. This method is used in the constant current hot- wire.

11.5.1 Constant Temperature Type

The circuit of a constant temperature hot-wire anemometer is shown in Figure 11.13. The wire element is held between the two needle supports projecting from the main body of the probe. The l/d ratio of the wire is kept at about 200; this reduces the conduction of heat from the wire to the supports or terminals to a negligible value. The terminals of the probe are connected to the wheatstone bridge circuit as shown in the figure. The heating current (for the chosen temperature) through the hot-wire is adjusted by the variable resistance R_5: thus the hot-wire resistance $R_w = R_4$ is fixed. R_2 and R_3 are fixed resistances. Resistance R_1 is initially varied to balance the bridge after which it is not changed. Due to change in the gas velocity and the increased convective heat transfer the resistance $R_w = R_4$ is changed. This is brought back to its initial value by readjusting the variable resistance R_5 and balancing the bridge. For each value of the gas velocity there is a different value of the current through the hot wire. Thus the different values of the current can be used to measure the gas velocities.

In a separate experiment a calibration curve (gas velocity versus current) is obtained by moving the hot wire element (on a rotating arm) at various speeds and measuring the corresponding value of the current. Such calibration curves at two temperatures are shown in Figure 11.14. The sensitivity of the hot-wire is high at higher temperatures. Therefore,

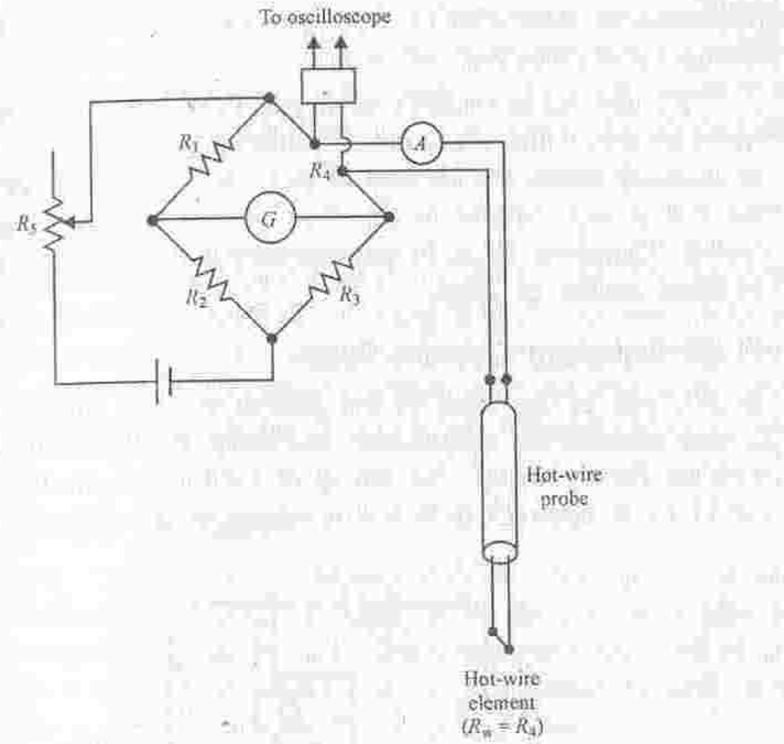

FIGURE 11.13 : Bridge circuit for a constant temperature hot-wire

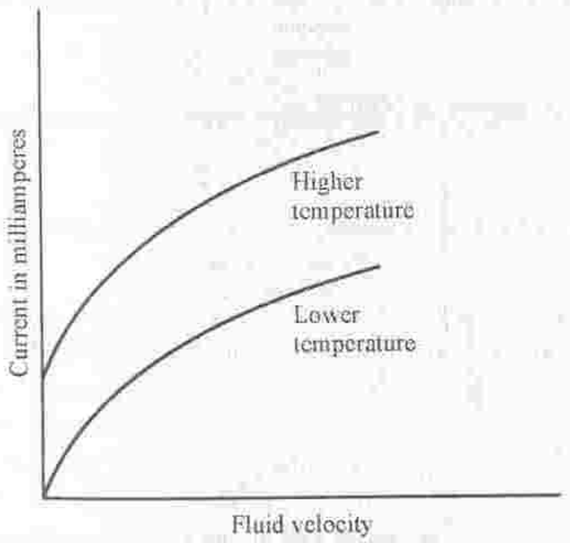

FIGURE 11.14 : Calibration curves for a constant temperature hot-wire

the probe wire temperature should be sufficiently high; the wire can be heated to about 700°C. Care should be taken against burning the wiring by overheating.

Besides measurements in steady flow constant temperature hot-wires are also widely used for measurements of turbulence, and velocity in unsteady flows. On account of the small size of the sensing element the disturbance caused in the flow is negligible compared to other probes. Therefore, it can be conveniently used in situations where other methods cannot be used.

11.5.2 Constant Current Type

In this type as the value of the current through the hot-wire element is kept constant the temperature and hence the wire resistance changes with the flow velocity. The circuit of such a hot wire is shown in Figure 11.15. A micro or milli voltmeter across the wire records the variation of the voltage with the gas velocity. The calibration curve for this anemometer is shown in Figure 11.16. The frequency response of the constant current anemometers is limited; therefore, they are not as versatile as the constant temperature type. However, their performance in fluctuating flows can be improved to some extent by employing dynamic compensation.

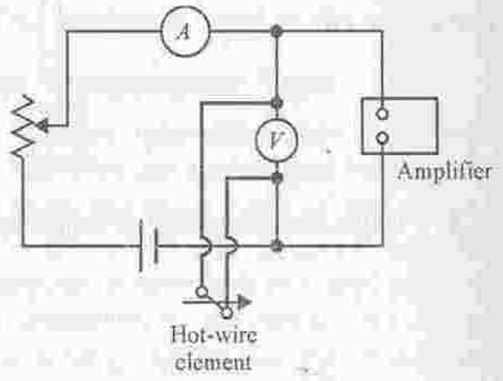

FIGURE 11.15 : Constant current hot-wire anemometer

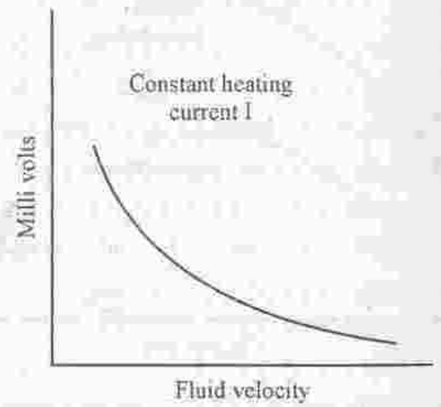

FIGURE 11.16 : Calibration curve for a constant current hot-wire

11.5.3 Hot Films

Hot films are obtained by depositing a thin film of metal like platinum on glass tube. This is mechanically stronger than the hot-wire element, and can be used at higher temperatures. The bridge for the hot film is similar to that used for a constant temperature hot-wire. Hot films can also be used to measure the direction and temperature in a flow field.

11.6 DIRECTION OF FLOW

General direction of flow on a surface can be observed by cotton streamers as described in Section 11.9.1. Flow direction can also be observed by introducing smoke in it. For quantitative estimate of the flow direction a number of instruments called yawmeters have been developed. Some of them are briefly described here.

11.6.1 Claw Type Yawmeter

The measuring head of this instrument is shown in Figure 11.17. It consists of two identical hypodermic tubes bent to from a claw with

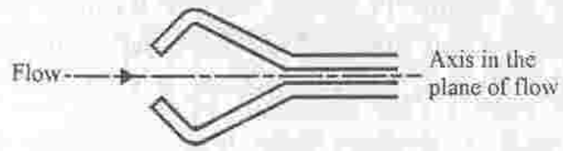

FIGURE 11.17 : Claw type yawmeter (direction probe)

symmetrical sides about its axis. The stem of the claw is perpendicular to the plane of the flow and carries the two hypodermic tubes for connections to the manometer. The stem passes through a suitable traversing device outside the flow duct. Thus the probe can be rotated about its vertical axis besides vertical movement in the duct. The probe head is rotated till its horizontal axis is parallel to the direction of flow; in this position the manometer tubes connected to the two tubes of the probe (claw) register the same deflection. Alternatively, the two sides of the claw can be connected to a U-tube manometer and a null method

is used; for greater accuracy the U-tube is kept in an inclined position. On account of the slight asymmetry of the claw about its axis, the probe is calibrated for its zero position. This can be done on a wind tunnel.

11.6.2 Wedge Probe

The basic principle of working of this instrument is same as that of the claw type. A small wedge has two tiny holes in symmetrical positions on its vertical faces as shown in Figure 11.18 (a). The holes are connected to the manometer; the probe head is carried by a vertical stem as before. If the two sides of the wedge and the holes are perfectly symmetrical the flow direction coincides with the bisector of the wedge angle.

Sometimes a pitot tube is combined with the wedge (Figure 11.18) or the claw probes.

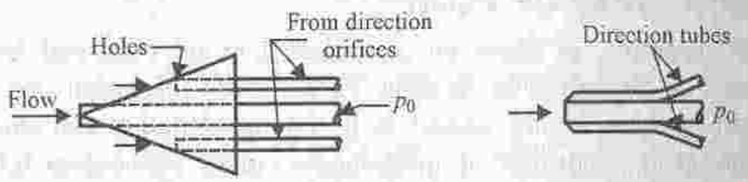

(a) Wedge probe (b) Cobra probe

FIGURE 11.18 : Wedge and Cobra type yawmeters

11.6.3 Cobra Probe

This is shown in Figure 11.18 (b). In this the two yaw or direction tubes are chamfered and silver soldered symmetrically on the two sides of the pitot tube. Rest of the arrangement is same as in the aforementioned types.

In yet another type (Conrad yaw meter) the two chamfered yaw tubes are soldered back to back.

In order to minimize the disturbance created due to the introduction of these probes in the flow the sizes of their sensing heads and the stem are kept as small as practicable.

11.6.4 Hot-wire Yawmeter

Various arrangements of hot-wire are used to measure the direction of flow.

(a) A single wire can be used to measure the direction of flow because the convective heat transfer from the wire depends upon its relative position in the flow. This method is convenient and dependable only when the flow direction is roughly known. Comparatively more reliable results are obtained when the angle between the wire and the flow direction is between 25 and 90 degrees.

(b) Hot-wire direction probe can also make use of two identical wires fixed at a given included angle ($\approx 90^\circ$) as shown in Figure 11.19 (a). The two wire elements W_1 and W_2 are fixed on the three

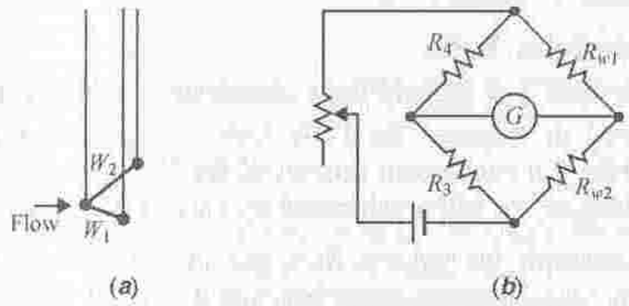

(a) (b)

FIGURE 11.19 : A hot-wire yawmeter

supports and form the two arms (R_{w1} and R_{w2}) of the bridge (Figure 11.19 (b)). The bridge null point is obtained when the wires are symmetrically placed relative to the flow direction.

11.7 FLOW RATE

Steady rates of flow of both liquids and gases are generally determined by measuring the static pressure difference across a constriction introduced into the flow passage. These devices are the orifice meter, venturimeter and the flow nozzle. The introduction of such devices causes stagnation pressure loss in the flow; too high a value of this loss is undesirable. Besides these many other methods of flow measurement are used; they make use of different gadgets like the pitot-static tube, rotameter, electric flow meter, hot-wire and the soap film.

The flow rate of a gas is given by

$$q = A\bar{c} \text{ m}^3/\text{s} \tag{11.17}$$

$$\dot{m} = \rho q = \rho A \bar{c} \text{ kg/s} \tag{11.18}$$

The area of cross-section A for a duct or the constriction is known. Therefore, the determination of mass flow rate involves measurement of the mean velocity $\bar{c}$ and the density

$$\rho = \frac{p}{RT}$$

Density can be obtained by very accurate pressure and temperature measuring devices described in Sections 11.1 and 11.2.

The fluid velocity $\bar{c}$ can be obtained by the head (pressure difference) across the constriction or by a direct measurement, for example by a pitot-static tube, soap film method or hot-wire anemometer.

It is often convenient and advisable to reduce the velocity of flow before it enters a flow measuring device; this can simply be done by using a passage of larger area of cross-section.

11.7.1 Pitot-static Tube

A pitot-static tube has already been described in Section 11.4.1. This is widely used to measure the flow rates in ducts by obtaining the velocity profile at a convenient section of the flow passage. Other flow measuring devices are often calibrated by traversing a pitot-static tube.

As an example the volume flow rate in a circular duct is considered; the discharge through an infinitesimal ring of flow in the duct is given by

$$dq = c\,dA = c\,(2\pi r\,dr) \tag{11.19}$$

Therefore, the total volume flow rate is obtained by integration.

$$q = \bar{c}\,\pi R^2 = \int_0^R c\,(2\pi r\,dr) \tag{11.20}$$

For the purpose of determining the value of the above integral the expression is rewritten in the following forms:

$$q = 2\pi \int_0^R cr\,dr \tag{11.21}$$

$$q = \pi \int_0^R cd\,(r^2) \tag{11.22}$$

The pitot-static traverse gives the values of the fluid velocity c at a large number of points along one or more diameters; for determining the values of the integrals in Equations (11.21) and (11.22) graphically the values of c and cr are plotted as shown in Figure 11.20. Alternatively, the integrals can be evaluated by using any numerical integration method, e.g., the well known Simpson's rule or the Trapezoidal rule.

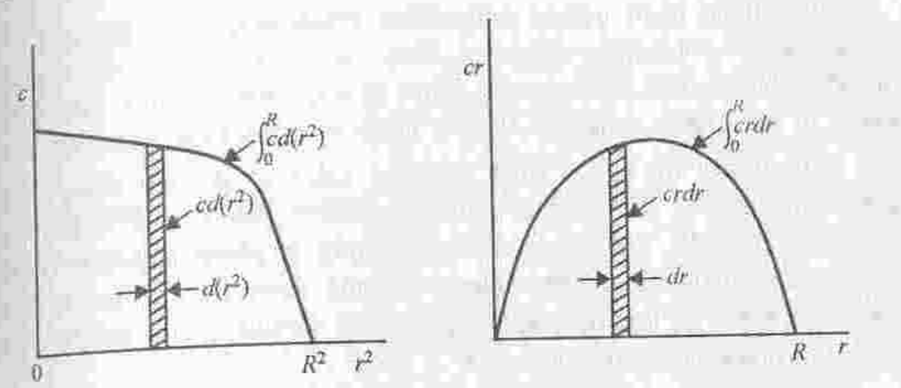

FIGURE 11.20 : Methods of integration for determining the flow rate by a pitot tube

11.7.2 Orifice Meter

This is one of the simpler devices which can easily be introduced in a flow system. An orifice plate of standard shape is shown in Figure 11.21; this is bolted between the flanges of the two pipes. Various dimensions are given in terms of the pipe diameter D. The location of the pressure tappings for determining the head ($\Delta p = p_1 - p_2$) across the orifice is critical. Corner tappings and D, $D/2$ tappings (as shown in the figure) are recommended. To ensure correct measurement of the pressures p_1 and p_2 more than one tappings at upstream and downstream sections are used. The static holes and the tappings should conform to the specifications given in Section 11.1.1. The material for the orifice plate should be such that its sharp edges and surfaces are not deformed due to erosion and corrosion (in case of corrosive gases).

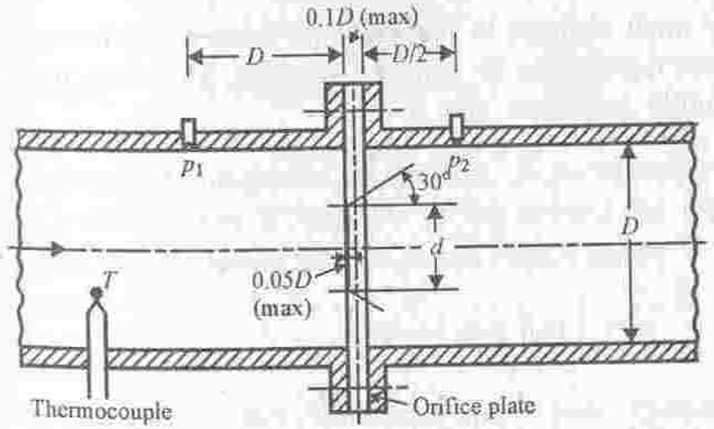

FIGURE 11.21 : A plate orifice meter

The head (Δp) across the orifice depends on the ratio d/D; its value for the minimum expected flow rate should be easily readable on an inclined tube manometer. For a given range of flow rate a high value of Δp due to small d/D ratio leads to unnecessary pressure loss.

To obtain the mass flow rate the value of density close to the upstream edge of the orifice is also required. This can be determined by measuring the pressure and temperature prevailing in this region. Temperature is measured by either a thermocouple or a mercury in glass thermometer. The location of these devices should not disturb the flow near the static pressure tappings.

Orifice meters have been satisfactorily used in circular ducts of 5 cm to 100 cm diameters. The orifice diameter for small diameter pipes should not be less than 6 mm. The maximum value of the ratio $n = d^2/D^2$ is recommended as 0.7.

Calculation of the flow rate: Let the flow be considered between sections upstream of the orifice and the venacontracta downstream of the orifice. The corresponding areas of cross-section are

$$A = \frac{\pi}{4} d^2$$

$$A_1 = \frac{\pi}{4} D^2$$

$$A_2 = C_c A = C_c \frac{\pi}{4} d^2$$

$$\frac{A_2}{A_1} = C_c \frac{A}{A_1} = C_c \left(\frac{d}{D}\right)^2 = nC_c \tag{11.23}$$

For small changes in pressure and temperature between the two sections the density can be assumed constant. Therefore, the continuity and Bernoulli equations give

$$\dot{m} = \rho A_1 c_1 = \rho A_2 c_2$$

$$\frac{c_1}{c_2} = \frac{A_2}{A_1} \tag{11.24}$$

$$p_1 + \frac{1}{2}\rho c_1^2 = p_2 + \frac{1}{2}\rho c_2^2$$

$$\frac{1}{\rho}(p_1 - p_2) = \frac{1}{2} c_2^2 \left(1 - \frac{c_1^2}{c_2^2}\right) \tag{11.25}$$

Equations (11.24) and (11.25) give

$$\frac{1}{\rho}(p_1 - p_2) = \frac{1}{2} c_2^2 \left(1 - \frac{A_2^2}{A_1^2}\right)$$

Therefore, the theoretical velocity c_2 at a section where the area of cross-section is A_2 is given by

$$c_2 = \sqrt{\frac{2(p_1 - p_2)}{\rho\left(1 - \frac{A_2^2}{A_1^2}\right)}} \tag{11.26}$$

The actual velocity is $C_v c_2$.

Therefore, the mass flow rate is given by

$$\dot{m} = \rho (C_v c_2) A_2$$

Substituting values for c_2 and A_2

$$\dot{m} = \rho C_v C_c A \sqrt{\frac{2}{\rho} \frac{(p_1 - p_2)}{1 - n^2 C_c^2}}$$

$$\dot{m} = \frac{C_v C_c A}{\sqrt{1 - n^2 C_c^2}} \sqrt{2\rho (p_1 - p_2)} \tag{11.27}$$

Now the coefficient of discharge for the orifice is defined by

$$C_d = \frac{C_v C_c}{\sqrt{1 - n^2 C_c^2}} \tag{11.28}$$

Therefore, $$\dot{m} = C_d A \sqrt{2\rho (p_1 - p_2)} \tag{11.29}$$

The discharge coefficient depends on the area ratio (n), Reynolds number (Re) and the roughness of the pipe. Experimentally obtained values of C_d are available in literature on this subject and hand books. A typical plot of C_d versus area ratio for orifice plates is shown in Figure 11.22.

11.7.3 Venturimeter

A convergent-divergent duct introduced into a flow system can also be used for measuring flow rates of fluids. This is used in a device

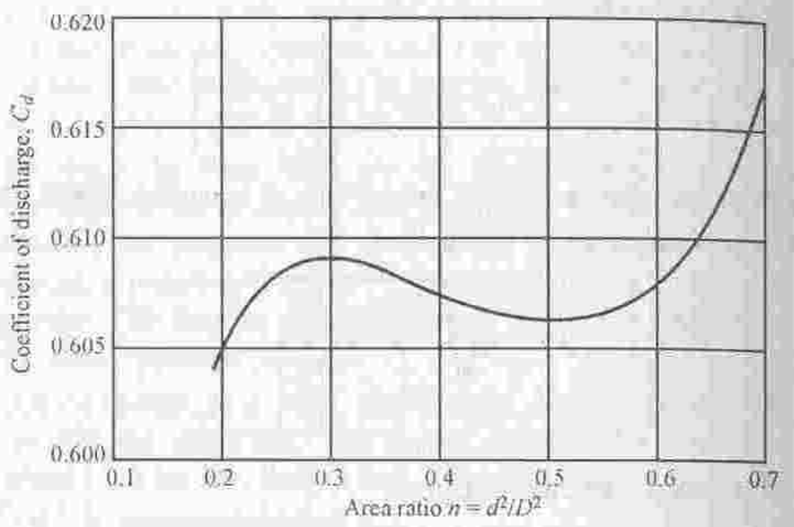

FIGURE 11.22 : Coefficient of discharge for plate orifice meters (D, $D/2$ tappings)

called the venturimeter (or venturi tube) known after its inventor. The convergent section can be made shorter by employing a larger cone angle; but the diverging part should not have a very large divergence on account of the decelerating flow. The recommended value of the cone angle for this section is 5 to 15 degrees.

A venturimeter tube with standard dimensions is shown in Figure 11.23. The length of the throat is equal to its diameter (d) which

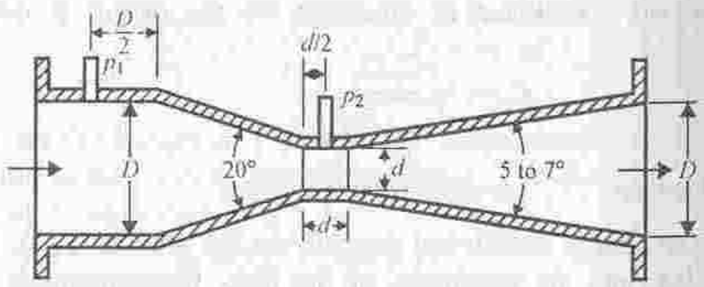

FIGURE 11.23 : A venturi-meter

should not be less than 2 cm. The recommended range of area ratio $n = (d/D)^2$ is from 0.05 to 0.55. The variation in the discharge coefficient with area ratio and Reynolds number for venturi tubes is small. For conical venturi tubes of $n = 0.1 - 0.55$ and $\text{Re} = 5 \times 10^3 - 3 \times 10^5$ the discharge coefficient is between 0.985 and 0.900.

Equation (11.27) derived for the orifice plate is also valid for the venturimeter. But on account of the ability to measure the pressure p_2 at the well defined throat in this case $C_c = 1$ and

$$A = A_2 = \frac{\pi}{4} d^2$$

$$\dot{m} = \frac{C_d A}{\sqrt{1 - n^2}} \sqrt{2\rho (p_1 - p_2)} \tag{11.30}$$

The difference between the value of C_d in Equations (11.29) and (11.30) should be noted.

The venturitube differs from the orifice or the nozzle mainly due to the fact that the jet after passing through the minimum cross-sectional area (throat) does not suddenly expand to a large area. Therefore, the flow in this device experiences much lesser pressure loss compared to other constrictions. Therefore, if this is an important consideration use of venturimeter is preferred. On the other hand this device requires larger space between the pipes, which may be a disadvantage in some situations.

11.7.4 Nozzle Meter

A standard nozzle for metering the flow rate is shown in Figure 11.24. Various dimensions in terms of the pipe diameter (D) and the nozzle throat diameter (d) are shown. The nozzle, like the previously described

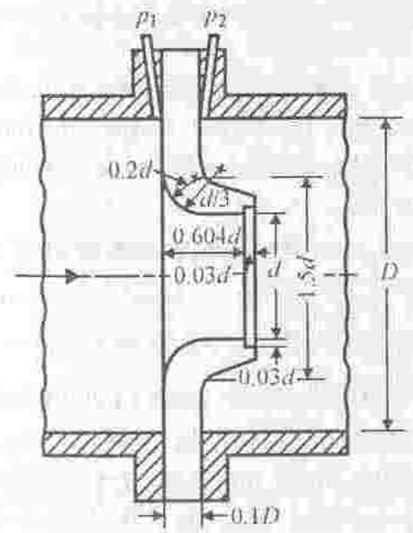

FIGURE 11.24 : A standard nozzle

devices is bolted between the pipe flanges. The head across the nozzle is measured through corner pressure tappings. It is obvious from the arrangement that these pressures (p_1 and p_2) will appreciably differ from the mean values upstream and downstream of the nozzle. Therefore, the value of the discharge coefficient for the nozzle covers this aspect.

Values of the various critical parameters for the nozzle meters are given below:

$$n = 0.05 \text{ to } 0.55$$
$$d \nless 1.2 \text{ cm}$$
$$D \nless 5.0 \text{ cm}$$

The discharge coefficient of a nozzle meter is higher than that of the orifice meter. Its values for a standard nozzle are shown in Figure 11.25. For the same value of the area ratio (n) the nozzle by virtue

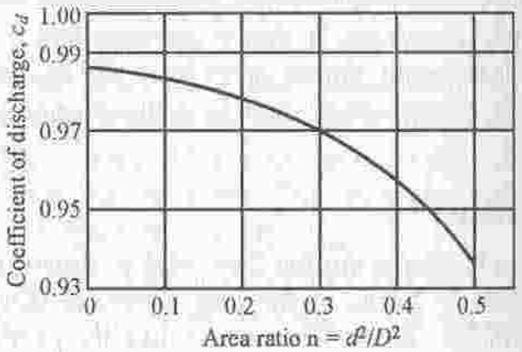

FIGURE 11.25 : Coefficient of discharge for a flow nozzle

of its higher discharge coefficient introduces lesser resistance in the flow passage. Besides this the value of the discharge coefficient of a nozzle is less sensitive to erosion caused by solid particles generally present in the gas or air.

Flow nozzles can also be used at the end of a pipe, and the discharge opening from a reservoir.

11.7.5 Rotameter

Rotameters are used to measure the flow rates of both liquids and gases in a wide range (1.25×10^{-4} m^3/h to 5000 m^3/h). This device is an advanced version of the "ball and tube type" flow meter developed by Ewing; in this the position of a steel ball in a vertical tapered tube was utilized as a measure of the flow rate through the tube.

In the present designs the steel ball is replaced by a float as shown in Figure 11.26. The position of the float in the transparent and graduated section of the vertical tube is a measure of the flow rate as explained below:

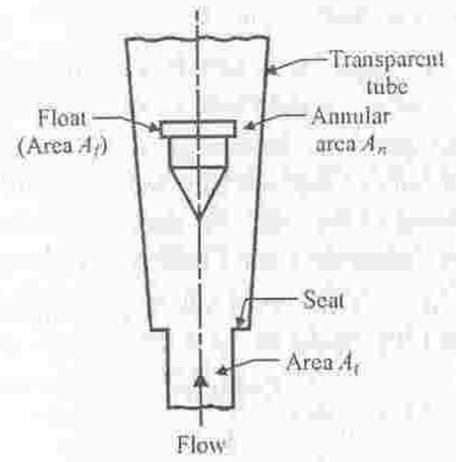

FIGURE 11.26 : A Rotameter

When there is no flow through the rotameter the float rests on the seat; the cross-sectional area (A_t) of the vertical tube below the seat is a little smaller than the maximum float area (A_f) perpendicular to the upward flow.

When a steady flow is established the float rises from the seat and stops at a certain height in the tapered section; this happens when the upward and the downward forces acting on the float are equal. The upward force due to the flow is

$$F_1 = K \frac{\rho A_f c^2}{g} \qquad (11.31)$$

(K = resistance coefficient)

The upward buoyant force

F_2 = (density of the fluid) × (volume of the float)

$$F_2 = \rho V_f$$

The weight of the float

W_f = (density of the float) × (volume)

$$W_f = \rho_f V_f$$

For equilibrium $F_1 + F_2 = W_f$

$$K\rho A_f \frac{c^2}{g} + \rho V_f = \rho_f V_f$$

$$K\rho A_f c^2 = (\rho_f - \rho)\, g\, V_f \tag{11.32}$$

Fluid velocity (c) required to satisfy Equation (11.32) depends on the annular area (A_n) between the float and the tapered tube. Therefore, at a given flow rate the float attains an equilibrium position at such a section in the tube where the velocity (c) satisfies Equation (11.32). Thus the float positions in the tube for specified values of temperature and pressure can be calibrated for fluid velocity or the flow rate.

If the density of the float material is much greater than the fluid density, Equation (11.32) reduces to

$$c = \frac{\text{constant}}{\sqrt{\rho}} \tag{11.33}$$

The flow rate is given by

$$\dot{m} = \rho A_n c$$

$$\dot{m} = \text{constant}\ \sqrt{\rho} \tag{11.34}$$

11.7.6 Electrical Flow Meter

In this method the flowing air or gas is heated in an insulated pipe by an electrical heating element as shown in Figure 11.27. The heat

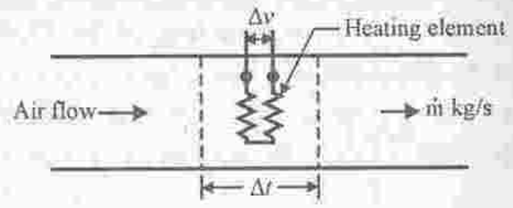

FIGURE 11.27 : Electrical flow meter

Q required to maintain a specified temperature difference (Δt) between the two sections of the duct for a given mass flow rate is given by

$$Q = \dot{m} c_p \Delta t \tag{11.35}$$

The heat Q is supplied by passing an electric current (I) through the resistance R. The corresponding voltage drop across the heating element is ΔV. Therefore, Equation (11.35) is rewritten as

$$\dot{m} = \frac{Q}{c_p \Delta t}$$

$$\dot{m} = \frac{I^2 R}{c_p \Delta t}$$

$$\dot{m} = \frac{(\Delta V)^2}{R c_p \Delta t} \tag{11.36}$$

In this equation values of R and c_p are known. To determine the mass flow rate the voltage drop ΔV or the current I is adjusted to obtain the desired temperature difference Δt. The value of Δt can be so chosen that it is accurately determined, preferably by an array of thermocouples.

This is a very convenient method of measuring velocity and flow rate without causing appreciable pressure drop in the flow passage. Flow rates as low as 1 litre/hour can be measured by this method.

11.7.7 Soap Film Method

This simple method is particularly suitable for very small flow rates. The arrangement adopted is shown in Figure 11.28 (*a*). The flow enters

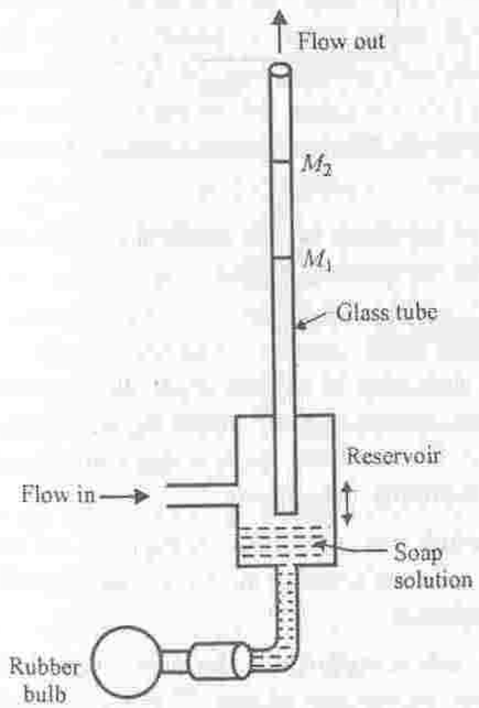

FIGURE 11.28 (*a*) : Soap film method of flow measurement

a reservoir which is partly filled with soap solution; the reservoir is in communication with a rubber bulb which is used to raise or lower the solution surface in the reservoir. The gas leaves the measuring arrangements through a vertical glass tube.

To measure the flow rate or the velocity in the vertical glass tube a soap film is sent through it along with the flow by raising the level of the solution to its lower end in the reservoir. The speed of the soap film (fluid velocity) is easily determined by recording its time of travel in the glass tube between the two marks M_1 and M_2. This with the area of cross-section of the tube gives the flow rate. A calibration curve as shown in Figure 11.28 (*b*) can be prepared for quick determination of the flow rate.

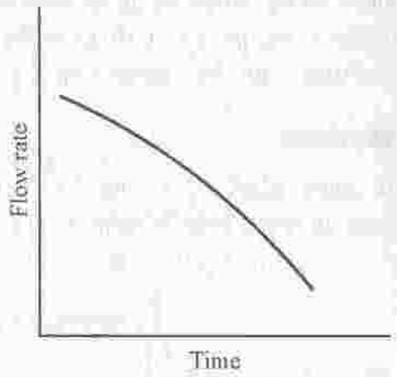

FIGURE 11.28 (*b*) : Calibration for soap film method

The degree of accuracy of this method is high and mainly depends on the accuracy in measuring time.

11.8 WIND TUNNELS

A wind tunnel is a device in which a jet of air or any other suitable gas (freon, nitrogen, steam etc.) of uniform properties across the cross-section is produced. This is used for aerodynamically testing the models under the given standard conditions.

All wind tunnels are generally comprised of the driving unit, a settling chamber, an accelerating duct (contraction or nozzle), the test section and the diffuser.

The driving unit consists of the fan, blower or a compressor, generally driven by an electric motor. The location of the driving unit depends on the type of the tunnel. If a large electric motor is kept

in the flow circuit it will heat the flow raising its temperature continuously.

The flow from the compressor/blower or a fan is settled in a large chamber called the settling chamber; this is provided with wire gauzes and arrays of honeycombs to straighten the flow and remove irregularities in it. On account of very low flow velocity, near stagnation conditions exist in the settling chamber.

The settling chamber supplies the flow to the contraction located downstream. This is carefully designed to accelerate the flow from the settling chamber to the test section velocity with minimum disturbance.

The contraction or the nozzle feeds the test section with a jet of uniform velocity. The model to be tested is fixed here with suitable supports. A transparent window of strong glass is often provided on one or both the side walls of the test section. This facilitates in handling the model and the instruments and also permits optical measurements in the flow over the model surfaces.

The diffuser collects the flow from the test section and raises the pressure of the air for discharging it into the atmosphere or the return circuit in case of a closed circuit tunnel. Boundary layer thickening and separation on account of strong pressure gradients in the diffuser should be minimized. The diffuser throat is often made flexible; this allows the throat to be varied for starting and running conditions. After starting the diffuser throat area is reduced for optimum running conditions. If the jet from the diffuser is discharged into the atmosphere a distributor and a silencer are often used after the diffuser to reduce the noise level in the area.

In high speed tunnels the temperature in the test section is very low and the moisture in air will condense on the flow surfaces. To prevent this air is passed through a drier. In a closed circuit tunnel this can be done by passing only a part of the main flow through the drier. But in the open circuit types all the air should pass through the drier, thus increasing its size.

Some types of wind tunnels are described here.

11.8.1 Blower Tunnels

The arrangement adopted in a blower tunnel is shown in Figure 11.29. The air from an axial fan enters the settling chamber through a diffuser to reduce the pressure losses. The diffuser cannot always have a small divergence angle on account of impractical lengths. Therefore, wider

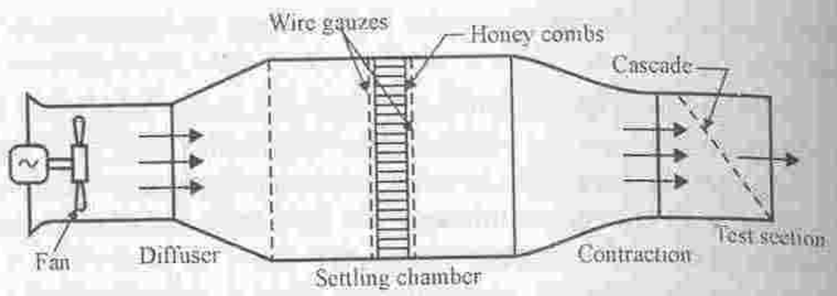

FIGURE 11.29 : A blower type wind tunnel

angle diffusers provided with a number of small compartments are used. The contraction feeds the test section with an air jet at near ambient conditions; this is a special advantage of this type of the tunnel because models and instruments can be easily manipulated during the operation of the tunnel.

Blower tunnels are specially useful for conducting low speed ($M < 1$) tests on cascades of turbine and compressor blades; in these tests the cascade is mounted on the oblique exit end of the test section as shown in the figure. This becomes necessary to take care of the entry blade angles.

Since the air from the test section is exhausted into the atmosphere it is an open circuit tunnel.

11.8.2 Suction Tunnels

Another low speed open circuit tunnel is shown in Figure 11.30. Air is sucked into the tunnel through the contraction, honeycombs, test sec-

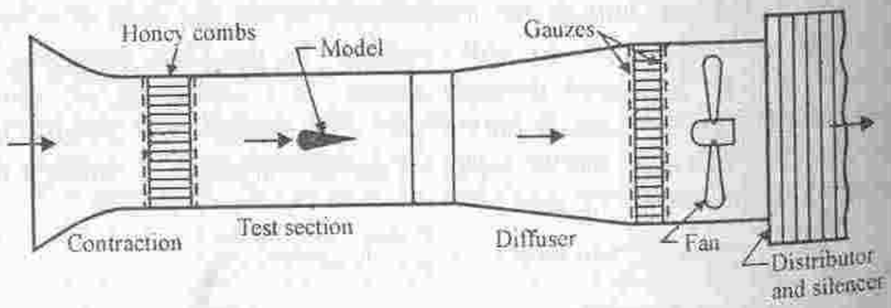

FIGURE 11.30 : A suction type wind tunnel

tion etc. by an exhaust fan. The air jet in the entire tunnel is slightly below atmospheric pressure; therefore for a given velocity in the test

section the power required to drive the fan is comparatively lesser. The fan exhausts the air into the atmosphere through a distributor which may also act as a silencer. Since the model is located inside the closed test section, manipulation of the instruments is slightly difficult.

11.8.3 Open Jet Tunnels

In an open jet wind tunnel the test sections in Figure 11.29 and 11.30 are kept open on all sides. In the open jet return circuit tunnels this jet is collected and returned back to the fan. This arrangement makes the handling of the model and the instruments easy.

Return circuit tunnels, whether open or closed circuit type, occupy much more space compared to the straight open circuit type.

11.8.4 Induction Tunnels

An induction tunnel is shown in Figure 11.31. The flow in the test section is induced by introducing high pressure air downstream of the test section through an annular nozzle. Such a tunnel is used when there is a relatively small quantity of high pressure air available.

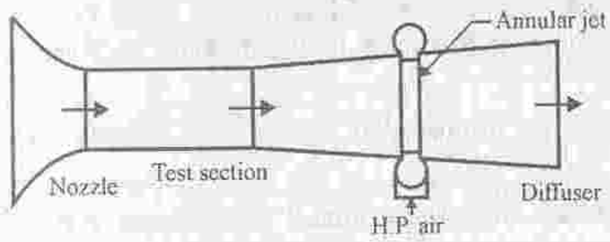

FIGURE 11.31 : An induction type wind tunnel

The great advantage of an induction tunnel is that its operation is independent of the compressor characteristic. The compressors are used to fill large reservoirs at the required pressure. The tunnel may then be operated at any convenient time even when the power is not available to run the compressors. It may be noted that such tunnels are of the blowdown or intermittent type and the duration of operation is very short.

These tunnels by proper design can be used in a wide range of subsonic and supersonic Mach numbers ($M < 2.5$). The mass of the air flowing through the test section is of the order of about ten times the mass of the high pressure air. This value would obviously depend on the Mach number, and the area ratio of the nozzle and the test section.

11.8.5 Supersonic Tunnels

Supersonic tunnels are those in which the test section Mach numbers are greater than unity.

Section 6.15 has already dealt with some aspects of the flow in supersonic tunnels. Figure 6.10 and 6.11 show the shock locations in starting and steady running positions. Figure 6.12 shows the difference of power required between the starting and steady running operations. Any of the following arrangements can be adopted in supersonic tunnels:

(*i*) continuous open circuit type,

(*ii*) blow-down or intermittent type,

(*iii*) continuous closed circuit type.

To obtain higher values of the Mach number in the test section at low gas velocities a suitable gas of higher molecular weight is used. For example, Freon-21 has the following properties:

$$p = 1.0 \text{ bar},\ T = 293 \text{ K},\ R = 0.095 \text{ kJ/kg K},$$

$$\text{velocity of sound } a = 181.4 \text{ m/s}$$

It is observed that the sound velocity in Freon-21 is about half its corresponding value in air. Thus for the same flow velocity Mach number obtainable in Freon-21 is about twice its corresponding value in air.

This aspect is discussed in Section 5.2. Equation (5.13) explains this point.

Open circuit supersonic tunnel (Continuous type): Figure 11.32 shows the arrangement used in an open circuit tunnel. Air is continuous-

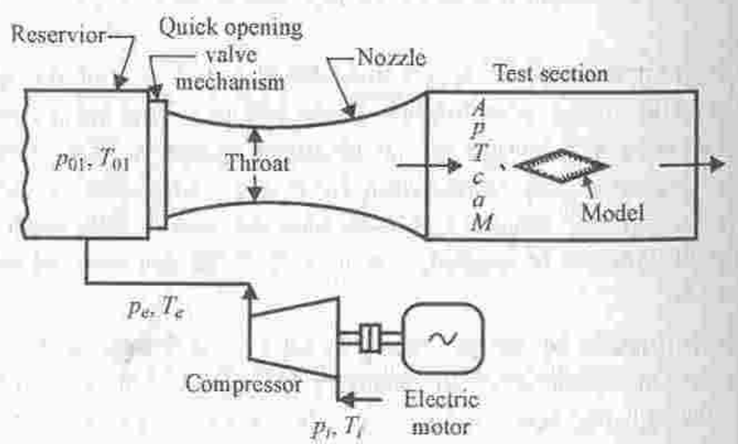

FIGURE 11.32 : An open circuit supersonic wind tunnel

ly supplied to the reservoir by a compressor which may be either reciprocating, centrifugal or axial type; this depends on the type of the tunnel, the test section size and the Mach number. High pressure air is continuously expanded from the stagnation state (p_{01}, T_{01}) to the test section pressure p through the convergent-divergent nozzle.

Various flow parameters in the test section are shown in the figure. It may be noted that the test section Mach number is only a function of the pressure ratio across the nozzle.

$$M = f\left(\frac{p}{p_{01}}\right) \tag{11.37}$$

Therefore, for the desired values of the test section Mach number and the temperature the stagnation temperature (T_{01}) is also fixed. In the present setup shown the air temperature (T_e) at the compressor exit may be lower or higher than the required temperature in the reservoir. Therefore, the correct value of the temperature T_{01} is obtained by either heating or cooling the air from the compressor.

The cross-sectional area (A) of the test section is determined by the capacity of the compressor, and the state of air in it;

$$\frac{T}{T_{01}} = f(M) \tag{11.38}$$

Equations (11.37) and (11.38) give the density of air in the test section.

$$\rho = \frac{p}{RT}$$

Velocity of sound in the test section is

$$a = \sqrt{\gamma RT}$$

$$c = Ma = M\sqrt{\gamma RT}$$

The mass flow rate is given by

$$\dot{m} = \rho Ac$$

$$A = \frac{\dot{m}}{\rho c} = \frac{\dot{m}}{pM}\sqrt{\frac{RT}{\gamma}} \tag{11.39}$$

It is obvious that the arrangement described here is not the best way of obtaining a continuous supersonic flow; some of the shortcomings of this method are:

(*a*) All the air from the compressor has to pass through the drier (not shown in Figure 11.32).

(*b*) The test section throws away a considerable quantity of energy into the atmosphere. Thus the compressor pressure ratio and the power required for a given Mach number are very high.

(*c*) The exit of the high velocity jet has its own nuisance.

To overcome some of these problems the same arrangement can be used as a blowdown or intermittent tunnel.

Blow-down tunnel: The operation of this tunnel is intermittent. This makes use of the high pressure air stored in large reservoirs. A quick opening valve between the reservoir and the nozzle is used to start the tunnel. The high pressure air is expanded to the atmosphere through the supersonic nozzle and the test section in an intermittent operation of a very short duration; the operation time is of the order 1/4 to 5 min. depending on the test section size, Mach number and the reservoir capacity. Some time is required for filling the reservoirs before another run; this reduces the availability of the tunnel. Since the only power required is to fill the reservoirs between test runs, operation of such tunnels is economical.

A specially designed constant pressure valve is used for maintaining pressure at the nozzle entry constant.

Blow-down concept can also be used by employing high vacuum in a reservoir downstream of the diffuser. The supply to the test section is from the infinite reservoir of the atmosphere upstream of the nozzle; thus the supply conditions are constant during the operation of this tunnel. Besides this advantage the entire body of the tunnel is of a cheaper construction as it is not required to operate at high pressures.

Closed circuit supersonic tunnel (Continuous type): A closed circuit continuous supersonic wind tunnel is shown in Figure 11.33 (*a*). This overcomes some of the problems confronted in the open circuit tunnels described earlier. The complete arrangement in this tunnel consists of a compressor, the reservoir (supply section), the supersonic nozzle, test section, the diffuser, the downstream reservoir (receiver), the drier and the cooler. On account of the closed circuit any gas besides air can also be used; the open circuit continuous and the blow-down tunnels do not have this advantage.

The high kinetic energy at the exit of the test section is partly recovered by the supersonic diffuser; thus the compressor receives the air (or gas) at a much higher pressure than in an open circuit tunnel.

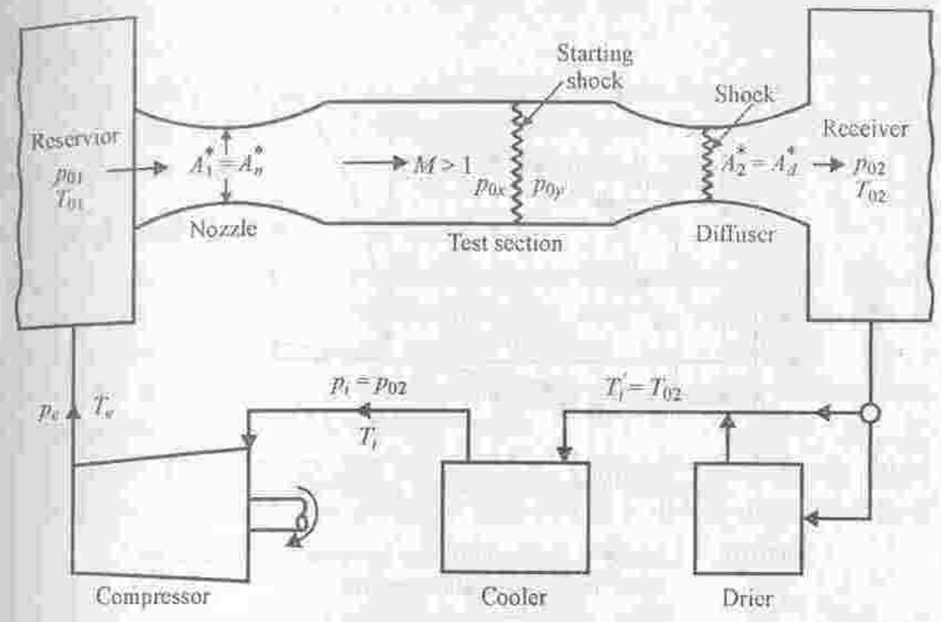

FIGURE 11.33 (*a*) : A closed circuit continuous type supersonic wind tunnel

This greatly reduces the compressor pressure ratio and the power. If loss only due to the shock wave is considered the pressure ratio across the compressor is p_{01}/p_{02}; this assumes constant pressure drying and cooling of the air.

On account of the high rate of dissipation of energy in such tunnels the stagnation temperature T_{01} of the air will continuously rise. Therefore, to keep it constant at the required value the air is cooled before entering the compressor.

Alternatively, the cooler can be located at the exit of the compressor but it should be noted that it is advantageous for the compressor to cool the air before compression.

The temperature-entropy diagrams of the compression processes before and after the cooling are shown in Figure 11.33 (*b*). If the pressure losses in the drier, cooler and the connecting passages are ignored and the temperature change in the drier is negligible,

$$\left.\begin{aligned} p_{02} &\approx p_i \\ T_i' &\approx T_{02} \\ p_{01} &\approx p_e \\ T_{01} &\approx T_e \end{aligned}\right\} \qquad (11.40)$$

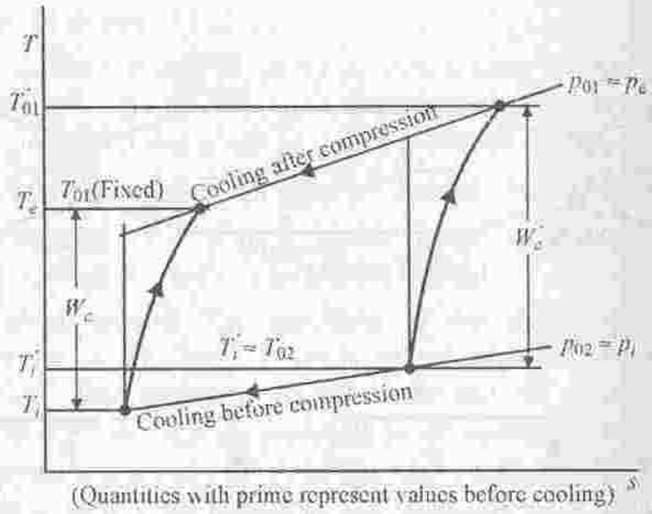

FIGURE 11.33 (*b*) : *T-s* diagrams for compression processes before and after cooling

The compressor pressure ratio is given by

$$p_r = \frac{p_{01}}{p_{02}} = \frac{p_e}{p_i} \tag{11.41}$$

Above relations have been written assuming that the flow velocities from the receiver to the reservoir are small and the values of the static and stagnation properties are identical.

The values of the work done by the compressor before and after the cooling are

$$W_c' = \dot{m} c_p (T_{01}' - T_i')$$

$$W_c' = \dot{m} c_p T_i' [p_r^{(\gamma-1)/\gamma} - 1] \tag{11.42}$$

$$W_c = \dot{m} c_p (T_{01} - T_i)$$

$$W_c = \dot{m} c_p T_i [p_r^{(\gamma-1)/\gamma} - 1] \tag{11.43}$$

Since $T_i' > T_i$ Equations (11.42) and (11.43) show that the work of compression after cooling is lesser than its corresponding value before cooling.

$$W_c < W_c'$$

Some air from the receiver is passed through the drier which contains an array of anhydrous materials (calcium chloride, alumina etc.). The tunnel being closed circuit all the air need not pass through the

drier; this is a great advantage because the size of the drier can be kept much smaller.

For changing the test section Mach number the tunnel may be provided with replaceable nozzle blocks or liners. Flexible nozzle and diffuser allow continuous variation of the Mach number.

11.8.6 Shock Tubes

A shock tube is another form of a blow-down or an intermittent tunnel. As the term indicates the shock tube is a duct in which high Mach number flow is generated by passing a shock wave through it. Sections 5.4.2 and 6.16 explain how a stagnant gas is set in motion due to the passage of a strong shock wave.

Figure 11.34 shows the arrangement adopted for a shock tube; it consists of high and low pressure sections in a strong duct separated

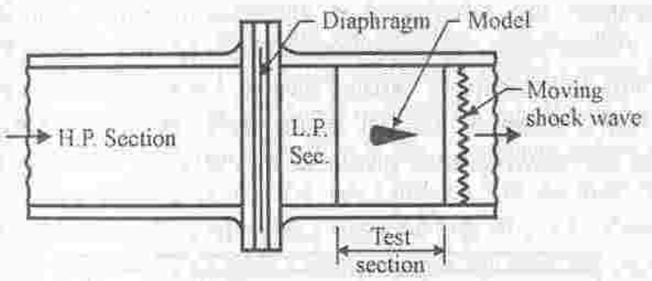

FIGURE 11.34 : A shock tube

by a diaphragm. The pressure in the high pressure section is increased to many atmospheres while the low pressure section is maintained at a high vacuum. The model to be tested is kept in the test section located in the low pressure section. All the automatic recording instruments and photographic equipment (if any) are kept ready before a test run.

For operating the shock tube the pressure in the high pressure section is further increased to rupture the diaphragm; after the rupture due to the high pressure difference a strong shock wave moves into the initially stagnant gas in the low pressure section imparting a high velocity (high Mach number) to the gas in the test section. The time of operation in shock tubes is very short, generally in terms of milliseconds.

In some shock tubes on account of very high vacuum on the low pressure side ambient air forces its way into the low pressure section through joints and porous walls of the shock tube. This is a serious

practical problem in high Mach number shock tubes and can be resolved by using specially designed joints and non-porous materials.

One great advantage of testing models in shock tubes is the absence of low temperature in the test section. On the contrary the high stagnation temperature occurring in the test section are representative of the actual conditions.

11.8.7 Gun Tunnels

The conventional high Mach number supersonic tunnels suffer from a serious disadvantage of low temperature in the test section: this is overcome in the shock tube by accelerating the flow by a shock wave. The same principle in a slightly different way is employed in the gun tunnels. Here very strong shock waves are generated by a moving piston.

In a typical gun tunnel a multistage compressor raises the pressure of nitrogen to about 10,000 bar in a strong reservoir. One or more 5 mm thick diaphragms are punctured in succession which forces the flow in a thick walled cylinder provided with a piston. The movement of the piston and the resulting strong shock waves downstream generate very high Mach numbers (≈ 10) in the test section as shown in Figure 11.35. If the downstream pressure in the duct is reduced to a very

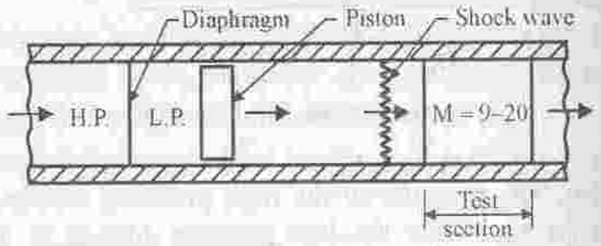

FIGURE 11.35 : A Gun tunnel

small value still higher Mach numbers (≈ 20) can be obtained. Such tunnels are used for studying hypersonic and non-equilibrium flows, and meteorological problems.

11.9 Flow Visualization

Visual study of a given flow pattern is convenient and useful in many practical situations. For example, in a steady laminar flow the streamline pattern can be made visible by introducing dense smoke into the flow. Visualization of the flow pattern, wherever possible, gives the real picture of the flow phenomena. In yet another example the nature of flow,

laminar or turbulent, transition, separation and the presence of vortices can be observed and studied by adopting a number of flow visualization techniques developed till date. Some of these methods are discussed here.

11.9.1 Streamers

Small streamers or surface tufts of wool, silk or cotton attached at one end to the surface of the model give the general direction of the flow. If the flow is steady and laminar the tufts remain steady in a particular direction whereas in the turbulent flow region (as on the suction surface of an aerofoil blade nearer the trailing edge) free ends of the streamers leave the surface and exhibit violent fluttering. This phenomenon along with the rotating movement of the tufts indicate the presence of circulatory flows in the region.

11.9.2 Liquid Films

This method makes use of the contrast obtained on account of the unequal rates of evaporation of a liquid film in the laminar and turbulent regions. A film of some volatile oil is applied on the surface of the model prior to starting the flow. When the air flow takes place over this surface the evaporation of the oil film in the turbulent region is faster than in the laminar region. A clearer contrast is obtained by using black paint on the surface. This method can be easily employed for aerofoil blade surfaces in wind tunnels.

11.9.3 Smoke

Dense smoke introduced into a flow field by a smoke generator can make the streamline pattern visible. Smoke is generally injected into the flow through an array of nozzles or holes.

Kerosene oil can be conveniently used in a smoke generator. The oil is heated to its boiling point by an electric coil; the smoke is formed by introducing the vapours into the air stream. Smoke can also be produced by many other methods. For better results smoke should be light, non-poisonous and free of deposits.

11.10 OPTICAL METHODS

Optical method for studying a flow field is a valuable and widely used technique. As pointed out earlier on many occasions variation of density in a compressible flow field is appreciable. The refractive index of the medium (flow field) and the velocity of light through it are functions

of the density field. For a given medium and wave length of light refractive index is a function of density.

$$n = f(\rho) \tag{11.44}$$

For compressible flows this can be approximately expressed as

$$n = 1 + \beta\left(\frac{\rho}{\rho_{ref}}\right) \tag{11.45}$$

The basis of all the optical methods of study of compressible flow is the variation of the density to a lesser or greater degree. Figure 11.36 (*a*) shows the variation of density along the width of test section of a wind tunnel; Figure 11.36 (*b*) and (*c*) give corresponding variations of the first and the second derivatives of the density.

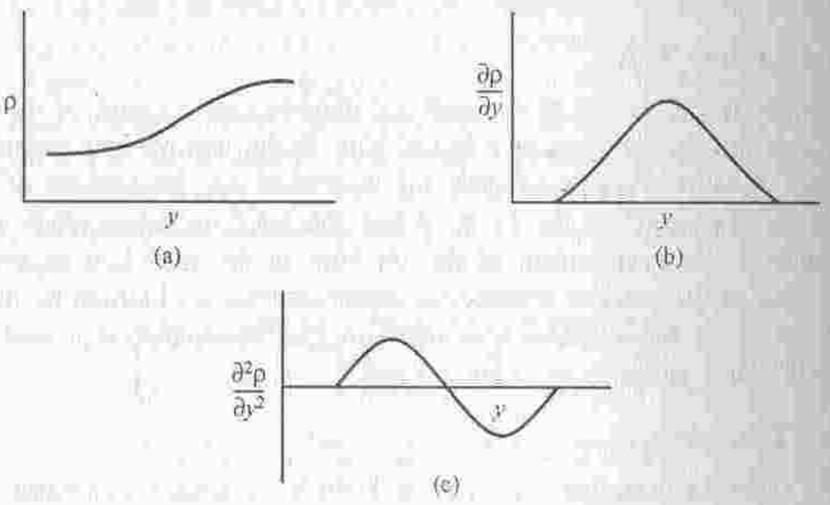

FIGURE 11.36 : Variation of density and its first and second derivatives

The three optical techniques described here are:

(*i*) the shadowgraph,

(*ii*) the interferometer and

(*iii*) the Schlieren system

Each of these techniques is based on either of the variations shown in Figure 11.36.

If the variations of refractive index in the flow field are measured the corresponding density variations can be determined from this. Density along with pressure can yield the values of temperature, velocity of sound, Mach number etc.

By using these techniques the flow field can either be observed on a screen or its permanent record is obtained on a photographic plate. The great advantage of optical methods over other methods is that the instruments are not inserted into the flow; thus the flow is undisturbed in this method of flow investigation.

Various optical and mechanical details employed in these techniques have not been given here; only the basic principles of operations are given.

Though the working of these methods is described here with reference to a model in the wind tunnel test section, they can no doubt be used in a variety of other situations. The flow direction in the test section is considered perpendicular (x-direction) to the plane of the paper, while the light beam is parallel to the span (z-direction) of the model—an aerofoil or a wedge. These directions are shown in Figure 11.37.

11.10.1 Shadow Technique

The arrangement adopted in this technique is shown in Figure 11.37 and is often referred to as a shadowgraph. The collimating lens provides

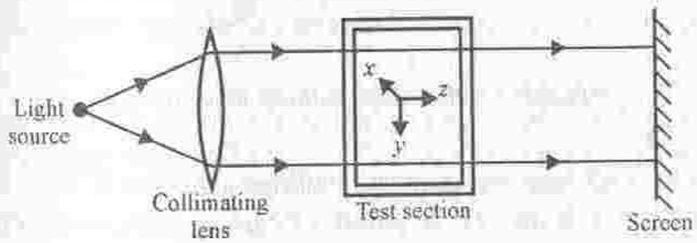

FIGURE 11.37 : Shadow technique

a collimated beam of light from the source. This beam passes through the transparent walls of the test section. The shadow picture of the flow is directly obtained on a white screen placed on the other side of the test section. The degree of brightness on the screen is proportional to the second derivative of the density, $\frac{\partial^2 \rho}{\partial x^2}$ (see Figure 11.36 (*c*)). The varying degree of brightness is a measure of the variations in the density field.

This technique gives clear pictures of the density variation in flows with shocks and combustion. The method is convenient because the required equipment is inexpensive and easy to operate.

10.10.2 Interferometer Technique

In this technique the variation of density in the flow field is directly determined from the interference pattern obtained on the screen or a photographic plate.

The most widely used apparatus based on this technique is the Mach-Zehnder interferometer which is shown in Figure 11.38. It consists

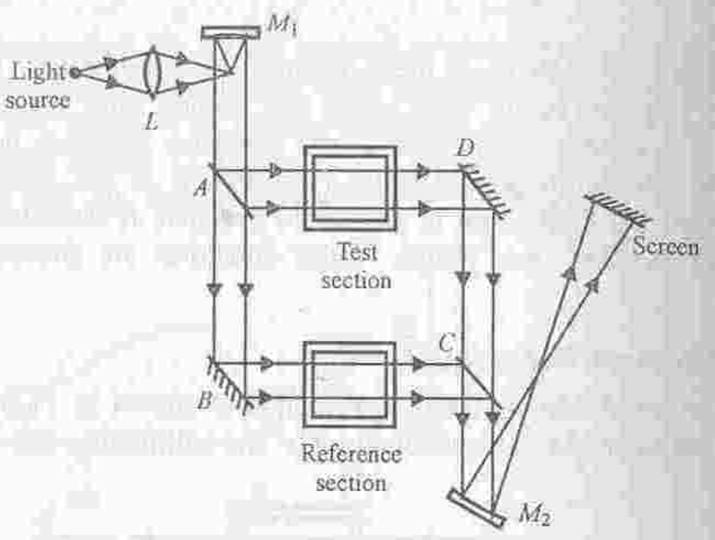

FIGURE 11.38 : Mach Zehnder interferometer

of two plane half silvered mirrors (splitters) A and C, and two fully reflecting mirrors B and D. A parallel beam of light is obtained from the light source through the lens L and concave mirror M_1. The splitter A reflects a part of this beam to the transparent section of the test section; the rays of light from the test section are reflected by the mirror D to a concave mirror M_2 through the splitter C.

The part of the beam from M_1 which passes through the splitter A is reflected by the mirror B to the reference section; this has transparent walls identical to those of the test section. Therefore, these walls act as compensating plates. The rays from the reference section also reach the concave mirror M_2 after reflection from the splitter C. Thus the mirror M_2 collects the rays coming separately from the test section and the reference section and directs them on the screen or a photographic plate. After emerging from the splitter C the two parts of the light beam merge into one single coherent beam before reaching

the mirror M_2; thus the pattern of illumination reflected on the screen would be uniform when there is no flow in the test section like the reference section. When the flow is established in the test section the beam of light passing through its density field will be out of phase with the beam coming through the reference section; in this case the mirror M_2 will reflect an interference pattern on the screen; this represents the variable density pattern in the flow field.

While the interferometer is suitable for quantitative measurement of the density variation in a flow field it requires expensive equipment which is difficult to operate.

11.10.3 Schlieren Technique

In this technique the density gradient $(\partial\rho/\partial x)$ in the flow field is obtained in terms of the varying degree of the brightness on the screen; the degree of brightness or intensity of illumination is proportional to the density gradient in the flow field.

The arrangement adopted in the Schlieren technique is shown in Figure 11.39. A beam of light is sent through the test section from the light source by a properly oriented concave mirror M_1. The beam coming from the test section is reflected on to the screen or a photographic plate through two suitably located concave mirrors M_2 and M_3.

A sharp knife edge is inserted at the focal point of the mirror M_2 to intercept about half the light. Thus in the absence of flow through

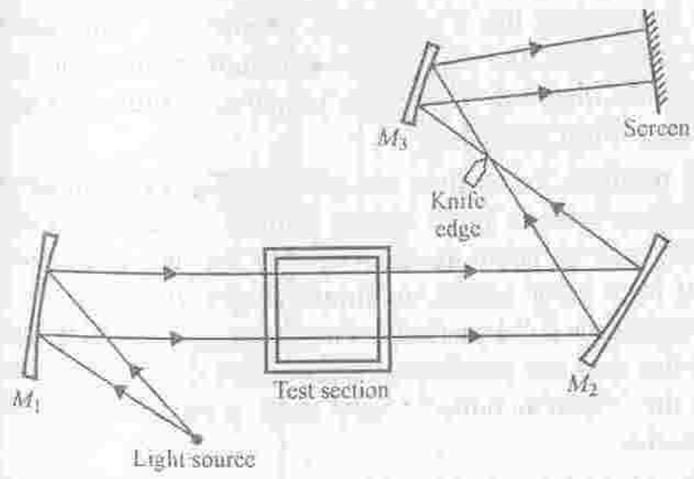

FIGURE 11.39 : Schlieren technique

the test section the screen is illuminated uniformly by the light escaping the knife edge. But in the presence of flow the rays of light are differently deflected (as in a prism) on account of the variable density and the refractive index in the flow field. Therefore, greater or lesser part of the light beam will now escape the knife edge. This gives a varying intensity of the illumination on the screen.

11.11 LASER TECHNIQUES

Application of lasers has provided the most powerful and reliable optical method of measuring velocity, direction and turbulence in liquids and gases over a wide range. In this method a laser beam is focussed in the flow field (test section) where measurement of velocity, turbulence etc., is required. The scattered light from the minute solid particles in the flow is utilized as a signal for velocity measurement by employing a number of optical and electronic equipment such as special lenses, beam splitters, photo detectors, signal processors, timing devices, data acquisition system and a computer.

Laser is an acronym for Light Amplification by Stimulated Emission of Radiation; this is a strong source of monochromatic and coherent light. In this light emitted from one atom of the gas is employed to amplify the original light. Helium-Neon lasers are commonly used in the range 0.5-100 milli watts; they have comparatively lower cost and higher degree of reliability. Argon-ion lasers are used in higher power range *i.e.*, 5 m watts-15 watts. CO_2 lasers have a range of power between 1 and 100 watts. Higher power lasers produce greater noise level in the system which interferes with the signal.

The laser beam has a very high intensity of light which can be damaging to the eyes and skin. It can also start spontaneous combustion of inflammable material. Therefore, proper precautions must be taken while using a laser system.

Solid particles in the flow act as scattering points at the measuring stations. If they are too small having density close to that of the flow their velocity can be taken as equal to the flow velocity; this condition is satisfied to a great extent, in liquid flows. In air flows the small naturally occurring solid particles should act as scattering point. Very small particles may not produce a signal of sufficient strength and would be lost in the "system noise"; very large size particles will give erraneous results.

Artificial seeding plant can also be employed to supply solid particles of the desired size (about one micron).

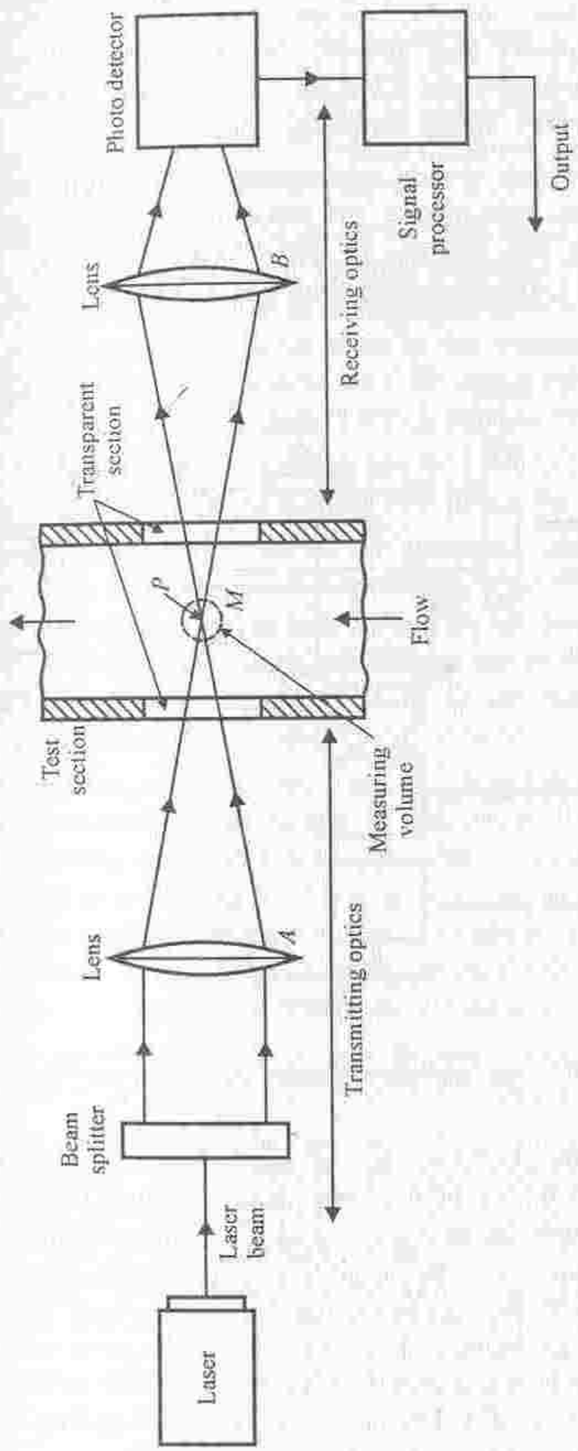

FIGURE 11.40 : Dual-beam laser doppler velocimeter (with forward scatter)

Two widely used laser systems for flow measurement are (*a*) The Laser Doppler velocimeter or anemometer (LDV or LDA) based on the Doppler frequency shift and (*b*) The Dual focus velocimeter based on the flight time of solid particles between two beams. These will be described briefly in the following sections.

In these methods several components of the opto-electronic equipment including the transmitting and receiving lenses are placed on both the sides of the test section. In the forward scattering mode (Figures 11.40 and 11.42) the transmitting and receiving optical equipment

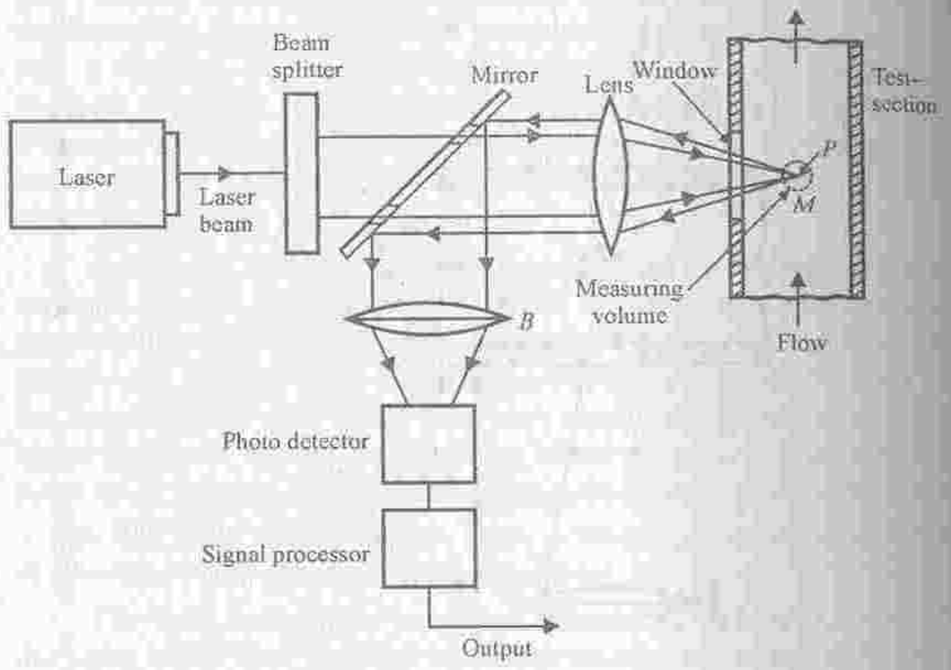

FIGURE 11.41 : Dual-beam laser doppler velocimeter (with back scatter)

and accessories are placed on the two sides of a transparent test section or windows. The power of the laser beam required in this method is comparatively lower. However, in a majority of cases where flow measurements are required it is not possible or convenient to place the receiving optics alongwith the accessories on the other side of the test section. Therefore, ingenious methods have been developed to receive the optical signal through the backscattered light on the same side of the test section (Figures 11.41 and 11.43). The power of the laser required in the "back scattering mode" is comparatively more.

11.11.1 Laser Doppler Velocimeter

When light is scattered by a moving particle there is a frequency shift between the original light and the scattered light; this "shift" or difference in frequencies is proportional to the particle velocity. This is the well known "Doppler effect" which was first employed for measurement of fluid velocity in the sixties.

Various optical arrangements have been successfully used. One of them is the Dual-beam laser Doppler velocimeter or anemometer (LDV/LDA); the layout of such an arrangement is shown in Figure 11.40. The laser source provides a laser beam to the transmitting optics consisting of the beam splitter, lenses etc., the beam splitter provides the two beams (dual-beam) to the lens *A* which focuses them at the measuring point *P* within a very small region [$< 1\,(\text{mm})^3$] of the flow *M*; this is also known as the measuring-volume or the probe-volume.

A fringe-pattern is formed by the scattering of light by the solid particles passing through the probe-volume; this is projected to the photodetector by the collecting lens *B*. The signal in terms of the Doppler frequency shift is processed in the signal processor which provides the output corresponding to the velocity of the solid particle (fluid velocity) passing through the measuring volume.

A transparent section or windows are provided in the test-section where the measurements are required. This allows the passage of the incoming and outgoing beams during a series of measurements. Measurements at other points in the flow region can be taken by moving the beamwaist and the probe-volume containing it to the required measuring station; this can be done by moving either the test-section or the entire laser system mounted on a movable table.

The layout of a Dual-beam laser Doppler velocimeter with backscatter is shown in Figure 11.41. The two beams emerging from the beam splitter pass through the apertures in the mirror inclined at 45° to the optical axis. Lens *A* focuses the beams at the measuring point *P* within the probe-volume *M*. The scattered light from the passing solid particles through the probe volume is collected back by the same lens *A* and transmitted to the lens *B* by the mirror. The fringe-pattern from the lens *B* is received by the photodetector and processed as before.

The great advantage of this system is that the entire "laser system" is located only on one side of the test-section; this makes the traversing of the laser system or the test-section comparatively easier for measurements at different point in the flow. The transparent window

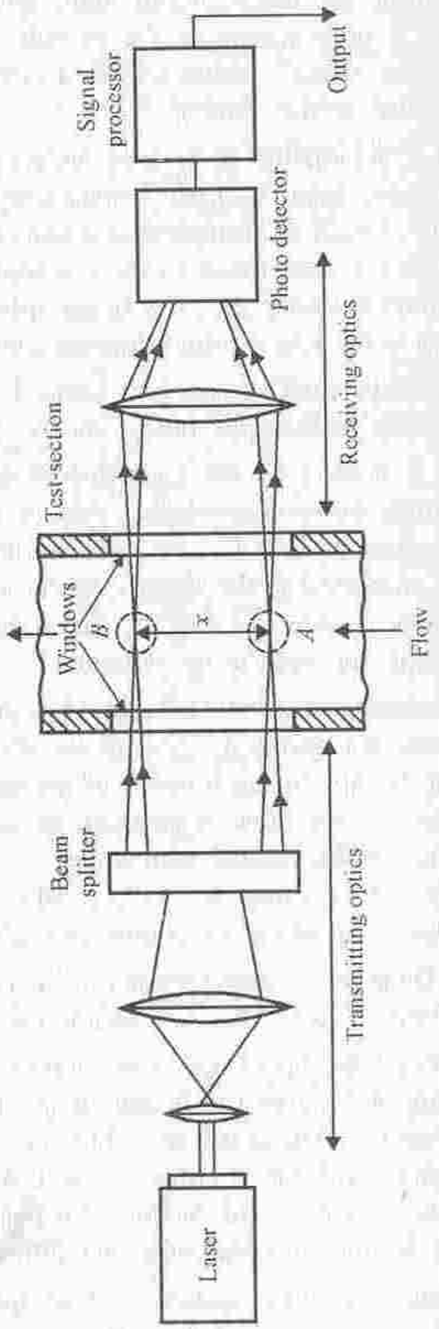

FIGURE 11.42 : Dual focus laser velocimeter (with forward scatter)

is also required only in one of the walls of the test section as shown in the figure.

11.11.2 Dual-focus Laser Velocimeter

The layout of a dual-focus laser velocimeter with forward scatter is shown in Figure 11.42. The transmitting optics consists of two cylindrical lenses and a beam splitter; two identical beams of equal power are focused at the measuring or probe volume in the flow occurring through the test-section as shown in the figure. The beam waists at the focal volumes A and B within the probe volume have microscopic widths (say of the order of 10 micron); the distance (x) between them is comparatively large, say twenty times the width of the beam waists. The total width of the probe volume in the flow direction is only a fraction of a milli-meter.

At the receiving end the beams are collected by a lens and photodetector. A solid particle in the flow passing through the focal volume A scatters light which is employed as a signal in the photodetector which passes it on to a time measuring device or a clock via the signal processor; this is the "start signal". The same sequence of events take place when the same particle passes through the focal volume B. In this case the opto-electronic equipment provides the "stop signal" to the clock. The start and stop signals thus obtained give the transit time (t) of the solid particle from A to B. Therefore, the particle or the fluid velocity at the measuring station or the probe-volume is simply given by $c = x/t$.

As pointed out earlier it is more convenient to adopt a laser velocimeter in the backscatter mode. The backscatter version of the dual-focus laser velocimeter is shown in Figure 11.43. The details of the transmitting and receiving optics have already been shown in the earlier figures. The two beams emerging from the beam splitter have been shown greatly enlarged to depict the beam waists and the focal volumes more clearly. As stated before light is scattered in all the directions by the solid particles passing through the focal volumes A and B. The light scattered backwards in the directions BC and AD is collected back by the receiving optics and photodetectors as shown in the figure. The signal processors and the time measuring device give the time of flight of the solid particle over the distance x. Thus the fluid velocity in the probe volume is obtained.

The entire optical and electronic equipment can be assembled in a casing to facilitate safe handling and traversing during measurements at a number of stations in the flow field.

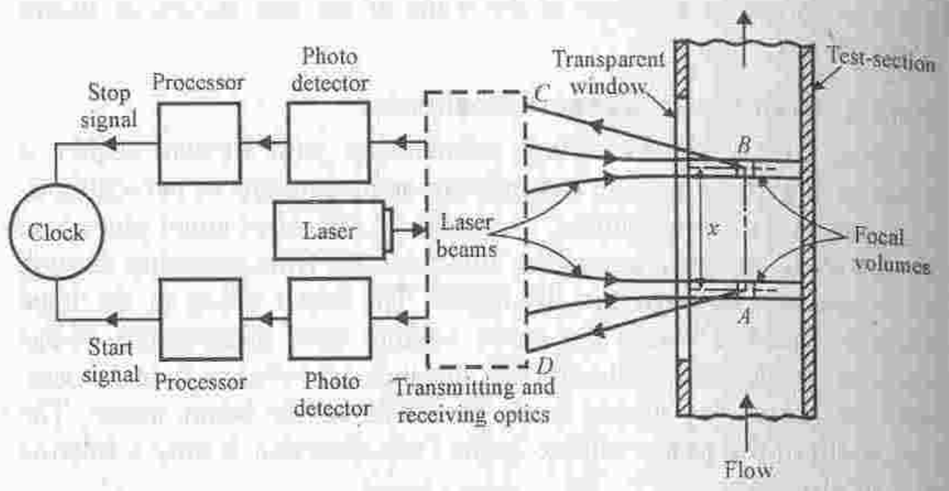

FIGURE 11.43 : Dual-focus laser velocimeter with backscatter

11.11.3 Advantages of Laser Techniques

Laser velocimeters have wide applications in measurements in turbomachinery, wind tunnels, water tunnels, combustion studies, heat exchangers and many areas in aerospace and nuclear engineering. Their main advantages are:

1. They employ a non-intrusive method which does not disturb the flow.
2. They can measure velocities in regions which are inaccessible by other devices. They offer valuable device for boundary layer measurements.
3. No calibration is required; their working is independent of pressure, temperature and the density of the fluid.
4. They can be used in a wide range of velocity (0.1 – 300 m/s); their frequency response is very high.
5. Velocity varies linearly with the signal over wide range.
6. They can be easily interfaced with a computer.

Some of the disadvantages include their high cost, complex optical and electronic equipment, and requirement of well trained and skilled operators. Installation of a laser system requires considerable preparation. In some cases a seeding plant is also needed which further adds to the already prohibitively high cost.

NOTATION FOR CHAPTER 11

A	Area of cross-section, ammeter	p_r	pressure ratio
		$\Delta p = p_0 - p$	pressure difference
a	velocity of sound	q	volume flow rate
c	air or gas velocity	Q	heat transfer
c_p	specific heat at constant pressure	r	radius
		R	pipe radius, gas constant, electrical resistance
$C_1, C_2, \ldots$	constants		
C_c	contraction coefficient	R_1, R_2, R_3, R_4	arms of the wheatstone bridge
C_d	discharge coefficient		
C_v	velocity coefficient	R_f	recovery factor
d, D	diameters	s	entropy
$f( )$	function of	S^*	entropy transport coefficient
F	force	T	absolute temperature
g	acceleration due to gravity	Δt	temperature rise
G	galvanometer	W	work, weight or hot wire element
Δh	manometer deflection		
I	electric current	V	volume or voltage
K	constant, resistance coefficeint or correction factor	ΔV	voltage drop
		X, Y, Z	rectilinear co-ordinates
$\dot{m}$	mass or mass flow rate	ρ	density
M	Mach number	$\gamma = c_p/c_v$	ratio of specific heats
$n =$	d^2/D^2, area ratio or refractive index	β	constant
		δ	half wedge angle
p	pressure		

SUBSCRIPTS AND SUPERSCRIPTS

o	reference or stagnation value	i	inlet
$*$	corresponding to $M = 1$	n	annular or nozzle
1	initial	r	recorded
2	final	ref	reference
$-$	mean	t	tube
aw	adiabatic wall	T	at temperature T
c	compressor	W	hot-wire element
d	diffuser	x	upstream of the shock
e	exit	y	downstream of the shock
f	float		

SOLVED EXAMPLES

Example 11.1. Air enters a circular duct ($D = 40$ cm) through a measuring nozzle; then it passes through a venturimeter and an orifice meter located at suitable distances. Determine from the following data the mass flow rate through the duct.

	Nozzle	Venturimeter	Orifice meter
area ratio	0.500	0.5625	0.700
coefficient of discharge	0.935	0.990	0.617
head across the device	—	—	100 mm W.G.

Determine the head in millimeters of water column across the nozzle and the venturimeter. Take ambient conditions as $p = 1.013$ bar, $T = 295$ K. Changes in density at the various devices may be considered negligible.

Solution. $\rho = \dfrac{p}{RT} = \dfrac{1.013 \times 10^5}{287 \times 295} = 1.196 \text{ kg/m}^3$

Orifice meter:

$$\Delta p = 100 \times 9.807 = 980.7 \text{ N/m}^2$$

$d^2/D^2 = 0.7$;

$$A = \frac{\pi}{4} d^2 = \frac{\pi}{4} \times 0.7 \times 0.4^2 = 0.0879 \text{ m}^2$$

$$\dot{m} = C_d A \sqrt{2\rho \, \Delta p}$$

$$\dot{m} = 0.617 \times 0.0879 \times \sqrt{2 \times 1.196 \times 980.7}$$

$$\dot{m} = 2.615 \text{ kg/s} \quad \textbf{Ans.}$$

Venturimeter:

$$n = d^2/D^2 = 0.5625$$

$$A = \frac{\pi}{4} d^2 = \frac{\pi}{4} \times 0.5625 \times 0.4^2 = 0.07 \text{ m}^2$$

$$\dot{m} = \frac{C_d A}{\sqrt{1 - n^2}} \sqrt{2\rho \, \Delta p}$$

$$\sqrt{\Delta p} = \frac{m}{C_d A} \sqrt{\frac{1 - n^2}{2\rho}}$$

$$\sqrt{\Delta p} = \frac{2.615}{0.99 \times 0.07} \sqrt{\frac{1 - 0.5625^2}{2 \times 1.196}} = 20.176$$

$$\Delta p = 407.07 \text{ N/m}^2$$

$$\Delta h = \frac{\Delta p}{9.807} = \frac{407.07}{9.807} = 41.5 \text{ mm WG} \quad \textbf{Ans.}$$

Nozzle:

$$A = 0.5 \times \frac{\pi}{4} D^2 = 0.5 \times \frac{\pi}{4} 0.16 = 0.0628 \text{ m}^2$$

$$\sqrt{\Delta p} = \frac{2.615}{0.935 \times 0.0628} \sqrt{\frac{1 - 0.25}{2 \times 1.196}} = 24.937$$

$$\Delta p = 621.854 \text{ N/m}^2$$

$$\Delta h = \frac{621.854}{9.807} = 63.409 \text{ mm WG} \quad \textbf{Ans.}$$

Example 11.2. Determine the air velocities and the Mach numbers from the given data in each of the following cases:

	Pitot-tube pressure (gauge)	Free stream static pressure (gauge)	Free stream temperature
(*a*)	1.4 bar	– 274 mbar	265 K
(*b*)	195 mm Hg	– 5 mm Hg	298 K
(*c*)	56 mm Hg	6 mm Hg	305 K

Ambient pressure 1.013 bar.

Solution. (*a*) $p_o = 1.013 + 1.4 = 2.413$ bar

$$p = 1.013 - 0.274 = 0.739 \text{ bar}$$

$$p/p_o = 0.739/2.413 = 0.306$$

It is seen from isentropic gas tables that at this value of p/p_o the Mach number is greater than unity. Therefore, the deceleration of flow at the mouth of the pitot-tube is no longer isentropic due to presence of a standing shock wave upstream of the pitot. The pitot-tube will record the stagnation pressure p_{oy} downstream of the normal shock.

$$p_o = p_{oy} = 2.413 \text{ bar}$$

$$p = p_x = 0.739 \text{ bar}$$

$$p_{oy}/p_x = 2.413/0.739 = 3.265$$

From normal shock tables Mach number at this value is

$$M_x = 1.46 \quad \textbf{Ans.}$$

Velocity of sound upstream of the shock is

$$a_x = \sqrt{\gamma R T_x} = 20.04 \sqrt{T_x}$$

$$a_x = 20.04 \sqrt{265} = 326.3 \text{ m/s}$$

Therefore, the gas velocity is

$$c_x = M_x c_x$$

$$c_x = 1.46 \times 326.3 = 476.4 \text{ m/s} \quad \textbf{Ans.}$$

(*b*) 1 mm Hg $= 1.334$ mbar

$$p_o = 1.013 + 0.195 \times 1.334 = 1.273 \text{ bar}$$

$$p = 1.013 - 0.005 \times 1.334 = 1.006 \text{ bar}$$

$$\frac{p}{p_o} = \frac{1.006}{1.273} = 0.79$$

The flow at this value of p/p_o is compressible; therefore, instead of using Bernoulli equation the Mach number can simply be read from the isentropic gas tables for $\gamma = 1.4$ at $p/p_o = 0.79$

$$M = 0.59 \quad \textbf{Ans.}$$

$$a = 20.04\sqrt{298} = 345.94 \text{ m/s} \quad \textbf{Ans.}$$

$$c = Ma = 0.59 \times 345.94$$

$$c = 204.1 \text{ m/s} \quad \textbf{Ans.}$$

(*c*)
$$p_o = 1.013 + 0.056 \times 1.334 = 1.088 \text{ bar}$$

$$p = 1.013 + 0.006 \times 1.334 = 1.021 \text{ bar}$$

$$\rho = \frac{p}{RT} = \frac{1.021 \times 10^5}{287 \times 305} = 1.167 \text{ kg/m}^3$$

Since the difference in p and p_o is small, Bernoulli equation can be used.

$$c = \sqrt{\frac{2(p_o - p)}{\rho}}$$

$$c = \sqrt{\frac{2 \times 0.067 \times 10^5}{1.167}} = 107.16 \text{ m/s} \quad \textbf{Ans.}$$

$$a = 20.04\sqrt{305} = 349.98 \text{ m/s}$$

$$M = \frac{107.16}{349.98} = 0.306 \quad \textbf{Ans.}$$

Alternatively, $p/p_o = 1.021/1.088 = 0.9384$

This gives a Mach number of 0.302 from the isentropic tables. The difference is small.

Example 11.3. The data of a Mach-2 supersonic wind tunnel is given below:

pressure in the test section	0.69 bar
area of cross-section of the nozzle throat	1000 cm^2
ambient pressure	1.02 bar
ambient temperature	311 K

The air is taken from the atmosphere and compressed continuously in a multistage compressor to the reservoir pressure. The test section of tunnel directly exhausts into the altmosphere.

Determine:

(*a*) temperature of air in the test section,

(*b*) mass flow rate of air,

(*c*) cross-sectional area of the test section,

(*d*) power required to drive the compressor.

Assume reversible flow throughout.

Solution. From isentropic gas tables ($\gamma = 1.4$) at

$$M = 2.0$$

$$\frac{p}{p_{01}} = 0.128, \quad \frac{T}{T_{01}} = 0.555, \quad \frac{A}{A^*} = 1.687$$

Refer to Figure 11.32,

$$p_{01} = 0.69/0.128 = 5.39 \text{ bar}$$

$$T_{01} = \left(\frac{p_{01}}{p_i}\right)^{(\gamma-1)/\gamma} \times T_i$$

$$T_{01} = \left(\frac{5.39}{1.02}\right)^{0.286} \times 311 = 500.7 \text{ K}$$

(*a*) Since there is no cooling after compression, this is the temperature of air in the reservoir. Therefore, the test section temperature is

$$T = 0.555 T_{01}$$

$$T = 0.555 \times 500.7 = 277.8 \text{ K}$$

$$t = 4.8^\circ\text{C} \quad \textbf{Ans.}$$

(*b*) at $M = 2$, the nozzle is passing maximum flow of air; this is given by the Fliegner's formula,

$$\frac{\dot{m}\sqrt{T_{01}}}{A^* p_{01}} = 0.0404$$

$$\dot{m} = \frac{0.0404 \times 0.1 \times 5.39 \times 10^5}{\sqrt{500.7}}$$

$$\dot{m} = 97.317 \text{ kg/s} \quad \textbf{Ans.}$$

(*c*) The area of cross-section of the test section is

$$A = 1.687 \times A^* = 1.687 \times 1000$$

$$A = 1687 \text{ cm}^2 \quad \textbf{Ans.}$$

(*d*) Taking compressor efficiency as 100% and $c_p = 1.005$ kJ/kg K, compressor power is

$$W = \dot{m} c_p (T_{01} - T_i)$$

$$W = 97.317 \times 1.005 (500.7 - 311)$$

$$W = 18553.34 \text{ kW} \quad \textbf{Ans.}$$

Example 11.4. A closed circuit supersonic wind tunnel provided with a diffuser and a cooler has the following data:

area of cross-section of the nozzle throat 1000 cm^2

area of cross-section of the test section 1687 cm^2

test section pressure	0.69 bar
test section temperature	277.8 K
test section Mach number	2.0

Determine:

(*a*) the diffuser throat area for minimum power during running,

(*b*) the power required to start the flow through the tunnel,

(*c*) the power required during steady flow operation of the tunnel.

Solution. Refer to Figure 11.33 (*a*).

From normal shock tables ($\gamma = 1.4$) at

$$M_x = 2.0$$

$$M_y = 0.578, \quad \frac{p_{oy}}{p_{ox}} = 0.721$$

(*a*) At the time of starting the shock has to first pass through the test section.

Therefore, $A_n^* = A_1^* = 1000 \text{ cm}^2$

$$A_2^* = A_d^*$$

$$A_1^* p_{ox} = A_2^* p_{oy}$$

$$A_d^* = A_2^* = A_1^* \frac{p_{ox}}{p_{oy}}$$

$$A_d^* = \frac{1000}{0.721} = 1387 \text{ cm}^2 \quad \textbf{Ans.}$$

$$\frac{p_{ox}}{p_{oy}} = \frac{1}{0.721} = 1.387$$

$$p_{01} = p_{ox} = p_e$$

$$p_{oy} = p_{02} = p_i$$

Pressure ratio required at the time of starting is

$$p_r = \frac{p_e}{p_i} = \frac{p_{ox}}{p_{oy}} = 1.387$$

(*b*) Power required to start the flow is

$$W = \dot{m} c_p (T_{01} - T_i)$$

Here the values of $\dot{m}$ and T_{01} are same as Example 11.3, but on account of closed circuit T_i will be higher.

$$\frac{T_{01}}{T_i} = p_r^{0.286} = 1.387^{0.286} = 1.098$$

$$T_i = \frac{500.7}{1.099} = 456 \text{ K}$$

$$W = 97.317 \times 1.005 \times 456 (1.098 - 1)$$

$$W = 4370.64 \text{ kW} \quad \textbf{Ans.}$$

This value is much less compared to its corresponding value in the previous example.

(*c*) After the shock is swallowed by the diffuser the Mach number (M_x) before the shock is its value in the isentropic deceleration.

$$(A/A^*)_2 = 1.387$$

The Mach number corresponding to this value from the isentropic table is

$$M = 1.75$$

$$M_x = M = 1.75$$

From shock tables at $M_x = 1.75$

$$p_{oy}/p_{ox} = 0.835$$

Therefore, the pressure ratio during steady running operation is

$$p_r = \frac{p_{ox}}{p_{oy}} = \frac{1}{0.835} = 1.1976$$

$$p_r^{0.286} = 1.1976^{0.286} = 1.0529$$

$$T_i = T_{01}/1.0529 = 500.7/1.0529$$

$$T_i = 475.5^{\circ}\text{K}$$

Due to the decrease in the pressure ratio the power required will also be less.

$$W = \dot{m} c_p (T_{01} - T_i)$$

$$W = 97.317 \times 1.005 (500.7 - 475.5)$$

$$W = 2464.65 \text{ kW} \quad \textbf{Ans.}$$

Example 11.5. A closed circuit subsonic wind tunnel has a Mach number of 0.8 in its test section of 15 cm × 30 cm cross-section. The condition of air in the test-section is maintained at $p = 1.02$ bar $T = 288$ K. The stagnation pressure loss in the precooler and the ducts upstream of the compressor is 100 mbar. The compressor efficiency is 79 per cent. The flow in the nozzle and the diffuser is isentropic. Determine:

(*a*) compressor pressure ratio,

(*b*) mass flow rate through the tunnel,

(*c*) temperature drop of air required in the precooler, and

(*d*) the power required by the compressor.

Solution. From isentropic flow tables ($\gamma = 1.4$) at $M = 0.8$,

$$\frac{p}{p_{01}} = 0.656, \quad \frac{T}{T_{01}} = 0.886$$

Therefore, the settling chamber stagnation pressure and temperature are

$$p_{01} = \frac{1.02}{0.656} = 1.5548 \text{ bar}$$

$$T_{01} = \frac{288}{0.886} = 325.056 \text{ K}$$

Refer to Figures 11.33 (*a*) and (*b*)

The static pressure and temperature at the diffuser exit for very small velocity are also $p_{01} = 1.5548$ and $T_{01} = 325.056$ K.

(*a*) The static pressure at the compressor inlet on account of losses in the inter-cooler and ducts is

$$p_i = p_{01} - \Delta p_0$$

$$p_1 = 1.5548 - 0.100 = 1.4548 \text{ bar}$$

Therefore, the compressor pressure ratio is

$$p_r = \frac{p_{01}}{p_i} = \frac{1.5548}{1.4548} = 1.0687 \quad \textbf{Ans.}$$

(*b*) Velocity of air in the test section is

$$c = Ma = 0.8 \sqrt{1.4 \times 287 \times 288} = 340.174 \text{ m/s}$$

Test section area of cross-section is

$$A = 15 \times 30 = 450 \text{ cm}^2$$

Density of air in the test-section is

$$\rho = \frac{p}{RT} = \frac{1.02 \times 10^5}{287 \times 288} = 1.234 \text{ kg/m}^3$$

The mass flow rate through the tunnel is $\dot{m} = \rho A c$

$$\dot{m} = 1.234 \times 0.045 \times 340.174$$

$$\dot{m} = 18.889 \text{ kg/s} \quad \textbf{Ans.}$$

(*c*) For maintaining test-section temperature as 288 K, the stagnation temperature in the settling chamber/compressor exit should be $T_{01} = 325.056$.

The actual temperature rise through the compressor is given by

$$T_{01} - T_i = \frac{1}{\eta_c}(T_{01s} - T_i) = \frac{T_i}{\eta_c}\left(\frac{T_{01s}}{T_i} - 1\right)$$

$$\frac{T_{01s}}{T_i} = \left(\frac{p_{01}}{p_i}\right)^{(\gamma-1)/\gamma} = (1.0687)^{0.286} = 1.0192$$

Therefore, $325.056 - T_i = \frac{T_i}{0.79}(1.0192 - 1)$

$$T_i = 317.343 \text{ K}$$

The temperature of air at the entry of the cooler is $T_{01} = 325.056$; therefore, temperature drop in the pre-cooler is

$$\Delta T = T_{01} - T_i$$

$$\Delta T = 325.056 - 317.343 = 7.713 \text{ K} \quad \textbf{Ans.}$$

(*d*) Compressor power is given by

$$W = \dot{m} c_p (T_{01} - T_i)$$

$$W = 18.889 \times 1.0045 \times 7.713$$

$$W = 146.346 \text{ kW} \quad \textbf{Ans.}$$

QUESTIONS AND PROBLEMS

11.1 Describe the working principles of devices which are used for measuring the following pressures:

(*a*) pressure on the aerofoil surface of the order of 0.1 mbar,

(*b*) pressure in a reservoir in the range of 2000-5000 bar and

(*c*) pressure in the L-P section of a shock tube in the range of $10^{-3} - 10^{-2}$ mbar.

11.2 How are the mean values of the static and stagnation pressures determined in a large circular duct if the gas parameters vary over the cross-section?

11.3 (*a*) What is the basic principle of an electrical pressure transducer? In what situations is it superior to manometric measurements?

(*b*) Describe a low pressure transducer.

11.4 (*a*) What is the difference between the static, stagnation and the recorded temperatures of a gas stream?

(*b*) Describe a stagnation temperature measuring instrument.

11.5 What is adiabatic wall temperature? Show that the Mach number is given by $M^2 = \dfrac{2}{\gamma - 1}\left(\dfrac{T_{aw}}{T} - 1\right)\dfrac{1}{R_f}$

11.6 Describe the temperature measuring devices for the following temperature ranges:

(*a*) -100 to 5°C (*b*) 0 to 1000°C

(*c*) 1500 to 2000°C.

11.7 How is the density of a gas determined by measuring the velocity of sound in it?

11.8 (*a*) Describe how the pitot-static tube is used to determine the mass flow weighted mean value of the velocity in a large duct.

(*b*) What are the methods of determining the gas velocity in supersonic flow?

11.9 Describe the working principles of the following devices:

(*a*) constant temperature and constant current hot-wires for velocity measurement,

(*b*) hot-films for direction, velocity and temperature measurement,

(*c*) hot-wire for direction measurement.

11.10 What are the relative advantages and disadvantages of the orifice meter, venturimeter and the flow nozzle for measuring flow rates of gases?

11.11 Explain briefly the working principles of the following flow measuring devices:

(*a*) rotameter,

(*b*) electrical flow meter,

(*c*) soap film.

What are the flow ranges in each of the above devices?

11.12 What are the various types of wind tunnels used for low and high speed testing of models? Describe briefly the special problems of the supersonic tunnels.

11.13 Describe with the aid of a schematic diagram the working of a closed circuit continuous supersonic wind tunnel. Why is a high molecular weight gas sometimes preferred for high Mach number tests?

11.14 Why is cooling of air necessary in a closed circuit supersonic tunnel? Show that the compressor power required is lower if cooling of air is done before compression.

11.15 Show illustrative sketches of the following:

(*a*) Vacuum type blow-down tunnel,

(*b*) induction tunnel,

(*c*) shock tube and

(*d*) gun tunnel.

What are the special advantages of the shock tube and the gun tunnel over the other types of supersonic tunnels?

11.16 How are nylon surface tufts and smoke used for determining the general direction of flow? What are the methods by which the correct direction of flow is determined?

11.17 What is the basic principle employed in the working of optical devices for obtaining a density field of a gas stream?

11.18 Draw a neat sketch of an interferometer. How is it used to determine the gas velocity and its Mach number?

11.19 Following data refers to a standard nozzle:

throat diameter 50 mm; area ratio 4; head across the nozzle 100 mm Hg; static pressure at the throat 80 mm Hg below atmospheric pressure; temperature at the throat 295 K; atmospheric pressure 980 mbar.

Determine the mass flow rate. (0.327 kg/s)

11.20 A 200 mm diameter standard orifice plate with D, $D/2$ pressure tappings is fitted in a 300 mm diameter pipe. Static pressures measured across the orifice are 250 and 100 mm W.G. The temperature measured upstream of the orifice plate is 300 K. If the atmospheric pressure is 1029 mbar determine the mass flow rate through the orifice. (1.144 kg/s)

11.21 Determine the flow rate of air in kg/s from the following data on a venturimeter:

Pipe diameter 250 mm; area ratio 2.5; static pressure at the throat 1049 mbar (absolute); temperature at the throat 25°C; manometer deflection between the entry and the throat 65 mm W.G; discharge coefficient 0.99. (0.835 kg/s)

11.22 Compute the velocities of air from the following data for a pitot-static tube:

(*a*) total pressure 150 mm W.G.
static pressure 50 mm W.G.

(*b*) total pressure 500 mm Hg (gauge)
static pressure 105 mm Hg (gauge)

(*c*) total pressure 101.3 cm Hg (gauge)
wall static pressure

51 mm Hg (gauge) upstream of the pitot-tube
Ambient pressure 980 mbar,

Take temperature of air upstream of the pitot in each case as 288 K. (40.77 m/s, 259.62 m/s, 386.02 m/s)

11.23 A low pressure fan supplies ambient air ($p = 1.015$ bar, $T = 300$ K) to a circular duct of 30 cm diameter. The dynamic head measured in the free stream inside the duct is 4.81 mm W.G. on a manometer tube inclined at 11.53° to the horizontal.

The mean velocity in the duct is 0.765 times the free stream velocity. Determine (*a*) free stream velocity in the duct (*b*) volume and mass flow rate through the fan.

[(*a*) 4 m/s, (*b*) 0.216 m^3/s, 0.255 kg/s]

11.24 A mixture of air and freon is used in a closed circuit supersonic tunnel; this has the following data:

cross-section of the test-section	25 × 25 cm
test-section Mach number	1.6
settling chamber pressure	5 bar
settling chamber temperature	425 K

For freon-air mixture take $\gamma = 1.3$,
$R = 135$ J/kg K.

Determine (*a*) areas of cross-section of the nozzle and diffuser throats (*b*) power required to start the tunnel and (*c*) power required for steady running.

[(*a*) 491.738 cm^2, 553.136 cm^2, (*b*) 578.98 kW, (*c*) 233.255 kW].

11.25 If the compressor in the wind tunnel of Example 11.5 takes in ambient air ($p = 1.013$ bar, $T = 288$ K) determine the following quantities for an open circuit tunnel:

(*a*) mass flow rate required,
(*b*) compressor pressure ratio,
(*c*) compressor power, and
(*d*) the temperature drop in the cooler before the compressor.

Comment on these values as compared to those for the closed circuit wind tunnel.

Ans. [(*a*) 18.889 kg/s (*b*) 1.6335 (*c*) 1041.67 kW (*d*) 17.844°C]

On account of the compression of the ambient air in the compressor its pressure ratio and power are much higher than their corresponding values in the closed circuit tunnel.

PART-III

12

Aircraft Propulsion

Man had always dreamed of flying like birds. Flying required lifting off the ground and propelling the craft forward (propulsion). After several attempts with ingenious devices man finally succeeded in lifting his primitive flying vehicle or craft and propelling it at modest speeds.

With the introduction of the aerofoil (Figure 12.1) in the beginning of the twentieth century all that was necessary was to propel the craft

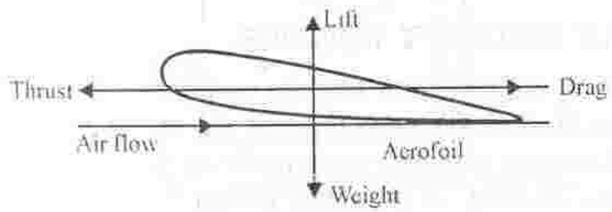

FIGURE 12.1 : Forces acting on the aerofoil wing of an aircraft

(aeroplane or the aircraft) at a speed high enough to produce the required lift on the aerofoil wings. Once the craft lifts (takes off) off the ground it is free from the surface friction of the wheels; now the propelling force (thrust) has only to overcome a much smaller drag force due to air resistance (Figure 12.2).

At constant speed level flight the propelling force equals the drag force; at this speed the lift on the wings (and other lifting surfaces) balances the total weight of the craft including the weight of men, material and the fuel. In a flying machine the weight and size of the propulsion device (engine) for a given thrust (propelling force) must be as small as possible.

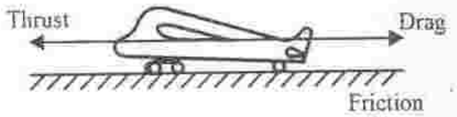

(*a*) Take off roll

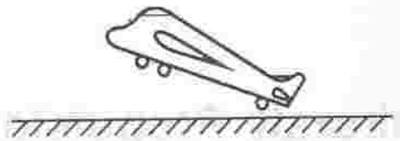

(*b*) Take off

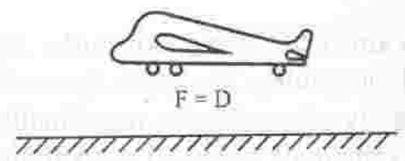

(*c*) Level flight

FIGURE 12.2 : Take-off roll, take-off and level flight

12.1 EARLY AIRCRAFT ENGINES

Besides gliders, balloons and airships were the first airborne vehicles and therefore first to be propelled; in the beginning they flew with the winds. Later on attempts were made to propel them by means of propellers (air screws). A propeller driven by a 3 h.p. steam engine was employed in 1852 for the first time to propel a balloon in France. Later on a 9 h.p. battery operated electric motor was used for driving the propeller.

For bigger and faster aeroplanes (heavier than air flying vehicles) more advanced, powerful and reliable engines were required. Developments in the piston type petrol engines and gas turbines in the later half of the nineteenth century gave fresh impetus to the art and craft of aircraft propulsion.

Early aircrafts employed successfully the reciprocating internal combustion engine (petrol engine) for driving the aircraft propellers. Engine cylinders were arranged in various configurations such as "in line", radial and V-arrangements. The petrol or gasoline engine which is lighter in construction due to its low compression ratio was ideally

suited for aircraft propulsion. The supercharged engines worked satisfactorily inspite of low density ambient air at high altitudes.

12.1.1 Jet Propulsion

The reciprocating piston engine, on account of limitations of size and speed could not be employed for generating much higher flow rates of hot gases required in jet propulsion for the aircrafts.

The squid fish can be considered as the first ever jet propulsion device that existed in the world; it employs "hydraulic jet propulsion" to move forward by taking in water and ejecting it rearward.

Man's first effort to employ jet propulsion can be traced back to Hero's reaction turbine called the "aeolipile" (Figure 12.3) which

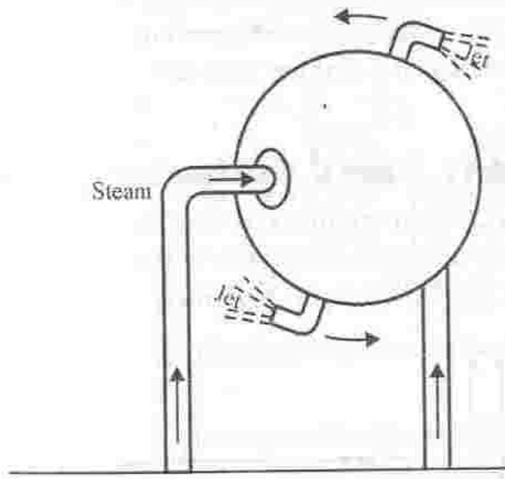

FIGURE 12.3 : Hero's reaction turbine (aeolipile)

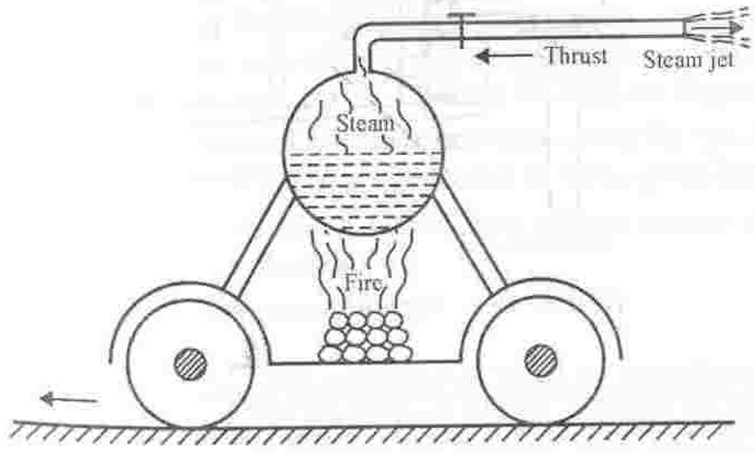

FIGURE 12.4 : Steam-jet propelled carriage

was developed in 100 B.C. in Egypt; steam jets issuing from two diametrically opposite nozzles attached to a spherical vessel provided the torque for rotation. Much later in 1687 a Dutchman employed the reaction of steam jet to drive a carriage (Figure 12.4).

In 1940 an attempt was made in Italy to operate a jet propelled aircraft with a piston engine; however the results were disappointing.

With the developments of gas turbines in nineteen thirties and forties mainly in Britain, France, Germany and the United States of America they were successfully employed in the turbo-prop and turbojet aircraft engines.

12.2 TYPES OF AIRCRAFT ENGINES

All aircraft engines are airbreathing in contrast to rocket engines which carry their own supply of fuel and oxidizer. Internal combustion engines of both the reciprocating and turbine type are used for aircraft propulsion.

12.2.1 Reciprocating Internal Combustion Engines

As stated earlier the piston engine was widely employed to drive the propellers in the early aircrafts; the power to the propeller is transmitted through a reduction gear (Figure 12.5). Since the mass of air inducted

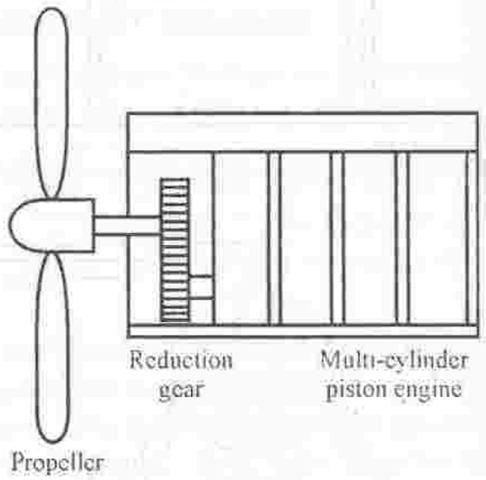

FIGURE 12.5 : Piston engine driven propeller

into the engine depends on its density their performance drops at higher altitudes. This is on account of the reduced quantity of oxygen available for combustion. This problem is overcome in supercharged engines; an

air compressor driven by the crankshaft or an exhaust gas turbine supplies the correct quantity of air to the engine. However, with increasing speeds and size of the aircrafts the reciprocating I.C. engine became too complicated and unwieldy. Therefore, now its use is restricted in the propulsion of only comparatively small and low speed aircrafts flying at lower altitudes.

12.2.2 Gas Turbine Engines

Bigger and faster aircrafts operating at higher altitudes employ the gas turbine engines (Figure 12.6) for their propulsion. These engines are

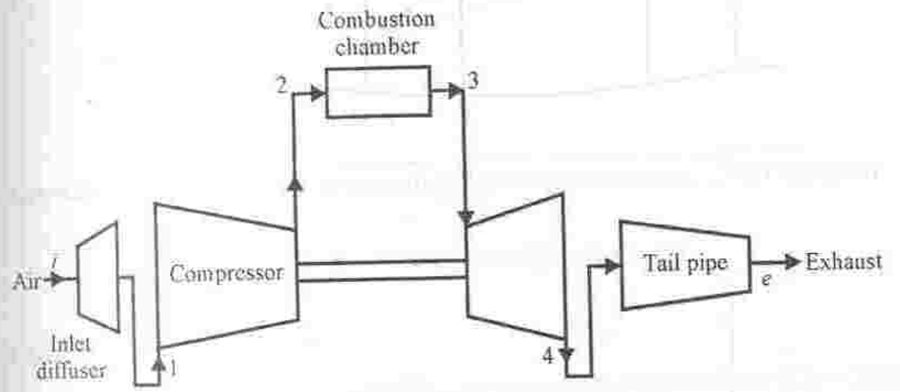

FIGURE 12.6 : Gas turbine power plant for aircraft propulsion

much simpler in construction compared to the piston engines and operate at higher speeds handling much larger flow rates of air and fuel. A simple gas turbine power plant widely used for aircraft propulsion is shown in Figures 12.6 and 12.7; this works on a simple open circuit Joules or Brayton cycle. The ideal and actual cycles are shown in Figure 12.8 and 12.9. Processes occurring in the inlet diffuser and the exhaust nozzle are represented by $(i-1_s)$ and (4_s-e_s) in Figure 12.8. In the actual cycle (Figure 12.9) they are represented by $(i-1)$ and $(4-e)$ respectively; They are not significant in turbo-prop engines.

Principal components of an aircraft gas turbine engine are described in the following sections:

Compressor

Ambient air is sucked by the compressor (axial or centrifugal type) through an inlet diffuser; the pressure of the air is raised by the compressor besides a small rise through the diffuser. This adiabatic com-

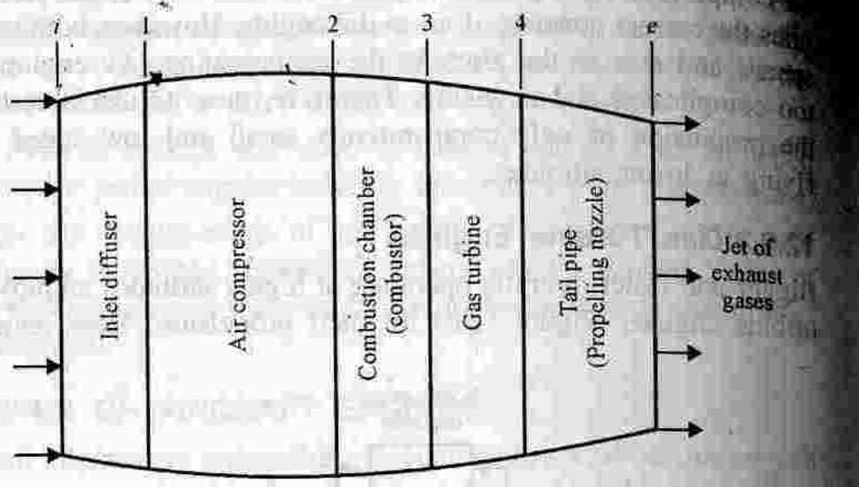

FIGURE 12.7 : Layout of the principal components in an aircraft gas turbine engine

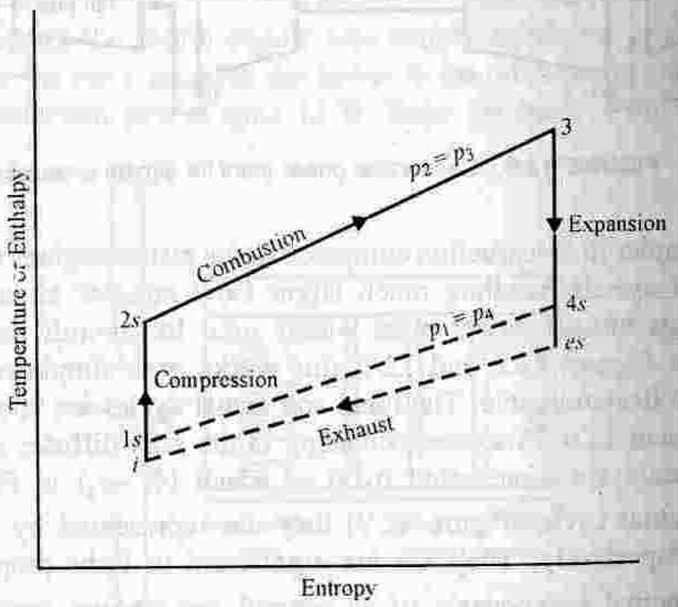

FIGURE 12.8 : Simple open circuit Joules or Brayton cycle (ideal)

pression is represented by $1-2s$ on the $T-s$ or $h-s$ diagram; suff
s represents isentropic or constant entropy process. The irreversible co
pression and expansion processes and the static pressure drop in
combustion chamber are depicted in Figure 12.9.

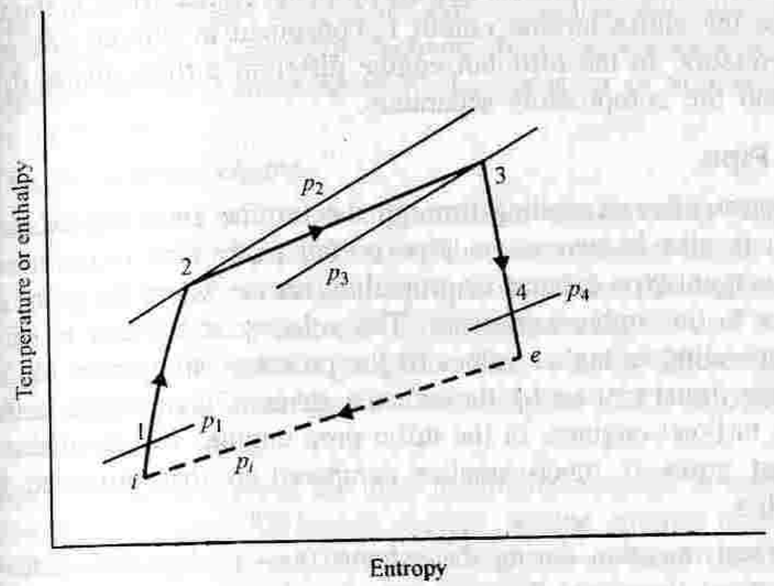

FIGURE 12.9 : Actual Joule or Brayton cycle

Combustion Chamber

High pressure air from the compressor supports combustion ($2s-3$) in the combustion chamber; this occurs at constant pressure in the ideal cycle. The air is supplied in three streams-(a) primary air which is about 15 per cent of the total, initiates the combustion of the atomised fuel entering the combustion chamber. About 30 per cent of air (secondary air) is introduced to complete the combustion; the remaining quantity of air (about 55 per cent) known as tertiary air is used only to dilute the high fuel-air ratio mixture and lowering down its temperature to safe limits for the turbine. The air-fuel ratio of the high pressure and temperature gases entering the turbine may approximately vary from 50 to 150.

The fuel-air mixture is ignited by means of a high voltage device at the time of starting the engine. Once a flame is established it propagates to other sections of the combustion chamber. Various methods are employed to stabilize the flame.

Turbine

The hot gases from the combustion chamber at the designed pressure and temperature expand ($3-4s$) adiabatically through one or more turbine stages and the exhaust nozzle. In the turboprop engine the turbine

stages drive the compressor and the propeller respectively. In the turbojet engine the entire turbine output is consumed in driving one or more compressors. In the turbofan engine different turbine stages drive the fan and the compressors separately.

Tail Pipe

Hot gases after expanding through the turbine enter the exhaust pipe which is also known as jet pipe or tail pipe. This is provided with a convergent type exhaust or propelling nozzle where the gases expand further to the ambient pressure. The velocity at the exit is very high corresponding to higher values of the pressure ratio across the nozzle; thus the thrust caused by the exhaust gases is high which is the case in the turbojet engines. In the turbo prop engines the thrust due to the exhaust gases is much smaller compared to that produced by the propeller.

Heat rejection during the exhaust $(4s-1)$ does not occur within the engine; therefore, this is not a closed circuit cycle.

After Burner

Exhaust gases from the last turbine stage have a large quantity of oxygen which can support the combustion of additional fuel. If the thrust of the engine is desired to be increased without changing the physical dimensions of the compressor, turbine etc. additional quantity of fuel can be burnt in a section of the jet pipe to increase the velocity of the jet; this process is known as reheating. In order to obtain favourable conditions for efficient combustion the velocity of the gases is reduced in the reheat section by providing a diffuser after the turbine exit as shown in Figure 12.10.

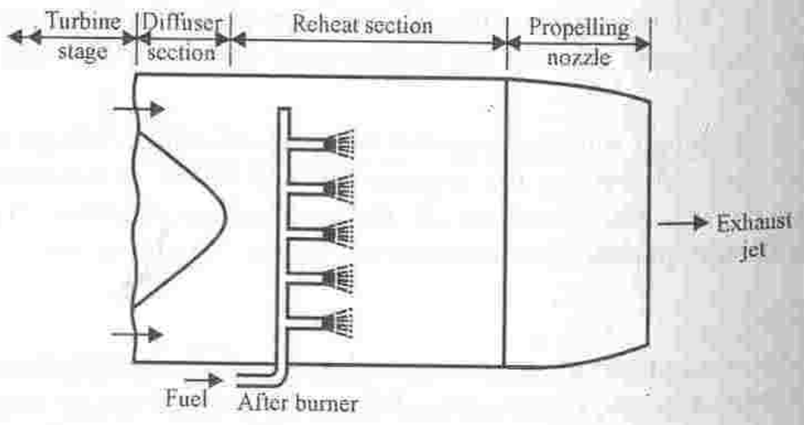

FIGURE 12.10 : Jet pipe with after burner

Reheating can also be used for a short time to obtain increased thrust for special purposes such as military operations and take-off. It should be possible to increase or decrease the cross-sectional area of the propelling nozzle corresponding to the variation of volume flow rate due to reheat.

(a) The turbo-prop engine

As stated before the gas turbine engine drives the propeller (through a reduction gear) in a turboprop engine. Therefore, the turbine develops enough power to be able to drive the propeller besides the compressor. Thrust is produced by the increase in the momentum flux of a large mass of air passing through the propeller. The velocity differential between the upstream and downstream flows (Figure 12.15) is comparatively small.

Since turboprop engines are used in smaller aircrafts at comparatively lower speeds ($u < 800$ kmph) the gas turbine engines employed are small. For low power and flow rates one or two stage centrifugal compressors are commonly used. The turbine is of the axial type; separate turbine stages are sometimes employed to drive the compressors and the propeller.

The turbine exhaust is allowed to expand in the propelling nozzle but the jet thrust is much smaller compared to the propeller thrust.

The large diameter propellers cannot run at high speeds on account of mechanical and aerodynamic limitations. As will be seen later the propulsive efficiency of propellers falls at higher speeds.

Some advantages of the turboprop engines are:

1. On account of higher thrust at low speeds the take-off roll is short requiring shorter runway.
2. The specific fuel consumption (TSFC) based on thrust is low.
3. Propulsive efficiency within the range of operation is high.
4. Thrust reversal is easily achieved with variable pitch propeller blades.

The disadvantages are:

1. Application is limited to lower speeds and altitudes.
2. On account of large diameter propeller the landing gears have to be longer.
3. Engine is heavier and more complicated.
4. Use of centrifugal compressor stages increases the frontal area.
5. Higher weight per unit thrust.

(*b*) The turbojet engine

The gas turbine plant (Figure 12.6) employed in the turbojet engine has already been described in Section 12.2.2. The entire engine is housed in a cylindrical shell like casing (Figure 12.7) which is attached to the wings or the nacelle.

The power developed in the turbine stages is wholly consumed in driving the compressor or compressors and the auxilliaries. The high pressure and temperature gas from the combustion chamber expands through the turbines and the propelling nozzle with considerable pressure drop. If the gases do not expand to the ambient pressure (under expansion) in the propelling nozzle the engine will experience a pressure thrust in addition to the large thrust produced by the increase in the momentum flux through the engine.

On account of the large overall pressure ratio required across the turbine stages and the propelling nozzle the compressor section has many stages; in some designs the low pressure and high pressure multistage compressors are driven separately by separate turbine stages. Since the turbojet engine is employed in high speed aircrafts the static pressure rise through the inlet diffuser is significant.

The turbojet engine handles comparatively smaller quantities of air flow through a large velocity differential.

Some advantages of the turbojet engine are:

1. Suitable for long distance flights at higher speeds and altitudes.
2. Lower frontal area and shorter landing gears.
3. Lower weight per unit thrust at design speed and altitude.
4. Pressure rise through the inlet diffuser is significant.
5. Reheat can be employed for increased thrust.

The disadvantages are:

1. Take-off roll is longer requiring longer runway.
2. TSFC is comparatively higher at lower speeds and altitudes.
3. Uneconomical on short distance flights.
4. Lower thrust and propulsive efficiency at lower speeds.

(*c*) The turbofan engine

The turbofan engine is a combination of the turboprop and the turbojet engines combining the advantages of both. In the turbo-prop system the quantity of air flowing through the propeller (low pressure fan) is

much greater than that passing through the engine while in the turbojet system the entire air passes through the engine.

Figure 12.11 shows a turbofan engine system employing a low pressure ducted fan. The air after passing through the fan is divided

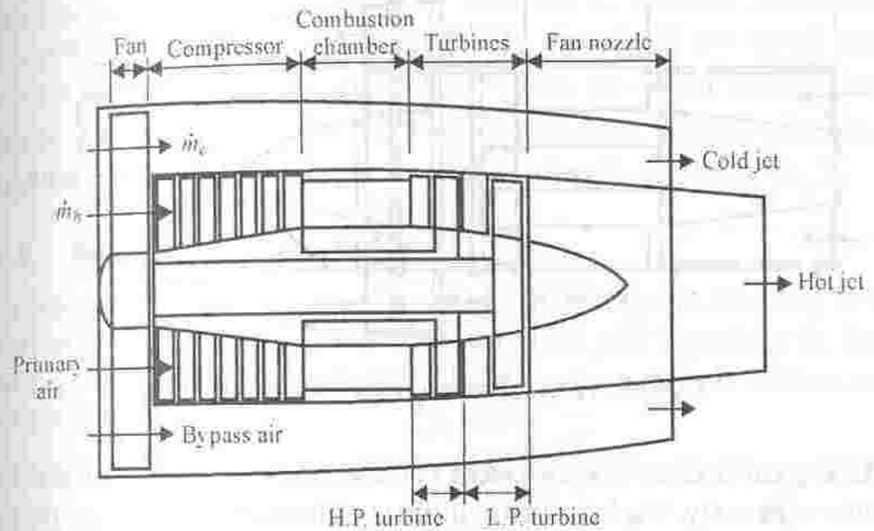

FIGURE 12.11 : Turbofan engine with front fan

into two streams: (*a*) The primary stream ($\dot{m}_h$) goes through the conventional turbojet engine consisting of the compressors, combustion chamber, turbines and the exhaust nozzle; (*b*) the secondary stream or the bypass air ($\dot{m}_c$) at relatively lower pressure is ducted around the aforementioned turbojet engine (core engine) for expansion through the annular fan nozzle. Thus the thrust is developed by the bypass air issuing as a cold jet at lower velocity and by the primary air issuing as a hot jet of gas at much higher velocity. In some engines the two stream mix at the rear. The ratio of the mass flow rates of cold air and the hot air streams is known as the bypass ratio ($B = \dot{m}_c / \dot{m}_h$). In modern turbofan engines the bypass ratio is high (of the order of 8.0 or higher). Therefore, a large fraction of the total thrust is developed by the cold jet at lower velocity which reduces the noise level and increases the propulsive efficiency.

The arrangement in Figure 12.11 shows the low pressure turbine driving the fan. In a large engine a multistage turbine consisting of a few stages drives the fan or fan stages; here the compressor is driven by the high pressure turbine.

Figure 12.12 shows a turbofan engine with a fan mounted at the rear of the engine. The fan blades are an extension of the low pressure

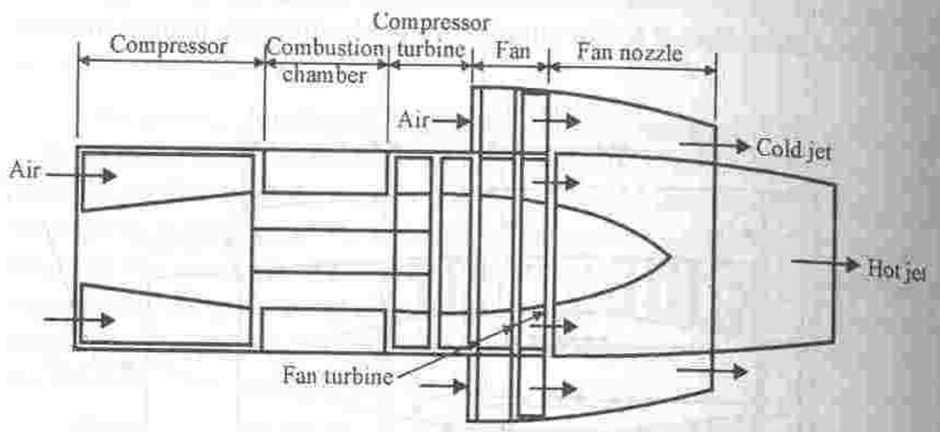

FIGURE 12.12 : Turbofan engine with an aft-fan

turbine rotor blades. The air enters the core engine compressor and the aft-fan separately. Various configurations of fans and compressor drives have been employed. Recently unducted fans have also been used in some engines. In some ducted fans inlet guide vanes are not provided in order to reduce fan noise. Some advantages of the turbofan engines are:

1. Short take-off roll due to increased thrust at low speeds.
2. Comparatively quieter engine.
3. More efficient flow in fan nozzle on account of short length and low speed.
4. Weight per unit thrust is lower than the turboprop system.
5. Thrust is higher than that in turbojet engine.

The disadvantages are:

1. Increased frontal area and drag.
2. Separate thrust reversers are needed for the hot and cold jets, if they are separate.
3. TSFC is higher compared to the turboprop engine.
4. Engine is heavier and more complicated compared to the turbojet engine.
5. Lower speed limit ($M < 1$) than that of the turbojet engine.

12.3 AIRCRAFT PROPULSION THEORY

In this section theoretical relations are developed for various quantities affecting the design and performance of aircraft gas turbine engines and propulsion devices. Reciprocating internal combustion engines have not been included here. The quantities that are of interest are—thrust (F), specific thrust (F_s) or impulse (I), aircraft to jet speed ratio ($\sigma = u/c_j$), specific fuel consumption based on thrust (TSFC) and various efficiencies such as cycle efficiency (η_J), thermal efficiency (η_{th}) propulsive efficiency (η_p) and the overall efficiency (η_o).

12.3.1 Energy Relations

Various processes occurring in a turbojet engine (Figures 12.6 and 12.7) have been depicted in Figures 12.8 and 12.9 and described in Section 12.2.2. The energy equations for these processes are written and discussed in this section.

Following relations are applicable to the ideal cycle (Figure 12.8);

Inlet diffuser

The state of air at the compressor inlet is denoted by 1 instead of 1*s*.

$$h_{oi} = h_{o1}$$

$$h_i + \frac{1}{2} c_i^2 = h_1 + \frac{1}{2} c_1^2 \tag{12.1}$$

$$T_i + \frac{c_i^2}{2c_p} = T_1 + \frac{c_1^2}{2c_p}$$

$$\frac{T_1}{T_i} = \left(\frac{p_1}{p_i} \right)^{(\gamma-1)/\gamma}$$

Pressure ratio, $$\frac{p_1}{p_i} = \left(\frac{T_1}{T_i} \right)^{\gamma/(\gamma-1)} \tag{12.2}$$

Compressor

Work $$w_c = h_{o2s} - h_{o1} = c_p (T_{o2s} - T_{o1}) \tag{12.3}$$

Pressure ratio, $$\frac{p_2}{p_1} = \left(\frac{T_{2s}}{T_1} \right)^{\gamma/(\gamma-1)} \tag{12.4}$$

Combustion chamber

Heat supplied is given by

$$Q_s = Q_f = h_{o3} - h_{o2s} = c_p\,(T_{o3} - T_{o2s}) \tag{12.5}$$

Turbine

Work, $$w_T = h_{o3} - h_{o4s} = c_p\,(T_{o3} - T_{o4s}) \tag{12.6}$$

Pressure ratio $$\frac{p_3}{p_4} = \left(\frac{T_3}{T_{4s}}\right)^{\gamma/(\gamma-1)} \tag{12.7}$$

Exhaust nozzle

$$h_{04s} = h_{oes}$$

$$h_{4s} + \frac{1}{2}c_{4s}^2 = h_{es} + \frac{1}{2}c_{es}^2$$

$$T_{4s} + \frac{c_{4s}^2}{2c_p} = T_{es} + \frac{c_{es}^2}{2c_p} \tag{12.8}$$

Pressure ratio $$\frac{p_4}{p_e} = \left(\frac{T_{4s}}{T_{es}}\right)^{\gamma/(\gamma-1)} \tag{12.9}$$

Air standard efficiency

The thermal efficiency or the air standard efficiency of the ideal cycle $1-2s-3-4s$ (Figure 12.8) is given by

$$\eta_J = \frac{\text{Work}}{\text{Heat supplied}}$$

$$= \frac{\text{Heat supplied} - \text{heat rejected}}{\text{Heat supplied}} = \frac{Q_s - Q_r}{Q_s}$$

$$\eta_J = 1 - \frac{Q_r}{Q_s} \tag{12.10}$$

Considering static temperatures in the cycle, $1-2s-3-4s$,

$$Q_s = c_p\,(T_3 - T_{2s})$$

$$Q_r = c_p\,(T_{4s} - T_1)$$

Therefore, Equation (12.10) gives

$$\eta_J = 1 - \frac{T_{4s} - T_1}{T_3 - T_{2s}} \tag{12.11}$$

The pressure ratio in the compressor and turbine is same

$$r = \frac{p_2}{p_1} = \frac{p_3}{p_4} \tag{12.12}$$

Therefore, the corresponding temperature ratios are given by

$$t = \frac{T_{2s}}{T_1} = \frac{T_3}{T_{4s}} = r^{(\gamma-1)/\gamma} \tag{12.13}$$

Equation (12.13) in (12.11) gives

$$\eta_J = 1 - \frac{1}{t} = 1 - \frac{1}{r^{(\gamma-1)/\gamma}} \tag{12.14}$$

The actual work that is considered in aircraft propulsion is propulsive work = thrust × aircraft speed.

Therefore, the efficiency in Equation (12.14) is used only for turboshaft and turboprop engines. The efficiencies of various components besides the propulsive efficiency and thermal efficiency of the actual power plant are of greater importance in aerospace propulsion.

12.3.2 Component Efficiencies

The departure of actual processes from the ideal in various components of the turbojet engine is shown in Figure 12.9. Efficiencies of the inlet diffuser, compressor, combustion chamber, turbine and the exhaust or the propelling nozzle will be separately considered in this section.

Inlet diffuser

Adiabatic compression of air through the inlet diffuser $(i-1)$ and the compressor $(1-2)$ is shown in Figure 12.13.

Ambient air enters the diffuser at pressure p_i, temperature T_i and velocity $c_i = u$. The pressure rises to p_1 at the diffuser exit where the velocity is reduced to c_1. There is no energy transfer; only energy transformations takes place here. The performance and diffuser efficiency can be considered in different ways. Only two methods of analysis are presented here.

(a) Small pressure Rise

Here the static pressure rise in the diffuser for a given change in the kinetic energy $\frac{1}{2}(c_i^2 - c_1^2)$ is considered. The efficiency is defined as

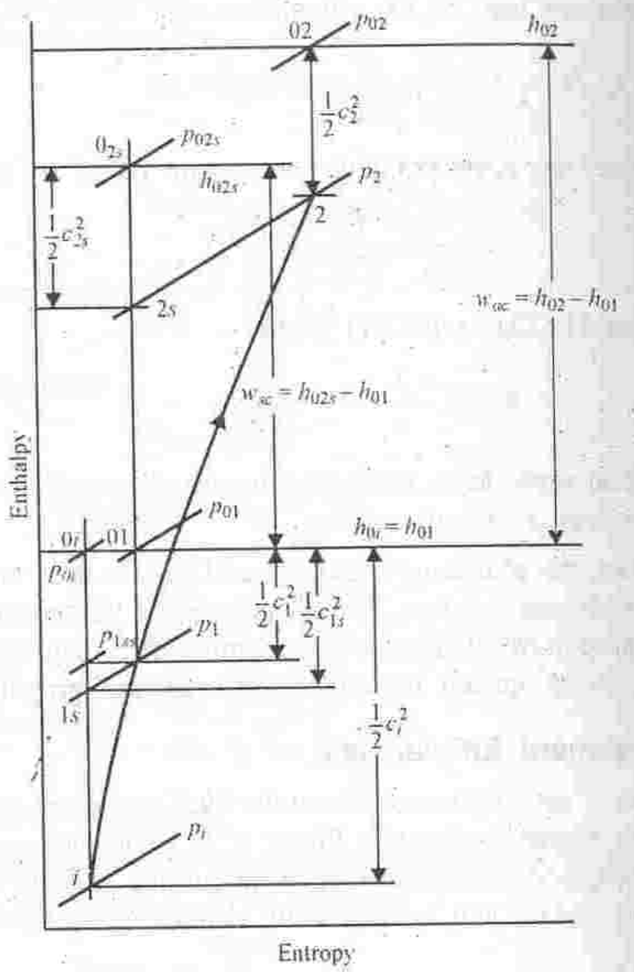

FIGURE 12.13 : Compression through the inlet diffuser and the compressor

$$\eta_D = \frac{\text{Static pressure rise in the actual process}}{\text{Static pressure rise in the isentropic process}}$$

$$\eta_D = \frac{p_1 - p_i}{p_{1ss} - p_i} \tag{12.15}$$

Considering incompressible flow, $\rho \approx$ constant

$$p_1 - p_i = p_{o1} - \frac{1}{2}\rho c_1^2 - p_{oi} + \frac{1}{2}\rho c_i^2$$

$$p_1 - p_i = \frac{1}{2}\rho\,(c_i^2 - c_1^2) - (p_{oi} - p_{o1}) \tag{12.16}$$

Stagnation pressure loss across the diffuser

$$(\Delta p_o)_D = p_{oi} - p_{o1} \tag{12.17}$$

For the isentropic process $i - 1ss$,

$$p_{1ss} - p_i = p_{oi} - \frac{1}{2}\rho c_1^2 - p_{oi} + \frac{1}{2}\rho c_i^2$$

$$p_{1ss} - p_i = \frac{1}{2}\rho\,(c_i^2 - c_1^2) \tag{12.18}$$

Equations (12.15) and (12.18) give

$$\eta_D = \frac{p_1 - p_i}{\frac{1}{2}\rho\,(c_i^2 - c_1^2)} \tag{12.19}$$

Above expressions are fairly accurate for subsonic flows. For higher Mach numbers at entry following definition may be adopted.

(*b*) Large pressure rise

$$\eta_D' = \frac{\text{Enthalpy change in isentropic diffusion}}{\text{Enthalpy change in actual diffusion for the same exit pressure}}$$

$$\eta_D' = \frac{h_{1s} - h_i}{h_1 - h_i} = \frac{T_{1s} - T_i}{T_1 - T_i} \tag{12.20}$$

Here the exit velocity in the isentropic process is greater than that in the actual process

$$c_{1s} > c_1$$

The values of the diffuser efficiency in Equations (12.19) and (12.20) are nearly the same for small pressure rise in the diffuser.

Efficiency in Equation (12.20) can be expressed as a function of the Mach number at the diffuser inlet or the flight Mach number.

$$\eta_D' = \frac{\left[\frac{T_{1s}}{T_i} - 1\right]}{\left[\frac{T_1}{T_i} - 1\right]}$$

Assuming $T_1 \approx T_{o1} = T_{oi}$

$$\frac{T_1}{T_i} - 1 = \frac{T_{oi}}{T_i} - 1 = \frac{\gamma - 1}{2} M_i^2, \text{ therefore,}$$

$$\eta_D' = \frac{\left(\frac{p_1}{p_i}\right)^{(\gamma-1)/\gamma} - 1}{\frac{\gamma-1}{2} M_i^2} \tag{12.21}$$

Compressor

Air enters the compressor at a reduced velocity (c_1) and Mach number (M_1). Its pressure and enthalpy are raised to p_2 and h_2 in the actual process (1 – 2). Stagnation pressures and enthalpies at the exit in the isentropic and actual processes are also shown in Figure 12.13. Both energy transformation and transfer occur in this process.

The actual work done by the compressor on the air is

$$w_{ac} = h_{o2} - h_{o1} = c_p (T_{o2} - T_{o1}) \tag{12.22}$$

Work or energy transfer in the isentropic process (1 – 2s) is lesser than the actual on account of losses; this is given by

$$w_{sc} = h_{o2s} - h_{o1} = c_p (T_{o2s} - T_{o1}) \tag{12.23}$$

The efficiency of the compressor based on Equations (12.22) and (12.23) is known as the total-to-total efficiency; this is given by

$$\eta_c = \frac{w_{sc}}{w_{ac}} = \frac{h_{o2s} - h_{o1}}{h_{o2} - h_{o1}} = \frac{T_{o2s} - T_{o1}}{T_{o2} - T_{o1}} \tag{12.24}$$

The stagnation pressure ratio for the compressor, assuming $p_{o2s} \approx p_{o2}$ is

$$r_{oc} = \frac{p_{o2}}{p_{o1}}$$

Therefore, $$\eta_c = \frac{T_{o1} (r_{oc}^{(\gamma-1)/\gamma} - 1)}{T_{o2} - T_{o1}} \tag{12.25}$$

Combustion Chamber

Air enters the combustion chamber from the compressor at pressure p_2, temperature T_2 and velocity c_2. The combustion of the fuel increases the enthalpy of the air-fuel mixture. The mass of high temperature gases flowing from the combustion chamber to the turbine and the propelling nozzle is $\dot{m}$ kg/s.

$$\dot{m} = \dot{m}_a + \dot{m}_f$$

$$m = \dot{m}_a (1 + f) \tag{12.26}$$

All the energy of the fuel is not available for increasing the enthalpy of gases in the combustion chamber; this is on account of incomplete combustion and heat losses. The efficiency of the combustion or fuel burning is defined as

$$\eta_B = \frac{\text{increase in the enthalpy of gases}}{\text{energy supplied in the fuel}}$$

$$\eta_B = \frac{(\dot{m}_a + \dot{m}_f) h_{o3} - \dot{m}_a h_{o2}}{\dot{m}_f Q_f} \tag{12.27}$$

This can be approximated to the following expression for very small values of fuel-air ratio:

$$\eta_B = \frac{h_{o3} - h_{o2}}{f \cdot Q_f} \tag{12.28}$$

Combustion efficiency can also be defined by

$$\eta_B = \frac{\text{theoretical fuel-air ratio}}{\text{actual fuel-air ratio}}$$

$$\eta_B = \frac{f'}{f} \tag{12.29}$$

Turbine

The products of combustion from the combustion chamber enter the turbine at pressure p_3, temperature T_3 and velocity c_3. Properties (γ, c_p etc.) of these gases are different from those of air flowing through the inlet diffuser and the compressor. Expansion of the gases through the turbine and the propelling nozzle is shown in Figure 12.14. The actual stagnation enthalpy change across the turbine (3-4) appears as actual work. Both energy transformation and transfer occur in this process. The values of turbine work in actual and ideal processes are:

$$w_{aT} = h_{o3} - h_{o4} = c_p (T_{o3} - T_{o4}) \tag{12.30}$$

$$w_{sT} = h_{o3} - T_{o4s} = c_p (T_{o3} - T_{o4s}) \tag{12.31}$$

Total-to-total efficiency of the turbine is given by

$$\eta_T = \frac{w_{aT}}{w_{sT}} = \frac{h_{o3} - h_{o4}}{h_{o3} - h_{o4s}} = \frac{T_{o3} - T_{o4}}{T_{o3} - T_{o4s}} \tag{12.32}$$

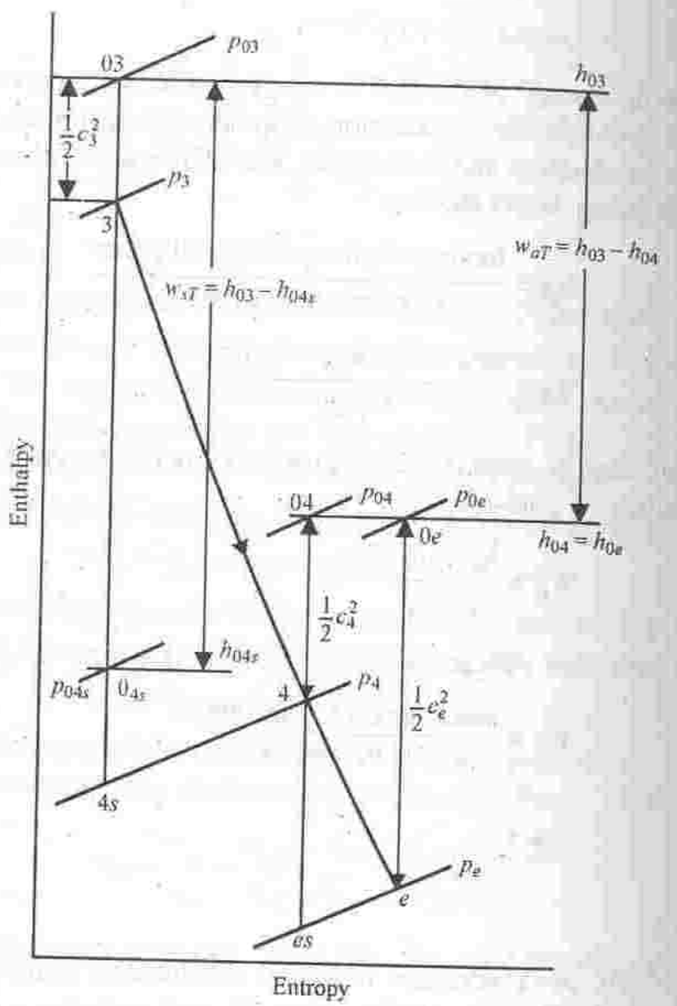

FIGURE 12.14 : Expansion through the turbine and the propelling nozzle

The stagnation pressure ratio for the turbine assuming $p_{o4s} \approx p_{o4}$ is $r_{oT} = \dfrac{p_{o3}}{p_{o4}}$.

Therefore, $$\eta_T = \frac{T_{o3} - T_{o4}}{T_{o3}\left[1 - \dfrac{1}{r_{oT}^{(\gamma-1)/\gamma}}\right]} \tag{12.33}$$

Exhaust or Propelling Nozzle

Exhaust gases from the turbine enter the propelling nozzle at pressure p_4, temperature T_4 and velocity c_4. The gases expand adiabatically to the exit pressure p_e. There is no energy transfer; only energy transformation occurs here. As stated before only convergent nozzles are employed. Gases expand either to the ambient pressure (p_a) or a slightly higher value. Nozzle efficiency is defined as the ratio of actual and isentropic values of the enthalpy drop between pressures p_{o4} and p_e.

$$\eta_j = \frac{h_{o4} - h_e}{h_{o4} - h_{es}} = \frac{T_{o4} - T_e}{T_{o4} - T_{es}} \tag{12.34}$$

$$\eta_j = \frac{T_{o4} - T_e}{T_{o4}\left[1 - \left(\dfrac{p_e}{p_{o4}}\right)^{(\gamma-1)/\gamma}\right]} \tag{12.35}$$

If the velocity at the nozzle entry is small, $T_{o4} \approx T_4$; therefore,

$$\eta_j = \frac{T_4 - T_e}{T_4\left[1 - \left(\dfrac{p_e}{p_4}\right)^{(\gamma-1)/\gamma}\right]} \tag{12.36}$$

Energy equation gives

$$h_{04} = h_{oe} = h_e + \frac{1}{2}c_e^2$$

$$\frac{1}{2}c_e^2 = h_{o4} - h_e = \eta_j (h_{o4} - h_{es})$$

$$c_e^2 = 2\eta_j c_p (T_{o4} - T_{es})$$

$$c_e^2 = 2\eta_j c_p T_{o4}\left[1 - \left(\frac{p_e}{p_{o4}}\right)^{(\gamma-1)/\gamma}\right] \tag{12.37}$$

12.3.3 Thrust

The force which propels the aircraft forward at a given speed is called thrust or propulsive force. This is developed by the jet at the exit of the propelling nozzle in the turbojet and turbofan engines as explained before; the main propulsive force (thrust) in turboprop engines comes from the propeller. Analytical expressions for the thrust by these engines will be developed in the following sections separately.

(*a*) Propeller Thrust

Figure 12.15 shows a model of air flow taking place across the propeller moving leftward at the speed of the aircraft. The action of the propeller accelerates the air and causes it to flow in a pattern shown in the figure. The flow across the propeller is separated from the fluid at rest by a boundary similar to the walls of a convergent duct.

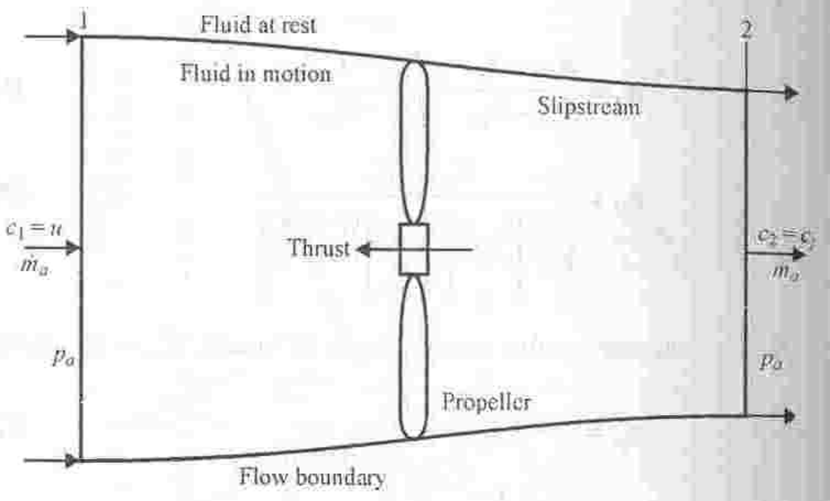

FIGURE 12.15 : Flow through an aircraft propeller

Stations 1 and 2 far upstream and downstream have uniform one-dimensional flow at velocities c_1 and c_2 respectively. The static pressure change within the boundary between stations 1 and 2 is governed by the Bernoulli equation; the pressure outside the boundary is ambient throughout. Therefore, the thrust on the propeller disc and the aircraft is wholly due to the change in the momentum flux between the two stations, which is given by

$$F = \dot{m}_a (c_2 - c_1)$$

Now $c_1 = u =$ flight speed

$c_2 = c_j =$ slip stream velocity or jet velocity

$$F = \dot{m}_a (c_j - u) \qquad (12.38)$$

The effective speed ratio or flight to jet velocity ratio is

$$\sigma = \frac{u}{c_j}$$

Therefore, $$F = \dot{m}_a u \left(\frac{1}{\sigma} - 1 \right) = \dot{m}_a c_j (1 - \sigma) \qquad (12.39)$$

The non-dimensional value of thrust is given by

$$\frac{F}{\dot{m}_a u} = \frac{1}{\sigma} - 1 \qquad (12.40\ (a))$$

$$\frac{F}{\dot{m}_a c_j} = 1 - \sigma \qquad (12.40\ (b))$$

The actual flow through the propeller differs considerably from the model depicted in Figure 12.15. The propeller works in an "infinite sea of air"; there is no well defined boundary between the fluid at rest and fluid in motion; therefore, the actual thrust will differ considerably from the values in the above expressions.

(*b*) Jet Thrust

Figure 12.16 shows the internal and external flows for a turbojet engine (propulsive device) occurring through an imaginary control surface with

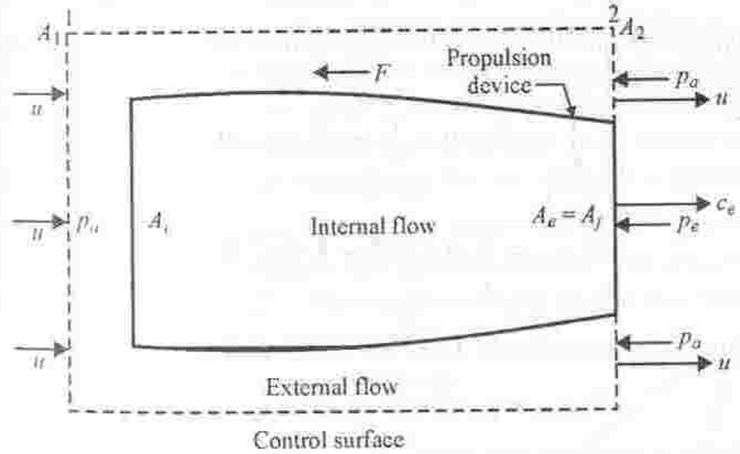

FIGURE 12.16 : Internal and external flows for a propulsion device

very large areas of cross-section A_1 and A_2 at entry and exit. The flow of air and gases (internal flow) through the engine is separated from the external flow of air by the solid boundaries of the engine casing.

Ambient air enters the engine at pressure p_a and velocity u; hot gases leave the engine at pressure p_e and high velocity c_e. In case of complete expansion of gases in the propelling nozzle $p_e = p_a$ and

$c_e = c_j$. The flow rate at the engine inlet (cross-sectional area $= A_i$) is $\dot{m}_a$ kg/s; and at the engine exit (cross-sectional area $= A_e = A_j$) it is $(\dot{m}_a + \dot{m}_f)$ kg/s.

Part of the air flow at ambient conditions at station 1 (far upstream of the inlet) is swallowed by the engine and experiences change in the momentum flux by the action of the engine; the remaining flow passes over the engine without any change in the momentum flux.

Thrust on the engine (and the aircraft) is exerted on account of changes in the momentum flux as well as pressure.

Net thrust = momentum thrust + pressure thrust

$$F = F_{\text{mom}} + F_{pr} \tag{12.41}$$

For steady flow parallel to the direction of flight Equation (3.25) (Chapter 3) gives

$$F_{\text{mom}} = \int_{A_e} \rho c_e^2 \, dA + \int_{A_2 - A_e} \rho u^2 \, dA - \int_{A_i} \rho u^2 \, dA - \int_{A_1 - A_i} \rho u^2 \, dA \tag{12.42}$$

The external flow does not experience any change in the momentum flux; therefore,

$$\int_{A_2 - A_e} \rho u^2 \, dA - \int_{A_1 - A_i} \rho u^2 \, dA = 0$$

$$F_{\text{mom}} = \int_{A_e} \rho c_e^2 \, dA - \int_{A_i} \rho u^2 \, dA \tag{12.43}$$

For one-dimensional flow at stations 1 and 2,

$$F_{\text{mom}} = \rho_e c_e^2 A_e - \rho_i u^2 A_i \tag{12.44}$$

From continuity equation

$$\dot{m}_a = \rho_i u A_i \tag{12.45}$$

$$\dot{m} = \dot{m}_a + \dot{m}_f = \rho_e c_e A_e \tag{12.46}$$

Equations (12.44), (12.45) and (12.46) give

$$F_{\text{mom}} = (\dot{m}_a + \dot{m}_f) c_e - \dot{m}_a u$$

Neglecting $\dot{m}_f$ as negligible compared to $\dot{m}_a$

$$F_{\text{mom}} = \dot{m}_a (c_e - u) \tag{12.47}$$

Pressure force on the control surface for the external flow outside the cross-sectional area A_i (assuming $A_i > A_e$) is zero; therefore,

$$F_{pr} = p_e A_e + p_a (A_i - A_e) - p_a A_i$$

$$F_{pr} = (p_e - p_a) A_e \tag{12.48}$$

Same result is obtained by writing the above relations for $A_e \geq A_i$. Equations (12.47) and (12.48) in Equation (12.41) give

$$F = \dot{m}_a (c_e - u) + (p_e - p_a) A_e \tag{12.49}$$

A reference velocity known as "effective jet velocity" (c_j) is defined by the following relation through Equation (12.49):

$$F = \dot{m}_a (c_j - u) = \dot{m}_a (c_e - u) + (p_e - p_a) A_e \tag{12.50}$$

When the pressure at the jet exit plane is same as the ambient pressure $c_e = c_j$; in this case Equations (12.38) and (12.50) are identical.

12.3.4 Propulsive, Thermal and Overall Efficiencies

Performance of an aircraft propulsion system can be judged by various efficiencies besides some specific quantities. The performance of the engine can be rated in terms of an energy conversion efficiency or thermal efficiency. The performance of the turbojet engine or the propeller as a propulsive device can be rated in terms of a propulsive efficiency. The overall efficiency of the propulsion system is a measure of the utilization of fuel energy in propelling the aircraft at a given speed.

Figure 12.17 depicts the utilization of power of the fuel in a turbojet engine in different stages. The power input to the engine or the propulsion system is $\dot{m}_f . Q_f$. The engine output is the increase in the

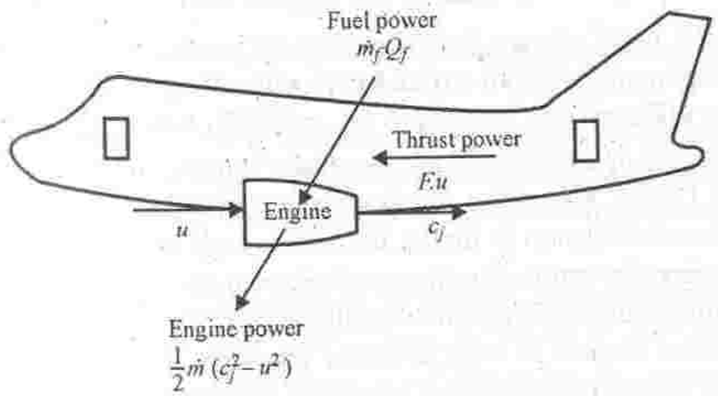

FIGURE 12.17 : Power utilization in aircraft propulsion

rate of kinetic energy of gases *i.e.*, $\frac{1}{2}\dot{m}\,(c_j^2 - u^2)$. The net outcome of the propulsion system is the rate of work or thrust power F.u.

For convenience the flow rate through the engine is taken as

$$\dot{m} \approx \dot{m}_a \text{ kg/s}.$$

Propulsive Efficiency

The propulsive efficiency is given by

$$\eta_p = \frac{\text{Propulsive power or thrust power}}{\text{Power output of the engine}}$$

Substituting for thrust in terms of the effective jet velocity from Equation (12.50)

$$\eta_p = \frac{\dot{m}\,(c_j - u)\,u}{\frac{1}{2}\dot{m}\,(c_j^2 - u^2)} = \frac{2u}{c_j + u}$$

$$\eta_p = \frac{2}{\frac{c_j}{u} + 1} = \frac{2}{\frac{1}{\sigma} + 1}$$

$$\eta_p = \frac{2\sigma}{1 + \sigma} \qquad (12.51)$$

The above analysis is applicable for the turboprop engine also: in that case the increase in the kinetic energy $\frac{1}{2}(c_j^2 - u^2)$ of air is caused through the propeller instead of the engine itself.

Figure 12.18 shows the variations of propulsive efficiency and the thrust (Equations 12.40 (*a*) and (*b*)) with effective speed ratio. The propulsive efficiency is maximum ($\eta_p = 100\%$) when the flight speed is equal to the jet velocity; this condition corresponds to zero thrust (Equation 12.39). Therefore, this is only a hypothetical case. However, an important conclusion is drawn from this: high propulsive efficiency can be obtained by employing jet speed close to the flight speed whereas thrust can be increased by increasing the flow rate of air or gas through the propulsive device. A large diameter propeller with a small velocity differential ($u \approx c_j$) comes close to such a device. High speed turbojet engines are located at the other end of the scale. On account of low

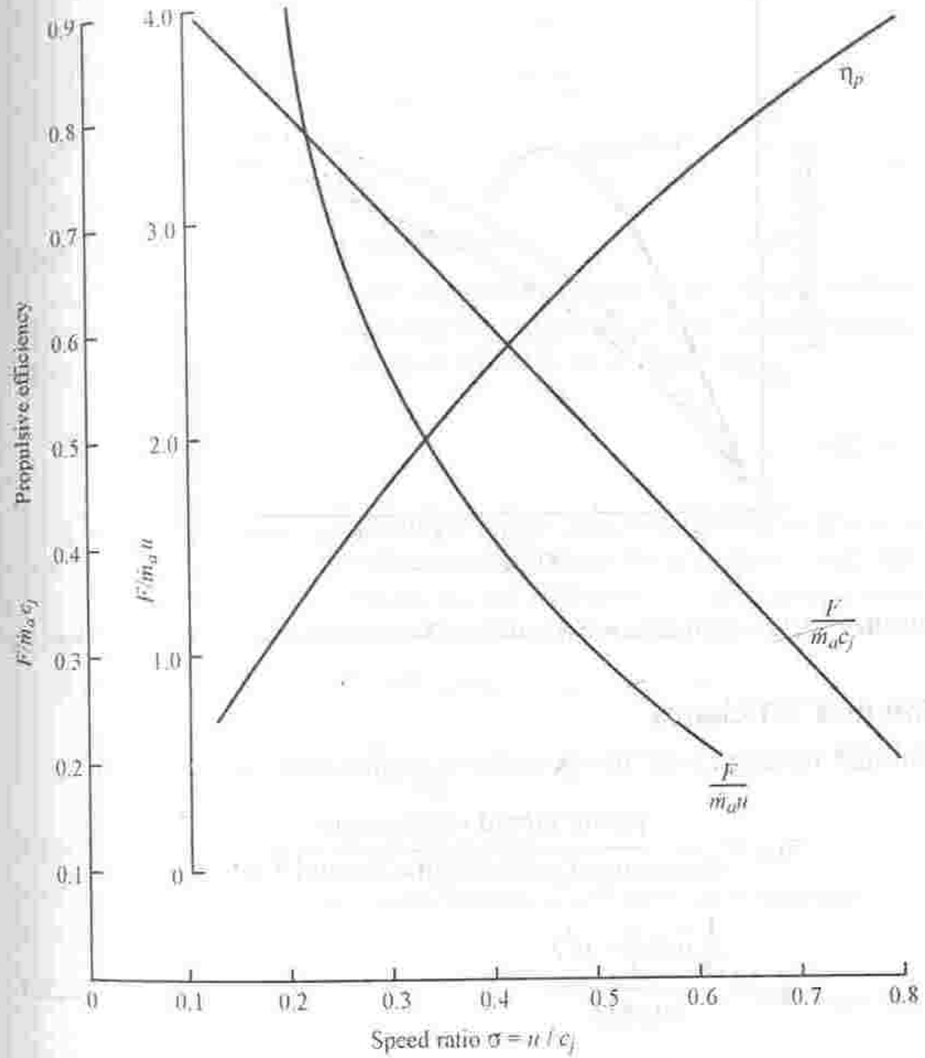

FIGURE 12.18 : Variation of thrust and propulsive efficiency with speed ratio

values of σ (higher velocity differential) the propulsive efficiencies are poor but the thrust is high. Turbofan engine performance comes in between the turboprop and turbojet engines in terms of propulsion as stated before.

The propulsive efficiencies of the various engines with flight speed are shown in Figure 12.19. The turboprop system is preferable in the lower range of speed. Performance of turbojet and turbofan engines continues to improve with speed.

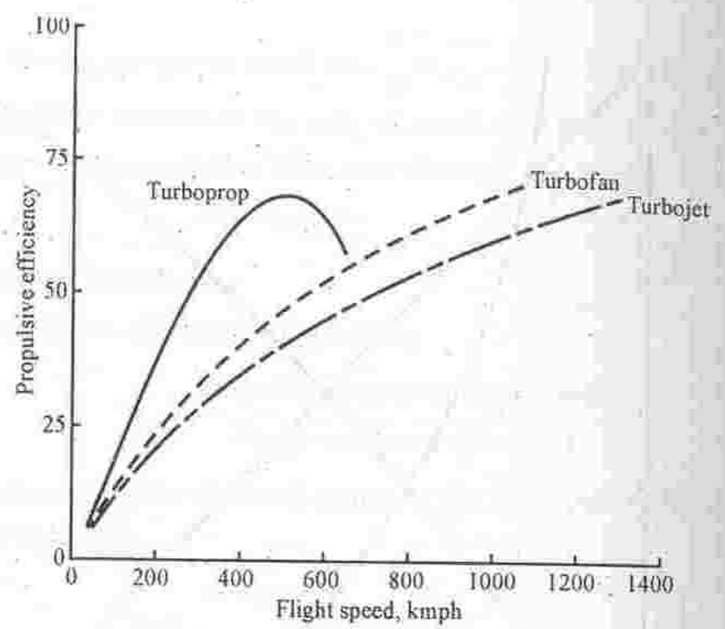

FIGURE 12.19 : Comparison of propulsive efficiencies of various propulsive devices

Thermal Efficiency

Thermal efficiency of the propulsive engine can be defined by

$$\eta_{th} = \frac{\text{power output of the engine}}{\text{power input to the engine through fuel}}$$

$$\eta_{th} = \frac{\frac{1}{2}\dot{m}\,(c_i^2 - u^2)}{\dot{m}_f\, Q_f} \tag{12.52}$$

$$\eta_{th} = \frac{1}{2}\,\frac{c_j^2}{f Q_f}(1 - \sigma^2) \tag{12.53}$$

Overall Efficiency

Overall efficiency of the propulsion system is defined by

$$\eta_o = \frac{\text{Propulsive power}}{\text{power input to the engine through fuel}}$$

$$\eta_o = \frac{\dot{m}\,(c_j - u)\,u}{\dot{m}_f\, Q_f} \tag{12.54}$$

$$\eta_o = \frac{\dot{m}\,(c_j - u)\,u}{\frac{1}{2}\dot{m}\,(c_j^2 - u^2)} \times \frac{\frac{1}{2}\dot{m}\,(c_j^2 - u^2)}{\dot{m}_f\, Q_f}$$

$$\eta_o = \eta_p \times \eta_{th} \tag{12.55}$$

12.3.5 Specific Fuel Consumption

Specific fuel consumption is an important parameter in engine performance. In aircraft propulsion, since the output is in the form of thrust, a thrust specific fuel consumption (TSFC) is defined by

$$\text{TSFC} = \frac{\dot{m}_f}{F} \tag{12.56}$$

This gives the fuel consumption rate per unit thrust; it gives a better idea of the entire propulsion system than the efficiency and can be used to compare the performance of different types of propulsion systems.

Equation (12.56) in (12.54) gives

$$\eta_o = \frac{u}{\text{TSFC} \times Q_f} \tag{12.57}$$

12.3.6 Specific Thrust and Impulse

Specific thrust is defined as thrust produced per unit flow rate through the propulsive device.

$$F_s = \frac{F}{\dot{m}} \tag{12.58}$$

This is useful in comparing the size of the different types of the propulsion devices.

Equations (12.56) and (12.58) give

$$\text{TSFC} = \frac{f}{F_s} \tag{12.59}$$

Another useful performance parameter in aerospace propulsion is the specific impulse. This is thrust developed per unit weight flow rate through the propulsive device.

$$I_s = \frac{F}{\dot{w}} \tag{12.60}$$

$$I_s = \frac{\dot{m}\,(c_j - u)}{\dot{m} g}$$

$$I_s = \frac{u}{g}\left(\frac{c_j}{u} - 1\right)$$

$$I_s = \frac{u}{g}\left(\frac{1}{\sigma} - 1\right) \tag{12.61}$$

If $\dot{w} = \dot{w}_a$ the quantity in Equation (12.60) is known as air specific impulse.

Specific thrust and specific impulse are identical quantities expect for the units. Specific impulse is simply expressed in seconds.

Figure 12.20 shows the variation of specific impulse with flight speed for various values of the flight to jet speed ratio (and propulsive

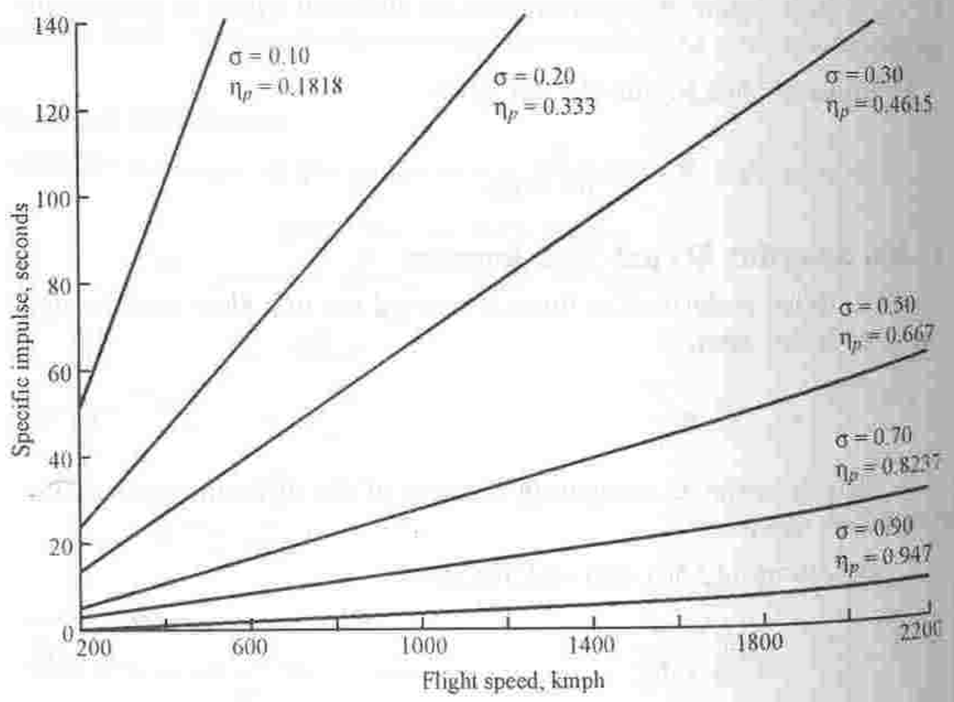

FIGURE 12.20 : Variation of specific impulse with flight speed for various aircraft propulsion systems

efficiency). For a given speed ratio specific impulse increases with flight speed; this gives higher values of specific impulse for turbojet engines on account of their high speeds; turboprop engines have comparatively

lower specific impulse on account of their lower speeds and higher values of speed ratio. At a given flight speed higher value of specific impulse can be obtained by decreasing the speed ratio and paying the penalty in propulsive efficiency.

12.4 RAMJET ENGINE

When the flight speed of a turbojet engine is very high, say in the range of Mach number 2 to 4 the pressure rise in the diffuser (ram pressure) is very high; at this flight speed the contribution of the compressor to the total static pressure rise is insignificant. Therefore, it can be removed from the engine along with its prime mover—the turbine. In this manner a thrust producing device (engine) is obtained which does not have compressor and turbine.

12.4.1 Main Components and Operation

Figure 12.21 shows such a device known as ramjet engine. On account of high flight speed (generally supersonic) the static pressure rise in

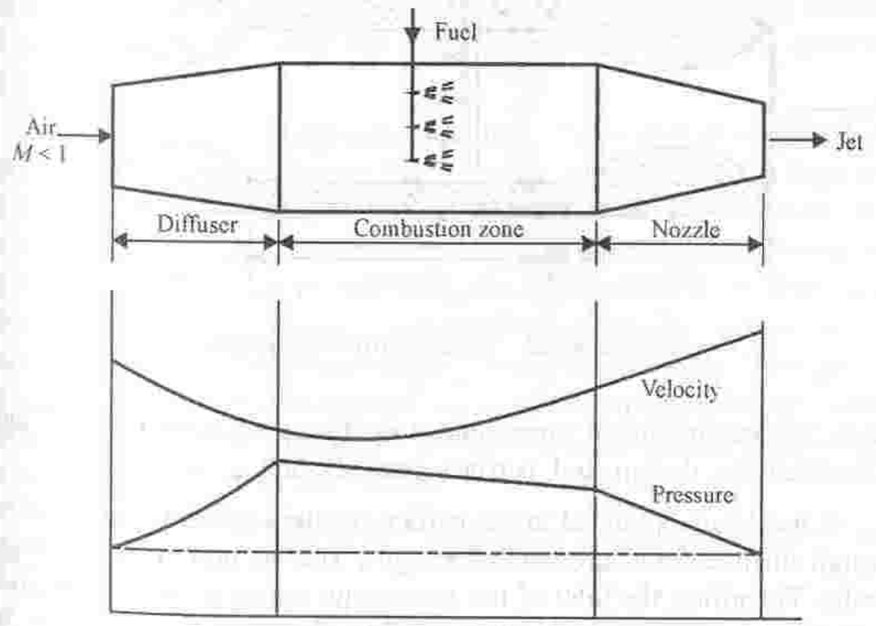

FIGURE 12.21 : A subsonic ramjet engine

the inlet diffuser is high enough to support combustion of fuel in the combustion zone. The diffuser must decrease the velocity of incoming air to a sufficiently low value so that addition of the required quantity

of heat is possible before choking (see Section 9.5); low velocity also increases the stability of the flame. The high pressure and temperature gas then expands to very high velocity in the nozzle. A high thrust is developed on account of large change in the momentum flux through the engine.

Variation of pressure and velocity of the air and gas through the engine is also shown in Figure 12.21. The pressure drop across the nozzle is lower than the ram pressure on account of decrease in the static pressure in the combustion chamber due to heat addition.

Experience and tests have shown that a subsonic flow system is not the right choice for a ramjet engine. Since the pressure rise in the engine is wholly due to the "ram effect" it can be increased by employing supersonic flow of high Mach number at the diffuser entry. Figure 12.22 shows such an arrangement with supersonic diffuser and

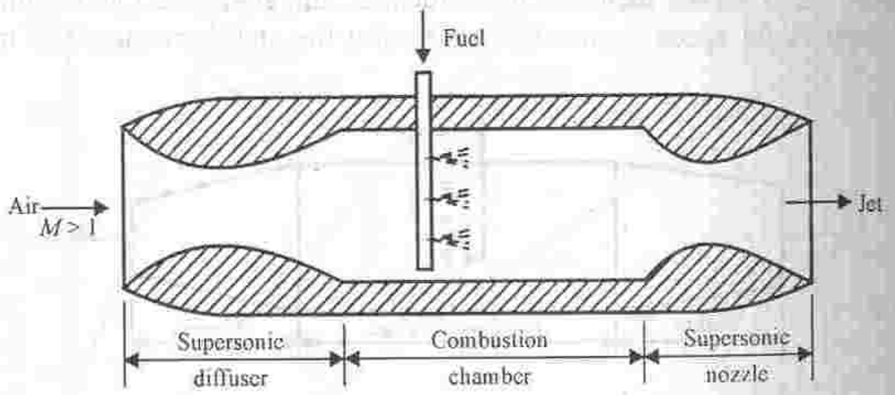

FIGURE 12.22 : A supersonic ramjet engine

nozzle. Characteristics of supersonic flow discussed in Sections 4.7 and 6.15 effect the design and performance of such an engine.

It has been explained in the earlier chapters that supersonic flows through diffusers and around bodies give rise to normal and oblique shocks. Therefore, the inlet of the supersonic ramjet engine is designed carefully in order to reduce losses. Different configurations can be employed in obtaining diffusion at supersonic flight speeds. Figure 12.23 shows one such arrangement. Here diffusion takes place in many stages; first the flow is decelerated through a conical shock at the nose of the engine; then it is diffused in the subsonic diffuser after passing through normal shock. Static pressure rise occurs across the

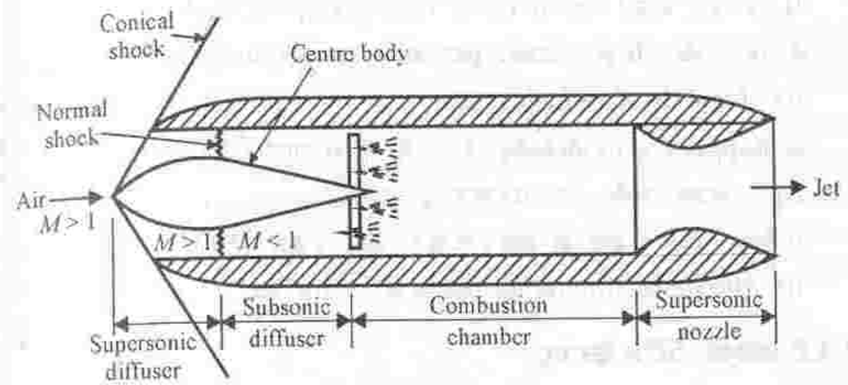

FIGURE 12.23 : Supersonic ramjet engine with Oswatitsch type annular diffuser

oblique and normal shocks besides supersonic and subsonic diffusion of flow in the diffuser passages as shown in the figure.

On account of the absence of the turbine and compressor high temperatures of the order of 2000°C can be employed in the combustion chamber to obtain very high values of thrust at high Mach numbers. Ramjet engines are ideal for missiles and propulsion of hypersonic aircrafts.

The stagnation temperature at the diffuser exit is very high corresponding to very high inlet Mach numbers; as a result the high combustor temperatures lead to the dissociation of fuel and failure of the vehicle structure. The remedy lies in keeping the stagnation temperature low at the diffuser exit by restricting the deceleration of the flow within the supersonic range. In this case the flow enters the combustor at supersonic velocity and comparatively lower temperature. This prevents the aforementioned problems but the combustion at supersonic velocity requires greater care. The static pressure is high enough to provide the required expansion in the nozzle.

This device is called as "supersonic combustion ramjet" or in short Scramjet.

The main advantages of the ramjet engine are:

1. High temperatures can be employed.
2. In the absence of rotating machinery its construction is very simple and cheap.
3. It can operate efficiently at high supersonic Mach numbers.

4. It is not very sensitive to the quality of fuel.
5. It provides high thrust per unit weight and frontal area.

Its main disadvantages are:

1. It requires a launching device at supersonic speed.
2. It is unsuitable for subsonic speeds.
3. It has low thermal efficiency and high TSFC.
4. Its maximum operating altitude is limited.

12.4.2 Ideal Efficiency

Various processes occurring in the ramjet engine can also be represented by an open circuit Brayton cycle (Figure 12.24). This cycle is considered here with the following assumptions:

1. Steady one-dimensional flow,
2. Isentropic compression and expansion, $\Delta s = 0,\ \Delta p_o = 0,$
3. Perfect gas,

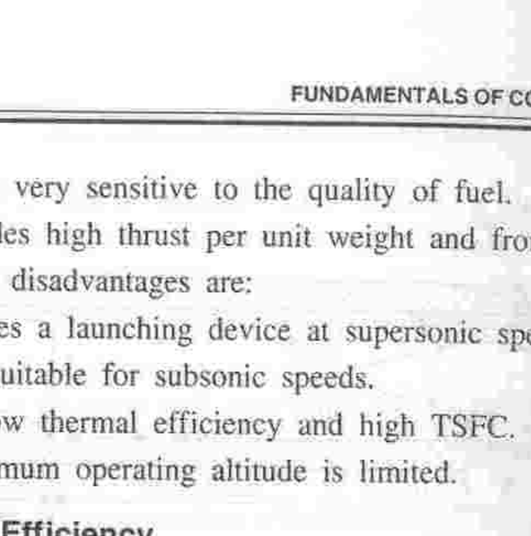

FIGURE 12.24 : Ideal Brayton cycle for ramjet engine

4. Constant pressure heat addition in the combustion chamber,

$$p_2 \approx p_3.$$

5. Very low Mach number in the combustion chamber.

$$p_2 \approx p_{o2} \approx p_{o3}$$

$$T_2 \approx T_{o2} \approx T_{o1}$$

Compression and expansion processes here are thermodynamically different from those shown in Figure 12.8 for a turbojet engine. These processes here experience only energy transformation; there is no energy transfer such as compressor and turbine work within the engine. Thrust work is obtained from the energy supplied in the fuel during process 2-3. Heat is rejected during process 4-1 outside the engine. However, the ideal efficiency of the ramjet engine is still given by Equation (12.14):

$$\eta_i = 1 - \frac{1}{t} = 1 - \frac{1}{r^{(\gamma-1)/\gamma}} \tag{12.14}$$

Here, the temperature ratio, with the above assumptions is given by

$$t = \frac{T_2}{T_1} = \frac{T_{o2}}{T_1} = \frac{T_{o1}}{T_1} = 1 + \frac{\gamma - 1}{2} M_1^2 \tag{12.62}$$

Substituting the value of t from Equation (12.62) into (12.14) we get

$$\eta_i = 1 - \frac{1}{1 + \frac{\gamma-1}{2} M_1^2} = \frac{\frac{\gamma-1}{2} M_1^2}{1 + \frac{\gamma-1}{2} M_1^2}$$

$$\eta_i = \frac{1}{1 + \frac{2}{\gamma-1} \frac{1}{M_1^2}} = f(M_1) \tag{12.63}$$

Though the actual thermal efficiency of the ramjet engine will be much lower than the value given by Equation (12.63) it demonstrates an important characteristic *i.e.*, the efficiency increases with the flight Mach number and has a high value (76.19% at $M_1 = 4$) at higher operating Mach numbers.

Other performance parameters and efficiencies defined in Section 12.3 are also applicable for the ramjet engine.

12.5 PULSEJET ENGINE

Pulsejet engine is also a thrust producing device without turbine and compressor. Compression is achieved in the diffuser due to the ram-effect.

Therefore, it offers favourable conditions for employing high temperatures. This engine is shown in Figure 12.25. The engine consists

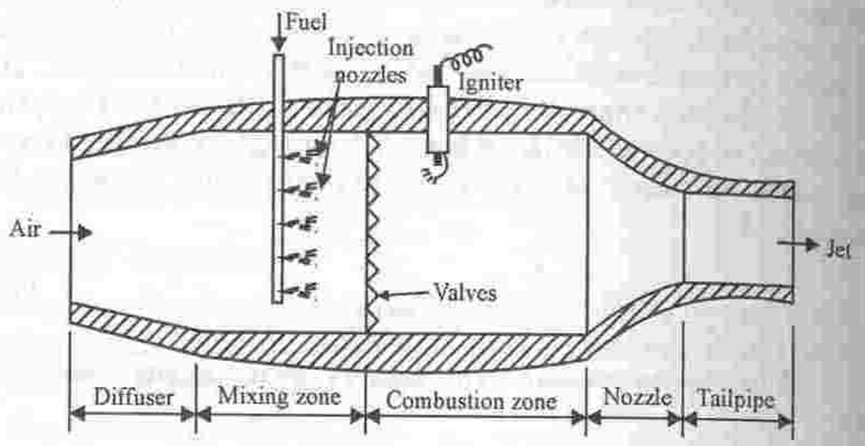

FIGURE 12.25 : A pulse jet engine

of an inlet diffuser which supplies air after compression, to the combustion chamber. Fuel is supplied to the high pressure air in a mixing zone upstream of the combustion chamber. The fuel-air mixture enters the combustion chamber through a bank of valves.

The fuel-rich mixture is exploded by a spark plug in the combustion chamber; this generates high pressure and temperature. The valves close due to the momentary pressure rise and the gases expand to high velocity in the nozzle and the tail pipe. The short burst of expansion of gases creates a vacuum in the combustion chamber; therefore the high pressure fuel-air mixture upstream forces the valves open starting a new cycle of recharging the combustion chamber, explosion, expansion and suction. Thus the thrust is not steady; it is produced in short pulses, hence the name "pulsejet". The combustion can be considered to occur at constant volume though the actual process deviates considerably from this. The frequency of explosions can be as high as 300 per second.

Pulsejet engine once started can work at any flight speed. Its performance does not improve at high speeds; the maximum flight speed is about 1000 kmph. On account of low air density its performance deteriorates with altitude.

Pulsejet engine has the following main advantages:

1. It is simple in construction and cheap; therefore, it can be mass produced in a short time.

2. It does not have the turbine and compressor, allowing it to employ high temperatures.
3. It is suitable for one-time military use. It was used by Germany in the world war as buzz-bomb or V-1 missile.

Its chief disadvantages are:

1. High vibration and noise level.
2. Limited altitude and flight speed.

NOTATION FOR CHAPTER 12

a	velocity of sound	p	pressure
A	area of cross-section	P	power
B	bypass ratio $= \dot{m}_c/\dot{m}_h$	Δp_o	stagnation pressure loss
c	velocity of air or gas	Q	lower calorific value of the fuel or heat transfer
c_p	specific heat at constant pressure	r	pressure ratio
d	diameter	R	gas constant
D	drag force	s	specific entropy
f	fuel-air ratio $= \dot{m}_f/\dot{m}_a$	Δs	change of entropy
F	force or thrust	t	time, temperature ratio
g	acceleration due to gravity	T	absolute temperature
h	specific enthalpy	$TSFC$	thrust specific fuel consumption
I	specific impulse		
L	lift force	u	aircraft or flight speed
$\dot{m}$	mass flow rate	w	specific work
M	Mach number	$\dot{w}$	weight flow rate
		Z	altitude

GREEK SYMBOLS

γ	specific heat ratio $= c_p/c_v$	ρ	density
η	efficiency	σ	speed ratio, u/c_j

SUBSCRIPTS

0	stagnation value	j	jet or nozzle
1, 2, 3.4	stations shown in the text	J	Joule or Brayton cycle
a	adiabatic, actual, air	max	maximum
B	burner or combustion chamber	mom	momentum
		o	overall
c	cold stream, compressor	p	propulsive
D	diffuser	p_r	pressure
e	exit	r	rejected
f	fuel	s	isentropic, specific, supplied
h	hot stream	ss	isentropic
i	inlet, ideal	T	turbine
		th	thermal

SOLVED EXAMPLES

Example 12.1. A turboprop engine operates at an altitude of 3000 meters above mean sea level and an aircraft speed of 525 kmph. The data for the engine is given below:

Inlet diffuser efficienc $= 0.875$
Compressor efficiency $= 0.790$
Velocity of air at compressor entry $= 90$ m/s
Temperature rise through the compressor $= 230^{\circ}$C
Properties of air: $\gamma = 1.4$, $c_p = 1.005$ kJ/kg K

From the above data calculate (*a*) pressure rise through the inlet diffuser (*b*) pressure ratio developed by the compressor (*c*) power required by the compressor per unit flow rate of air and (*d*) the air-standard efficiency of the engine.

Solution. At $Z = 3000$ m

$$T_i = 268.65K,\ p_i = 0.701,\ \rho_i = 0.909 \text{ kg/m}^3$$

$$a_i = 328.7 \text{ m/s}$$

$$u = 525/3.6 = 145.833 \text{ m/s}$$

$$M_i = u/a_i = 145.833/328.7 = 0.4436$$

$$\frac{T_{oi}}{T_i} = 1 + \frac{\gamma - 1}{2} M_i^2 = 1 + 0.2 \times 0.4436^2 = 1.03936$$

$$T_{oi} = T_{o1} = 1.03936 \times 268.65 = 279.244 \text{ K}$$

$$T_1 = T_{o1} - c_1^2/2c_p = 279.244 - 8100/2 \times 1005 = 275.194 \text{ K}$$

For the inlet diffuser,

$$T_{1s} - T_i = \eta_D (T_1 - T_i)$$

$$\frac{T_{1s}}{T_i} = 1 + \eta_D \left(\frac{T_1}{T_i} - 1 \right) = \left(\frac{p_{1s}}{p_i} \right)^{(\gamma-1)/\gamma} = \left(\frac{p_1}{p_i} \right)^{(\gamma-1)/\gamma}$$

$$\left(\frac{p_1}{p_i} \right)^{(\gamma-1)/\gamma} = 1 + 0.875 \left(\frac{275.194}{268.65} - 1 \right) = 1.0213$$

$$p_1/p_i = (1.0213)^{3.5} = 1.0766$$

$$p_1 = 1.0766 \times 0.701 = 0.7547 \text{ bar}$$

(*a*) Pressure rise through the inlet diffuser

$$p_1 - p_i = 0.7547 - 0.7010 = \mathbf{0.0537 \text{ bar}} \quad \textbf{Ans.}$$

(*b*) Compressor efficiency is given by

$$\eta_c = T_{o1} (r_{oc}^{(\gamma-1)/\gamma} - 1)/(T_{o2} - T_{o1})$$

$$r_{oc}^{(\gamma-1)/\gamma} = \frac{\eta_c}{T_{o1}} (T_{o2} - T_{o1}) + 1$$

$$= \frac{0.79 \times 230}{279.224} + 1 = 1.6507$$

$$r_{oc} = \frac{p_{o2}}{p_{o1}} = (1.6507)^{3.5} = 5.779 \quad \textbf{Ans.}$$

(*c*) Power required by the compressor is

$$\dot{m}_a c_p (T_{o2} - T_{o1}) = 1 \times 1.005 \times 230$$

$$= 231.15 \text{ kW/(kg/s)} \quad \textbf{Ans.}$$

(*d*) Air-standard efficiency of the engine for the pressure ratio of 5.779 is

$$\eta_J = 1 - \frac{1}{(r_{oc})^{(\gamma-1)/\gamma}} = 1 - \frac{1}{(5.770)^{0.286}}$$

$$\eta_J = 0.3942 \quad \textbf{Ans.}$$

Example 12.2. The diameter of the propeller of an aircraft is 2.5 m. It flies at a speed of 500 kmph at an altitude of 8000 m. For a flight to jet speed ratio of 0.75 determine (*a*) the flow rate of air through the propeller, (*b*) thrust produced, (*c*) specific thrust, (*d*) specific impulse and (*e*) the thrust power.

Solution. Area of cross-section of the propeller disc

$$A = \frac{\pi}{4} d^2 = \frac{\pi}{4} \times 2.5^2 = 4.908 \text{ m}^2$$

Air density at $Z = 8000$ m is

$$\rho = 0.525 \text{ kg/m}^3$$

Flight speed $u = 500$ kmph $= 138.89$ m/s

$$\sigma = u/c_j = 0.75$$

$$c_j = 138.89/0.75 = 185.18 \text{ m/s}$$

(*a*) Velocity of air flow at the propeller disc is

$$c = \frac{1}{2}(u + c_j)$$

$$c = 0.5\ (138.89 + 185.18) = 162.035\ \text{m/s}$$

Theoretical value of the flow rate is given by

$$\dot{m}_a = \rho A c = 0.525 \times 4.908 \times 162.035$$

$$\dot{m}_a = 417.516\ \text{kg/s} \quad \textbf{Ans.}$$

(*b*) $$F = \dot{m}_a\ (c_j - u)$$

$$F = 417.516\ (185.18 - 138.89) \times 10^{-3}$$

$$F = 19.3268\ \text{kN} \quad \textbf{Ans.}$$

(*c*) $$F_s = \frac{F}{\dot{m}_a} = \frac{19326.8}{417.516} = 46.29\ \text{N/(kg/s)} \quad \textbf{Ans.}$$

(*d*) $$I_s = \frac{F}{\dot{w}_a} = \frac{F}{\dot{m}_a g} = \frac{46.29}{9.81} = 4.718\ \text{s} \quad \textbf{Ans.}$$

(*e*) Thrust power is $P = F \times u$

$$P = 19.3268 \times 138.89 = 2684.3\ \text{kW} \quad \textbf{Ans.}$$

Example 12.3. An aircraft flies at 960 kmph. One of its turbojet engines takes in 40 kg/s of air and expands the gases to the ambient pressure. The air-fuel ratio is 50 and the lower calorific value of the fuel is 43 MJ/kg. For maximum thrust power determine (*a*) jet velocity (*b*) thrust (*c*) specific thrust (*d*) thrust power (*e*) propulsive, thermal and overall efficiencies and (*f*) TSFC.

Solution. $u = 960 \times 1000/3600 = 266.7$ m/s

(*a*) For maximum thrust power $\sigma = u/c_j = 0.5$

$$c_j = 266.7/0.5 = 533.4\ \text{m/s}$$

(*b*) $$\dot{m} = \dot{m}_a + \dot{m}_f = \dot{m}_a \left(1 + \frac{\dot{m}_f}{\dot{m}_a}\right)$$

$$\dot{m} = 40 \left(1 + \frac{1}{50}\right) = 40.8\ \text{kg/s}$$

$$F = \dot{m} c_j - \dot{m}_a u$$

$$F = (40.8 \times 533.4 - 40 \times 266.7) \times 10^{-3}$$

$$F = 11.094\ \text{kN} \quad \textbf{Ans.}$$

(*c*) Specific thrust based on air intake

$$F_s = F/\dot{m}_a$$

$$F_s = 11094/40 = 277.35\ \text{N/(kg/s)} \quad \textbf{Ans.}$$

(*d*) Thrust power $P = F \times u$

$$P = 11.094 \times 266.7 = 2958.77\ \text{kW} \quad \textbf{Ans.}$$

(*e*) $$\eta_p = \frac{1}{1 + c_j/u} = \frac{2}{1+2} = 0.666 \text{ or } 66.6\% \quad \textbf{Ans.}$$

$$\eta_{th} = \frac{\frac{1}{2}\dot{m}\,(c_j^2 - u^2)}{\dot{m}_f\, Q_f}$$

$$\dot{m}_f = \frac{1}{50}\dot{m}_a = \frac{40}{50} = 0.8\ \text{kg/s}$$

$$\eta_{th} = \frac{0.5 \times 40.8\ (533.4^2 - 266.7^2)}{0.8 \times 43 \times 10^6}$$

$$\eta_{th} = 0.1265 \text{ or } 12.65\% \quad \textbf{Ans.}$$

$$\eta_o = \eta_p \times \eta_{th} = 0.666 \times 0.1265$$

$$\eta_o = 0.0842 \text{ or } 8.42\% \quad \textbf{Ans.}$$

(*f*) $$\text{TSFC} = \dot{m}_f \times 3600/\text{F}$$

$$= 0.8 \times 3600/11094$$

$$= 0.2596\ \text{kg/kN} \quad \textbf{Ans.}$$

Example 12.4. A turbojet engine propels an aircraft at a Mach number of 0.8 in level flight at an altitude of 10 km. The data for the engine is given below:

Stagnation temperature at the turbine inlet = 1200 K,

Stagnation temperature rise through the compressor = 175 K,

Calorific value of the fuel = 43 MJ/kg,

Compressor efficiency = 0.75,

Combustion chamber efficiency = 0.975,

Turbine efficiency = 0.81,

Mechanical efficiency of the power transmission between turbine and compressor = 0.98,

Exhaust nozzle efficiency = 0.97,

Specific impulse = 25 seconds,

Assuming the same properties for air and combustion gases calculate:

(*a*) fuel-air ratio,

(*b*) compressor pressure ratio,

(*c*) turbine pressure ratio,

(*d*) exhaust nozzle pressure ratio, and

(*e*) Mach number of exhaust jet.

Solution. Temperature and velocity of sound at the engine entry at $Z = 10$ km are:

$$T_i = 223.15 \text{ K}, \; a_i = 299.6 \text{ m/s}$$

$$T_{o1} = T_{oi} = \left(1 + \frac{\gamma - 1}{2} M_i^2 \right) T_i$$

$$T_{o1} = \left(1 + \frac{1.4 - 1}{2} \times 0.8^2 \right) 223.15 = 251.71 \text{ K}$$

$$T_{o2} - T_{o1} = 175, \; T_{o2} = 175 + 251.71 = 426.71 \text{ K}$$

(*a*) For the combustion chamber,

$$(\dot{m}_a + \dot{m}_f)\, c_p\, T_{o3} - \dot{m}_a\, c_p\, T_{o2} = \eta_B\, \dot{m}_f\, Q_f$$

$$\left(\frac{1}{f} + 1 \right) T_{o3} - \frac{1}{f} T_{o2} = \eta_B\, Q_f / c_p$$

$$\frac{1}{f}(1200 - 426.71) = \frac{0.975 \times 43 \times 10^6}{1005} - 1200$$

$$f = \frac{\dot{m}_f}{\dot{m}_a} = 0.01908 \quad \textbf{Ans.}$$

(*b*) For the compressor,

$$T_{o2} - T_{o1} = \frac{T_{o1}}{\eta_c} \left\{ \left(\frac{p_{o2}}{p_{o1}} \right)^{(\gamma-1)/\gamma} - 1 \right\}$$

Stagnation pressure ratio across the compressor

$= p_{o2}/p_{o1} = r_{oc}$; therefore,

$$r_{oc} = \left\{ 1 + \eta_c \frac{(T_{o2} - T_{o1})}{T_{o1}} \right\}^{\gamma/(\gamma-1)}$$

$$r_{oc} = \left\{ 1 + \frac{0.75 \times 175}{251.71} \right\}^{3.5} = (1.5214)^{3.5}$$

$$r_{oc} = 4.344 \quad \textbf{Ans.}$$

(*c*) Compressor power required = power supplied by the turbine; therefore.

$$\eta_m (\dot{m}_a + \dot{m}_f)\, c_p\, (T_{o3} - T_{o4}) = \dot{m}_a\, c_p\, (T_{o2} - T_{o1})$$

$$\eta_m (1 + f)\; (T_{o3} - T_{o4}) = T_{o2} - T_{o1}$$

$$T_{o3} - T_{o4} = 175/0.98 \times 1.01908 = 175.228$$

$$T_{o3} \left\{ 1 - \left(\frac{1}{r_{oT}} \right)^{(\gamma-1)/\gamma} \right\} \eta_T = 175.228$$

$$T_{oT} = \left\{ 1 - \frac{175.228}{1200 \times 0.81} \right\}^{\gamma/(\gamma-1)} = 2.005 \quad \textbf{Ans.}$$

(*d*)

$$I_s = \frac{u}{g} \left(\frac{1}{\sigma} - 1 \right)$$

$$u/a_i = M_i$$

$$u = M_i\, a_i = 0.8 \times 299.6 = 239.68 \text{ m/s}$$

$$25 = \frac{239.68}{9.81} \left(\frac{1}{\sigma} - 1 \right)$$

$$\sigma = u/c_e = 0.4942$$

$$c_e = 239.68/0.4942 = 484.93 \text{ m/s}$$

For the exhaust or propelling nozzle,

$$T_{oe} = T_{o4} = T_e + c_e^2/2c_p$$

$$T_{o4} = 1200 - 175.228 = 1024.772 \text{ K}$$

$$T_e = 1024.772 - 484.93^2/2 \times 1005$$

$$T_e = 907.778 \text{ K}$$

$$T_{o4} - T_e = \eta_n (T_{o4} - T_{es}) = \eta_n T_{o4} \left\{ 1 - \left(\frac{1}{r_n} \right) \right\}^{(\gamma-1)/\gamma}$$

$$1024.772 - 907.778 = 0.97 \times 1024.772 \left\{ 1 - \left(\frac{1}{r_n} \right) \right\}^{(\gamma-1)/\gamma}$$

$$r_n = \frac{p_{o4}}{p_e} = 1.55 \quad \textbf{Ans.}$$

(*e*) Velocity of sound at the nozzle exit

$$a_e = (\gamma R T_e)^{1/2} = (1.4 \times 287 \times 907.778)^{1/2} = 603.94 \text{ m/s}$$

The exit Mach number is given by

$$M_e = c_e / a_e = 484.93/603.94$$

$$M_e = 0.803 \quad \textbf{Ans.}$$

The Mach number corresponding to the isentropic flow will be higher than this value. Using isentropic flow tables for $\gamma = 1.4$

$M = 0.816$ at $p_e/p_{o4} = 1/1.55 = 0.645$.

Example 12.5. A ramjet engine operates at $M = 1.5$ at an altitude of 6500 m. The diameter of the inlet diffuser at entry is 50 cm and the stagnation temperature at the nozzle entry is 1600 K. The calorific value of the fuel used is 40 MJ/kg. The properties of the combustion gases are same as those of air ($\gamma = 1.4$, $R = 287$ J/kg K). The velocity of air at the diffuser exit is negligible.

Calculate (*a*) the efficiency of the ideal cycle (*b*) flight speed (*c*) air flow rate (*d*) diffuser pressure ratio (*e*) fuel-air ratio (*f*) nozzle pressure ratio (*g*) nozzle jet Mach number (*h*) propulsive efficiency (*i*) and thrust. Assume the following values: $\eta_D = 0.90$, $\eta_B = 0.98$, $\eta_j = 0.96$, stagnation pressure loss in the combustion chamber = $002 p_{o2}$.

Solution. Refer to Figure 12.24.

At $Z = 6500$ m the properties of air are

$T_1 = 245.90$ K, $p_1 = 0.440$, $a_1 = 314.50$ m/s

$\rho_1 = 0.624$ kg/m^3

(*a*) Ideal cycle efficiency

$$\eta_i = \left(1 + \frac{2}{\gamma - 1} \frac{1}{M_1^2} \right)^{-1}$$

$$\eta_i = \left(1 + \frac{2}{1.4 - 1} \times \frac{1}{1.5^2} \right)^{-1} = 0.310 \quad \textbf{Ans.}$$

(*b*) $$M_1 = \frac{u}{a_1}$$

$$u = 1.5 \times 314.50 = 471.75 \text{ m/s}$$

$$u = 1698.3 \text{ kmph} \quad \textbf{Ans.}$$

(*c*) Area of cross-section of the diffuser inlet

$$A_1 = \frac{\pi}{4} \times 0.5^2 = 0.1963 \text{ m}^2$$

$$\dot{m}_a = \rho_1 u A_1$$

$$\dot{m}_a = 0.624 \times 471.48 \times 0.1963$$

$$\dot{m}_a = 57.752 \text{ kg/s} \quad \textbf{Ans.}$$

(*d*) For negligible velocity at the diffuser exit, $p_{o2} = p_2$,

$$\eta_D = \frac{c_p (T_{2s} - T_1)}{\frac{1}{2} c_1^2} = \frac{(r_D)^{(\gamma-1)/\gamma} - 1}{\frac{\gamma - 1}{2} M_1^2}$$

$$(r_D)^{(\gamma-1)/\gamma} = 1 + \eta_D \frac{\gamma - 1}{2} M_1^2 = 1 + 0.9 \times \frac{1.4 - 1}{2} \times 1.5^2$$

$$r_D = (1.405)^{3.5} = 3.2875 \quad \textbf{Ans.}$$

$$p_2 = p_{o2} = r_D \cdot p_1 = 3.2875 \times 0.440 = 1.446$$

(*e*) $$\frac{T_{o1}}{T_1} = 1 + \frac{\gamma - 1}{2} M_1^2 = 1 + 0.2 \times 1.5^2 = 1.45$$

$$T_{o2} = T_{o1} = 1.45 \times 245.90 = 356.55 \text{ K}$$

$$\dot{m}_a c_p (T_{o3} - T_{o2}) = \eta_B \dot{m}_f Q_f$$

$$f = \frac{\dot{m}_f}{\dot{m}_a} = c_p (T_{o3} - T_{o2}) / \eta_B \cdot Q_f$$

$$f = 1.005 (1600 - 356.55) / 0.98 \times 40000$$

$$f = 0.03188 \quad \textbf{Ans.}$$

(*f*) $$p_{o3} = p_{o2} - 0.02 p_{o2} = 0.98 p_{o2}$$

$$p_{o3} = 0.98 \times 1.446 = 1.417 \text{ bar}$$

Nozzle pressure ratio

$$r_j = \frac{p_{o3}}{p_4} = \frac{1.417}{0.440} = 3.22 \quad \textbf{Ans.}$$

(*g*) The Mach number at the nozzle exit for a pressure ratio of 3.22 in an isentropic expansion would be $M_{4s} = 1.41$; however, on account of irreversible expansion ($\eta_j = 0.96$) the exit velocity and Mach number will be slightly lower.

$$\frac{T_{o4}}{T_{4s}} = 1 + \frac{\gamma - 1}{2} M_{4s}^2 = 1 + 0.2 \times 1.41^2 = 1.3976$$

$$T_{4s} = 1600/1.3976 = 1144.82 \text{ K}$$

$$T_{o4} - T_4 = \eta_j (T_{o4} - T_{4s}) = 0.96\,(1600 - 1144.82)$$

$$T_4 = 1600 - 436.973 = 1163.027 \text{ K}$$

$$T_{o4} = T_4 + c_4^2/2c_p$$

$$c_4^2 = 2c_p (T_{o4} - T_4) = 2 \times 1005 \times 436.973$$

$$c_4 = 937.185 \text{ m/s}$$

$$a_4 = (1.4 \times 287 \times 1163.027)^{1/2} = 683.596 \text{ m/s}$$

$$M_4 = \frac{c_4}{a_4} = \frac{937.185}{683.596} = 1.371 \quad \textbf{Ans.}$$

(*h*) $$\sigma = u/c_4 = 471.48/937.185 = 0.503$$

$$\eta_p = \frac{2\sigma}{1+\sigma} = \frac{2 \times 0.503}{1 + 0.503} = 0.6693 \quad \textbf{Ans.}$$

(*i*) $$\dot{m}_f = 57.752 \times 0.03188 = 1.841 \text{ kg/s}$$

$$\dot{m} = \dot{m}_a + \dot{m}_f = 57.752 + 1.841 = 59.593 \text{ kg/s}$$

$$F = \dot{m} c_4 - \dot{m}_a u$$

$$F = (59.593 \times 937.185 - 57.752 \times 471.75)\, 10^{-3}$$

$$F = 28.614 \text{ kN} \quad \textbf{Ans.}$$

QUESTIONS AND PROBLEMS

12.1 What is jet propulsion? Give two examples of early and modern jet propulsion devices.

12.2 How is forward motion of an aircraft achieved by propeller action? How does the aircraft lift off the ground? Explain with the help of illustrative sketches.

12.3 What are the main components of a gas turbine engine used for turbojet aircrafts? Show the various processes occurring in the engine on a *T-s* diagram.

12.4 What is "after burning" in turbojet engines? Explain briefly with the aid of a diagram.

12.5 What is a by pass engine? What are its main advantages and disadvantages?

12.6 Describe the working of a ramjet engine. Depict the various thermodynamic processes occurring in it on *h-s* diagram. What is the effect of flight Mach number on its efficiency?

12.7 Draw the sketch of a pulse jet engine. Write down its main advantages and disadvantages.

12.8 Describe the working of a scramjet engine. What is its advantage over the ramjet?

12.9 (*a*) Draw a neat sketch of a supersonic diffuser for a ramjet engine with oblique and normal shocks.

(*b*) Depict variation of the static pressure through the diffuser from its entry to exit.

12.10 Derive an expression for the air-standard efficiency of a turbojet engine in terms of the pressure ratio. Depict graphically its variation with the temperature ratio.

12.11 How are efficiencies of the inlet diffuser and the propelling nozzle of a turbojet engine defined? Write down their formulas.

12.12 Derive the following relations for aircraft engines:

(*a*) Combustion chamber efficiency

= ratio of the theoretical to actual fuel – air ratio.

(*b*) Flight to jet speed ratio

$$\sigma = 1 - \frac{F}{\dot{m}_a c_j}$$

(*c*) Thrust in a turbojet engine

$$F = \dot{m}_a (c_j - u) = \dot{m}_a (c_e - u) + (p_e - p_a) A_e$$

(*d*) $\text{TSFC} = \dfrac{\text{fuel-air ratio}}{\text{specific thrust}}$

(*e*) Specific impulse $I_s = \dfrac{u}{g}\left(\dfrac{1}{\sigma} - 1\right)$

State the assumptions used in the derivation of the above expressions.

12.13 Diameter of an aircraft propeller is 4.0 metres. The speed ratio is 0.8 at a flight speed of 450 kmph. If the ambient conditions of air at the flight altitude are $T = 256$ K and $p = 0.54$ bar determine (*a*) propulsive efficiency (*b*) thrust and (*c*) thrust power.

Ans. 0.888, 40.583 kN, 5072.875 kW.

12.14 A turbojet aircraft flies at 875 kmph at an altitude of 10,000 m above mean sea level. Calculate (*a*) air flow rate through the engine (*b*) thrust (*c*) specific thrust (*d*) specific impulse (*e*) thrust power and (*f*) TSFC from the following data:

diameter of the air inlet section = 0.75 m,
diameter of jet pipe at exit = 0.5 m,
velocity of the gases at the exit of the jet pipe = 500 m/s,
pressure at the exit of the jet pipe = 0.30 bar,
air to fuel ratio = 40.

Ans. (*a*) 44.23 kg/s, (*b*) 12.628 kN, (*c*) 278.55 N per (kg/s), (*d*) 28.395*s*, (*e*) 3069.3 kW, (*f*) 0.315 kg/hN.

12.15 A turbojet engine operates at a flight speed of 903.312 kmph and an altitude of 12 km ($T = 216.65$ K, $p = 0.193 \times 10^5$ N/m^2, $\rho = 0.311$ kg/m^3, $a = 295.2$ m/s). The engine has the following data:

Stagnation temperature at the turbine inlet = 1500 K,
temperature drop in the turbine = 200°C
calorific value of the fuel = 43 MJ/kg,
turbine efficiency = 0.91, compressor efficiency = 0.75,
combustion chamber efficiency = 0.96,
exhaust nozzle efficiency = 0.94,
Velocity of gases at the exit of the jet pipe is sonic.

Assume the properties of the combustion gases same as those of air and no stagnation pressure loss in the inlet diffuser. Stagnation pressure at the turbine entry = 0.98 × stagnation pressure at the compressor exit.

Calculate from the above data:

(*a*) flight Mach number,
(*b*) air-fuel ratio,
(*c*) compressor stagnation pressure ratio,
(*d*) turbine stagnation pressure ratio,
(*e*) exhaust nozzle pressure ratio, and
(*f*) the velocity of the exhaust jet.

Ans. (*a*) 0.85 (*b*) 39.246 (*c*) 5.417 (*d*) 1.741 (*e*) 1.974 (*f*) 660 m/s.

12.16 Calculate the air flow rate through the engine, cross-section area of the propelling nozzle exit, thrust, thrust power, propulsive and overall efficiencies for a turbojet engine from the following data:

flight Mach number = 0.85,
flight altitude = 12000 m
cross-sectional area of the inlet-diffuser at entry = 0.5 m^2
air-fuel ratio = 60
conditions at the exit of the exhaust jet:
pressure = 477 mbar, temperature = 1000 K
velocity = 660 m/s
calorific value of the fuel = 43 MJ/kg

Ans. $\dot{m}_a = 38.942$ kg/s, $A_e = 0.3609$ m^2,
$F = 26.608$ kN, $P = 6676.48$ kW
$\eta_p = 0.5507$, $\eta_o = 0.2392$

12.17 A ramjet engine has the following data:

Altitude = 6.5 km, flight Mach number = 4.0, Air fuel ratio = 50, calorific value of the fuel used = 44.18 MJ/kg.

Diffuser inlet diameter = 0.5 m, $\gamma = 1.4$, $R = 287$ kJ/kg K for both air and the products of combustion. Efficiencies of the diffuser, combustor and the nozzle are 0.85, 0.98 and 0.95 respectively.

Determine:

(*a*) ideal cycle efficiency,
(*b*) flight speed,
(*c*) air and fuel consumptions,

(*d*) diffuser pressure ratio,
(*e*) maximum temperature in the engine,
(*f*) nozzle pressure ratio and exit Mach number,
(*g*) thrust and
(*h*) air specific impulse.

Ans. (*a*) 0.762, (*b*) 4526.2 kmph, (*c*) 154.0 kg/s, 3.08 kg/s (*d*) 99.289, (*e*) 1894.4 K, (*f*) 99.289, 3.379, (*g*) 62.022 kN, (*h*) 41.05 s.

13

Rocket Propulsion

It has been observed in the previous chapter that the functioning of the air breathing propulsive devices is dependent on the ambient air; they cannot operate in vacuum. Therefore, their operation and performance depend on the altitude. The thrust of air breathing engines is also dependent on flight speed since the ambient air is admitted at the front of the engine at this speed.

Turbojet and ramjet engines can operate at supersonic speeds, the latter achieving a maximum speed of about Mach 4. For very high speeds in the hypersonic range rockets are employed which carry their own fuel and oxidizer supply; therefore, their operation and performance do not depend on the ambient air and altitude. They can operate in vacuum and achieve any altitude. The thrust of rocket engines is independent of the flight speed.

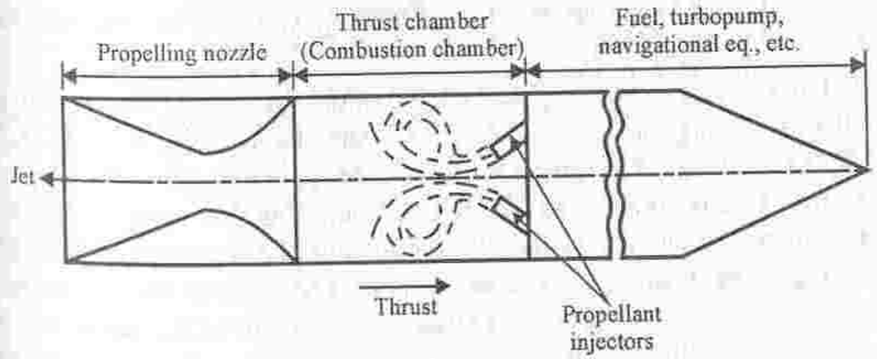

FIGURE 13.1 : A liquid propellant rocket

A rocket engine (Figure 13.1) mainly consists of a container or containers for propellants, combustion chamber (frequently called as a thrust chamber) and a propulsion or exhaust nozzle besides control and navigational equipment, payload etc. The fuel and the oxidizer (known as propellants) are introduced into the thrust chamber for chemical reaction (combustion) at high pressure and temperature. The products of combustion expand through the propelling nozzle to very high velocities. High flow rate of exhaust gases at high velocities gives very high values of thrust; this is due to a large change in the momentum flux as well as the difference between the nozzle exhaust pressure and the ambient pressure.

Both liquid and solid propellants can be used in rocket engines. The larger and long range rockets are generally liquid propellant engines whereas the smaller ones are solid propellant type. In a hybrid type a solid fuel is used with a liquid oxidizer or vice-versa. A monopropellant engine uses only one chemical (propellant) which dissociates after ignition. Conventionally liquid propellant rockets are known as 'engines' whereas the solid propellant type are referred to as 'motors'.

On account of limited quantity of the propellants stored in the rockets the exhaust jet velocities must be very high (of the order of 3000 m/s) for given operation time and targeted altitude. This requires very high pressures and temperatures of gases in the thrust chamber; their maximum values are over 200 bar and 4000K respectively.

13.1 EARLY ROCKET ENGINES

On account of the invention of gun powder or black powder the primitive rockets were operated by solid propellants. Early Greeks and Chinese were using nitre, sulphur and charcoal in their artillery. The use of solid propellant rockets or rocket launchers was only an extension of the well established application of such propellants in guns and cannons.

Historical records suggest that rockets were first developed by Greeks as 'flying fire' in 350 B.C. and later by Chinese in 1232 A.D. Chinese are reported to have used rocket propelled arrows (fire-arrows) in battles against the Mongols. A Chinese, Wan Hu tried to fly in a rocket propelled chair but died in the explosion before taking off. Tatars and Moors are said to have employed rockets against their European enemies during battles in the Thirteenth century. In the later part of the eighteenth century Hyder Ali and his son Tipu Sultan employed rockets in large numbers against the British in the battle of Srirangapatnam (Mysore, India).

Early rockets were mainly used as weapons and signals besides display of fire works on special occasions.

With the rapid and widespread advances in various sciences a renewed interest developed in rocket propulsion in the beginning of the twentieth century. Prominent names of the pioneers in this field are Oberth and Von Braun of Germany, Ziolkousky of Russia, Robert Goddard of Unites States of America and Robert Pelterie of France. World's first liquid propellant rocket engine was designed and built by Robert Goddard in 1926. The fuel and oxidizer used were gasoline and liquid oxygen (LOX) respectively. He developed and perfected the designs of various components of the single and multistage rocket engines; a rocket for 'Rocket or Jet assisted take-off' (JATO) aircraft was developed in 1945.

A great impetus to the rocket technology in various European countries was given by the appearance of the German V-2 missile or rocket during the second world war in 1942; a number of these missiles were showered by Germany on Britain. It was also a liquid propellant rocket which used alcohol as fuel and LOX as oxidizer. Some specifications of this engine designed by Von Braun are given below:

Total weight with propellants		12 tons
Length	15 metres	(46 ft)
Diameter	1.68 metres	(5 ½ ft)
Maximum speed	5600 kmph	(3500 mph)
Maximum altitude	96 km	(60 miles)
Maximum range	320 km	(200 miles)

It carried large quantities of explosives and was regarded as the most dreaded and major weapon in the second world war. After the war a large number of these missiles were captured and taken to Russia and the United States of America for further developments in rocketry in these countries. After the war in 1952 Von Braun tried to employ rockets for launching artificial satellites into the outer space.

Efforts to develop rockets in Russia were first pioneered by Ziolkovsky in 1903; he developed theories for rocket propulsion and space travel.

The post-war developments in the field of rocket propulsion were much faster and substantial compared to the pre-war times. Rockets were developed to launch ramjet engines and models for high speed aerodynamic research and JATO planes; now the attention shifted from weapon applications to space travel. Several different types of multi-

stage rockets were designed, developed and launched in a number of western countries. The first rocket powered aircraft X-15 flew at hypersonic speed in the U.S. Continuous efforts in Russia and the U.S. finally succeeded in the launchings of the Russian satellites 'sputniks' in 1957 and the U.S. satellite explorer in 1958.

Some important events in 'space flights' are given in Appendix A.10.

13.2 TYPES OF ROCKET ENGINES

Rocket engines or simply rockets can be classified in the following manner:

A. On the basis of source of energy employed
A.1 Chemical rockets
A.2 Solar rockets
A.3 Nuclear rockets
A.4 Electrical rockets
B. On the basis of propellants used
B.1 Liquid propellant rockets
B.2 Solid propellant rockets
B.3 Hybrid propellant rockets
C. On the basis of application
C.1 Space rockets
C.2 Military rockets (missiles)
C.3 Weather or Sounding rockets
C.4 Aircraft propulsion, turbo-rocket engines, ramjet-rocket engines,
C.5 Booster rockets
C.6 Sustainer rockets
C.7 Retro rockets
D. On the basis of number of stages
D.1 Single stage rockets
D.2 Multi-stage rockets
E. On the basis of size and range
E.1 Short range small rockets
E.2 Long range large rockets

Some of these rockets are described here. Liquid and solid propellant rockets are again described in detail separately in Sections 13.3 and 13.4.

13.2.1 Liquid Propellant Rockets

Rocket engines in which liquid fuels and oxidizers are used are known as liquid propellant rocket engines; one such engine is shown in Figure 13.1. The propellants are fed into the thrust chamber (combustor or combustion chamber) from their containers for combustion or chemical reaction. For better mixing and efficient combustion the fuel and the oxidizer are atomised through the injectors. The feed system regulates the optimum mixture ratio for a given set of propellants.

Some commonly used liquid fuels are liquid hydrogen, UDMH, hydrazine, alcohol etc. The oxidizers used are liquid oxygen, red fuming nitric acid (RFNA), liquid fluorine, WFNA etc., most of the liquid propellants are toxic and require very high combustion temperatures; this demands special materials and handling system. One of the propellants is circulated through the outer shell of the exhaust nozzle and the inner walls of the thrust chamber before injection for combustion. Besides cooling the high temperature components it also achieves regenerative heating of the propellant giving an increase in the thermal efficiency.

Ignition is achieved electrically or by a pilot flame obtained by burning a small charge in the thrust chamber.

Besides the propellant tanks, thrust chamber and the exhaust nozzle which occupy a large proportion of the rocket space there are several other things that a rocket engine carries such as the propellant pumping and control system, navigational equipment, auxiliary power unit and the payload.

13.2.2 Solid Propellant Rockets

Rockets which use solid fuels and oxidizers (solid propellants) are known as solid propellant rocket engines or motors. Figure 13.2 shows a simple sketch of such a rocket. Solid fuel (plastic or resin material) and oxidizer (nitrates, perchlorates, etc.) are mixed in a single propellant grain and packed into the steel shell or case of the rocket. The method of casting the fuel and the oxidizer mixture in fluid state into the rocket shell is widely employed. A cylindrical star-shaped cavity is provided for combustion in the centre along the axis of the shell. Different shapes of this cavity can be employed to obtain several patterns of the thrust-burning time profiles.

A liner provided between the case and the propellant protects the case from high temperatures developing inside the propellant layers. The igniter located at the top starts the combustion or the chemical

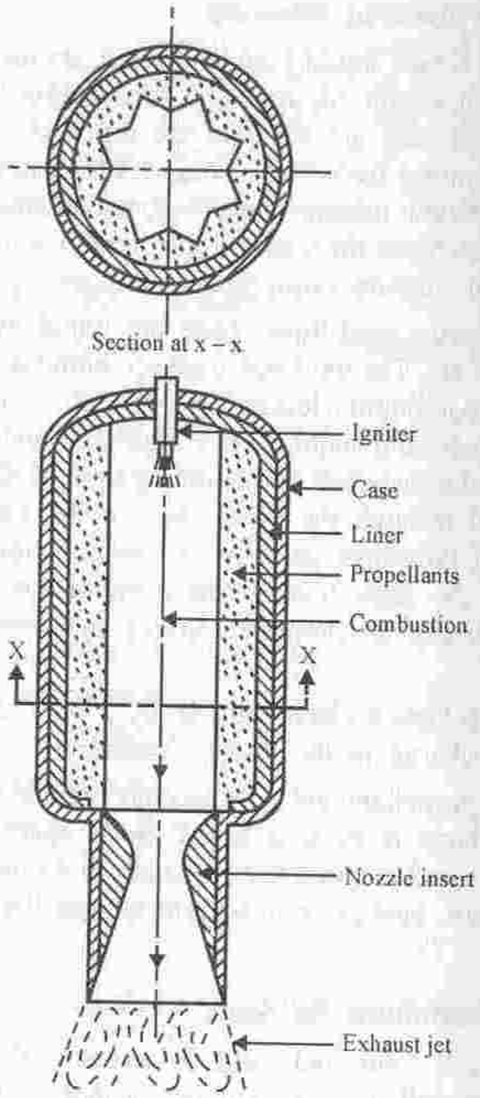

FIGURE 13.2 : A solid propellant rocket

reaction between the fuel and oxidizer. Once the flame front is established combustion is self sustaining. The rate of burning for a given fuel-oxidizer mixture depends on the internal shape of the cast propellant shell besides other factors.

Several solid propellant charges can be designed for different pressures and burning rates. Excessive pressures which are a serious problem in solid propellant rockets can be kept lower by suitably choosing the fuel and oxidizer combinations.

Solid propellant rockets are comparatively simpler and lighter. They are widely used in small sizes; however, recent developments have made it possible to design large size solid propellant rockets also for space vehicles.

13.2.3 Hybrid Propellant Rockets

Hybrid rocket engines employ a combination of liquid and solid propellants; in a large number of experiments and comparatively fewer actual flights of hybrid rockets the fuel is solid and the oxidizer a liquid. This type of rocket combines the advantages of both the liquid and solid propellant rockets.

Figure 13.3 shows the arrangement employed in a hybrid rocket. The liquid oxidizer is injected into the central region of the solid fuel shell where the chemical reaction between the two propellants takes place. For some combinations ignition is not required to start the reac-

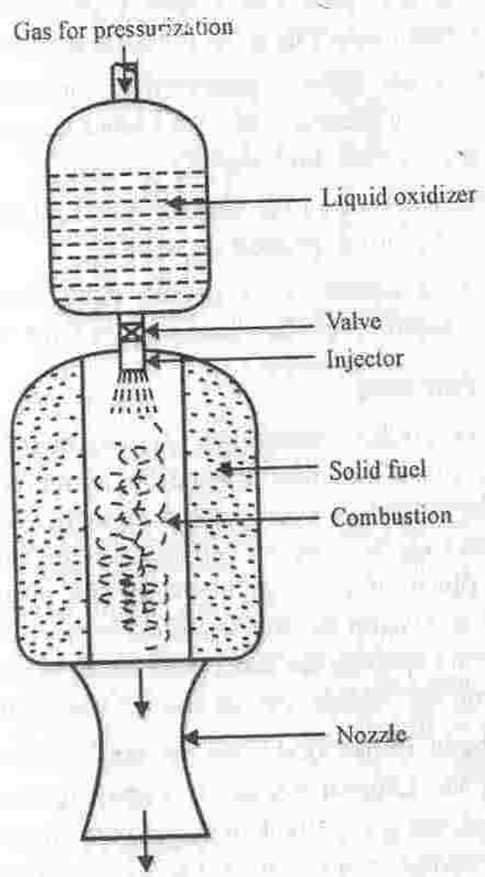

FIGURE 13.3 : A hybrid rocket

tion; merely a contact between the fuel and the oxidizer starts the required reaction. Such propellants are known as hypergolic. Rocket engines with hypergolic propellants are easy to fire, and the reaction can be started and stopped as desired in a given operation.

Some fuel-oxidizer combinations for hybrid propellant rockets are:

Beryllium hydride (Be-H_2)	— Fluorine (F_2)
Lithium hydride (Li H)	— Chlorine Trifluoride (ClF_3)
Lithium hydride (Li H)	— Nitrogen tetroxide (N_2O_4)
Hydrocarbon $(CH_2)_n$	— Nitrogen tetroxide (N_2O_4)

Hybrid rockets would be prefered over other types in view of their simplicity and other advantages some of which are given here:

1. Thrust control is comparatively easier because only the flow of the liquid oxidizer need be regulated.
2. Since the fuel and the oxidizer are kept separate the chemical deterioration that occurs in solid propellant rockets is absent here.
3. Hybrid rockets are lighter compared to the corresponding liquid propellant type on account of less elaborate propellant pumping equipment and higher fuel density.
4. There is greater choice in the selection of fuel grain configuration compared to the solid propellant rockets.
5. In case of an accident or crash the explosion (if any) is less destructive compared to the liquid propellant rocket engines.

13.2.4 Nuclear Rockets

In a nuclear rocket nuclear energy is used to heat the propellant or the working fluid to obtain high stagnation temperature in the thrust chamber. Liquid hydrogen is widely used in such rockets. Figure 13.4 shows a general arrangement employed in a nuclear rocket. A nuclear reactor takes the place of the combustor in the thrust chamber. The reactor with nuclear fission of the uranium fuel consists of the conventional components such as the fuel, moderator, reflector, shield, control rods etc., some of which are shown in the figure.

Liquid hydrogen is pumped from its tank to the reactor through the shell jacketing the exhaust nozzle as shown in the figure. A small portion of the heated gas (propellant) is tapped out for driving the turbine which in turn drives the propellant pump. The turbine exhaust is also expanded in a small nozzle providing a fraction of the total thrust.

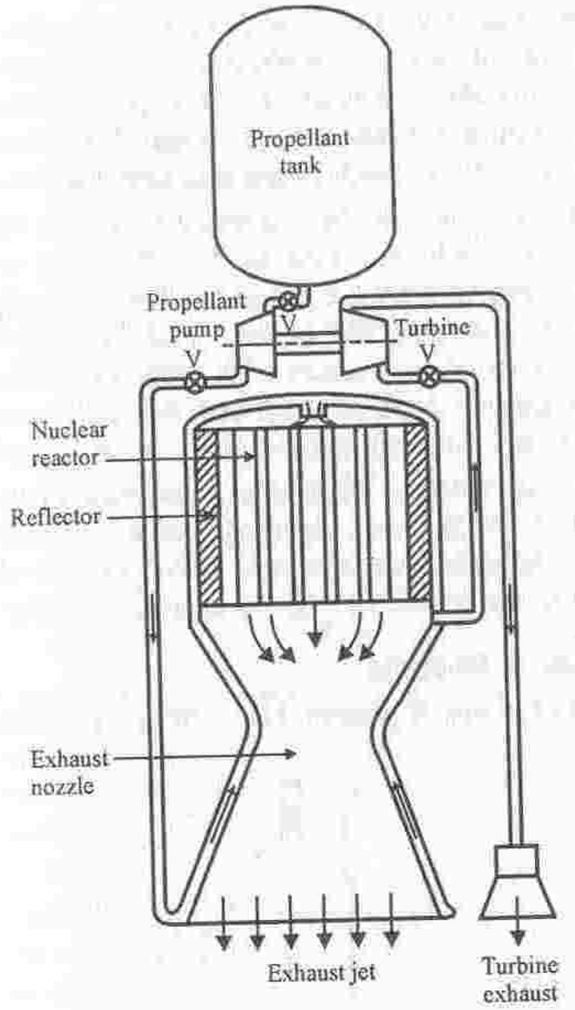

FIGURE 13.4 : Main components of a nuclear rocket engine

A solid-core nuclear fission reactor employing hydrogen as propellant can give a specific impulse of about 1000 seconds at thrust chamber temperature of little over 2000°C.

Nuclear rockets can also employ a Rankine power cycle for generating electricity which in turn can be employed to heat the propellant as described in Section 13.2.6.

13.2.5 Solar Rockets

Heat energy from solar radiation can be used for heating a propellant such as hydrogen. Sun rays are focussed on the heat exchanger by a large parabolic reflector. The propellant is pumped through the heat

exchanger and then expanded in the exhaust nozzle. Since solar energy is very thinly distributed large surface areas are required to capture it. This makes it impractical to build large solar-powered rockets; however, small rockets with low thrust can be designed and built for auxiliary operations in space flights such as attitude control and course correction.

Solar energy can also be converted first into electrical energy through solar cells, which is then used in electrical rockets. Another concept which does not require the expansion of a propellant through the nozzle for propulsion is that of the "solar sail" much like the "sail boats"; here the radiation pressure of the sun rays is employed for obtaining the propulsion force or the thrust. Since there is no propellant such a device will have an infinite value of the specific impulse.

Besides large surface areas solar powered rockets have another severe limitation. Solar energy captured is inversely proportional to the square of the distance from the sun. Therefore, the thrust of solar-powered rocked varies with the distance from the sun.

13.2.6 Electrical Rockets

Rockets in which thrust is produced by employing the electrical energy

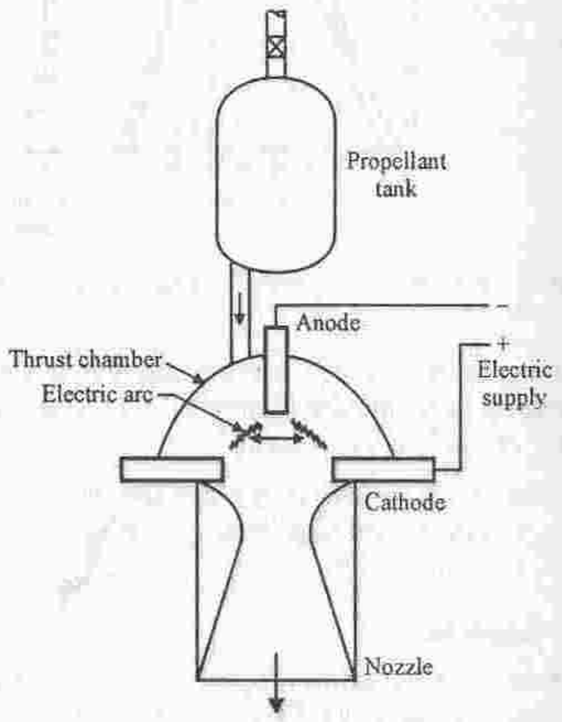

FIGURE 13.5 : Main components of an electric rocket engine (arc-heating type)

are called electrical rockets. In nuclear-electric rocket engines nuclear energy is converted into electrical energy. In the solar-electric type rocket electrical energy is obtained from solar radiation.

Electrical energy is used to generate thrust in the rockets by different methods. In an electro-thermal rocket (Figure 13.5), the propellant is heated by an electric arc struck between the central anode and an annular cathode housed in the thrust chamber. Very high temperatures of the propellant in the thrust chamber can be obtained in this type; this arrangement gives low values of mass ratio with very high specific impulse ($\approx$ 20,000 seconds).

In magnetrohydro dynamic (MHD) rocket propulsion the propellant at very high temperatures is accelerated by a magnetic field.

In an electrostatic or ion propulsion rocket engine the propellant is ionized. The ions are then accelerated by an electric field. Heavy metals such as mercury and cesium are suitable for generating an "ion beam" which gives maximum specific impulse of the order of 20,000 seconds.

13.3 LIQUID PROPELLANT ROCKET ENGINES

The main components of a liquid propellant rocket engine are the fuel and oxidizer tanks, gas pressure or turbopump feed system, the injectors, combustion chamber or the combustor (also known as thrust chamber) and the exhaust nozzle.

In the most widely used bipropellant system two propellants (fuel and oxidizer) are injected into the combustion chamber for the release of the thermochemical energy; this develops high temperature and pressure in the combustion chamber required for expansion of gases to high velocity through the exhaust nozzle. Many combinations of the fuel and oxidizer require ignition while others (called hypergolic) do not. Some chemicals decompose with the generation of heat; such substances can be used as monopropellants in rocket propulsion. However, the choice of choosing a bipropellant combination is very wide compared to the monopropellants.

Both "storable" and cryogenic propellants are used in liquid rocket engines. Storable propellants (fuels and oxidizers) can be stored in the liquid state at normal ambient temperatures whereas cryogenic propellants (at very low temperature) require special arrangements for storage and handling.

Cryogenic propellants are in the gaseous state at normal temperatures and require extremely low temperature to maintain them in the

liquid state; they release much higher heat energy in the thrust chamber and offer better performance compared to the storable type. Some commonly used cryogenic propellants are liquid oxygen, hydrogen, fluorine and ammonia.

13.3.1 Liquid Propellants

The number of liquid propellant combinations that can be employed for a given rocket engine is very large. Only a brief description of some propellants is given in this section. Some of them can be used as monopropellants and others as bipropellants.

Monopropellants

A liquid propellant which contains both the fuel and oxidizer in a single chemical is known as a ''monopropellant''; this is stable at normal ambient conditions and liberates thermo-chemical energy on heating or igniting. A monopropellant should decompose easily and rapidly on injection and ignition into the combustion chamber. The number of chemicals which satisfy the aforementioned properties is small. Hydrogen peroxide (H_2O_2), hydrazine (N_2H_4), nitroglycerine [$C_3H_5(O\,NO_2)_3$], nitromethane (CH_3NO_2) are some of the monopropellants used for rocket propulsion.

Liquid monopropellant rocket engines are considerably simpler compared to the bipropellant engines as they require only one turbopump (or gas pressure) feed system. Such engines are generally small. Monopropellants are more suitable for auxiliary and turbopump power plants in a rocket engine.

Bipropellants

A number of fuel and oxidizer combinations can be found to fit a given application. The main considerations are the properties discussed in the proceeding section and the thermodynamic parameters such as combustion temperature and pressure and the molecular weight of the product of combustion. The number of liquid rocket fuels is much large compared to the liquid oxidizers. For given oxidizer there are a number of fuel options available. Some bipropellant combinations which are widely used in liquid propellant rocket engines are given in Table 13.1: combustion temperatures and the corresponding values of the mixture ratio are also given.

TABLE 13.1: Some liquid fuel and oxidizer combinations

Oxidizer	Fuel	Mixture ratio $\dot{m}_{ox}/\dot{m}_f$	Combustion temperature (Kelvins)
Liquid Oxygen (LOX)	Gasoline	2.5	3294
	Hydrazine	0.92	3400
	UDMH	1.65	3600
	Liquid hydrogen	4.0	2922
	Ethyl alcohol (Ethnol)	1.8	3422
Hydrogen peroxide H_2O_2	Gasoline		
	Ethnol		
	Hydrazine	1.84	2817
	UDMH	4.54	2922
	Organic fuels	—	—
Nitrogen tetroxide N_2O_4	Hydrogen	5.20	2661
	UDMH	2.50	3355
	Hydrazine	1.33	3246
	Ethnol	2.80	3242
Nitric acid (RFNA)	Aniline	3.00	3045
	Gasoline	4.80	
	Hydrazine	1.47	3083
	Alcohol	1.90	3045
	UDMH (50%)	1.73	2997

Properties of some of the oxidizers and fuels are described here briefly.

Oxidizers

(*a*) **Liquid Oxygen (LOX):** This is a cryogenic propellant (Boiling point = 90 K at atmospheric pressure); therefore, it requires proper insulation of containers and feed lines to prevent evaporation. It is non-corrosive but harmful to personnel. It can explode under impact when mixed with oils and organic substances. Liquid oxygen is used with a large number of rocket fuels some of which are mentioned in Table 13.1. Its specific gravity is 1.14, molecular weight 32.0 and vapour pressure 51.7 mbar (at 88.8 K).

(*b*) **Hydrogen Peroxide:** It is a highly reactive liquid requiring special materials and handling system. Besides some catalysts such as manganese dioxide, calcium permanganate and potassium permanganete many impurities in the containers or feed system act as catalysts decomposing it into steam (H_2O) and oxygen in an ex-

othermic reaction. It is therefore often employed as monopropellant also.

Highly concentrated solution of hydrogen peroxide is used in rocket engines; this is harmful to the skin of the personnel and suffers from hazards of fire and explosion. However, it is preferred in many applications due to its higher specific gravity (≈ 1.4).

Its boiling point is 423.5 K, vapour pressure 17.23 mbar (327.78 K) and molecular weight 34.

(*c*) **Nitrogen Tetroxide:** It is a storable propellant (B.P = 294.4 K) used in combination with a number of rocket fuels such as hydrogen, unsymmetrical dimethyl hydrazine etc. Besides being hypergolic with several rocket fuels it also ignites easily with other materials such as wood and paper while its higher specific gravity (≈ 1.44) is an advantage its high vapour pressure (0.958 bar) is a serious disadvantage for the feed system. Its molecular weight is 92.0.

(*d*) **Nitric Acid:** Two important types among a large variety of nitric acids used as oxidizers in rockets are the red fuming nitric acid (RFNA) and white fuming nitric acid (WFNA); they are used with a large number of rocket fuels. Nitric acid is preferred in many applications on account of its high specific gravity (≈ 1.5).

RFNA contains a significant percentage of nitrogen tetroxide; its molecular weight is about 60 and vapour pressure 0.1378 bar at 293.3 K. It is highly reactive, corrosive and poisonous causing storage and handling problems.

Fuels

Some fuels given in Table 13.1 are described here:

(*a*) **Liquid Hydrogen:** This is a cryogenic propellant (B.P. = 20 K). Its low specific gravity (0.07) and extremely low temperatures present several technological problems. It requires larger and well insulated storage tanks. Besides this low temperatures create material and strength problems. Its mixture with air due to leakage can cause explosion. Its vapour pressure is 82.7 mbar (at 13.9 K).

(*b*) **Ethyl alcohol or ethnol:** Ethyl alcohol or ethnol (C_2H_5OH) along with some water is used as a rocket fuel with several oxidizers such as LOX, H_2O_2, N_2O_4 RFNA, etc. It gives lower combustion temperature with slightly lower performance.

Its molecular weight is 46.06 and specific gravity 0.79. Its vapour pressure at 289 K is 58.6 mbar. Ethnol can dissolve a number of lubricants; therefore they are carefully selected for ethnol engines.

(*c*) **Hydrazine:** This is also a storable rocket fuel widely used with several oxidizers. On leakage it forms explosive mixture with air leading to fires and accidents. It is harmful to personnel. Another problem with hydrazine is its higher freezing point (274.7 K); therefore, some chemicals are added to lower this temperature.

Hydrazine is decomposed by employing a catalyst. Therefore, it can also be used as a monopropellant specially in auxiliary or turbopump power units and small rocket engines. A mixture of hydrazine and UDMH is also employed as rocket fuel.

Hydrazine (N_2H_4) has a molecular weight of 32 and specific gravity of about unity. Its vapour pressure is 13.79 mbar at 293.3 K.

(*d*) **Unsymmetrical dimethyl-hydrazine:** This is also known as UDMH. It is a derivative of hydrazine. Its chemical formula is $(CH_3)_2\ NNH_2$ with a molecular weight of 60. As stated before it is used as a 50 : 50 mixture with hydrazine in combination with the oxidizer nitrogen tetroxide or Red fuming nitric acid.

Some important data for UDMH is given in the following:

Specific gravity = 0.66 (at 227.8 K)

Freezing point = 216 K

Boiling point = 336.7 K

Vapour pressure = 1.117 bar (at 338.9 K)

This high value of the vapour pressure can cause cavitation if proper measures in the design of the feed system are not taken.

13.3.2 Properties of Liquid Propellants

Following important properties of the liquid fuels and oxidizers require consideration for their application in rocket engines:

1. Energy released during combustion per unit mass of the propellant combination should be high.
2. High density propellants are preferred; they require smaller tanks and structures offering lower values of the mass ratio and aerodynamic drag.

3. The propellants should have lower freezing point; this makes the handling of propellants, particularly cryogenic propellants easier in various rocket components. Low freezing point rules out any possibility of freezing of the propellants at high altitudes and in cold weather.
4. They must be non-corrosive so that their handling is easier and less demanding on materials used in various parts of the rocket.
5. They should be chemically stable. Their properties should not deteriorate with time. They should not absorb moisture. Small amounts of impurities should not change their chemical properties.
6. Propellants should have low values of vapour pressure and viscosity. Lower vapour pressure avoids cavitation problems in the feed pumping system. Lower viscosity decreases the power required for pumping.
7. Propellants must have higher specific heat and thermal conductivity for better performance.
8. They should not be poisonous and hazardous. Some propellants are poisonous; they are dangerous for personnel if inhaled or touched. Others ignite easily when they come in contact with air. Such propellants may explode if not carefully stored and handled. Handling, transportation and storage should be simple, convenient and safe.
9. Propellants chosen should be cheap and abundantly available. The raw materials required for their large scale manufacture should be easily available. The manufacturing process required for producing propellants should be simple and inexpensive.
10. Products of combustion must have lower values of the molecular weight and gas constant.

13.3.3 Propellant Feed System

Liquid propellants are required to be injected at a pressure slightly above the combustor pressure. Two types of feed systems can be employed; they are (*i*) Gas pressure feed system, and (*ii*) the pump feed system. The former is much simpler and widely used for low thrust and short range operations. The latter is used in large engines.

Gas Pressure Feed System

Figure 13.6 shows a schematic diagram of a liquid propellant rocket employing the ''gas pressure feed system''. An inert gas is separately

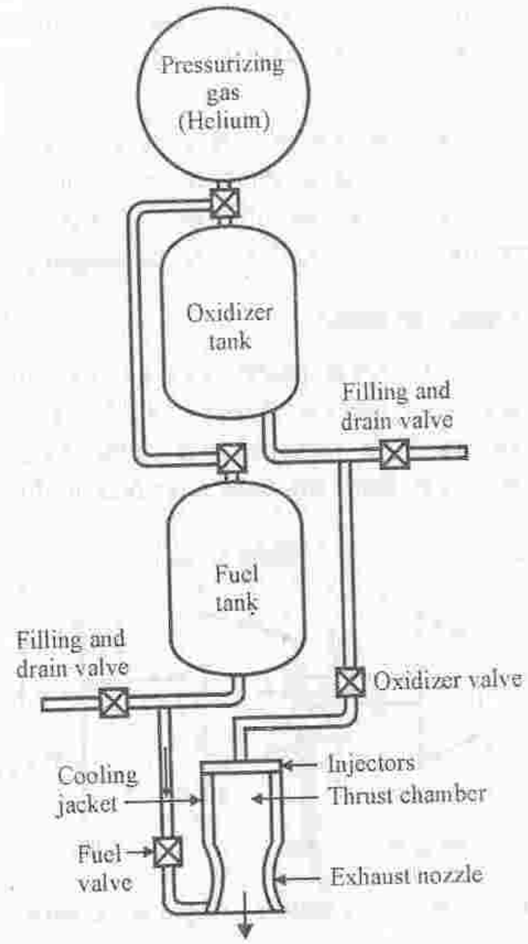

FIGURE 13.6 : Gas pressure feed system for liquid propellant rocket engines

carried at a pressure much higher than the injection pressure; this is used to exert the required pressure in the propellant tanks. The pressurizing gas is chosen on the basis of its chemical properties, density, pressure and the total weight of the gas and the tank. A gas which is ideal for one propellant may be quite unsuitable for another. Nitrogen, Helium and air have been used for pressurization. The propellants under high pressure are forced to flow into the thrust chamber through valves, feed lines and injectors. Several regulating and check valves are used for filling, draining, starting and checking the flow of propellants.

In this method no moving parts such as pumps and turbines are used. Therefore, the system is considerably simpler. However, the pressurization of the propellant tanks requires them to be comparatively

much heavier and introduces a weight penalty besides other problems. Therefore, this system is unsuitable for large rocket engines and long range missions.

Pressure for injection can also be generated within the propellant tank or tanks by introducing a small quantity of a gas which reacts exothermally with the propellant; this produces the high pressure gas required to force the propellant into the combustor.

Turbo-pump Feed System

In the turbopump feed system propellants from the tanks are pumped into the combustor by gas turbine driven centrifugal pumps. The turbine or turbines work on high pressure and temperature gas generated separately or tapped out from the main combustor. Figure 13.7 depicts

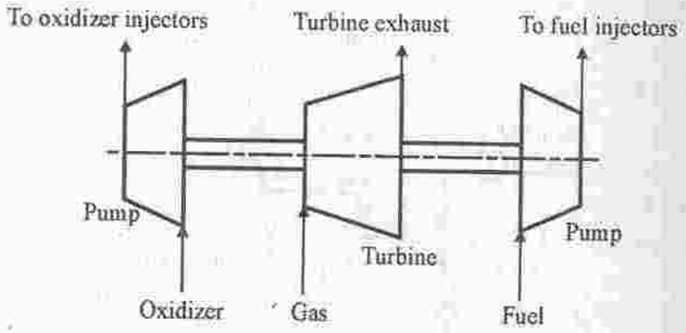

FIGURE 13.7 : Turbo-pump system for liquid propellant rocket engines

a general arrangement of a turbopump system. Here both the fuel and oxidizer pumps are driven by a single turbine. In order to achieve flexibility in choosing the design and operating parameters the fuel and oxidizer pumps can be driven separately by their turbines.

Figure 13.8 depicts a turbopump feed system employing a single turbine driving the fuel and oxidizer pumps through a reduction gear. The turbine operates on a separate gas stream generated from the propellants in an independent gas generator as shown. A pressurizing gas can be used to increase the pressure of the propellants at the pump suctions to avoid cavitation and the resulting instability in pump operation.

Generally turbine speeds are high; therefore, propellant pumps can be driven at optimum speeds through reduction gears with an additional weight penalty. The working gas for the turbine can also be generated at the optimum temperature and pressure. The gas generator also has

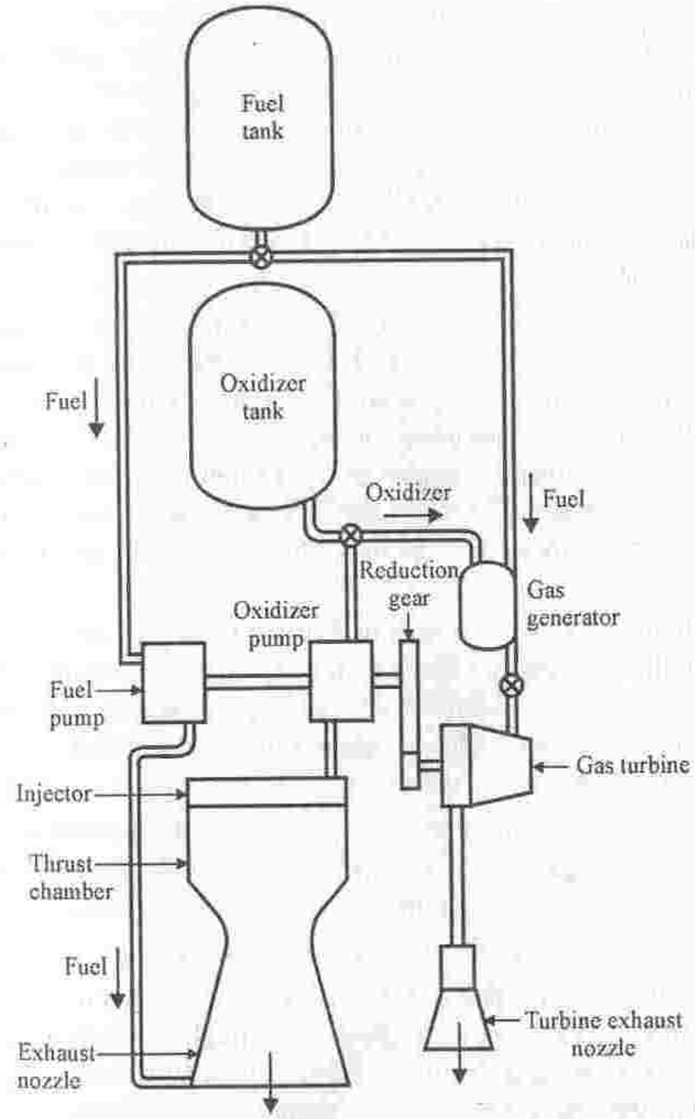

FIGURE 13.8 : Principal components of a turbo-pump feed system

its own injection and ignition systems. The flow of propellants to the gas generator occurs (in the system shown in Figure 13.8) due to the action of the pressurizing gas. If gas pressurization is not employed the propellants can be bled from the delivery lines of the pumps. The propellants flow required for driving the turbine is of the order of 1.5 to 5 per cent of the main flow. The turbine exhaust is also expanded through an exhaust nozzle to provide an additional thrust as shown in the figure.

An auxiliary power unit is also needed in a rocket engine. A single turbine can develop sufficient power to drive the propellant pumps as well as the electric generator. Besides working on high energy gases bled from the main thrust chamber or combustor it can also employ its own combustor with a gas pressure feed system. An alternate method which is comparatively simpler is to generate the working gases by burning solid propellants in a manner similar to the solid propellant rocket (see Section 13.4).

The turbines and pumps for rocket applications are designed to meet some special requirements. There are enormous temperature differences within a turbo-pump unit. The high pressure gas at the turbine inlet is at a high temperature of the order of 1500 K whereas the temperature of some of the cryogenic propellants may be as low as 100 K at the pump inlet. Many propellants are highly reactive. Therefore, the sealing arrangement in propellant pumps should be perfect and resistant to corrosion.

Both positive displacement and turbopumps can be used for delivering propellants from the tanks to the combustion chamber. However, centrifugal pumps are widely used. For a given peripheral speed of the pump impeller it is preferable to employ higher rotational speed in order to restrict the size of the pump.

Several types of turbines can be employed to match given pump requirements. Weight, speed and space considerations are important. For a given value of the rotor peripheral speed u the specific power output is u^2 for a single stage fifty per cent reaction turbine, $2u^2$ for a single stage impulse turbine and $8u^2$ for a two stage velocity compounded impulse turbine. Since the enthalpy drop through the turbine is generally very high the flow rate of the working gas is too small for a full admission turbine. In view of the aforementioned factors a multi-stage impulse turbine with partial admission is often used. Such a turbine has a low efficiency on account of high gas velocities over the blades ($M > 1$) and additional losses due to shock waves and partial admission.

13.3.4 Combustion

Combustion of a liquid propellant (fuel and oxidizer mixture) in the combustor or thrust chamber of a rocket engine requires the following basic processes-injection, atomization, mixing, vapourization, ignition and the exothermic chemical reaction between the fuel and oxidizer. Mixing and chemical reactions may also take place before vapourization.

Complete combustion depends besides other factors, on the oxidizer-fuel ratio ($\dot{m}_{ox}/\dot{m}_f$), combustion temperature and time and space available, degree of atomization and mixing. In contrast to air breathing engines the oxidizer-fuel ratio in liquid propellant rockets is lower than the stoichiometric value to give a fuel rich mixture. The combustion temperatures corresponding to stoichiometric ratios are very high.

The propellants are injected into the thrust chamber through fine orifices for proper atomization. Various methods are employed to atomize and mix the fuel and oxidizer. Figure 13.9 shows some injector

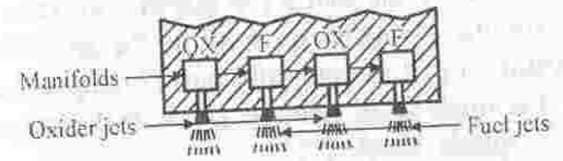

(*a*) Parallel stream type

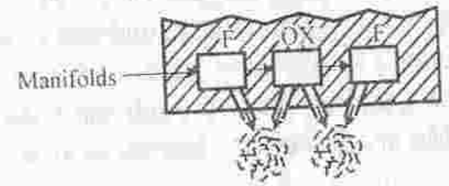

(*b*) Impinging stream type

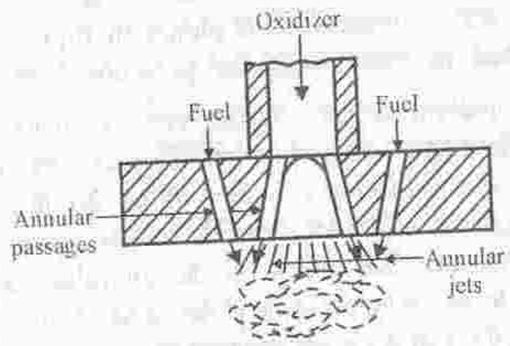

(*c*) Spray injection type

FIGURE 13.9 : Different designs of propellant injectors

designs for liquid propellants. The parallel stream type injector shown in Figure 13.9 (*a*) employs alternate parallel streams of fuel (F) and oxidizer (OX); mixing of the stream occurs due to diffusion and eddies. The fuel and oxidizer manifolds and the jets are shown in the figure.

Figure 13.9 (*b*) shows the configuration employed in an impinging stream type injector. The fuel and oxidizer jets impinge on each other providing thorough mixing. A conical outlet housing the jets is also employed to collect the streams and supply a well mixed propellant charge to the combustor.

In another type annular jets of fuel and oxidizer are directed on each other in a pattern shown in Figure 13.9 (*c*). The operation of the rocket engine starts with the arrival of one of the propellants in the combustor slightly earlier than the other; in order to obtain a low value of the oxidizer-fuel ratio the fuel jet is allowed to enter the combustor first. In the beginning a smaller quantity of the propellants is allowed into the combustor so that the partially burnt charge on account of low temperature and ignition delay remains small. If the mass of this charge is large it can explode suddenly.

The temperature and pressure in the combustor increase rapidly after firing; this also increases the gas flow rate through the exhaust nozzle to its steady state value. The equilibrium combustion pressure and temperature depend on the flow rates of the propellants, the combustion rate and the gas flow rate through the exhaust nozzle. During the steady state stable operation the aforementioned flow rates are identical.

The propellant flow rate through the injector depends on the pressure drop across it, besides its orifice size and geometry. A typical characteristic curve for an injector is depicted in Figure 13.10. It is seen that the flow rate increases with the pressure drop.

Liquid propellant rocket engines very often experience pressure fluctuations in the combustion chamber. This excites vibrations of varying frequencies and amplitudes in the engine structure. The propellant flow rate through the injectors depends on the combustor pressure. If the combustor pressure falls below the design value the propellant flow rate increases. On account of some delay period in the combustion of the excess propellant and its sudden combustion subsequently there is an instantaneous pressure rise in the combustor above the design value; this decreases the propellant flow rate corresponding to the reduced pressure drop across the injectors. These events decrease the propellant combustion rate, again resulting into a low combustion pressure thus starting the next cycle. Several types of vibrations occur on account of combustor pressure fluctuations. Range of frequencies of such vibrations is very wide, and lies between 50 and 10,000 c/s.

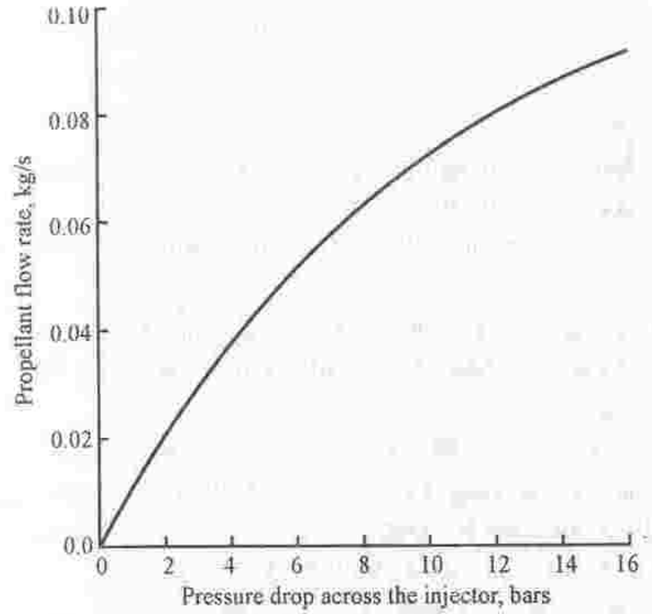

FIGURE 13.10 : Variation of propellant flow rate with pressure drop across the injector for a given orifice size and geometry

Except hypergolic propellants all the propellant combinations require an ignition system for starting the reaction or combustion in the thrust chamber. The ignition system employed depends on the propellants used; this should be reliable and start combustion with minimum loss of unreacted or unburnt propellants. Any delay in combustion leads to the accumulation of the unburnt mixture in the thrust chamber. If the delay period is long the accumulated mixture explodes suddenly with a possibility of an accident.

A convenient method of ignition is to use a hypergolic fluid for a short time which starts combustion after coming into contact with one of the propellants (fuel or oxidizer) which is injected first in the combustor.

Ignition by spark plug is also employed in rocket combustion chambers. This requires an ignitable mixture of propellant vapours.

In pyrotechnic ignition a small mass of solid propellant is ignited electrically. The solid propellant pellet is introduced at a convenient location in the combustor.

13.3.5 Advantages and Disadvantages

For many applications liquid propellant rocket engines have some ad-

vantages over other types. Some of the important ones are briefly described here.

Advantages

1. Liquid propellant engines can be reused after recovery. This offers considerably economic benefits.
2. They offer more flexible and greater control over the thrust. The operation is more stable.
3. The propellants are not stored in the thrust chamber. Therefore, aerodynamically and structurally better and safer thrust chambers can be designed.
4. Higher values of specific impulse are obtained.
5. Wreckage on account of some defect or malfunctioning is not sudden allowing time for corrective and rescue measures. This offers greater degree of safety to the crew.
6. It is much easier to stop the operation in case of an impending catastrophe.
7. Regenerative heating of the propellant before combustion along with the cooling of the nozzle and thrust chamber is possible. This offers thermodynamic and structural advantages.
8. It is much easier to run an auxiliary power plant.
9. Liquid propellant rockets are more economical for long range space and military operations.

Disadvantages

1. Liquid propellant rockets are more complicated compared to solid propellant rockets. There is greater probability of problems arising on account of malfunctioning of the turbo-pump system, valves, leakage, vibrations etc.
2. Many liquid propellants are cryogenic which require special arrangements for heat insulation, solar radiation shields and handling at low temperatures.
3. There are additional handling and safety problems if the propellants are poisonous and corrosive.
4. They require propellant feed pumping system or tank pressurization increasing the total weight of the rocket.
5. On account of lower density of the liquid propellants compared to solid propellants large storage space is required increasing the size and weight of the structures.

6. It takes much longer to design, manufacture and test liquid propellant rockets. They cannot be mass produced in a short time for military applications.

13.4 SOLID PROPELLANT ROCKET MOTORS

As stated earlier the solid propellant rockets are much older compared to the other types. Therefore, large variety of fuels and oxidizers have been developed since their use in ancient times. It will be observed in the following sections that the fuel and oxidizer system and the pattern of combustion (chemical reactions) in solid propellant rockets are quite different from those in liquid propellant rockets; this has its own advantages and disadvantages.

Till recently solid propellant rockets were generally looked upon as small engines or motors meant for short duration and small operations. However, recent developments in solid propellants and design of rockets have made it possible to develop large and long range solid propellant rocket motors both for military and space applications. A cluster of several solid propellant rocket motors has been employed in the first or booster stage of a number of large multi-stage rockets for space flights. Comparatively smaller rocket motors have been used for JATO aircrafts and missiles; they have also been employed in the upper stages for propulsion of space vehicle.

13.4.1 Solid Propellants

Two types of solid propellants (fuels and oxidizers) which are widely used are:

(*a*) heterogeneous or composite propellants and

(*b*) homogeneous mixtures of organic substances.

Composite solid propellants generally employ nitrates and perchlorates (NH_4NO_3, KNO_3, $KClO_4$, NH_4ClO_4) as oxidizers with comparatively smaller ($\simeq$ 25 per cent) quantities of fuels such as polymers, plastics and PVC (polyvinyl chloride) and some metals. Besides fuels and oxidizers other materials such as additives and inhibitors are also added to the propellants mixture. The burning rate and the processes for fabricating the propellant grain are influenced by the additives. Some substances act as binders and catalysts; others stabilize the chemical reactions in the propellants.

Inhibitors or restrictors are also used to regulate or prevent burning of the propellant grain or some sections of its surface.

Some metals, such as Aluminium and Beryllium when used with other propellants increase the combustion temperature giving higher values of the specific impulse. Besides this their addition increases the grain density; this decreases the volume required for a given value of the total impulse. High energy composite propellants can also be obtained by the addition of some metallic hydrides.

Other group of solid propellants widely used in rockets are the double-base type which are homogeneous mixtures of organic substances such as nitroglycerine (NG) and nitrocellulose (NC) and some stabilizers; they combine the properties of fuels as well as oxidizers. This mixture can be shaped into solid propellant grain either by casting or extrusion.

Nitroglycerine (NG) or glycerol trinitrate is an organic nitrate $[C_3H_5(ONO_2)_3]$ which is a colourless liquid. This is produced by the nitration of glycerine by a mixture of nitric and sulphuric acids. It can easily explode with shock; however, it is less dangerous when mixed with materials such as charcoal and sawdust.

Nitrocellulose (NC) or cellulose nitrate $[C_6H_7O_2(ONO_2)_3]$ is also an unstable organic compound which looks like cotton. It can be obtained by the nitration of wood or cotton. Gun cotton is also a from of cellulose nitrate.

The molecules of both NG and NC contain sufficient oxygen required for combustion and have properties of both fuels and oxidizers. After ignition chemical energy is released by the combustion of carbon and hydrogen in the propellants to carbon dioxide and steam respectively; other gases present in the exhaust are nitrogen, carbon monoxide and the hydroxyl group (OH).

13.4.2 Properties of Solid Propellants

Some of the important properties of solid propellants desired are briefly described here:

1. It should be possible to produce propellants from abundantly available raw materials which are cheap and safe to handle.
2. It should be easily possible and safe to grind, mix, heat, trim, pack and store the propellants. It should also be practicable to cast or extrude the solid propellants in desired shapes and sizes.
3. Physical and chemical properties should not change considerably during processing.

4. Chemical reaction between the fuel and oxidizer must release large amount of heat energy giving higher values of combustion temperature and specific impulse.
5. The useful properties of the propellants should not deteriorate with time. They should be chemically inert before ignition and not ignite with slight impact, shock or pressure.
6. The propellant grain must have high mechanical strength.
7. They must have comparatively lower molecular weight and higher density which yield higher values of specific impulse and need lighter structures.
8. The products of combustion or exhaust gases should be smokeless and colourless. This makes detection difficult in military operations.
9. The fuel-oxidizer mixture should not experience any chemical reaction (slow or brisk) with the atmospheric air and moisture; it should not be hygroscopic.
10. There should be no possibility of any slow undetected chemical reaction between the various constituents of the propellant and with the metallic liner or the case before ignition.

13.4.3 Combustion

The hardware and methods employed for the combustion of solid propellants in the thrust chamber of a rocket are quite different from those of the liquid propellants. Well-mixed fuel and oxidizer (known as propellant grain) are already present in the thrust chamber; they do not need injection and mixing during the combustion. Regenerative heating of the propellant and cooling of the thrust chamber and the nozzle walls are not practicable.

The burning rate of the propellant grain depends on the initial temperature of the grain before combustion, equilibrium combustion pressure, and the ratio of grain surface area and the exhaust nozzle throat area. The cross-sectional areas in rocket thrust chambers are generally large. Therefore, the flow of combustion gases upstream of the exhaust nozzle is at low Mach numbers and the equilibrium combustion pressure can be assumed to be identical with the stagnation pressure.

Linear Burning Rate

A solid propellant grain burns at its exposed surface (area = A_c). As a result of the combustion the grain surface recedes in the direction

perpendicular to itself. The rate at which it recedes is known as the "linear burning rate" (r) expressed in millimeters or centimeters per second. Linear burning rate mainly depends on the combustion pressure (p_c) and the propellant grain temperature (T_p) before combustion; the velocity of combustion gases and the elapsed time can be assumed to have only slight effect. The linear burning rate is given by the following empirical formula:

$$r = K_1 p_c^{n1} \tag{13.1}$$

The coefficient K_1 and the exponent n_1 depend on the chemical composition and the pressure range; the value of the exponent n_1 is approximately between 0.2 and 0.8. The coefficient K_1 also depends on the propellant grain temperature, T_p. Burning rate is found to be higher for higher initial temperatures of the propellant. However, initial temperature of the propellant grain has other important effects. At some temperatures the grain becomes weak or develops cracks; at other values it may become soft, or deformed or even flow blocking the nozzle passage. Cracks and deformations change the burning surface area which changes the burning and propellant consumption rates causing fluctuations in the pressure p_c.

The propellant consumption rate is given by:

$$\dot{m}_c = \rho r A_c \tag{13.2}$$

$$\dot{m}_c = K_1 \rho A_c p_c^{n1} \tag{13.3}$$

Obviously this is not the same as propellant flow rate ($\dot{m}_p$) through the exhuast nozzle because a part of it is contained in the free space of the combustion chamber which is continuously increasing. Therefore,

$$\dot{m}_p = \dot{m}_c - \frac{d}{dt}(\rho V) \tag{13.4}$$

Combustion Pressure

The pressure p_c at which combustion of the propellant grain takes place increases rapidly after firing until the propellant consumption rate ($\dot{m}_c$) and flow rate ($\dot{m}_p$) through the exhaust nozzle satisfy Equation (13.4); after this p_c remains constant. This constant value of pressure is known as the "equilibrium combustion pressure". This remains constant during burning for perfectly homogeneous propellant grain and constant burning surface area. Reference to combustion pressure in the

text generally implies its equilibrium value; changes in pressure p_c cause variations in other parameters. If these changes occur intermittently vibrations of the propellant grain and the structures may assume serious proportions. Fluctuations in the combustion pressure lead to corresponding fluctuations in the propellant flow rate and the thrust.

A solid propellant grain requires a certain minimum value of the combustion pressure for stable combustion. Combustion is not satisfactory below this minimum value; this minimum value of the pressure is known as the "combustion limit" which depends on the type of the propellant employed. The value of this limiting pressure lies approximately between 5 and 55 bar. It is observed from Equation (13.1) that the burning rate increases with the combustion pressure. At very high pressures burning rate increases spontaneously with slight increase in pressure; the corresponding propellant consumption rate is also very high which in turn again leads to an abrupt increase in pressure. This may cause explosion. Thus it is necessary to limit the maximum value of the combustion pressure.

The aforementioned lower and upper limits of combustion pressure for a given propellant help in choosing a safe operating range in view of stable combustion and structural strength.

Propellant Area Ratio

The ratio of the surface area available for burning of a propellant grain and the throat area of the exhaust nozzle is known as the propellant area ratio.

$$K_p = \frac{A_c}{A^*} \tag{13.5}$$

The relation between the area ratio and the equilibrium combustion pressure is given by the following empirical expression:

$$K_p = K_2 p_c^{n2} \tag{13.6}$$

The coefficient K_2 is a function of the propellant grain temperature before burning. The index n_2 is constant. For some propellants it can be shown that the combustion pressure varies approximately with the fourth power of the propellant area ratio:

$$p_c \propto K_p^4 \tag{13.7}$$

This shows that the combustion pressure is very sensitive to even small changes in the area ratio K_p. Any increase in K_p due to cracks

in the propellant grain or damage to the inhibitor material can increase combustion pressure and the burning rate abruptly leading to explosion.

Figure 13.11 depicts graphically the variation of the burning rate and the propellant area ratio with the equilibrium combustion pressure.

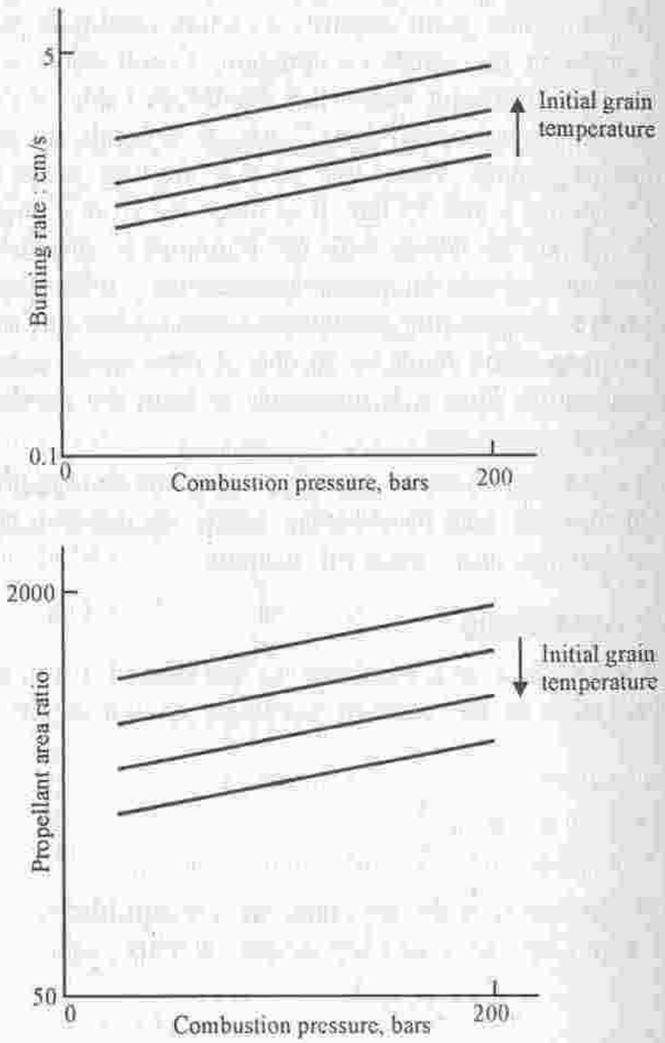

FIGURE 13.11 : Variation of area ratio and burning rate with combustion pressure in solid propellant rockets

As stated before both r and K_p increase with the combustion pressure at the given propellant grain temperature before burning. For a given combustion pressure the burning rate is higher for higher grain temperature and the corresponding area ratio required is lesser.

Figure 13.12 depicts typical thrust-time profiles for regressive, neutral and progressive burning of the solid prepellant grain. For given

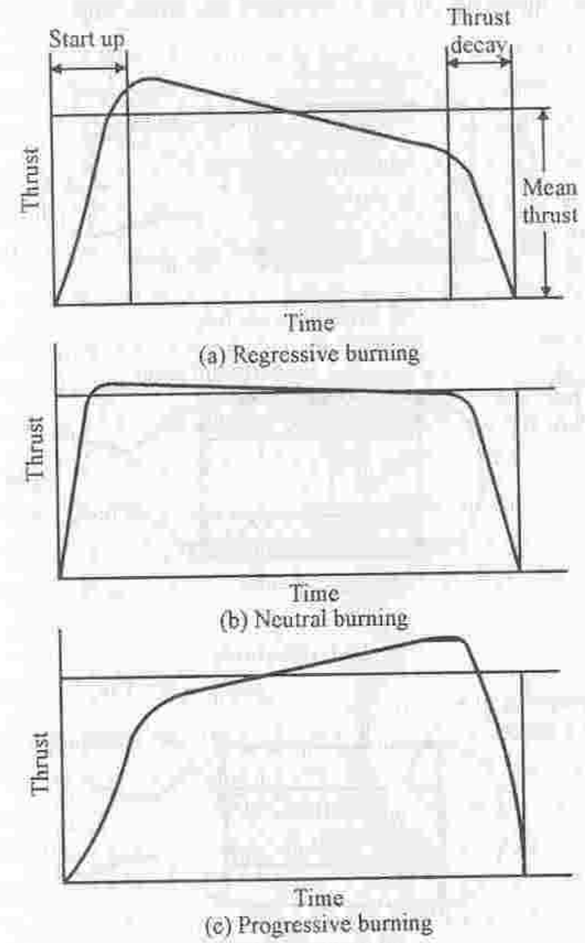

FIGURE 13.12 : Typical thrust-time curves for solid propellant rockets

values of the grain temperature and the combustion pressure burning rate and the propellant flow rate through the exhaust nozzle depend on the propellant area ratio. Therefore, a regressive burning is obtained when the area ratio decreases with time; this can be obtained by employing a suitable geometrical configuration of the propellant grain.

If the burning surface is kept constant during rocket operation an approximately constant thrust profile can be obtained through neutral burning.

If the grain configuration employed is such that its burning surface increases with time a progressive burning profile is obtained.

13.4.4 Restricted Burning

Several grain configurations (shown in Figure 13.13) are employed to obtain restricted burning of the solid fuel-oxidizer mixture at the desired

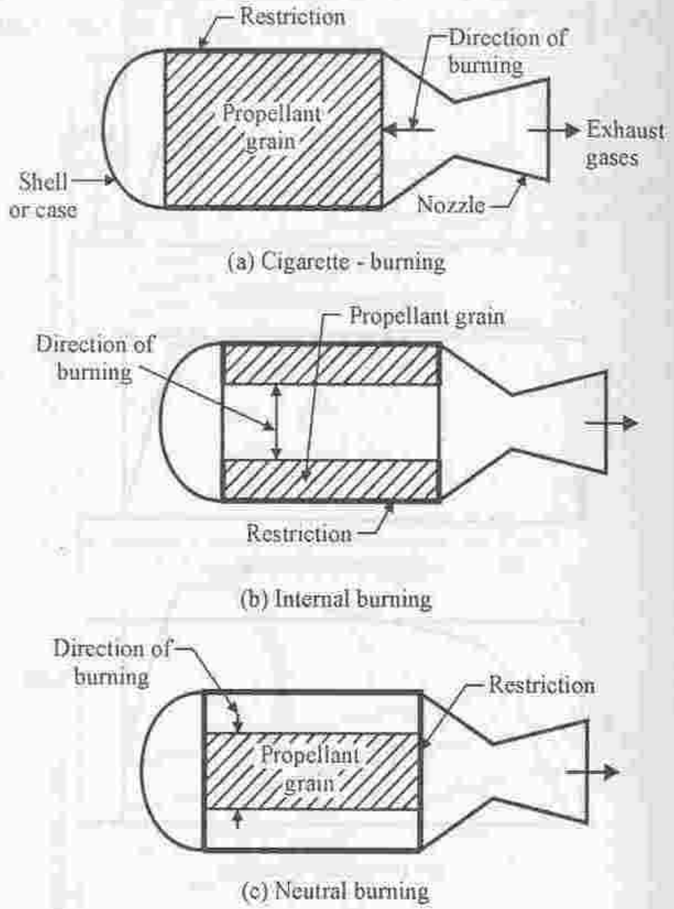

FIGURE 13.13 : Solid propellant grain configurations for restricted burning

rate. The inhibiting material or restrictions prevent the propellant grain from burning in all directions. Very often the restrictions assume the form of a liner between the propellant grain and the thrust chamber case or shell. The inhibiting material should not start burning along with the grain or before.

An older practice employs "cigarette burning" pattern as shown in Figure 13.13 (*a*); here the grain is ignited at one end upstream of the nozzle from where the combustion starts and proceeds in the direction shown. The burning surface progressively recedes leftward. In this pattern of burning the entire thrust chamber is heated to a high temperature throughout the operation. This causes high temperature material and strength problems. Since the burning surface area remains constant a constant thrust profile is obtained.

An improvement over this method is the internal burning pattern shown in Figure 13.13 (*b*). Combustion of the propellant takes place on the surface of the internal passage (of star shape cross-section as shown in Figure 13.2) or perforations provided along the whole length of the propellant grain. Different geometrical shapes of the internal passages offer different surface areas or propellant area ratio (A_c/A^*) values. Thus several thrust-time profiles can be obtained.

A propellant grain with the configuration of a cross in the middle of the annular void space is shown in Figure 13.13 (*c*). Here the burning takes place only at the cylindrical surface of the grain. The gas pressure is same all around the grain. This can also give neutral burning.

In restricted burning rockets, particularly in cigarette burning pattern a larger quantity of propellants can be packed into a given volume of the combustion chamber. This offers better utilization of the available space.

13.4.5 Unrestricted burning

If the propellant grain surface is not restricted from burning and all surfaces except those with supports are exposed to the flame or hot gases the mode of combustion is known as "unrestricted burning". This requires perforations and hollow spaces running along the length of the propellant grain as shown in Figure 13.14. This arrangement requires larger volume of empty spaces to permit the flow of combustion gases and provision of supports. Therefore, the quantity of propellant that can be packed into a given volume of the combustion chamber is considerably reduced; however, large values of the propellant burning surface area can be obtained by employing a number of grain configurations.

Figure 13.14 (*a*) shows a tubular grain shape; the hollow cylindrical grain is supported within the shell on three or more sufficiently strong webs. During combustion the outer cylindrical surface area of the grain decreases while the area of the inner surface increases. Neutral burning can be obtained if the overall area of the burning surfaces remains constant.

Figure 13.14 (*b*) shows a multiple hole grain. Burning takes place at both the outer and inner surfaces of the grain. In this configuration also burning surface area can be kept constant to obtain constant thrust.

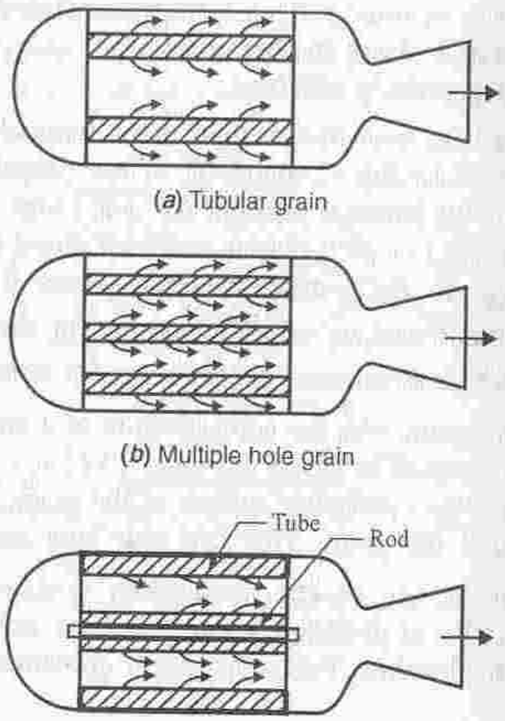

(*a*) Tubular grain

(*b*) Multiple hole grain

(*c*) Rod and tube type grain

FIGURE 13.14 : Solid propellant grain configurations for unrestricted burning

The aforementioned configurations suffer from a serious problem of differential combustion pressure. The combustion pressure and hence the burning rate on the outer and inner surfaces are different. If the pressure difference is large the grain may crack or break. In order to avoid this the pressure on different surfaces is equalised by providing holes through the grain thickness.

The rod and tube type grain shown in Figure 13.14 (*c*) evercomes this problem. Burning takes place at the inner surface of the tube and outer surface of the rod. The combustion pressure in the annular space is same. Thus the burning rate is same. Since the surface area of the tube increases and that of the rod decreases during burning any desired thrust profile is obtained by choosing different sizes and the propellants for the tube and the rod.

13.4.6 Advantages and Disadvantages

Some of the important advantages and disadvantages of the solid propellant rockets are given in the following:

Advantages

1. Solid propellant rockets are simple in design and construction. Therefore, a large number of small size rockets for military use can be mass produced at short notice.
2. They do not require feed system. Therefore, they are free from the problems of moving parts such as pumps, turbines, valves, etc.
3. They are comparatively lighter for short range and small size.
4. On account of high density much larger quantity of propellants can be packed into a small space. The specific gravity of solid propellant grains ranges from approximately 1.5 to 2.0.
5. Solid propellant rockets have much fewer and less frequent servicing problems.
6. Problems arising from the sudden emptying of propellant tanks are absent.
7. Vibration problems originating from turbo-pump and liquid flow system are absent.

Disadvantages

1. In case of emergency it is difficult or almost impossible to turn off the operation midway.
2. Minor malfunctioning or accident generally leads to wreckage or abondoning the mission.
3. It is comparatively more difficult to control combustion and regulate thrust.
4. Solid propellant rockets have comparatively lower values of the specific impulse.
5. At the end of an operation the burnt up debries cannot be reused; this renders large operations uneconomical.
6. Nozzle cooling is not possible.
7. Long range large size solid propellant rockets are comparatively heavier.
8. Transportation and handling of these rockets before firing require greater care because of the presence of propellants throughout.
9. Refuelling in long duration mission is not possible.
10. On account of the presence of solid particles in the high temperature and high speed gases exhaust nozzle suffers erosion.

13.5 ROCKET PROPULSION THEORY

Some of the main and basic parameters in rocket propulsion are the thrust (F), specific impulse (I_s), specific propellant consumption (SPC) and the exhaust gas velocity (c_e) or the 'effective exhaust velocity' (c_j). Pressure ratio across the nozzle and its area ratio obviously effect the above quantities.

In energy conversion systems efficiencies are also important. The efficiencies that are considered here are the propulsive efficiency (η_p), thermal efficiency (η_{th}) and the overall efficiency (η_o).

High pressure and temperature gases are produced in the combustion or thrust chambers as a result of the chemical reaction between the fuel and the oxidizer. Since the combustion pressure is very high and the ambient pressure low gases are expanded through a convergent-divergent nozzle; the adiabatic or isentropic flow through the nozzle are governed by the relations derived in chapters two and four.

The exhaust gases in the jet are produced by the propellants *i.e.*, the fuel and the oxidizer; therefore, the mass rate of flow of gases is equal to the rate of flow of the propellants.

$$\dot{m}_p = \dot{m}_f + \dot{m}_{ox} \tag{13.8}$$

$$\dot{m}_p = \frac{\dot{w}_p}{g} = \dot{m}_f \left(1 + \frac{\dot{m}_{ox}}{\dot{m}_f}\right) \tag{13.9}$$

The total weight of the propellants required for the duration of powered flight of the operation time (t_p) is given by

$$W_p = \int_o^{t_p} \dot{w}_p \, dt \tag{13.10}$$

On account of the choking conditions at the throat of the convergent-divergent nozzle the propellant flow rate is maximum.

13.5.1 Thrust

The force that propels the rocket at a given velocity is known as the thrust; this is produced due to the change in the momentum flux of the outgoing gases as well as the difference between the nozzle exit pressure and the ambient pressure. In contrast to the airbreathing engines (Section 12.3.3) here a comparatively small quantity of gases or matter carried within the engine is ejected at very high velocity.

Rocket thrust is employed to overcome the drag and gravitational forces besides providing the acceleration.

Figure 13.15 shows a control surface enclosing the rocket. Unlike the airbreathing engines since there is no inflow of air into the rocket

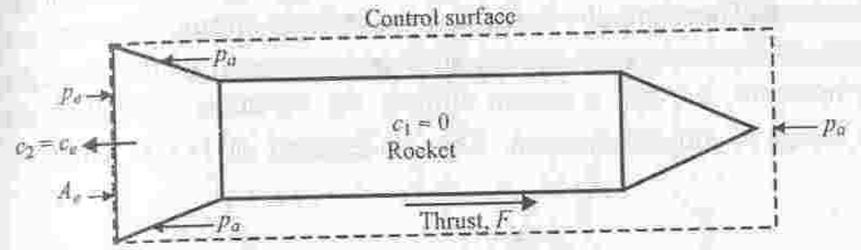

FIGURE 13.15 : Development of thrust in a rocket

engine the initial velocity of the gases before expansion in the nozzle is almost zero ($c_1 \simeq 0$). The final velocity at the end of adiabatic expansion through the nozzle is $c_2 = c_e$. Therefore, for one-dimensional steady flow at the nozzle exit the rate of change of momentum flux is

$$F_{mom} = \int_{A_e} \rho_e c_e^2 \, dA = \rho_e c_e^2 A_e \tag{13.11}$$

Continuity equation at the nozzle exit gives

$$\dot{m}_p = \rho_e c_e A_e \tag{13.12}$$

Therefore, $F_{mom} = \dot{m}_p c_e$ (13.13)

The pressure acting on the entire rocket surface is equal to the ambient pressure p_a. If the expansion through the nozzle is not complete, $p_e \neq p_a$. Therefore, the pressure force acting on the rocket in the direction of motion is given by

$$F_{pr} = p_e A_e - p_a A_e$$

$$F_{pr} = (p_e - p_a) A_e \tag{13.14}$$

Equations (13.13) and (13.14) in Equation (12.41) give the value of the net thrust.

$$F = F_{mom} + F_{pr}$$

$$F = \dot{m}_p c_e + (p_e - p_a) A_e \tag{13.15}$$

The method of analysis in Section 12.3.3 applied to a rocket will give the same result as in Equation (13.15). However, it should be noted here that the flight speed term 'u' is absent in Equation (13.15); therefore, the thrust is independent of the flight speed.

For a given design of the nozzle the value of the exit pressure p_e is fixed. Therefore, the thrust during the flight through the atmosphere continuously increases with the altitude on account of the decrease in p_a; however, beyond a certain altitude the variation is negligible and the thrust is almost constant. This is depicted in Figure 13.16.

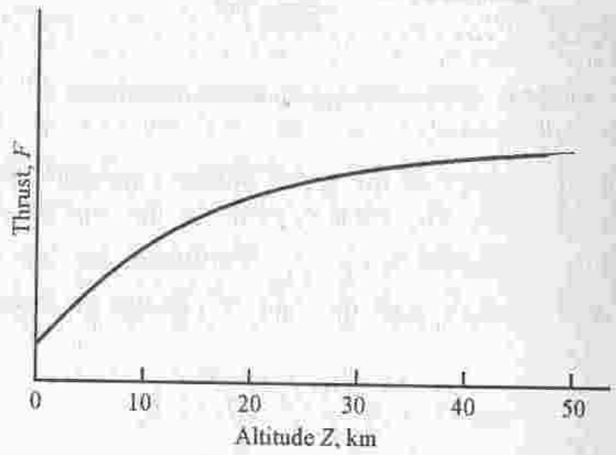

FIGURE 13.16 : Variation of thrust with altitude

If $p_a > p_e$ the pressure thrust is negative decreasing the net thrust which is not desirable.

In view of the aforementioned problem it is convenient to employ a hypothetical or reference jet velocity known as the "effective jet velocity", c_j; this is the velocity of the jet when the gases through the nozzle expand to the ambient pressure. Then the value of the thrust in Equation (13.15) can be written as

$$F = \dot{m}_p c_j = \dot{m}_p c_e + (p_e - p_a) A_e \qquad (13.16\ (a))$$

$$F = \frac{\dot{w}_p}{g} c_j \qquad (13.16\ (b))$$

13.5.2 Specific Impulse

Specific impulse of a rocket engine is the thrust per unit weight flow rate of the propellant. This is given by

$$I_s = \frac{F}{\dot{w}_p} \left[\text{units: } \frac{N}{N/s} = s \right] \qquad (13.17)$$

It will be seen later that specific impulse is a characteristic parameter of a rocket engine for a given propellant (fuel-oxidizer combination); this can also be defined as the thrust acting on a hypothetical rocket discharging unit weight of the propellant per second as shown in Figure 13.17 (a).

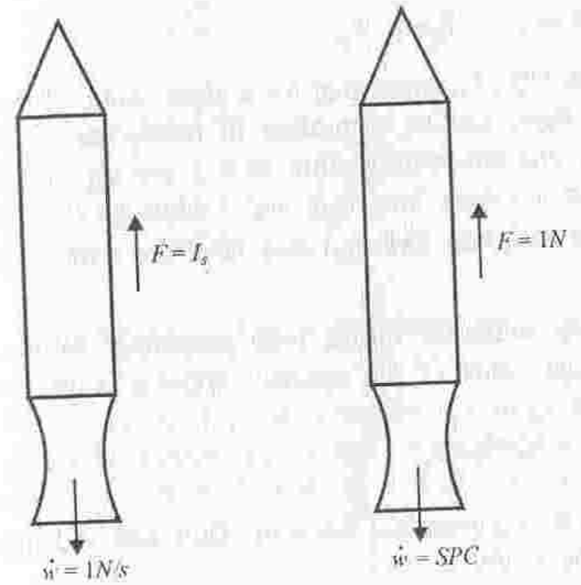

FIGURE 13.17 : Specific impulse and specific propellant consumption

Equations (13.16 (b)) and (13.17) give the following relation:

$$I_s = \frac{c_j}{g} \qquad (13.18)$$

The value of c_j depends on the exhaust gas properties (γ, R) and the thrust chamber pressure (p_o) and temperature (T_o). Therefore, values of specific impulse for various propellant combinations are known fairly accurately. The total impulse for a rocket engine during the powered flight or burning time t_p is given by

$$I_t = \int_o^{t_p} F \, . \, dt \qquad (13.19)$$

$$I_t = \int_o^{t_p} I_s \dot{w}_p \, dt \tag{13.20}$$

Assuming I_s = constant Equation (13.10) in Equation (13.20) gives

$$I_t = I_s \int_o^{t_p} \dot{w}_p \, dt$$

$$I_t = I_s W_p \tag{13.21}$$

Equation (13.21) shows that for a given value of the total impulse (or impulse) there can be a number of combinations of the specific impulse value and the burning time; thus a low specific impulse rocket operating over a longer time (t_p), and a high specific impulse rocket operating over a shorter time (t_p) may have the same value of the total impulse.

For given values of thrust, total propellant weight and burning time an average value of the specific impulse is defined by

$$\bar{I}_s = \frac{F}{W_s / t_p} \tag{13.22}$$

This figure is convenient when the flow rate and specific impulse vary during the flight.

13.5.3 Specific Propellant Consumption

The weight flow rate of the propellant required to produce a thrust of one Newton is known as the specific propellant consumption (SPC). This is given by

$$\text{SPC} = \frac{\dot{w}_p}{F} = \frac{1}{F/\dot{w}_p} \tag{13.23}$$

$$\text{SPC} = \frac{1}{I_s} \tag{13.24}$$

A hypothetical rocket developing a thrust of one Newton is shown in Figure 13.17 (*b*) here

$$\dot{w}_p = \text{SPC}$$

SPC value for a rocket determines the size of the propellant tanks and hence its total size; this is also valid for the specific impulse.

13.5.4 Flow Through Rocket Nozzles

Relations for Ideal or isentropic flow through nozzles have been dealt with in detail in Chapter 4; some of them are summarised here. Various flow parameters in a rocket nozzle are shown in Figure 13.18. On ac-

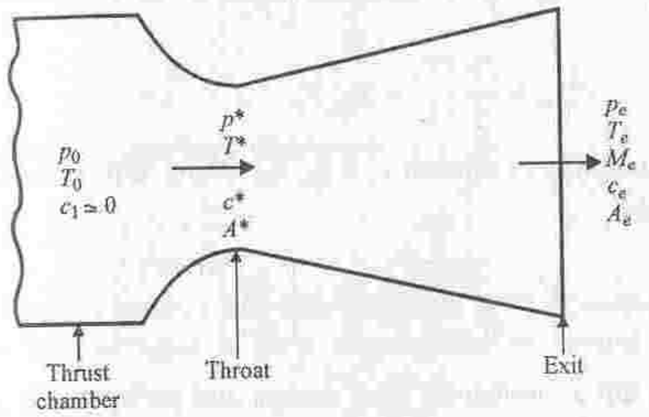

FIGURE 13.18 : Flow through a rocket nozzle

count of low Mach number the gas is assumed at stagnation conditions in the thrust chamber. Following relations for one-dimensional steady flow of a perfect gas are applicable to a rocket nozzle:

$$\frac{T^*}{T_o} = \frac{2}{\gamma + 1} \tag{13.25}$$

$$\frac{p^*}{p_o} = \left(\frac{2}{\gamma + 1} \right)^{\gamma/(\gamma-1)} \tag{13.26}$$

$$c^* = \sqrt{\gamma R T^*} \tag{13.27}$$

$$\dot{m}_p = \rho^* c^* A^* = \rho_e c_e A_e \tag{13.28}$$

$$\frac{\dot{m}_p \sqrt{T_o}}{A^* p_o} \sqrt{\frac{R}{\gamma}} = \left(\frac{2}{\gamma + 1} \right)^{(\gamma+1)/2(\gamma-1)} \tag{13.29}$$

$$\frac{T_o}{T_e} = 1 + \frac{\gamma - 1}{2} M_e^2 \tag{13.30}$$

$$\frac{p_o}{p_e} = \left(1 + \frac{\gamma - 1}{2} M_e^2 \right)^{\gamma/(\gamma-1)} \tag{13.31}$$

$$\frac{A_e}{A^*} = \frac{1}{M_e}\left(\frac{2}{\gamma+1} + \frac{\gamma-1}{\gamma+1}M_e^2\right)^{(\gamma+1)/2(\gamma-1)} \tag{13.32}$$

$$c_e^2 = \frac{2\gamma}{\gamma-1}RT_o\left\{1-\left(\frac{p_e}{p_o}\right)^{(\gamma-1)/\gamma}\right\} \tag{13.33}$$

$$c_{\max}^2 = \frac{2\gamma RT_o}{\gamma-1} = 2c_p T_o \tag{13.34}$$

For complete expansion $c_e = c_j$, therefore, Equations (13.18) and (13.33) yield

$$I_s^2 = \frac{2\gamma RT_o}{(\gamma-1)g^2}\left\{1-\left(\frac{p_e}{p_o}\right)^{(\gamma-1)/\gamma}\right\} \tag{13.35}$$

There are a number of other design and performance parameters, coefficients, and correction factors which require discussions at length. However, in an introductory treatment such as this only some important quantities are included. They can be determined experimentally and also predicted theoretically with some degree of accuracy.

(*a*) **Weight Flow coefficient:** This is the ratio of the gas or propellant flow rate and the force term $p_o A^*$

$$C_w = \frac{\dot{w}_p}{p_o A^*} \tag{13.36}$$

This is not a dimensionless quantity; it has the same unit as specific propellant consumption *i.e.*, s^{-1}.

All the quantities $\dot{w}_p$, p_o and A^* in Equation (13.29) can be measured.

(*b*) **Thrust coefficient:** This is the ratio of the thrust and the force term $p_o A^*$

$$C_F = \frac{F}{p_o A^*} \tag{13.37}$$

This is a dimensionless quantity; it is used for determining the thrust with known values of the combustion pressure and the nozzle throat area.

Equations (13.36) and (13.37) give

$$\dot{w}_p = C_w p_o A^*$$

$$F = C_F p_o A^*$$

Therefore, specific impulse is readily given by

$$I_s = \frac{F}{\dot{w}_p} = \frac{C_F}{C_w} \tag{13.38}$$

The specific propellant consumption is

$$\text{SPC} = \frac{1}{I_s} = \frac{C_w}{C_F} \tag{13.39}$$

Thrust coefficient is a function of several thermodynamic parameters; effects of some of them are depicted in Figures 13.19 and

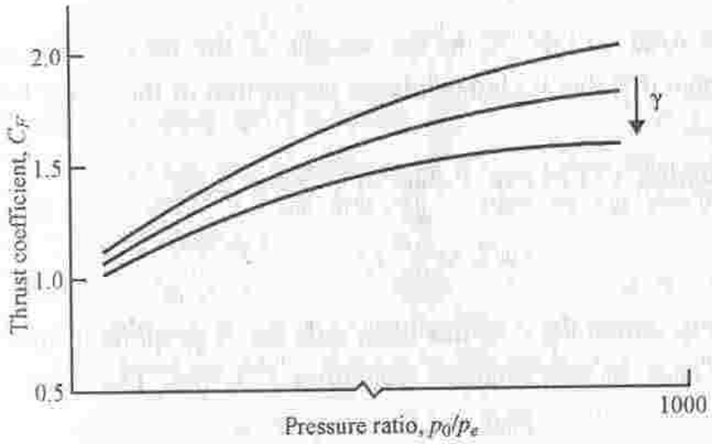

FIGURE 13.19 : Variation of thrust coefficient with pressure ratio

13.20. As expected it increases with the pressure ratio; there is a decrease with the increase in the specific heat ratio. It also increases with the area ratio. However, there is an optimum value of area ratio for a given value of the pressure ratio.

(*c*) **Impulse to weight ratio:** This is the ratio of the total impulse of the rocket and the total weight of the rocket vehicle system.

$$\text{IWR} = \frac{I_t}{W_t} \tag{13.40}$$

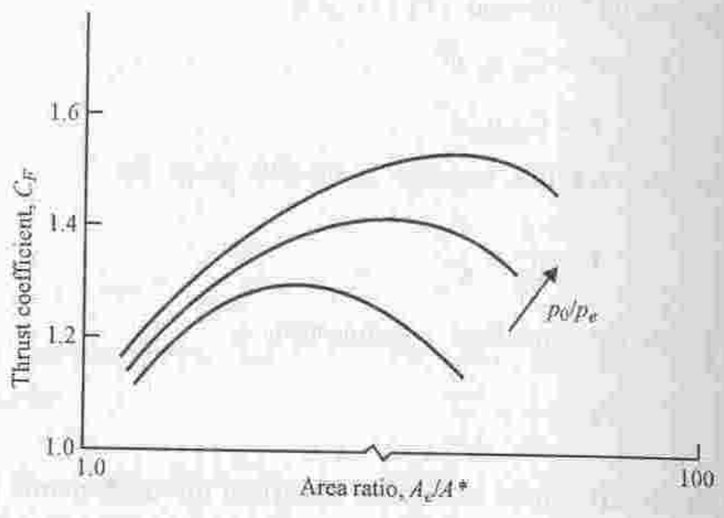

FIGURE 13.20 : Variation of thrust coefficient with area ratio

The total weight W_t is the weight of the rocket vehicle system at take off; this includes a large proportion of the propellant weight (W_p).

Equation (13.21) in Equation (13.40) gives

$$\text{IWR} = \frac{W_p}{W_t} I_s$$

The quantity W_p / W_t has been defined as propellant mass fraction (ζ) later in this chapter (Equation (13.56)). Therefore,

$$\text{IWR} = \zeta I_s \tag{13.41}$$

The space or volume required for storing the propellants depends on its density; and the total weight of the structure depends on the overall design skill. Therefore, IWR is an overall index of perfection achieved in the design and performance of the rocket vehicle system.

(*d*) **Characteristic velocity:** Rocket performance is also frequently expressed in terms of a characteristic velocity which is defined as

$$v^* = \frac{\text{effective jet velocity}}{\text{thrust coefficient}}$$

$$v^* = \frac{c_j}{C_F} \tag{13.42}$$

Characteristic velocity is equal to the effective jet velocity for a thrust coefficient of unity.

$$v^* = \frac{c_j}{g} \frac{g}{C_F}$$

Replacing $\frac{c_j}{g}$ by I_s, we get

$$v^* = \frac{g I_s}{C_F} \tag{13.43}$$

Equation (13.24) in the above expression gives

$$v^* = \frac{g}{C_F \, \text{SPC}} \tag{13.44}$$

Further, Equation (13.39) yields

$$v^* = \frac{g}{C_w} \tag{13.45}$$

13.5.5 Losses and Efficiencies

Figure 13.21 depicts the utilization of energy, and the various losses occurring in chemical rocket engines employing the thermo-chemical energy of the propellants.

Energy is supplied to the rocket engine or motor through the chemical reaction of the propellants in the combustion chamber, combustor or the thrust chamber. Energy in the gases at the combustor exit

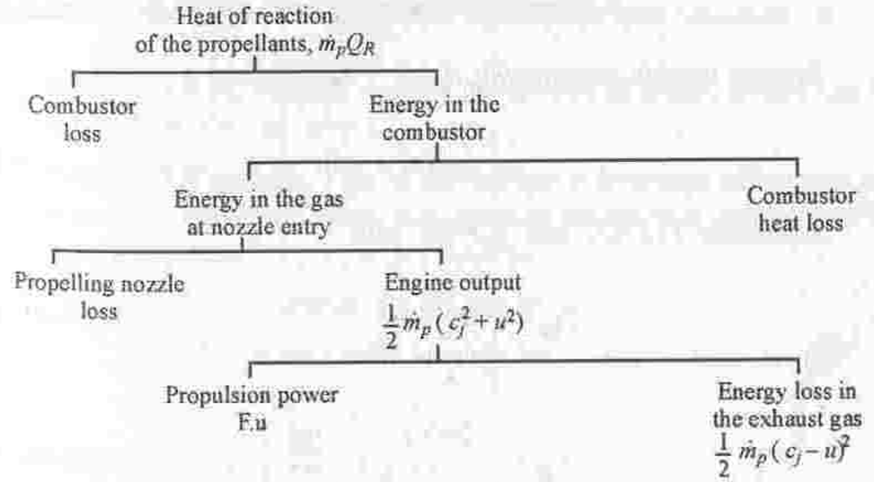

FIGURE 13.21 : Utilization of energy, and losses in thermo-chemical rocket engines

or entry of the propelling nozzle is less than the heat of reaction on account of energy losses in combustion, and combustor heat losses.

The rocket engine output is less than the energy at the nozzle entry due to energy losses in the nozzle. Energy required for propelling the rocket or the vehicle is equal to the propulsion work ($F.u$); the remaining part of the engine output is the residual kinetic energy lost in the exhaust gases.

Various efficiencies in rocket propulsion are defined here in order to understand and optimize the energy conversion process and method of propulsion. These efficiencies are defined on the same lines as presented in Section 12.3.4 for air breathing engines.

(a) **Propulsive Efficiency:** This is defined by

$$\eta_p = \frac{\text{propulsion or thrust power}}{\text{engine output power}}$$

$$\text{Propulsion power} = F.u \tag{13.46}$$

Substituting for F in terms of the effective jet velocity from Equation (13.16 (a))

$$\text{Propulsion power} = \dot{m}_p\, c_j\, u \tag{13.47}$$

Kinetic energy loss in the exhaust gas is $\frac{1}{2}(c_j - u)^2$

Therefore, the rate of energy or power loss is $\frac{1}{2}\dot{m}_p (c_j - u)^2$

Now engine output power

= propulsion power + power loss in the exhaust gas.

$$\text{Engine output power} = \dot{m}_p\, c_j\, u + \frac{1}{2}\dot{m}_p (c_j - u)^2$$

$$= \frac{1}{2}\dot{m}_p (c_j^2 + u^2) \tag{13.48}$$

Equations (13.47) and (13.48) give

$$\eta_p = \frac{c_j\, u}{\frac{1}{2}(c_j^2 + u^2)} \tag{13.49 (a)}$$

$$\eta_p = \frac{2u/c_j}{1 + u^2/c_j^2} = \frac{2\sigma}{1 + \sigma^2} \tag{13.49 (b)}$$

Equation (13.49) yield

$$\eta_p = 1 \text{ at } u = c_j \text{ or } \sigma = u/c_j = 1$$

For this condition the thrust power is given by

$$\dot{m}_p\, c_j^2 = \dot{m}_p\, u^2 \tag{13.50}$$

Figure 13.22 shows the variation of the propulsive efficiency with the flight to jet speed ratio. It should be noted here that unlike

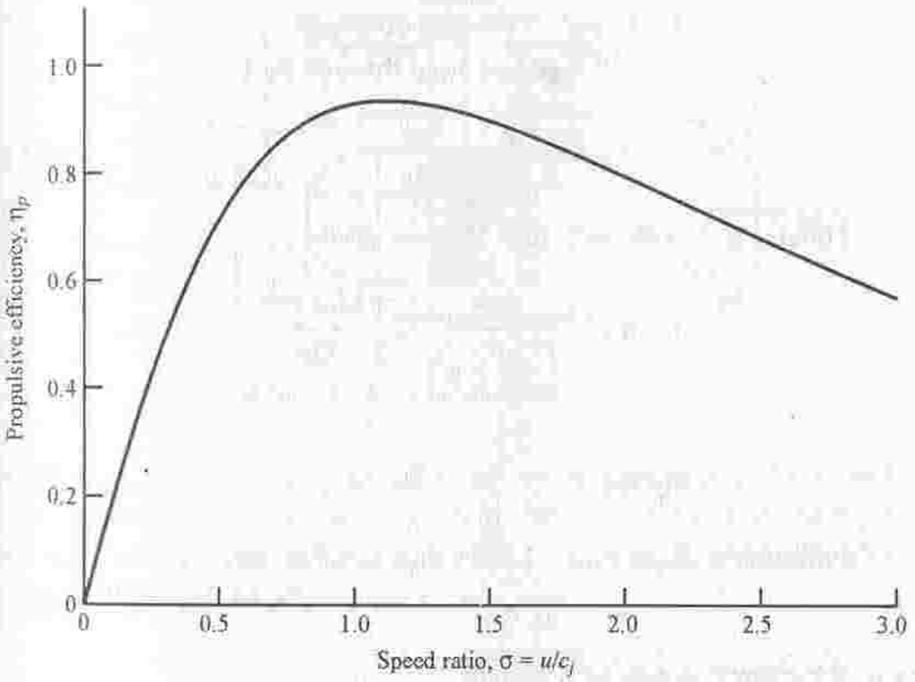

FIGURE 13.22 : Variation of propulsion efficiency of a rocket with speed ratio

the air breathing engines rockets do operate at flight speeds much greater than the jet speed.

(b) **Thermal Efficiency:** This is the energy conversion efficiency of the rocket engine and takes into account the thermal losses. Referring to Figure 13.21 it is defined as

$$\eta_{th} = \frac{\text{engine output power}}{\text{power input through fuel}}$$

$$\eta_{th} = \frac{\frac{1}{2}\dot{m}_p (c_j^2 + u^2)}{\dot{m}_p\, Q_R}$$

$$\eta_{th} = \frac{c_j^2 + u^2}{2Q_R} \tag{13.51}$$

(*c*) **Overall efficiency:** It is seen from Figure 13.21 that the power input to the rocket engine is $\dot{m}_p Q_R$. Here Q_R is the heat of reaction per kg of the products of combustion or the propellants (fuel and oxidizer); the net output is the propulsion power $F.u$. Therefore, the overall efficiency is given by

$$\eta_o = \frac{\text{propulsion power}}{\text{power input through fuel}}$$

$$\eta_o = \frac{Fu}{\dot{m}_p Q_R} = \frac{c_j u}{Q_R} \tag{13.52}$$

Equations (13.49 (*a*)) and (13.51) give

$$\eta_p \eta_{th} = \frac{c_j u}{\frac{1}{2}(c_j^2 + u^2)} \times \frac{1}{2} \frac{c_j^2 + u^2}{Q_R}$$

$$\eta_p \eta_{th} = \frac{c_j u}{Q_R} \tag{13.53}$$

Comparing Equations (13.52) and (13.53) we get

$$\eta_o = \eta_p \eta_{th} \tag{13.54}$$

13.6 ROCKET APPLICATIONS

Rockets have several applications in military and peace time operations such as space exploration, weather prediction, communication, aircraft propulsion and scientific investigations. A brief summary of these applications is given here.

13.6.1 Aircrafts

Rockets have been used in aircrafts as propulsion as well as auxiliary devices. Rocket propelled aircrafts have been used for both military, and high speed research aircrafts. Aircrafts with very heavy payloads require high values of thrust at take-off; such a high thrust is not required during level flight. Therefore, rocket propulsion is employed for a short duration during take-off. Thus "rocket-assisted take off" planes can employ much lighter engines; this mode of take-off is frequently referred

to as RATO or JATO. Solid fuel rocket motors are generally used for this purpose on account of their smaller size and simplicity.

A turbo-rocket engine is shown in Figure 13.23. It is the combination of a rocket and turbo jet engine. The engine starts with the supply of hot gases from the rocket combustor, which drive the turbine and the air compressor. The compressor supplies combustion air directly to a reheater located upstream of the main propulsion nozzle.

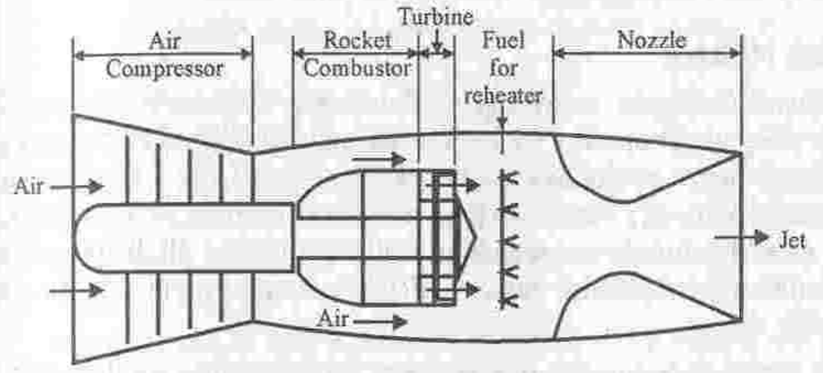

FIGURE 13.23 : A turbo-rocket engine

Military aircrafts can take-off with the conventional turbojet and achieve high rate of climb with rocket propulsion; cruising on turbojet it can again employ rocket engines for short duration supersonic flights for intercepting the target.

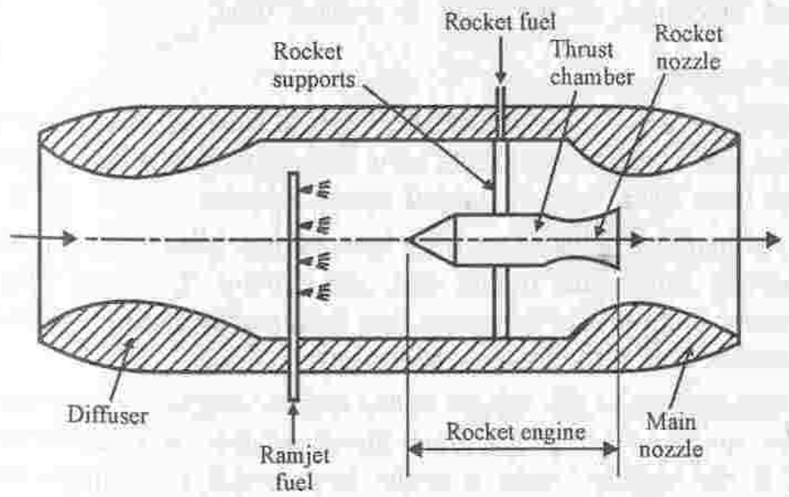

FIGURE 13.24 : A ramjet-rocket engine

Rockets are also used for the ejection of crew escape capsules and stores. Military aircrafts employ rocket propulsion for firing various types of missiles.

Ramjet engines are also launched at supersonic speeds by rockets. Figure 13.24 shows a ramjet-rocket engine. The operation of the rocket engine upstream of the main nozzle produces the thrust required for launching the ramjet engine. After achieving the desired Mach number ($M > 1$) the ramjet engine flies on its own thrust.

13.6.2 Military

Besides V-2 bombs many types of missiles with warheads have been used; they are propelled by both solid and liquid fuel rockets in short and long range operations; some of the missiles are (*i*) surface to air missile (SAM), (*ii*) surface to surface missile (SSM), (*iii*) air to air missile (AAM), (*iv*) Intercontinental ballistic missile (ICBM), (*v*) intermediate range ballistic missile (IRBM), and (*vi*) guided air missile (GAM).

Small short range missiles are propelled by solid fuel rocket motors; they are more compact and light. They rise faster through the lower atmosphere. Large and long range missiles till recently have been using liquid propellant rocket engines; these are ballistic missiles such as ICBMs and IRBMs and rise at comparatively lower speeds and burnout takes place at much higher altitudes. The inter continental ballistic missiles can travel a maximum distance equal to about one quarter of the earth's circumference. Global missiles in orbit can be made to hit a target anywhere on the earth in a short time.

13.6.3 Space

As stated before rocket propulsion was a stepping stone for space launches and space travels. Both solid and liquid propellant multi-stage rockets have been used to propel space vehicles.

All space vehicles or satellites have to pass through the atmosphere overcoming forces due to the drag and gravity. To avoid very high drag losses and prevent excessive skin temperatures space vehicles rise at a slower rate through the atmosphere.

The first stage lifts off the entire rocket-vehicle system; therefore, it is the most powerful stage, often known as the "booster" or booster stage. It can employ either a single large liquid propellant rocket or a number of smaller rockets operating simultaneously in parallel as shown in Figure 13.25. The last stage or the "sustainer" is generally

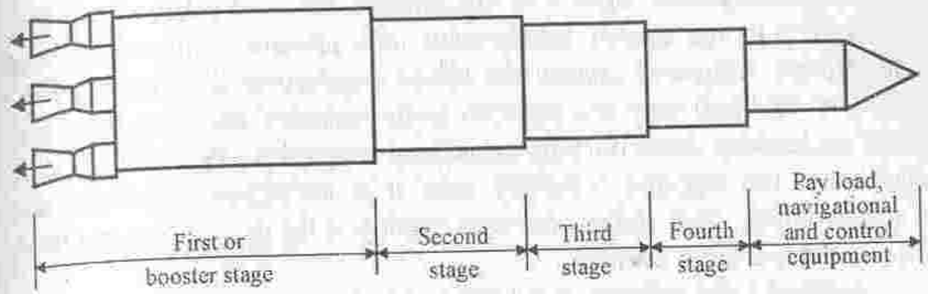

FIGURE 13.25 : A multi-stage rocket vehicle system

the smallest. The thrust required for propulsion along the inter planetary trajectory is much smaller. Small rockets are used on the way for various minor operations such as trajectory correction, attitude control and stage separation. Retro-rockets are small rockets fired in the direction of motion of the space vehicle to achieve braking or deceleration. A rocket vehicle system may have as many as 50 to 100 big and small rockets.

Several types of spacecrafts are launched and propelled by rockets such as Earth satellites, Lunar satellites, interplanetary satellites, manned and unmanned satellites, Figure 13.26 depicts an interplanetary flight of a rocket vehicle between the earth and a given planet. The take-off begins on earths surface with the operation of the booster rocket; after

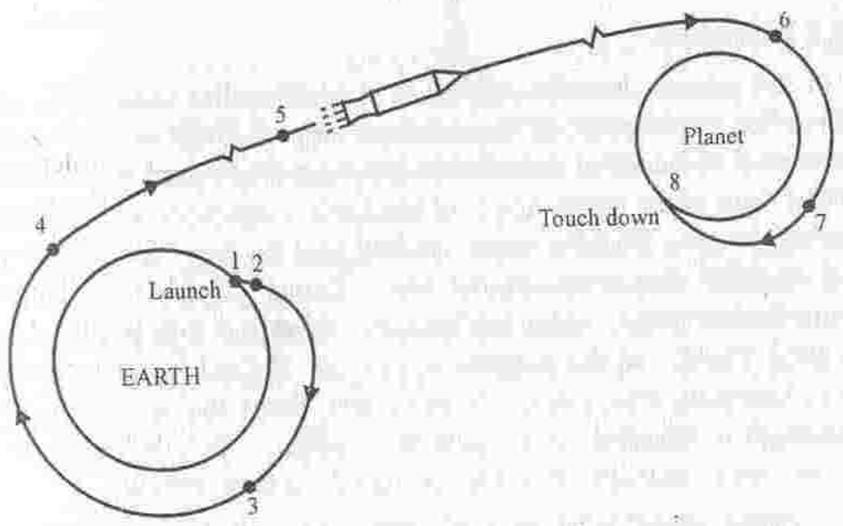

1	Launch or take-off	5 – 6	Coasting in interplanetary trajectory
1 – 2	Acceleration to orbital velocity	6 – 7	De-orbiting
2 – 3	Transfer to earth orbit	7 – 8	Decelerated flight for landing
3 – 4	Coasting in earth orbit	8	Touch down
4 – 5	Acceleration		

FIGURE 13.26 : Interplanetary flight of a rocket vehicle

the powered flight for some time the vehicle coasts in earth orbit before accelerating to the interplanetary orbit. On account of the absence of atmosspheric drag and gravity the thrust required in the interplanetary trajectory is small and the vehicle to jet velocity ratio is very high. Small rockets are fired only for trajectory correction. When the vehicle approaches the targeted planetary orbit it is decelerated by the action of retro-rockets; such rockets are also employed for de-orbiting and landing on the planet's surface.

Refuelling of rocket engines in transit at other planets can make them much lighter and simpler in design. Refuelling can be attempted at the moon surface and other distant planets for return and long journeys through space; many planets have hostile environment preventing such a facility. Some of them have either too high or too low ambient temperatures; others are enveloped by a thick layer of opaque and dense gases.

Gravitational force of other planets in addition to rocket thrust can also be employed for accelerating space vehicles during long journeys; this would require comparatively smaller rocket engines. It is estimated that a rocket must be launched at a velocity of 16,616 m/s (54,500 fps) in the direction of earth's rotation for escaping from the solar system. By employing "Jupiter fly by" the launch velocity can be reduced considerably.

13.6.4 Scientific

One of the greatest benefits of rocket propulsion has been in the area of scientific exploration of the surface and environment of various planets. Rocket launched space-crafts are extensively used for collecting scientific data of the upper layers of the earth's atmosphere, outer space and other planets. Besides moon landing rockets have been employed to put satellites into orbits around Mars, Venus and Jupiter. Elaborate instrumentation gives useful information about the topographical and geological aspects of the planets. Rocks are studied for the presence of new materials and water; physical data about the soil, its quality and strength is required for a "possible landing", installation of structures and movement of specially designed surface vehicles.

Orbiting space vehicles can carry probes for measurement of temperature pressure and density. Several other quantities which are important for data collection and study are the physical characteristics of the atmosphere close to the planet's surface, its chemical composition, magnetic field, wind patterns, etc.

Rockets meant for taking instruments to high altitudes for meterological measurements are called "sounding rockets"; global surveys of weather conditions are conducted by these instruments. The data thus collected helps in predicting weather in various regions of the world. Weather charts are prepared with the aid of detailed photographic records of clouds.

13.7 SPACE FLIGHTS

Man's interest in the heavens beyond the skies and the infinite number of stars dates back thousands of years before Christ. Sumerians (3500 B.C.) and other ancient civilizations had legends of non-human creatures coming occasionally to the Earth from the heavens in their flying vehicles. Sumerians and Babylonians of Mesopotamia (present Iraq) made revealing studies of the stars. Later on Greeks (300 B.C.) also made considerable progress in astronomy.

Space fiction describes journeys beyond the Earth on birds, and capsules fired by gigantic cannons; some kind of rockets have also been mentioned. Man had also been preoccupied with interest in the existence of intelligent civilizations on other planets. Various attempts were made to communicate with them by sending messages to these creatures, real or imaginary. However, no such contacts have been successful and they only remain a dream or "space fiction". Earth's man still feels lonely in the universe.

The long distances to the various heavenly bodies in astronomical magnitudes provoked the interest of the twentieth century scientists and engineers to develop high speed propulsive devices in the form of several different types of rockets some of which have already been described.

Operation of the modified V-2 missile by the United States in 1949 can be regarded as the first attempt towards space flights; the missile entered the ionosphere reaching an altitude of 400 km.

As stated earlier rocket propelled bodies such as space crafts and satellites can reach any altitude. Very high speeds of flight of the order of 30,000 kmph can be achieved in airless space between the earth and other planets. Theoretically the maximum achievable speed by a body is the speed of light *i.e.*, 186,000 miles/s (297,600 km/s).

On account of very long distances involved in space travel rockets have several stages (upto ten) which are successively dropped after their operations. This eliminates the problem of carrying the structures of the "spent up" rockets over long distances. Besides this each individual

rocket must have the largest proportion of the propellant weight compared to the total weight.

Besides putting weather and communication satellites into various orbits rockets have been taking spacecrafts to orbits around other planets for data collection and landing, if possible. The historic moon-landing took place in September 1959. In future special "super rockets" may take space ships to distant planets, stars and other galaxies for exciting explorations. Future techniques in propulsion will achieve new dimensions and science and technology will be at the threshold of yet another revolution.

The following sections deal with some elementary aspects of the performance of rockets and dynamics of high altitude and space flights.

13.7.1 Relative Masses

A rocket-propelled vehicle system consists of the rocket engine/motor with its propellant tanks, turbo pump system (in a liquid propellant type), pay load and navigational and auxiliary equipment. The mass ratio (MR) of a rocket is defined by

$$MR = \frac{\text{final mass of the rocket after burnout}}{\text{total mass of the rocket at take-off}}$$

$$MR = \frac{m_2}{m_1} \tag{13.55}$$

A good design and careful selection of construction materials should give a small value of the mass ratio. It will be seen later that small values of mass ratio give higher flight speeds of the rocket.

Another quantity that is often used in rocket calculations is the "propellant mass fraction" (ζ). This is defined by

$$\zeta = \frac{\text{propellant mass at take-off}}{\text{total mass of the rocket at take-off}}$$

$$\zeta = \frac{m_p}{m_1} \tag{13.56}$$

$$\zeta = \frac{m_1 - m_2}{m_1} = 1 - \frac{m_2}{m_1}$$

$$\zeta = 1 - MR \tag{13.57}$$

The propellant mass fraction should be as high as practicable coupled with a small value of the burning time (t_p) of the propellant.

13.7.2 Vertical Flight of a Rocket

Figure 13.27 depicts a simplified model of the flight of a rocket within the gravitational field with g = constant. The mass and acceleration of the rocket are also assumed constant. The powered flight takes place during the burn out time t_p achieving an altitude Z_p and velocity u_p. After burn out the rocket coasts to zero upward velocity reaching an altitude Z_{max}. After this the rocket starts falling down. For simplicity in analysis atmospheric drag will be neglected.

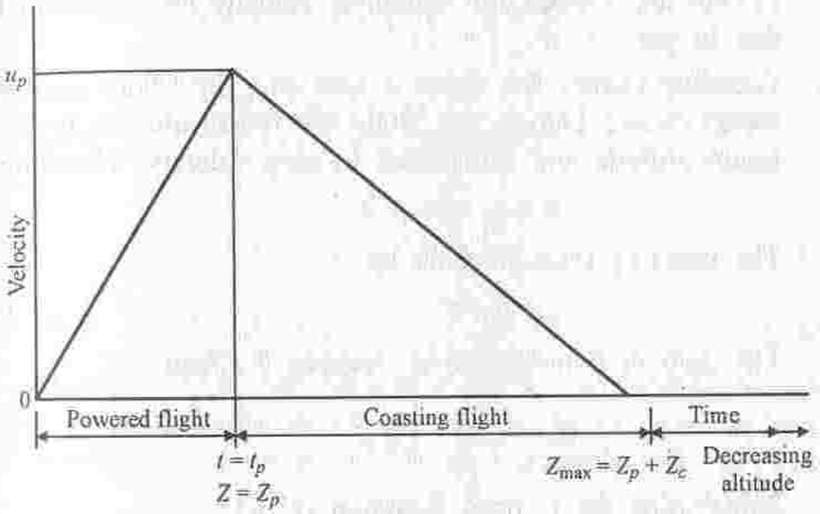

FIGURE 13.27 : Powered and coasting flights of a rocket within the gravitational field

(*a*) **Powered flight:** In the absence of drag force the accelerating force ($m_1 a$) is given by

$$m_1 a = F - m_1 g$$

Therefore, acceleration of the rocket is given by

$$a = \frac{F}{m_1} - g \tag{13.58}$$

Assuming constant acceleration, maximum value of the flight velocity of the rocket at burn out is given by

$$u_p = a t_p$$

$$u_p = \left(\frac{F}{m_1} - g \right) t_p = \frac{F t_p}{m_1} - g t_p \tag{13.59}$$

The altitude attained is given by

$$Z_p = \frac{1}{2} a t_p^2$$

$$Z_p = \frac{1}{2}\left(\frac{F}{m_1} - g\right) t_p^2 = \frac{1}{2}\frac{F}{m_1} t_p^2 - \frac{1}{2} g t_p^2 \qquad (13.60)$$

The quantities $g t_p$ in Equation (13.59) and $\frac{1}{2} g t_p^2$ in Equation (13.60) are respectively known as velocity loss and altitude loss due to gravity.

(*b*) **Coasting flight:** The thrust is zero after the "burn out" and the rocket coasts. During this flight the rocket ascends to the maximum altitude and decelerates to zero velocity. Therefore,

$$u = u_p - g t_c = 0$$

The coasting time is given by

$$t_c = u_p / g \qquad (13.61)$$

The gain in altitude during coasting is given by

$$Z_c = u_p t_c - \frac{1}{2} g t_c^2$$

Substituting for t_c from Equation (13.61)

$$Z_c = \frac{u_p^2}{g} - \frac{1}{2}\frac{u_p^2}{g}$$

$$Z_c = \frac{1}{2}\frac{u_p^2}{g} = \frac{1}{2}\left(\frac{F}{m_1} - g\right)^2 \frac{t_p^2}{g} \qquad (13.62)$$

The total gain in altitude from Equations (13.60) and (13.62) is given by

$$Z = Z_p + Z_c$$

$$Z = \frac{1}{2}\left(\frac{F}{m_1} - g\right) t_p^2 + \frac{1}{2}\left(\frac{F}{m_1} - g\right)^2 \frac{t_p^2}{g}$$

$$Z = \frac{1}{2} t_p^2 \left(\frac{F^2}{g m_1^2} - \frac{F}{m_1}\right) \qquad (13.63)$$

Replacing mass term by weight

$$Z = \frac{1}{2} g t_p^2 \left(\frac{F^2}{w_1^2} - \frac{F}{w_1}\right) \qquad (13.64)$$

Now $$F = I_s \dot{w}_p = I_s \frac{W_p}{t_p}$$

Therefore, $$Z = \frac{1}{2} g t_p^2 \left(\frac{I_s^2}{t_p^2}\frac{W_p^2}{w_1^2} - \frac{I_s}{t_p}\frac{W_p}{w_1}\right)$$

Now $$\frac{W_p}{w_1} = \frac{m_p}{m_1} = \zeta, \text{ therefore,}$$

$$Z = \frac{1}{2} g \,.\, I_s \zeta (\zeta I_s - t_p) \qquad (13.65\ (a))$$

Thus $$Z = f(I_s,\ \zeta,\ t_p) \qquad (13.65\ (b))$$

Equations (13.65 (*a*)) through a simple and approximate analysis shows that the maximum altitude attained can be increased by increasing specific impulse and the propellant mass fraction, and decreasing the burn out time. Both velocity loss ($g t_p$) and altitude loss $\left(\frac{1}{2} g t_p^2\right)$ can be kept low by keeping the burning time low.

13.7.3 Vertical Flight of a Multi-Stage Rocket

Figure 13.28 depicts the velocity increments during the successive operations of the three stages of a rocket followed by coasting. The total masses of the individual stages at take-off are m_1, m_2 and m_3; altitude gains at the end of operation of each stage are Z_1, Z_2 and Z_3. The acceleration is assumed constant and drag is ignored during each operation. Therefore,

$$u_1 = \left(\frac{F_1}{m_1} - g\right) t_1$$

$$u_2 = \left(\frac{F_2}{m_2} - g\right) t_2$$

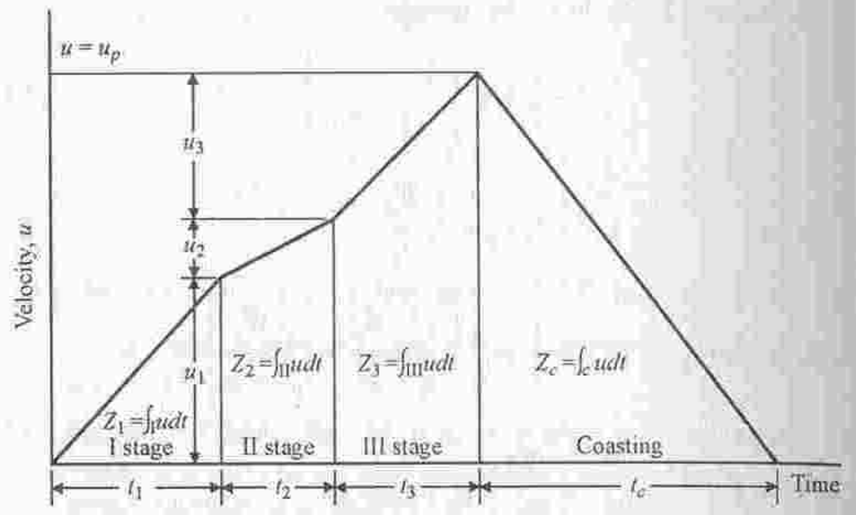

FIGURE 13.28 : Ascent of a three-stage rocket within the gravitational field

$$u_3 = \left(\frac{F_3}{m_3} - g \right) t_3$$

In general the velocity increment for the nth stage is given by

$$u_n = \left(\frac{F_n}{m_n} - g \right) t_n$$

Therefore, the final velocity after complete burn out or the operation of the nth stage is

$$u_p = u_1 + u_2 + u_3 + \ldots + u_n$$

$$u_p = \left(\frac{F_1}{m_1} - g \right) t_1 + \left(\frac{F_2}{m_2} - g \right) t_2 + \left(\frac{F_3}{m_3} - g \right) t_3 + \ldots + \left(\frac{F_n}{m_n} - g \right) t_n \quad (13.66)$$

The altitude gains in each operation are given by the areas under the velocity-time curves for each stage as shown in Figure 13.28.

$$Z_1 = \int_I u dt = \frac{1}{2} u_1 t_1 \quad (13.67)$$

$$Z_1 = \frac{1}{2} \left(\frac{F_1}{m_1} - g \right) t_1^2 \quad (13.68)$$

$$Z_2 = \int_{II} u dt = u_1 t_2 + \frac{1}{2} u_2 t_2$$

$$= \left(u_1 + \frac{1}{2} u_2 \right) t_2 \quad (13.69)$$

$$Z_2 = \left(\frac{F_1}{m_1} - g \right) t_1 t_2 + \frac{1}{2} \left(\frac{F_2}{m_2} - g \right) t_2^2 \quad (13.70)$$

$$Z_3 = \int_{III} u dt = (u_1 + u_2) t_3 + \frac{1}{2} u_3 t_3$$

$$Z_3 = \left(u_1 + u_2 + \frac{1}{2} u_3 \right) t_3 \quad (13.71)$$

$$Z_3 = \left(\frac{F_1}{m_1} - g \right) t_1 t_3 + \left(\frac{F_2}{m_2} - g \right) t_2 t_3 + \frac{1}{2} \left(\frac{F_3}{m_3} - g \right) t_3^2 \quad (13.72)$$

$$Z_n = \left(u_1 + u_2 + u_3 + \ldots + u_{n-1} + \frac{1}{2} u_n \right) t_n \quad (13.73)$$

$$Z_n = u_{n-1} t_n + \frac{1}{2} a_n t_n^2$$

$$Z_n = \left[\left(\frac{F_1}{m_1} - g \right) t_1 + \left(\frac{F_2}{m_2} - g \right) t_2 + \left(\frac{F_3}{m_3} - g \right) t_3 + \ldots + \left(\frac{F_{n-1}}{m_{n-1}} - g \right) t_{n-1} + \frac{1}{2} \left(\frac{F_n}{m_n} - g \right) t_n \right] t_n \quad (13.74)$$

The altitude gain at the end of coasting is

$$Z_c = \int_c u dt = \frac{1}{2} u_p \cdot t_c \quad (13.75)$$

The velocity at the end of coasting is zero and the altitude is maximum. Therefore,

$$0 = u_p + (-g) t_c$$

$$t_c = u_p/g$$

$$Z_c = \frac{1}{2}\frac{u_p^2}{g} \tag{13.76}$$

The maximum altitude gained at the end of powered and coasting flights is

$$Z_{max} = Z_p + Z_c$$

$$Z_{max} = Z_1 + Z_2 + Z_3 + \ldots + Z_n + Z_c \tag{13.77}$$

13.7.4 The Rocket Equation

The limitations of the simplified analyses in Sections 13.7.2 and 13.7.3 are quite obvious from the several assumptions used. A more accurate expression for the maximum velocity of the rocket at burn out is developed here under the following assumptions:

(*a*) constant gravitational force,
(*b*) drag force is negligible,
(*c*) specific impulse is constant,
(*d*) steady flow through the rocket nozzle.

During the operation of the rocket its mass decreases due to the propellant combustion and outflow of exhaust gases; therefore,

$$-\frac{dm}{dt} = -\frac{dm_p}{dt} = \dot{m}_p \tag{13.78}$$

The rocket thrust provides the accelerating force besides overcoming the gravitational pull. Therefore,

$$F = ma + mg$$

$$F = m\frac{du}{dt} + mg$$

Now $F = \dot{w}_p \,.\, I_s = \dot{m}_p\, g\, I_s$, therefore,

$$m\frac{du}{dt} + mg = \dot{m}_p\, g\, I_s$$

Substituting for $\dot{m}_p$ from Equation (13.78)

$$m\frac{du}{dt} + mg = -gI_s\frac{dm}{dt}$$

$$du + g\,dt = -gI_s\frac{dm}{m} \tag{13.79}$$

This is the differential form of the rocket equation.

At $t = 0,\ u = 0,\ m = m_1$

$t = t_p,\ u = u_p,\ m = m_2$

Therefore, integrating Equation (13.79) we get

$$\int_o^{u_p} du + g\int_o^{t_p} dt = -gI_s\int_{m_1}^{m_2}\frac{dm}{m}$$

$$u_p + gt_p = gI_s \ln\frac{m_1}{m_2} \tag{13.80 (a)}$$

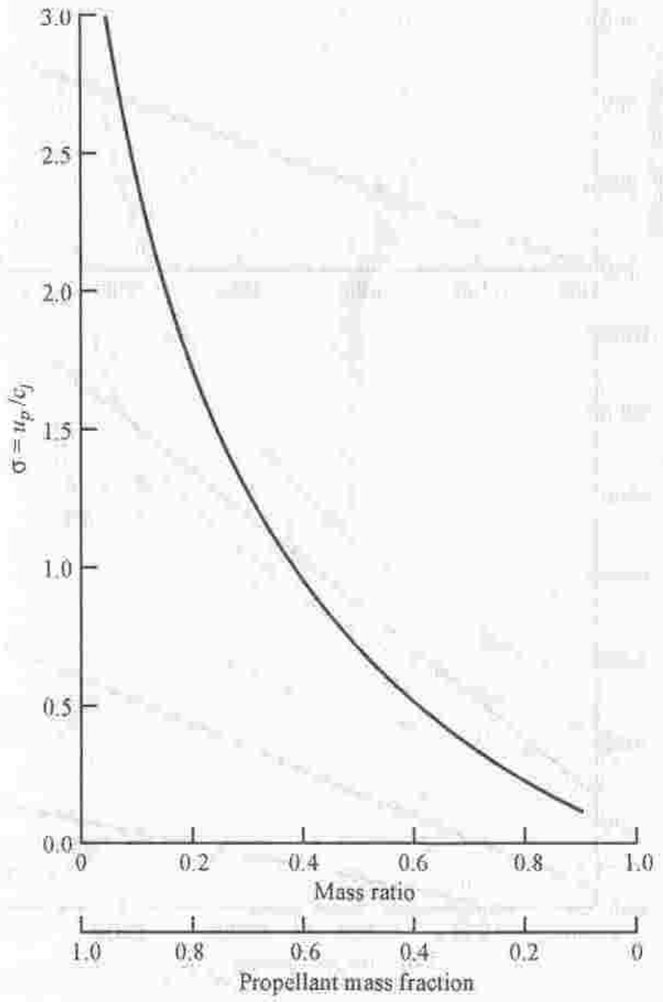

FIGURE 13.29 : Variation of the maximum speed ratio with mass ratio

$$u_p = g I_s \ln \frac{1}{MR} - g t_p \qquad (13.80\ (b))$$

Since $g I_s = c_j$ [Equation (13.18)]

$$u_p = c_j \ln \frac{1}{MR} - g t_p \qquad (13.80\ (c))$$

The value of the term $g t_p$ is negligible for large values of c_j and $1/MR$. Therefore, maximum flight to jet speed ratio is given by

$$\sigma = \frac{u_p}{c_j} = \ln \frac{1}{MR} \qquad (13.81)$$

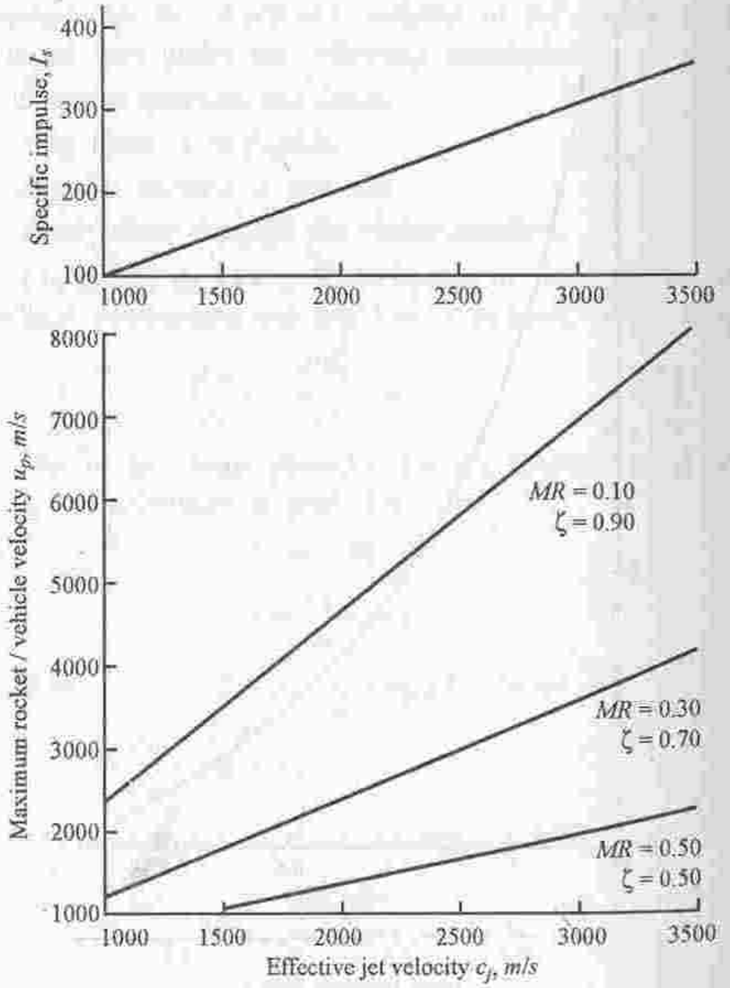

FIGURE 13.30 : Variation of specific impulse and maximum rocket velocity with the effective jet velocity

This is plotted in Figure 13.29. It is observed that for low values of the mass ratio flight speeds at burn out are considerably greater than the effective jet speed.

Figure 13.30 depicts the variation of the maximum rocket or vehicle velocity with the effective jet velocity for various values of mass ratio and the propellant mass fraction. If the propellant weight is close to the total rocket weight at take off the burn out velocity of the rocket is much higher compared to the effective jet velocity.

Equation (13.18) fixes the specific impulse for a given value of the effective jet velocity; this is also shown in Figure 13.30. Since specific impulse is an important performance parameter of a rocket its influence on the maximum velocity is depicted in Figure 13.31. In order

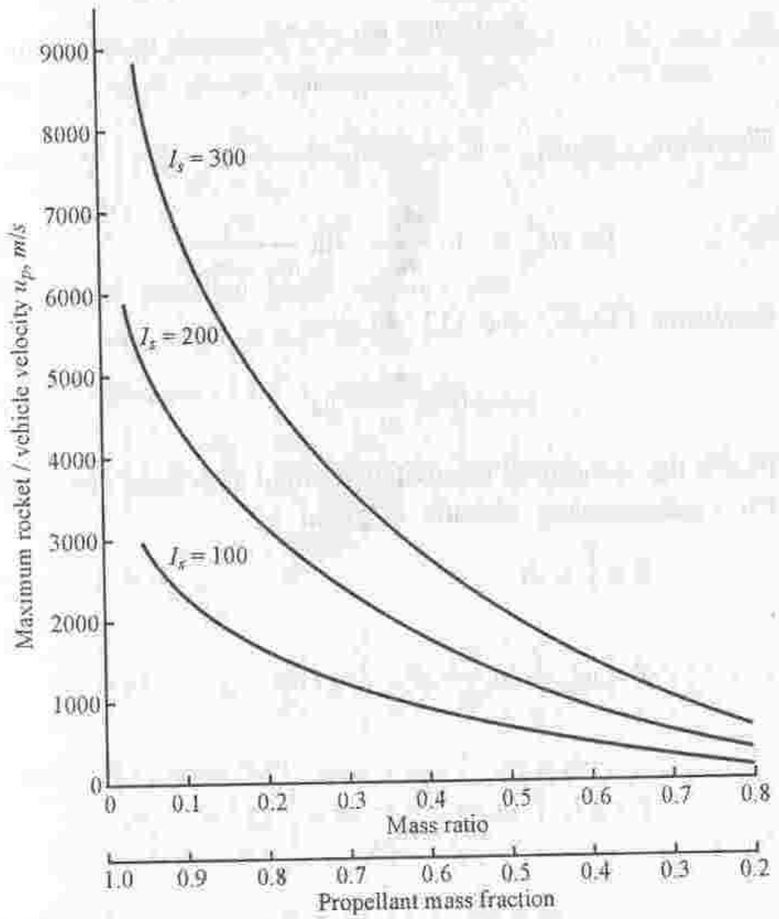

FIGURE 13.31 : Effect of specific impulse, mass ratio and propellant mass fraction on maximum rocket or vehicle velocity

to achieve high rocket velocity at burn out high value of specific impulse with low mass ratio should be employed.

13.7.5 Altitude Gain During Rocket Flight

Expressions for altitude gains during powered and coasting flights of a rocket or a missile are developed in this section employing the rocket equation (Equation (13.79)).

(*a*) **Powered vertical flight**: Equation (13.79) is

$$du = -g\,dt - g I_s \frac{dm}{m}$$

This on integration yields

$$u = -gt - g I_s \, [\ln m]_0^t \tag{13.82}$$

at $t = 0,\ m = m_1,\ u = 0$

$t = t,\ m = m_1 - \dot{m}_p t,\ u = u$

Therefore, $[\ln m]_0^t = \ln (m_1 - \dot{m}_p t) - \ln m_1$

or $$[\ln m]_o^t = -\ln \frac{m_1}{m} = -\ln \frac{m_1}{m_1 - \dot{m}_p t} \tag{13.83}$$

Equations (13.82) and (13.83) give

$$u = g I_s \ln \frac{m_1}{m} - gt \tag{13.84}$$

This is the velocity of the rocket attained after time t from take-off. The corresponding altitude is given by

$$Z = \int u\,dt$$

$$Z = g I_s \int_0^t \ln \frac{m_1}{m}\,dt - \int_o^t gt\,dt$$

$$Z = g I_s \int_o^t \ln \frac{m_1}{m_1 - \dot{m}_p t}\,dt - \frac{1}{2} g t^2$$

$$Z = g I_s \int_0^t \ln m_1\,dt - g I_s \int_o^t \ln (m_1 - \dot{m}_p t)\,dt - \frac{1}{2} g t^2$$

$$Z = g I_s t \ln m_1 - g I_s \int_0^t \ln (m_1 - \dot{m}_p t)\,dt - \frac{1}{2} g t^2 \tag{13.85}$$

The second term with the integral sign can be dealt with separately.

$$\int_o^t \ln (m_1 - \dot{m}_p t)\,dt$$

$$= \left[\frac{m_1 - \dot{m}_p t}{-\dot{m}_p} \ln (m_1 - \dot{m}_p t) - t \right]_o^t$$

$$= \left(t - \frac{m_1}{\dot{m}_p} \right) \ln (m_1 - \dot{m}_p t) - t + \frac{m_1}{\dot{m}_p} \ln m_1 \tag{13.86}$$

Substituting from Equation (13.86) in Equation (13.85) and simplifying the value of the altitude Z at time t is obtained.

$$Z = g I_s \left\{ t \ln \frac{m_1}{m_1 - \dot{m}_p t} - \frac{m_1}{\dot{m}_p} \ln \frac{m_1}{m_1 - \dot{m}_p t} \right\} + g I_s t - \frac{1}{2} g t^2 \tag{13.87}$$

At the end of powered flight or burn out.

$t = t_p,\ m_1 - \dot{m}_p t_p = m_2,\ Z = Z_p,$

Therefore, Equation (13.87) reduces to

$$Z_p = g I_s \left\{ t_p \ln \frac{m_1}{m_2} - \frac{m_1}{\dot{m}_p} \ln \frac{m_1}{m_2} + t_p \right\} - \frac{1}{2} g t_p^2 \tag{13.88 (a)}$$

Putting $\frac{m_2}{m_1} = MR$

$$Z_p = g I_s \left\{ \left(t_p - \frac{m_1}{\dot{m}_p} \right) \ln \frac{1}{MR} + t_p \right\} - \frac{1}{2} g t_p^2 \tag{13.88 (b)}$$

Introducing the propellant mass ratio ζ through

$$m_1 = \frac{m_p}{\zeta} = \frac{\dot{m}_p t_p}{\zeta} \tag{13.89}$$

Equation (13.88 (*b*)) yields a simpler relation

$$Z_p = c_j t_p \left\{ 1 + \left(1 - \frac{1}{\zeta} \right) \ln \frac{1}{MR} \right\} - \frac{1}{2} g t_p^2 \tag{13.90 (a)}$$

Since $\zeta = 1 - MR$

$$Z_p = f(c_j,\ t_p,\ MR) \qquad (13.90\ (b))$$

It may be observed that Equations (13.65 (*b*)) and (13.90 (*b*)) are identical.

(*b*) **Coasting vertical flight:** The velocity at the end of powered flight is given by Equation (13.80 (*b*)) and the altitude gain during coasting by Equation (13.76). Therefore,

$$Z_c = \frac{1}{2}\frac{u_p^2}{g} = \frac{1}{2}g\left(I_s \ln\frac{1}{MR} - t_p\right)^2 \qquad (13.91)$$

The maximum altitude gained is

$$Z_{\max} = Z_p + Z_c$$

13.7.6 Orbital Velocity of the Earth-satellite

Rockets are used to launch space stations or satellites into earth-orbit; they revolve round the earth at an altitude beyond the earth's atmosphere where the drag force is absent. Therefore, such satellites can remain in the orbit forever without any expenditure of energy.

If the orbital velocity of an earth-satellite is equal to the angular velocity of the earth it has zero velocity relative to the earth. Such a satellite is known as a stationary satellite which can be usefully employed for several purposes.

Earth satellites are used for several scientific and technological programmes such as observation of space phenomena, study of weather, military missions and communication.

The orbital velocity of the satellite can be found by equating the centrifugal force acting on it to the gravitational pull. The velocity of the satellite is u_{orb} at a radius R from the centre of the earth. Therefore,

$$m\frac{u_{\text{orb}}^2}{R} = mg$$

$$u_{\text{orb}} = \sqrt{Rg} \qquad (13.92)$$

The variation of the gravitational force along the radius $R = R_o + Z$ is given by

$$g = \left(\frac{R_o}{R}\right)^2 g_o = \left(\frac{R_o}{R_o + Z}\right)^2 g_o \qquad (13.93)$$

Figure 13.32 shows the plot of the acceleration due to gravity (in the dimensionless form g/g_o) against the altitude. Comparing Figure 1.10 with this plot it is seen that there is only little decrease in the gravitational pull with altitude even in the upper regions of the atmosphere such as the ionosphere and the exosphere.

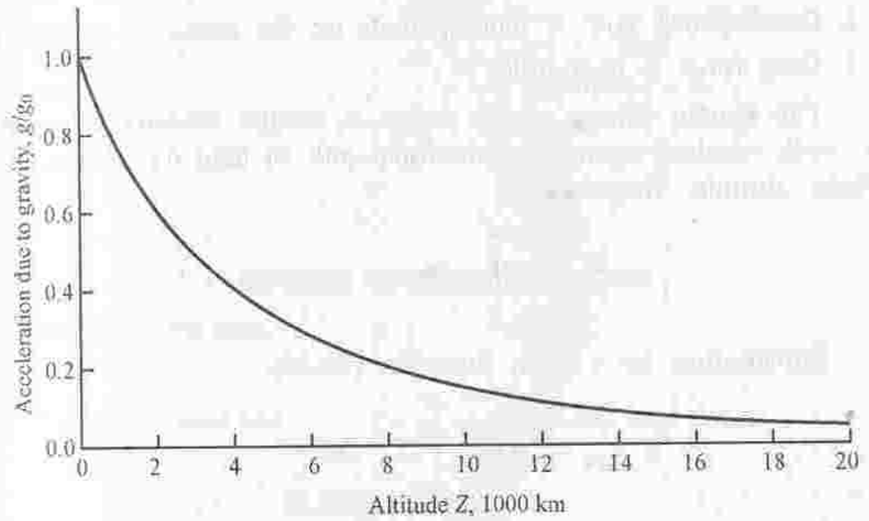

FIGURE 13.32 : Variation of acceleration due to gravity with altitude

Substitution from Equation (13.93) into Equation (13.92) yields the expression for the orbital velocity in terms of the earth's radius at mean sea level, and altitude.

$$u_{\text{orb}} = \sqrt{\frac{g_o R_o^2}{R}} = R_o\sqrt{\frac{g_o}{R_o + Z}} \qquad (13.94)$$

13.7.7 Escape Velocity

A rocket vehicle system destined to travel in the outer space to other planets or their orbits must escape from the earth's gravitational field. The thrust should be able to accelerate the rocket to a velocity at which its kinetic energy equals the work required to overcome gravitational force.

The escape velocity at the earth's surface is about 11.2 km/s. If the rocket-vehicle systems are accelerated to this velocity within the earth's atmosphere the frictional heating will be excessive leading to unsurmountable problems. Therefore, a practical and safer method is

first to accelerate the rocket at lower velocities through the atmosphere; the rocket is finally accelerated to the escape velocity at a much higher altitude where the atmospheric drag and heating are absent. An expression for the escape velocity of the rocket at altitude Z is derived under the following assumptions:

1. Vertical flight of the rocket,
2. Gravitational pull of other planets on the rocket is negligible,
3. Drag force is negligible.

The kinetic energy of the rocket at escape velocity is equal to the work required against gravitational pull to take the rocket to an infinite altitude. Therefore,

$$\frac{1}{2} m u_{esc}^2 = m \int_R^\infty g dR$$

Substitution for g from Equation (13.86)

$$u_{esc}^2 = 2 g_o R_o^2 \int_R^\infty R^{-2} dR$$

$$u_{esc}^2 = 2 g_o R_o^2 \left(\frac{1}{R}\right)_\infty^R = 2 g_o R_o^2 \left(\frac{1}{R}\right)$$

$$u_{esc} = R_o \sqrt{\frac{2 g_o}{R_o + Z}} \qquad (13.95)$$

Comparison of Equations (13.94) and (13.95) yields

$$u_{esc} = \sqrt{2}\, u_{\text{orb}}$$

NOTATION FOR CHAPTER 13

a	velocity of sound or acceleration	$MR = m_2/m_1$	mass ratio
A	area of cross-section	n	number of rocket stages
c	gas velocity	n_1, n_2	indices explained in the text
C_F	thrust coefficient	p	static pressure
C_w	weight flow rate coefficient	Q_R	heat of reaction of the propellants
d	diameter	r	linear burning rate
D	drag force	R_o	radius of earth at mean sea level
f	$\dot{m}_f/\dot{m}_{ox}$ fuel to oxidizer ratio	R	radius around earth at altitude Z
F	force or thrust		

g	acceleration due to gravity	SPC	specific propellant consumption
g_o	acceleration due to gravity at mean sea level	t	time
		T	absolute temperature
I	impulse	u	flight speed
K_1, K_2	constants explained in the text	u_{esc}	escape velocity
K_p	propellant area ratio	u_{orb}	orbital velocity
IWR	impulse to weight ratio	u_p	velocity of the rocket at burn out or the end of powered flight
m	mass		
$\dot{m}$	mass flow rate		
M	Mach number	v^*	characteristic velocity
		$w = mg$	weight
		$\dot{w}$	weight flow rate
		W	total weight
		Z	altitude

GREEK SYMBOLS

$\gamma = c_p/c_v$	ratio of specific heats	ρ	density
η	efficiency		
$\sigma = u/c_j$	flight to jet speed ratio	$\zeta = \frac{m_p}{m_1}$	propellant mass fraction

SUBSCRIPTS

o	stagnation values	max	maximum
1	initial or at take-off	mom	momentum
2	final or at burn out	n	nth
a	ambient	o	overall
c	coasting, combustion	orb	orbital
En	engine	ox	oxidizer
e	nozzle exit	p	propellant or powered flight, propulsive
esc	escape		
f	fuel	pr	pressure
F	thrust	s	specific
j	effective jet	t	total
		th	thermal

SUPERSCRIPTS

throat conditions or characteristic value

SOLVED EXAMPLES

Example 13.1. A rocket has the following data:

Propellant flow rate = 5.0 kg/s
Nozzle exit diameter = 10 cm
Nozzle exit pressure = 1.02 bar

Ambient pressure = 1.013 bar

Thrust chamber pressure = 20 bar

Thrust = 7 kN

(*a*) Determine the effective jet velocity, actual jet velocity, specific impulse and the specific propellant consumption.

(*b*) Recalculate the values of thrust and sp. impulse for an altitude where the ambient pressure is 10 mbar.

Solution. (*a*) Specific impulse $I_s = \dfrac{F}{\dot{w}_p}$

$$\dot{w}_p = 5 \times 9.81 = 49.05 \text{ N/s}$$

$$I_s = \frac{7000}{49.05} = \mathbf{142.71} \text{ seconds} \quad \textbf{Ans.}$$

Effective jet velocity $c_j = \dfrac{F \times g}{\dot{w}_p}$

$$c_j = 7000 \times 9.81/49.05 = \mathbf{1400} \text{ m/s} \quad \textbf{Ans.}$$

$$A_e = A_j = \frac{\pi}{4} d^2 = \frac{\pi}{4} \times 100 = 78.54 \text{ cm}^2$$

$$F = \dot{m}_p c_e + (p_e - p_a) A_e$$

$$7000 = 5 \times c_e + (1.02 - 1.013) \times 10^5 \times 78.54 \times 10^{-4}$$

$$c_e = \mathbf{1398.9} \text{ m/s} \quad \textbf{Ans.}$$

$$\text{SPC} = \frac{1}{I_s} = \frac{1}{142.71} = \mathbf{0.007} s^{-1} \quad \textbf{Ans.}$$

(*b*) The change in the ambient pressure to 10 mbar does not alter the nozzle exit pressure, velocity and propellant flow rate. Thrust due to decrease in the ambient pressure increases.

$$F' = \dot{m}_p c_e + (p_e - p_a') A_e$$

$$= 5 \times 1398.9 + (1.02 - 0.01) \times 10^5 \times 78.54 \times 10^{-4}$$

$$= 6994.5 + 793.254 = 7787.754 \text{ N}$$

$$F' = \mathbf{7.787 \text{ kN}} \quad \textbf{Ans.}$$

$$I_s' = 7787.754/49.05 = \mathbf{158.77 \text{ seconds}} \quad \textbf{Ans.}$$

Example 13.2. If the propellant (exhaust gases) in Example 13.1 has specific heat ratio value of 1.3 determine the following quantities for the exit pressure of 1.02 bar:

Exit Mach number, nozzle area ratio, thrust and propellant weight flow coefficients, and the characteristic velocity.

Solution. $p_e/p_o = 1.02/20 = 0.051$

From isentropic flow gas tables for $\gamma = 1.3 at$

$$p_e/p_o = 0.051$$

$$M_e = \mathbf{2.56} \quad \textbf{Ans.}$$

$$A_e/A^* = \mathbf{3.154} \quad \textbf{Ans.}$$

$$A^* = 78.54/3.154 = 24.90 \text{ cm}^2$$

Thrust coefficient $C_F = F/p_o A^*$

$$C_F = 7 \times 1000/20 \times 10^5 \times 24.90 \times 10^{-4}$$

$$C_F = \mathbf{1.405} \quad \textbf{Ans.}$$

The propellant weight flow coefficient

$$C_w = \dot{w}_p/p_o A^*$$

$$C_w = 49.05/20 \times 249$$

$$C_w = \mathbf{0.00985} s^{-1} \quad \textbf{Ans.}$$

The characteristic velocity $v^* = \dfrac{c_j}{C_F}$

$$v^* = \frac{1400}{1.405} = \mathbf{996.44 \text{ m/s}} \quad \textbf{Ans.}$$

Example 13.3. (*a*) Starting from isentropic relations for an ideal exhaust nozzle with discharge coefficient of unity prove that its thrust coefficient is given by

$$C_F = \gamma \sqrt{\frac{2}{\gamma - 1}} \left(\frac{2}{\gamma + 1} \right)^{(\gamma+1)/2\,(\gamma-1)} \sqrt{1 - \left(\frac{p_e}{p_o} \right)^{(\gamma-1)/\gamma}}$$

(*b*) Determine the values of thrust coefficient for a gas with $\gamma = 1.2$ at pressure ratios 2.0 and 5.0.

Solution. (*a*) Gas velocity at the nozzle exit for isentropic flow is given by

$$c_e = \sqrt{\frac{2\gamma}{\gamma-1} RT_o \left\{1 - \left(\frac{p_e}{p_o}\right)^{(\gamma-1)/\gamma}\right\}}$$

Assuming the flow to have reached critical conditions at the throat corresponding to a nozzle pressure ratio (p_e/p_o) lesser than

$$\frac{p^*}{p_o} = \left(\frac{2}{\gamma+1}\right)^{\gamma/(\gamma-1)}$$

The propellant flow rate through the nozzle is given by

$$\dot{m}_p = \rho^* c^* A^* = \frac{p^*}{RT^*} A^* \sqrt{\gamma RT^*}$$

$$\dot{m}_p = p^* A^* \frac{\sqrt{\gamma}}{\sqrt{RT^*}}$$

Now $F = \dot{m}_p \times c_e$

$$F = \frac{p^* A^* \sqrt{\gamma}}{\sqrt{RT^*}} \sqrt{\frac{2\gamma}{\gamma-1} RT_o \left\{1 - \left(\frac{p_e}{p_o}\right)^{(\gamma-1)/\gamma}\right\}}$$

$$C_F = \frac{F}{p_o A^*} = \gamma \left(\frac{p^*}{p_o}\right)\left(\frac{T_o}{T^*}\right)^{1/2} \sqrt{\frac{2}{\gamma-1}\left\{1 - \left(\frac{p_e}{p_o}\right)^{(\gamma-1)/\gamma}\right\}}$$

Substituting for p^*/p_o and T^*/T_o

$$C_F = \gamma \left(\frac{2}{\gamma-1}\right)^{1/2} \left(\frac{2}{\gamma+1}\right)^{(\gamma+1)/2(\gamma-1)} \sqrt{1 - \left\{\frac{p_e}{p_o}\right\}^{(\gamma-1)/\gamma}}$$

(proved)

(*b*) For $\gamma = 1.2$, $\dfrac{\gamma-1}{\gamma} = \dfrac{1}{6}$

$$C_F = 2.246 \sqrt{1 - \left(\frac{p_e}{p_o}\right)^{(\gamma-1)/\gamma}}$$

For $p_e/p_o = 1/2$

$$C_F = 2.246 \sqrt{1 - (0.5)^{1/6}}$$

$$C_F = \mathbf{0.7418} \quad \textbf{Ans.}$$

For $p_e/p_o = 1/5$

$$C_F = 2.246 \sqrt{1 - (0.2)^{1/6}}$$

$$C_F = \mathbf{1.089} \quad \textbf{Ans.}$$

Example 13.4. (*a*) Derive the following relations for the characteristic velocity:

$$(i) \quad v^* = \frac{a_o}{\gamma \left(\dfrac{2}{\gamma+1}\right)^{(\gamma+1)/2(\gamma-1)}}$$

$$(ii) \quad v^* = \frac{\sqrt{\bar{R} T_o / \bar{M}}}{\sqrt{\gamma} \left(\dfrac{2}{\gamma+1}\right)^{(\gamma+1)/2(\gamma-1)}}$$

(*b*) Calculate the values of the characteristic velocity for

(*i*) $\gamma = 1.25$, $\bar{M} = 18.3$ and $T_o = 3300$ K

(*ii*) $\gamma = 1.33$, $\bar{M} = 29.0$ and $T_o = 3508$ K.

Solution. (*a*) By definition $v^* = c_j / C_F$

Assuming complete isentropic expansion through the exhaust nozzle, we have

$$c_j = \sqrt{\frac{2\gamma}{\gamma-1} RT_o \left\{1 - \left(\frac{p_e}{p_o}\right)^{(\gamma-1)/\gamma}\right\}}$$

$$C_F = \gamma \left(\frac{2}{\gamma-1}\right)^{1/2} \left(\frac{2}{\gamma+1}\right)^{(\gamma+1)/2(\gamma-1)} \left\{1 - \left(\frac{p_e}{p_o}\right)^{(\gamma-1)/\gamma}\right\}^{1/2}$$

Therefore, $v^* = \dfrac{\sqrt{\dfrac{2}{\gamma-1}} \times \sqrt{\gamma RT_o}}{\gamma \left(\dfrac{2}{\gamma-1}\right)^{1/2} \left(\dfrac{2}{\gamma+1}\right)^{(\gamma+1)/2(\gamma-1)}}$

Let $a_o = \sqrt{\gamma RT_o}$

$$v^* = \frac{a_o}{\gamma\left(\frac{2}{\gamma+1}\right)^{(\gamma+1)/2(\gamma-1)}} \qquad \text{(proved)}$$

Now $a_o = \sqrt{\gamma \frac{\overline{R}}{\overline{M}} T_o}$

Therefore, $v^* = \dfrac{\sqrt{\frac{\overline{R}}{\overline{M}} T_o}}{\sqrt{\gamma}\left(\frac{2}{\gamma+1}\right)^{(\gamma+1)/2(\gamma-1)}}$ (proved)

(*b*) (*i*) $\gamma = 1.25,\ \overline{M} = 18.3,\ T_o = 3300$ K

$$\sqrt{\frac{\overline{R}T_o}{\overline{M}}} = \sqrt{\frac{8314.3 \times 3300}{18.3}} = 1224.459$$

$$\sqrt{\gamma}\left(\frac{2}{\gamma+1}\right)^{(\gamma+1)/2(\gamma-1)} = \sqrt{1.25}\left(\frac{2}{2.25}\right)^{2.25/2\times.25} = 0.6577$$

Therefore, $v^* = 1224.459/0.6577$

$v^* = \mathbf{1861.73\ m/s}$ **Ans.**

(*ii*) $\gamma = 1.33,\ \overline{M} = 29.0,\ T_o = 3508$ K

$R = 8314.3/29 = 286.7$ J/kg K

$a_o = \sqrt{\gamma R T_o} = \sqrt{1.33 \times 286.7 \times 3508}$

$a_o = 1156.56$ m/s

$$\gamma\left(\frac{2}{\gamma+1}\right)^{(\gamma+1)/2(\gamma-1)} = 1.33\left(\frac{2}{2.33}\right)^{2.33/0.66} = 0.7758$$

$$v^* = \frac{1156.56}{0.7758} = \mathbf{1490\ m/s} \quad \textbf{Ans.}$$

Example 13.5. A rocket flies at 10,080 kmph with an effective exhaust jet velocity of 1400 m/s and propellant flow rate of 5.0 kg/s. If the heat of reaction of the propellants is 6500 kJ/kg of the propellant mixture determine:

(*a*) Propulsion efficiency and propulsion power,

(*b*) engine output and thermal efficiency, and

(*c*) overall efficiency.

Solution. (*a*) $c_j = 1400$ m/s

$u = 10{,}080 \times 1000/3600 = 2800$ m/s

$\sigma = u/c_j = 2800/1400 = 2.0$

$$\eta_p = \frac{2\sigma}{1+\sigma^2} = \frac{2\times 2}{1+4} = 0.80 \quad \textbf{Ans.}$$

$F = \dot{m}_p \times c_j = 5 \times 1400 = 7000$ N

Propulsive power $= F \times u$

$P_p = 7000 \times 2800 \times 10^{-6}$

$P_p = \mathbf{19.6\ MW}$ **Ans.**

(*b*) $P_{En} = P_p/\eta_p$

$P_{En} = 19.6/0.8 = \mathbf{24.5\ MW}$ **Ans.**

Alternatively, $P_{En} = \frac{1}{2}\dot{m}_p (c_j^2 + u^2)$

$= 0.5 \times 5\,(1.4^2 + 2.8^2) \times 10^6$ watts

$= 2.5 \times 9.8 = \mathbf{24.5\ MW}$ **Ans.**

$$\eta_{th} = \frac{P_{En}}{\dot{m}_p Q_R}$$

$\dot{m}_p Q_R = 5 \times 6500 \times 1000$ watts

$\dot{m}_p Q_R = 32.5$ MW

$\eta_{th} = 24.5/32.5 = \mathbf{0.7538}$ **Ans.**

$\eta_o = \eta_p \times \eta_{th} = 0.8 \times 0.7538 = \mathbf{0.603}$ **Ans.**

Example 13.6. Determine the maximum velocity of a rocket and the altitude attained from the following data:

Mass ratio	= 0.15
Burn out time	= 75 s
Effective jet velocity	= 2500 m/s

What are the values of the velocity and altitude losses due to gravity? Ignore drag and assume vertical trajectory.

Solution. The maximum velocity is given by

$$u_p = c_j \ln \frac{1}{MR} - g\,t_p$$

$$u_p = 2500 \ln \frac{1}{0.15} - 9.81 \times 75$$

$$u_p = 4742.8 - 735.75 = \mathbf{4007.05\ m/s} \quad \textbf{Ans.}$$

The altitude gain is given by

$$Z = Z_p + Z_c$$

$$Z_p = c_j t_p \left\{ 1 + \left(1 - \frac{1}{\zeta} \right) \ln \frac{1}{MR} \right\} - \frac{1}{2} g t_p^2$$

$$\zeta = 1 - MR = 1 - 0.15 = 0.85$$

$$\frac{1}{2} g t_p^2 = \frac{9.81 \times 75^2 \times 0.5}{1000} = 27.59 \text{ km}$$

$$Z_p = \frac{2500 \times 75}{1000} \left\{ 1 + \left(1 - \frac{1}{0.85} \right) \ln \frac{1}{0.15} \right\} - 27.59$$

$$Z_p = 124.72 - 27.59 = 97.13 \text{ km}$$

$$Z_c = \frac{1}{2} \frac{u_p^2}{g} = \frac{0.5}{9.81} \times \frac{4007.03^2}{1000} = 818.36 \text{ km}$$

$$Z = 97.13 + 818.36 = \mathbf{915.49\ km} \quad \textbf{Ans.}$$

Velocity loss due to gravity is

$$g t_p = 735.75 \text{ m/s} \quad \textbf{Ans.}$$

Altitude loss due to gravity is

$$\frac{1}{2} g t_p^2 = 27.59 \text{ km} \quad \textbf{Ans.}$$

Example 13.7. A missile has a maximum flight speed to jet speed ratio of 0.2105 and specific impulse equal to 203.88 seconds. Determine for a burn out time of 8 seconds:

(*a*) effective jet velocity,

(*b*) mass ratio and propellant mass fraction,

(*c*) maximum flight speed, and

(*d*) altitude gain during powered and coasting flights.

Solution. (*a*) $c_j = g I_s$

$$c_j = 9.81 \times 203.88 = \mathbf{2000.06\ m/s} \quad \textbf{Ans.}$$

(*b*)
$$u_p = c_j \ln \frac{1}{MR} - g t_p$$

$$\frac{u_p}{c_j} = \ln \frac{1}{MR} - g t_p / c_j$$

$$0.2105 = \ln \frac{1}{MR} - 9.81 \times \frac{8}{2000.06}$$

$$\ln \frac{1}{MR} = 0.2105 + 0.0392 = 0.2497$$

$$\frac{1}{MR} = 1.281, \quad MR = \mathbf{0.780} \quad \textbf{Ans.}$$

$$\zeta = 1 - MR = 1 - 0.780 = \mathbf{0.220} \quad \textbf{Ans.}$$

(*c*)
$$u_p / c_j = 0.2105$$

$$u_p = 0.2105 \times 2000.06 = 2121 \text{ m/s}$$

$$u_p = \mathbf{1515.65\ kmph} \quad \textbf{Ans.}$$

(*d*)
$$Z_p = c_j t_p \left\{ 1 + \left(1 - \frac{1}{\zeta} \right) \ln \frac{1}{MR} \right\} - \frac{1}{2} g t_p^2$$

$$Z_p = 2000.06 \times 8 \left\{ 1 + \left(1 - \frac{1}{0.22} \right) \ln \frac{1}{0.780} \right\} - \frac{1}{2} \times 9.81 \times 8^2$$

$$Z_p = 1593.94 \text{ m} = \mathbf{1.594\ km} \quad \textbf{Ans.}$$

$$Z_c = \frac{1}{2} \frac{u_p^2}{g}$$

$$Z_c = 0.5 \times 421^2 / 9.81 \times 1000$$

$$Z_c = 9.0336 \text{ km} \quad \textbf{Ans.}$$

Example 13.8. Calculate the orbital and escape velocities of a rocket at mean sea level and an altitude of 300 km from the following data:

Radius of earth at mean sea level = 6341.6 km

Acceleration due to gravity at mean sea level = 9.809 m/s^2

Solution. At $Z = 0$

$$u_{orb} = \sqrt{g_o R_o} = (9.809 \times 6341.6 \times 1000)^{1/2}$$

$$u_{orb} = \mathbf{7887\ m/s} \quad \textbf{Ans.}$$

$$u_{esc} = \sqrt{2}\, u_{orb} = \sqrt{2} \times 7887$$

$$u_{esc} = \mathbf{11{,}154\ m/s} \quad \textbf{Ans.}$$

At $Z = 300$ km

$$R = R_o + Z = 6341.6 + 300 = 6641.6 \text{ km}$$

$$u_{orb} = R_o \sqrt{\frac{g_o}{R_o + Z}} = 6341.6 \times 1000 \sqrt{\frac{9.809}{6641.6 \times 1000}}$$

$$u_{orb} = 7706.8 \text{ m/s} \quad \textbf{Ans.}$$

$$u_{esc} = \sqrt{2} \times 7706.8 = \mathbf{10{,}899.96\ m/s} \quad \textbf{Ans.}$$

QUESTIONS AND PROBLEMS

13.1 (*a*) Describe briefly three early rockets.

(*b*) Enumerate five methods of modern rocket propulsion.

13.2 What is rocket propulsion? Why is a rocket called a non-airbreathing engine?

13.3 Draw neat sketches explaining the general working of the following rocket engines:

(*a*) Liquid propellant engine,
(*b*) Solid propellant engine,
(*c*) Hybrid engine,
(*d*) Electrical rocket,
(*e*) Nuclear rocket.

13.4 Describe briefly three important applications of rocket propulsion.

13.5 Draw a simple sketch of a multi-stage rocket vehicle depicting clearly (*i*) the booster stage, (*ii*) propellant tanks and exhaust nozzle, (*iii*) instruments and navigational equipment, and (*iv*) the space craft.

13.6 What is gas pressurization and its purpose in rocket engines? Describe with the aid of a sketch.

13.7 (*a*) Draw a neat sketch of a turbo-pump feed system employed in rockets.

(*b*) How does cavitation occur in this system and what measures are taken to prevent it?

(*c*) What is the effect of cavitation on the operation of the rocket?

13.8 (*a*) State briefly five important properties desired in a liquid propellant.

(*b*) Write down five advantages of liquid propellant rockets and three disadvantages.

13.9 Explain briefly what is meant by

(*a*) monopropellants,
(*b*) hypergolic propellants,
(*c*) bipropellants,
(*d*) UDMH,
(*e*) RFNA,
(*f*) JATO.

13.10 Write down names, chemical formulas and molecular weights of seven liquid propellants with their oxidizers.

13.11 (*a*) What is regenerative heating of a propellant in a liquid propellant rocket?

(*b*) What is the purpose of injectors in rocket engines? Describe an injector with the aid of a sketch.

13.12 (*a*) What are the various methods of ignition employed in liquid propellant rockets?

(*b*) What is ignition delay?

(*c*) Describe the events leading to pressure oscillations in a rocket combustor.

13.13 (*a*) What are cryogenic propellants?

(*b*) Give names and important properties of two such propellants.

(*c*) State the main advantages and disadvantages of cryogenic propellants.

13.14 What are composite and homogeneous organic solid propellants for rockets?

Describe ten important properties of the solid propellants desired for rocket propulsion.

13.15 Explain briefly the following terms in solid propellant rockets:

(*a*) Linear burning rate,
(*b*) combustion rate,
(*c*) propellant area ratio,

(*d*) equilibrium combustion pressure,
(*e*) cigarette burning.

13.16 Describe with the aid of illustrative diagrams two arrangements of solid propellant grains employed for restricted and unrestricted burning. Indicate the directions of burning and flow of gases.

13.17 Draw curves to depict the variation of the following quantities in solid propellant rockets:

(*a*) burning rate and propellant area ratio with combustion pressure,

(*b*) thrust vs time.

13.18 How are regressive, neutral and progressive burning of the solid propellant grain achieved? Explain with the aid of diagrams.

13.19 (*a*) State seven advantages and five disadvantages of solid propellant rockets.

(*b*) Give three examples in which they are preferred to other types.

13.20 Explain briefly the meanings of the following terms:

(*a*) Booster rocket stage,
(*b*) Retro-rockets,
(*c*) Sustainer stage,
(*d*) Earth satellite,
(*e*) Stationary satellite,
(*f*) coasting,
(*g*) Burnt out,
(*h*) ICBM,
(*i*) IRBM.

13.21 Show graphically the variation of the following quantities in rocket propulsion:

(*a*) Rocket thrust with altitude,
(*b*) Thrust coefficient vs exhaust nozzle pressure ratio, p_o/p_e,
(*c*) Thrust efficiency vs speed ratio of the rocket,
(*d*) Propulsive efficiency vs speed ratio of the rocket,
(*e*) Maximum rocket velocity vs mass ratio,
(*f*) Acceleration due to gravity vs altitude.

13.22 Define the following quantities; write down their formulas and units: Specific impulse, total impulse, average impulse and specific propellant consumption.

13.23 Derive the following expressions for rockets:

(*a*) $$I_s = \frac{c_{max}}{g}\left\{1 - \left(\frac{p_e}{p_o}\right)^{(\gamma-1)/\gamma}\right\}^{1/2}$$

(*b*) $$\text{Propulsive efficiency} = \frac{2\sigma}{1+\sigma^2}$$

where σ = speed ratio of the rocket

(*c*) Thermal efficiency of the rocket engine

$$= \frac{c_j^2}{2Q_R}(1+\sigma^2)$$

13.24 Define the following quantities in space rocket propulsion: Mass ratio, propellant mass fraction, velocity loss and altitude loss due to gravity.

13.25 (*a*) Derive an expression for the velocity of a rocket-vehicle at the end of the powered flight.

(*b*) What is the effect of mass ratio, specific impulse and burn out time on the maximum velocity attained by the rocket-vehicle?

(*c*) Using the above expression for maximum velocity derive the following relation for the altitude gain during the powered flight:

$$Z_p = c_j t_p \left\{1 + \left(1 - \frac{1}{\zeta}\right)\ln\frac{1}{MR}\right\} - \frac{1}{2} g t_p^2$$

13.26 (*a*) Prove that the overall efficiency of a rocket engine is given by $\sigma c_j^2/Q_R$

(*b*) Calculate thrust, specific impulse, propulsive, thermal and overall efficiencies of a rocket engine from the following data:

Effective jet velocity	= 1250 m/s
Flight to jet speed ratio	= 0.80
Oxidizer flow rate	= 3.5 kg/s

Fuel flow rate = 1.0 kg/s
Heat of reaction per kg of the exhaust gases = 2500 kJ/kg

Ans. $F = 5.625$ kN, $I_s = 127.42$ s, $\eta_p = 0.975$, $\eta_{th} = 0.5125$, $\eta_o = 0.50$.

13.27 A rocket nozzle has a throat area of 18 cm^2 and combustion chamber pressure of 25 bar. If the specific impulse is 127.42 seconds and weight flow rate 44.145 N/s. Determine:

(*a*) the thrust coefficient,
(*b*) propellant weight flow coefficient,
(*c*) specific propellant consumption, and
(*d*) the characteristic velocity.

Ans. $C_F = 1.25$, $C_w = 0.00981$, SPC = 0.00785, $v^* = 1000$ m/s.

13.28 The data for a rocket engine is given below:

combustion chamber pressure = 38 bar
combustion chamber temperature = 3500 K
oxidizer flow rate = 41.67 kg/s
mixture ratio = 5.0
properties of the exhaust gases $\gamma = 1.3$, $R = 287$ J/kg K

If the expansion in the rocket nozzle takes place to the ambient pressure 583.59 N/m^2 calculate:

(*a*) nozzle throat area,
(*b*) thrust,
(*c*) thrust coefficient,
(*d*) characteristic velocity,
(*e*) exit velocity of exhaust gases,
(*f*) maximum possible exhaust velocity.

Ans. (*a*) 197.65 cm^2, (*b*) 129.940 kN, (*c*) 1.730, (*d*) 1502.02 m/s. (*e*) 2598.9 m/s, (*f*) 2950.5366 m/s.

13.29 (*a*) How does the development of thrust in a rocket engine differ from that in a turbojet engine? Explain briefly.

(*b*) Write down expression for the forces acting on a rocket due to

(*i*) change in momentum flux and

(*ii*) the pressure difference between the ambient and the nozzle exhaust pressure.

(*c*) Calculate the thrust, effective jet velocity and the specific impulse for a rocket operating at an altitude of 20 km with the following data:

Propellant flow rate = 1.0 kg/s
Thrust chamber pressure = 27.5×10^5 N/m^2
Thrust chamber temperature = 2400 K
Nozzle area ratio = 10.2
Thermodynamic properties of the exhaust gases:
$\gamma = 1.3$, $R = 355$ J/kg K

Ans. $F = 2.309$ kN, $c_j = 2309$ m/s, $I_s = 235.37$ s.

13.30 A rocket has an initial mass of 3600 kg at take-off. The effective jet velocity for the duration of powered flight of 80 seconds remains constant at 2070 m/s. The maximum velocity of the rocket during the flight (assumed vertical) is twice the effective jet velocity.

Calculate the flow rate of the propellants, thrust in kilo Newtons and the values of the altitude gains during powered and coasting flights.

Ans. 40.831 kg/s, 84.52 kN, 94 km, 873.58 km.

13.31 A rocket engine has the following data:

thrust coefficient = 1.2
propellant flow rate = 20 N/s
combustion chamber pressure = 15×10^5 N/m^2
Exhaust nozzle throat diameter = 5 cm

From the above data compute the values of thrust, specific impulse, effective jet velocity and the characteristic velocity.

Ans. $F = 3.5343$ kN, $I_s = 176.715$ s, $c_j = 1733.574$ m/s, $v^* = 1444.645$ m/s.

13.32 (*a*) Define orbital and escape velocities of a rocket-vehicle. Derive the following relation:

$$u_{esc} = \sqrt{2}\, u_{orb} = R_o \left(\frac{2g_o}{R_o + Z} \right)^{1/2}$$

(*b*) Depict graphically the variations of orbital and escape velocities with altitude.

(*c*) The diameter of earth at the mean sea level is 12,683.2 km and the acceleration due to gravity 9.809 m/s^2; determine the values of the orbital and escape velocities of a rocket-propelled space craft at an altitude of 500 km.

Ans. 7.593 km/s, 10.739 km/s.

14

Miscellaneous Problems in Compressible Flow

The solved examples in this chapter cover the entire subject matter of compressible flow included in this book. For convenience and reference, examples are given almost in the same order as the main chapters. Notation used is the same as in the previous chapters.

For air following values have been used in the calculations:

$$\gamma = 1.4,\ R = 287\ \text{J/kg K}\ \ c_p = 1005\ \text{J/kg K}$$

The examples are designed to provide a deeper and wider understanding of the compressible flow problems and practical applications. In some problems the results of calculations have been presented in tabular form for useful comparisons.

Figures, sketches and graphical depictions have been generously employed to support the calculations in the examples.

Example 14.1. A rectangular duct has a cross-section of 15 cm × 20 cm. Air flows in the duct at a velocity of 60 m/s. If the kinematic viscosity of air is 17.90×10^{-6} Ns/m^2 calculate the friction factor by Falkner's formula.

Solution. Hydraulic mean diameter of the duct is given by

$$d = 4\frac{A}{P} = \frac{4\,(15 \times 20)}{2\,(15 + 20)} = 17.142\ \text{cm}$$

The Reynolds number of the flow is

$$\text{Re} = \frac{cd}{\nu}$$

$$\text{Re} = \frac{60 \times 0.17142}{17.9} \times 10^6 = 5.745 \times 10^5$$

By Falkner's formula friction factor is given by

$$f = \frac{0.0306}{\text{Re}^{1/7}}$$

$$f = 0.0306/(574500)^{1/7}$$

$$\boldsymbol{f = 0.00462} \quad \textbf{Ans.}$$

Example 14.2. Calculate the height (in metres) above mean sea level for

(*a*) the atmospheric temperature (absolute) to fall to 0.774 times its value at the *msl*.

(*b*) the atmospheric pressure to decrease to 0.30 times its value of the *msl*.

The *msl* value of the temperature is 288.2 K.

Solution. (*a*) $T = T^0 - \alpha Z = 0.774T^o$

$$\alpha Z = 0.226T^0$$

$$Z = 0.226 \times 288.2/6.5 = 10.020 \text{ km}$$

$$\boldsymbol{Z = 10{,}020 \text{ metres}} \quad \textbf{Ans.}$$

(*b*) $$\frac{p}{p^0} = \left(1 - \frac{\alpha Z}{T^0}\right)^{g/\alpha R}$$

$$1 - \frac{\alpha Z}{T^0} = \left(\frac{p}{p^0}\right)^{\alpha R/g}$$

$$\alpha R/g = 0.0065 \times 287/9.81 = 0.19$$

$$1 - \frac{0.0065Z}{288.2} = 0.3^{0.19} = 0.7955$$

$$Z = 0.2045 \times 288.2/0.0065 = \textbf{9067.2 m} \quad \textbf{Ans.}$$

Example 14.3. Using equations of continuity and state obtain the following relation for steady flow of an ideal gas:

$$\frac{dp}{p} - \frac{dT}{T} + \frac{dA}{A} + \frac{dc}{c} = 0.$$

Solution. Continuity equation gives $\dot{m} = \rho Ac = \text{constant}$

Taking logs we have

$$\ln \rho + \ln A + \ln c = \ln (\text{constant})$$

Differentiating $$\frac{d\rho}{\rho} + \frac{dA}{A} + \frac{dc}{c} = 0 \qquad (1)$$

The equation of state for an ideal gas gives

$$pv = RT$$

Now $$v = \frac{1}{\rho}$$

Therefore, $$p = \rho RT$$

By logarithmic differentiation we get

$$\ln p = \ln \rho + \ln R + \ln T$$

$$\frac{dp}{p} = \frac{d\rho}{\rho} + \frac{dT}{T}$$

$$\frac{d\rho}{\rho} = \frac{dp}{p} - \frac{dT}{T} \qquad (2)$$

Equation (2) in (1) gives

$$\frac{dp}{p} - \frac{dT}{T} + \frac{dA}{A} + \frac{dc}{c} = 0$$

Example 14.4. An air-jet has a velocity temperature equal to twice its static temperature ($T = 300$ K); the static pressure is 2.0 bar. Determine:

(*a*) Mach numbers M and M^* of the jet,

(*b*) stagnation pressure and temperature, and

(*c*) the critical velocity of flow and sound.

Solution. $T = 300$ K, $p = 2.0$ bar

Stagnation temperature is given by

$$T_0 = T + \frac{c^2}{2c_p}$$

$$T_0 = T + 2T = 3T$$

$$\frac{T_0}{T} = 1 + \frac{\gamma - 1}{2} M^2 = 3$$

$$1+\frac{1.4-1}{2}M^2=3$$

$$M^2=10$$

$$M=\sqrt{10}=\mathbf{3.162}\quad\textbf{Ans.}$$

$$T_0=3T=3\times300=\mathbf{900\ K}\quad\textbf{Ans.}$$

Stagnation pressure is given by

$$\frac{p_0}{p}=\left(\frac{T_0}{T}\right)^{\frac{\gamma}{\gamma-1}}=3.0^{3.5}=46.765$$

$$p_0=2\times46.765=\mathbf{93.53\ bar}\quad\textbf{Ans.}$$

$$M^{*2}=\frac{\frac{\gamma+1}{2}M^2}{1+\frac{\gamma-1}{2}M^2}=\frac{1.2\times10}{1+0.2\times10}=4$$

$$M^*=2\quad\textbf{Ans.}$$

$$\frac{T_0}{T^*}=\frac{\gamma+1}{2}=1.2,\ T^*=\frac{T_0}{1.2}=\frac{900}{1.2}=750\ \text{K}$$

$$c^*=a^*=\sqrt{\gamma RT^*}$$

$$c^*=\sqrt{1.4\times287\times750}=\mathbf{548.95\ m/s}\quad\textbf{Ans.}$$

Example 14.5. A centrifugal fan has radially tipped rotor blades. The inner and outer diameters of the blade ring are 15 cm and 25 cm respectively. The breadth of the blades at exit is 10 cm and density of air 1.3 kg/m^3. The fan runs at 1450 rpm and has an efficiency of 75 per cent.

The blades have an angle of 30 degrees (from the tangential direction) at entry. The flow has no tangential component of the absolute velocity at entry and has a constant value of the normal component.

Calculate for this fan (*a*) the flow rate of air, (*b*) power required, and (*c*) the pressure developed.

Solution. Figure 14.1 (*a*) shows the control surface enclosing the fan rotor blade ring. The tangential and normal velocity vectors at the entry and exit of the rotor blades are shown. Notation of Chapter 3 is used here.

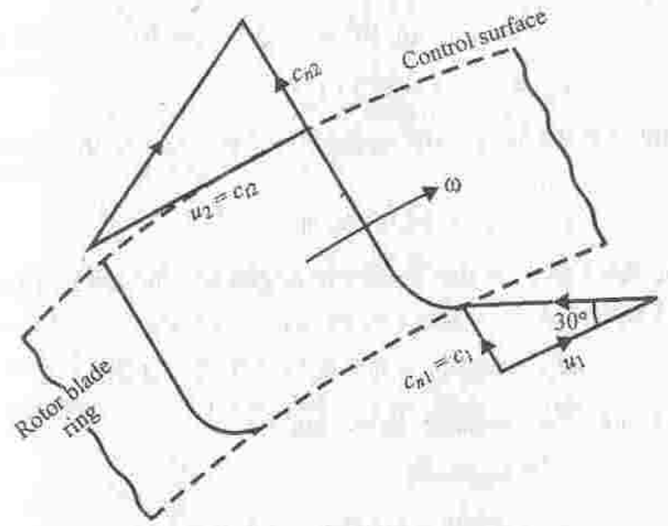

(*a*) Control surface enclosing the fan rotor blade ring (Example 14.5)

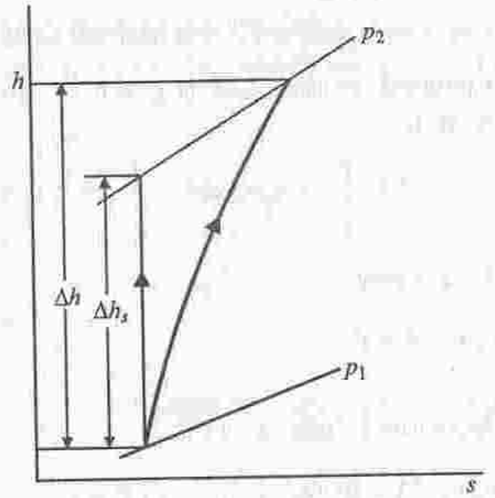

(*b*) Isentropic and actual values of enthalpy rise in the fan (Example 14.5)

FIGURE 14.1

The peripheral velocities at the entry and exit are

$$u_1=\pi d_1 N/60=\pi\times0.15\times1450/60=11.388\ \text{m/s}$$

$$u_2=\pi d_2 N/60=\pi\times0.25\times1450/60=18.98\ \text{m/s}$$

At the entry $c_{t1}=0$, $\dfrac{c_{n1}}{u_1}=\tan 30^\circ$

$$c_{n1} = u_1 \times \tan 30^\circ = 11.388 \tan 30^\circ = 6.575 \text{ m/s}$$

$$c_{n1} = c_{n2} = 6.575 \text{ m/s}$$

At the exit the tangential component is equal to the rotor peripheral velocity.

$$c_{t2} = u_2 = 18.98 \text{ m/s}$$

(*a*) If the thickness of the blades is neglected the area of cross-section at exit is

$$A_2 = \pi d_2 b_2 = \pi \times 0.25 \times 0.10 = 0.0785 \text{ m}^2$$

Therefore, the volume flow rate is

$$Q = c_{n2} \times A_2$$

$$Q = 6.575 \times 0.0785 = 0.516 \text{ m}^3/\text{s}$$

$$= \mathbf{30.96 \text{ m}^3/\text{min}} \quad \textbf{Ans.}$$

The mass flow, rate is

$$\dot{m} = \rho_2 c_{n2} A_2 = 1.3 \times 0.516 = \mathbf{0.6708 \text{ kg/s}} \quad \textbf{Ans.}$$

(*b*) The torque exerted on the fluid is given by Equation (3.31). For steady flow it is

$$\tau = \int_{\text{out}} \rho r c_n c_t \, dA - \int_{\text{in}} \rho r c_n c_t \, dA$$

Since $c_t = 0$ at entry

$$\int_{\text{in}} \rho r c_n c_t \, dA = 0$$

For one-dimensional flow at exit

$$\int_{\text{out}} \rho r c_n c_t \, dA = (\rho_2 c_{n2} A_2) r_2 c_{t2} = \dot{m} r_2 c_{t2}$$

Therefore, $\tau = \dot{m} r_2 c_{t2} = 0.6708 \times 0.125 \times 18.98$

$$\tau = 15.917 \text{ mN}$$

The rotational speed $\omega = \dfrac{2\pi N}{60}$

$$\omega = 2\pi \times 1450/60 = 151.84 \text{ rad/s}$$

Therefore, power required to drive the fan is

$$P = \tau \times \omega$$

$$P = 15.917 \times 151.84/1000 = \mathbf{2.416 \text{ kW}} \quad \textbf{Ans.}$$

(*c*) The actual enthalpy rise is

$$\Delta h = 2416/0.6708 = 3601.67 \text{ J/kg}$$

The isentropic enthalpy rise is

$$\Delta h_s = \eta \times \Delta h$$

$$\Delta h_s = 3601.67 \times 0.75 = 2701.25 \text{ J/kg}$$

Figure 14.1 (*b*) shows the isentropic and actual values of enthalpy rise.

For incompressible flow and small pressure rise

$$\Delta h_s = \frac{\Delta p}{\rho}$$

$$\Delta p = \rho \times \Delta h_s = 1.3 \times 2701.25 = 3511.62 \text{ N/m}^2$$

$$\Delta p = 357.96 \text{ kgf/m}^2 \text{ or } \mathbf{\text{mm W.G.}} \quad \textbf{Ans.}$$

Example 14.6. Using equations of continuity, state and energy obtain the following relations for steady isentropic flow of a gas:

(*a*) $\dfrac{dA}{A} = \dfrac{1}{2}(M^2 - 1)\dfrac{dc^2}{c^2}$

(*b*) $\dfrac{dA}{A} = \dfrac{(M^2 - 1)}{2\left(1 + \dfrac{\gamma - 1}{2} M^2\right)} \dfrac{dM^2}{M^2}$

Solution. (*a*) In the absence of shaft work adiabatic energy equation is

$$h + \frac{1}{2} c^2 = h_0 = \text{constant}$$

Differentiating $dh + c\,dc = 0$

For isentropic flow $dh = \dfrac{dp}{\rho}$

Therefore, $dp = -\rho c \, dc$ (1)

Continuity equation is

$$\dot{m} = \rho A c = \text{constant}$$

Taking logs and differentiating

$$dc = -c\left(\frac{d\rho}{\rho} + \frac{dA}{A}\right) \tag{2}$$

Equations (1) and (2) give

$$\frac{dA}{A} = \frac{dp}{\rho c^2}\left(1 - \frac{d\rho}{dp}c^2\right)$$

Substituting $a^2 = \frac{dp}{d\rho} = \left(\frac{\partial p}{\partial \rho}\right)_s$ for isentropic flow

$$\frac{dA}{A} = \frac{dp}{\rho c^2}\left(1 - \frac{c^2}{a^2}\right) = \frac{dp}{\rho c^2}(1 - M^2) \tag{3}$$

Substituting for dp in Equation (3) from Equation (1)

$$\frac{dA}{A} = (M^2 - 1)\frac{dc}{c}$$

$$\frac{dA}{A} = \frac{1}{2}(M^2 - 1)\frac{dc^2}{c^2} \tag{4}$$

(*b*) $$T_0 = T\left(1 + \frac{\gamma - 1}{2}M^2\right)$$

By logarithmic differentiation and noting that

$$dT_0 = 0$$

$$\frac{dT}{T} = -\frac{\gamma - 1}{2}\frac{dM^2}{1 + \frac{\gamma - 1}{2}M^2} \tag{5}$$

Mach number is given by

$$M^2 = \frac{c^2}{a^2} = \frac{c^2}{\gamma RT}$$

By logarithmic differentiation and noting that

$$\gamma R = \text{constant}$$

$$\frac{dM^2}{M^2} = \frac{dc^2}{c^2} - \frac{dT}{T}$$

Substituting from Equation (5) for $\frac{dT}{T}$ and simplifying

$$\frac{dc^2}{c^2} = \frac{dM^2}{M^2\left(1 + \frac{\gamma - 1}{2}M^2\right)} \tag{6}$$

Equation (6) in (4) yields

$$\frac{dA}{A} = \frac{M^2 - 1}{2\left(1 + \frac{\gamma - 1}{2}M^2\right)}\frac{dM^2}{M^2}$$

Example 14.7. Air is supplied to a convergent-divergent nozzle ($A^* = 10\ \text{cm}^2$) at $p_0 = 5$ bar, $T_0 = 1000$ K. What is the maximum flow rate of air in kg/s? The same nozzle is used for carbon dioxide ($\gamma = 1.18$, $R = 189$ J/kg K) at $T_0 = 1000$ K. What is the value of p_0 required for the same value of maximum flow rate?

Solution. $$\frac{\dot{m}_{\max}\sqrt{T_0}}{A^* p_0} = \sqrt{\frac{\gamma}{R}}\left(\frac{2}{\gamma + 1}\right)^{\frac{\gamma + 1}{2(\gamma - 1)}} = 0.0404 \text{ (for air)}$$

For air, $$\dot{m}_{\max} = 0.0404 \times 10 \times 10^{-4} \times 5 \times 10^5/\sqrt{1000}$$

$$\dot{m}_{\max} = \mathbf{0.6387\ kg/s} \quad \textbf{Ans.}$$

For carbon dioxide,

$$\sqrt{\frac{\gamma}{R}}\left(\frac{2}{\gamma + 1}\right)^{\frac{\gamma + 1}{2(\gamma - 1)}} = \sqrt{\frac{1.18}{189}}\left(\frac{2}{2.18}\right)^{\frac{2.18}{2 \times 0.18}} = 0.04687$$

$$p_0 = \dot{m}_{\max}\sqrt{T_0}/0.04687A^*$$

$$= \frac{0.6387\sqrt{1000}}{0.0468 \times 10 \times 10^{-4}}$$

$$= \mathbf{4.309 \times 10^5\ N/m^2} \quad \textbf{Ans.}$$

Example 14.8. An accelerating duct increases the Mach number of air from 0.2 to 0.9 between stations 1 and 2. Determine the area ratio A_1/A_2 of the duct. If the static temperature of air at station 1 is 500 K calculate:

(*a*) stagnation temperature,
(*b*) critical temperature,
(*c*) maximum possible velocity, and
(*d*) the static temperature at station 2.

Assume isentropic flow.

Solution. From isentropic flow gas tables ($\gamma = 1.4$)

At $M_1 = 0.2$,

$$A_1/A^* = 2.964 \quad T_1/T_0 = 0.992$$

At $M_2 = 0.9$,

$$A_2/A^* = 1.009 \quad T_2/T_0 = 0.861$$

The area ratio

$$\frac{A_1}{A_2} = \frac{A_1/A^*}{A_2/A^*} = \frac{2.964}{1.009} = \mathbf{2.937} \quad \textbf{Ans.}$$

(*a*) $T_0 = T_1/0.992 = 500/0.992 = \mathbf{504.03\ K}$ **Ans.**

(*b*) $$T^* = \frac{2}{\gamma+1} T_0$$

$$T^* = \frac{2}{1.4+1} \times 504.03 = \mathbf{420.025\ K} \quad \textbf{Ans.}$$

(*c*) $$c_{max} = \sqrt{\frac{2\gamma}{\gamma-1} RT_0}$$

$$= \left(\frac{2 \times 1.4}{0.4} \times 287 \times 504.03 \right)^{1/2}$$

$$= \mathbf{1006.2\ m/s} \quad \textbf{Ans.}$$

(*d*) $$T_2 = \frac{T_2/T_0}{T_1/T_0} \times T_1$$

$$= \frac{0.861}{0.992} \times 500$$

$$= \mathbf{433.97\ K} \quad \textbf{Ans.}$$

Example 14.9. A supersonic diffuser has the following data: At entry $p_1 = 1.0$ bar, $T_1 = 300$ K, $M_1 = 2.0$. The area ratio of the diffuser

is 1.5945. Determine the exit Mach number, pressure and temperature of air for isentropic flow.

Solution. See Figure 14.2.

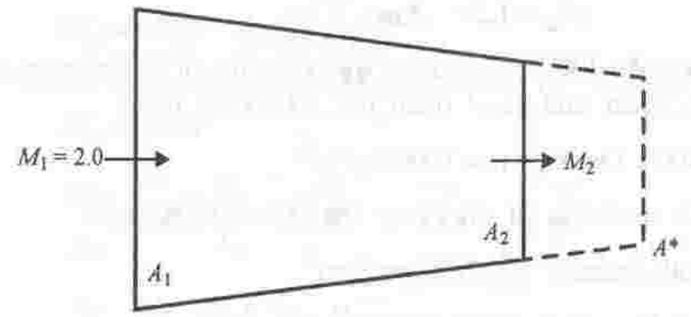

FIGURE 14.2 : Isentropic flow through a diffuser (Example 14.9)

From Isentropic flow gas tables ($\gamma = 1.4$) at $M_1 = 2.0$,

$$\frac{A_1}{A^*} = 1.687, \quad \frac{p_1}{p_{01}} = 0.128, \quad \frac{T_1}{T_{01}} = 0.555$$

$$p_{01} = p_1/0.128 = 1.0/0.128 = 7.8125 \text{ bar}$$

$$T_{01} = T_1/0.555 = 300/0.555 = 540.54 \text{ K}$$

$$\frac{A_2}{A^*} = \frac{A_2}{A_1} \times \frac{A_1}{A^*}$$

$$A_1/A_2 = 1.5945, \quad A_1/A^* = 1.687$$

$$\frac{A_2}{A^*} = \frac{1.687}{1.5945} = 1.058$$

From isentropic flow gas tables ($\gamma = 1.4$) at

$$\frac{A_2}{A^*} = 1.058$$

$$M_2 = 1.28, \quad \frac{p_2}{p_{02}} = 0.371, \quad \frac{T_2}{T_{02}} = 0.753$$

For isentropic flow

$$p_{02} = p_{01} = 7.8125 \text{ bar}$$

$$T_{02} = T_{01} = 540.54 \text{ K}$$

Therefore, $p_2 = 0.371 \times 7.8125 = \mathbf{2.898 \text{ bar}}$ **Ans.**

$$T_2 = 0.753 \times 540.54 = \mathbf{407.027 \text{ K}} \quad \textbf{Ans.}$$

$$M_2 = \mathbf{1.28} \quad \textbf{Ans.}$$

Example 14.10. Calculate the velocity of infinitesimal pressure waves in water and steel from the following data:

(*a*) **Water:** Density $\rho = 1000 \text{ kg/m}^3$

Bulk modulus of elasticity $K = 2.9 \times 10^9 \text{ N/m}^2$

(*b*) **Steel:** Density $\rho = 7.86 \text{ gm/cm}^3$

Modulus of elasticity $2 \times 10^{11} \text{ N/m}^2$.

Solution. (*a*) Water

$$a = \sqrt{\frac{K}{\rho}} = \left(\frac{2.9 \times 10^9}{1000} \right)^{1/2} = \mathbf{1702.9 \text{ m/s}} \quad \textbf{Ans.}$$

(*b*) Steel $a = \sqrt{\dfrac{E}{\rho}} = \left(\dfrac{2 \times 10^{11}}{7860} \right)^{1/2} = \mathbf{5044.3 \text{ m/s}}$ **Ans.**

Example 14.11. Calculate the velocity of sound in Freon at 373 K. Take $c_p = 0.678 \text{ kJ/kg K}$, $c_v = 0.593 \text{ kJ/kg K}$.

Solution. $\gamma = c_p/c_v = 0.678/0.593 = 1.1433$

$$R = c_p - c_v = 0.678 - 0.593 = 0.085 \text{ kJ/kg K}$$

Assuming ideal gas

$$a = \sqrt{\gamma RT}$$

$$a = (1.1433 \times 85 \times 373)^{1/2}$$

$$a = \mathbf{190.39 \text{ m/s}} \quad \textbf{Ans.}$$

Example 14.12. Calculate the Mach number upstream of a normal shock which would decelerate the flow of air downstream to half its velocity upstream of the shock. Verify the velocity ratio through pressure and temperature ratios across the shock.

Solution.
$$\frac{c_y}{c_x} = \frac{1 + \dfrac{\gamma - 1}{2} M_x^2}{\dfrac{\gamma + 1}{2} M_x^2} = 0.5$$

$$1 + \frac{\gamma - 1}{2} M_x^2 = 0.5 \left(\frac{\gamma + 1}{2} M_x^2 \right)$$

$$M_x^2 = 2.5$$

$$M_x = \mathbf{1.581} \quad \textbf{Ans.}$$

Verification: From normal shock gas tables ($\gamma = 1.4$) at

$$M_x = 1.581$$

$$\frac{p_y}{p_x} = 2.75, \quad \frac{T_y}{T_x} = 1.375$$

$$\frac{c_y}{c_x} = \frac{\rho_x}{\rho_y} = \frac{p_x}{p_y} \times \frac{T_y}{T_x}$$

$$\frac{c_y}{c_x} = \frac{1.375}{2.75} = 0.5 \text{ (verified)}$$

Example 14.13. Calculate the pressure and temperature of stagnant air in a duct initially at $p_1 = 1.2$ bar, $T_1 = 283$ K which has been traversed by (*a*) a non-steep finite pressure wave, (*b*) a steep pressure wave (normal shock wave). Take the wave velocity in both the cases as 405 m/s, (*c*) what is the value of the Mach number of the flow induced by these waves.

Solution. $a_1 = (\gamma RT_1)^{1/2} = (1.4 \times 287 \times 283)^{1/2} = 337.2 \text{ m/s}$

$$c_w = 405 \text{ m/s}$$

(*a*) See Figure 5.7

From Equation (5.38 (*a*)),

$$\frac{c_w}{a_1} = \frac{\gamma + 1}{\gamma - 1} \left(\frac{p_2}{p_1} \right)^{\frac{\gamma - 1}{2\gamma}} - \frac{2}{\gamma - 1} = \frac{405}{337.2} = 1.2$$

$$\frac{1.4 + 1}{1.4 - 1} \left(\frac{p_2}{p_1} \right)^{\frac{1.4 - 1}{2 \times 1.4}} - \frac{2}{1.4 - 1} = 1.2$$

$$\frac{p_2}{p_1} = 1.258, \quad p_2 = 1.258 \times 1.2 = \mathbf{1.509 \text{ bar}} \quad \textbf{Ans.}$$

The non-steep wave is an isentropic wave. Therefore,

$$\frac{T_2}{T_1} = \left(\frac{p_2}{p_1}\right)^{\frac{\gamma-1}{\gamma}} = 1.258^{1/3.5} = 1.068$$

$$T_2 = 1.068 \times 283 = \mathbf{302\ K} \quad \textbf{Ans.}$$

(*b*) See Figure 6.15

$$c_x = c_w,\ a_x = a_1,\ M_x = \frac{c_x}{a_x} = \frac{405}{337.2} = 1.2$$

From normal shock tables ($\gamma = 1.4$) at $M_x = 1.2$,

$$p_y/p_x = 1.513,\ T_y/T_x = 1.128$$

$$p_y = 1.513 \times 1.2 = \mathbf{1.815\ bar} \quad \textbf{Ans.}$$

$$T_y = 1.128 \times 283 = \mathbf{319.2\ K} \quad \textbf{Ans.}$$

Here the gas on *Y*-side of the wave has been traversed by the finite wave. The flow on the *X*-side appears to be occurring through the stationary wave at a velocity c_x.

(*c*) The Mach number of the induced flow for non-steep waves is given by Equation (5.39).

$$M = \frac{2}{\gamma - 1}\left[1 - \left(\frac{p_1}{p_2}\right)^{\frac{\gamma-1}{2\gamma}}\right]$$

$$M = 5\,(1 - 1.258^{-1/7}) = \mathbf{0.161} \quad \textbf{Ans.}$$

The Mach number of the induced flow for steep waves (normal shocks) is given by Equation (5.54).

$$M = \frac{p_2/p_1 - 1}{\left[\gamma\left(\frac{\gamma-1}{2}\right)\frac{p_2}{p_1}\left(\frac{\gamma+1}{\gamma-1} + \frac{p_2}{p_1}\right)\right]^{1/2}}$$

$$M = \frac{1.513 - 1}{[1.4 \times 0.2 \times 1.513\,(6 + 1.513)]^{1/2}} = \mathbf{0.287} \quad \textbf{Ans.}$$

For comparison the values are presented here in tabular form.

TABLE 14.1: Comparison of non-steep and steep pressure waves

Flow parameters	Non-steep wave	Steep wave (Normal shock)
c_w	405 m/s	405 m/s
p_2/p_1	1.258	1.513
M	0.161	0.287

Example 14.14. A supersonic diffuser has the following data for air flow ($\gamma = 1.4$):

Inlet Mach number $M_1 = 2.5$

Exit Mach number $M_2 = 0.30$

Area ratio $A_2/A_1 = 2.52$

(*a*) A normal shock occurs within the diffuser at Mach number M_x and area ratio A_x/A_1. Calculate the values of M_x and A_x/A_1 and the pressure ratio p_2/p_1.

(*b*) Calculate the values of area and pressure ratios A_2/A_1 and p_2/p_1 in an isentropic process for the same Mach numbers at the inlet and exit.

(*c*) Show the variation of static pressure along the diffuser in the above two cases.

Solution. Refer to Figure 14.3 (*a*).

From Isentropic flow gas tables ($\gamma = 1.4$) at $M_x = 2.5$

$$\frac{p_1}{p_{o1}} = \frac{p_1}{p_{ox}} = 0.0585,\ \frac{A_1}{A_1^*} = \frac{A_1}{A_x^*} = 2.637$$

At $M_2 = 0.30$

$$\frac{p_2}{p_{o2}} = \frac{p_2}{p_{oy}} = 0.939,\ \frac{A_2}{A_2^*} = \frac{A_2}{A_y^*} = 2.035$$

(*a*) From the above values we get

$$\frac{p_{o2}}{p_{o1}} = \frac{p_{oy}}{p_{ox}} = \frac{A_x^*}{A_y^*} = \frac{A_1/2.637}{A_2/2.035} = \frac{1}{2.52} \times \frac{2.035}{2.637} = 0.3062$$

From normal shock tables ($\gamma = 1.4$) at $\dfrac{p_{oy}}{p_{ox}} = 0.3062$

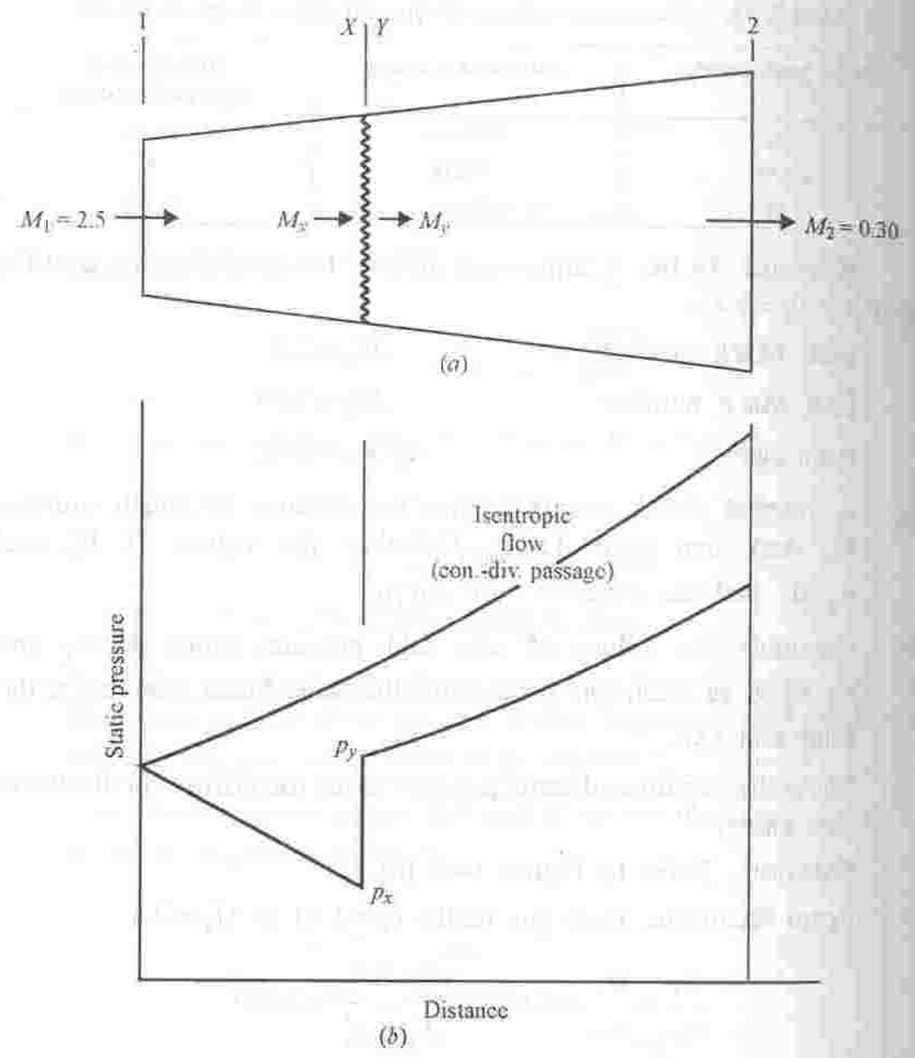

FIGURE 14.3 : Normal shock in a supersonic diffuser (Example 14.14)

$$M_x = 3.07,\ M_y = 0.470,\ \frac{p_y}{p_x} = 10.90$$

From Isentropic flow gas tables ($\gamma = 1.4$) at $M_x = 3.07$

$$A_x/A_x^* = 4.527$$

From the above values we get

$$\frac{A_x}{A_1} = \frac{A_x/A_x^*}{A_1/A_1^*} = \frac{4.527}{2.637} = \mathbf{1.716} \quad \textbf{Ans.}$$

$$M_x = \mathbf{3.07} \quad \textbf{Ans.}$$

The pressure ratio p_2/p_1 is given by

$$\frac{p_2}{p_1} = \frac{0.939\,p_{oy}}{0.0585\,p_{ox}}$$

Here $p_{o1} \neq p_{o2}$ on account of shock

$$p_{o1} = p_{ox} \text{ and } p_{o2} = p_{oy},\ \frac{p_{oy}}{p_{ox}} = 0.3062$$

Therefore, $$\frac{p_2}{p_1} = \frac{0.939 \times 0.3062}{0.0585} = \mathbf{4.915} \quad \textbf{Ans.}$$

(*b*) For isentropic flow for the same Mach numbers at inlet and exit,

$$\frac{A_2}{A_1} = \frac{A_2/A_2^*}{A_1/A_1^*} = \frac{2.035}{2.637} = \mathbf{0.7717} \quad \textbf{Ans.}$$

$$\frac{p_2}{p_1} = \frac{p_2/p_{o2}}{p_1/p_{o1}} = \frac{0.939}{0.0585} = \mathbf{16.05} \quad \textbf{Ans.}$$

Note that in isentropic flow

$$A_1^* = A_2^* \text{ and } p_{o1} = p_{o2}$$

(*c*) Variation of static pressure along the diffuser in the two cases in shown in Figures 14.3 (*b*).

Example 14.15. Air at Mach number 2.0 flows over three convex corners of a wall. The wall deflects by 5 degrees (clockwise) at each corner. Depict the isentropic expansion waves at these corners and the accelerating flow over the wall.

Calculate the Mach numbers downstream of these waves and the pressure and temperature ratios across them.

Solution. Refer to Figure 14.4 ($\delta = -5^o$)

From gas tables ($\gamma = 1.4$) for Prandtl-Meyer flow at

$$M_1 = 2.0,\ \omega_1 = 26.38$$

$$\omega_1 - \omega_2 = \delta$$

$$\omega_2 = \omega_1 - \delta = 26.38 - (-5) = 31.38^o$$

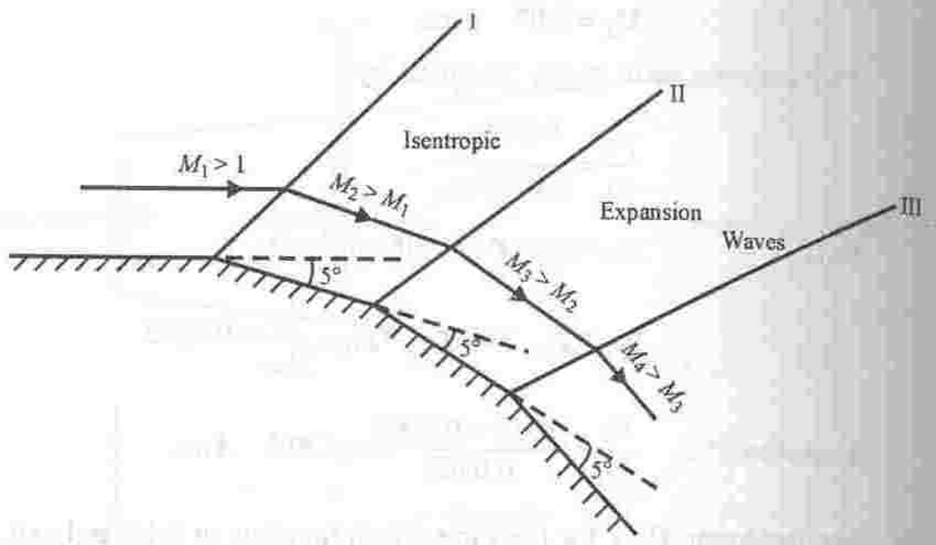

FIGURE 14.4 : Flow through isentropic expansion waves at the corners of a convex wall (Example 14.15)

ω_1 and ω_2 are the values of the Prandtl-Meyer functions upstream and downstream of the first wave corresponding to the Mach numbers M_1 and M_2.

From the gas tables Mach number M_2 corresponding to $\omega_2 = 31.38^\circ$ is $M_2 = 2.18$.

The values of the Prandtl-Meyer functions (ω) and the Mach numbers downstream of the II and III waves are also obtained as shown above.

The values of the pressure ratio p/p_0 and temperature ratio T/T_0 corresponding to the Mach numbers are obtained from isentropic flow tables. These values yield the values of pressure ratio and temperature ratio across the waves. As an example, for the first wave

$$\frac{p_1}{p_2} = \frac{(p/p_0)_1}{(p/p_0)_2} = \frac{0.128}{0.0965} = 1.326$$

$$\frac{T_1}{T_2} = \frac{(T/T_0)_1}{(T/T_0)_2} = \frac{0.555}{0.513} = 1.0818$$

Table 14.2 presents various values of ω, M, p_1/p_2 and T_1/T_2. Subscripts 1 and 2 represent the upstream and downstream values for the

waves. Values of the Prandtl-Meyer functions are given downstream of the waves I, II and III.

TABLE 14.2: Variation of flow parameters across isentropic waves

	Initial values	I wave	II wave	III wave	Overall values
δ	—	-5°	-5°	-5°	-15°
ω	26.38	31.38	36.38	41.38	41.38
M	2.0	2.18	2.38	2.60	2.6
p/p_0	0.128	0.0965	0.0706	0.0501	—
T/T_0	0.555	0.0513	0.469	0.425	—
p_1/p_2	—	1.326	1.367	1.409	2.555
T_1/T_2	—	1.0818	1.0938	1.1035	1.305

Example 14.16. Supersonic flow over a concave corner is deflected inwards by 15 degrees downstream of the wave. Assuming Prandtl-Meyer flow calculate the values of the downstream Mach number, pressure ratio and temperature ratio across the wave for upstream Mach numbers of 2.0 and 3.0.

Compare, these values with the corresponding values for oblique shocks.

Solution. Assume the wave as an isentropic compression wave. This is shown in Figure 14.5.

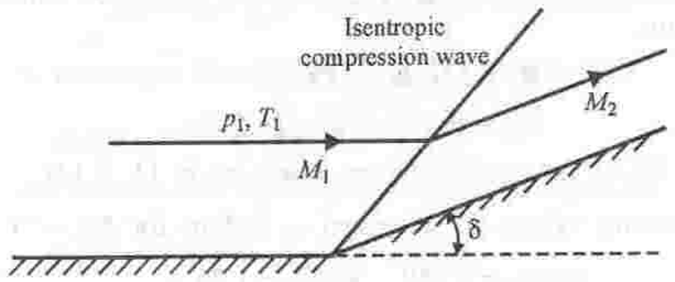

FIGURE 14.5 : Flow through isentropic compression wave (Example 14.16)

From gas tables ($\gamma = 1.4$) for Prandtl-Meyer function, at

$$M_1 = 2.0, \ \omega_1 = 26.38^\circ$$

$$\delta = \omega_1 - \omega_2$$

$$\omega_2 = \omega_1 - \delta = 26.38 - 15 = 11.38^\circ$$

From gas tables for Prandtl-Meyer function the Mach number M_2 corresponding to $\omega_2 = 11.38^\circ$ is 1.48.

The Mach number downstream of a weak oblique shock wave is 1.448 (see Example 7.1 (*a*) for the weak shock).

From isentropic flow tables ($\gamma = 1.4$)

$$\text{at } M_1 = 2.0,\ T_1/T_0 = 0.555,\ p_1/p_0 = 0.128$$

$$\text{at } M_2 = 1.48,\ T_2/T_0 = 0.695,\ p_2/p_0 = 0.280$$

p_0 and T_0 are constant in isentropic flow. Therefore,

$$\frac{p_2}{p_1} = \frac{p_2/p_0}{p_1/p_0} = \frac{0.28}{0.128} = 2.1875$$

$$\frac{T_2}{T_1} = \frac{T_2/T_0}{T_1/T_0} = \frac{0.695}{0.555} = 1.252$$

These values for weak oblique shock (Example 7.1 (*a*)) are

$$p_2/p_1 = 2.191, \quad T_2/T_1 = 1.267$$

Values of Mach number, pressure, temperature, etc. downstream of the isentropic wave at the corner can only be compared with their corresponding values in a flow through a weak oblique shock.

Since the deflection angle in this case is large compression wave/waves generated at the corner will be strong; therefore, the flow across them is far from isentropic. Thus the calculated values are only approximate.

At $M_1 = 3.0,\ \omega_1 = 49.757$

$$\omega_2 = 49.757 - 15 = 34.757$$

$M_2 = 2.32$ (2.25 for weak oblique shock as in Q. 7.14)

Following values are obtained as before for $M_1 = 2.0$

$$p_2/p_1 = 2.849, \quad T_2/T_1 = 1.35$$

For comparison the calculated values are presented in the Table 14.3.

TABLE 14.3: Comparison of Prandtl-Meyer flow with weak oblique shock flow ($\delta = 15^\circ$)

	Prandtl-Meyer flow	Weak oblique shock flow
M_1	2.0	2.0
M_2	1.48	1.448
p_2/p_1	2.1875	2.191
T_2/T_1	1.252	1.267

	Prandtl-Meyer flow	Weak oblique shock flow
M_1	3.0	3.0
M_2	2.32	2.25
p_2/p_1	2.849	2.80
T_2/T_1	1.350	1.40

Example 14.17. A 30 cm diameter, 2 meter long duct has a convergent-divergent nozzle fitted at its exit. It receives compressed air at $M_1 = 2.0$, $p_1 = 4.0$ bar, $T_1 = 300$ K. The friction factor for the duct is 0.003. The flow in the duct is adiabatic and isentropic in the nozzle.

A normal shock occurs in the duct at a Mach number $M_x = 1.8$. Determine:

(*a*) The length of the duct between the normal shock and the nozzle inlet.

(*b*) The throat and exit diameters of the nozzle for a Mach number of 2.0 at the nozzle exit.

(*c*) Nozzle exit pressure.

(*d*) Depict the variation of stagnation and static pressures along the duct and the nozzle.

Solution. Refer to Figure 14.6 (*a*), (*b*)

$$A_1 = A_2 = \frac{\pi}{4} D^2 = \frac{\pi}{4} \times 30^2 = 706.858 \text{ cm}^2$$

From isentropic flow tables ($\gamma = 1.4$) at $M_1 = 2.0$

$$p_1/p_{o1} = 0.128,\ A_1/A_1^* = 1.687$$

As the nozzle exit Mach number is also $M_F = 2.0$

$$p_E/p_{oE} = 0.128,\ A_E/A_E^* = 1.687$$

$$p_{o1} = p_1/0.128 = 4/0.128 = 31.25 \text{ bar}$$

$$A_1^* = A_1/1.687 = 706.858/1.687 = 419 \text{ cm}^2$$

From Fanno flow tables ($\gamma = 1.4$) at $M_1 = 2.0$

$$p_{o1}/p_{o1}^* = 1.687,\ \left(\frac{4\bar{f}L_{\max}}{D}\right)_1 = 0.305$$

$$p_{o1}^* = p_{o2}^* = p_{o1}/1.687 = 31.25/1.687 = 18.524 \text{ bar}$$

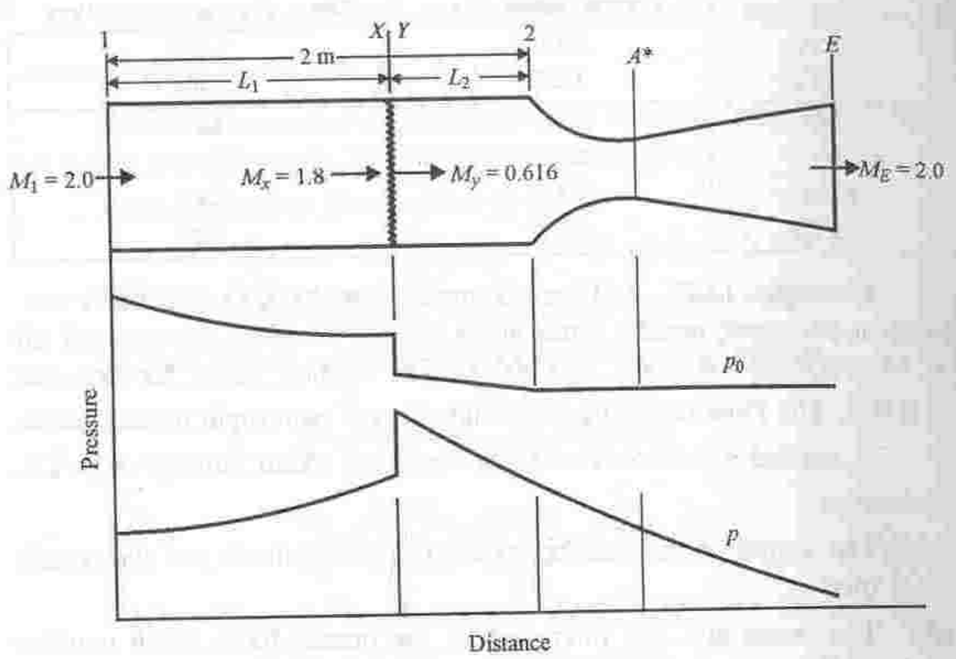

(*a*) Flow with friction and normal shock (Example 14.17)

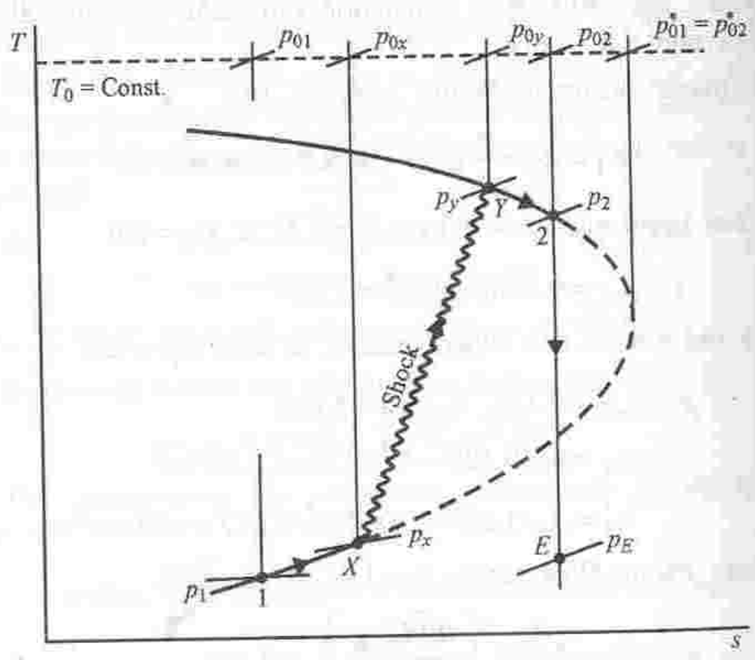

(*b*) Flow with friction and normal shock (Example 14.17)

FIGURE 14.6

At $M_x = 1.8$, $\left(\dfrac{4\bar{f}L_{\max}}{D}\right)_1 = 0.242$

For Fanno flow between 1 and X

$$\frac{4\bar{f}L_1}{D} = \left(\frac{4\bar{f}l_{\max}}{D}\right)_1 - \left(\frac{4\bar{f}L_{\max}}{D}\right)_x = 0.305 - 0.242 = 0.063$$

$$L_1 = 0.063 \times 0.3/4 \times 0.003 = 1.575 \text{ metre}$$

(*a*) Therefore, $L_2 = 2.0 - 1.575 = 0.425$ metre **Ans.**

$$\frac{4\bar{f}L_2}{D} = 4 \times 0.003 \times 0.425/0.3 = 0.017$$

(*b*) From normal shock tables ($\gamma = 1.4$) at $M_x = 1.8$, $M_y = 0.616$

From Fanno flow tables ($\gamma = 1.4$) at $M_y = 0.616$

$$\left(\frac{4\bar{f}L_{\max}}{D}\right)_y = 0.435$$

For Fanno flow between sections Y and 2

$$\left(\frac{4\bar{f}L_{\max}}{D}\right)_2 = \left(\frac{4\bar{f}L_{\max}}{D}\right)_y - \frac{4\bar{f}L_2}{D} = 0.435 - 0.017 = 0.418$$

From Fanno flow tables ($\gamma = 1.4$) at $\dfrac{4\bar{f}L_{\max}}{D} = 0.418$

$$M_2 = 0.62,\ p_{o2}/p_{o2}^* = 1.166$$

From isentropic flow tables ($\gamma = 1.4$) at $M_2 = 0.62$

$A_2/A_2^* = 1.166$, therefore,

$$A_2^* = A_2/1.166 = 706.858/1.166 = 606.22 \text{ cm}^2$$

For isentropic flow $A_E^* = A_2^* = 606.22 \text{ cm}^2$

This throat area can also be obtained directly from

$$A_1^* p_{o1} = A_e^* p_{oE}$$

$$\frac{\pi}{4} D_2^{*2} = 606.22 \text{ cm}^2,\ D_2^* = D_E^* = 27.789 \text{ cm} \quad \textbf{Ans.}$$

Now $A_E/A_E^* = 1.687$

$$A_E = 1.687 \times 606.22 = 1022.693 \text{ cm}^2$$

$$\frac{\pi}{4} D_E^2 = 1022.693, \quad D_E = 36.094 \text{ cm} \quad \textbf{Ans.}$$

Again the exit area A_E can also be determined from

$$A_E = \frac{A_E/A_E^*}{A_2/A_2^*} \times A_2 = \frac{1.687}{1.166} \times 706.858 = 1022.7 \text{ cm}^2$$

(*c*) The nozzle exit pressure is given by

$$p_E = 0.128 p_{oE} = 0.128 p_{o2} = 0.128\ (1.166 p_{o2}^*)$$

$$p_E = 0.128 \times 1.166 \times 18.524$$

$$p_E = 2.7645 \text{ bar} \quad \textbf{Ans.}$$

(*d*) Stagnation and static pressures and their variations are shown in Figure 14.6 (*a*), (*b*).

Example 14.18. A nozzle accelerates the flow of air to supersonic velocity upstream of a constant area duct ($\bar{f} = 0.0025$). The nozzle exit diameter is the same as duct diameter. Following pressures have been measured:

Stagnation pressure at the nozzle entry $p_0 = 10.0$ bar

Static pressure at station 1 downstream of the nozzle

$$p_1 = 1.50 \text{ bar}$$

Static pressure at station 2 further downstream in the duct

$$p_2 = 2.3 \text{ bar}$$

The cross-sectional areas of the nozzle throat and the duct are 188 cm^2 and 314 cm^2 respectively. The flow is isentropic upto the nozzle throat and adiabatic throughout downstream of the throat.

Calculate the Mach numbers at stations 1 and 2 and the distance between the two stations in terms of the ratio L/D.

Show the pressures p_1, p_2, p^* and p_{o1}, p_{o2}, p_o^* on the Fanno line.

Solution. See Figures 14.7 (*a*), (*b*)

For isentropic and adiabatic flows

$$\frac{p}{p_o} \times \frac{A}{A^*} = f(M)$$

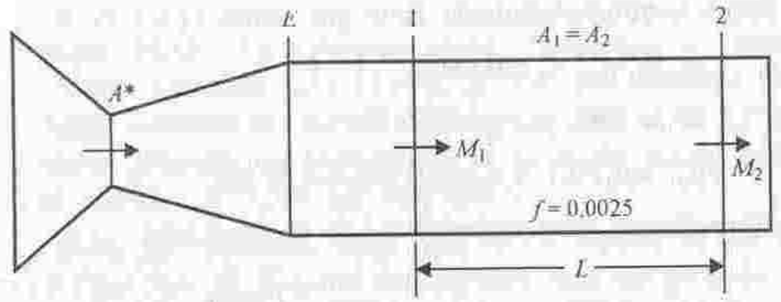

(a)

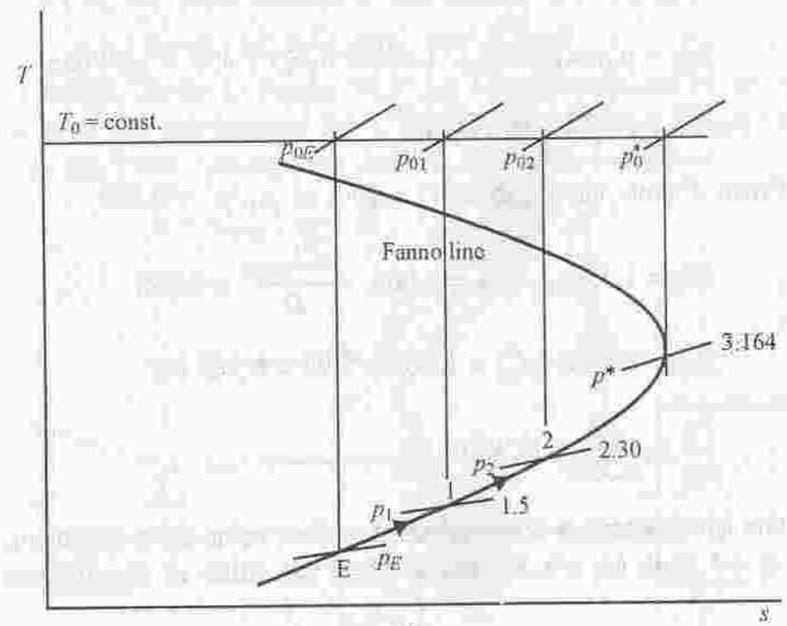

(b)

FIGURE 14.7 : Supersonic duct downstream of a nozzle (Example 14.18)

Since the flow upto the throat is isentropic and the rest of the flow is supersonic and adiabatic

$$\frac{\dot{m}_{\max} \sqrt{T_0}}{A^* p_0} = \frac{\dot{m}_{\max} \sqrt{T_{o1}}}{A_1^* p_{o1}} = \frac{\dot{m}_{\max} \sqrt{T_{o2}}}{A_2^* p_{o2}}$$

Therefore, $A^* p_0 = A_1^* p_{o1} = A_2^* p_{o2}$

At station 1, $\frac{p_1}{p_{o1}} \times \frac{A_1}{A_1^*} = \frac{1.5 \times 314}{p_{o1} A_1^*} = \frac{1.5 \times 314}{10 \times 188} = 0.2505$

From isentropic/adiabatic flow gas tables ($\gamma = 1.4$) at

$$p_1 A_1/p_{o1} A_1^* = 0.2505$$

$$\mathbf{M_1 = 1.80},\ p_1/p_{o1} = 0.174$$

$$p_{o1} = p_1/0.174 = 1.5/0.174 = 8.62 \text{ bar}$$

From Fanno flow tables ($\gamma = 1.4$) at $M_1 = 1.8$

$$p_1/p^* = 0.474,\ p_{o1}/p_{o1}^* = 1.439,\ \frac{4\bar{f}L_{max}}{D} = 0.242$$

$$p^* = p_1/0.474 = 1.5/0.474 = 3.164 \text{ bar}$$

$$p_{o1}^* = p_{o2}^* = p_o^* = p_{o1}/1.439 = 8.62/1.439 = 5.99 \text{ bar}$$

$$p_2/p^* = 2.3/3.164 = 0.727$$

From Fanno flow tables ($\gamma = 1.4$) at $p_2/p^* = 0.727$

$$\mathbf{M_2 = 1.3},\ p_{o2}/p_{o2}^* = 1.066,\ \frac{4\bar{f}L_{max}}{D} = 0.065$$

$$p_{o2} = 1.066 \times p_{o2}^* = 1.066 \times 5.99 = 6.385 \text{ bar}$$

$$\frac{p_2}{p_{o2}} = \frac{2.3}{6.385} = 0.3602$$

The Mach number corresponding to this value from isentropic flow tables ($\gamma = 1.4$) is $M_2 = 1.3$. This verifies the value of M_2 obtained earlier.

$$\left(\frac{4\bar{f}L_{max}}{D}\right)_1 - \left(\frac{4\bar{f}L_{max}}{D}\right)_2 = \frac{4\bar{f}L}{D}$$

$$0.242 - 0.065 = 4 \times 0.0025 \left(\frac{L}{D}\right)$$

$$\frac{L}{D} = 17.7 \quad \textbf{Ans.}$$

The Mach numbers at stations 1 and 2 are

$$\mathbf{M_1 = 1.8} \qquad \mathbf{M_2 = 1.3} \quad \textbf{Ans.}$$

Various static and stagnation pressures are shown in Figure 14.7 (*b*).

Example 14.19. An exhauster sucks air through a convergent nozzle of throat diameter ($D = 15$ cm). A constant diameter pipe of length L meters connects the nozzle to the suction side of the exhauster. The stagnation pressure and temperature of air at the nozzle entry are maintained constant at 1.789 bar and 400 K.

Calculate, for maximum flow rate, Mach number at the nozzle exit, mass flow rate of air, and the pressure and temperature of air at the inlet of the exhauster.

Assume isentropic flow in the nozzle and frictional flow ($\bar{f} = 0.003$) in the pipe. Compute the above values for

$$L = 0,\ 17.34D,\ 89D \text{ and } 1211D.$$

Solution. Refer to Figure 14.8. Let the exit sections of the nozzle and the pipe be represented by 1 and 2 respectively. For maximum flow rate the flow corresponds to the choking conditions *i.e.*,

$$\dot{m} = \dot{m}_{max},\ p_2 = p^*,\ T_2 = T^*,\ M_2 = 1$$

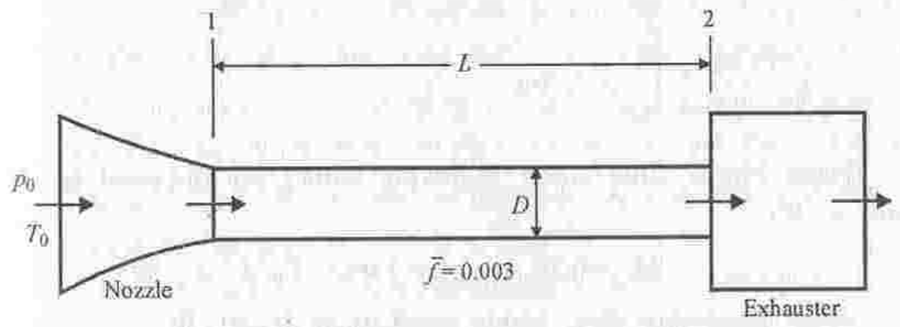

FIGURE 14.8 : Flow of air through convergent nozzle and pipe at the entry of an exhauster (Example 14.19)

In the absence of the pipe ($L = 0$), sections 1 and 2 are the same and

$$M_1 = M_2 = 1,\ T_1 = T_2 = T^*,\ p_1 = p_2 = p_n^*$$

It should be noted that $p_n^* \neq p^*$ (for Fanno line).

Here subscript n represents isentropic flow in the nozzle in the absence of the pipe. For such a flow, from gas tables ($\gamma = 1.4$) at $M = 1$

$$p_n^*/p_0 = 0.528,\ p_n^* = 0.528 \times 1.789 = 0.945 \text{ bar}$$

$$T^*/T_0 = 0.834,\ T^* = 0.834 \times 400 = 333.6 \text{ K}$$

$$\dot{m}_{max}\sqrt{T_0}/p_0 A^* = 0.0404$$

$$A^* = \frac{\pi}{4}D^2 = \frac{\pi}{4} \times 0.15^2 = 0.01767 \text{ m}^2$$

$$\dot{m}_{max} = 0.0404 \times 1.789 \times 10^5 \times 0.01767/\sqrt{400} = 6.385 \text{ kg/s}$$

In the presence of pipe Mach number at the nozzle exit would not be unity. For maximum flow rate ($M_2 = 1$). The state of air at the pipe exit is defined by p^*, T^*, c^* on the Fanno line.

For $L/D = 17.34$

$$\left(\frac{4\bar{f}L_{max}}{D}\right)_{M_1} - \left(\frac{4\bar{f}L_{max}}{D}\right)_{M_2} = \frac{4\bar{f}L}{D} = 4 \times 0.003 \times 17.34 = 0.208$$

For sonic flow at the pipe exit $\left(\frac{4\bar{f}L_{max}}{D}\right)_{M_2} = 0$. Therefore,

$$\left(\frac{4\bar{f}L_{max}}{D}\right)_{M_1} = 0.208$$

From Fanno flow tables following values are obtained for the value 0.208:

$$M_1 = 0.70,\ p_1/p^* = 1.493,\ T_1/T^* = 1.093$$

From isentropic flow tables ($\gamma = 1.4$) at $M_1 = 0.70$

$$p_1/p_{o1} = 0.721,\ p_1 = 0.721 \times 1.789 = 1.289 \text{ bar}$$

$$T_1/T_{o1} = 0.911,\ T_1 = 0.911 \times 400 = 364.4 \text{ K}$$

From these values,

$$p^* = p_1/1.493 = 1.289/1.493 = 0.8634 \text{ bar}$$

$$T^* = T_1/1.093 = 364.4/1.093 = 333.39 \text{ K}$$

This temperature has already been calculated as 333.60 K. The small difference is due to calculation error.

$$\rho^* = \frac{p^*}{RT^*} = \frac{0.8634 \times 10^5}{287 \times 333.60} = 0.9018 \text{ kg/m}^3$$

$$\dot{m}_{max} = \rho^* c^* A^*$$

$$c^* = (\gamma RT^*)^{1/2} = (1.4 \times 287 \times 333.60)^{1/2}$$
$$= 366.1 \text{ m/s}$$
$$\dot{m} = 0.9018 \times 366.11 \times 0.01767 = 5.833 \text{ kg/s}$$

Values of M_1, p^*, T^* and $\dot{m}$ for $L/D = 89$ and 1211 are calculated by the same method. The values are tabulated in Table 14.4 for comparison.

TABLE 14.4: Effect of pipe length on the gas dynamic parameters of flow with friction

L/D	0	17.34	89	1211
p_0	1.789	1.789	1.789	1.789
T_0	400	400	400	400
M_2	1.0	1.0	1.0	1.0
M_1	1.0	0.70	0.50	0.20
p^*	0.945	0.8634	0.705	0.3191
T^*	333.6	333.6	333.6	333.6
$\dot{m}$	6.385	5.833	4.761	2.154

For convenience in comparison given values of p_0, T_0 and M_2 are also included in the table. Following conclusions are drawn:

1. The maximum value of the maximum flow rate is obtained in the absence of the pipe between the nozzle and the exhauster.
2. The quantities M_1, p^* and $\dot{m}$ decrease significantly with the increase in the pipe length or L/D.

Example 14.20. In a compressed air system a variable area convergent nozzle is employed to limit the maximum flow rate. Following three cases are considered:

(*a*) A frictionless duct of 15 cm diameter is fitted with the variable area nozzle at its exit. Air enters the duct at $M_1 = 0.20$, $p_1 = 4.0$ bar, $T_1 = 400$ K. Calculate the flow rate and the nozzle exit area for maximum flow rate.

(*b*) Heat is supplied to the air raising the stagnation temperature of air in the duct to twice its value at entry. Recalculate the new value of nozzle throat area for the same value of the maximum flow rate.

(*c*) The duct ($d = 15$ cm) upstream of the nozzle is 63 meters long and has a friction factor of 0.006. If the entry to the duct remains at $M_1 = 0.2$, $p_1 = 4.0$ bar, $T_1 = 400$ K calculate the nozzle throat area for maximum flow rate value in (*a*) and (*b*).

Solution. (*a*) Refer to Figure 14.9 (*a*).

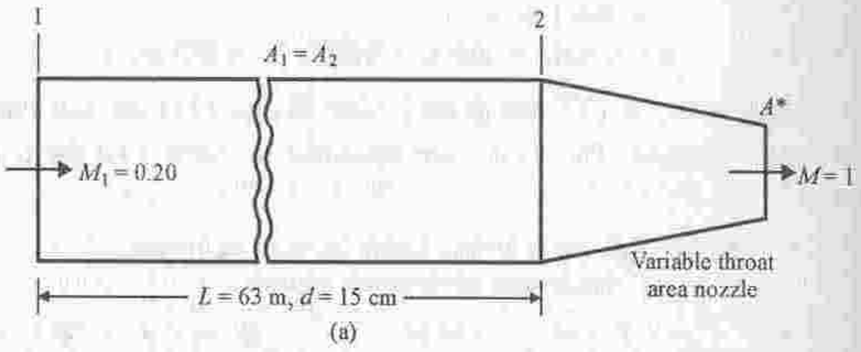

FIGURE 14.9 : Sonic nozzle downstream of a long duct (Example 14.20)

The area of cross-section of the duct is

$$A_1 = A_2 = \frac{\pi}{4} d^2 = \frac{\pi}{4} \times 15 \times 15 = 176.71 \text{ cm}^2$$

From isentropic flow tables ($\gamma = 1.4$) at

$$M_1 = 0.20$$

$$T_1/T_{o1} = 0.992,\ p_1/p_{o1} = 0.973,\ A_1/A_1^* = 2.964$$

$$T_{o1} = T_1/0.992 = 400/0.992 = 403.22 \text{ K}$$

$$p_{o1} = p_1/0.973 = 4.0/0.973 = 4.111 \text{ bar}$$

$$A_1^* = A_1/2.964 = 176.71/2.964 = \mathbf{59.618 \text{ cm}^2} \quad \textbf{Ans.}$$

In the frictionless duct $A_1^* = A_2^*$ = nozzle throat area

Maximum flow rate is given by

$$\dot{m}_{max} \sqrt{T_{o1}}/A_1^* p_{o1} = 0.0404$$

$$\dot{m}_{max} = 0.0404 \times 59.618 \times 10^{-4} \times 4.111 \times 10^5/\sqrt{403.22}$$

$$\dot{m}_{max} = \mathbf{4.934 \text{ kg/s}} \quad \textbf{Ans.}$$

This is also given by

$$\dot{m}_{max} = \rho_1 A_1 c_1$$

$$\rho_1 = \frac{p_1}{RT_1} = 4 \times 10^5/287 \times 400 = 3.484$$

$$c_1 = M_1 \sqrt{\gamma RT_1} = 0.2 \sqrt{1.4 \times 287 \times 400} = 80.18$$

$$\dot{m}_{max} = 3.484 \times 176.71 \times 10^{-4} \times 80.18 = \mathbf{4.936 \text{ kg/s}} \quad \textbf{Ans.}$$

The difference in the two values is due to small calculation error.

(*b*) Refer to Figure 14.10 (*a*), (*b*).

From Rayleigh flow tables ($\gamma = 1.4$) at $M_1 = 0.20$

$$p_{o1}/p_o^* = 1.235,\ T_{o1}/T_o^* = 0.174$$

$$p_o^* = p_{o1}/1.235 = 4.111/1.235 = 3.328 \text{ bar}$$

$$T_o^* = T_{o1}/0.174 = 403.22/0.174 = 2317.35 \text{ K}$$

$$T_{o2} = 2 \times T_{o1} = 2 \times 403.22 = 806.44 \text{ K}$$

$$T_{o2}/T_o^* = 806.44/2317.35 = 0.348$$

From Rayleigh flow tables ($\gamma = 1.4$) at

$$T_{o2}/T_o^* = 0.348$$

$$M_2 = 0.30,\ p_{o2}/p_o^* = 1.198$$

$$p_{o2} = 1.198 \times p_o^* = 1.198 \times 3.328 = 3.987 \text{ bar}$$

Nozzle throat area for maximum flow rate is given by

$$\dot{m}_{max} \sqrt{T_{o2}}/A^* p_{o2} = 0.0404$$

$$A^* = 4.934 \sqrt{806.44}/0.0404 \times 3.987 \times 10^5$$

$$= 8.69876 \times 10^{-3} \text{ m}^2$$

$$= \mathbf{86.9876 \text{ cm}^2} \quad \textbf{Ans.}$$

This can also be calculated from the isentropic value of A_2^*/A_2 at Mach number M_2.

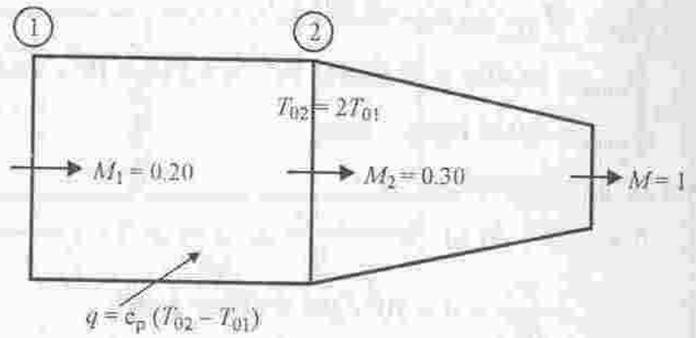

(a)

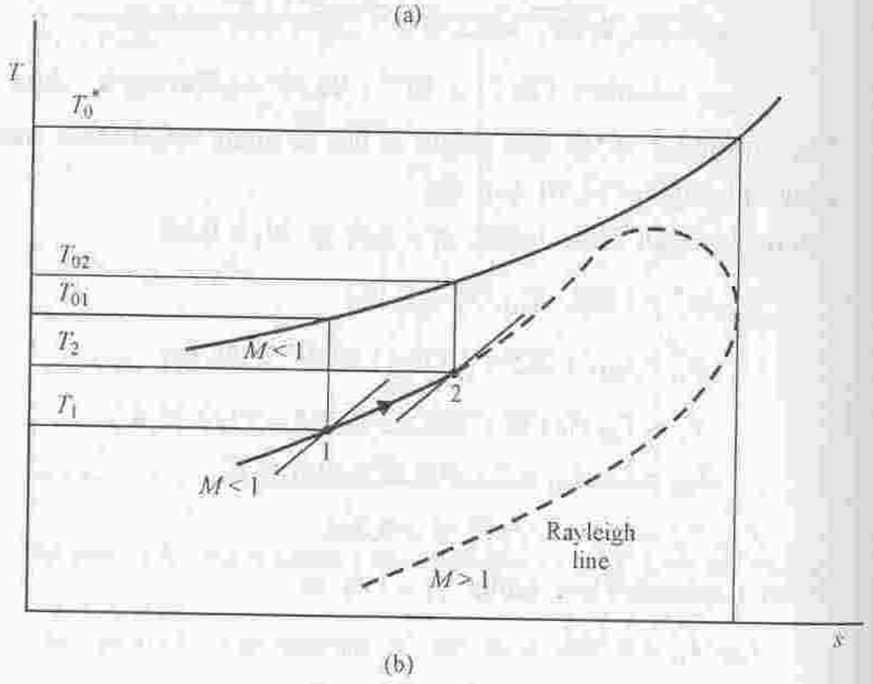

(b)

FIGURE 14.10 : Sonic nozzle with heat transfer upstream (Example 14.20 (*b*))

From isentropic flow tables ($\gamma = 1.4$) at $M_2 = 0.3$

$$A_2/A_2^* = 2.035$$

$$A_2^* = 176.71/2.035$$

$$A_2^* = 86.835 \text{ cm}^2$$

(*c*) Refer to Figure 14.9 (*a*), (*b*)

From Fanno flow tables ($\gamma = 1.4$) at $M_1 = 0.20$

$$p_{o1}/p_o^* = 2.964, \quad p_o^* = p_{o1}/2.964 = 4.111/2.964 = 1.3869 \text{ bar}$$

$$\left(\frac{4\bar{f}L_{max}}{D}\right)_1 = 14.533$$

$$\left(\frac{4\bar{f}L_{max}}{D}\right)_1 - \left(\frac{4\bar{f}L_{max}}{D}\right)_2 = \frac{4\bar{f}L}{D}$$

$$\frac{4\bar{f}L}{D} = 4 \times 0.006 \times 6300/15 = 10.08$$

$$\left(\frac{4\bar{f}L_{max}}{D}\right)_2 = 14.533 - 10.08 = 4.453$$

From Fanno flow tables ($\gamma = 1.4$) at $\dfrac{4\bar{f}L_{max}}{D} = 4.453$

$$M_2 = 0.32, \quad p_{o2}/p_o^* = 1.922$$

$$p_{o2} = 1.922 \times 1.3869 = 2.6658 \text{ bar}$$

$$T_{o2} = T_{o1} = 403.22 \text{ K}$$

These values for maximum flow rate give

$$\mathbf{A_2^* = 91.93 \text{ cm}^2} \quad \textbf{Ans.}$$

Example 14.21. Air enters a combustion chamber at $M_1 = 2.5$, $p_1 = 2$ bar, $T_1 = 288$ K. A normal shock occurs at the end of the combustion chamber; the static pressure before the shock is 4.0 bar. Determine (*a*) Mach number, (*b*) static pressure, and (*c*) static temperature at the exit of the combustion chamber. What are these values in the absence of shock?

Calculate the heat supplied and its maximum value in the two cases.

Solution. Refer to Figure 14.11 (*a*), (*b*)

From isentropic flow gas tables ($\gamma = 1.4$) at $M_1 = 2.5$,

$$T_1/T_{o1} = 0.444$$

$$T_{o1} = 288/0.444 = 648.65 \text{ K}$$

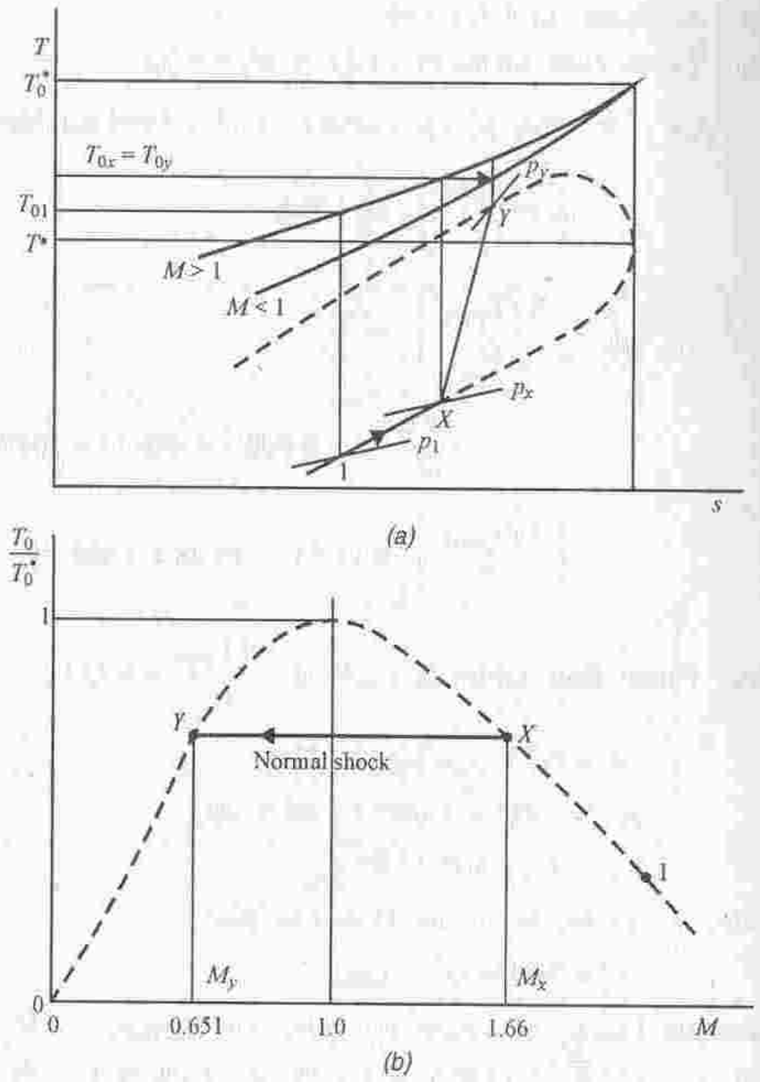

FIGURE 14.11 : Normal shock at the exit of the combustion chamber (Example 14.21)

From Rayleigh flow gas tables ($\gamma = 1.4$) at $M_1 = 2.5$

$$T_1/T^* = 0.379,\ T_{o1}/T_o^* = 0.71,\ p_1/p^* = 0.246$$

$$T^* = \frac{288}{0.379} = 759.89 \text{ K},\ T_o^* = \frac{648.65}{0.71} = 913.59 \text{ K},$$

$$p^* = \frac{2.0}{0.246} = 8.13 \text{ bar}$$

Figures 14.11 (*a*), (*b*) show the states of air on the Rayleigh line at the entry (1) of combustion chamber, before (X) and after (Y) the shock. Exit conditions are represented by the state at Y.

(*a*) At the state X on the Rayleigh line,

$$p_x/p^* = 4/8.13 = 0.492$$

From Rayleigh flow gas tables ($\gamma = 1.4$) at

$$p_x/p^* = 0.492 \text{ (say } 0.494)$$

$$M_x = 1.66,\ T_x/T^* = 0.673,\ T_{ox}/T_o^* = 0.869$$

From normal shock tables ($\gamma = 1.4$) at $M_x = 1.66$

$$p_y/p_x = 3.048,\ T_y/T_x = 1.43,\ M_y = 0.651$$

This gives the Mach number of the flow at the exit of the combustion chamber

$$\boldsymbol{M_y = 0.651} \quad \textbf{Ans.}$$

(*b*) The exit pressure is

$$p_y = 3.048 p_x = 3.048 \times 4.0$$

$$p_y = 12.192 \text{ bar} \quad \textbf{Ans.}$$

(*c*) The exit temperature is

$$T_y = 1.43 T_x = 1.43\ (0.673 T^*) = 1.43 \times 0.673 \times 759.89$$

$$T_y = 731.3 \text{ K} \quad \textbf{Ans.}$$

In the absence of shock

Exit temperature $= T_x = 0.673 \times 759.89 = \mathbf{511.4\ K}$ **Ans.**

Exit Mach number $= M_x = 1.66$ **Ans.**

Exit pressure $= p_x = \mathbf{4.0\ bar}$

Heat Transfer

Refer to Figure 14.11.

The heating process with shock is represented by the path 1 – X – Y. There is no heat transfer during $X - Y$ as $T_{ox} = T_{oy}$. Therefore,

$$q = c_p\ (T_{ox} - T_{o1})$$

$$T_{ox} = 0.869 T_o^* = 0.869 \times 913.59 = 793.9 \text{ K}$$

$$q = 1.005\ (793.9 - 648.65)$$

$$\boldsymbol{q = 145.97 \text{ kJ/kg}} \quad \textbf{Ans.}$$

The value of heat transfer is same in the absence of shock. Its maximum value is also the same in the two cases.

$$q_{\max} = c_p (T_o^* - T_{o1})$$
$$= 1.005 (913.59 \times 648.65)$$
$$= \mathbf{266.26\ kJ/kg} \quad \textbf{Ans.}$$

Example 14.22. Air is to be heated in a constant area duct from a stagnation temperature of 500 K in a subsonic or supersonic flow to obtain the same value of the maximum stagnation temperature. The initial Mach number in supersonic heating is 2.0. Compare the heating processes at $M < 1$ and $M > 1$. What are the values of:

(*a*) initial Mach number in the subsonic flow,

(*b*) maximum stagnation temperature and the corresponding static temperature, and

(*c*) the values of static temperature rise for $M < 1$ and $M > 1$?

(*d*) if the value of the heat transfer is reduced to half its maximum value what are the final values of Mach numbers in subsonic and supersonic flows?

Solution. Refer to Figures 14.12 (*a*), (*b*)

For comparison calculations are presented in the tabular form (Table 14.5).

For the same stagnation temperature (T_{o1}) at $M > 1$ and $M < 1$ the corresponding Mach number in subsonic flow is $M_y = 0.577$ obtained from normal shock tables at $M_x = 2.0$. This is shown in Figure 14.12 (*a*), (*b*). M_y can also be obtained from Rayleigh gas tables.

The heating process in the duct of constant cross-section is represented by the subsonic and supersonic branches of the Rayleigh line.

The initial value of the stagnation temperature (T_{o1}) is same in the two cases. The final temperature ($T_{o2} = T_o^* = T_{o\,\max}$) is also same for the same Rayleigh line. Therefore, the values of the heat transfer are also same for both $M > 1$ and $M < 1$.

TABLE 14.5: Comparison of heating processes in subsonic and supersonic flows

Flow parameters	Subsonic flow	Supersonic flow
M	0.577 (obtained from N. shock tables at $M_x = 2.0$)	2.0 (given)

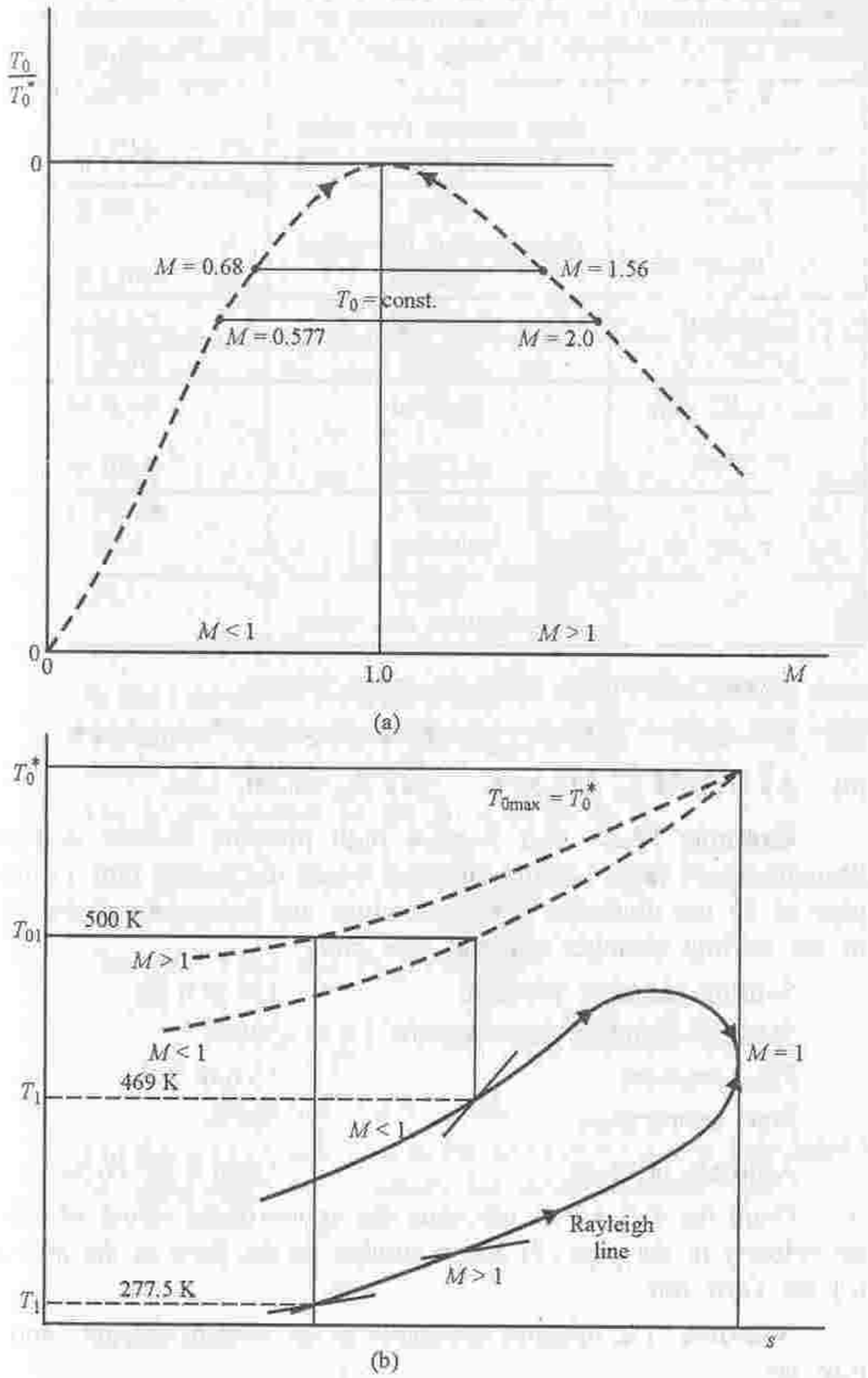

FIGURE 14.12 : Comparison of heat transfer in subsonic and supersonic flows (Example 14.22)

Flow parameters	Subsonic flow	Supersonic flow
T_{o1}	500 K	500 K
T_1/T_{o1}	0.938 (From isentropic flow tables)	0.555
T_1	469 K	277.5 K
T_{o1}/T_o^*	0.793 (From Rayleigh flow tables)	0.793 K
T_o^*	630.5 K	630.5 K
$T^* = 0.834 T_o^*$	525.84 K	525.84 K
$\Delta T = T^* - T_1$	56.84 K	248.34 K
$q_{max} = c_p (T_o^* - T_{o1})$	131.15 kJ	131.15 kJ
$q = \frac{1}{2} q_{max}$	65.575 kJ	65.575 kJ
T_{o2}	565.252 K	565.252 K
T_{o2}/T_o^*	0.896	0.896
M_2	0.68 (From Rayleigh flow tables)	1.56

Answers from the table are given below:

(*a*) $M = 0.577$ (*b*) $T_{o\,max} = T_o^* = 630.5$ K, $T^* = 525.84$ K

(*c*) $\Delta T = 56.84$ K, 248.34 K (*d*) $M_2 = 0.68$, 1.56.

Example 14.23. Air from a high pressure blower is passed through a very large settling chamber which discharges into a circular pipe of 15 cm diameter. Static pressures and temperatures measured in the settling chamber and the pipe are:

Settling chamber pressure	137 mm Hg
Settling chamber temperature	320 K
Pipe pressure	15 mm W.G.
Pipe temperature	305 K
Ambient pressure	1.015×10^5 N/m^2

From the above data calculate the approximate values of (*a*) the air velocity in the pipe (*b*) Mach number of the flow in the pipe and (*c*) the flow rate.

Solution. The absolute pressures in the settling chamber and the pipe are

$$p_0 = 1.015 + 137 \times 1.334 \times 10^{-3} = 1.1977 \text{ bar}$$

$$p = 1.015 + 15 \times 0.098 \times 10^{-3} = 1.0165 \text{ bar}$$

On account of the very large size of the settling chamber the pressure and temperature of air inside it can be assumed to have stagnation values. Therefore,

$$\rho_0 = \frac{p_0}{RT_0} = 1.1977 \times 10^5 / 287 \times 320 = 1.304 \text{ kg/m}^3$$

$$\rho = \frac{p}{RT} = 1.0165 \times 10^5 / 287 \times 305 = 1.161 \text{ kg/m}^3$$

(*a*) Using Bernoulli equation for compressible flow (Equation (11.16)) air velocity in the pipe is given by

$$c = \left\{ \frac{2\gamma}{\gamma - 1} \left(\frac{p_0}{\rho_0} - \frac{p}{\rho} \right) \right\}^{1/2}$$

$$= \left\{ \frac{2 \times 1.4}{0.4} \left(\frac{1.1977 \times 10^5}{1.304} - \frac{1.0165 \times 10^5}{1.161} \right) \right\}^{1/2}$$

$= 173.392$ m/s **Ans.**

In this calculation the acceleration of air from the settling chamber to the pipe has been assumed isentropic. Therefore, this value of velocity is approximate.

(*b*) The Mach number of the flow is given by

$$M = \frac{c}{\sqrt{\gamma RT}} = 173.392 / (1.4 \times 287 \times 305)^{1/2} = 0.495 \quad \textbf{Ans.}$$

(*c*) The mass flow rate is given by

$$\dot{m} = \rho A c = 1.161 \times \frac{\pi}{4} \times 0.0225 \times 173.392$$

$$\dot{m} = 3.557 \text{ kg/s} \quad \textbf{Ans.}$$

For the sake of comparison the air velocity is also calculated here by using Bernoulli equation for incompressible flow

$$p_0 = p + \frac{1}{2} \rho c^2$$

$$0.5 \times 1.161 c^2 = (1.1977 - 1.0165) \times 10^5$$

$$c = 176.676 \text{ m/s}$$

This is obviously not the correct value as the Mach number of the flow is much higher than 0.30.

Example 14.24. (*a*) Calculate the static and stagnation temperatures and velocity of air in a duct from the following data:

Mach number	0.60
Adiabatic wall temperature	400 K
Recovery factor	0.89

(*b*) Compare this velocity with the value obtained from the following manometer readings:

Static pressure 150 mm W.G. (below atmospheric).

Dynamic pressure measured from the deflection in a *U*-tube manometer 188.2 mm Hg.

Ambient pressure $p_a = 1.013$ bar.

Solution. (*a*) The static temperature of air is given by

$$\frac{T_{aw}}{T} = 1 + R_f \frac{\gamma - 1}{2} M^2$$

$$\frac{400}{T} = 1 + 0.89 \times \frac{1.4 - 1}{2} \times 0.6^2 = 1.064$$

$$T = \mathbf{375.94\ K} \quad \textbf{Ans.}$$

From isentropic flow tables ($\gamma = 1.4$) at $M = 0.60$

$$\frac{T}{T_0} = 0.933, \text{ therefore,}$$

$$T_0 = T/0.933 = 375.94/0.933 = \mathbf{402.936\ K} \quad \textbf{Ans.}$$

$$c = M\sqrt{\gamma RT}$$

$$= 0.6\,(1.4 \times 287 \times 375.94)^{1/2} = \mathbf{233.193\ m/s} \quad \textbf{Ans.}$$

(*b*) Absolute static pressure of air is given by

$$p = 1.013 - 150 \times 9.81 \times 10^{-5} = 1.013 - 0.0147 = 0.9983 \text{ bar}$$

Stagnation pressure is $p_0 = p + \frac{1}{2}\rho c^2$

$$p_0 = 0.9983 + 188.2 \times 13.6 \times 9.81 \times 10^{-5} = 1.2494 \text{ bar}$$

$$\frac{p}{p_0} = \frac{0.9983}{1.2494} = 0.799 \ (M_2 = 0.585 \text{ from isentropic flow tables})$$

$$c = 0.585 \times (1.4 \times 287 \times 375.94)^{1/2}$$

$$= \mathbf{227.36\ m/s} \quad \textbf{Ans.}$$

It can also be determined directly from the dynamic head.

$$\rho = \frac{p}{RT} = \frac{0.9983 \times 10^5}{287 \times 375.94} = 0.9252 \text{ kg/m}^3$$

$$\frac{1}{2}\rho c^2 = 188.2 \times 13.6 \times 9.81 = 2.51 \times 10^4$$

$$0.5 \times 0.9252 c^2 = 2.51 \times 10^4$$

$$c = \mathbf{232.93\ m/s} \quad \textbf{Ans.}$$

Example 14.25. If the aircraft in Example 12.1 flies at 400 kmph recalculate (*a*) pressure rise in the inlet diffuser, (*b*) compressor pressure ratio, (*c*) air flow rate, (*d*) power required by the compressor, and (*e*) the air standard efficiency of the engine. Take the inlet diameter of the diffuser as 60 cm.

Compare the values for the two flight speeds (400 and 525 kmph) at the same attitude, $Z = 3$ km.

Solution. Refer to the solved Example 12.1. Same notation is used here.

At $Z = 3$ km from gas tables for the standard atmosphere,

$$T_i = 268.65 \text{ K}, \ p_i = 0.701 \text{ bar}, \ \rho_i = 0.909 \text{ kg/m}^3$$

$$a_i = 328.7 \text{ m/s}$$

$$\text{Aircraft speed} = \text{engine speed} = \frac{400}{3.6} = 111.11 \text{ m/s}$$

This is the velocity of air at the diffuser entry.

$$c_i = u = 111.11 \text{ m/s}$$

$$M_i = c_i/a_i = 111.11/328.7 = 0.338$$

$$\frac{T_{oi}}{T_i} = 1 + \frac{\gamma - 1}{2} M_i^2 = 1 + 0.2 \times 0.338^2 = 1.02286$$

$$T_{oi} = T_{o1} = 1.02286 \times 268.65 = 274.791 \text{ K}$$

$$T_1 = T_{o1} - c_1^2/2c_p$$

$$T_1 = 274.791 - 8100/2 \times 1005 = 270.76 \text{ K}$$

(*a*) Pressure ratio of the inlet diffuser is obtained from

$$T_{is} - T_i = \eta_D\,(T_1 - T_i)$$

$$\left(\frac{p_1}{p_i}\right)^{\frac{\gamma-1}{\gamma}} = \frac{T_{is}}{T_i} = 1 + \eta_D \left(\frac{T_1}{T_i} - 1\right)$$

$$\left(\frac{p_1}{p_i}\right)^{\frac{1}{3.5}} = 1 + 0.875\left(\frac{270.76}{268.65} - 1\right) = 1.00687$$

$$p_1/p_i = 1.0242$$

$$p_1 = 1.0242 \times 0.701 = 0.718 \text{ bar}$$

$$(\Delta p)_D = 0.718 - 0.701 = 0.017 \text{ bar} = 17 \text{ mbar} \quad \textbf{Ans.}$$

(*b*) Compressor pressure ratio is given by

$$r_{oc} = \left[1 + \frac{\eta_c}{T_{o1}}(T_{o2} - T_{o1})\right]^{\frac{\gamma}{\gamma-1}}$$

$$r_{oc} = \left[1 + \frac{0.79 \times 230}{274.791}\right]^{3.5} = \mathbf{5.9088} \quad \textbf{Ans.}$$

(*c*) Air flow rate is given by

$$\dot{m}_a = \rho_i c_i A_i = \rho_i u A_i$$

$$A_i = \frac{\pi}{4} D^2 = \frac{\pi}{4} \times 0.36 = 0.2827 \text{ m}^2$$

At the same altitude $Z = 3$ km, $\rho_i = 0.909$ kg/m^3

Therefore, $\dot{m}_a = 0.909 \times 111.11 \times 0.2827 = 28.5527$ kg/s

at $u = 400$ kmph

$$\dot{m}_a = 0.909 \times 145.833 \times 0.2827 = 37.475 \text{ kg/s} \quad \textbf{Ans.}$$

at $u = 525$ kmph

(*d*) The power, required to drive the air compressor is proportional to the air flow rate for the same temperature rise.

$$P = \dot{m}_a c_p (T_{o1} - T_{o2})$$

$$P = 1.005 \times 230 \dot{m}_a = 231.15 \dot{m}_a \text{ kW}$$

For $u = 400$ kmph

$$P = 28.5527 \times \frac{231.15}{1000} = \mathbf{6.599 \text{ MW}} \quad \textbf{Ans.}$$

For $u = 525$ kmph

$$P = 31.475 \times \frac{231.15}{1000} = \mathbf{8.662 \text{ MW}} \quad \textbf{Ans.}$$

(*e*) The air standard efficiency or the ideal Joule cycle efficiency is a function of only the compressor pressure ratio.

$$\eta_J = 1 - \left(\frac{1}{r_{oc}}\right)^{\frac{\gamma-1}{\gamma}}$$

$$\eta_J = 1 - \left(\frac{1}{5.9088}\right)^{\frac{1}{3.5}}$$

$$\eta_J = \mathbf{0.39802 \ (39.802\%).}$$

The calculated values are presented in table 14.6 for comparison at the two aircraft speeds.

TABLE 14.6: Comparison of turbo prop engine diffuser and compressor at two aircraft speeds

Parameters	$u = 400$ kmph	$u = 525$ kmph
Altitude	3 km	3 km
Compressor temperature rise	230 K	230 K
Diffuser pressure rise	17.0 mbar	53.7 mbar
Compressor pressure ratio	5.9088	5.779
Air flow rate	28.5527 kg/s	37.475 kg/s
Compresor power	6.599 MW	8.662 MW
Air standard efficiency	39.80%	39.42%

Example 14.26. The aircraft in Example 12.4 flies at an altitude of 8 km at the same Mach number 0.80. Assuming the same data for the engine calculate (*a*) fuel-air ratio (*b*) compressor pressure ratio (*c*) turbine pressure ratio (*d*) exhaust nozzle pressure ratio and (*e*) the Mach number of the exhaust jet.

If the cross-sectional area of the engine at inlet is 0.5 m^2 calculate the air mass flow rate at the two attitudes (8 and 10 km). Compare the engine parameters at these attitudes.

Solution. Notation used here is the same as in the solved Example 12.4.

From the tables of standard atmosphere at $Z = 8$ km, $p = 0.356$ bar, $T = 236.15$ K, $\rho = 0.525$ kg/m^3, $a = 308.2$ m/s.

The speed of the aircraft and the engine is

$$u = M_i\, a_i = 0.8 \times 308.2 = 246.56 \text{ m/s} = 887.62 \text{ kmph}$$

From isentropic flow tables ($\gamma = 1.4$) at $M = 0.8$,

$T/T_o = 0.886$, therefore,

$$T_{o1} = T_{oi} = 236.15/0.886 = 266.535 \text{ K}$$

Temperature rise in the compressor is given as

$T_{o2} - T_{o1} = 175$; therefore,

$$T_{o2} = 175 + 266.535 = 441.535 \text{ K}$$

(*a*) The fuel-air ratio is calculated from

$$\frac{1}{f}(T_{o3} - T_{o2}) = \eta_B\, Q_f/c_p - T_{o3}$$

$$\frac{1}{f}\,(1200 - 441.535) = \frac{0.975 \times 43 \times 10^6}{1005} - 1200 = 40516.418$$

$$\boldsymbol{f = 0.01872} \quad \textbf{Ans.}$$

(*b*) Compressor pressure ratio is given by

$$r_{oC} = \left[\, 1 + \eta_C \frac{T_{o2} - T_{o1}}{T_{o1}} \,\right]^{\frac{\gamma}{\gamma - 1}}$$

$$r_{oC} = \left[\, 1 + \frac{0.75 \times 175}{266.535} \,\right]^{3.5} = \textbf{4.061} \quad \textbf{Ans.}$$

(*c*) The entire power output of the turbine is utilized in driving the compressor. The pressure ratio of the turbine is obtained from

$$\eta_m\,(1 + f)\;(T_{o3} - T_{o4}) = T_{o2} - T_{o1}$$

This assumes the same thermodynamic properties for air and the gas.

$$T_{o3}\left\{1 - \left(\frac{1}{r_{oT}}\right)^{\frac{\gamma-1}{\gamma}}\right\}\eta_T = 175/0.98 \times 1.01872 = 175.29$$

$$1 - \left(\frac{1}{r_{oT}}\right)^{\frac{\gamma-1}{\gamma}} = 175.29/1200 \times 0.81 = 0.1803$$

$$r_{oT} = (1 - 0.1803)^{-3.5} = \textbf{2.0056} \quad \textbf{Ans.}$$

(*d*) $$T_{o4} = T_{o3} - 175.29 = 1200 - 175.29 = 1024.71 \text{ K}$$

The velocity of gas (c_e) at the exhaust nozzle is obtained from the specific impulse.

$$I_s = \frac{u}{g}\left(\frac{1}{\sigma} - 1\right)$$

$$25 = \frac{246.56}{9.81}\left(\frac{1}{\sigma} - 1\right)$$

$$\sigma = u/c_e = 0.501$$

$$c_e = 246.56/0.501 = 492.135 \text{ m/s}$$

Gas temperature at the exit of the exhaust nozzle is given by

$$T_e = T_{o4} - c_e^2/2c_p = 1024.71 - 492.135^2/2 \times 1005$$

$$T_e = 904.2 \text{ K}$$

$$T_{o4} - T_e = \eta_n\,(T_{o4} - T_{es}) = \eta_n \left\{1 - \left(\frac{1}{r_n}\right)^{\frac{1}{3.5}}\right\} T_{o4}$$

$$1 - \left(\frac{1}{r_n}\right)^{1/3.5} = 120.51/0.97 \times 1024.71 = 0.1212$$

$$\boldsymbol{r_n = 1.572} \quad \textbf{Ans.}$$

(*e*) $$M_e = c_e/\sqrt{\gamma RT_e} = 492.135/(1.4 \times 287 \times 904.2)^{1/2}$$

$$M_e = 0.816$$

The flow rate of air through the engine is given by

$$\dot{m} = \rho_i\, A_i\, c_i = \rho_i\, A_i\, u$$

At $Z = 10$ km

$$\dot{m} = 0.413 \times 0.5 \times 239.68 = 49.494 \text{ kg/s} \quad \textbf{Ans.}$$

At $Z = 8$ km

$$\dot{m} = 0.525 \times 0.5 \times 246.56 = 64.722 \text{ kg/s} \quad \textbf{Ans.}$$

The comparison of the engine parameters at the two altitudes is presented in Table 14.7.

TABLE 14.7: Comparison of turbojet engine parameters at two values of the altitude

Engine Parameters	$Z = 8$ km	$Z = 10$ km
M	0.80	0.80
u	887.62 kmph	862.85 kmph
f	0.01872	0.01908
r_{oc}	4.061	4.344
r_{oT}	2.0056	2.005
r_n	1.572	1.55
M_e	0.816	0.803
$\dot{m}_a$	64.722 kg/s	49.494 kg/s

Example 14.27. For isothermal flow in constant area duct with friction

(*a*) Starting from $\dfrac{dp}{p} = -\dfrac{1}{2}\dfrac{dM^2}{M^2}$

prove $\gamma p_1^2 M_1^2 = \gamma p_2^2 M_2^2 = \gamma p^2 M^2 = (p^{*t})^2$

(*b*) Starting from $\dfrac{\gamma M^2}{2} 4f\dfrac{dx}{D} = \gamma M^2 \dfrac{dp}{p} - \dfrac{dp}{p}$

prove $$\frac{4fL}{D} = \ln\frac{p_2^2}{p_1^2} + \frac{1}{\gamma M_1^2}\left(1 - \frac{p_2^2}{p_1^2}\right)$$

Solution. (*a*) Integrating the quantities on both sides of the given equation between Mach numbers M and $M^{*t} = 1/\sqrt{\gamma}$

$$\int_p^{p^{*t}} \frac{dp}{p} = -\frac{1}{2}\int_M^{M^{*t}} \frac{dM^2}{M^2}$$

$$\ln\frac{p^{*t}}{p} = -\frac{1}{2}\ln\frac{M^{*t\,2}}{M^2} = \ln\left(\frac{M^2}{M^{*t\,2}}\right)^{1/2} = \ln\frac{M}{M^{*t}}$$

Therefore, $$\frac{p^{*t}}{p} = \frac{M}{M^{*t}} = \sqrt{\gamma}\,M$$

Squaring both sides

$$\gamma p_1^2 M_1^2 = \gamma p_2^2 M_2^2 = \gamma p^2 M^2 = p^{*t\,2}$$

(*b*) The given expression is rewritten as

$$4f\frac{dx}{D} = \frac{2dp}{p} - \frac{2}{\gamma p^2 M^2}p\,dp$$

Replacing $\gamma p^2 M^2$ with $\gamma p_1^2 M_1^2$ and integrating

$$\frac{4f}{D}\int_1^2 dx = 2\int_{p_1}^{p_2}\frac{dp}{p} - \frac{2}{\gamma p_1^2 M_1^2}\int_{p_1}^{p_2} p\,dp$$

$$\int_1^2 dx = L = \text{distance between the two stations}$$

Therefore, $$\frac{4fL}{D} = [\ln p^2]_1^2 - \frac{1}{\gamma p_1^2 M_1^2}[p^2]_{p_1}^{p_2}$$

$$\frac{4fL}{D} = \ln\frac{p_2^2}{p_1^2} + \frac{1}{\gamma p_1^2 M_1^2}(p_1^2 - p_2^2)$$

$$\frac{4fL}{D} = \ln\frac{p_2^2}{p_1^2} + \frac{1}{\gamma M_1^2}\left(1 - \frac{p_2^2}{p_1^2}\right)$$

Example 14.28. A gas is transmitted isothermally over a long distance in a system of compressors and pipe sections each of 50 km length. The increase in the static pressure through the compressors (at the pumping stations) compensates the static pressure drop in the pipe-lines. The data for two pipe-lines A and B is given in the following table:

Parameters	Pipe-line *A*	Pipe-line *B*
Pipe length, L	50 km	50 km
Pipe diameter, D	40 cm	60 cm
Friction factor, f	0.003	0.0022
Static pressure at entry, p_1	25 bar, 30 bar	25 bar, 30 bar
Mach number at entry, M_1	0.02	0.02
Gas/pipe temperature, T (constant)	310 K	310 K

Calculate for the two pipe-lines (*a*) mass flow rate of the gas (*b*) maximum possible distance between two compressor/pumping stations (*c*) Mach number and velocity of the gas at the exit of the pipe-line (*d*) compressor pressure ratio and the power required, and (*e*) the stagnation pressure loss.

Take for the gas $\gamma = 1.26$, $c_p = 2.0$ kJ/kg K, $R = 410$ J/kg K

Solution. Figure 14.13 shows the pipe-line between two pumping stations. Gas conditions at entry and exit of the pipe-line are designated by the subscripts 1 and 2 respectively.

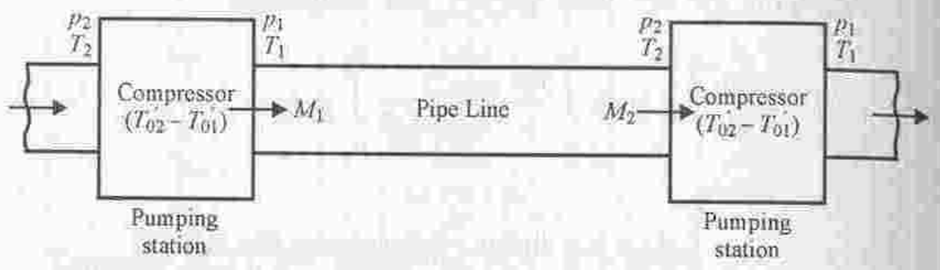

FIGURE 14.13 : Gas pipe-line between two pumping stations (Inside diameter = D, length = L), (Example 14.28)

The pressure drop in the pipe-line is $(p_1 - p_2)$; this is assumed equal to the pressure rise through the compressor. For isothermal flow through the pipe-line,

$$T = T_1 = T_2 = \text{constant}$$

Velocity of sound is also constant. Therefore,

$$a = a_1 = a_2 = \sqrt{\gamma RT}$$

$$a = (1.26 \times 410 \times 310)^{1/2} = 400.182 \text{ m/s}$$

$$c_1 = M_1 \times a_1 = 0.02 \times 400.182 = 8.004 \text{ m/s}$$

$$\gamma M_1^2 = 1.26 \times 0.02^2 = 0.000504$$

$$1/\gamma M_1^2 = 1984.127$$

$$\ln \gamma M_1^2 = -0.7592$$

Pipe-line *A*

(*a*) Area of cross-section $= \frac{\pi}{4} D^2 = \frac{\pi}{4} \times 0.4^2 = 0.1257 \text{ m}^2$

Density of gas at entry $\rho_1 = \frac{p_1}{RT} = \frac{25 \times 10^5}{410 \times 310} = 19.669 \text{ kg/m}^3$

Therefore, the flow rate (for $p_1 = 25$ bar) is

$$\dot{m} = \rho_1 A c_1 = 19.669 \times 0.1257 \times 8.004 = 19.789 \text{ kg/s}$$

$$\dot{m} = 71.24 \text{ t/h} \quad \textbf{Ans.}$$

For $p_1 = 30$ bar

$$\rho_1 = \frac{30 \times 10^5}{410 \times 310} = 23.603 \text{ kg/m}^3$$

$$\dot{m} = 23.603 \times 0.1257 \times 8.004 = 23.747 \text{ m/s}$$

$$\dot{\boldsymbol{m}} = \mathbf{85.489 \text{ t/h}} \quad \textbf{Ans.}$$

(*b*) $$\left(\frac{4fL_{\max}}{D}\right)_{M_1} = \frac{1 - \gamma M_1^2}{\gamma M_1^2} + \ln \gamma M_1^2 = \frac{1}{\gamma M_1^2} - 1 + \ln \gamma M_1^2$$

$$\left(\frac{4fL_{\max}}{D}\right)_{M_1} = 1984.127 - 1 - 7.592 = 1975.535$$

$$L_{\max} = 1975.535 \times 0.4/4 \times 0.003 \times 1000$$

$$\boldsymbol{L_{\max}} = \mathbf{65.851 \text{ km}} \quad \textbf{Ans.}$$

(*c*) $$\frac{4fL}{D} = 4 \times 0.003 \times 50{,}000/0.4 = 1500$$

$$\left(\frac{4fL_{\max}}{D}\right)_{M_2} = \left(\frac{4fL_{\max}}{D}\right)_{M_1} - \frac{4fL}{D} = 1975.535 - 1500$$

$$= 475.535$$

Therefore, $$\frac{1}{\gamma M_2^2} - 1 + \ln \gamma M_2^2 = 475.535$$

$$\frac{1}{\gamma M_2^2} + \ln \gamma M_2^2 = 476.535$$

By trial and error, $\boldsymbol{M_2 = 0.0405}$ **Ans.**

Since the change in Mach number is very small the flow is incompressible. Therefore, the exit Mach number can also be determined by

$$\frac{1}{\gamma}\left(\frac{1}{M_1^2} - \frac{1}{M_2^2}\right) = \frac{4fL}{D}$$

$$\frac{1}{0.02^2} - \frac{1}{M_2^2} = 1.26 \times 1500$$

$$M_2 = 0.040489$$

The exit velocity, $c_2 = M_2 \times a$

$$c_2 = 0.0405 \times 400.182 = 16.207 \text{ m/s} \quad \textbf{Ans.}$$

(*d*) The compressor pressure ratio required is

$$p_1/p_2 = M_2/M_1 = 0.0405/0.02 = 2.025 \quad \textbf{Ans.}$$

This is same for both the values of inlet pressure.

$$p_2 = 25/2.025 = 12.345 \text{ bar (for } p_1 = 25 \text{ bar)}$$

$$p_2 = 30/2.025 = 14.815 \text{ bar (for } p_1 = 30 \text{ bar)}$$

$$\frac{\gamma - 1}{\gamma} = \frac{1.26 - 1}{1.26} = 0.2063 \text{ and } \frac{\gamma}{\gamma - 1} = 4.846$$

For calculating the power of the compressor at the pumping station it is assumed that the gas enters the compressor at pressure p_2 and temperature T. For isentropic compression power is given by

$$P = \dot{m} c_p (T_{o2}' - T_{o1}')$$

$(T_{o2}' - T_{o1}')$ is the stagnation temperature rise of the gas during compression. Assuming $T_{o1}' = T_1 = T$

$$P = \dot{m} c_p T \left\{ \frac{T_{o2}'}{T} - 1 \right\}$$

For small gas velocity at the compressor exit

$$\frac{T_{o2}'}{T} = \left(\frac{p_1}{p_2} \right)^{\frac{\gamma-1}{\gamma}} = 2.025^{0.2063} = 1.1567$$

Therefore, $P = 2 \times 310 \times 0.1567 \dot{m} = 97.154 \dot{m}$ kW

$$P = 97.154 \times 19.789 = 1922.58 \text{ kW (for } p_1 = 25 \text{ bar)}$$

$$P = 97.154 \times 23.747 = 2307.12 \text{ kW (for } p_1 = 30 \text{ bar)}$$

(*e*)
$$p_{o1} = p_1 \left(1 + \frac{\gamma - 1}{2} M_1^2 \right)^{\frac{\gamma}{\gamma-1}} = 25 \left(1 + \frac{0.26}{2} \times 0.02^2 \right)^{4.846}$$

$$= 25.0063 \text{ bar}$$

$$p_{o2} = 12.345 \times 1.000213^{4.846} = 12.3577 \text{ bar}$$

The stagnation pressure loss (for $p_1 = 25$ bar)

$$\Delta p_0 = p_{o1} - p_{o2} = 25.0063 - 12.3577 = 12.648 \text{ bar} \quad \textbf{Ans.}$$

This is almost equal to $(p_1 - p_2)$ an account of much lower values of the Mach numbers.

$$\Delta p_0 = 30 - 14.815 = 15.185 \text{ bar (for } p_1 = 30 \text{ bar)} \quad \textbf{Ans.}$$

Pipe-line *B*

(*a*) Area of cross-section

$$A = \frac{\pi}{4} \times 0.6^2 = 0.2827 \text{ m}^2$$

$$\rho_1 = 19.669 \text{ kg/m}^3$$

Mass flow rate for $p_1 = 25$ bar,

$$\dot{m} = 19.669 \times 0.2827 \times 8.004 = 44.505 \text{ kg/s}$$

$$\dot{m} = 160.2 \text{ t/h} \quad \textbf{Ans.}$$

Mass flow rate for $p_1 = 30$ bar,

$$\dot{m} = 23.603 \times 0.2827 \times 8.004 = 53.408 \text{ kg/s}$$

$$\dot{m} = 192.27 \text{ t/h} \quad \textbf{Ans.}$$

(*b*)
$$\left(\frac{4 f L_{\max}}{D} \right)_{M_1} = 1975.535$$

$$L_{\max} = 1975.535 \times 0.6/4 \times 0.0022 \times 1000$$

$$L_{\max} = 134.696 \text{ km} \quad \textbf{Ans.}$$

(*c*)
$$\frac{4 f L}{D} = 4 \times 0.0022 \times 50{,}000/0.6 = 733.33$$

$$\left(\frac{4 f L_{\max}}{D} \right)_{M_2} = 1975.535 - 733.33 = 1242.205$$

In this case the choking length ($L_{\max}$) is much larger than the actual length (50 km). Therefore, the flow can be assumed incompressible and the following formula can be used:

$$\frac{1}{\gamma} \left(\frac{1}{M_1^2} - \frac{1}{M_2^2} \right) \simeq \frac{4 f L}{D}$$

$$\frac{1}{0.02^2} - \frac{1}{M_2^2} = 1.26 \times 733.33$$

$$M_2 = 0.025$$

This also nearly satisfies the following relation:

$$\frac{1}{\gamma M_2^2} + \ln \gamma M_2^2 - 1 = 1242.205$$

$$M_2 = 0.0252 \quad \textbf{Ans.}$$

The exit velocity $c_2 = 0.0252 \times 400.182 = 10.08$ m/s **Ans.**

(*d*) The compressor pressure ratio is

$$p_1/p_2 = M_2/M_1 = 0.0252/0.02 = 1.26 \quad \textbf{Ans.}$$

$p_2 = 25/1.26 = 19.84$ bar, and $p_2 = 30/1.26 = 23.809$ bar

for the two values of the entry pressure.

The power required is

$$P = \dot{m} \times 2 \times 310\,(1.26^{0.2063} - 1) = 30.277\dot{m} \text{ kW}$$

For $p_1 = 25$ bar

$$P = 30.277 \times 44.505 = 1347.48 \text{ kW} \quad \textbf{Ans.}$$

For $p_1 = 30$ bar

$$P = 30.277 \times 53.408 = 1617.034 \text{ kW} \quad \textbf{Ans.}$$

(*e*) For incompressible flow, $\Delta p_0 \simeq \Delta p = p_1 - p_2$

$\Delta p_0 = 25 - 19.84 = 5.16$ bar (for $p_1 = 25$ bar) **Ans.**

$\Delta p_0 = 30 - 23.809 = 6.191$ bar (for $p_1 = 30$ bar) **Ans.**

The results of the calculations are presented in the following Table No. 14.8.

TABLE 14.8: Comparison of gas pipe-lines and compressors

Parameters	Pipe-line *A*	Pipe-line *B*
Pipe length, L	50 km	50 km
Pipe diameter, D	40 cm	60 cm
Friction factor, f	0.003	0.0022
Entry Mach number	0.02	0.02
Mass flow rate ($\dot{m}$) for		
$p_1 = 25$ bar	71.24 t/h	160.2 t/h
$p_1 = 30$ bar	85.489 t/h	192.27 t/h

Parameters	Pipe-line *A*	Pipe-line *B*
Max. pipe length, L_{max}	65.851 km	134.696 km
Exit Mach number	0.0405	0.0252
Compressor pressure ratio, $\frac{p_1}{p_2}$	2.025	1.26
Compressor power, P for		
$p_1 = 25$ bar	1922.58 kW	1347.48 kW
$p_1 = 30$ bar	2307.02 kW	1617.034 kW
Stagnation pressure loss for		
$p_1 = 25$ bar	12.648 bar	5.16 bar
$p_2 = 30$ bar	15.185 bar	6.191 bar

Following conclusions can be drawn from the table:

1. Use of larger diameter pipe leads to lower static pressure drop, stagnation pressure loss and pumping power.
2. Larger diameter pipe-lines require fewer pumping stations on account of much longer pipe lengths which can be employed between pumping stations.
3. The rate of transmission of the gas can be significantly increased by employing higher pressures at the compressor outlet and larger pipe diameters.

Example 14.29. Prove that the pressure gradient in the radial direction of flow through an axial fan is given by

$$\frac{dp}{dr} = \rho \frac{c_\theta^2}{r}$$

Assume radial equilibrium.

Solution. Momentum Equation (10.72) in the radial direction for steady flow in the absence of body forces is

$$c_r \frac{\partial c_r}{\partial r} + \frac{c_\theta}{r} \frac{\partial c_r}{\partial \theta} + c_x \frac{\partial c_r}{\partial r} - \frac{c_\theta^2}{r} = -\frac{1}{\rho} \frac{\partial p}{\partial r}$$

Putting $c_r = 0$ for radial equilibrium,

$$\frac{c_\theta^2}{r} = \frac{1}{\rho} \frac{dp}{dr}$$

$$\frac{dp}{dr} = \rho \frac{c_\theta^2}{r}$$

This is the pressure gradient in the radial direction.

Example 14.30. Derive the following relations for steady and inviscid flow in radial equilibrium:

(*a*) $\dfrac{dh_0}{dr} = \dfrac{dh}{dr} + c_\theta \dfrac{dc_\theta}{dr} + c_x \dfrac{dc_x}{dr}$

(*b*) $c_\theta \dfrac{dc_\theta}{dr} + c_x \dfrac{dc_x}{dr} + \dfrac{c_\theta^2}{r} = 0$

(*c*) $\dfrac{1}{r^2}\dfrac{d}{dr}(rc_\theta)^2 + \dfrac{d}{dr}(c_x^2) = 0.$

Solution. (*a*) $h_0 = h + \dfrac{1}{2}c^2$

For three dimensional flow $c^2 = c_r^2 + c_\theta^2 + c_x^2$

For radial equilibrium, $c_r = 0$, therefore,

$$h_0 = h + \frac{1}{2}(c_\theta^2 + c_x^2)$$

Differentiating w.r.t. r,

$$\frac{dh_0}{dr} = \frac{dh}{dr} + c_\theta \frac{dc_\theta}{dr} + c_x \frac{dc_x}{dr} \qquad (1)$$

(*b*) For isentropic flow, $dh = \dfrac{dp}{\rho}$

$$\frac{dh}{dr} = \frac{1}{\rho}\frac{dp}{dr}$$

For radial equilibrium ($c_r = 0$). Therefore,

$$\frac{dh}{dr} = \frac{1}{\rho}\frac{dp}{dr} = \frac{c_\theta^2}{r} \qquad (2)$$

Assuming constant stagnation enthalpy in the radial direction

$$\frac{dh_0}{dr} = 0$$

Therefore, Equation (2) in Equation (1) gives

$$\frac{c_\theta^2}{r} + c_\theta \frac{dc_\theta}{dr} + c_x \frac{dc_x}{dr} = 0 \qquad (3)$$

(*c*) Equation (3) can be rewritten as

$$\frac{1}{r^2}\left(c_\theta^2 \,.\, 2r\frac{dr}{dr} + r^2 \,.\, 2c_\theta \frac{dc_\theta}{dr}\right) + 2c_x \frac{dc_x}{dr} = 0$$

The quantity in brackets on the left hand side is the differential coefficient of the product of two quantities r^2 and c_θ^2. Therefore,

$$\frac{1}{r^2}\frac{d}{dr}(rc_\theta)^2 + \frac{d}{dr}(c_x^2) = 0$$

APPENDICES

APPENDICES

A.1

Prandtl-Meyer Function (Section 7.11.2)

$$\omega(M) = \int \frac{\sqrt{M^2 - 1}}{1 + \frac{\gamma - 1}{2} M^2} \frac{dM}{M}$$

Let $x^2 = M^2 - 1$

$$M^2 = 1 + x^2$$

$$2M\, dM = 2x\, dx$$

$$\frac{dM}{M} = \frac{xdx}{M^2} = \frac{xdx}{1 + x^2}$$

$$\omega(M) = \int \frac{x}{1 + \frac{\gamma - 1}{2}(1 + x^2)} \frac{x}{1 + x^2} dx$$

$$\omega(M) = \int \frac{2x^2}{\{(\gamma + 1) + (\gamma - 1)x^2\}(1 + x^2)} dx$$

$$\omega(M) = \int \frac{(\gamma + 1)}{(\gamma + 1) + (\gamma - 1)x^2} dx - \int \frac{dx}{1 + x^2}$$

The above integrals are of the form

$$\int \frac{dx}{a^2 + b^2 x^2} = \frac{1}{ab} \tan^{-1} \frac{b}{a} x$$

The first integral is

$$\int \frac{1}{1+\frac{\gamma-1}{\gamma+1}x^2}\,dx$$

$$a = 1,\ b = \sqrt{\frac{\gamma-1}{\gamma+1}}$$

The second integral is straight forward.

After integration and rearrangement following expression is obtained:

$$\omega(M) = \sqrt{\frac{\gamma+1}{\gamma-1}}\tan^{-1}\sqrt{\frac{\gamma-1}{\gamma+1}(M^2-1)} - \tan^{-1}\sqrt{M^2-1} \qquad (A.1)$$

A.2

Integration of Fanno Flow Equations

VELOCITY

(Section 8.4.1)

$$I = \int \frac{dM^2}{2M^2\left(1+\frac{\gamma-1}{2}M^2\right)}$$

Let $1+\frac{\gamma-1}{2}M^2 = X,\ M^2 = x,\ 1 = a,$

$$\frac{\gamma-1}{2} = b,\ X = a+bx$$

$$I = \frac{1}{2}\int \frac{dx}{xX} = -\frac{1}{a}\ln\left(\frac{X}{x}\right)$$

$$I = -\frac{1}{2}\ln\frac{1+\frac{\gamma-1}{2}x}{x} = -\frac{1}{2}\ln\frac{1+\frac{\gamma-1}{2}M^2}{M^2}$$

$$I = \ln\frac{M}{\sqrt{1+\frac{\gamma-1}{2}M^2}}$$

$$\int_1^M (\,)\,dM^2 = \left[\ln\frac{M}{\sqrt{1+\frac{\gamma-1}{2}M^2}}\right]_1^M$$

$$= \ln M \sqrt{\frac{(\gamma+1)}{2\left(1+\frac{\gamma-1}{2}M^2\right)}} = \ln \frac{c}{c^*}$$

$$\frac{c}{c^*} = M\left[\frac{\gamma+1}{2\left(1+\frac{\gamma-1}{2}M^2\right)}\right]^{1/2} \tag{A.2}$$

Temperature (Section 8.4.3)

$$I = -\int \frac{\gamma-1}{2+(\gamma-1)M^2}\, dM^2$$

Let $M^2 = x,\ z = 2+(\gamma-1)x$

$$I = -\int \frac{(\gamma-1)\,dx}{2+(\gamma-1)x} = -\int \frac{dz}{z} = -\ln z = \ln\{2+(\gamma-1)M^2\}^{-1}$$

$$\int_1^M (\,)\,dM = \left[\ln \frac{1}{2\left(1+\frac{\gamma-1}{2}M^2\right)}\right]_1^M$$

$$= \ln \frac{\gamma+1}{2\left(1+\frac{\gamma-1}{2}M^2\right)} = \ln \frac{T}{T^*}$$

$$\frac{T}{T^*} = \frac{\gamma+1}{2\left(1+\frac{\gamma-1}{2}M^2\right)} \tag{A.3}$$

Pressure (Secion 8.4.4)

$$I = -\int \frac{1+(\gamma-1)M^2}{2M^2+(\gamma-1)M^4}\, dM^2$$

Let $M^2 = x$

$$I = -\frac{1}{2}\int \frac{1+(\gamma-1)x}{x+\frac{\gamma-1}{2}x^2}$$

Putting $z = x+\frac{\gamma-1}{2}x^2$

$$I = -\frac{1}{2}\int \frac{dz}{z} = -\frac{1}{2}\ln z$$

$$I = -\frac{1}{2}\ln\left(x+\frac{\gamma-1}{2}x^2\right) = \ln\left(M^2+\frac{\gamma-1}{2}M^4\right)^{-1/2}$$

$$\int_{M=1}^{M=M} (\,)\,dM^2 = -\left[\ln M\left(1+\frac{\gamma-1}{2}M^2\right)^{1/2}\right]_1^M$$

$$\int_1^M (\,)\,dM^2 = \ln\frac{1}{M}\sqrt{\frac{\gamma+1}{2\left(1+\frac{\gamma-1}{2}M^2\right)}} = \ln\frac{p}{p^*}$$

$$\frac{p}{p^*} = \frac{1}{M}\sqrt{\frac{\gamma+1}{2\left(1+\frac{\gamma-1}{2}M^2\right)}} \tag{A.4}$$

Stagnation pressure (Section 8.4.5)

$$I = -\frac{1}{2}\int \frac{1-M^2}{M^2\left(1+\frac{\gamma-1}{2}M^2\right)}\, dM^2$$

Let $M^2 = x,\ 1 = a,\ \frac{\gamma-1}{2} = b,\ X = a+bx$

$$I = -\frac{1}{2}\int \frac{(1-x)\,dx}{x(a+bx)} = -\frac{1}{2}\int \frac{dx}{x(a+bx)} + \frac{1}{2}\int \frac{dx}{a+bx}$$

$$I = \frac{1}{2a}\ln\frac{X}{x} + \frac{1}{b}\ln X$$

$$I = \frac{1}{2}\ln\frac{1+\frac{\gamma-1}{2}M^2}{M^2} + \frac{2}{\gamma-1}\ln\left(1+\frac{\gamma-1}{2}M^2\right)$$

$$I = \frac{1}{2}\ln\frac{1}{M^2}\left\{1+\frac{\gamma-1}{2}M^2\right\}^{(\gamma+1)/(\gamma-1)}$$

$$\int_1^M ( )\, dM^2 = \left[\ln \frac{1}{M} \left\{ 1 + \frac{\gamma - 1}{2} M^2 \right\}^{(\gamma+1)/2\,(\gamma-1)} \right]_1^M$$

$$\int_1^M ( )\, dM^2 = \ln \frac{1}{M} \left[\frac{2\left(1 + \frac{\gamma - 1}{2} M^2 \right)}{\gamma + 1} \right]^{(\gamma+1)/2\,(\gamma-1)} = \ln \frac{p_o}{p_o^*}$$

$$\frac{p_0}{p_0^*} = \frac{1}{M} \left[\frac{2\left(1 + \frac{\gamma - 1}{2} M^2 \right)}{\gamma + 1} \right]^{(\gamma+1)/2\,(\gamma-1)} \tag{A.5}$$

Impulse function (Section 8.4.6)

$$I = -\int \frac{(1 - M^2)}{2M^2 (1 + M^2) \left(1 + \frac{\gamma - 1}{2} M^2 \right)} dM^2$$

Let $x = M^2$

$$I = -\int \frac{1 - x}{x\,(1 + \gamma x)\ \{2 + (\gamma - 1)\, x\}} dx$$

$$I = -\int \frac{dx}{2x} + \int \frac{\gamma}{1 + \gamma x} dx + \int \frac{\gamma - 1}{4 + 2\,(\gamma - 1)\, x} dx$$

$$I = -\frac{1}{2} \ln x + \ln (1 + \gamma x) - \frac{1}{2} \ln \{2 + (\gamma - 1)\, x\}$$

$$I = \ln \frac{1 + \gamma x}{\sqrt{x\,\{2 + (\gamma - 1)\, x\}}}$$

$$I = \ln \frac{1 + \gamma M^2}{\sqrt{2M^2 \left(1 + \frac{\gamma - 1}{2} M^2 \right)}}$$

$$\int_1^M ( )\, dM^2 = \left[\ln \frac{1 + \gamma M^2}{M \sqrt{2 \left(1 + \frac{\gamma - 1}{2} M^2 \right)}} \right]_1^M$$

$$\int_1^M ( )\, dM^2 = \ln \frac{1 + \gamma M^2}{\sqrt{M \left(1 + \frac{\gamma - 1}{2} M^2 \right)}} - \ln \sqrt{\gamma + 1}$$

$$\int_1^M ( )\, dM^2 = \ln \frac{1 + \gamma M^2}{M \left[2\,(\gamma + 1) \left(1 + \frac{\gamma - 1}{2} M^2 \right) \right]^{1/2}} = \ln \frac{F}{F^*}$$

$$\frac{F}{F^*} = \ln \frac{1 + \gamma M^2}{M \left[2\,(\gamma + 1) \left(1 + \frac{\gamma - 1}{2} M^2 \right) \right]^{1/2}} \tag{A.6}$$

Maximum length parameter (Section 8.5)

$$I = \int \frac{1 - M^2}{\gamma M^4 \left(1 + \frac{\gamma - 1}{2} M^2 \right)} dM^2$$

Let $x = M^2,\ a = 1,\ b = \frac{\gamma - 1}{2},\ X = 1 + \frac{\gamma - 1}{2} x = a + bx$

$$I = \frac{1}{\gamma} \int \frac{1 - x}{x^2 X} dx$$

$$I = \frac{1}{\gamma} \int \left[\frac{dx}{x^2 X} - \frac{dx}{xX} \right]$$

$$I = -\frac{1}{\gamma} \left[\frac{X}{x} - b \ln \frac{X}{x} \right] + \frac{1}{\gamma} \ln \frac{X}{x}$$

$$I = \frac{1}{\gamma} \left[-\frac{1 + \frac{\gamma - 1}{2} M^2}{M^2} + \frac{\gamma - 1}{2} \ln \frac{1 + \frac{\gamma - 1}{2} M^2}{M^2} + \ln \frac{1 + \frac{\gamma - 1}{2} M^2}{M^2} \right]$$

$$I=\frac{1}{\gamma}\left[-\frac{1+\frac{\gamma-1}{2}M^2}{M^2}+\frac{\gamma+1}{2}\ln\frac{1+\frac{\gamma-1}{2}M^2}{M^2}\right]$$

$$\int_{M^2}^{1}(\,)\,dM^2=\frac{1}{\gamma}\left[-\frac{1+\frac{\gamma-1}{2}M^2}{M^2}+\frac{\gamma+1}{2}\ln\frac{1+\frac{\gamma-1}{2}M^2}{M^2}\right]_{M^2}^{1}$$

$$\int_{M^2}^{1}(\,)\,dM^2=\frac{1}{\gamma}\left[-\frac{\gamma+1}{2}+\frac{\gamma+1}{2}\ln\frac{\gamma+1}{2}\right]$$

$$-\frac{1}{\gamma}\left[-\frac{1+\frac{\gamma-1}{2}M^2}{M^2}+\frac{\gamma+1}{2}\ln\frac{1+\frac{\gamma-1}{2}M^2}{M^2}\right]$$

This on simplification and rearrangement gives

$$\int_{M^2}^{1}(\,)\,dM^2=\frac{1-M^2}{\gamma M^2}+\frac{\gamma+1}{2\gamma}\ln\frac{(\gamma+1)M^2}{2\left(1+\frac{\gamma-1}{2}M^2\right)} \qquad \text{(A.7)}$$

A.3

Isentropic flow of a perfect gas ($\gamma = 1.4$)

M	M^*	T/T_0	p/p_0	A/A^*	F/F^*	Ap/A^*p_0
0.00	0.000	1.000	1.000	∞	∞	∞
0.05	0.0548	0.999	0.998	11.592	9.158	11.571
0.10	0.1094	0.998	0.993	5.822	4.624	5.781
0.15	0.1640	0.996	0.984	3.910	3.132	3.849
0.20	0.218	0.992	0.973	2.964	2.400	2.882
0.25	0.272	0.987	0.957	2.403	1.973	2.301
0.30	0.326	0.982	0.939	2.035	1.698	1.912
0.35	0.378	0.976	0.918	1.778	1.509	1.634
0.40	0.431	0.969	0.895	1.590	1.375	1.424
0.45	0.483	0.961	0.870	1.448	1.276	1.261
0.50	0.534	0.954	0.843	1.339	1.203	1.129
0.55	0.585	0.943	0.814	1.255	1.147	1.022
0.60	0.635	0.933	0.784	1.188	1.105	0.932
0.65	0.684	0.922	0.753	1.135	1.073	0.855
0.70	0.732	0.910	0.721	1.094	1.049	0.789
0.75	0.779	0.898	0.688	1.062	1.031	0.731
0.80	0.825	0.886	0.656	1.038	1.018	0.681
0.85	0.870	0.874	0.623	1.020	1.009	0.636
0.90	0.914	0.860	0.591	1.009	1.004	0.596
0.95	0.958	0.847	0.559	1.002	1.001	0.560
1.00	1.000	0.833	0.528	1.000	1.000	0.528
1.10	1.081	0.805	0.468	1.008	1.003	0.472
1.20	1.158	0.776	0.412	1.030	1.011	0.425
1.30	1.231	0.747	0.361	1.066	1.022	0.385
1.40	1.300	0.718	0.314	1.115	1.034	0.350
1.50	1.364	0.689	0.272	1.176	1.048	0.320
1.60	1.425	0.661	0.235	1.250	1.063	0.294

M	M^*	T/T_0	p/p_0	A/A^*	F/F^*	Ap/A^*p_0
1.70	1.482	0.634	0.202	1.337	1.078	0.271
1.80	1.536	0.607	0.174	1.439	1.093	0.250
1.90	1.586	0.581	0.149	1.555	1.108	0.232
2.00	1.633	0.555	0.128	1.687	1.123	0.215
2.25	1.737	0.497	0.0865	2.096	1.156	0.181
2.50	1.826	0.444	0.0585	2.637	1.187	0.154
2.75	1.900	0.398	0.0397	3.337	1.213	0.133
3.00	1.964	0.357	0.027	4.234	1.236	0.115
3.50	2.064	0.289	0.013	6.789	1.274	0.089
4.00	2.138	0.238	0.00658	10.719	1.303	0.0706
4.50	2.194	0.198	0.00346	16.562	1.325	0.057
5.00	2.236	0.166	0.00189	25.000	1.341	0.047

A.4

Normal Shocks in a Perfect Gas ($\gamma = 1.4$)

M_x	M_y	p_y/p_x	T_y/T_x	p_{oy}/p_{ox}	p_{oy}/p_x
1.00	1.000	1.000	1.000	1.000	1.893
1.05	0.953	1.119	1.033	0.999	2.008
1.10	0.912	1.245	1.065	0.999	2.133
1.12	0.896	1.297	1.077	0.998	2.185
1.14	0.882	1.349	1.090	0.997	2.239
1.16	0.868	1.403	1.103	0.996	2.294
1.18	0.855	1.458	1.115	0.995	2.350
1.20	0.842	1.513	1.128	0.993	2.407
1.22	0.829	1.569	1.140	0.991	2.466
1.24	0.818	1.627	1.153	0.988	2.526
1.26	0.807	1.686	1.166	0.98	2.587
1.28	0.796	1.745	1.178	0.983	2.650
1.30	0.786	1.805	1.191	0.979	2.714
1.32	0.776	1.866	1.203	0.976	2.778
1.34	0.766	1.928	1.216	0.972	2.844
1.36	0.757	1.991	1.229	0.967	2.911
1.38	0.748	2.055	1.242	0.963	2.979
1.40	0.739	2.120	1.255	0.958	3.049
1.42	0.731	2.186	1.267	0.953	3.119
1.44	0.723	2.253	1.281	0.947	3.192
1.46	0.716	2.320	1.294	0.942	3.264
1.48	0.708	2.389	1.307	0.936	3.338
1.50	0.701	2.458	1.320	0.929	3.413
1.52	0.694	2.529	1.333	0.923	3.489
1.54	0.687	2.600	1.347	0.916	3.567
1.56	0.681	2.672	1.361	0.907	3.645
1.58	0.675	2.746	1.374	0.903	3.725

M_x	M_y	p_y/p_x	T_y/T_x	p_{oy}/p_{ox}	p_{oy}/p_x
1.60	0.668	2.820	1.388	0.895	3.805
1.70	0.641	3.205	1.458	0.856	4.224
1.75	0.628	3.406	1.495	0.834	4.443
1.80	0.616	3.613	1.532	0.813	4.669
1.85	0.605	3.826	1.569	0.790	4.902
1.90	0.595	4.045	1.608	0.767	5.142
2.00	0.577	4.500	1.687	0.721	5.641
2.50	0.513	7.125	2.137	0.499	8.526
3.00	0.475	10.333	2.679	0.328	12.061
3.50	0.451	14.125	3.315	0.213	16.242
4.00	0.435	18.500	4.047	0.138	21.068
4.50	0.423	23.548	4.875	0.0917	26.539
5.00	0.415	29.000	5.800	0.0617	32.654

A.5

Initial Mach Number as Function of Oblique Shock Wave Angles and deflections ($\gamma = 1.4$)

σ/δ	2	3	4	5	10	15	20	25	30
15	4.232	4.457	4.718	5.031	8.823				
20	3.132	3.251	3.385	3.536	4.734	9.830			
25	2.505	2.582	3.667	2.757	3.382	4.697	14.925		
30	2.100	2.158	2.217	2.280	2.681	3.348	4.900		
35	1.824	1.869	1.915	1.962	2.253	2.678	3.424	5.454	
40	1.624	1.662	1.698	1.738	1.965	2.275	2.748	3.635	6.812
45	1.475	1.507	1.541	1.575	1.767	2.015	2.359	2.905	4.055
50	1.362	1.391	1.422	1.453	1.625	1.837	2.115	2.515	3.198
55	1.276	1.305	1.334	1.363	1.526	1.718	1.959	2.287	2.788
60	1.211	1.240	1.270	1.300	1.460	1.645	1.870	2.165	2.582
65	1.165	1.195	1.227	1.257	1.425	1.615	1.840	2.125	2.520
70	1.135	1.169	1.204	1.240	1.426	1.635	1.878	2.187	2.608
75	1.125	1.165	1.208	1.252	1.478	1.733	2.035	2.418	2.970

A.6

Initial and Final Mach Numbers and Deflections from Normal Shock Tables ($\gamma = 1.4$)

M_x	M_y	σ	M_1	δ	M_2
1.00	1.00	15	3.863	0	3.863
1.05	0.593	15	4.057	1.11	3.972
1.10	0.912	15	4.250	2.09	4.081
1.20	0.842	15	4.636	3.70	4.278
1.30	0.786	15	5.023	4.97	4.515
1.40	0.739	15	5.409	5.989	4.723
1.50	0.701	15	5.795	6.811	4.922
2.00	0.577	15	7.727	9.26	5.775
2.50	0.513	15	9.659	10.40	6.402
3.00	0.475	15	1.591	11.02	6.857
1.00	1.00	30	2.000	0	2.000
1.05	0.953	30	2.100	1.96	2.027
1.10	0.912	30	2.200	3.71	2.059
1.20	0.842	30	2.400	6.72	2.131
1.30	0.786	30	2.600	9.15	2.208
1.40	0.739	30	2.800	11.13	2.288
1.50	0.701	30	3.000	12.77	2.368
2.00	0.577	30	4.000	17.78	2.728
2.50	0.513	30	5.000	20.17	3.006
3.00	0.475	30	6.000	21.48	3.210
1.00	1.00	45	1.414	0	1.414
1.05	0.953	45	1.485	2.30	1.405
1.10	0.912	45	1.555	4.45	1.403
1.20	0.842	45	1.697	8.30	1.409
1.30	0.786	45	1.838	11.58	1.427

M_x	M_y	σ	M_1	δ	M_2
1.40	0.739	45	1.980	14.38	1.452
1.50	0.701	45	2.121	16.76	1.482
2.00	0.577	45	2.828	24.44	1.644
2.50	0.513	45	3.535	28.30	1.785
3.00	0.475	45	4.243	30.46	1.893
1.00	1.00	60	1.154	0	1.154
1.05	0.953	60	1.212	2.04	1.124
1.10	0.912	60	1.270	4.02	1.100
1.20	0.842	60	1.385	7.76	1.065
1.30	0.786	60	1.501	11.19	1.044
1.40	0.739	60	1.616	14.29	1.033
1.50	0.701	60	1.732	17.07	1.029
2.00	0.577	60	2.309	26.99	1.060
2.50	0.513	60	2.887	32.54	1.113
3.00	0.475	60	3.464	35.82	1.160
1.00	1.00	75	1.035	0	1.035
1.05	0.953	75	1.087	1.19	0.993
1.10	0.912	75	1.139	2.39	0.955
1.20	0.842	75	1.242	4.77	0.895
1.30	0.786	75	1.345	7.10	0.848
1.40	0.739	75	1.449	9.36	0.812
1.50	0.701	75	1.553	11.52	0.783
2.00	0.577	75	2.071	20.55	0.709
2.50	0.513	75	2.588	26.77	0.687
3.00	0.475	75	3.106	30.94	0.683

A.7

Flow of a Perfect gas with Friction (Fanno Line, $\gamma = 1.4$)

M	p/p^*	$c/c^* = \rho^*/\rho$	T/T^*	p_0/p_0^*	F/F^*	$4\bar{f}L_{max}/D$
0.00	∞	0	1.200	∞	∞	∞
0.05	21.903	0.0547	1.199	11.592	9.158	280.02
0.10	10.944	0.1094	1.197	5.822	4.624	66.922
0.12	9.116	0.131	1.1965	4.864	3.875	45.408
0.14	7.809	0.153	1.195	4.182	3.343	32.511
0.16	6.829	0.175	1.194	3.673	2.947	24.198
0.18	6.066	1.196	1.192	3.278	2.642	18.543
0.20	5.455	0.218	1.1905	2.963	2.400	14.533
0.25	4.355	0.272	1.185	2.403	1.973	8.483
0.30	3.619	0.3257	1.178	2.035	1.698	5.299
0.35	3.092	0.379	1.171	1.778	1.509	3.453
0.40	2.696	0.431	1.163	1.590	1.375	2.308
0.45	2.386	0.483	1.153	1.448	1.276	1.566
0.50	2.138	0.534	1.143	1.340	1.203	1.069
0.52	2.052	0.555	1.138	1.303	1.178	0.917
0.54	1.972	0.575	1.134	1.270	1.157	0.787
0.56	1.897	0.595	1.129	1.240	1.138	0.673
0.58	1.828	0.615	1.124	1.213	1.120	0.576
0.60	1.763	0.635	1.119	1.188	1.105	0.491
0.65	1.618	0.684	1.106	1.135	1.073	0.325
0.70	1.493	0.732	1.093	1.094	1.049	0.208
0.75	1.385	0.779	1.078	1.062	1.031	0.127
0.80	1.289	0.825	1.064	1.038	1.918	0.072
0.85	1.205	0.870	1.048	1.020	1.0097	0.0363
0.90	1.129	0.914	1.0327	1.009	1.004	0.0145
0.95	1.061	0.958	1.0165	1.002	1.001	0.0033
1.00	1.000	1.000	1.000	1.000	1.000	0.000

M	p/p^*	$c/c^* = \rho^*/\rho$	T/T^*	p_0/p_0^*	F/F^*	$4\bar{f}L_{max}/D$
1.20	0.804	1.158	0.932	1.030	1.011	0.0336
1.50	0.606	1.365	0.827	1.176	1.048	0.136
1.60	0.557	1.425	0.794	1.250	1.063	0.172
1.70	0.513	1.483	0.760	1.338	1.078	0.208
1.80	0.474	1.536	0.728	1.439	1.0935	0.242
1.90	0.439	1.586	0.697	1.555	1.108	0.274
2.00	0.408	1.633	0.667	1.687	1.123	0.305
2.50	0.292	1.826	0.533	2.637	1.187	0.432
3.00	0.218	1.964	0.428	4.235	1.237	0.522
3.50	0.1685	2.064	0.348	6.789	1.274	0.586
4.00	0.134	2.138	0.286	10.719	1.303	0.633
4.50	0.108	2.194	0.237	16.562	1.325	0.667
5.00	0.0894	2.236	0.200	25.000	1.342	0.694

A.8

Flow of a Perfect gas with heat transfer (Rayleigh line $\gamma = 1.4$)

M	p/p^*	p_0/p_0^*	T/T^*	T_0/T_0^*	$c/c^* = \rho^*/\rho$
0.00	2.400	1.268	0.000	0.000	0.000
0.05	2.392	1.266	0.0143	0.0119	0.00598
0.10	2.367	1.259	0.056	0.0468	0.0237
0.12	2.353	1.255	0.079	0.0667	0.0339
0.14	2.336	1.251	0.107	0.089	0.0458
0.16	2.317	1.246	0.137	0.115	0.0593
0.18	2.296	1.241	0.1708	0.143	0.0744
0.20	2.273	1.235	0.2066	0.1735	0.091
0.25	2.207	1.218	0.304	0.257	0.138
0.30	2.131	1.198	0.409	0.3468	0.192
0.35	2.048	1.178	0.514	0.439	0.251
0.40	1.961	1.157	0.615	0.529	0.314
0.45	1.870	1.135	0.708	0.614	0.378
0.50	1.778	1.114	0.790	0.691	0.444
0.52	1.741	1.106	0.819	0.720	0.470
0.54	1.704	1.098	0.847	0.747	0.497
0.56	1.668	1.090	0.872	0.772	0.523
0.58	1.632	1.083	0.896	0.796	0.549
0.60	1.596	1.075	0.917	0.819	0.574
0.65	1.508	1.058	0.961	0.868	0.637
0.70	1.424	1.043	0.993	0.908	0.697
0.75	1.343	1.030	1.014	0.940	0.755
0.80	1.266	1.019	1.025	0.964	0.810
0.85	1.193	1.011	1.028	0.981	0.862
0.90	1.125	1.045	1.0245	0.992	0.911
0.95	1.060	1.001	1.0146	0.998	0.957
1.00	1.000	1.000	1.000	1.000	1.000

M	p/p^*	p_0/p_0^*	T/T^*	T_0/T_0^*	$c/c^* = \rho^*/\rho$
1.20	0.796	1.0194	0.912	0.978	1.146
1.50	0.578	1.122	0.753	0.909	1.301
1.60	0.523	1.176	0.702	0.884	1.340
1.70	0.475	1.240	0.654	0.859	1.375
1.80	0.433	1.316	0.609	0.836	1.405
1.90	0.396	1.403	0.567	0.814	1.431
2.00	0.363	1.503	0.529	0.794	1.455
2.50	0.246	2.222	0.378	0.710	1.538
3.00	0.176	3.424	0.280	0.654	1.588
3.50	0.132	5.328	0.214	0.616	1.619
4.00	0.1025	8.227	0.168	0.589	1.641
4.50	0.0818	12.502	0.135	0.569	1.656
5.00	0.0667	18.634	0.111	0.555	1.667

A.9

Important Events in the Development of Aircraft Engines and Propulsion Systems

100 B.C.	Jet propulsion utilized for the first time by Hero of Alexandria (Egypt) in his engine called "aeolipile".
1500 A.D.	Leonardo Vinci employed hot air from the chimney to drive a rotor (chimney jack).
1687 A.D.	Newton's steam jet propelled wagon developed by a Dutchman.
1783 A.D.	First manned flight in a hot-air balloon in Paris.
1783 A.D.	Propeller drive for an airship was suggested first in France.
1791 A.D.	John Barbar obtained patent for his gas turbine (first in the world).
1838 A.D.	Screw propeller used in Britain.
1852 A.D.	Henri Giffard flew an airship by a 3 h.p. steam engine in France.
1860 A.D.	First internal combustion engine constructed by Lenoir in France.
1872 A.D.	Stoltze obtained patent for a gas turbine engine; it was tested during 1901-1904 but failed to operate successfully.
1876 A.D.	Otto's gas engine constructed in Germany.
1884 A.D.	9 h.p. electric motor was employed in France to propel an airship.
1903 A.D.	12 h.p. I.C. engine developed for flying by Wright brothers. Flight speeds 28-500 miles/hr. Power 12-2200 h.p. Type Reciprocating and radial engines.
1903 A.D. -1906 A.D.	A number of gas turbine power plants built in France by Societe des Turbomoteurs.
1917	Eight cylinder Liberty engine was built for aviation in the U.S.
1930	Frank Whittle (in Britain) developed a jet engine for aircraft propulsion.
1939	Hans von Ohain of Germany developed a jet engine.

1940	Secundo Campini employed the reciprocating I.C. engine for a jet propelled aircraft in Italy.
1942	First jet propelled aircraft flown in the United States.
1944	Operation of the first jet fighter by Germans.
1950	Sonic flights made by jet propelled aircrafts.

A.10

Some Important Events is Space Flights

4th Oct. 1957	World's first satellite sputnik I put into orbit by Russia.
3rd Nov. 1957	Russian satellite sputnik II put into orbit with a dog-Laika.
31st Jan. 1958	Satellite Explorer I launched by the U.S. for the first time.
11th Oct. 1958	Pioneer 1 was launched by the U.S. for placing probes in lunar orbit; could not achieve the target.
2nd Jan. 1959	Luna 1 (first spacecraft to escape from the earth) launched by Russia.
3rd March 1959	Pioneer 4 (first U.S. spacecraft to escape from the earth) launched.
12th Sept. 1959	Luna 2 launched by Russia. First man made satellite to touch the moon.
2nd March 1960	Pioneer 5 launched by U.S. for deep interplanetary probe.
19th Aug. 1960	Russian spacecraft for the first time took dogs, rats and flies (biological payload) in its ''zoo flight''.
12th April 1961	First manned orbital flight by Russian astronaut Maj. Yuri Gagarin in the spacecraft Vastok I.
5th May 1961	First space flight by the U.S. astronaut Alan B. Shapherd, Jr. in spacecraft Freedom-7.
21st July 1961	Astronaut Virgil I. Grissom (2nd U.S. astronaut) went into space in spacecraft Liberty Bell-7.
6th Aug. 1961	Russian cosmonaut Major Titov completed 17 ½ orbits in spacecraft Vastok-II.
20th Feb. 1962	U.S. Astronaut John H. Glenn completed three orbits in spacecraft Friendship-7.
23rd April 1962	Ranger IV, first U.S. spacecraft touched the moon surface on 26th April 1962.
10th July 1962	First successful attempt at T.V. transmissions through satellite Telstar-I
27th Aug. 1962	U.S. launched Mariner-2 for Venus probe.

2nd April 1963	Luna-4 launched by Russia for soft landing on Moon but missed moon surface by 8000 km.
16th June 1963	Russian cosmonaut Valentia V. Tereshkova (first woman in space) completed 48 orbits in Vastok VI.
30th Jan. 1964	U.S. spacecraft Ranger-VI launched; reached Moon surface on 2.2.64 at the sea of Tranquility.
28th Jan. 1964	Ranger-VII launched by U.S.; thousands of pictures of the lunar surface obtained.
12th Oct.1964	Russian spacecraft Voskhod I launched with three cosmonauts.
5th Nov. 1964	Mariner 3 launched by U.S. for attempting Mars fly by; target could not be achieved.
17th Feb. 1965	U.S. spacecraft Ranger VIII launched for probing lunar surface; landed on Moon at the sea of Tranquility on 20th Feb. 1965.
18th March 1965	Russian spaceship Voskhod-II launched with two cosmonauts; one of them walked in space outside the spaceship.
3rd June 1965	U.S. spacecraft Gemini-IV made 62 orbits with two astronauts; one of them performed a 'space-walk' outside the craft.
4th Oct. 1965	Luna 7 launched by Russia for lunar soft landing crashed in the ocean of storms.
16th Nov. 1965	Venera 3 launched by Russia for probing Venusian atmosphere; target could not be achieved.
31st Jan. 1966	Luna 9 launched by Russia for lunar soft landing. First successful lunar landing on 3rd Feb. 1966 by Russia.
30th May 1966	Surveyor I launched by U.S. for lunar soft landing. First successful lunar soft-landing by U.S. on Ist June 1966.
10th Aug. 1966	Lunar Orbiter 1 launched by U.S.: first U.S. lunar satellite.
21st Dec. 1966	Luna-13 launched by Russia; soft-landed on moon on 24th Dec. 1966.
16th April 1967	Surveyor-3 launched by U.S. for lunar soft-landing; trench-digging experiments performed.
12th June 1967	Venera-4 launched by Russia for probing Venusian atmosphere.
8th Sept. 1967	Surveyor-5 launched by U.S. for lunar soft-landing. Examination of chemical composition of lunar soil conducted.
7th Jan. 1968	Surveyor-7 launched by U.S. for lunar soft-landing; T.V. photography and laser communication tests performed.
15th Sept. 1968	Zond-5 launched by Russia; flew within 1950 km of the lunar surface.
21st Dec. 1968	Apollo-8 launched by U.S. spacecraft with a crew of three astronauts went into lunar orbit for visual and photographic studies.
5th Jan. 1969	Venera-5 launched by Russia for Venus soft-landing.
24th Feb. 1969	Mariner-6 launched by U.S. for Mars flyby; flew within 3400 km of Martian surface.
18th May 1969	Apollo-10 (U.S.) performed rendezvous and docking with LEM in lunar orbit with crew of three astronauts. LEM went within 15 km of the lunar surface.

16th July 1969 Neil Armstrong, Edwin Aldrin and Michael Collins flew in Apollo-11 (U.S.) for the first manned landing on the moon. Landed on 20th July 1969.

11th April 1970 Apollo-13 with 3 men crew launched for moon landing. Mission was abandoned due to an explosion.

17th Aug. 1970 Venera-7 (USSR) was launched for Venus soft landing. Landed on Venus on 15th Dec. 1970. Transmitted data.

31st Jan. 1971 Apollo-14 took a crew of three for Moon-landing (on 5th Feb. 1971). A distance of 3.4 km was traversed during a total stay of 33 hours on the moon.

19th May 1971 Russia launched the combined Mars orbiter and lander. First spacecraft to land on Martian surface.

17th Aug. 1971 Mariner-9 sent into Martian orbit. Transmitted photographs of volcanoes and canyons on Martian surface.

26th March 1972 Russian spacecraft Venera-8 entered Venusian atmosphere. Data on pressure, temperature, atmosphere and soil was obtained.

7th Dec. 1972 Apollo-17 took 3 men crew for Moon landing (on 11th Dec. 1972); total stay on Moon = 75 hours, distance traversed on lunar surface = 26 km.

8th Jan. 1973 Luna-21 sent by Russia for lunar landing; automatic lunar rover used on the lunar surface.

5th May 1973 Pioneer-11 launched by the U.S. for the study of planets of the outer solar system; flew past Jupiter and Saturn.

5th Aug. 1973 Landing capsule and "Mars flyby bus" launched by Russia; landing capsule reached Martian surface but lost communication.

28th Oct. 1974 Luna-23 launched by Russia; landed on Moon on 6th Nov. 1974 at the Sea of Crises.

10th Dec. 1974 Helio-1 (joint venture of West Germany and U.S.) launched to study solar phenomenon such as solar winds, magnetic field, radio waves etc.

8th June 1975 Venera-9 launched by Russia; successful landing of the lander on Venusian surface on 22nd Oct. 1975. Measurements of wind speed and soil composition were made. The main spacecraft went into the venus orbit becoming its artificial satellite.

20th Aug. 1975 Viking-1 (combined orbiter and lander) launched by the U.S. Lander reached Martian surface on 20th July 1976. Measurements of wind speed, soil composition, pressure, temperature etc. were made.

15th June 1976 Joint U.S. West German Helios-2 launched for the study of solar phenomena. Measurements of solar wind, magnetic field, radio waves etc. were made.

5th Sept. 1977 Voyager-1 launched by the U.S. for the study of the outer planets of the solar system. Flew past Jupiter and Saturn and sent thousands of photographs of Jupiter, Galilean moons and Saturn.

20th May 1978 U.S. launched Pioneer-Venus-1 for the study of Venusian atmosphere and mapping the surface. Photographs of comet Halley were also obtained.

9th Sept. 1978 Russia sent Venera-11 (combined Venus flyby probe and lander); the lander reached Venusian surface on 21st Dec. 1978 and conducted chemical analysis of the Venusian atmosphere. Flyby bus flew within 35,000 km of Venus.

4th Nov. 1981 Russia sent combined Venus fly-by bus and lander (Venera-14). Lander touched down Venus on 5th March 1982 and functioned for 53 minutes on its surface. Chemical examination of the venusian soil conducted.

7th June 1983 Russia launched Venera-16 (Venus orbiter and surface mapper); entered Venus orbit on 14th Oct. 1983 mapping a large area of the Venusian surface.

15th Dec. 1984 Vega-1 (combined Venus and comet Halley probe) launched by Russia. Conducted examination and measurements of plasma, magnetic field, dust and gas. Venus lander operated on the surface for 56 minutes. Flew past comet Halley on 6th March 1986.

19th Aug. 1985 Japanese-Suisei (planet-A mission) launched towards comet Halley. Flew within 151,000 km of Halley's nucleus on 8th March 1986 and conducted scientific studies.

A.11

Glossary of Terms in Rocket Propulsion and Space Flights

A.11.1 Rocket Propulsion

Artillery rockets

Rockets used in terrestrial (military) applications; they have a maximum velocity of about 1500 m/s.

Auxiliary power plant

Power plant (turbo-generator set) used for supplying electric power to the rocket and spacecraft.

Ballistic missile

A long range missile which follows a ballistic path. It does not have wings; its course cannot be deflected. It is used as surface to surface missile.

Bipropellants

Propellants consisting of two chemicals-fuel and oxidizer; they react to release thermal energy.

Booster rocket

High thrust first stage powerful rocket or rockets.

Burning rate

The rate at which a solid propellant grain burns in terms of millimeters per second.

Burnout time

Operation time of a rocket engine or a stage; duration of powered flight of a rocket.

Burnout velocity

Velocity attained by the rocket at the end of the powered flight; it is also called cut-off velocity.

Cigarette burning

Burning of the solid propellant grain at one end like a cigarette.

Composite propellants

Solid propellant grain made of a mixture of crystalline fuel and oxidizer material.

Coasting

Free flight of a space vehicle during which the thrust acting on it is zero.

Cryogenic material

Materials (propellants) which are in liquid state at very low temperature and in the gaseous state at normal temperature.

Effective exhaust velocity

This is a hypothetical or fictious velocity at the exit of the rocket nozzle (with complete expansion) which would produce the same thrust as the actual jet.

Electrical rockets

Rockets which employ electrical energy for their propulsion.

Gas pressurization

Use of high pressure gas for feeding liquid propellants into the combustion chamber.

Guided missile

A missile which is controlled throughout its mission.

Hybrid rockets

Rockets employing both liquid and solid propellants.

Hypergolic propellants

Propellants which ignite on coming into contact with each other; they do not require an ignition device.

Impulsive velocity

Velocity reached by a rocket in the absence of gravity and drag.

Infinite staging

Continuous discarding of used up or burnt out rocket stages.

Inhibitors

Materials used on the surface of solid propellant grains to restrict burning.

JATO

Jet assisted take off.

LOX

Liquid oxygen.

Mass ratio

Ratio of the final mass of the rocket (or stage) at burnout and its initial mass.

Mixture ratio
Flow rate of the oxidizer per unit flow rate of the fuel.

MMH
Monomethyl hydrazine.

Mono propellant
A single propellant composed of both the combustible substance and the oxidizer.

Nuclear rocket
A rocket using nuclear energy for its propulsion.

Photon rocket
A rocket propelled by a beam of photons.

Propellant grain
The solid mass of fuel and oxidizer in different geometrical shapes used in solid propellant rockets.

Propellant mass fraction
Ratio of propellant mass and the initial mass of the rocket at take-off.

Pyro technique
Ignition of a small mass of solid propellants by electrical device.

Ramjet-rocket
A combination of a rocket and a ramjet engine.

RATO
Rocket-assisted take-off.

Retro-rockets
Rockets fired in the direction of flight of space vehicles for achieving their deceleration.

Restricted burning
Burning of solid propellant grain only at some surfaces while other surfaces are prevented from burning.

RFNA
Red-fuming nitric acid.

Rocket stage
A propulsion unit or engine consisting of its fuel and oxidizer tanks (or the solid propellant grain), propulsion nozzle, etc.

Solar rocket
A rocket which employs solar energy for its propulsion.

Solar sail
A sail which employs radiation pressure of the sun on it for providing thrust to a spacecraft.

Sounding rocket
A rocket used for collecting data on weather.

Specific impulse
Thrust per unit weight flow rate of the propellant; this is measured in seconds.

Storable propellants
Rocket fuels and oxidizers which remain in liquid state at normal temperature.

Sustainer rocket
A rocket which imparts low thrust for long duration for supplying additional energy to the space vehicle.

Thrust decay
Reduction of thrust to zero towards burnout of a rocket

TVC
Thrust vector control.

Tripropellant
Combination of three liquid chemicals employed for rocket propulsion.

Turbo-rocket
A combination of turbojet and rocket engines.

UDMH
Unsymmetrical dimethyl hydrazine; a liquid fuel for rocket propulsion.

Vernier rocket
A small rocket employed for accurate adjustment of the magnitude and direction of the thrust of the main rocket or missile.

WFNA
White-fuming nitric acid.

Zero stage
The stage parallel to the first stage; it is fired first and employs a number of rockets surrounding the first stage rocket.

A.11.2.Space Flights

Artificial satellite
A man made space vehicle or spacecraft which orbits around earth or other heavenly bodies.

Asteroid
Small heavenly body in orbit intersecting the orbits of Mars and Jupiter.

Astronaut/cosmonaut
One who goes in the outer space or to other heavenly bodies such as moon and Mars.

Astronomical unit
Unit of distance in space science which is equal to the average distance between the earth and sun; this is equal to about 92.96×10^6 miles.

Attitude control
Governing the orientation of a space vehicle during its flight.

Capture orbit
The orbit of a body in which its energy is only slightly less than the escape energy.

Celestial
Heavenly, belonging to heaven.

Comet
Small object in the solar system which is visible only when it approaches the sun; it has a bright nucleus and a tail formed of space dust and gases.

Drag loss
Rocket thrust required to overcome atmospheric drag force which is not available for acceleration of the rocket.

Earth satellite
A space vehicle orbiting around earth.

Earth time
The time that passes on earth during space flights.

Escape rocket
A rocket which overcomes the gravitational pull to travel an infinite distance away from the earth.

Escape velocity
The velocity of a rocket required to escape from the earth's gravity; this is equal to about 11,200 m/s corresponding to gravitational force at the earth's surface.

Fixed satellite
An earth satellite with zero velocity relative to the earth.

Flight path angle
Angle made by the tangent at the flight trajectory with the horizontal.

Flyby
Flying close to a planet for utilizing its gravitational field in order to accelerate a space vehicle.

Galaxy
Large clusters of stars such as ours which include billions of stars and the milky way.

Gravity loss
The thrust required to overcome gravitational force which is not available for accelerating the rocket.

Heliocentric orbit
Orbit with sun as the centre.

Hohmann transfer
Transfer from one circular orbit to the other along an elliptical trajectory with minimum energy.

Inner solar system
Region of the solar system lying within the Mars orbit.

Intergalactic space
Space between various galaxies.

Inter stellar space
Space between various stars.

LEM
Lunar excavation module.

Light year
Distance travelled by light in one year; this is equal to 5.9×10^{12} miles or 9.44×10^{12} kilometers.

Mass annihilation rocket
A rocket which converts all its fuel (nuclear) into energy.

Meteors
Small bodies in the interplanetary space.

Natural satellite
Small heavenly bodies (moons) revolving around larger bodies (planets) in the solar system.

Orbit
The path of a spacecraft or a heavenly body moving about another body under its gravitational attraction.

Orbital velocity
Velocity of the satellite to maintain it in an orbit.

Outer solar system
Region of the solar system which lies outside the Mars orbit.

Payload
The net weight of the equipment and crew carried by a space vehicle in a space mission; this excludes the weight of the rocket engine and fuel.

Satellite
A smaller body (man made or natural) revolving round a bigger body under its gravitational force.

Solar system

The sun and the planetary system consisting of its nine planets (Earth, Mars, Venus, Jupiter, Saturn, Uranus, Pluto, Neptune and Mercury) and a number of moons, comets, asteroids and meteors.

Space

Infinite extension or regions remote from the earth; interplanetary distance.

Spacecraft

A vehicle or craft that goes into space or to the heavenly bodies; it is also referred to as spaceship.

Terrestrial

Earthly, belonging to the Earth.

Trajectory

Path of flight of a rocket, missile or a spacecraft.

Bibliography

Thermodynamics

1. Gibbings, J.C., *Thermomechanics; The governing equations*, Pergamon Press, 1970.
2. Hall, N.A., *Thermodynamics of Fluid Flow*. Prentice-Hall, 1951.
3. Hatsopoulos, G.N. and Keenan, J.H., *Principles of General Thermodynamics*, Wiley, 1965.
4. Holman, J.P., *Thermodynamics*, 2nd ed. McGraw-Hill (Kogakusha), 1974.
5. Reynolds, W.C. and Perkins, H.C., *Engineering Thermodynamics*, 2nd ed. McGraw-Hill, 1977.
6. Saad, M.A., *Thermodynamics for Engineers*, Prentice-Hall, New Delhi, 1976.
7. Spalding, D.B. and Cole, E.H., *Engineering Thermodynamics*, Arnold, 1973.
8. Wark, K., *Thermodynamics*, 3rd ed. McGraw-Hill, 1977.
9. Zemansky, M.W. et. al., *Basic Engineering Thermodynamics*, 2nd ed., McGraw-Hill, 1975.

Fluid Mechanics, Fluid Dynamics and Aerodynamics

10. Bradshaw, P., *Experimental Fluid Mechanics*, 2nd ed., Pergamon Press, 1970.
11. Fox, J.A., *An Introduction to Engineering Fluid Mechanics*, Macmillan Press, 1974.
12. Howarth, L., (Ed), *Modern Development in Fluid Dynamics*, Oxford, 1953.
13. Kuethe, A.M. and Schetzer, *Fundamentals of Aerodynamics*, Wiley, 1959.
14. McLeod, E.B., Jr., *Introduction to Fluid Dynamics*, Macmillan, 1955.
15. Reynolds, A.J., *Thermofuid Dynamics*, Wiley-interscience, 1971.
16. Streeter, V.L., *Fluid Mechanics*, 5th ed. McGraw-Hill, 1971.
17. Streeter, V.L., (Ed), *Hand Book of Fluid Dynamics*, McGraw-Hill, 1961.
18. Yuan, S.W., *Foundations of Fluid Mechanics, Prentice-Hall, New Delhi, 1969.*

Gas Dynamics/Compressible Flow

19. Cambel, A.B. and Jennings, B.H., *Gas Dynamics*, McGraw-Hill, 1958.
20. Chapman, A.J. and Walker, W.F., *Introductory Gas Dynamics*, Holt Rinehart and Winston, 1971.
21. Imrie, B.W., *Compressible Fluid Flow*, Butterworths, 1973.
22. Joh, J.E.A., *Gas Dynamics*, Allyn and Bacon, Boston, 1969.

23. Liepmann, H.W. and Roshko, A., *Elements of Gas Dynamics*, Wiley, 1957.
24. Oswatitsch, K., *Gas Dynamics*, Academic Press, 1956.
25. Owczarek, J.A., *Fundamentals of Gas Dynamics*, International Text Book Co., 1964.
26. Pai, S.I., *Introduction to the Theory of Compressible Flow*, Van Nostrand, 1959.
27. Rotty, R.M., *Introduction to Gas Dynamics*, Wiley, 1962.
28. Shapiro, A.H., *The Dynamics and Thermodynamics of Compressible Fluid Flow*, (Vol. I and II), Ronald Press, 1953.
29. Tsien, H.S., *Equations of Gas Dynamics*, Princeton University Press, 1958.
30. Thompson, P.A., *Compressible Fluid Dynamics*, McGraw-Hill, 1972.
31. Zucker, R.D. *Fundamentals of Gas Dynamics*, Matrix Publishers, Champaign, 1977.
32. Zucrow, M.J. and Hoffman, J.D., *Gas Dynamics*, (Vol. I and II), Wiley, 1977.

Method of Measurement

33. Beckwith, T.G. and Buck, N.L. *Mechanical Measurements*, 2nd ed., Addison-Wesley, 1973.
34. B.S. 1042, Part 2A, *Methods for the Measurement of Fluid Flow in Pipes*, British Standard Institution, London, 1973.
35. Clark, N.J., *Flow Measurement*, Pergamon Press, 1965.
36. Doebelin, E.O., *Measurement Systems: Application and Design*, McGraw-Hill (Kogakusha), 1966.
37. *Fluid Meters: Their theory and applications*, A.S.M.E. Research Committee on Fluid Meters, 6th ed. 1977.
38. Lion, K.S.,*Instrumentation in Scientific Research*, New York, McGraw-Hill 1959.
39. Neubert, H.K.P., *Instrument Transducers*, Oxford University Press, 1968.
40. Ower, E. and Pankhurst, R.C. *The Measurement of Air Flow*, 5th ed. Pergamon Press, 1977.
41. Pankhurst, R.C., and Holder, D.W., *Wind Tunnel Techniques*, Pitman, 1952.
42. Patranabis, D., *Principles of Industrial Instrumentation*. Tata McGraw-Hill, New Delhi, 1976.
43. Pope, A., *Wind Tunnel Testing*, Wiley, 1954.

Aerospace Propulsion

44. Aerospace year book, 1961. *American Aviation Publications*, Inc.
45. Emme, Eugene M. *History of Space flight. Holt*, Rinehart and Winston Inc. 1965.
46. Hesse, W.I. and Mumford, N.V.S., *Jet Propulsion for Aerospace Applications*, Pitman, 1964.
47. Hill and Peterson, *Mechanics and Thermo-dynamics of Propulsion*, Addison-Wesley, Reading, Mass, 1965.
48. Hunter, Maxwell W., *Thrust into Space*, Holt, Rinehart and Winston Inc., 1966.
49. Kerrebrock, J.L., *Aircraft Engines and Gas Turbines*, The M.I.T. Press, 1977.
50. Shephard, D.G., *Aerospace Propulsion*, Am. Elsevier Pub. Co. Inc.
51. Spaceflight journal of the British Interplanetary Society, Missiles and Rockets.

52. Sutton, George, P., and Ross, D.P., *Rocket Propulsion Elements*, 4th edn. John Wiley, 1976.
53. Whittle, F., *The Early History of Whittle Jet Propulsion Gas Turbines*, Proc. Instn. Mech. Engrs., 152, 1945.

Gas Tables

54. Houghton, E.L. and Brock, A.E., *Tables for the compressible Flow of Dry Air*, Arnold, 1970.
55. Keenan, J.H. and Kaye, J., *Gas Tables*, Wiley, 1948.
56. Yahya, S.M., *Gas Tables* , 3rd ed. Wiley Eastern, 1990.

Index

A

Acceleration 343, 354
Adiabatic process 17, 88, 90
Adiabatic wall temperature 389
Aerofoil 220, 453
Aeolipile 455
After burner 460
Aircrafts 550
Aircraft propulsion 453, 465
Air standard efficiency 466
Alcohol 515
Altitude loss 559
Altitude gain 558, 566
Aniline 515
Area ratio 96, 531
Artillery rockets 670
Artificial sattelite 673
Attached shock 249
Attitude control 674
Atmosphere 30, 31
Axial flow fan 85
Axisymmetric flow 353, 359

B

Back scatter 432
Ballistic missile 552, 670
Bernoulli equation 59, 395
Beryllium hydride 510
Bipropellants 514, 670
Blowdown tunnel 420
Blower tunnel 416
Body forces 328, 344, 359
Booster rocket 552, 670
Boundary 4
Bourdon-tube gauges 386
Brayton cycle 458
Bridge circuit 387, 391
Bulk modulus 18
Burning rate 529
Burnout velocity 557
Burnout time 557, 590

C

Calibration curves 392, 399
Cartesian coordinates 338
Centrifugal fan 590
Change of entropy 17, 186, 278
Characteristic velocity 546, 573
Cigarette burning 534, 671
Circulation 346
Claw type yawmeter 401
Closed circuit tunnel 442, 444
Coasting flight 558, 671

Cobra probe 402
Coefficient of
—compressibility 20
—discharge 408
—skin friction 27
—viscosity 25
Combustion 458
—chamber 459
Compressed an system 615
Compressible flow 21
Compression wave 141, 157, 605
Component efficiencies 467
Compressor 457, 465
Conical diffuser 115
Conical shock 220
Continuity equation 73, 338, 350
Continuum 5
Control surface 73, 82
Control volume 4, 45
Constant current hot-wire 400
Constant enthalpy lines 314
Constant entropy lines 313
Constant temperature hot-wire 398
Convergent-divergent nozzles 107
Convergent nozzle 106
Correction factor 388
Corocco number 58
Critical velocity 55, 94
Cryogenic material 671
Curved shock 220
Cylindrical coordinates 350
Cycle 5

D

Darcy's friction factor 28
Definitions 3
Deflection angle 234
Degree of tubulence 27
Density 6, 393
—ratio 232
Detached shock 220, 249
Diffusers 92, 110
Diffuser efficiency 196
Diffuser throat 195
Downstream Mach number 178, 242
Drag 453
—loss 674
Dual-beam laser 431
Dual-focus laser velocimeter 435

E

Early rockets 504
Earth satellite 568
Effect of compressibility 60
Effective jet velocity 477, 540
Effective speed ratio 474
Equation of state 13
Equilibrium 6
Elastic medium 130
Electrical flow meter 412
Electrical rockets 512
Electrostatic propulsion 513
Elemental cube 339
Energy 7
—equation 45, 78
—transformation 48
Enthalpy 10
Entropy 17
—equation 80
Escape velocity 569, 674
Ethnol 515
Exhaust jet 508
Exhaust nozzle 466
Expansion wave 153, 155, 604
Exosphere 32
Extensive property 13

External flow 475
Euler's equations 342

F

Fan 463
Fanning's coefficient 27
Fanno equations 268, 647
Fanno line 173, 660
Feed system 518, 521
Finite wave 141
First law 3, 8
Flow process 22, 47
Flow through nozzles 105
Flow visualization 424
Fluid 4
Flying fire 504
Forward scatter 434

G

Gas charts 113, 193, 239
Gasoline 515
Gas pressure feed system 518
Gas pressurization 519
Gas tables 111, 192, 238
Gas turbine engines 457
Glycerine 528
Glycerol trinitrate 528
Gravity loss 674
Gravitional force 344, 568
Guided air missile 552
Gun powder 504
Gun tunnel 424

H

Heat 7
Heat transfer 8, 319
Hero's reaction turbine 455
Hodograph plane 247
Hot films 401
Hot-wire anemometer 397
Hot-wire yawmeter 403
Hybrid propellants 509
—rockets 509, 671
Hydrazine 517
Hydraulic mean diameter 587
Hydrogen peroxide 515
Hypersonic flow 53

I

ICBM 552
Ideal efficiency 486
Ideal gas 11
Impulse function 98
Impulse to weight ratio 545
Impulsive velocity 671
Incompressible flow 21, 53
Induction tunnel 417
Infinitesimal wave 131
Injectors 521
Inlet diffuser 467
Intensive property 13
Interferometer 428
Internal energy 10
International standard atmosphere 33
Interplanetary flight 553
Inward flow turbine 83
Ionosphere 32
Irreversible process 17
Isentropic process 18
Isentropic flow 59, 87, 653
Isothermal flow 282, 633

J

JATO planes 527, 551, 671
Jet pipe 460
Jet propulsion 455

Jet thrust 475
Joules cycle 458

K

Kinematic viscosity 25

L

Laminar flow 26
Lapse rate 32
Laplace's equation 367
Large pressure rise 469
Laser doppler velocimeter 433
Laser technique 430
Lift 453
Liquid hydrogen 516
Liquid oxygen 515
Liquid propellants 514
—rockets 507, 513
Linear burning rate 529
Line integral 346, 363
Lithium hydride 510
Losses and efficiencies 547

M

Mach angle 134
Mach cone 136
Mach lines 25
Mach number 56, 134
—variation 91
Mach waves 237, 248
Manometers 384
Mass flow density 266
Mass flow rate 100
Mass flow weighted mean value 383
Mass ratio 556, 671
Maximum altitude 562
Maximum deflection 249
Maximum duct length 651
Maximum heat transfer 321
Maximum rocket velocity 564
Maximum velocity 54, 64, 94
Mean coefficient of friction 279
Mesosphere 32
Minimum Mach number 240
Mixture ratio 672
Momentum equations 75, 356
Momentum flux 476, 539
Monopropellants 514
Moving shock 198, 210
Multi-stage rockets 559

N

Navier-stokes equations 349
Newton's second law 3
Newtonian fluid 24
Non-dimensional number 25
—heat transfer 319
—mass flow 100
Non-flow process 23, 46
Non-steep wave 141, 144, 601
Normal shock 169, 655
Nozzle 91
Nozzle meter 409
Nozzle throat 92
Nuclear rockets 510

O

Oblique shocks 219, 657
Off-design 108
Open-circuit tunnel 418
Open-jet tunnel 417
Open system 4, 23
Optical methods 425

Orbital velocity 568, 675
Orifice meter 405
One-dimensional flow 26, 75
Overall efficiency 480
Oswatitsch diffuser 220, 485
Oxidizers 515

P

Partial derivative 374
Path function 7
Perchlorates 527
Perfect gas 11
Photon rocket 672
Piston engine 456
Pitot-static tube 404
Pitot-tube 191
Plane of discontinuity 108
Polar diagram 243
Polymers 527
Potential function 363
Power utilization 477
Powered flight 557
Prandtl-Meyer relation 176, 254, 645
—equation 226
Pressure 6, 380
—coefficient 60
—forces 344, 358
—waves 129
Process 4
Progressive burning 533
Propellant 514
—area ratio 531
—grain 534, 672
—mass fraction 556
Propelling nozzle 472
Propeller 82, 474
Property 5
Propulsive efficiency 478, 548
Pulse-jet 487
Pumping stations 634
Pure substances 6
Pyro-technique 672

Q

Quasistatic process 17

R

Radial acceleration 354
Ram-jet engine 483, 496
Ram-jet rocket 672
Rankine-Hugoniot equation 181, 217
Rarefaction wave 171
Rate equations 73
RATO 551, 672
Rayleigh flow relations 317
—line 174, 309, 662
Real gases 13
Recovery factor 389, 626
Reference velocities 54
Resistance thermometer 390
Restricted burning 534
Retro-rocket 506, 554, 672
Reversible process 17
Reynolds number 25
Rockets 503
—applications 550
—equation 562
—fuels 516
—motors 507
—nozzle 543
—propulsion 503
—types 506
Rotameter 410

S

Schlieren technique 429
Second law 16

Shadow technique 427
Shock polar 243, 247
Shock wave 109, 169
Shock strength 188
Shock tube 423
Skin friction 27
Soap film method 413
Solar rockets 511
Solid propellants 527
—rockets 507
Sonic flow 53, 136
Sounding rockets 555
Sound waves 131, 135
Space flights 555
Specific
—fuel consumption 481
—heat 9
—impulse 481, 540
—propellant consumption 542
—thrust 481
Sputnik satellite 666
State 4, 51
Stagnation
—density 51
—enthalpy 49
—pressure 51
—state 51
—temperature 49
Standard atmosphere 33, 41
Standard pitot-tube 394
Static pressure 381
—tappings 381
Steady flow 21, 341
Steep wave 145, 152, 601
Stream function 370
Streamlines 21
Streamers 425
Stream tube 21
Stratosphere 32, 35
Strong shocks 190
Subsonic
—diffuser 92, 485
—flow 53, 396
—Mach number 97
—ramjet 483
Supersonic diffuser 484, 485, 596
—flow 53
—Mach number 97
—nozzle 484
—ramjet 484, 485
—wind tunnel 193, 418
Surface to air missile 552
Surface to surface missile 552
Sustainer rocket 552
System 4

T

Tall pipe 460
Take-off roll 454
Tangential acceleration 355
Temperature 7
—measurement 387
Thermal efficiency 480, 549
Thermocouple 391
Third law 18
Test section 195
Thrust 473, 538
—coefficient 544, 574
—decay 673
Transducers 386
Transonic flow 53
Transmission of gas 633
Troposphere 34
Turbo fan engine 462, 464
Turbojet engine 462
Turboprop engine 461
Turbopump feed system 520
Turbo-rocket 551, 673
Turbulent flow 26
Two-dimensional flow 341

U

UDMH 517, 673
Unrestricted burning 535
Universal gas constant 12
Unsteady flow 22
Use of gas tables 111, 192, 238
Utilization of energy 547
U-tube manometer 385

V

Vega-I 590
Vane anemometer 397
Van der Waal's equation 14
Van Driest's relation 35
Variation of
—gravity with altitude 569
—Mach number with duct length 279
—pressure and density with altitude 36
—Prandtl-Meyer function 255
—properties in Fanno flow 275, 281
—properties in Rayleigh flow 324
—propulsion efficiency 549
—specific impulse 481, 540
—thrust with altitude 554
—wave angle 240
Velocity 20, 393
—loss 559
—measurement 393
—of non-steep wave 142
—of steep wave 146
—of sound 54, 133
—profile 27
—triangles 224
Venera satellite 589
Venturi meter 407
Vernier rocket 673
Vertical flight 559
Vorticity components 347, 360
Viscosity 24
Viscous fluid 24
Viscous flow 27
V-2 missile 505

W

Wave 129
—angle 239
—front 130
—Mach number 143, 150
—motion 129
—propagation 129, 131
Wedge 220
—method 396
—probe 402
Weight flow coefficient 544
Wind tunnels 414
—blow-down type 420
—blower type 415
—induction type 417
—suction 416
—supersonic 418
Work 7
WFNA 673

X

X-15 hypersonic plane 506

Y

Yaw meter 401, 403

Z

Zero stage 673
Zeroth law 7
Zond-5 667
Zone of action 136
Zone of silence 136